

**FORM AND FUNCTION
IN THE HOMINOID TARSA
SKELETON**

William Harcourt-Smith

September 2002

Dissertation submitted to University College London in partial fulfilment of the requirements for the degree of Doctor of Philosophy

“..the most characteristic peculiarity in the Human structure.”

Richard Owen on the human foot, 1866, *Contributions to the Natural History of the Anthropoid apes.*

Abstract

This thesis explores form variation in the adult tarsal skeleton of extant and fossil hominoids. Three dimensional coordinate data were obtained from five bones of the foot: the calcaneus, talus, cuboid, navicular and medial cuneiform. The comparative sample was made up of *Homo sapiens*, *Pan troglodytes troglodytes*, *Pan paniscus*, *Gorilla gorilla gorilla* and *Pongo pygmaeus*. The fossil sample consisted of tarsal remains assigned to a number of Late Pliocene taxa: *Australopithecus afarensis*, *Australopithecus africanus*, *Paranthropus robustus* and *Homo habilis*. Statistical shape analysis was conducted using geometric morphometric techniques.

The first section of analysis explores sexual dimorphism in the extant hominoid foot. It is found that there is no shape dimorphism in the forefoot, and a marginal amount in the hindfoot of *Gorilla* and *Pongo* only. Such differences are likely to be linked to high degrees of body mass dimorphism in those taxa. The section concludes that shape dimorphism is unlikely to be an important factor in explaining differences between fossil hominin pedal remains.

The second section explores the inter-specific relationship between the tarsals of the extant hominoids. It is found that shape differences between taxa closely mirror those differences already described in the literature. However, it is found that the phenetic relationship between the taxa varies from bone to bone, and, furthermore, does not match the consensus molecular phylogeny. The section concludes that some tarsals are more specialised and remodelled than others, and thus great caution should be taken when considering isolated fossil pedal specimens.

The third section incorporates the fossil specimens into the study. It is found that the morphology of the *A.africanus* and *H.habilis* tarsals are very similar, and fall within extant hominoid intra-specific ranges of variation. However, the morphology of the *A.afarensis* tarsals are considerably distinct, and show a different overall pattern to those of *A.africanus* and *H.habilis*. The section concludes that all taxa were mosaic in their affinities, but were mosaic in different ways.

This thesis concludes that it is likely that there were at least two distinct ways in which the tarsals of different hominin taxa had adapted to bipedal locomotion. This finding supports recent new discoveries suggesting a far wider degree of taxonomic diversity in the African fossil hominin record than had previously been thought.

Acknowledgments

I would firstly like to thank my two supervisors Leslie Aiello and Paul O'Higgins for all their guidance, advice and considerable patience. I have enjoyed my time working with them tremendously, and there is no doubt that without them this thesis could not have happened. I would also like to thank Professor Christopher Dean for always giving excellent advice when it was most needed.

I would like to thank all the staff and students of the Evolutionary Anatomy Unit for helping to create such a lively and rewarding place to work in. I would especially like to thank Sam Cobb for all his help and support. I would also like to thank the following people: Gilles Berillon & Rebecca Fisher for stimulating conversation and helpful comments; Julia Boughner; Nick Jones; Marianne Macdonald for editorial advice; Brian Richmond & John Cant for useful pointers on primate locomotion.

Thanks are particularly due to the curators and assistants in the various museums and collections around the world where I gathered data. In no particular order: Malcolm Harman & John Harrison, of the Powell Cotton Museum, Birchington, Kent; Louise Humphrey, Paula Jenkins and Robert Kruszynski, of the Natural History Museum, London; Wendy Birch & Derek Dudley, of the Dept. Anatomy, UCL; Phillipe Menecier, of the Musée de l'Homme, Paris; Wim van Neer, of the Musée de l'Afrique Centrale, Tervuren, Belgium; Kevin Kuykendall, Beverley Kramer & Ron Clarke, of The University of the Witwatersrand, Johannesburg; Francis Thackeray, of the Transvaal Museum, Pretoria; Bob Randall of the American Museum of Natural History, New York; Linda Gordon, Richard Thorington & David Hunt, of the Smithsonian Institution (Natural History), Washington DC.

This work was funded by the Wellcome Trust Bioarchaeology Initiative. I am greatly indebted to their generosity. I also thank the UCL Graduate School for crucially funding several of my data collection trips.

I would like to thank my friends, particularly Gary Schwartz and Kate Graham for their general encouragement. Likewise my family for all their support (and good humour) throughout the course of this thesis. My final thanks goes to Amira Thoron, who has constantly inspired and encouraged me in equal amounts to finish this work.

Table of Contents

List of Figures	10
List of Tables	14
CHAPTER 1 INTRODUCTION AND LITERATURE REVIEW	17
1.1 Introduction	17
1.2 Morphometrics and its importance	18
1.3 Objectives of thesis	20
1.4 Structure of thesis	20
1.5 Notes on terminology	21
1.5.1 Overview of tarsal osteology	22
1.6 Locomotor differences in the extant hominoids	23
1.7 Foot function in locomotion	25
1.7.1 The modern human foot in bipedal locomotion	25
1.7.1.1 Force transmission	25
1.7.1.2 Overall foot movement	27
1.7.2 The great ape foot in locomotion	28
1.7.2.1 Terrestrial locomotion	28
1.7.2.2 Arboreal locomotion	29
1.8 Functional anatomy of the foot	29
1.8.1 Brief overview of anatomy of each bone	30
1.8.2 The foot as a series of functional units	34
1.8.2.1 Foot Proportions	34
1.8.2.2 Arches of the foot	36
1.8.2.3 The talo-crural joint	39
1.8.2.4 The sub-talar joint	40
1.8.2.5 Talar neck and neck-torsion angles	42
1.8.2.6 The calcaneocuboid complex	43
1.8.2.7 Cuboid morphology	45
1.8.2.8 The talo-navicular joint	45
1.8.2.9 The 1 st tarso-metatarsal joint	46
1.8.2.10 The 2 nd to 5 th rays	48

1.8.2.11	Summary	49
1.9	The foot in the hominin fossil record	49
1.9.1	The calcaneus in the fossil record	50
1.9.2	The calcaneo-cuboid joint in the fossil record	51
1.9.3	The talus in the fossil record	52
1.9.4	The navicular in the fossil record	55
1.9.5	The 1 st tarso-metatarsal joint in the fossil record	57
1.9.6	Rays II to V in the fossil record	60
1.9.7	Summary of fossil hominin pedal functional anatomy by taxon	61
1.9.8	Models of hominin foot evolution	64
1.10	Summary	67
 CHAPTER 2 MATERIALS AND METHODS		 68
2.1	Materials	68
2.2	Methods	73
2.2.1	Landmark choice	73
2.2.2	Data collection	84
2.2.3	The issue of size	85
2.2.4	Analysis of landmark data	86
2.2.4.1	Background	86
2.2.4.2	Recent approaches	86
2.2.4.2.1	EDMA	86
2.2.4.2.2	Superimposition	87
2.2.4.3	How GPA works	88
2.2.4.4	Statistical analysis of registered forms	89
2.2.4.5	Principal Components Analysis	90
2.2.4.6	Thin Plate Splines	90
2.2.4.7	Visualisation	91
2.2.4.8	Implementation of methods for this study	91
2.2.4.9	Procrustes distances	92
2.2.4.10	Procrustes distances between means	92
2.2.4.11	Permutation tests	92
2.2.4.12	UPGMA phenograms	93
2.2.4.13	Maximum Likelihood	93

CHAPTER 3 INTRA-SPECIFIC SHAPE VARIATION	94
3.1 Introduction	94
3.1.1 Sex differences in locomotor repertoires	95
3.1.2 Hypotheses	97
3.2 Materials	98
3.2.1 Sample size for intraspecific study	98
3.3 Methods	99
3.4 Results	101
3.4.1 Centroid size	101
3.4.2 <i>Pongo pygmaeus</i>	102
3.3.3 <i>Pan troglodytes troglodytes</i>	106
3.3.4 <i>Pan paniscus</i>	106
3.3.5 <i>Gorilla gorilla gorilla</i>	108
3.3.6 <i>Homo sapiens</i>	112
3.3.6.1 Zulus	112
3.3.6.2 Xhosa	113
3.5 Discussion	114
3.5.1 Functional considerations	115
CHAPTER 4 INTER-SPECIFIC SHAPE VARIATION	117
4.1 Introduction	117
4.1.1 Summary of anatomical differences between extant hominoid tarsals	117
4.1.2 Summary of locomotor differences between extant hominoids	119
4.1.3 Factors that may account for shape differences between species	120
4.1.4 Hypotheses	122
4.1.5 Summary of how results are laid out	123
4.2 Materials	124
4.3 Methods	124
4.4 Results	125
4.4.1 Centroid Size	125
4.4.2 Distribution of individual specimens	127
4.4.2.1 Calcaneus	127
4.4.2.2 Talus	129

4.4.2.3	Cuboid	130
4.4.2.4	Navicular	132
4.4.2.5	Medial Cuneiform	133
4.4.3	Shape variation between taxa	135
4.4.3.1	Calcaneus	135
4.4.3.2	Talus	138
4.4.3.3	Cuboid	140
4.4.3.4	Navicular	142
4.4.3.5	Medial Cuneiform	143
4.4.4	Statistical relationships between taxa	146
4.4.4.1	Phenograms	149
4.4.4.2	Maximum Likelihood	152f
4.5	Discussion	153
4.5.1	Size versus shape	153
4.5.2	Comparative anatomy	153
4.5.2.1	Calcaneus	153
4.5.2.2	Talus	154
4.5.2.3	Cuboid	156
4.5.2.4	Navicular	157
4.5.2.5	Medial Cuneiform	158
4.5.3	Relationships between taxa	159
4.5.4	Summary	161
CHAPTER 5	FOSSIL SHAPE VARIATION	173
5.1	Introduction	173
5.1.1	Which species were fully bipedal?	173
5.1.2	<i>Homo habilis</i> versus <i>Australopithecus africanus</i>	174
5.1.3	Did the feet of fossil taxa adapt to bipedalism in different ways?	175
5.2	Hypotheses	176
5.3	Materials	176
5.4	Methods	179
5.5	Results	181
5.5.1	Talus	181
5.5.2	Cuboid	190

5.5.3	Navicular	195
5.5.4	Medial Cuneiform	202
5.6	Discussion	208
5.6.1	Talus	208
5.6.2	Cuboid	209
5.6.3	Navicular	210
5.6.4	Medial Cuneiform	212
5.7	Hypotheses	213
5.8	Summary	214
CHAPTER 6 CONCLUSIONS		217
6.1	Summary of Results	217
6.2	Conclusions	220
6.2.1	How these findings relate to the “problem” taxon, <i>Homo habilis</i>	220
6.2.2	How these findings relate to various models of hominin foot evolution	222
6.2.3	How these findings relate to the origins of bipedalism	224
APPENDIX		228
BIBLIOGRAPHY		235

List of Figures

CHAPTER 1

Figure 1.1	Schematic of dorsiflexion/plantar flexion and abduction/adduction	21
Figure 1.2	Bones of the hominoid foot	22
Figure 1.3	Summary of locomotor affinities of extant hominoids	24
Figure 1.4	Centres of pressure in the foot during stance phase of walking	26
Figure 1.5	Vertical ground reaction forces during modern human stance phase	27
Figure 1.6	The Calcaneus	30
Figure 1.7	The Cuboid	31
Figure 1.8	The Talus	32
Figure 1.9	The Navicular	32
Figure 1.10	The Medial Cuneiform	33
Figure 1.11	Lateral view of the chimpanzee and modern human articulated foot	36
Figure 1.12	Path of leg over foot in chimpanzees and humans during walking	40
Figure 1.13	The sub-talar joint	41
Figure 1.14	Talar neck and neck torsion angles	42
Figure 1.15	The calcaneocuboid joint: lateral view	43
Figure 1.16	The calcaneocuboid joint: plantar-medial view	44
Figure 1.17	Metatarsal and hallucial torsion in the hominoids	47
Figure 1.18	Reconstruction of “Littlefoot” pedal assemblage	63
Figure 1.19	Morton’s hypothetical “prehuman foot”	65

CHAPTER 2

Figure 2.1	Diagrams of landmarks	79
Figure 2.1	Wireframe models	82
Figure 2.3	PC 1 vs. PC 2 for 40 Zulu naviculars versus 10 repeats	85

CHAPTER 3

Figure 3.1	Talus: PC 1 versus PC 2 for <i>Pongo pygmaeus</i> males and females	102
Figure 3.2	Talus: warped images of mean female vs. male shapes for <i>Pongo</i>	103

Figure 3.3	Calcaneus: PC 1 versus PC 2 for <i>Pongo pygmaeus</i> males and females	104
Figure 3.4	Calcaneus: warped images of mean female vs. male shapes for <i>Pongo</i>	105
Figure 3.5	Calcaneus: PC 1 versus PC 2 for <i>Pan paniscus</i> males and females	107
Figure 3.6	Calcaneus: warped images of mean female vs. male shapes for <i>P.paniscus</i>	107
Figure 3.7	Calcaneus: PC 1 versus PC 2 for <i>Gorilla gorilla</i> males and females	108
Figure 3.8	Calcaneus: warped images of mean female vs. male shapes for <i>Gorilla</i>	109
Figure 3.9	Talus: PC 1 versus PC 2 for <i>Gorilla gorilla</i> males and females	110
Figure 3.10	Talus: warped images of mean female vs. male shapes for <i>Gorilla</i>	111
Figure 3.11	Medial Cuneiform: PC 1 versus PC 2 for <i>Homo sapiens</i> males and females	112
Figure 3.12	Medial Cuneiform: warped images of mean female vs. male shapes for <i>H.sapiens</i>	113

CHAPTER 4

Figure 4.1	Summary of relative degrees of arboreality/terrestriality in hominoids	120
Figure 4.2	Consensus molecular relationships amongst extant hominoidea	121
Figure 4.3	Calcaneus: PC 1 versus PC 2	127
Figure 4.4	Calcaneus: PC 1 versus PC 3	128
Figure 4.5	Calcaneus: PC 2 versus PC 3	129
Figure 4.6	Talus: PC 1 versus PC 2	130
Figure 4.7	Cuboid: PC 1 versus PC 2	131
Figure 4.8	Navicular: PC 1 versus PC 2	132
Figure 4.9	Medial Cuneiform: PC 1 versus PC 2	133
Figure 4.10	Medial Cuneiform: PC 1 versus PC 3	134
Figure 4.11	Calcaneus means: PC 1 versus PC 2	135
Figure 4.12	Calcaneus means: PC 1 versus PC 3	137
Figure 4.13	Talus means: PC 1 versus PC 2	140
Figure 4.14	Cuboid means: PC 1 versus PC 2	141
Figure 4.15	Navicular means: PC 1 versus PC 2	143

Figure 4.16	Medial Cuneiform: PC 1 versus PC 2	145
Figure 4.17	Medial Cuneiform: PC 1 versus PC 3	146
Figure 4.18	Calcaneus: UPGMA phenogram using Procrustes distances between means	149
Figure 4.19	Talus: UPGMA phenogram using Procrustes distances between means	150
Figure 4.20	Cuboid: UPGMA phenogram using Procrustes distances between means	151
Figure 4.21	Navicular: UPGMA phenogram using Procrustes distances between means	151
Figure 4.22	Medial Cuneiform: UPGMA phenogram using Procrustes distances between means	152
Figure 4.23	Calcaneus: TPS grid A and warped means	163
Figure 4.24	Talus: TPS grid A and warped means	164
Figure 4.25	Talus: TPS grid B and warped means	165
Figure 4.26	Talus: TPS grid C and warped means	166
Figure 4.27	Cuboid: TPS grid A and warped means	167
Figure 4.28	Navicular: TPS grid A and warped means	168
Figure 4.29	Navicular: TPS grid B and warped means	169
Figure 4.30	Medial Cuneiform: TPS grid A and warped means	170
Figure 4.31	Medial Cuneiform: TPS grid B and warped means	171
Figure 4.32	Medial Cuneiform: TPS grid C and warped means	172
Figure 4.33	Calcaneus: Maximum Likelihood tree	152a
Figure 4.34	Talus: Maximum Likelihood tree	152b
Figure 4.35	Cuboid: Maximum Likelihood tree	152c
Figure 4.36	Navicular: Maximum Likelihood tree	152d
Figure 4.37	Medial Cuneiform: Maximum Likelihood tree	152e

CHAPTER 5

Figure 5.1	Map of Africa showing fossil localities	179
Figure 5.2	Talus: PC 1 versus PC 2. Lateral malleolar facet included	182
Figure 5.3	Talus: PC 1 versus PC 2. Lateral malleolar facet excluded	182
Figure 5.4	Talus: PC 1 versus PC 2. Trochlea and medial malleolar facet only	183
Figure 5.5	Talus: PC 1 versus PC 2. Extant means and fossils	185

Figure 5.6	Talus: PC 1 versus PC 3. Extant means and fossils	186
Figure 5.7	Talus: PC 2 versus PC 3. Extant means and fossils	187
Figure 5.8	Talus: PC 1 versus PC 4. Extant means and fossils	187
Figure 5.9	Talus: UPGMA phenogram using extant means and fossils	189
Figure 5.10	Talus: Frequency histogram of pairwise Procrustes distances	190
Figure 5.11	Cuboid: PC 1 versus PC 2	191
Figure 5.12	Cuboid: PC 1 versus PC 2. Extant means and OH 8	192
Figure 5.13	Cuboid: warped means (medial aspect)	193
Figure 5.14	Cuboid: UPGMA phenogram using extant means and OH 8	194
Figure 5.15	Navicular: PC 1 versus PC 2	195
Figure 5.16	Navicular: PC 1 versus PC 2. Extant means and fossils	196
Figure 5.17	Navicular: PC 1 versus PC 3. Extant means and fossils	198
Figure 5.18	Navicular: PC 2 versus PC 3. Extant means and fossils	199
Figure 5.19	Navicular: UPGMA phenogram using extant means and fossils	201
Figure 5.20	Navicular: Frequency histogram of pairwise Procrustes distances	201
Figure 5.21	Medial Cuneiform: PC 1 versus PC 2	203
Figure 5.22	Medial Cuneiform: PC 1 versus PC 3	203
Figure 5.23	Medial Cuneiform: PC 1 versus PC 2. Extant means and fossils	204
Figure 5.24	Medial Cuneiform: UPGMA phenogram using extant means and fossils	206
Figure 5.25	Medial Cuneiform: Frequency histogram of pairwise Procrustes distances	207

CHAPTER 6

Figure 6.1	Temporal distribution of hominin taxa	219
Figure 6.2	Schematic of possible trends in the hominin fossil pedal record	226

APPENDIX

Figure A.1	Calcaneus: PC 1 versus centroid size	228
Figure A.2	Calcaneus: PC 2 versus centroid size	229
Figure A.3	Calcaneus: PC 3 versus centroid size	229
Figure A.4	Talus: PC 1 versus centroid size	230
Figure A.5	Talus: PC 2 versus centroid size	230
Figure A.6	Cuboid: PC 1 versus centroid size	231

Figure A.7	Cuboid: PC 2 versus centroid size	231
Figure A.8	Navicular: PC 1 versus centroid size	232
Figure A.9	Navicular: PC 2 versus centroid size	232
Figure A.10	Medial Cuneiform: PC 1 versus centroid size	233
Figure A.11	Medial Cuneiform: PC 2 versus centroid size	233
Figure A.12	Medial Cuneiform: PC 3 versus centroid size	234

List of Tables

CHAPTER 2

Table 2.1	Sample numbers for each bone for each extant species	71
Table 2.2	Cuboid landmarks	74
Table 2.3	Talar landmarks	75
Table 2.4	Navicular landmarks	76
Table 2.5	Calcaneus landmarks	77
Table 2.6	Medial Cuneiform landmarks	78

CHAPTER 3

Table 3.1	Sample sizes for each bone and species, separated by sex	98
Table 3.2	Procrustes distances between means and significance values	100
Table 3.3	Correlation between PCs 1 to 3 and centroid size	101
Table 3.4	Talus: percentage variance explained by PC 1 to PC 4 for <i>Pongo</i>	103
Table 3.5	Calcaneus: percentage variance explained by PC 1 to PC 4 for <i>Pongo</i>	105
Table 3.6	Calcaneus: percentage variance explained by PC 1 to PC 4 for <i>Pan paniscus</i>	106
Table 3.7	Calcaneus: percentage variance explained by PC 1 to PC 4 for <i>Gorilla</i>	109
Table 3.8	Talus: percentage variance explained by PC 1 to PC 4 for <i>Gorilla</i>	111
Table 3.9	Medial Cuneiform: percentage variance explained by PC 1 to PC 4 for <i>Homo sapiens</i> (Zulus)	113

CHAPTER 4

Table 4.1	Sample size for each bone and each taxa	124
Table 4.2	Correlation between PCs 1 to 3 and Centroid Size for each tarsal	126
Table 4.3	Calcaneus: Percentage variance explained by PC 1 to PC 4	128
Table 4.4	Talus: Percentage variance explained by PC 1 to PC 4	130
Table 4.5	Cuboid: Percentage variance explained by PC 1 to PC 4	131
Table 4.6	Navicular: Percentage variance explained by PC 1 to PC 4	132
Table 4.7	Medial Cuneiform: Percentage variance explained by PC 1 to PC 4	134
Table 4.8	Calcaneus means: Percentage variance explained by PC 1 to PC 4	137
Table 4.9	Talus means: Percentage variance explained by PC 1 to PC 4	138
Table 4.10	Cuboid means: Percentage variance explained by PC 1 to PC 4	141
Table 4.11	Navicular means: Percentage variance explained by PC 1 to PC 4	142
Table 4.12	Medial Cuneiform means: Percentage variance explained by PC 1 to PC 4	144
Table 4.13	Calcaneus: Procrustes distances between means and significance values	147
Table 4.14	Talus: Procrustes distances between means and significance values	147
Table 4.15	Cuboid: Procrustes distances between means and significance values	148
Table 4.16	Navicular: Procrustes distances between means and significance values	148
Table 4.17	Medial Cuneiform: Procrustes distances between means and significance values	149

CHAPTER 5

Table 5.1	Talus: Percentage variance explained by PC 1 to PC 4	181
Table 5.2	Talus without lateral malleolar facet: Percentage variance explained by PC 1 to PC 4	183
Table 5.3	Talar trochlea and medial malleolar facet only: Percentage variance explained by PC 1 to PC 4	184
Table 5.4	Talus (fossils and extant means): Percentage variance explained by PC 1 to PC 4	184
Table 5.5	Talus: Pairwise Procrustes distances between fossils and extant means	188

Table 5.6	Cuboid: Percentage variance explained by PC 1 to PC 4	191
Table 5.7	Cuboid (OH 8 and extant means): Percentage variance explained by PC 1 to PC 4	192
Table 5.8	Cuboid: Pairwise Procrustes distances between fossils and extant means	194
Table 5.9	Navicular: Percentage variance explained by PC 1 to PC 4	195
Table 5.10	Navicular (fossils and extant means): Percentage variance explained by PC 1 to PC 4	197
Table 5.11	Navicular: Pairwise Procrustes distances between fossils and extant means	200
Table 5.12	Medial Cuneiform: Percentage variance explained by PC 1 to PC 4	204
Table 5.13	Medial Cuneiform (fossils and extant means): Percentage variance explained by PC 1 to PC 4	205
Table 5.14	Medial Cuneiform: Pairwise Procrustes distances between fossils and extant means	205
Table 5.15	Summary of fossil hominin tarsal affinities and inferred functions	216

Chapter 1

1.1 Introduction

In terms of human evolution in the broader context, it is now generally considered that the development of bipedal locomotion as the primary form of locomotor activity was one of the most significant adaptations to occur within the hominin lineage. Traditionally, it has been argued that there were a number of major steps in the evolution of *Homo sapiens*, such as upright walking, increased encephalisation, tool use and the development of language. Whilst the reality is undoubtedly more complex, the fact remains that knowledge about how and when bipedal locomotion developed in the hominins is crucial to our understanding of how we evolved.

When considering the human postcranial skeleton in terms of its evolution, the foot can be considered to be highly specialised in both its anatomy and function. This is due to the fact that of all extant primates humans are the only obligate bipeds, and this unique form of locomotion has resulted in some very specific adaptations; particularly within the lower limb complex, and especially throughout the foot. Compared to the hand, the human foot is considerably more remodelled. Laitman (1982) pertinently argues that it is the function of the human hand, and thus its subsequent role, that is so specialised, but with the human foot it is both structure *and* function that are so unique. This makes perfect sense, since in developing bipedal locomotion, the foot becomes the only structure that directly interfaces with the ground, and subsequently is under strong selection pressure to deal with both balance and propulsion in a highly efficient way. Even in the more arboreal great apes, the lower limb is always the principal limb of locomotion. As such, increased knowledge about the relationship between structure and function in the foot bones of our hominin ancestors, as well as extant primates, is central to our understanding of the origins of bipedalism.

There has been a considerable degree of debate surrounding locomotor affinities inferred from fossil hominin foot bones. It is well known that geologically more “recent” hominin species, such as *Homo antecessor*, *Homo neanderthalensis* and *Homo sapiens* were fully bipedal, and had feet that reflected this (Trinkhaus, 1983a;

Aiello & Dean, 1990; Lorenzo *et al.*, 1999). Although there are no associated foot bones for *Homo ergaster*, we also know from the rest of the postcranial skeleton that that taxon was also fully bipedal (Ruff & Walker, 1993). Beyond that there is still a large degree of disagreement. The details of this are discussed later on in this chapter, but in general, it has been suggested by some that hominin species as old as 5.8 million years may have manifested an early form of terrestrial bipedalism as part of their locomotor repertoire (Haile-Selassie, 2001), whereas others maintain that the far more recent *Homo habilis* (at 1.8 mya) still retained arboreal adaptations (Lewis, 1980b; Oxnard & Lisowski, 1980; Kidd *et al.*, 1996; McHenry & Berger, 1998; Wood & Collard, 1999). For taxa that lie between these two dates, there is also considerable debate. The *Australopithecus afarensis* finds from Hadar, Ethiopia, are described by some as having foot bones compliant with full bipedal locomotion (Latimer & Lovejoy, 1982; Latimer *et al.*, 1987; Latimer & Lovejoy, 1989; Latimer & Lovejoy, 1990a, 1990b), whereas others have suggested that the same fossils show traits that indicate a mosaic of terrestrial and arboreal locomotion (Susman & Stern, 1982; Stern & Susman, 1983; Susman, 1983; Susman *et al.*, 1985; Stern & Susman, 1991; Susman & Stern, 1991; Duncan *et al.*, 1994; Berillon, 1998, 1999, 2000). The issue is further complicated by the suggestion that the foot of the important new “Littlefoot” specimen, currently assigned to *Australopithecus africanus*, and possibly as old as 3.6 mya, reflected an individual mosaic in its locomotor affinities (Clarke & Tobias, 1995).

There are a couple of problems with most of these studies. They have either concentrated on one particular pedal element, such as the talus, or have concentrated on one particular taxon. No metrical study to date has incorporated *all* the bones of the foot from *all* available fossil hominin taxa from the Plio-Pleistocene. Exhaustive as this sounds, until such integrated studies are performed, we are left with a rather incomplete view of hominin foot evolution.

1.2 Morphometrics and its importance

The traditional way of comparing the anatomy of different primate taxa, both fossil and living, can be broken down into two types of methodology: quantitative and qualitative analysis. The majority of early comparative studies took the qualitative

approach, with discussion centring on the presence or absence of particular structures, or of the relative degree of prominence or orientation of anatomical features. These studies provided the principal groundwork for comparative anatomy and palaeontology, but it is also evident that a degree of subjectivity was inescapable. Such studies also tended to use very small sample sizes, and there was little discussion of the range of variation of certain morphologies. This is a particularly important issue when considering the affinities of fossil specimens. Unless there is noticeable pathology, researchers have to assume that fossil specimens are an “ideal” representation of their taxon. This may often not be the case, but unless sample sizes are large enough (which is certainly not the case in the hominin fossil record) the assumption cannot be avoided. This problem has led to an increased requirement to quantify morphology, so that large sample sizes of extant taxa can be objectively measured, and fossils compared accordingly using suitable statistical techniques. The traditional way of doing this has been to take interlandmark distances, and, where relevant, angles. These distances and angles are often used to directly infer particular functional adaptations. Combinations of these distances can be converted into indices, but the fact remains that both these distances and angles are one or two-dimensional measurements. Bones are three-dimensional objects, and any study trying to quantify a 3D structure using two-dimensional measurements is going to result in a lot of important information being lost.

Recent technology is making it possible to address this problem. Three-dimensional landmarks can be easily collected, and modern computer power makes it possible to statistically analyse comparative datasets of 3D shapes, as well as visualise 3D shape change from one taxon to another. This new methodology, termed 3D geometric morphometrics, greatly increases the resolution of quantitative analysis of anatomical structures (O'Higgins, 2000).

There has been much discussion on the comparative anatomy of the hominin foot, but very few quantitative analyses have been done. Those that have been done have all used two-dimensional measurements, and, to date, there has been no attempt to address the morphological affinities and subsequent function of fossil hominins, using the three dimensional approach.

1.3 Objectives of this thesis

The objectives of this thesis are several fold. Firstly, it intends to take an integrated approach to the foot, which means that rather than concentrate on one bone, a number of pedal elements are analysed. More specifically this thesis concentrates on the tarsal region of the foot, which, as discussed later on in this chapter, is responsible for the majority of specialised foot functions in both modern humans and the great apes. Secondly, this thesis aims to take an integrated approach to fossil taxa in the Plio-Pleistocene, and thus attempts to incorporate as many specimens as possible from the known fossil records. Specimens from *Homo habilis*, *Paranthropus robustus*, *Australopithecus afarensis* and *Australopithecus africanus* are all represented here. This greatly facilitates the task of actually being able to comment on trends and events in human evolution, rather than just commenting on the affinities of one specimen. It is important to note that this study represents the first study, comparative or otherwise, to metrically analyse the important new *A.africanus* find Stw 573 (Littlefoot).

Finally, this study aims to approach the foot from the three-dimensional perspective. As discussed above, contemporary technology makes it possible to easily analyse and statistically compare 3D representations of foot bones (as determined by landmarks), and this should greatly increase the resolution of any findings.

1.4 Structure of thesis

This chapter reviews the literature relevant to the evolution of the modern human foot. Within this chapter, section 1.5 introduces anatomical terminology relevant to the foot. Section 1.6 discusses the different types of locomotion that exist in the extant hominoids. Section 1.7 discussed how the foot specifically operates during these different types of locomotion. Section 1.8 addresses the comparative anatomy of the feet of the extant hominoids, and section 1.9 discusses the comparative context of fossilised hominin pedal remains. Chapter 2 discusses the materials and methodology used in this study. Chapter 3 addresses interspecific variation in the modern hominoid foot, and particularly tests hypotheses relating to sexual dimorphism. Chapter 4 addresses interspecific differences between modern hominoid taxa, and Chapter 5 incorporates the fossil specimens, and tests hypotheses relating to those fossils.

Chapter 6 draws together the findings of the previous three chapters, and attempts to present a number of conclusions about hominoid foot evolution

1.5 Notes on terminology

There is a degree of inconsistency over the precise use and definition of certain anatomical terms as regards the foot (McDonald & Tavener, 1999). In order to clarify the meaning of certain terms, the definitions below are used throughout this thesis:

- Medial & lateral:* Relative to the sagittal midline of the body.
Hindfoot: The talus and calcaneus.
Forefoot: The navicular, cuboid, cuneiforms, metatarsals and phalanges.
Plantar flexion: Downwards rotation of the foot at the ankle, away from the anterior surface of the tibia.
Dorsiflexion: Upwards rotation of the foot at the ankle, towards the anterior surface of the tibia.
Eversion: Raising of the lateral side of the foot relative to the medial side.
Inversion: Raising of the medial side of the foot relative to the lateral side.
Abduction : Deviation away from the midline of the foot.
Adduction: Deviation towards the midline of the foot.

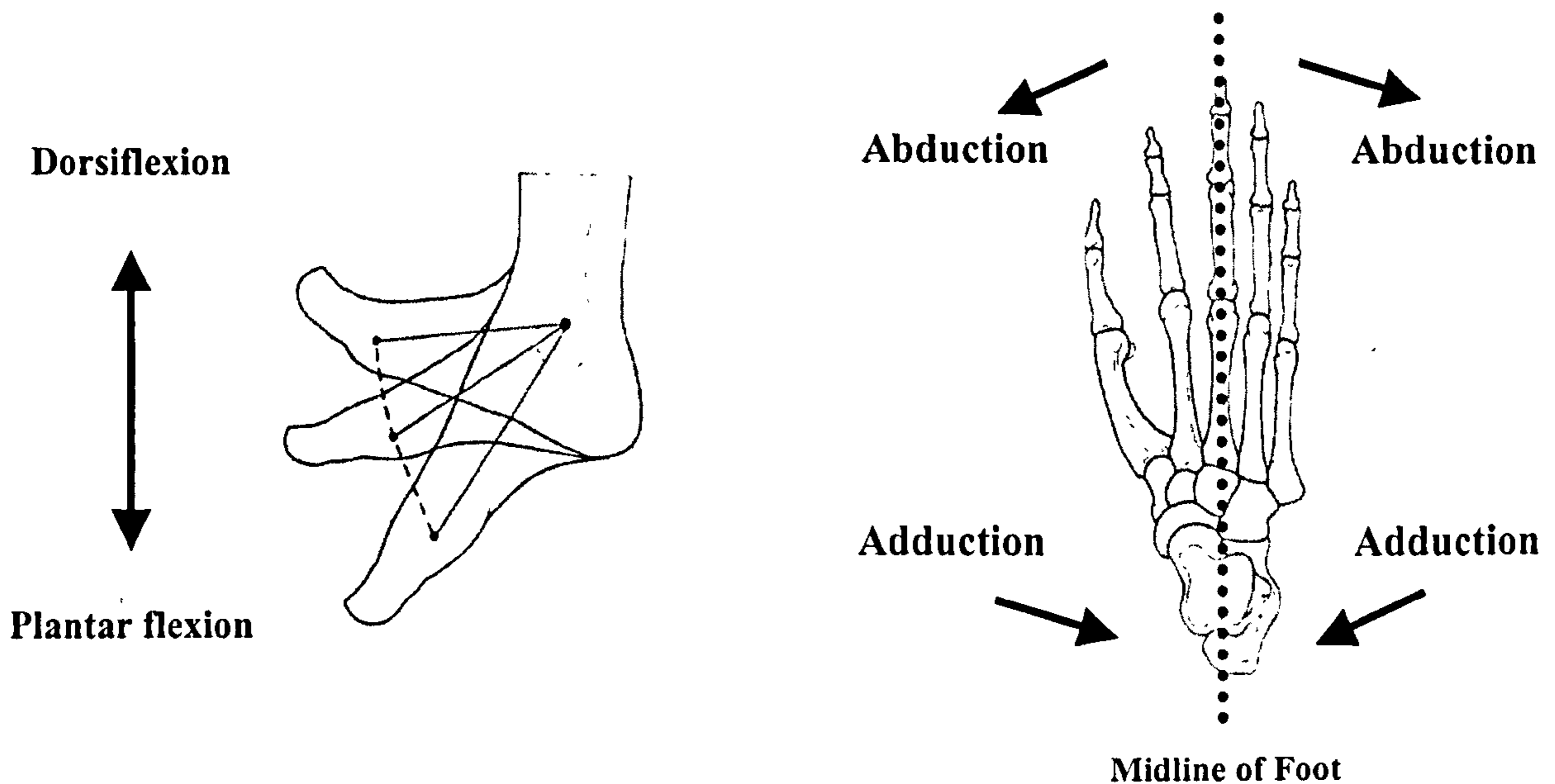


Figure 1.1 *Left:* Schematic of dorsiflexion versus plantar flexion
Right: Schematic showing abduction versus adduction
 (both adapted from Aiello & Dean, 1990)

1.5.1 Overview of osteology

The hominoid foot is usually made up of 26 bones. There is occasionally an extra number of accessory and sesamoid bones which can add to this total number. Figure 2 shows a dorsal view of a typical hominoid foot. The foot is divided into three sections: the tarsals, the metatarsals and the phalanges (Helal & Wilson, 1988; Aiello & Dean, 1990). There are seven tarsals: the calcaneus, the talus, the navicular, the cuboid, and the lateral, intermediate and medial cuneiforms. Collectively, they are sometimes referred to as the *tarsus*. The metatarsals and phalanges are broken down into five columns, or rays, with the phalanges of each ray making up the toe bones. There are five metatarsals, each forming the proximal segments of each ray. There are fourteen phalanges, with three each for rays 2 to 4, and only two for the first ray.

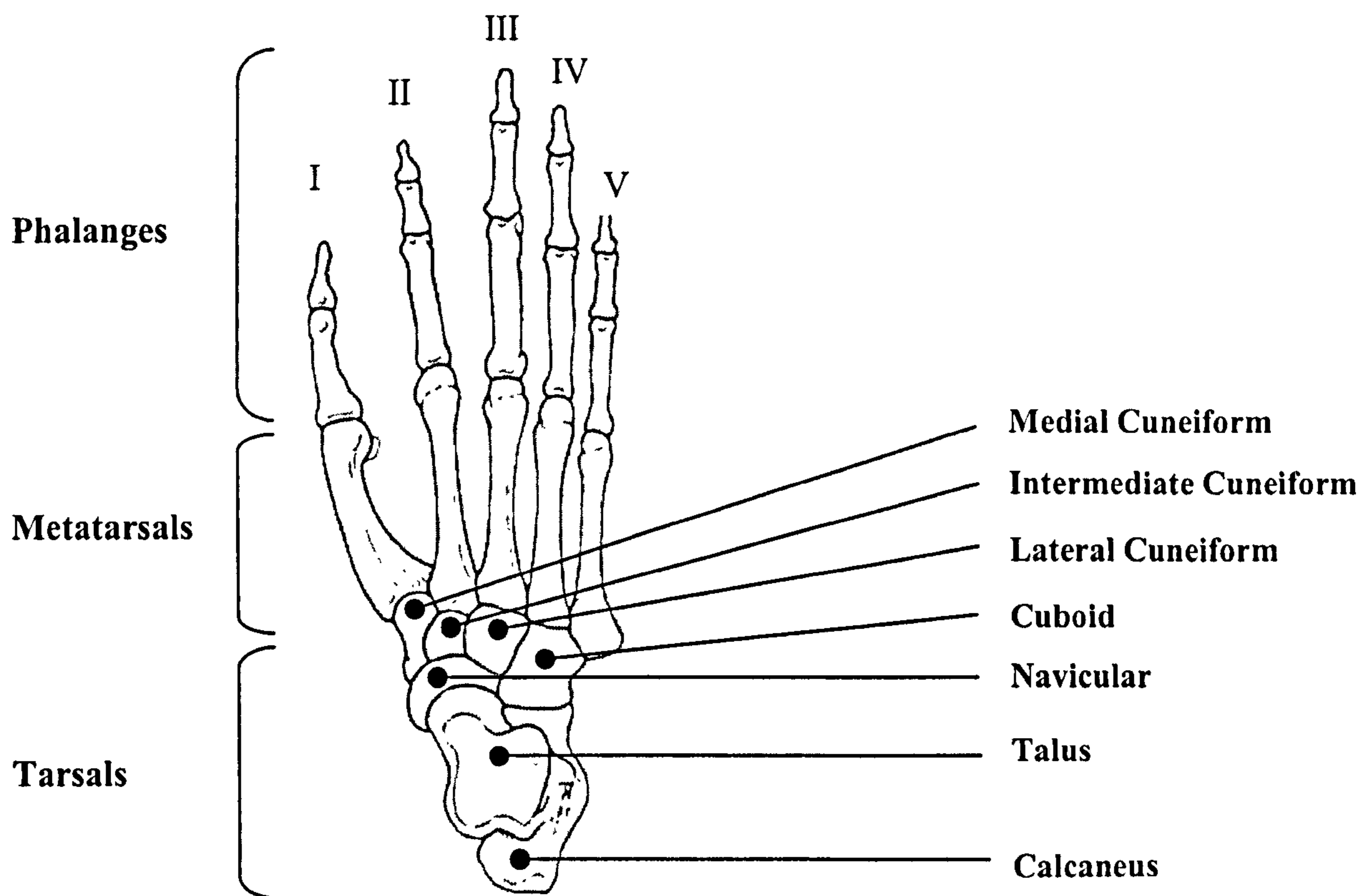


Figure 1.2 Dorsal view of a right hominoid foot. Numbers I – V represent each ray (adapted from Aiello & Dean, 1990).

1.6 Locomotor differences in the extant hominoids

Modern humans are almost exclusively bipedal. As discussed below, other species of ape can move bipedally (albeit for short periods of time), but no other extant primate uses this form of locomotion at the cost of all other types. Newborn modern humans cannot walk bipedally, and crawl to move, but within a few years bipedal walking has developed as the primary form of locomotion. In this respect modern humans can be considered to have an extremely specialised form of locomotion.

On the other hand, of the great apes being discussed here, *Pongo* is considered to be the most arboreal. Adult orangutans are almost exclusively arboreal, with the majority of their locomotor behaviour being taken up by clambering, vertical climbing, brachiation and arboreal quadrupedalism. They are also well known to have a predilection for suspensory posture (Tuttle, 1968). Clambering, which accounts for over 50% of observed locomotor behaviour mainly consists of forelimb suspension and hindlimb support and suspension (Tuttle, 1968; Cant, 1987). In this respect *Pongo* can be considered to be an arboreal specialist.

The most important aspect of the African apes is that, unlike *Pongo* and modern humans, their speciality lies not in their tendency to be *either* arboreal or terrestrial specialists, but rather on having a mosaic of different locomotor modes that suit different environments and situations. Field observations have shown that all three taxa of African ape spend considerable time in both the trees and on the ground. The principal form of terrestrial locomotion is fast and slow knuckle-walking, where the legs do most of the propulsive work, but a significant degree of body weight is borne by the upper limbs through the knuckles (Tuttle, 1970). African apes spend a small degree of time walking bipedally, but only for relatively short periods of time (Tuttle, 1970). When they are moving bipedally, the gait is an awkward “shuffling” movement, with marked mediolateral swaying of the body from step to step. *Pan* also spends a degree of time standing bipedally, mainly to collect fruit in tall bushes, but it is important to note that even when doing so, individuals are partially supporting themselves with their upper limbs, which are grasping onto branches (Hunt, 1994; Doran & Hunt, 1995). When in the trees, *Pan troglodytes* has a particular predilection for using knuckle-walking to move along large branches (Tuttle, 1970).

Within the African apes, *Pan paniscus* has been shown to be the most arboreal species. Although chimpanzees and bonobos show similar changes in locomotor behaviour during growth, adult bonobos have been observed to be more arboreal, and use more suspensory behaviour, than adult chimpanzees (Doran, 1992; Doran & Hunt, 1995). *Gorilla* has been shown to be the least arboreal of the non-human great apes, and field data shows that they are never as arboreal as chimpanzees or bonobos (Tuttle, 1968). However, smaller gorillas that are of a comparable size to chimpanzees have been shown to be as arboreal as the chimpanzees (Doran, 1997). This observation has led to suggestions that body size is the primary factor in explaining why bonobos are the most arboreal and gorillas the least arboreal of the African apes, since bonobos are the smallest in body size and gorillas the largest.

Figure 1.3 below summarizes the degrees of terrestriality/arboreality seen in the great apes.

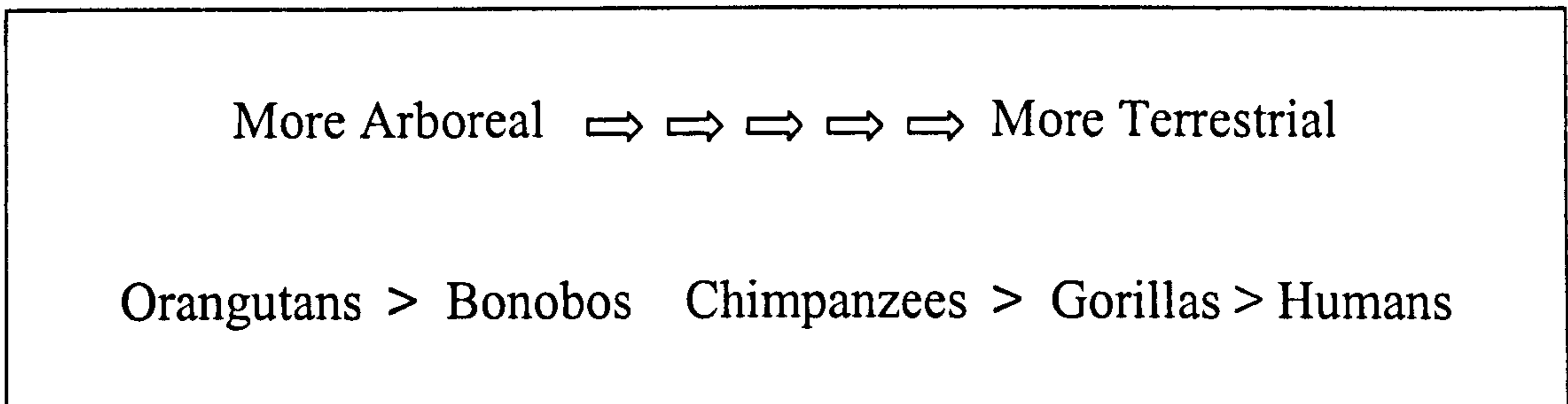


Figure 1.3 Summary of locomotor affinities of extant hominoids.

1.7 Foot function in locomotion

1.7.1 *The modern human foot in bipedal locomotion*

1.7.1.1 *Force transmission*

Before discussing this, there are a number of terms that need to be clarified. When the foot strikes the ground, this is known as *heel-strike*. At this point the foot enters the *stance phase*, and the other foot, now off the ground, is in the *swing phase*. The point when the body is directly over the weight bearing foot is known as the *mid-stance phase*, and the point at which the foot pushes off from the ground is referred to as *toe-off* (Helal & Wilson, 1988; Mann, 1988; Hutton & Stokes, 1991).

There has been a considerable amount of research into the patterns of force distribution through the modern human foot during locomotion, since knowledge about the distribution of forces exerted from the foot to the ground will give accurate information about foot movement and architecture. This has mainly come from studies of footprints and force plate studies. The initial force through the ground is transmitted through the heel, at heel strike, with the lateral margin of the heel contacting the ground first. The fifth metatarsal (and sometimes the fourth as well) usually strikes the ground next. Force is thus transmitted along the lateral side of the foot from heel strike through to the mid-stance phase. Force then rapidly shifts medially across the metatarsal heads to the ball of the foot, and by this point the heel has left the ground. The foot continues to roll medially, and the last part to leave the ground is the distal part of the hallux. This information has been summarised by a number of studies which show that the pathway for the centre of loading passes from directly under the lateral side of the calcaneus in a straight line distally, before shifting medially to the centre of the big toe, at which point the foot leaves the ground (see Figure 1.4) (Czerniecki, 1988; Helal & Wilson, 1988; Mann, 1988; Aiello & Dean, 1990; Mann, 1991).

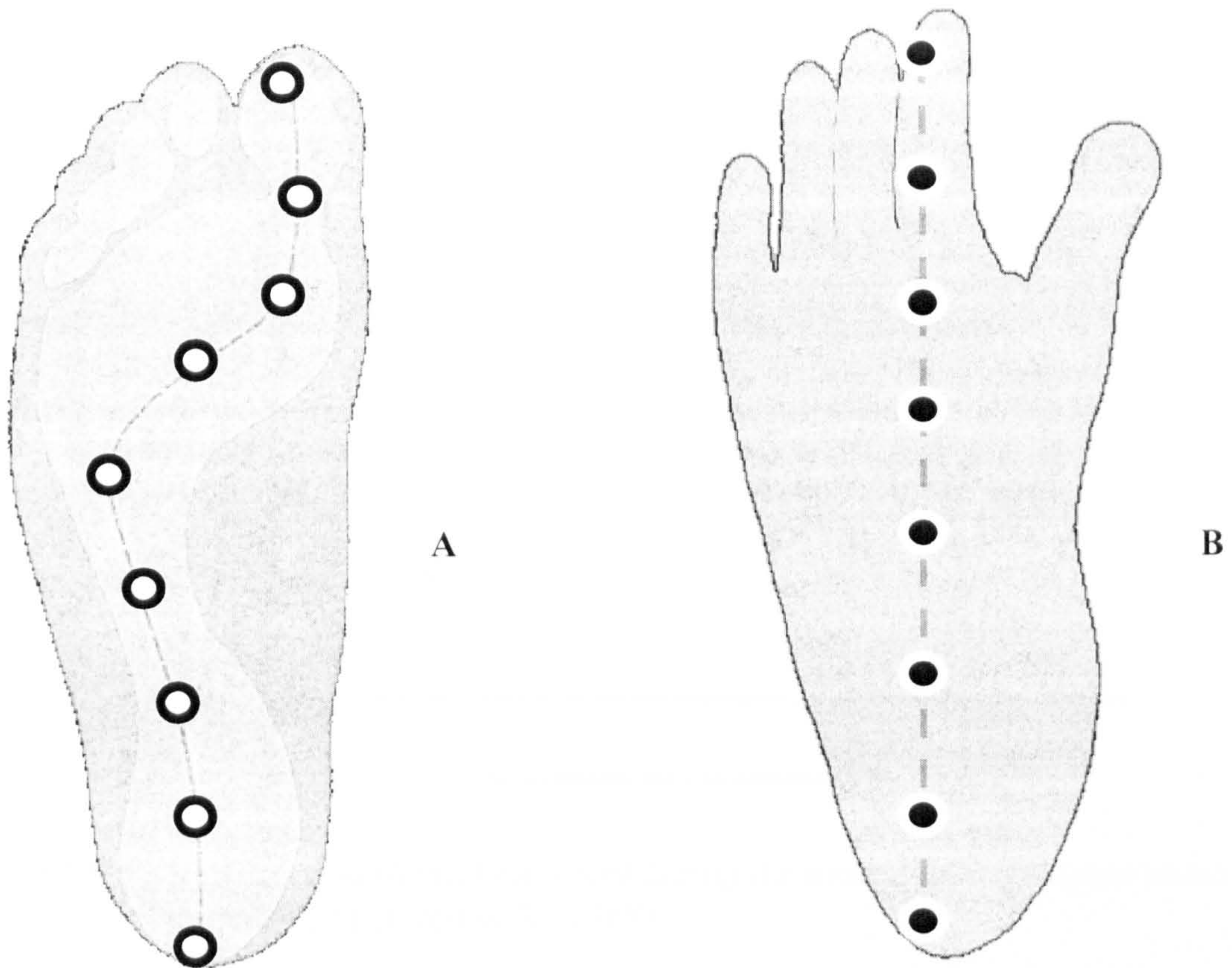


Figure 1.4 Centre of pressure in the foot throughout the stance phase in modern Humans (A) and chimpanzees (B) (adapted from Elftman & Manter, 1935; Napier, 1967; Clarke & Tobias, 1995).

In terms of the degree of force passing into the ground, as can be seen from Figure 1.5 (next page), the largest amount is transmitted in the initial part of the stance phase (i.e. heel strike), and at toe-off. At toe off, it has been shown that about two thirds of the total force is borne by the heads of the first and second metatarsals. For both force peaks, during walking, more than 100% of the body's weight is being transmitted through to the ground. During running, the force exerted at heel strike through to mid-stance is more than for walking, but the principal change is at toe-off, where the force is often more than 2.5 times body weight (Elftman & Manter, 1935a; Napier, 1967; Czerniecki, 1988; Mann, 1988; Aiello & Dean, 1990; Hutton & Stokes, 1991; Mann, 1991; Hayafune *et al.*, 1999).

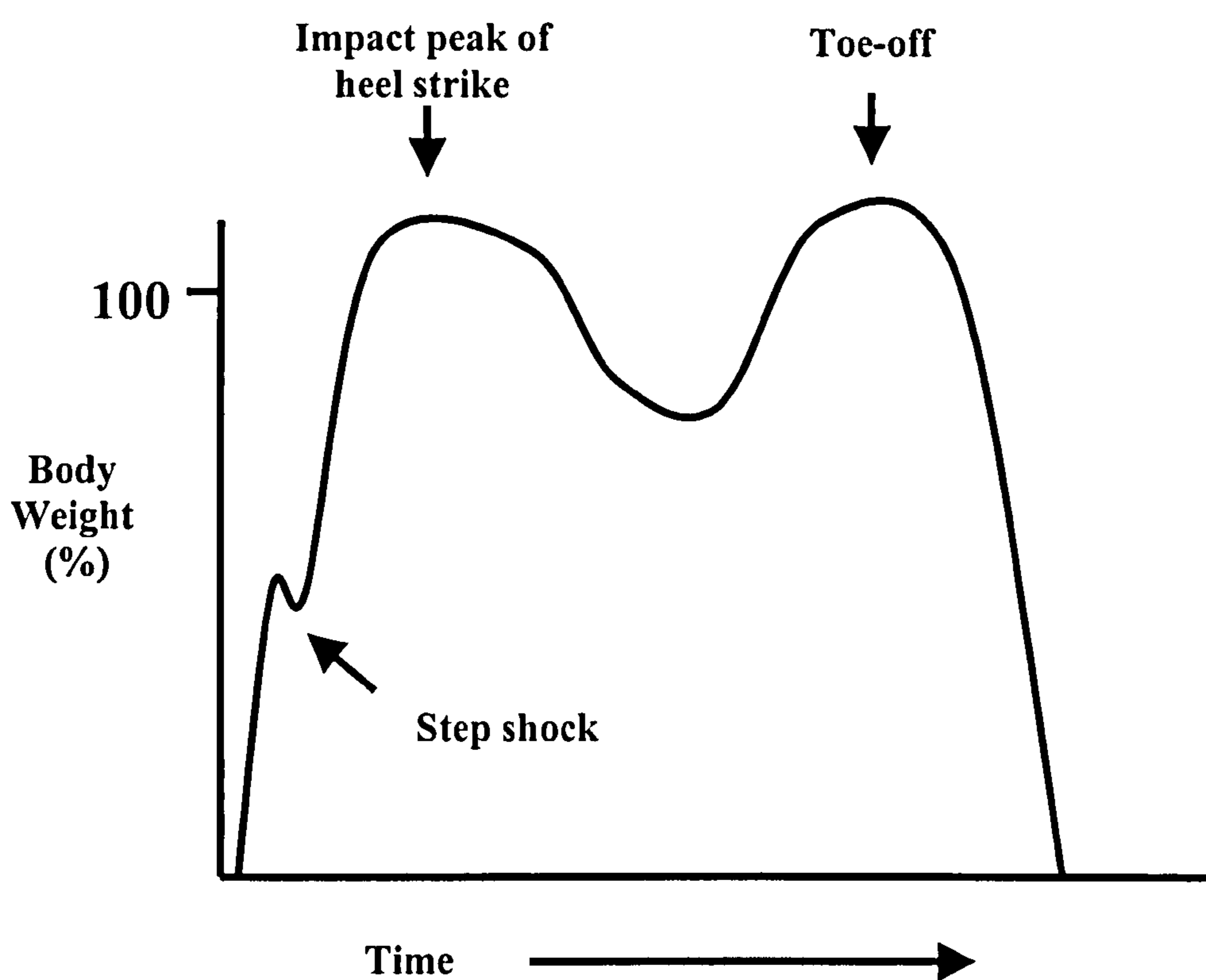


Figure 1.5 Vertical ground reaction forces during the modern human stance phase (adapted from Czerniecki, 1988).

1.7.1.2 Overall Foot movement

The general consensus is as follows: at heel strike, the foot is dorsiflexed and very slightly everted. During the heel strike to mid-stance phase, the foot undergoes rapid plantar flexion, as well as inversion. As discussed above, this results in the whole force of the body, up to mid-stance phase, passing along the lateral side of the foot. The foot then undergoes dorsiflexion as the body passes over the foot, and then rapid plantar flexion occurs again as the foot prepares for toe off. At the point of toe-off the foot is highly plantar flexed and everted (Czerniecki, 1988; Aiello & Dean, 1990; Hutton & Stokes, 1991; Mann, 1991). This is born out by electromyographic (EMG) studies of those muscles responsible for foot movement during the gait cycle. At heel strike the principal dorsiflexor of the foot, tibialis anterior, is still active, but this activity ceases rapidly. The following rapid plantar flexion and subsequent dorsiflexion are due mainly to the weight of the body beginning to be carried forward over the foot, but also to the inactivity of the dorsiflexors. At the same time as the foot begins to plantar flex in preparation for toe-off, there is a surge in activity in the calf muscles (soleus and gastrocnemius), which are strong plantar flexors, and the intrinsic muscles of the sole of the foot, which contract so as to help maintain arch support (Suzuki, 1985; Mann, 1988; Aiello & Dean, 1990). It is also important to

note that throughout the stance phase the muscles of the lower leg responsible for inversion and eversion (e.g. tibialis posterior and peroneus longus and brevis), are constantly working in relation to each other so as to fine-tune the position of the foot in order to cope with any unevenness in the substrate (Matsusaka, 1986).

1.7.2 *The great ape foot in locomotion*

1.7.2.1 *Terrestrial locomotion*

Compared to modern humans, there have been few *in vivo* studies on foot movement and pressure distribution in the extant great apes. Those studies that have been conducted have all had similar conclusions. When moving on the ground, both *Pan* and *Gorilla* do have a plantigrade foot (Gebo, 1992), but they do not have a true “exclusive” heel strike in the same way that modern humans do. The heel does strike before any other part of the foot makes contact with the ground, but only just, and this is very rapidly followed by the remaining lateral section of the foot striking the ground. In many cases the whole lateral side of the chimpanzee foot strikes the ground at the same time as the heel. The foot is highly inverted at this stage, with the toes of rays two to four curled under the foot. Tuttle (1970) argues that the hallux of *Pan* also makes contact with the ground, and bears weight, in the early part of the stance phase. The foot then rotates medially to become everted by the mid-stance phase, resulting in the medial side of the foot coming into contact with the ground far earlier than for modern humans. At this stage the navicular, medial cuneiform and the base of the first metatarsal are all in direct contact with the ground, and bear a considerable degree of body weight. In modern humans the tissues overlying the medial cuneiform and navicular do not contact the ground at any point during the stance phase. The chimpanzee heel also stays on the ground longer than for modern humans, and when it does lift up, there is no medial rotation to the ball of the foot and the big toe. Rather, the foot bends at the mid tarsal joint (the mechanics of which are discussed later) and the centre of loading continues in a straight line distally. The result is that at toe-off, the chimpanzee foot is pushing off from the middle of the foot rather than the medial side, and has all five rays in contact with the ground right up to the point that the foot actually lifts off. The overall conclusion is that the chimpanzee foot lacks the ability to efficiently transfer weight from the lateral to the medial side of the foot throughout the stance phase. It was also found that there is a great deal of

variation in foot position from step to step (far more so than modern humans) and that the reason for this was a varying position of the hallux (Elftman & Manter, 1935a; Morton, 1935; Tuttle, 1970; Susman, 1983).

With respect to the above findings, little work has been done on the feet of *Gorilla* and *Pongo*. Elftman and Manter (1935) asserted that preliminary analyses suggested that there was little difference between *Pan* and *Gorilla*. However, Morton (1935) argues that the foot of *Gorilla* shows a slightly more human-like pattern of movement during locomotion than that of *Pan*. This assertion is not backed up with evidence, and so can only be classed as speculative at best. On the rare occasions that *Pongo* does move along the ground, the foot is highly inverted, the main reason being that the markedly long toes of that taxon have to curl under the foot (Tuttle, 1970).

1.7.2.2 Arboreal locomotion

It has been observed that the foot of *Pongo* is engaged in almost exclusive arboreal locomotion. A large amount of this is spent in suspensory posturing, and the foot is often used in this context. As a result the foot of *Pongo* is often subjected to considerable tensile forces. A requirement for such needs would be a foot that is particularly capable of grasping for long periods of time. It has also been observed that when engaging in arboreal locomotion, both *Pan* and *Gorilla* rarely engage in suspensory behaviour (Tuttle, 1968). As discussed above, when in the trees, *Pan* usually knuckle-walks along large branches. In this case the foot is usually plantigrade, and such movement would subject the foot to compressive, rather than tensile, forces. On smaller branches the grasping capability of the African ape foot is used far more.

1.8 Functional anatomy of the foot

The importance, especially in relation to locomotion, of the anatomical differences between the foot of modern humans and that of the extant great apes has been noted in the literature for over three hundred years. Tyson (1699), in the first detailed anatomical description of a chimpanzee, wrote that "...the feet are particular; for they are like great hands..." and then went on to point out that the chimpanzee foot is used both in the capacity of a foot *and* hand. Tyson pertinently pointed out that, unlike

humans, the specimen had such features as an opposable hallux, which he described as “..like the thumb set off at a distance from the range of the other toes”. Since then a number of classic papers have built on these findings with increasing detail and resolution (e.g. Huxely, 1863; Volkov, 1903, 1904; Morton, 1922, 1924, 1927; Wood Jones, 1946; Lewis, 1980a, 1980b). This section will discuss and summarise the major known anatomical and subsequent functional differences between the feet of extant great apes and those of modern humans.

1.8.1 Brief overview of anatomy of each bone

The overviews given below are for applicable to all extant hominoid foot bones, and do not relate to any specific taxon. The detailed comparative anatomy (and associated function) of relevant bones and articular complexes, are discussed in the section preceding this one. Figures are only given for those bones analysed in this thesis.

Calcaneus

The calcaneus is the largest bone in the foot. It can be divided transversely into posterior and anterior sections. The anterior section is dominated by the sustentaculum tali, a medially projecting shelf that supports the head of the talus, and acts as a channel for the tendon of the flexor hallucis longus to pass under. It also acts as the attachment site for the spring ligament. Prominent on the dorsal surface are the posterior and anterior articular facets for the talus, forming the calcaneal part of the sub-talar joint. The anterior articular facet is sometimes comprised of two separate sections. On the anterior aspect of the bone, on the lateral side, is the cuboid facet, forming the calcaneal part of the calcaneal-cuboid joint.

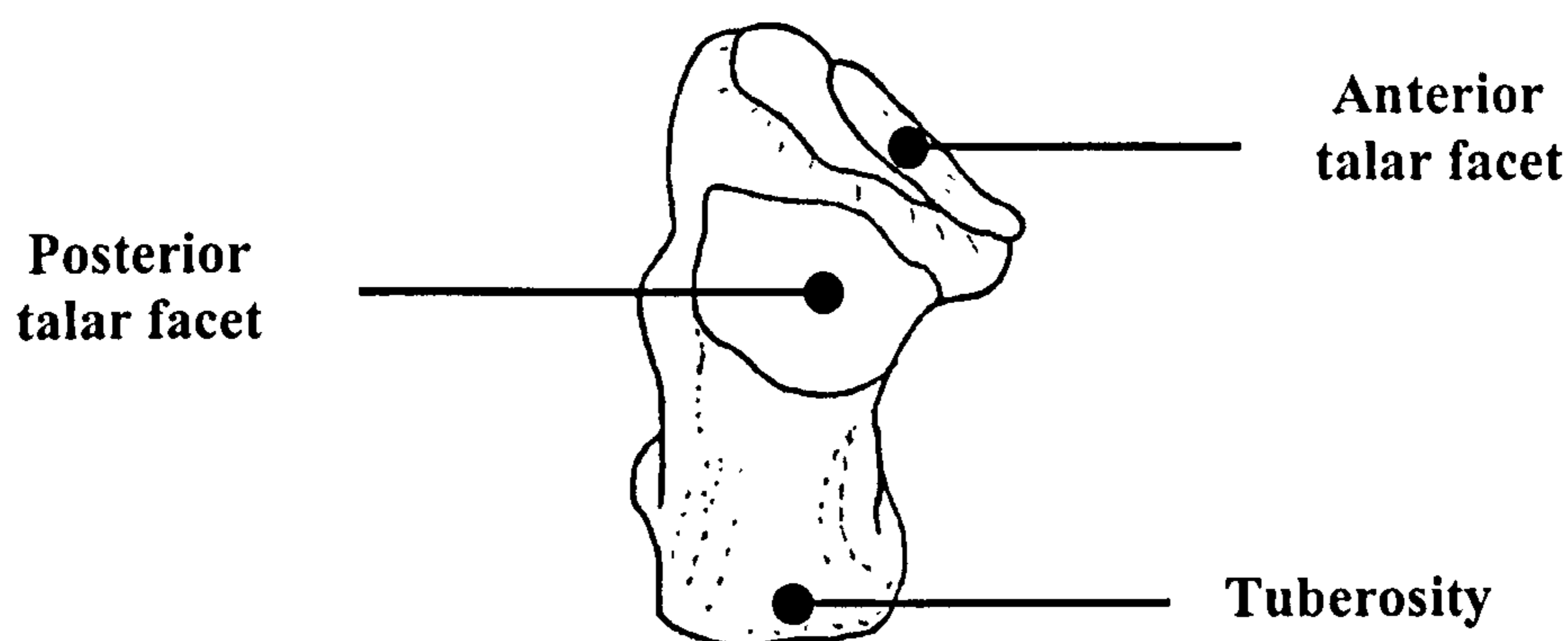


Figure 1.6 Left Calcaneus. Dorsal view.

The posterior section of the bone is dominated by the calcaneal tuberosity. The dorsal section of the posterior surface the tuberosity is the attachment site for the body's largest tendon, the tendocalcaneus, through which the soleus and gastrocnemius act as powerful plantar flexors. The plantar aspect of the tuberosity forms the bony part of the heel which is the part of the calcaneus that contacts the ground.

Cuboid

The cuboid articulates with the calcaneus proximally, and the 4th and 5th metatarsals distally. It also articulates with the lateral cuneiform medially, and there is an occasional adjacent facet for the navicular. The plantar surface is dominated by a marked groove for the tendon of the peroneus longus, an evertor of the foot.

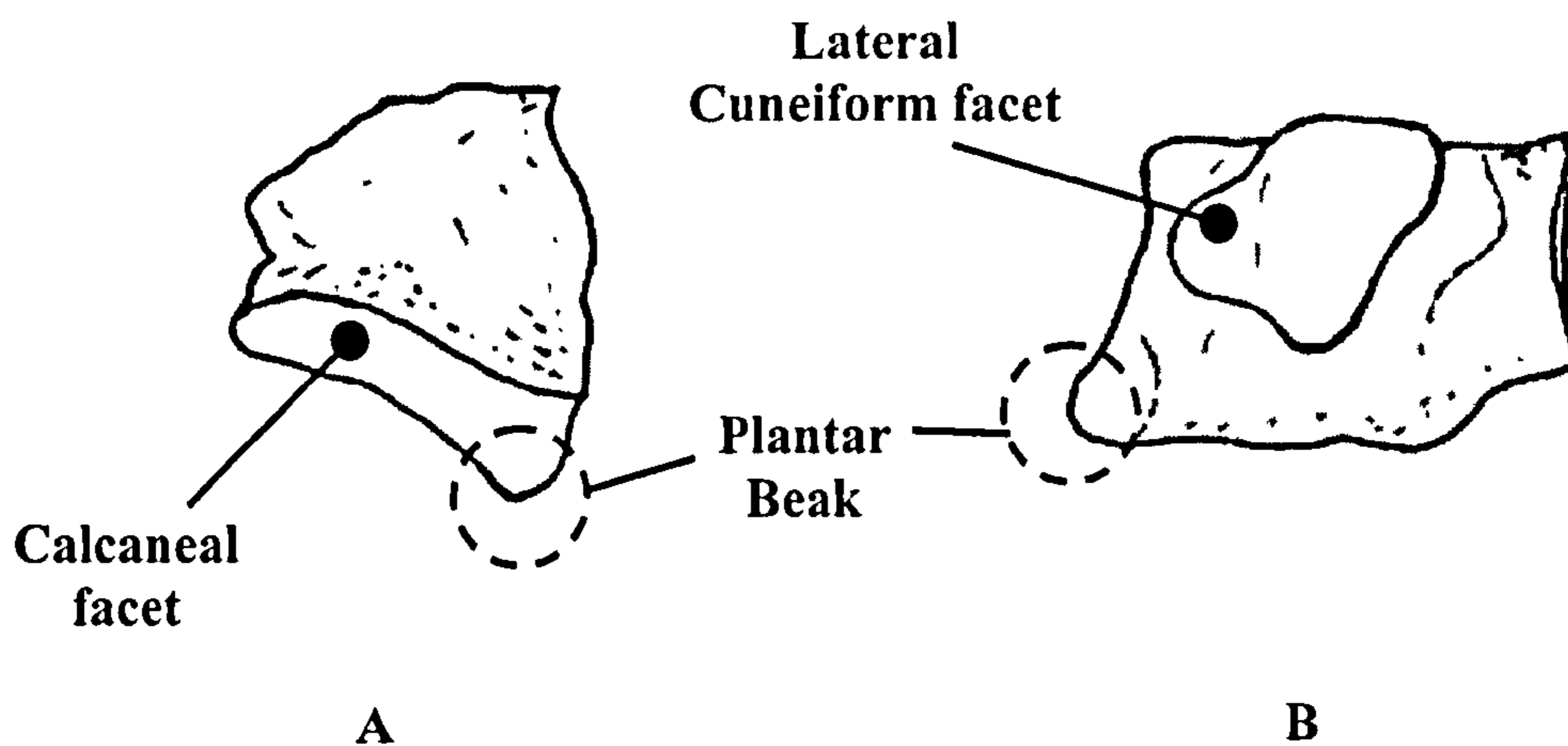


Figure 1.7 Left Cuboid. A: Dorsal view. B: Medial view.

Talus

The talus acts as the interface between the lower leg and the foot below. It is comprised of the talar body, and attached via the talar neck, is the talar head, which is situated mediodistally to the talar body. The dorsal surface of the talar body is covered by the talar trochlea, which articulates with the tibia, and thus forms the talar part of the talo-crural joint. The trochlea is comprised of the trochlear surface itself, and also, either side of it, the medial and lateral malleolar facets. The plantar surface of the talus articulates with the calcaneus, to form the sub-talar joint. The calcaneal facets are divided into an anterior and a posterior section. The anterior facet is convex, and is sometimes made up of two distinct sections, whilst the posterior facet is markedly concave. The convex head of the talus articulates with the concave

proximal facet of the navicular. The anterior calcaneal facet and the navicular facet, as well as the talar facet on the navicular, are sometimes collectively referred to as the calcaneotalonavicular joint, since they are all contained within the same joint capsule.

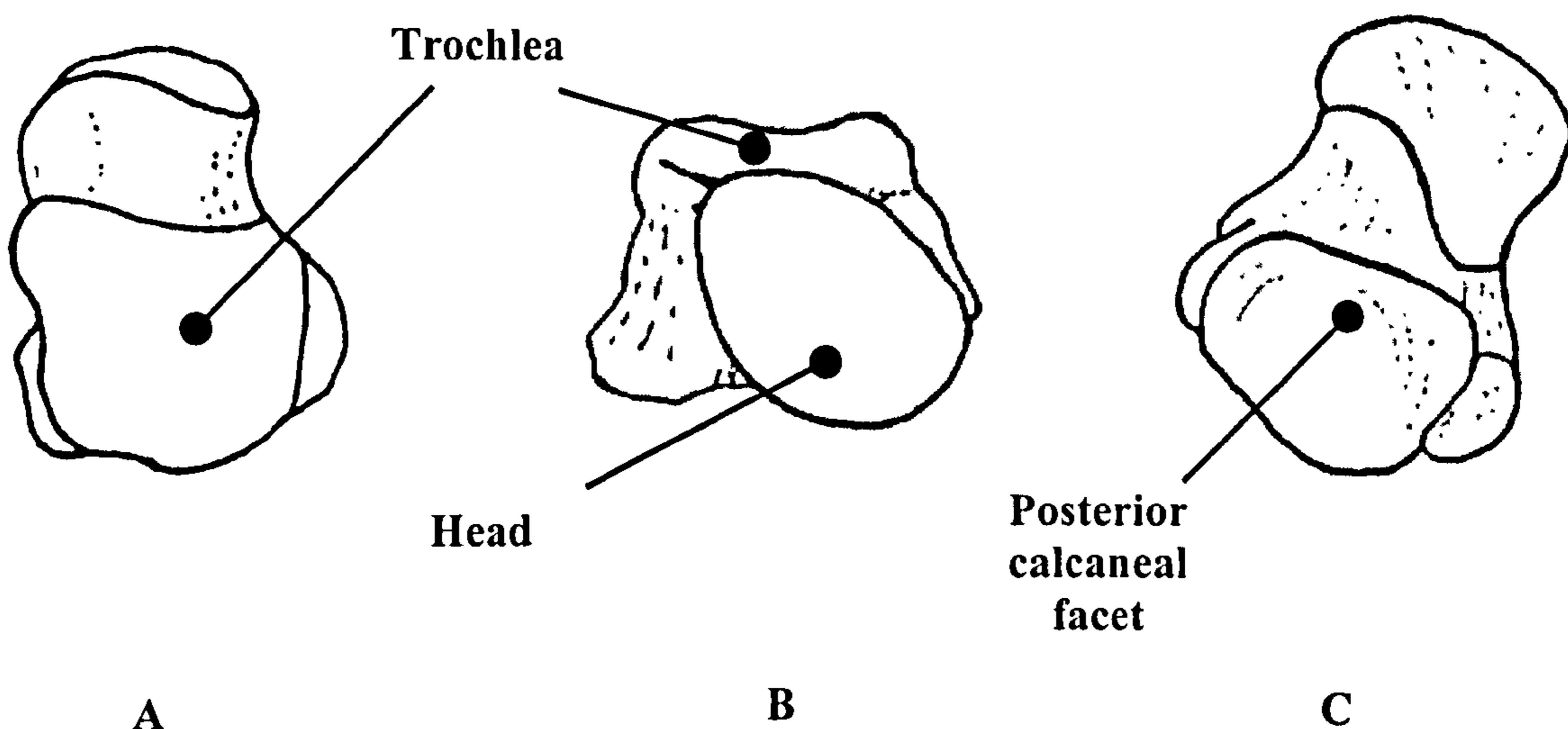


Figure 1.8 Right talus. A: Dorsal view. B: Distal view. C: Plantar view.

Navicular

The navicular articulates with the talus proximally and the three cuneiform bones distally. The talar facet is markedly concave, so as to accommodate the talar head. It occasionally articulates with the cuboid. On the medial side of the bone is a prominent tuberosity, which is the principal attachment site for the tibialis posterior, the principal invertor of the foot. The plantar side of the navicular tuberosity is also the attachment site for the spring ligament.

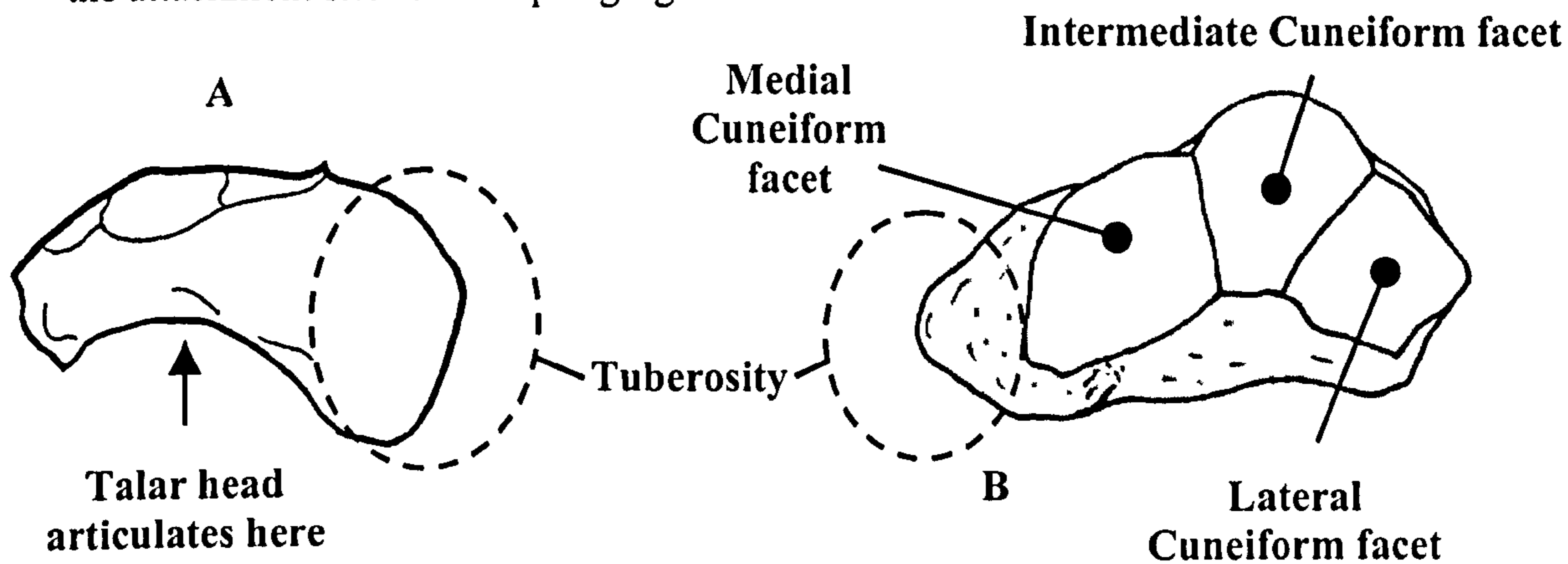


Figure 1.9 Left Navicular. A: Dorsal view. B: Distal view.

Medial Cuneiform

The medial cuneiform articulates with the navicular proximally, and the 1st metatarsal distally. Laterally it articulates with the intermediate cuneiform, and a small section of the medial part of the 2nd metatarsal base. The distoplantar part of the medial surface is a major attachment site for the tibialis anterior, one of the foot's main dorsiflexors.

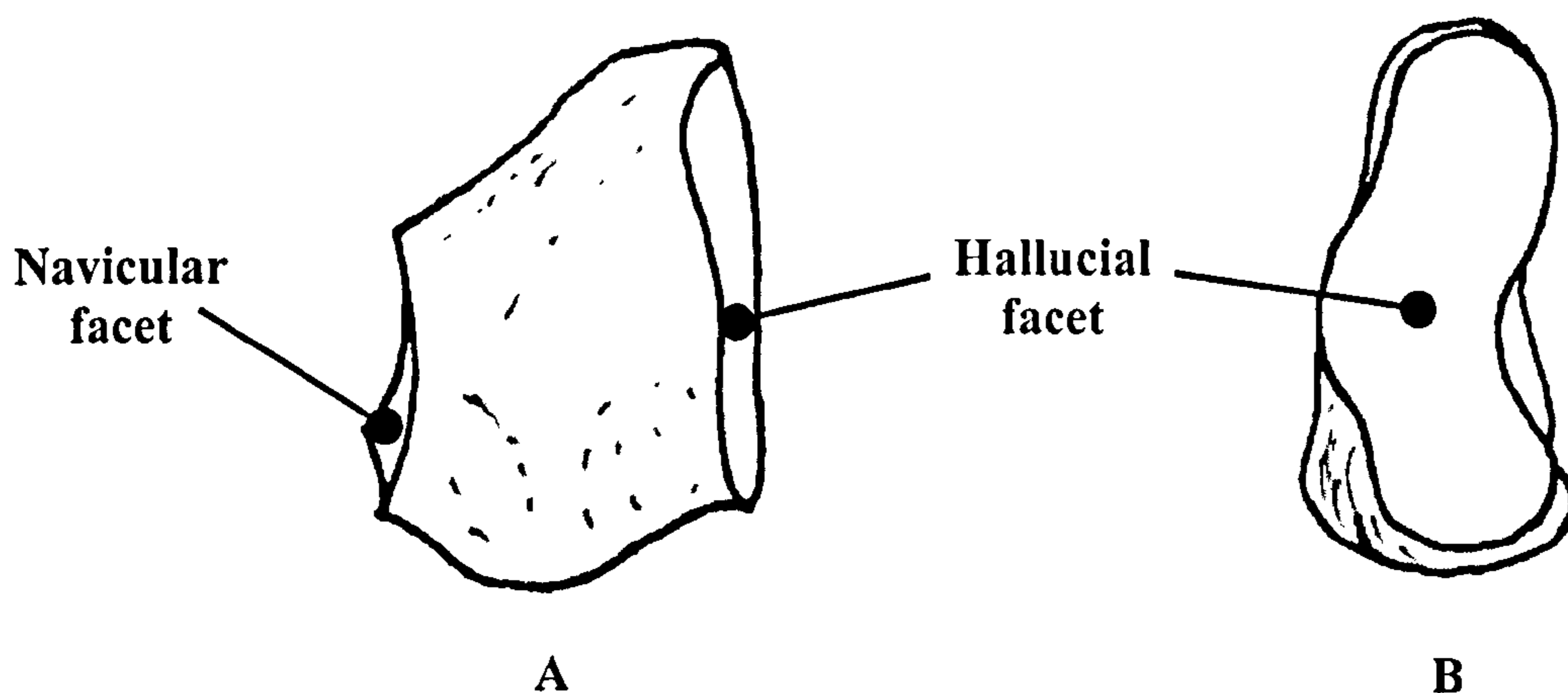


Figure 1.10 Left Medial cuneiform. A: Medial view. B: Distal view.

Intermediate Cuneiform

The smallest of the tarsals, the wedge-shaped intermediate cuneiform acts as the keystone for the transverse arch of the foot. It articulates with the 2nd metatarsal distally, and the navicular proximally. Mediolaterally it is surrounded by the medial and lateral cuneiforms respectively. The dorsal surface is approximately square, whilst the plantar surface is no more than a ridge running distoproximally. This gives the bone its wedge shape.

Lateral Cuneiform

The lateral cuneiform is longer than the intermediate cuneiform distoproximally, and is longer distoproximally than it is mediolaterally, making the dorsal surface rectangular. Otherwise it is still essentially wedge-shaped dorsoplantarly. It articulates distally with the 3rd metatarsal, proximally with the navicular, medially with the intermediate cuneiform, and laterally with the cuboid.

Metatarsals

Of the five metatarsals, the 1st (the hallux) is the most distinct, being the most robust, but also the shortest of the bones. Relative to the shafts, each metatarsal has expanded heads and bases. The bases articulate with the distal tarsal row (cuboid and the cuneiforms) and, also have small articulations with each other. The 2nd metatarsal is firmly wedged into the tarsal row, and is thus the least mobile of the bones. It is also usually the longest. The base of the fifth metatarsal has on its lateral side a prominent projection called the styloid process, which is the attachment site for the peroneus brevis, an evertor of the foot. The metatarsal heads are convex distoproximally, but are also expanded mediolaterally. This allows the proximal phalanges to both plantar flex and dorsiflex.

Phalanges

The phalanges for rays II to V are all fairly similar. There are three per ray, with the proximal phalanges being the longest, and the distal ones the shortest. They are smaller and more slender than in the hand, and taper distally. The proximal joints are concave, and the distal joints are correspondingly convex. The 1st ray only has two phalanges, and they are far more robust than for the remaining four rays. The 1st distal phalanx is considerably enlarged, which is reflective of its role in toe-off.

1.8.2 The foot as a series of functional units

1.8.2.1 Foot proportions

The relative proportions of the tarsals, the metatarsals and the phalanges differ between extant hominoid taxa. For modern humans, the tarsal region takes up over half the total length of the foot, whilst in *Pan* and *Gorilla* the average is 32% and 39% respectively, and it is a little less for *Pongo* (Keith, 1928). For all these taxa the metatarsals are all, relative to total foot length, similar in length. However, there is an exception with the hallux, which, relative to the length of the remaining metatarsals, is particularly short in *Pongo*, and relatively long in modern humans. The first ray of *Pongo* has reduced so much that as many as 60% of individuals lack both their 1st distal phalanges and nails (Tuttle & Rogers, 1966). This adaptation is thought to facilitate a specialised four digit grasp (Tuttle & Rogers, 1966). In modern humans

the overall length of the first ray is similar to that of the second and third rays (in fact usually it is the longest). In *Pongo* the first ray is 25% the length of the second and third rays. From a number of studies, it is also evident that modern humans have relatively short phalanges, particularly in the case of the intermediate phalanges (Tuttle, 1968; Morton, 1922; Keith, 1928; Schultz, 1963; Stern & Susman, 1983; Aiello & Dean, 1990).

These different foot proportions have important biomechanical consequences. The increased relative length of the tarsals in modern humans is probably a reflection of an increased requirement for the foot to act as an efficient lever rather than a grasping organ. The great apes only move bipedally occasionally. Modern humans are obligate bipeds, and the modern human foot is adapted to receive and transmit far larger forces over longer periods of time. One adaptation to sustained increased load is to enlarge the bones that will receive the majority of that load. Likewise, reducing the length of the phalanges increases the efficiency of toe-off. One of the problems the great apes have when walking bipedally, especially *Pongo*, is that their toes are so long (and their hallux so abducted) that they have to curl them under the foot. They thus have to strongly invert the foot so as to not trap the toes between the foot and the substrate (Morton, 1924, 1935; Elftman & Manter, 1935).

There is one other point in relation to proportions of bones in the foot. The talus acts as the pivot for the leg passing over the foot in the stance phase of bipedal walking. The section extending posteriorly from the middle of the talar trochlea to the most posterior point of the calcaneus essentially acts as the power arm of a lever. The lever can be considered to be the whole of the foot up to the metatarsal heads. The section extending anteriorly from the middle part of the trochlea to the metatarsal heads is the load arm. *Pongo* has the shortest power arm. This is followed by *Pan*, and then modern humans. Interestingly *Gorilla* has the longest power arm relative to the load arm (Schultz, 1963). One might expect modern humans to have the longest power arm, since they have a much more pronounced heel strike, and also for their foot to act as a more efficient lever than the ape foot does, but this is not the case. One possible explanation for this finding is that the relatively long power arm of the gorilla foot is a requirement for very large body size and this force transmitted through the

foot. Schultz's study (1963) did not take into account the large degree of body dimorphism in *Gorilla*, which would have helped address this hypothesis.

1.8.2.2 Arches of the foot

One of the most distinguishing features of the human foot is the presence of the longitudinal and transverse arches (Aiello & Dean, 1990). This longitudinal arch is considered to be made up of two sections, or columns: the lateral column, made up of the calcaneus, cuboid, and the 4th and 5th metatarsals, and the medial column, made up of the talus, navicular, cuneiforms and the first three metatarsals. Arching in the medial column is considerably more pronounced (Morton, 1935). In terms of contact with the ground at the normal standing position, the posterior part of the calcaneus (i.e. the heel) is in contact, and then the plantar surface of the foot arches dorsally. The foot does not usually retouch the ground until the head of the first metatarsal on the medial side, and the styloid process of the fifth metatarsal on the lateral side. The cuboid, navicular and cuneiforms do not usually come into contact with the ground. The transverse arch runs mediolaterally from the cuboid to the medial cuneiform. The feet of all extant great ape taxa possess a transverse arch, although it has been argued that it is slightly flatter than in modern humans (Morton, 1935; Oxnard & Lisowski, 1980). However, the great apes *do not* possess longitudinal arches. When a great apes stands on the ground, the foot is remarkably flat proximo-distally. Figure 1.11 clearly

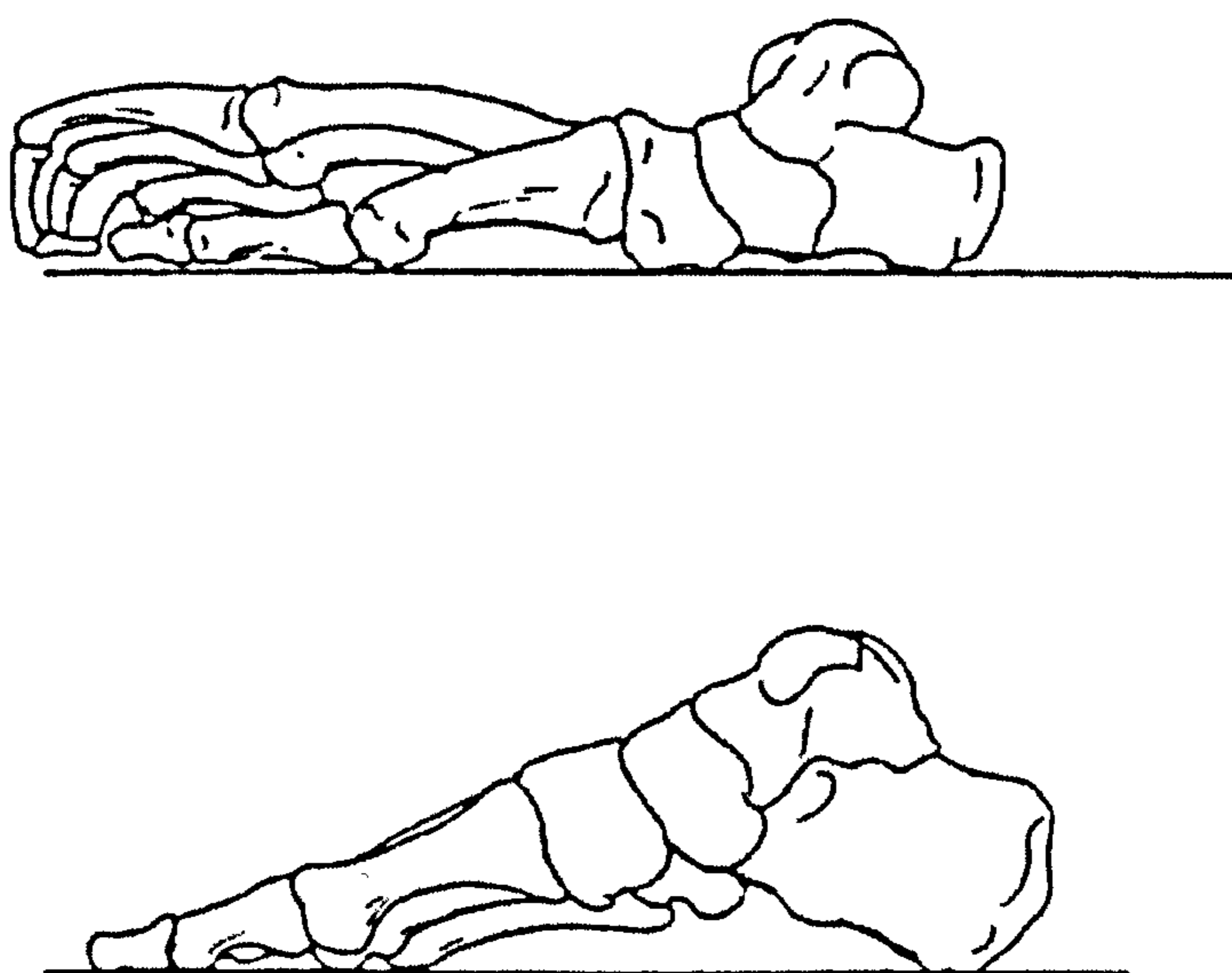


Figure 1.11 Articulated right chimpanzee (above) and modern human feet (below), viewed laterally (adapted from Kidd, 1999).

If viewed from the distal aspect, in *Pan* and *Gorilla* the metatarsal bases and heads are at the same elevation. In humans, due to the longitudinal arches, the bases are relatively elevated compared to the heads (Morton, 1922; Elftman & Manter, 1935b). On the medial side the navicular and medial cuneiform are all in contact with the ground, and on the lateral side the, in addition to the calcaneus, the base of the cuboid is also in contact with the ground (Elftman & Manter, 1935a). It is important to note that the medial tuberosity of the navicular is particularly pronounced in the African great apes (Kidd, 1999; Sarmiento, 2000). It has been suggested that this is an indication of an opposable hallux (Kidd, 1999). A more likely explanation is that it is a reflection of a lack of longitudinal arches in terrestrial great apes. Whilst all the great apes do not have longitudinal arches, only the African great apes engage in sustained terrestrial locomotion. As discussed earlier, this would require regular force transmission through the foot, and the lack of arches means that the navicular takes much of that force throughout the stance phase (Elftman & Manter, 1935a). The enlarged medial tuberosity is most likely, therefore, a reflection of an adaptation to increased loading.

The unique presence of the longitudinal arches in modern humans brings some important biomechanical advantages. The arch structure means that the foot can act more efficiently as a shock absorber during walking and running, and at the same time efficiently transfer weight from the ankle joint to the distal foot without wastefully dissipating force into the ground before toe-off is reached, as is the case with the ape foot. The two arches also provide a stable “tripod” base of support when standing. These benefits mean that the modern human foot is capable of prolonged bipedal posture (Morton, 1935; Olson & Seidel, 1983).

The longitudinal arches are maintained by a number of mechanisms and structures. In the resting position, the arch is partially maintained by the morphology of the bones and their articulations. The modern human calcaneus has two plantar tubercles that act as a stable base of support posteriorly. The cuboid is also wedged laterally, so that it acts as the “keystone” in the lateral arch. Within the sole of the foot, there are a number of crucial structures that maintain the modern human longitudinal arches. The most important of these are the plantar ligaments. The calcaneonavicular, or spring ligament is a short and very strong structure joining the plantar surface of the

sustentaculum tali and the plantar aspect of the navicular tuberosity. It has been noted that the attachment sites for this ligament are more developed in modern humans (Susman, 1983). As well as the spring ligament, there are the long and short plantar ligaments, that attach posteriorly to the anterior section of the calcaneal plantar tubercles, and anteriorly to the plantar ridge of the cuboid and metatarsal bases of rays two, three and four. These ligaments are some of the strongest in the body, and essentially act to tie the arches in place from underneath, and to prevent them from flattening when under pressure during the stance phase (Bojsen-Møller, 1979; Susman, 1983; Aiello & Dean, 1990). There is a further structure that acts in the same way, the plantar aponeurosis. This is a longitudinally running bundle of collagen fibres that lies within the sole of the foot, superficial to the intrinsic muscles and osteoligamentous framework of the plantar side of the foot, but deep to the skin. It runs between from the medial calcaneal plantar tubercle, where it is at its thickest, to the bases of the toes, where it anchors via in a complex network or attachments. So like the plantar ligaments, the plantar aponeurosis acts as a type of tie-rod (Bojsen-Møller & Flagstad, 1976; Aiello & Dean, 1990; Aquino & Payne, 1999). In addition to the collagen fibres, there are elastic fibres that act when the arch is stretched during the stance phase (Aquino & Payne, 1999). Because the plantar aponeurosis stretches under the toes, it also acts as a “windlass” mechanism, whereby when the foot is moving into toe-off, that part of the plantar aponeurosis between the toe-bones of the ball of the foot and the ground tightens (due to extension of the metatarsal phalangeal joints). This acts to anchor the aponeurosis between the ground and the heel, leading to a general tightening of the whole aponeurosis, which subsequently maintains (and even heightens) the arch during its maximum loading (Bojsen-Møller & Flagstad, 1976).

It has also been shown that the intrinsic flexors of the foot, which all lie plantar to the foot skeleton, are at their most active during the late stance phase. Contraction of these muscles, which mainly run longitudinally, essentially results in them functioning as tie-rods to maintain the longitudinal arch from beneath (Mann, 1988). In contrast, the plantar aponeurosis of the great apes has been shown to be highly variable in composition, and markedly less pronounced than that of modern humans (Susman, 1983). This means that the great apes lack an essential mechanism to efficiently support any longitudinal arch.

1.8.2.3 *The talo-crural joint*

The talo-crural joint, also known as the ankle joint, is the joint that directly joins the lower leg to the foot. As discussed above, the talus component is represented by three articular surfaces. The trochlear surface, which articulates with the inferior surface of the distal tibia, the medial malleolar facet, which articulates with the articular surface of the medial malleolus, and the lateral malleolar facet, which articulates with the lateral malleolus (on the fibula). The joint can be considered to be a “mitred hinge-joint”, that is to say, a joint that works like a hinge (i.e. principal movement in two directions in the same plane), but where one component (the talus in this case) is wedged in and surrounded on three sides by the other component (distal tibia and fibula) (Czerniecki, 1988).

As the principal weight distributing joint in the foot, the morphology of the talar component of the joint alone can provide considerable information about its functional nature (e.g. Lewis, 1980b; Latimer *et al.*, 1987; Aiello & Dean, 1990). The great ape trochlear surface has a considerably more raised lateral margin than medial margin. In modern humans the medial margin is relatively more raised than it is in apes (Elftman & Manter, 1935b), although one could argue that it is, in fact, the lateral margin that is relatively more depressed. Either way, both margins are at a similar height in humans. The result of this is that in modern humans, when the foot changes from being dorsiflexed to being plantarflexed (as it does from heel-strike to toe-off) the leg takes a straighter path over the foot than it would do in apes, where the leg takes a more arcuate path (Latimer *et al.*, 1987; Aiello & Dean, 1990). This allows for a more efficient transfer of weight from the hindfoot to the forefoot in the proximo-distal direction, since a more arcuate path would result in some force being dissipated laterally as well. Conversely, the ape foot, particularly that of the *Pongo* (Morton, 1924; Cant, 1987; Gebo, 1993), is usually inverted when engaged in terrestrial locomotion (Lewis, 1980a), and the morphology of the trochlear surface reflects this. Figure 1.12 illustrates these differences between modern humans and the great apes.

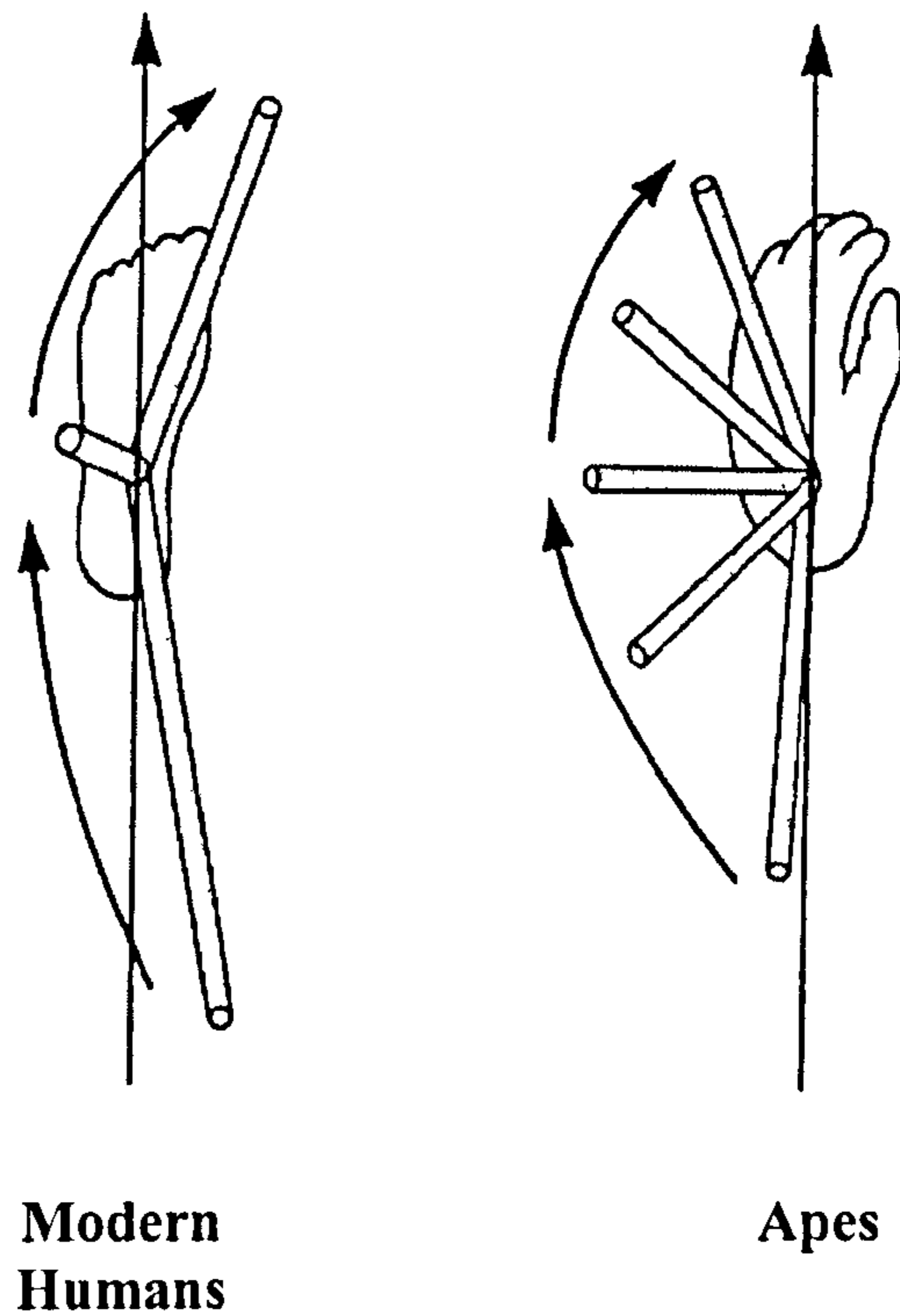


Figure 1.12 Path of lower leg over foot in modern humans and apes (adapted from Aiello & Dean, 1990).

1.8.2.4 The sub-talar joint

In humans and apes this joint can be divided into two major parts, the anterior part and the posterior part, and subsequently can be considered as a bicondylar joint. Both joints are found in separate synovial joint capsules, with the anterior talo-calcaneal joint sharing its capsule with the talo-navicular joint. As discussed earlier, in terms of morphology, the posterior section is made up of a concave facet on the talus and a convex facet on the calcaneus. For the anterior joint, it is reversed. From a biomechanical point of view, the joint has two main functions. Firstly, during the walking cycle, it transmits the body's weight from the talus to the calcaneus, and more specifically to the anterior part of the calcaneus. As the lower leg swings over the foot, and the foot enters the mid stance phase of the cycle, the joint (particularly the anterior part) also acts to transmit the force to the talo-navicular part of the transverse tarsal joint, and thus through the whole medial column.

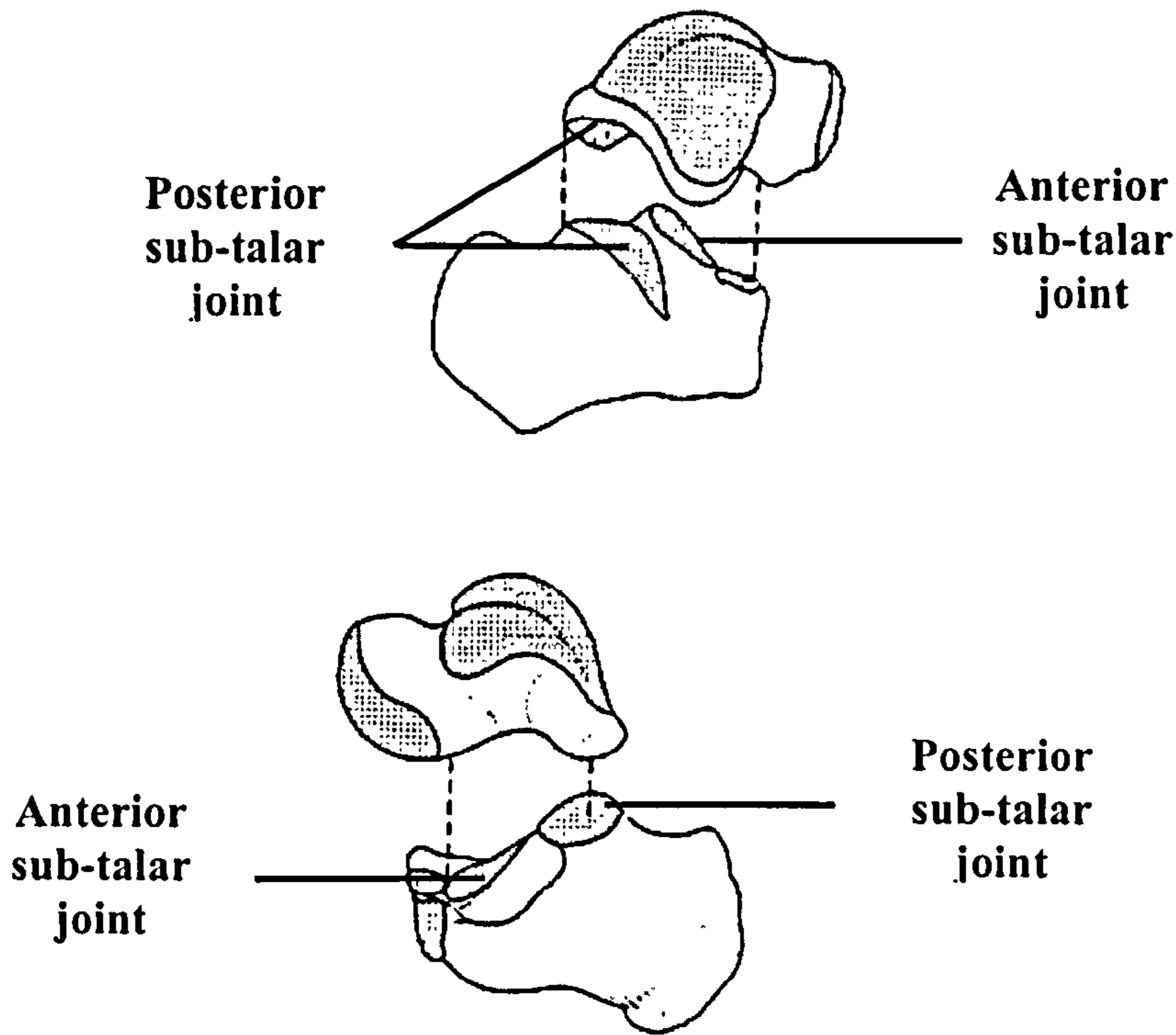


Figure 1.13 Lateral (above) and medial (below) views of the sub-talar joint (revised from Aiello & Dean, 1990).

Secondly, the joint is considered to be largely responsible for any degree of inversion and eversion that the foot undergoes during locomotion (Czerniecki, 1988; Aiello & Dean, 1990; Hall-Craggs, 1990; McMinn *et al.*, 1996). The reason for this is the nature of combination of the “mitred hinge” talo-crural joint, and the fact that the long axes of movement in the subtalar joint are essentially mediolateral. Since the talus is anchored into the distal tibia/fibula, when the tibia rotates laterally or medially, the result is that the subtalar joint is forced to invert or evert respectively. This is important when considering that the foot is essentially inverted at heel-strike, and then rolls through the joint to become everted at toe-off, since the leg is laterally rotated at that point. This movement in the foot, although relatively small, greatly facilitates the efficient transmission of force from the lateral to the medial side of the foot during the stance phase in modern humans (Czerniecki, 1988). It has been suggested that there is little difference between apes and modern humans in the morphology of the sub-talar joint (Lewis, 1980a; Aiello & Dean, 1990), and that the main difference is that the increased curvature of the human joint (especially the posterior section) accounts for the reduced degree of inversion and eversion observed

in the human foot. The increased degree of inversion and eversion found in apes is probably due to the requirement of a more flexible joint for arboreal locomotion.

1.8.2.5 Talar neck and neck-torsion angles

There has been much debate over these measurements. It has been often suggested that a high talar neck angle combined with a low neck-torsion angle indicated an abducted, opposable hallux (Le Gros Clark, 1967; Day & Wood, 1968; Preuschoft, 1971).

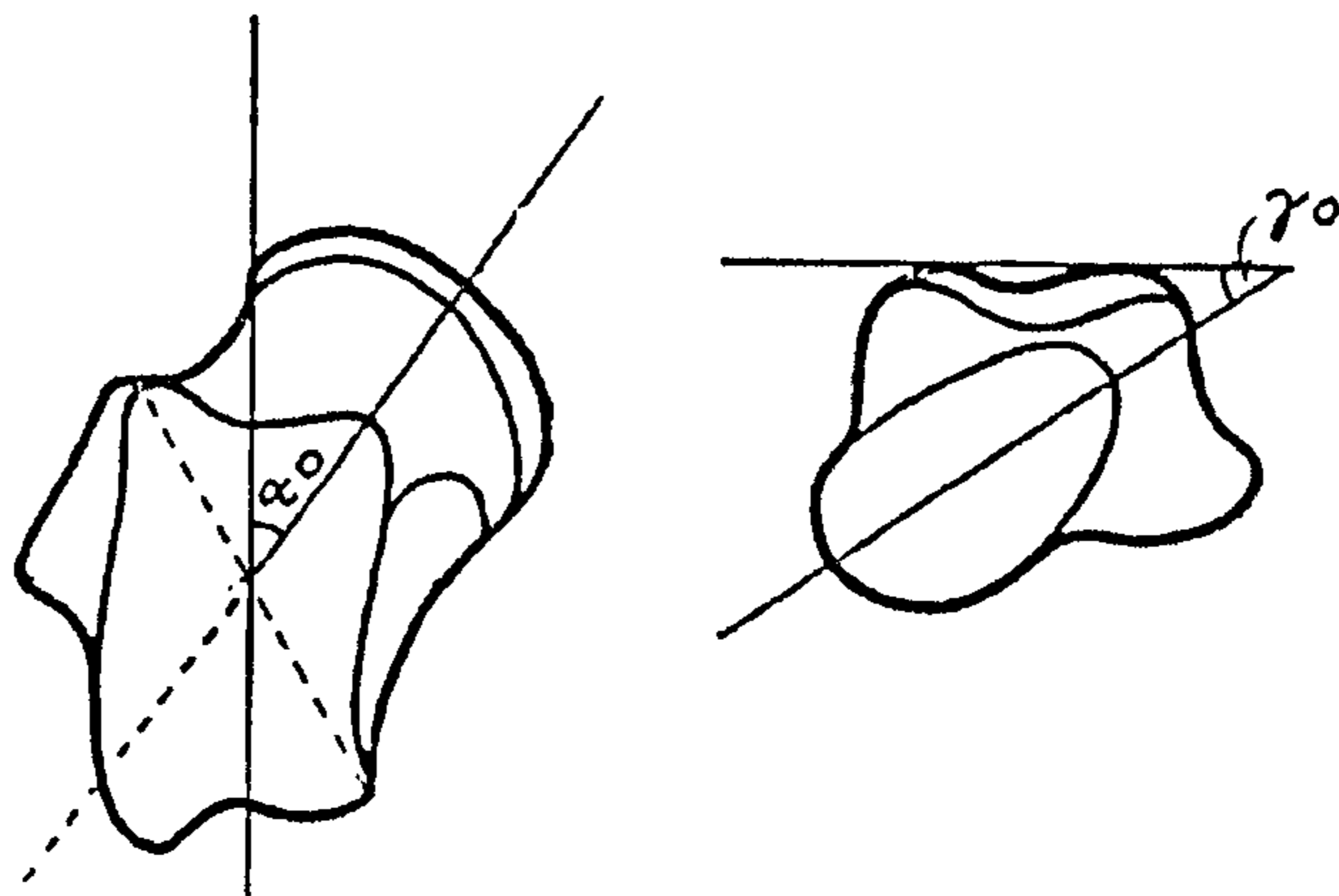


Figure 1.14 Dorsal and anterior views of the talus showing the talar neck angle (α) and the neck torsion angle (γ) (revised from Day & Wood, 1968).

However, Lewis has argued that “the talar neck angle is an expression of the orientation of the sub-talar axis and is not causally associated with the degree of divergence of the hallux” (1980b: p295), bringing into doubt the significance of the previous assumptions. Conflicting data on the OH 8 neck-torsion angle (Day & Napier, 1964; Lisowski, 1967; Lewis, 1980b; Kidd *et al.*, 1996) and Lewis’s assertion (1981) that it is not an easy angle to accurately measure also make it difficult to draw any clear cut assumptions about the degree of hallux abduction from these measurements. Perhaps most importantly, it is not unreasonable to assume that studying the morphology of the medial cuneiform distal facet (i.e. the *actual* articular surface that the hallux attaches to) is more likely to provide accurate information on hallux opposability than is studying the morphology of the talus.

1.8.2.6 *The calcaneocuboid complex*

The calcaneocuboid joint (see Figure 1.15) plays an important role in transforming the human foot into a propulsive platform during the middle to later parts of the stance phase.

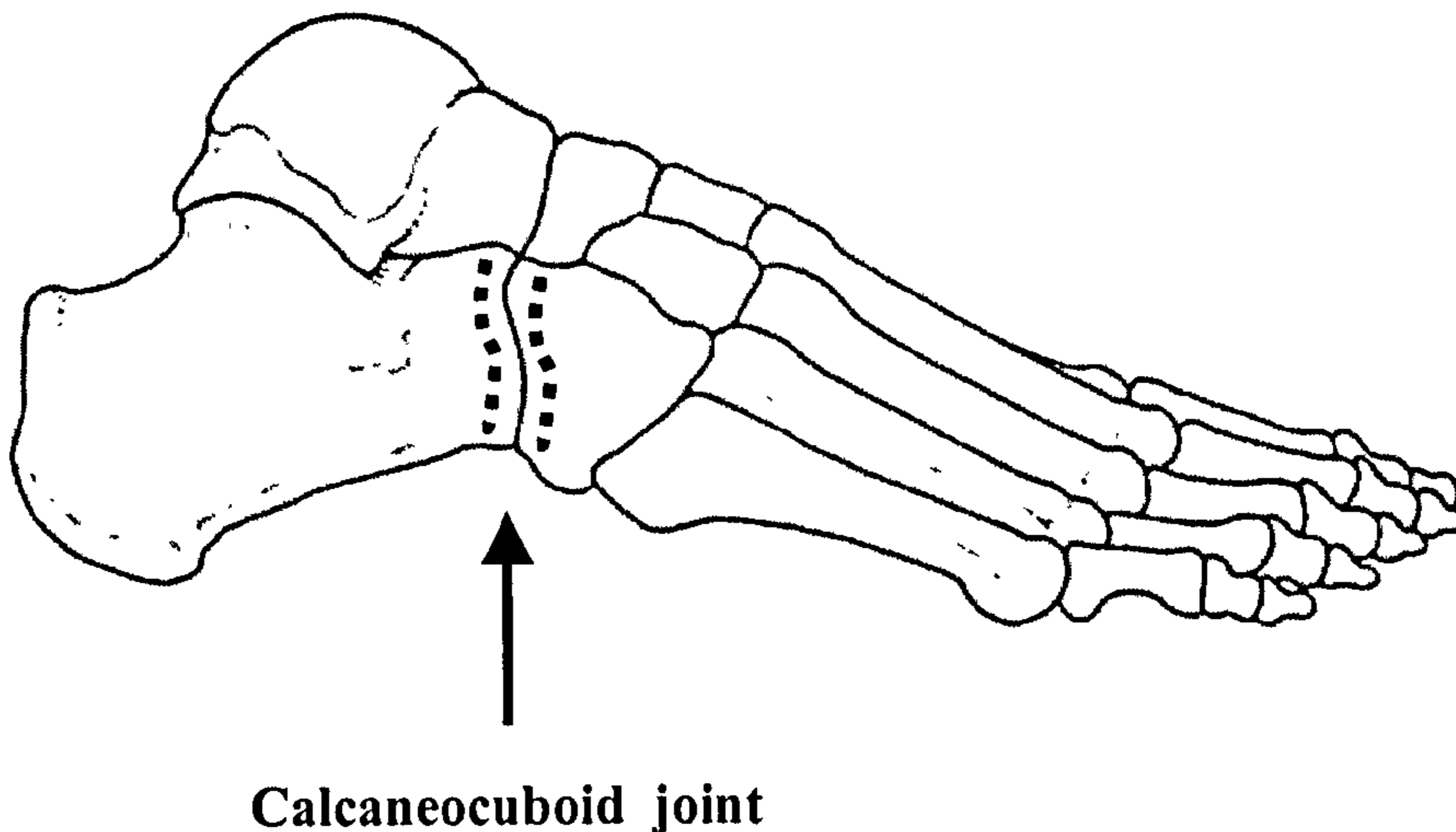


Figure 1.15 Lateral view of an articulated modern human foot, highlighting the calcaneocuboid joint (adapted from Aiello & Dean, 1990).

During the stance phase, as the body's weight is transferred to the medial side of the foot, the calcaneus swings laterally and rotates a little. This brings it into a firm, close-packed position with the cuboid. The result of this is to help transform the foot into a rigid lever as the heel leaves the ground and the foot enters the toe-off stage (Elftman & Manter, 1935a, 1935b; Lewis, 1980a, 1980b; Susman, 1983; Aiello & Dean, 1990; Kidd, O'Higgins & Oxnard, 1996). The reason that the joint is able to do this is that the cuboid has a marked projection, often referred to as a "beak", on its calcaneal facet (see Figure 1.16). The projection extends proximally, and is located on the plantar-medial part of the facet, resulting in the beak impacting under the sustentaculum tali of the calcaneus when the joint is in the close packed position. The highly three-dimensional nature of the joint essentially ensures that the articulation is very firm, and many researchers argue that it is the vital factor in decreasing the range of mobility of the whole complex (Bojson-Møller, 1979; Lewis 1980b, 1981; Susman, 1983; Kidd, O'Higgins & Oxnard, 1996). Subsequently, in humans the calcaneal-cuboid complex can be considered as a single, rigid unit during the mid to late stance

phase, and this is very important when considering the importance of maintaining the longitudinal arch throughout the cycle. It is worth noting that it has been suggested that flat-footed humans are so because they have a far more mobile calcaneal-cuboid joint (Elftman & Manter, 1935a).

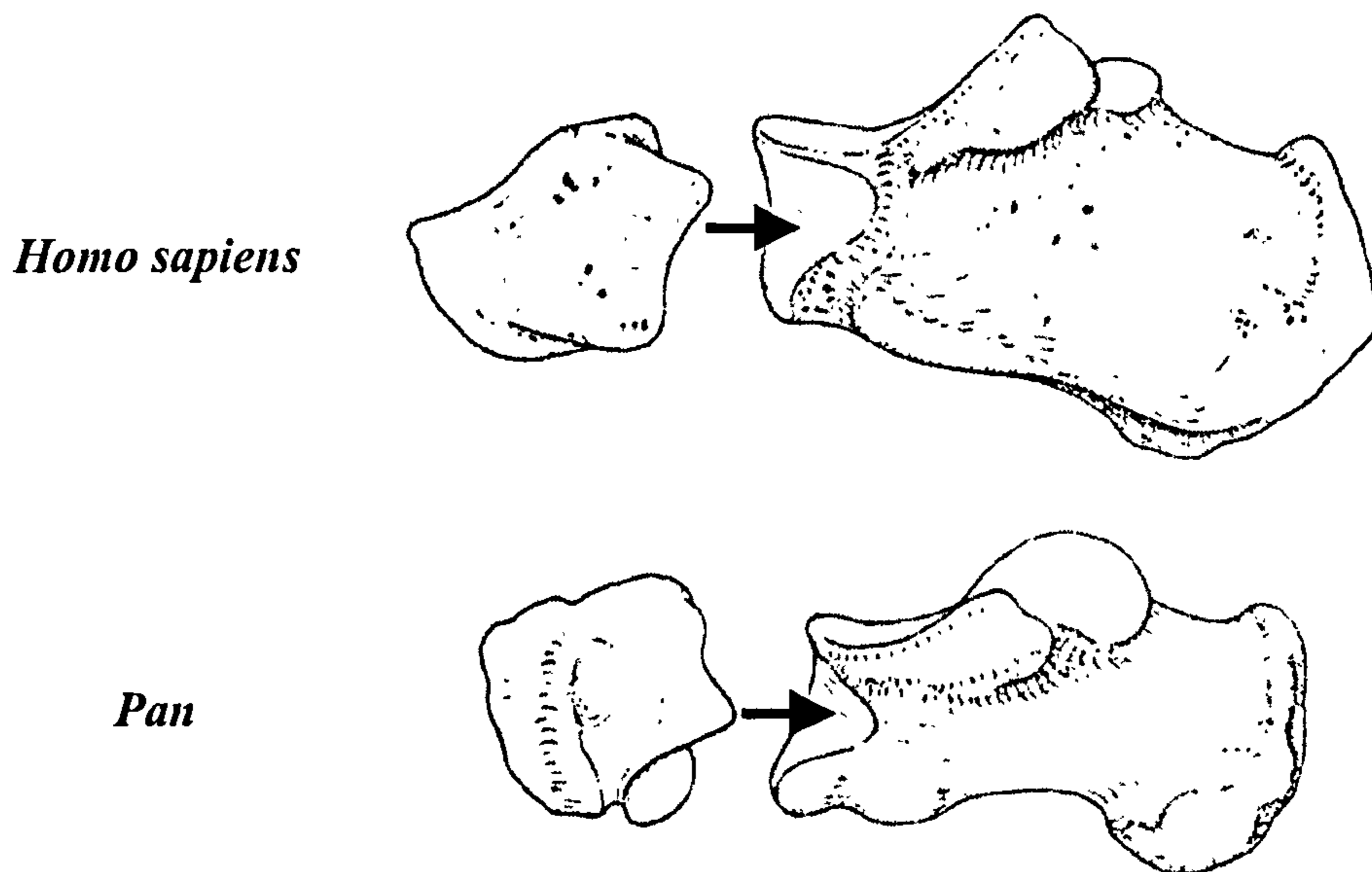


Figure 1.16 Plantar-medial view of the calcaneocuboid joints of modern humans (above) and *Pan* (below). The arrows show where the “beak” of the cuboid articulates into the corresponding depression on the calcaneus (adapted from Aiello & Dean, 1990).

In apes, the calcaneocuboid joint is able to rotate far more than in humans, but is unable to facilitate the lateral swing of the calcaneus. This has been borne out by anatomical studies of the joint surface of the ape cuboid, which indicates a considerably less pronounced, and more laterally orientated plantar beak. The result of this is a far more centrally orientated and symmetrical joint, which can rotate around the axis of the beak, but cannot properly lock into a close packed position. This increased degree of flexibility, at the cost of an inability to form a tightly packed and relatively stable joint, is responsible, along with the more flexible talo-navicular joint, for what is termed the “midtarsal break” along the ape transverse tarsal joint. During the mid-stance and toe-off phases, the ape foot cannot lock at the midtarsal joint so as to efficiently transmit force both distally and medially in preparation for toe-off. This effectively prevents the ape foot from acting as a rigid lever, and results

in an inability to efficiently transfer force from the lateral to medial side of the foot as in modern humans (Elftman & Manter, 1935a; Lewis, 1980a, 1980b; Susman, 1983; Aiello & Dean, 1990; Kidd, O'Higgins & Oxnard, 1996).

1.8.2.7 Cuboid morphology

One potentially important feature exclusive to the cuboid is the angle between the plane of the distal and proximal articular facets, since it may be a good indication of how "wedge-shaped" the cuboid is if looking at it laterally. As discussed earlier, in relation to the lateral longitudinal arch of the foot, the cuboid essentially acts as the "keystone" in the arch, just as the intermediate cuneiform does for the transverse arch (see Figure 1.10), and, as such, the more wedge-shaped it is, the more indicative that may be of an arch-like structure.

A second feature that is important to consider is the relative sizes of the distal facets that articulate with the 4th and 5th metatarsals. It has been shown that in the human foot the majority of weight is borne by the lateral column in the early to mid-stance phase, and by the medial column in the mid-stance phase to toe-off (Elftman & Manter, 1935a; Reeser *et al.*, 1983). This is also borne out by the metatarsal robusticity pattern that we see in humans, where the 5th metatarsal is the most robust after the first (Archibald *et al.*, 1972). This efficient transfer from the lateral to the medial side does not occur in the great apes, and the weight is transferred far more evenly throughout the whole foot in the stance phase. As a result, one might expect that, compared to the facet for the 4th metatarsal, the facet for the 5th metatarsal would be relatively larger in humans, since more force is transmitted through it. However, there is no quantitative research showing this, and consequently it is an issue that needs to be explored.

1.8.2.8 The talo-navicular joint

Along with the calcaneo-cuboid joint, the talo-navicular joint is an integral part of the transverse tarsal joint. However, by its very morphology (it is essentially a modified ball and socket joint) it lacks the ability to lock into a close-packed position like the calcaneo-cuboid joint can. It is subsequently the calcaneo-cuboid joint that forms the most active part of the transverse tarsal joint (Elftman, 1960; Lewis 1980a). Perhaps because of this observation, the talo-navicular joint has been little studied compared to

some of the other joints of the foot, but this does not demean its importance. During the mid to late part of the stance phase, as weight is transferred to the medial side of the foot in anticipation of toe-off, the talus transmits the majority of the propulsive force through the navicular. In this respect, the navicular can be considered as a structure that transmits that force into the three cuneiforms distal to it, and thus on into the subsequent metatarsals. Therefore, the morphology and orientation of the of the joint, as well as of the navicular bone as a whole, should give us important information relating to this force transmission. We know from kinematic studies (e.g. Elfman & Manter, 1935; Reeser et al., 1983) that in humans the vast majority of the force transmitted to the substrate in toe-off occurs through the first ray, whilst in the extant great apes this is markedly less so. A recent metrical study of the hominoid navicular (Harcourt-Smith, 1997; Harcourt-Smith & Aiello, 1999) indicates that the human navicular is considerably wider proximo-distally on its lateral side relative to that of the extant great apes. This effectively means that in modern humans it is less "wedge" shaped when viewing it dorsally. The possible explanation for this is that it is an adaptation to bipedal locomotion, since a less wedge-shaped navicular would result in any force from the talus being transmitted more medially (and thus more exclusively into the first ray) than in the apes. However, this finding is at best tentative, and far more analyses of the bone, and the talo-navicular joint, are needed before any clear conclusions can be made.

1.8.2.9 The 1st tarso-metatarsal joint

All primates except modern humans have an opposable hallux, and the difference between the opposable and abducted hallux in the extant apes and the fully adducted and non-opposable hallux in modern humans has been noticed and discussed since Tyson first wrote on the subject in 1699. It is considered to be one of the major differences between the human and non-human primate foot, and Owen (1866) described the loss of hallux abduction in modern humans as “..the most characteristic peculiarity in the Human structure” (p.256). The grasping hallux plays a fundamental role in arboreal locomotion, and is thus a particularly diagnostic when using the foot to infer the locomotor affinities of fossil taxa (Latimer & Lovejoy, 1990a). The distal articular facet of the medial cuneiform, which articulates with the hallux, can give a clear indication of how opposable the hallux is, and thus an indication of how much grasping potential an individual’s foot had. In humans, the surface is relatively flat

(sometimes even concave) and anterior facing, resulting in an adducted and essentially unopposable hallux that is in line with the rest of the metatarsals. In extant great apes, such as *Pan* and *Gorilla*, the facet is aligned in a more proximal and medial direction, and is far more convex on both the dorsal and plantar sections, indicating a marked increase in the possible range of motion, and thus allowing a significant degree of abduction and subsequent adduction (Huxely, 1863; Morton, 1922, 1924, 1927; Schultz, 1930; Morton, 1935; Lewis, 1980a, 1980b; Szalay & Langdon, 1986; Aiello & Dean, 1990). Schultz (1930) ascertains that both the set and curvature of the facet are equally important for effective hallux opposability. Furthermore, particularly in *Pan*, the plantar surface of the hallux is orientated at 90 degrees relative to the plane of the plantar surfaces of the remaining four digits of the foot, the reason for this being the relatively high degree of opposing torsion between the hallux and metatarsals 2 to 5. What this means is that when the hallux adducts from its "resting position" of relative abduction, it also, from a strict anatomical viewpoint, flexes as well. It is this combination of flexion and adduction that constitutes the arboreal grasp (Morton, 1922; Morton, 1935). Figure 1.17 illustrates what Morton was discussing.

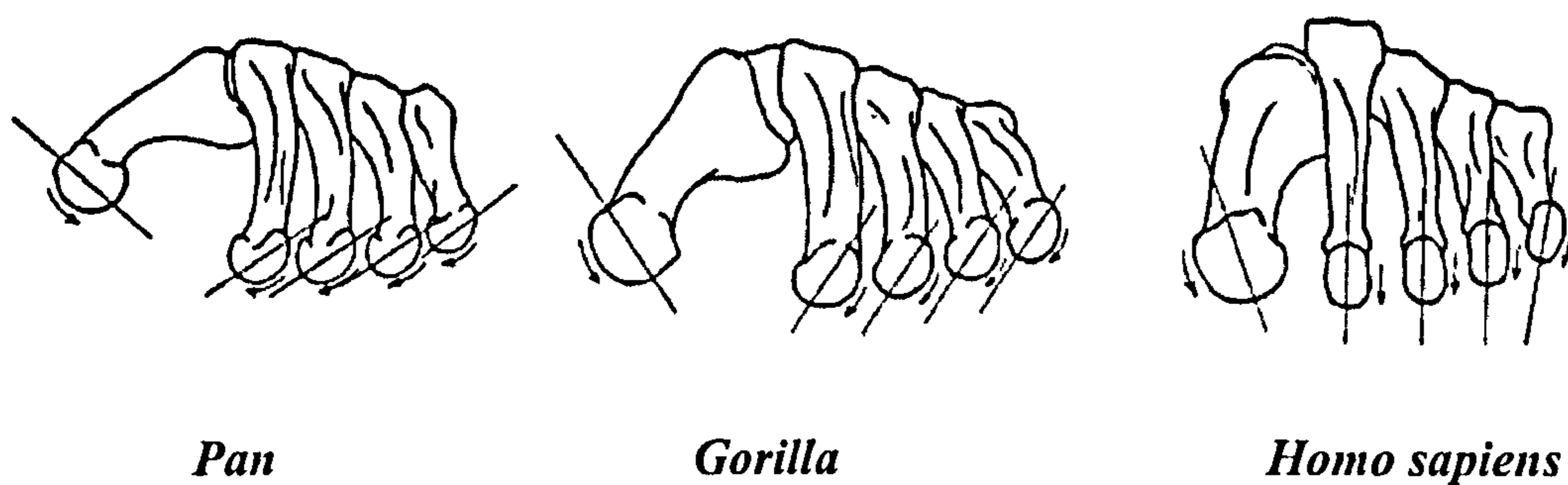


Figure 1.17 Relative metatarsal and hallucial torsion in the hominoids (Adapted from Morton, 1935).

In humans the angular difference between these planes is greatly reduced, and there is only a difference at all due to the presence of the transverse arch of the distal tarsal row. Morton (1935) also argues the reduced level of torsion between the hallux and remaining metatarsals of *Gorilla* is an adaptation to that taxon's increased terrestriality.

In terms of musculature, the hallux of the great apes is served by extremely well developed muscles that facilitate prehensile movement. This is most evident in *Pan* and *Gorilla* and least so in *Pongo*, which has relatively slighter hallucial abductor muscles than either species of African ape. This mainly due to the markedly reduced hallux in *Pongo*. Furthermore, the *Pongo* hallux does not usually receive a long flexor tendon, and this would reflect the specialised grasping capabilities of *Pongo*'s long, curved and strong 2nd through 5th rays, and the relatively reduced importance of its hallux (Boyer, 1935). Modern humans have hallucial abductor muscles that are considerably reduced in size and weight when compared to any great ape taxa (Tuttle, 1968, 1970).

1.8.2.10 The 2nd to 5th rays

One of the principal differences between modern humans and the great apes is the morphology of the metatarsophalangeal joints in rays two to five. In modern humans the metatarsal heads curve round more on the dorsal side, resulting in a greater degree of dorsiflexion at this joint. Aiello and Dean (1990) have pointed out that this is an adaptation to an increased requirement for a strong toe-off in modern humans. In the great apes, there is a pronounced dorsal ridge on the metatarsal heads that limits dorsiflexion. Conversely, the bases of the proximal phalanges are plantarly orientated in the great apes, and dorsally orientated in modern humans. This means that great ape metatarsophalangeal joints are capable of increased plantar flexion, which is most likely a requirement for increased gripping of the substrate, as in arboreal grasping (Latimer & Lovejoy, 1990b; Duncan *et al.*, 1994).

The intermediate phalanges are also considerably more curved in the great apes than in modern humans. This is also considered to be an adaptation for arboreal grasping (Stern & Susman, 1983). Within the great apes, *Pongo* has the most curved phalanges, and *Gorilla* the least. It is also important to note that *Pongo* has by far the most developed interosseous muscles in the foot, and this is thought to be as an adaptation for increased grasping in that taxon (Tuttle, 1968).

1.8.2.11 Summary

1. The human foot is a structure specially adapted for full, obligate bipedal locomotion. When compared to the great apes, there are a number of distinct features in the modern human foot that facilitate this mode of locomotion. Modern humans have: relatively short toes and relatively long tarsals, leading to a more efficient lever mechanism for the stance phase; the presence of a longitudinal arch, divided into medial and lateral columns; a more curved transverse arch; a talo-crural joint that allows the leg to pass directly over the foot; a highly stable calcaneo-cuboid joint that maintains foot rigidity during the stance phase; loss of opposability of the hallux; increased dorsiflexion at the metatarsophalangeal joints for rays two to five.
2. The African ape foot, by contrast, is adapted to both arboreal and terrestrial quadrupedalism, as well as arboreal grasping. Specialist features are: a strong, highly mobile and abducted hallux; an enlarged navicular tuberosity for weight-bearing during the stance phase; a mid-tarsal break to facilitate increased foot flexion/extension during grasping; curved phalanges and metatarsals. *Pan* typically has slightly more arboreal traits than *Gorilla*; an increased degree of plantar flexion at the metatarsophalangeal joints for rays two to five.
3. The foot of *Pongo* is that of an arboreal specialist. It has a greatly reduced, but still opposable hallux; elongated and highly curved phalanges; and relatively small tarsals.

1.9 The foot in the hominin fossil record

It has been suggested, on the basis of their morphology and thus assumed function, that fossilised pedal elements attributed to the taxon *Australopithecus afarensis*, from the Hadar Formation, Ethiopia, belonged to an essentially bipedal species of hominin (Latimer & Lovejoy, 1982; Latimer *et al.*, 1987; Latimer & Lovejoy, 1989; Latimer & Lovejoy, 1990a, 1990b). Combined with the discovery of at least two bipedal hominin tracks at Laetoli, Tanzania (Leakey & Hay, 1979) this evidence suggests that habitual bipedality may have been present in the east African australopithecines as early as 3.5 million year ago (mya). However, the recently discovered pedal elements

Sts 573, found at Sterkfontein, South Africa, have been initially described as having a mosaic of ape-like and human like affinities (Clarke & Tobias, 1995) and other researchers (e.g. Stern & Susman, 1983) have suggested that *A. afarensis* was more arboreal than has been suggested. Added to this is the well documented foot assemblage OH 8, found at Olduvai Gorge, Tanzania, dated at 1.75 mya and attributed to the taxon *Homo habilis*. Some researchers have suggested that it is essentially human like, was fully adapted to bipedal locomotion and had not retained any specialist arboreal adaptations (e.g. Day & Napier, 1964; Susman & Stern, 1982; Susman, 1983; Gebo, 1992; Berillon, 1998, 1999; Harcourt-Smith & Aiello, 1999), whilst others have suggested that it had a combination of human-like, ape-like and unique features indicating a mosaic lifestyle of terrestriality *and* arboreality (e.g. Oxnard & Lisowski, 1980; Lewis 1980b, 1981; Kidd, O'Higgins & Oxnard, 1996). There is therefore a significant degree of uncertainty over the exact locomotor affinities of the Plio-Pleistocene hominins. Furthermore, what is uncertain is how similar or different the morphology and function of the feet of these taxa were to each other.

This section reviews current opinion on the various morphologies, and associated functions, of fossilised hominin pedal remains. More recent hominin species that are known to be fully bipedal (such as the Neanderthals) are not considered in this review. There are no known *Homo erectus* foot bones, but the morphology of the remaining postcranial skeleton indicates a fully bipedal taxon (Ruff & Walker, 1993). The feet of the Neanderthals are considered to be virtually indistinguishable from those of modern humans (Trinkhaus, 1983a, 1983b).

1.9.1 The calcaneus in the fossil record

The *Australopithecus afarensis* calcaneus has been described as being human-like in its affinities, and thus fully adapted to bipedal locomotion (Latimer & Lovejoy, 1989). In all cases the known *A. afarensis* calcanei lack the cuboid articular facet due to post mortem damage. The authors have recently argued (1989) that the fossils have a lateral tubercle clearly present on the plantar surface of the tuberosity, a uniquely human characteristic that greatly facilitates a more stable heel-strike (Aiello & Dean, 1990; Susman & Stern, 1991), but they originally described the lateral tubercles as

“indistinct” or “small” (Latimer et al., 1982). The presence of this has also been disputed by a number of other studies (Deloison, 1985; Lewis, 1989; Susman & Stern, 1991), or has been described as being only “poorly developed” (Susman, 1983). Latimer and Lovejoy (1989) also argue that the *A. afarensis* calcaneus has a relatively large tuberosity (based on cross sectional area at the smallest circumference). The researchers argue that this is indicative of an expanded trabecular volume, which would be an adaptation for increased energy dissipation. They also suggest that there is a smaller, and thus more human-like, angle subtended by the posterior talar articular facet. A smaller angle is indicative of a more convex surface, and it has been argued that this results in a less mobile joint (Lewis, 1981). Finally, they suggest that the orientation of the posterior talar articular facet is human-like. It has been argued that both the posterior and the anterior talar articular facets are more orientated towards the central axis of the foot in modern humans than in the great apes (Morton, 1924), although some researchers argue that this is not the case for the anterior facet (e.g. Elftman & Manter, 1935b; Latimer and Lovejoy, 1989).

1.9.2 The calcaneo-cuboid joint in the fossil record.

There is one mention in the literature of a partial *A. afarensis* cuboid (Gomberg & Latimer, 1984). In a preliminary study, the authors state that the calcaneal facet is African-ape like in its morphology, and is indicative of a more mobile calcaneocuboid joint in *A. afarensis*. However, there has been no formal description of this fragment, so this finding can only be considered as speculative. Clarke (pers.comm) argues that the cuboid joint of *A. africanus*, as represented by a partial cuboid facet of the calcaneus of Stw 573, was ape like in having a mobile joint with a more laterally orientated and reduced plantar beak insertion. However, the Stw 573 partial calcaneus remains unpublished, and a formal description is awaited.

There is no cuboid bone associated with the Stw 573 (Littlefoot) pedal assemblage, but the partial calcaneus, as yet formally undescribed, is said to have a “bowl-shaped” cuboid facet reminiscent of that of the chimpanzee, and thus indicating a mobile calcaneocuboid joint incapable of the human-like locking mechanism (Clarke, 1998).

Only one *complete* fossil hominin cuboid exists in the record before the advent of species known to be fully bipedal (e.g. *Homo erectus*; *Homo sapiens*). This is the

cuboid of the *Homo habilis* specimen OH 8. The OH8 calcaneocuboid joint has some features that are markedly human-like. In particular, the calcaneal joint surface of the cuboid possesses a particularly prominent “beak”, which is orientated plantar-medially, as in humans (Lewis, 1980b; Susman & Stern 1982). As discussed in previous sections, this articulation is considered to be a vital factor in decreasing the range of mobility of this joint (Bojson-Møller, 1979; Lewis 1980b, 1981, 1989; Susman, 1983; Kidd, O’Higgins & Oxnard, 1996). The “beak” of the ape cuboid is located in a far more medially placed position (Aiello & Dean, 1990). Furthermore, a more recent multivariate investigation of the OH 8 cuboid has shown that it is essentially human-like in its morphology (Kidd, O’Higgins & Oxnard, 1996). However, Lewis (1980b, 1989) has argued that rotary movement of the OH 8 calcaneocuboid joint is far less than it is in humans, and that whilst the joint could lock in the close packed position as in humans, the calcaneus could not swing in the lateral direction nearly so much. This suggests that, whilst the midtarsal break did not occur in OH 8, the calcaneocuboid was not *fully* adapted to human-like bipedal locomotion. This may be the case, but quantitative analyses are needed to back this suggestion up. Lewis (1989) also asserts that the OH 8 calcaneocuboid joint was even more rigid (when in the close-packed position) than that of modern humans, suggesting that the locking mechanism in that joint was almost “ultra human-like”, and highly specialised for bipedal locomotion.

1.9.3 The talus in the fossil record

Much of the debate on the affinities of Plio-Pleistocene hominin pedal remains has been based on the morphology and function of the talus. This is partially due to its relative prominence in the fossil record. Based on the talus, distal fibula and distal tibia of AL 288-1 (“Lucy”) Latimer et al. (1987) have suggested that the *Australopithecus afarensis* talo-crural joint was fully adapted to habitual bipedal locomotion, and was anatomically/biomechanically constrained from having any particular adaptation to climbing. Their work rested on analyses of the relationship between the talar trochlear surface and the tibia and fibula. Specifically, they found that the medial border of the talar trochlear surface was raised to a human-like degree, meaning that the lower leg would pass in a straighter path over the foot, which, as discussed above, is an adaptation to efficient terrestrial bipedalism. It is also argued that the talar head angle of AL 288-1 is human-like (Langdon *et al.*, 1991), but the

study in question used very small sample sizes (two modern humans and one chimpanzee), and can only be considered as preliminary. However, a different study has suggested that the *A.afarensis* talus has features that are far from human-like. Susman (1983) argues that the *A.afarensis* talo-crural joint is “markedly ape-like” (p.373), having ape like features such as an enhanced range of plantar flexion at the joint, and an a short, high fibular malleolus. More recently, Lewis (1989) has argued that the AL 288-1 talar trochlea has ape like features. These features, he says, are an elevated lateral trochlear margin, a laterally flared lateral malleolar facet, “cupped” medial malleolar facet.

Clarke and Tobias have argued that the talus of *A.africanus*, as represented by the “Littlefoot” specimen Stw 573, is essentially human-like, with an elevated medial trochlear margin. This would make the talo-crural joints of *A.africanus* and *A.afarensis* very similar to each other in terms of their human-like morphology (if one is to believe the view on *A.afarensis* taken by Latimer *et al.* (1987)). However, there have been no metrical analyses on the Stw 573 foot, so such assertions need to be taken in that context.

There is only one tarsal element currently assigned to *Paranthropus robustus*, which is the right partial talus TM 1517 from Kromdraai, South Africa (Broom & Schepers, 1946). Only the head and the trochlea are complete enough to be commented on. The most interesting feature of the trochlea is that the medial and lateral margins are described as being level with each other, and it has been stated that this human-like feature is indicative of the leg passing directly over the talus, and thus of bipedal locomotion in *P.robustus* that is more human-like than ape-like (Broom & Schepers, 1946; Le Gros Clark, 1947; Robinson, 1972). However, the head of the Kromdraai talus is less human-like. It has a markedly long mediolateral dimension on the navicular facet, although the facet is not described as being markedly curved. This increased dimension on the talar head is seen by some to be indicative of increased movement at the talo-navicular joint, and thus of a more flexible paranthropine foot (Le Gros Clark, 1947; Robinson, 1972; Berillon, 2000). Multivariate studies of TM 1517 have indicated that the talus is similar to OH 8 (for the dimensions used in the study) and that it falls outside the range of variation of modern humans, and, although

also outside their ranges of variation, is more similar to the great apes (Day & Wood, 1968; Wood 1974; Lisowski *et al.*, 1974).

There has been much debate over the precise locomotor affinities of the hominin talus OH 8, currently assigned to *Homo habilis*. This may well be due to Day and Napier's (1964) positive assertion that whilst the OH 8 foot as a whole belonged to a fully bipedal individual, its talus was the least human-like of its tarsals, and may have has a mosaic of ape-like and human-like features. They observed that the talar neck and neck-torsion angles were similar to those of the Kromdraai talus TM 1517 (assigned to *Paranthropus robustus*), that the length and breadth measurements approached those of modern humans, but that the morphology of the trochlear surface was unlike that of modern humans. Metrical analysis by Lisowski (1967) confirmed that the neck and neck-torsion angles of the OH 8 talus were similar to those of Kromdraai. Lisowski (1967) also concluded that the OH 8 talus was significantly different to that of modern humans, and was essentially ape-like. Day and Wood's metrical analysis (1968) initially agreed with Lisowski (1967) that the OH 8 neck angle was essentially ape-like, but noted that this was compensated by an altered orientation of the head (in relation to the neck) in the lateral direction. Their measurement of the neck torsion angle disagreed with Lisowski's in that they found it to be essentially human-like.

Oxnard (1972) re-examined Day and Wood's multivariate analysis of the data (1968) and concluded that the OH 8 talus was equally different to both human and ape tali, but was similar to the talus from Kromdraai (and that of *Proconsul*). Wood (1973, 1974a) noted that metrical analysis of the talus KNM-ER 813, found at Koobi Fora, Kenya, and of a similar age to OH 8, showed it to be far more human-like than OH 8. Lisowski (Lisowski *et al.*, 1974) argued that the talus was closest in form to that of *Pongo*, a view recently supported by a multivariate analysis of 17 talar measurements (Kidd, O'Higgins & Oxnard, 1996). However, Henderson and Wood (1977) suggested that whilst this may be so, it is important to remember that the presence of a high lateral trochlear margin, robust lateral metatarsals and similar sub-talar angles suggested that the lateral part of the foot bears a high proportion of body weight in OH 8, *Pongo* and humans, and thus any similarities between the tali may be due to similar weight distribution patterns rather than locomotor affinities. However, as discussed earlier, other researchers have noticed that the lateral margin of the

trochlear surface in modern humans is not relatively high compared to that of the great apes (e.g. Elftman & Manter, 1935b). Perhaps the culmination of all this speculation was the conclusion by Wood (1973, 1974a, 1974b), and Lewis (1980b) that the affinities of the OH 8 talus lay with the genus *Australopithecus*, and not with the genus *Homo*. Lewis (1981) has also argued that the OH 8 talus had affinities with extant apes (*Pan* and *Gorilla*), since it had a relatively oblique sub-talar axis and was “squat and foreshortened”, both characteristics of the ape talus. In summary, it is likely that the OH 8 talus is unique in its morphology and function, but is possibly the least human-like of the OH 8 foot bones.

These findings relating to OH 8 are potentially at odds with some of the views discussed about the talus of *A. afarensis*. Essentially, it is being suggested that the habiline talus retained some ape-like characteristics and thus could be in fact more *Australopithecus*-like than *Homo*-like, whilst that of *Australopithecus afarensis* is essentially human-like.

1.9.4 The navicular in the fossil record

The navicular has received little attention in discussions over the affinities of hominin pedal elements. This may be due to the fact that it is considered to be one of the more conservative bones in the tarsus, and is thus less indicative of locomotor repertoire than, say, the talus or medial cuneiform (Aiello & Dean, 1990).

There are two naviculars from the AL 333 locality in Hadar, Ethiopia. They were originally described as being very similar to each other in morphology, and are assigned to *A. afarensis* (Latimer & Lovejoy, 1982). A preliminary report suggested that both naviculars were very similar to that of *Pan*, and differed from that of modern humans in having a relatively enlarged medial tuberosity, more ape like dimensions of the talar facet, and an ape-like articulation with the cuboid (Gomberg & Latimer, 1984). However, this study has not been followed up with a publication with in-depth analyses. A separate study described both specimens as being markedly flat dorsoplantarly, and thus very similar to the navicular of *Pan* (Stern & Susman, 1983). However, Susman (1983) also briefly mentioned that the Hadar specimens had strong attachments for the plantar ligaments, which may indicate the presence of a medial longitudinal arch, but this was not backed up with any further analyses. A recent

multivariate study by Sarmiento (Sarmiento, 2000), using 13 interlandmark distances and 7 angles on the navicular alone, concluded that the two Hadar specimens were most similar in overall morphology to *Pan* and *Gorilla*, the reason for this being that, compared to modern humans, they had an “inflated” medial tuberosity, a more dorsoplantarly curved talar facet, and a relatively large angle between the talar and lateral cuneiform facets. Berillon (1998) also conducted a multivariate study of the Hadar naviculars, and has made similar findings to Sarmiento (2000), although he also concluded that all the angles between the cuneiform facets were ape-like in the Hadar naviculars. Sarmiento used his own findings to assert that the Hadar foot “lacked the longitudinal plantar arch characteristic of modern humans” (p.29; Sarmiento, 2000). It is important to remember that this conclusion was made based on the navicular alone. Such a localised study can only have a limited say on the overall architecture of the foot.

The navicular of Stw 573 (Littlefoot) has not been formally described and measured to date. Preliminary description of the bone (Clarke & Tobias, 1994) states that the specimen is mosaic in its affinities, having both human-like and ape-like features. The medial tuberosity is described as being human-like, and by that the authors presumably mean that it is relatively reduced in prominence. However, the authors also say that the tuberosity is similar to that of the Hadar specimens, and as discussed above, those are described as being more prominent and ape-like. This apparent contradiction of possible affinities has yet to be resolved. In terms of ape-like affinities, Clark and Tobias (1994) argue that the orientation of the Stw 573 navicular’s cuneiform facets indicates that “the medial and intermediate cuneiform bones were orientated toward the axis of an abducted forefoot” (p.522). They also state that the distance between the lateral sections of the talar and lateral cuneiform facets is markedly small, as in apes.

The navicular of OH 8 has been under more scrutiny than those from Hadar, although compared with the OH 8 talus, there have been relatively few metrical studies. The first metrical study was by Kidd *et al.* (1996). Their study used nine interlandmark distances taken on the OH 8 navicular and a comparative sample. Using multivariate analysis (canonical variates) they showed that, for their measurements, the OH 8 navicular was most similar in morphology to the African great apes, and was very

different to both modern humans and *Pongo*. However, the study does not state *how* the OH 8 navicular is similar in morphology to the African great apes. Information on which measurements or indices strongly influenced the result is crucial if any functional interpretation of the OH 8 foot is to be made. Sarmiento (2000) in the same metrical study that he conducted on the Hadar specimens discussed earlier, concluded that the OH 8 navicular was far more human-like than either of the Hadar specimens. Specifically, the OH 8 navicular has, Sarmiento argues, a shallow talar facet, a relatively reduced medial tuberosity, and angles between the cuneiform facets that are similar to those found in the modern human navicular. The shallow talar facet might suggest more limited movement at the talo-navicular joint, and the reduced medial tuberosity may well be indicative of increased arching of the lateral column. It has also been argued that the OH 8 navicular has strong attachments on its plantar surface for the calcaneonavicular (spring) and cubonavicular (short plantar) ligaments. As discussed earlier in this chapter, this is a strong indication of human-like longitudinal arches in the OH 8 foot (Susman, 1983; Sarmiento, 2000).

1.9.5 The 1st tarso-metatarsal joint in the fossil record

Latimer *et al.* (1990) have argued, from metrical analyses, that the *Australopithecus afarensis* hallux was fully in-line with the remaining metatarsals, and that the hallucial-medial cuneiform joint morphology indicated that there was no significant degree of opposability. However, whilst they base this on the relatively adducted position of the medial cuneiform hallucial facet, they do note that the facet is “markedly convex” (Latimer *et al.*, 1982), and for their measurement of convexity, the *A. afarensis* specimen falls outside the range of modern human variation, and approaches the extreme of the *Gorilla* range. A convex articular facet is usually indicative of joint movement, the authors’ assertion that *A. afarensis* had a fully unopposable hallux has been questioned a number of times (Stern & Susman, 1983, 1991; Susman & Stern, 1991). It is certain that if the hallucial surface is in a more adducted position, that some movement would be constricted, but that still doesn’t explain why the *A. afarensis* specimen has such a curved facet. A recent study of this joint, using angles and measurements that reflected the orientation and curvature of the facet (Berillon, 1998; Berillon, 1999) concludes that there *was* a degree of opposability retained in the *A. afarensis*, and unpublished data collected by the author (from a cast of the fossil) concurs with this finding. In summary, the distal facet

appears to more convex than any modern human specimen observed, but it does appear to be orientated in an adducted position as in humans. Evidence for the relative degree of hallux opposability of the East African australopithecines also comes from the hominin footprints at Laetoli, Tanzania. The trails cannot be confidently assigned to a specific taxon, since they are not directly associated with any fossil material, but at 3.7 mya, they are approximately contemporaneous with *A. afarensis*, and, the type specimen for that taxon comes from Laetoli. There have been conflicting interpretations of the footprints, with some studies saying that they indicate that the hallucial impression appears fully adducted (Leakey & Hay, 1979; White & Suwa, 1987; Tuttle *et al.*, 1991), whilst others have argued that some of the foot prints indicate a clearly abducted hallux that was capable of a degree of opposability (Stern & Susman, 1983; Deloison, 1991).

More recently, Clarke and Tobias (1995) have suggested that the degree of curvature and orientation of the medial cuneiform hallucial facet of Stw 573, tentatively assigned to *Australopithecus africanus*, is intermediate between that of modern humans and the African great apes. They concluded that a wide range of movement was possible at this joint, and that it contained the close-packed locking mechanism that opposable 1st tarsometatarsal joints have, as described by Lewis (1980a, 1980b, 1989). This would suggest that that taxon had a foot that has a degree of grasping potential, and thus may well have had an owner that was partially arboreal, and definitely mosaic in its locomotor repertoire. The authors of that study also suggest that the foot of Stw 573 had a more abductable hallux than OH8. However, the study is the only published one to date on Stw 573, and there is no mention of comparative metrical analyses that would put the fossil in the context of extant hominoid ranges of variation.

The supposedly ape-like talar neck and neck-torsion angles of the *Paranthropus robustus* talus, TM 1517, are argued by Lisowski (1967) to indicate that that taxon had a degree of hallux abduction intermediate between modern humans and the African great apes. The relatively large navicular facet on TM 1517, is also argued as a feature that implies a degree of hallux abduction (Broom & Schepers, 1946; Le Gros Clark, 1947; Robinson, 1972). However, as has been argued earlier, it is medial cuneiform and hallux morphology that is going to give the clearest evidence of

whether a taxon had an opposable hallux or not, and it has also been argued that talar neck and neck-torsion angles should not be considered as features that are diagnostic of hallux abduction (Robinson, 1972; Lewis, 1980b). More recently, a *P.robustus* 1st metatarsal from the South African site of Swartkrans has been described as being very human like, especially with respect to the base of the bone (the head is described as being more ape-like when viewed distally). It is also described as being similar in morphology to that of OH 8. This finding has led to suggestions that *P.robustus* was a fully obligate biped, with no degree of hallux abduction and a strong, human-like toe-off (Susman & Brain, 1988; Susman, 1989).

Regarding the *Homo habilis* degree of hallux abduction, Day and Napier (1964) concluded that the OH 8 hallux would have lain in an adducted position, but Lewis (1972) has argued that “the form of the articular surface of the medial cuneiform...appeared to be strikingly conservative” and that “its architecture was comparable to that shown by *Gorilla gorilla*”. His evidence for this was his observation that the dorsal part of the distal facet was “markedly convex” and was confluent with a “concave cupped area” below, whilst the base of the hallux exhibited a cylindrical concavity. Lewis (1972) suggested that this meant that the hallux could be screwed, medially and slightly superiorly, into a close-packed position similar to that found in apes. In a grasping foot, this close-packed articulation causes the hallux to be abducted and somewhat flexed, resulting in maximum stabilisation of the joint (Lewis, 1972, 1980b). Subsequently, he concluded, OH 8 had “some residual grasping potential” (Lewis, 1972). However, several studies have argued against this suggestion, and have stated that the medial cuneiform distal articular surface is flat and anteriorly orientated in the human-like plane, and that as a result, the OH 8 hallux lacked the potential for ape-like abduction (Susman & Stern, 1982; Susman, 1983; Gebo, 1992). The main problem with both arguments is that until recently there have been no metrical analyses of the joint. Several recent studies (Berillon, 1998, 1999; Harcourt-Smith, 1997; Harcourt-Smith & Aiello, 1999) have attempted to resolve this issue, and both have clearly stated, using functionally relevant measurements, that in overall morphology and in distal articular facet curvature and orientation, the OH 8 medial cuneiform lies well outside the great ape range of variation and well within the modern human range of variation.

1.9.6 Rays II to V in the fossil record

Most recently, there has come the suggestion that an early form of terrestrial bipedalism existed in at least one hominin species from the Late Miocene. *Ardipithecus ramidus kadabba* is represented by a fragmentary series of remains dated at 5.2 mya. With respect to its lower limb it is solely represented by one, left, 4th proximal foot phalanx (Haile-Selassie, 2001). The phalanx is described as being curved similarly to *A.afarensis*, but also to have a dorsally canted proximal joint surface. As discussed earlier, this is a feature of later hominins, and is indicative of the increased degree of metatarsophalangeal dorsiflexion that bipeds require in the toe-off phase. The great apes have a more plantarly orientated joint surface that reflects an increased requirement for grasping (Aiello & Dean, 1990; Duncan *et al.*, 1994). The *A.ramidus kadabba* phalanx may have had these features, but the recent report on its discovery is based on visual comparison, and further metrical analysis is needed before any conclusion can be made.

There has been considerable debate over the degree of curvature and relative movement of the digits of *A.afarensis*. The proximal phalanges were originally described as being markedly curved (Latimer & Lovejoy, 1982), and studies soon after the original description concluded that they were more curved than those of either *Pan* or *Gorilla*. This was seen as a strong adaptation for powerful grasping (Stern & Susman, 1983; Susman, 1983; Susman *et al.*, 1985). Since then a metrical study by the original team that described the fossils has asserted that the proximal joint surfaces of the proximal phalanges were dorsally canted, like modern humans, rather than plantarly so as in the extant great apes. This would suggest that *A.afarensis* could dorsiflex its metatarsophalangeal joints to a human like degree (Latimer & Lovejoy, 1990b). However, a more recent metrical study has challenged this finding, and states that the orientation of the proximal joint surface is intermediate between extant great apes and modern humans. This would suggest that *A.afarensis* had a degree of grasping potential in rays II to V that was intermediate between humans and the great apes (Duncan *et al.*, 1994).

1.9.7 Summary of fossil hominin pedal functional anatomy by taxon

Late Miocene hominins

Ardipithecus ramidus kadabba is suggested as having “...a unique pedal morphology...” that is “...similar to that in Hadar” (Haile-Selassie, 2001). As discussed above, this is based on the morphology of the proximal end of one solitary phalanx. The *A.afarensis* pedal remains from Hadar are extensive compared to this, and provide insights into the relative degrees of hallux abduction, talo-navicular movement, calcaneal morphology and ankle movement. By itself, the *A.ramidus kadabba* phalanx does not provide enough evidence that its owner had any significant degree of terrestrial bipedalism. Only more pedal remains from the rest of the foot will alter this outcome.

The Paranthropines

There are very few pedal remains for the taxa *Paranthropus robustus*. There is still ambiguity over the affinities of the Kromdraai talus TM 1517, with researchers suggesting that it has a human-like trochlea (Broom & Schepers, 1946; Le Gros Clark, 1947; Robinson, 1972), but a more ape-like head (Le Gros Clark, 1947; Robinson, 1972; Berillon, 2000), thus being mosaic in its affinities. The 1st metatarsal from Swartkrans indicates that *P.robustus* had lost the ability to oppose its hallux, and in all probability was a full biped with a strong toe-off (Susman & Brain, 1988; Susman, 1989).

The Australopithecines

A.afarensis

There has been considerable debate over the foot of *A.afarensis*. It has been described as having all the prerequisites for a foot of an obligate biped: an adducted and unopposable hallux, human-like metatarsophalangeal joints, a human-like talo-crural joint, and a human-like calcaneus, with a lateral plantar tubercle (Latimer *et al.*, 1987; Latimer & Lovejoy, 1989; Latimer & Lovejoy, 1990a, 1990b). However, other researchers have suggested that the foot of was far more mosaic in its affinities, and had a degree of hallux opposability (Berillon, 1997; Berillon, 1998; Berillon, 1999), strong great-toe flexion and therefore gripping (Tuttle, 1981; Deloison, 1991) a more ape-like navicular (Sarmiento, 2000), a mobile talonavicular joint (Gomberg &

Latimer, 1984), an ape-like talo-crural joint (Susman, 1983), no lateral plantar tubercle on the calcaneus (Deloison, 1985; Lewis, 1989), an absence of longitudinal arches (Berillon, 1998), and curved phalanges more capable of ape-like plantar flexion (Stern & Susman, 1983; Susman, 1983; Duncan *et al.*, 1994).

The best compromise of these two differing schools of thought is that *A. afarensis* was probably fully capable of bipedal locomotion when travelling on the ground, but that it was not capable of sustained obligate bipedalism, and furthermore, engaged in a significant degree of arboreal locomotion, with a degree of grasping still available. Recent suggestions have argued that *A. afarensis* retained morphologies in its wrist that suggested a knuckle-walking ancestor (Richmond & Strait, 2000), although this has also been disputed (Dainton, 2001). It is not clear whether this morphology actually infers that *A. afarensis* included knuckle-walking in its own locomotor repertoire.

A. africanus

The only study to date on the foot of *A. africanus* is the preliminary description of the “Littlefoot” assemblage, Stw 573 (Clarke and Tobias, 1994). This study suggests, mainly from visual appraisal, that the Stw 573 foot was mosaic in its affinities, having an essentially human-like talus, a mosaic navicular, and a hallux capable of a significant degree of grasping. The specimen is currently dated at about 3.3 mya (Partridge *et al.*, 1999), making it approximately contemporary with the East African *A. afarensis*. However, some ambiguity rests over the dates of Sterkfontein Member 2 (from which Stw 573 came), with some researchers claiming that the fossil cannot be older than 3 mya, and may be considerably younger (McKee, 1996; McKee, pers.comm; Berger, pers.comm). Clarke and Tobias used a combination of the Stw 573 foot bones, a first and second metatarsal from Sterkfontein, and the *A. afarensis* phalanges from Hadar to suggest a hypothetical Stw 573 foot. As can be seen from Figure 1.18, the hallux is clearly in an abducted position.

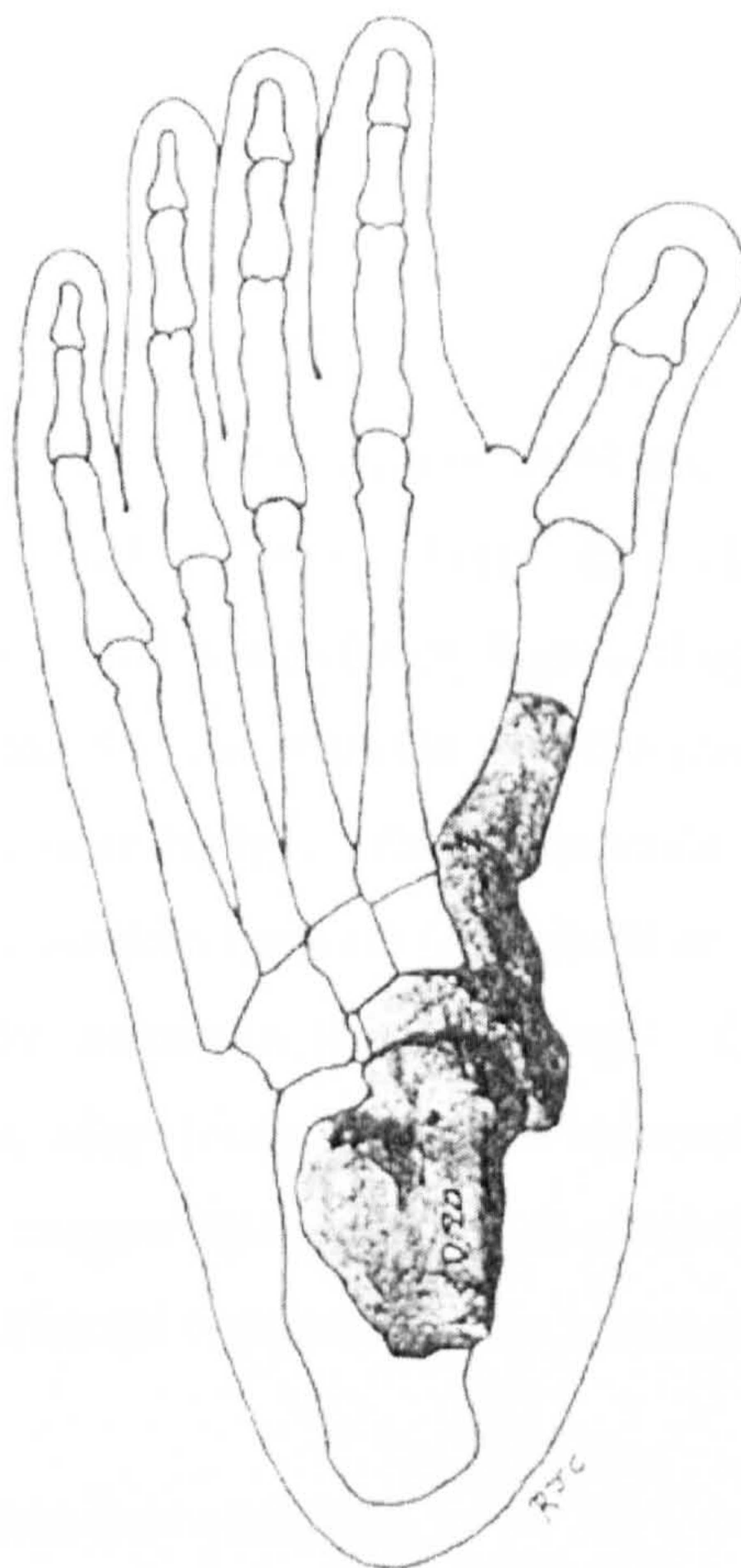


Figure 1.18 Reconstruction of “Littlefoot” by Clarke and Tobias (1994).

The Habiline foot

The *Homo habilis* foot is solely represented by the pedal assemblage OH 8. As has been discussed above, there has been a significant degree of debate surrounding the precise affinities of these foot bones. Most debate has surrounded the morphology of the talus, since it was originally described as being less human-like than the rest of the foot (Day & Napier, 1964). Some researchers have suggested that it is essentially human-like (Day & Wood, 1968; Wood, 1973; Wood, 1974a; Wood, 1974b), whilst others have postulated that it was markedly ape-like (Lisowski, 1967; Oxnard, 1972; Lisowski *et al.*, 1974; Lisowski *et al.*, 1976; Kidd *et al.*, 1996). Few doubt that the OH 8 calcaneocuboid joint was highly stable, and was capable of a human-like locking mechanism during the stance phase. However, Lewis (1989) asserts that the joint was could not facilitate the lateral swing of the calcaneus in the same fashion as modern humans. The OH 8 foot is also considered to have a lateral longitudinal arch

(Day & Napier, 1964), and this has been supported by metrical studies (Kidd *et al.*, 1996). The navicular has a considerably reduced medial tuberosity, a human-like trait, and indicative of a medial longitudinal arch (Susman, 1983; Sarmiento, 2000). The OH 8 great toe is described by many as being fully adducted and not capable of opposability (Day & Napier, 1964; Susman, 1983; Gebo, 1992), and this has been backed up by several recent metrical studies (Berillon, 1997; Harcourt-Smith, 1997; Berillon, 1998; Berillon, 1999; Harcourt-Smith & Aiello, 1999). However, Lewis (1972, 1980b, 1989) asserts that a significant degree of opposability was retained, and it has also been suggested that the possible ape-like morphology of the talus (Kidd, 1996) indicates an opposable hallux. The metatarsals of OH 8 have a robusticity pattern that is similar to modern humans (Archibald *et al.*, 1972). In summary, the habiline foot is probably mosaic in its morphology. Crucially it has a number of features that are specific adaptations to bipedal locomotion, but it has also retained some morphologies that suggest that it was not as efficient a biped as modern humans, and it *may* have had an arboreal component to its locomotor repertoire.

1.9.8 Models of hominin foot evolution

The most well known model of human foot evolution is Dudley Morton's synthesis (1935). Morton argued that the foot of the common ancestor of modern humans and the African great apes was that of a "hypothetical Dryopithecine". In terms of morphology, it was postulated that it would be intermediate between the foot of *Pan* and that of *Hylobates*, with relatively smaller tarsals than for *Pan*, but digits less elongated and curved than for *Hylobates*. Morton also suggested a hypothetical hominin foot, and postulated that it was intermediate between *Gorilla* and modern humans. The reason for this is that he concluded that since *Gorilla* is more terrestrial than *Pan*, then it must be more human-like in its foot, and Morton points to a suite of traits in the gorilloid foot that bears this out, such as a longer heel, decreased length of rays two to five, a slightly less abducted hallux and a decrease in the degree of torsion between the hallux and the remaining metatarsals. The last two observations effectively suggested a reduced grasping potential in *Gorilla*, relative to *Pan*. The hypothetical "prehuman foot" (Figure 1.19) is suggested by Morton (1935) to have still been a "flexible and muscular grasping organ", i.e. with an opposable hallux (although it would be relatively lengthened), but also an enlarged heel for increased weight bearing, shorter toes than *Gorilla*, but no longitudinal arches.

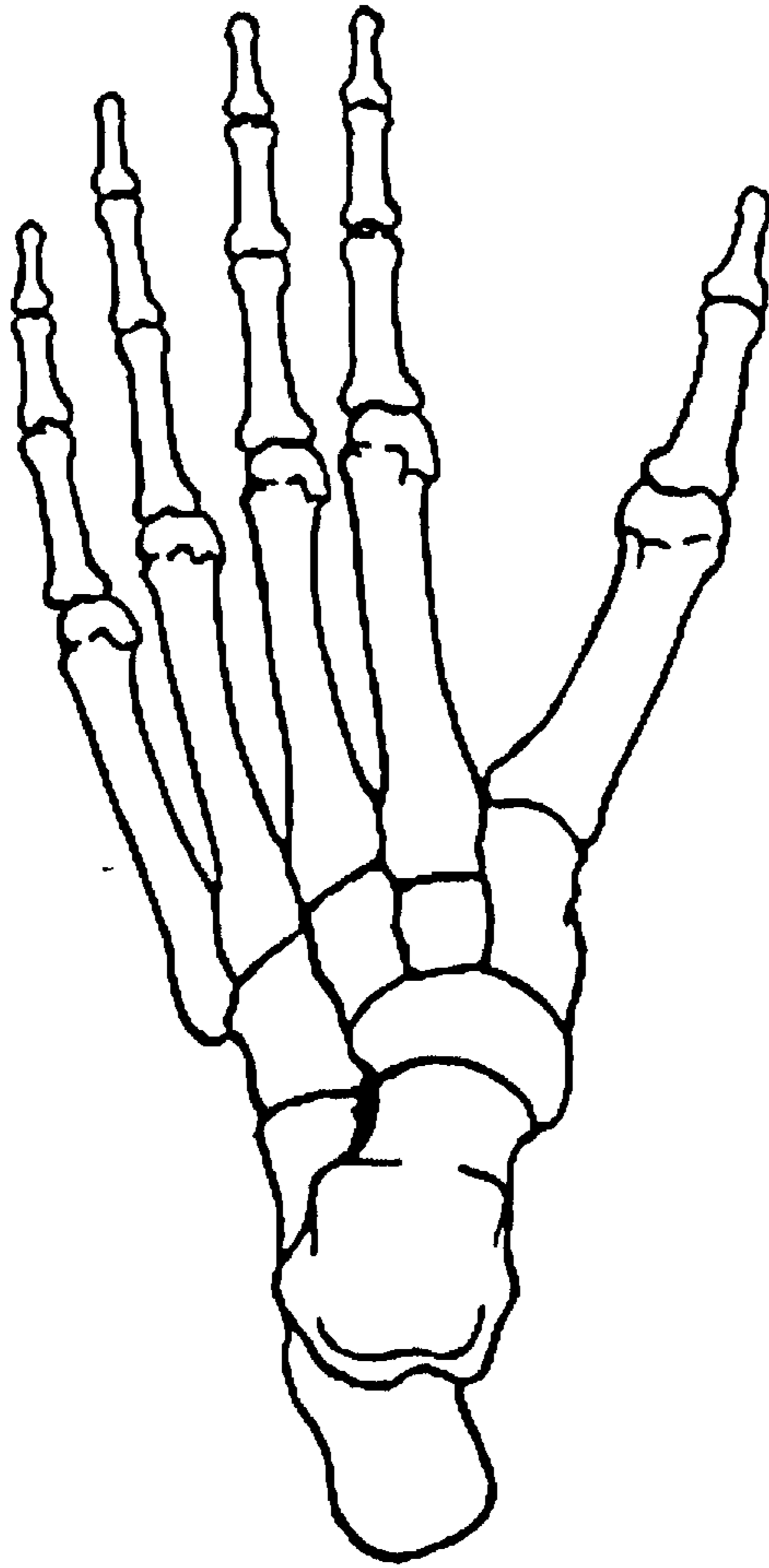


Figure 1.19 Morton's hypothetical "prehuman foot" (adapted from Morton, 1935).

Morton (1935) therefore suggested that our Plio-Pleistocene ancestors were essentially gorilloid rather than like *Pan*. He took no account of the fact that both *Gorilla* and *Pan* may well be highly derived in their pedal morphology, and that the terrestrial modifications seen in the foot of *Gorilla* (Sarmiento, 1994), could be structural modifications to cope with increased body weight, rather than modifications to becoming more bipedal. The other important fact to consider is that Morton had no fossils to work with, just modern comparative material.

More recent suggestions about hominin foot evolution have tended to be highly influenced by fossil finds. On the one hand this is advantageous, since the fossils provide hard evidence about particular morphologies at particular points in time. However, they also lead to hypotheses being "fossil driven", a constraint that would

not have influenced Morton (1936). Two recent models, by Lewis (1989) and Kidd (1999), stand out:

Lewis's model (1980a, 1980b, 1989) challenges what he refers to as the "traditional" model of how the ape foot remodels to become a human foot. This is described as the 1st ray adducting to become in line with the functional axis of the foot, and also the foot everting so that sole is flat on ground. Lewis argues that the problem with this is that by adducting the hallux, the 1st tarsometatarsal joint becomes unstable, due to moving into a loosely packed position. Lewis argues that instead, the hallux stayed in its close-packed position, and that the forefoot realigned towards this stabilised hallux. The problem here is that Lewis is assuming that the evolutionary changes in the foot would amount to the same changes that occur when an ape adducts its hallux. However, in evolutionary terms, with remodelling of the 1st ray so that it becomes more adducted, you would expect to get remodelling of the actual joint morphology so that maximum congruence (and therefore stability) would be retained between the medial cuneiform and the hallux. As discussed earlier, in modern humans the joint is essentially in the close-packed position permanently, and has very little ability to either abduct or adduct. This highlights the fact that the function of the close-packed position is different between apes to humans. In the great apes it is to facilitate a strong grip, whilst in modern humans it is to efficiently transfer weight during toe-off.

The other recent model by Kidd (Kidd, 1999), proposes a model of hominin foot evolution based solely on a study of the calcaneus, talus, cuboid and navicular of OH 8 (Kidd, 1995; Kidd *et al.*, 1996). As discussed earlier, these studies found that the talus and navicular of OH 8 were essentially ape-like, but that the calcaneocuboid articulation was markedly human-like. Kidd summarised that the medial column of OH 8 was still essentially ape-like, with no medial longitudinal arch and an opposable toe, but that the lateral column had remodelled to a human-like degree. Kidd (1999) proposes from this that the lateral side of the hominin foot evolved first, so as to stabilise mid-tarsal flexibility as an adaptation to increased terrestriality, and that the medial side followed, but at 1.8 mya still had a "mobile talonavicular joint" and an opposable hallux. Kidd's conclusions are problematic for several reasons. Firstly, the analysis of the OH 8 calcaneus is severely limited by the fact that the complete posterior section is missing. To add to this, crucially, Kidd did not measure the

medial cuneiform of OH 8, and yet concluded that the foot of OH 8 had an opposable hallux as part of its primitive medial column. As has been discussed at length in this chapter, it is the morphology of the medial cuneiform hallucial facet that gives the clearest indication of the degree of hallux abduction a taxon has. Finally, Kidd uses just one fossil specimen to drive a theory about hominin foot evolution. There is no consideration of the *A.afarensis* remains from Hadar, Ethiopia, or the various pedal remains from South Africa. As such, this model of foot evolution, whilst possible, can only be tentatively considered at this point.

1.10 Summary

As has been discussed throughout this chapter, there is widespread disagreement as to the affinities of Plio-Pleistocene pedal remains between 3.7 and 1.8 mya. We know that *Homo erectus* and more recent hominin species were fully bipedal, but cannot be any more certain than that. As represented by OH 8, the foot of *Homo habilis* may have retained certain arboreal capabilities, including a slight degree of hallux abduction and a more ape-like talo-crural joint. This ties in with findings based on analysis of the partial skeleton OH 62, which postulate that *Homo habilis* had more ape-like limb proportions (McHenry & Berger, 1998).

There is considerable debate over the affinities of *Australopithecus afarensis* pedal bones, and metrical research has not been published on bones belonging to *Australopithecus africanus*, especially with regards to Stw 573. There is also ambiguity over the nature of pedal function in *Paranthropus robustus*, but that debate rests on only one talus. The most parsimonious conclusion about these taxa, from fossil studies to date, is that their feet were all, in most likelihood, mosaic in their affinities, but that they may well have been so in different ways to each other. To date there have been no studies that incorporate all these taxa within one single analysis.

Chapter 2

2.1 Materials

Tarsals measured

The tarsals measured in this study are: the **talus, calcaneus, navicular, cuboid and medial cuneiform.**

Measurement criteria

All individuals were checked for pathologies. Those individuals with osteoarthritic growth around joint surfaces, fractures or recently healed fractures were not measured. Where possible, the bones measured all came from the left foot, but in a number of cases not all the bones of the left foot were present, and the right foot was measured instead.

All individuals measured were adults. Full adulthood was determined by:

- Full eruption of the 3rd permanent molar.
- Full epiphyseal fusion in the limb bones.
- Collection records.

Samples

The specimens included in this study represent two populations of modern humans, and four species of extant great apes. Where possible, the same number of males as females was measured for each population or species. Table 2.1 summarises the sample sizes by bone and species.

Modern Humans

Zulus

The Zulus are a southern African population, who, prior to European colonization, lived in the present day Kwazulu-Natal province in the eastern part of South Africa. Characterization of whether an individual in the collection was “Zulu” or not was

based on identification papers and/or language group at time of death. The Zulu sample was collected from the Dart Collection, Department of Anatomical Sciences, University of the Witwatersrand, South Africa. All bones measured in this study came from dissecting room cadavers, and have very accurate records of age at death, sex, cause of death, ethnic group, and in some cases height and body mass. This sample represents individuals who died between 1932 and 1990. Most individuals died of pulmonary related diseases, tuberculosis, heart problems or “natural causes”.

Xhosa

The Xhosa are also a southern African population. Prior to European colonization they are from the south-eastern region of present day South Africa, living in what used to be the Transkei and Ciskei homelands and is now the Eastern Province. As for the Zulus, all individuals measured came from dissecting room cadavers and represent individuals who died between 1932 and 1990.

Extant Great Apes

Pan troglodytes

The common chimpanzee sample comes from the Powell Cotton Museum, Birchington-on-Sea, Kent, UK. The collection is very well documented, and records show that all individuals measured in this study were wild shot members collected in the first half of the 20th century from localities in what is now modern day Cameroon, the Republic of Congo and the Democratic Republic of the Congo (former Zaire). All specimens came from west of the River Congo, and east of the Cameroon Highlands, and can therefore be confidently assigned to the subspecies *Pan troglodytes troglodytes* (Hill, 1969; Shea & Coolidge, 1988; Jenkins, 1990; Gonder *et al.*, 1997).

Pan paniscus

The *Pan paniscus* sample were all wild-shot individuals collected in the former Belgian Congo and are now housed in the Musée Royale de l’Afrique Centrale, Tervuren, Belgium. Careful inspection of the museum and expedition records shows that the specimens came unequivocally from that region south and east of the River Congo, north of the Rivers Kasai and Sankuru and west of the River Lualaba. This boxed-in region is known to be the specific habitat of *Pan paniscus* to the exclusion of the common chimpanzee (Fenart & Deblock, 1973; de Waal, 1997).

Gorilla

The *Gorilla* sample comes from two different collections. All but two individuals come from the Powell-Cotton Museum, Kent. The remaining two individuals come from the Peabody Museum, Yale, USA. As for the chimpanzees, all samples were wild shot in well documented localities in what is now modern day Cameroon, Gabon, the Republic of Congo and eastern parts of the Democratic Republic of the Congo. Inspection of collection records indicates that all individuals came from west of the River Congo, and can therefore be confidently assigned to the western lowland subspecies, *Gorilla gorilla gorilla* (Groves, 1970, 1971; Jenkins, 1990).

Pongo

The orangutan sample represents individuals from both subspecies of this taxon: the Sumatran orangutan, *Pongo pygmaeus abelli* and the Bornean orangutan, *Pongo pygmaeus pygmaeus*. Close inspection of collection records showed that nearly all individuals collected were wild shot from a variety of forest locations on both islands, but a small number (collected to supplement the sample size) were animals that had been caught in the wild but died in zoos. Of a total of 46 individuals measured (not all with complete feet) only 4 had died in zoos. The majority of the sample (29 individuals) came from the Smithsonian Museum of Natural History, Washington DC. The remaining specimens came from The American Museum of Natural History, New York (6 individuals) and The Natural History Museum, London (11 individuals).

Table 2.1 Sample numbers for each bone for each extant species

	Medial Cuneiform	Navicular	Cuboid	Talus	Calcaneus
<i>Pongo pygmaeus</i>	29	26	43	41	32
<i>Pan troglodytes</i>	40	40	42	44	40
<i>Pan paniscus</i>	15	15	16	16	16
<i>Gorilla gorilla gorilla</i>	41	41	42	41	41
<i>Homo sapiens</i> (Zulu)	77	80	80	80	81
<i>Homo sapiens</i> (Xhosa)	33	34	34	33	34

*Fossil specimens**Australopithecus africanus*

All measurements for the *A.africanus* material came from the original fossils, courtesy of the Department of Anatomical Sciences, the University of the Witwatersrand, Johannesburg, South Africa. The specimens measured were Stw 88 (a right talus), Stw 363 (a left talus) and the talus, navicular and medial cuneiform of Stw 573 (“Littlefoot”), which are assumed to all come from the left foot of one individual (Clarke & Tobias, 1995). The lateral malleolar facet is sheared off in the Stw 573 talus, so that structure could not be measured.

Australopithecus afarensis

All measurements of *A.afarensis* material came from original and accurate casts courtesy of Musée de l’Homme, Paris, France. All the casts measured represented fossils found in the AL 288 and Al 333 localities in Hadar, Ethiopia (Latimer & Lovejoy, 1982). Casts measured were the right talus AL 288-1as (from “Lucy”), and the two right naviculars AL 333-36 and AL 333-47.

Paranthropus robustus

Only one specimen from this taxon could be measured for this study, the talus TM 1517, found at the site of Kromdraai, South Africa (Broom & Schepers, 1946). The talus is missing both calcaneal facets, so only the trochlear surface was measured.

Measurements for this specimen were taken from the original fossil, courtesy of the Transvaal Museum, Pretoria, South Africa.

Australopithecus sp.

Original casts of two tali from Koobi Fora, Kenya (Leakey *et al.*, 1978), that are tentatively considered to be australopithecine, but are not assigned to a species, were measured. The specimens are KNM-ER 1464 (right talus) and KNM-ER 1476A (left talus).

Homo habilis

The only specimen measured belonging to this taxon that could be measured, was Olduvai Hominid 8 (OH 8). OH 8 consists of all the tarsals and metatarsals of a left foot (Day & Napier, 1964). Of the bones measured for this study, the calcaneus is badly damaged, and only the anterior half is preserved. Only those parts present were measured for the OH 8 calcaneus. The talus is missing the posteromedial part of its posterior calcaneal facet. This missing part of the facet was reconstructed using modelling clay. This particular facet is always very symmetrical in hominoids, so accurate reconstruction of the missing facet can be done with confidence if more than half of it is actually present. The OH 8 medial cuneiform, navicular and cuboid are all intact and undistorted. The original was not available, so measurements were taken from original and accurate casts housed in the Natural History Museum, London. Three different sets of casts were measured so as to ensure any morphological discrepancies between the original fossil and the casts were kept to a minimum.

Homo sp.

One right talus from Koobi Fora is assigned to the genus *Homo*, but is not assigned to a species (Leakey *et al.*, 1978). The specimen measured is KNM-ER 813A.

2.2 Methods

2.2.1 Landmark choice

This study is concerned with the analysis of 3D shapes representing the tarsals. 3D Cartesian landmarks were chosen to accurately reflect both the overall shape *and* the function of each bone. As discussed in Chapter 1, tarsal function is mainly concerned with the transmission of forces through joint complexes, and is thus dominated by facet morphology. As such, the majority of landmarks in this study represent the articular facets. The other main reason that most landmarks were facet based, is one of homology. All the tarsals of the hominoids possess homologous major facets. There is minor variation of additional facets, but otherwise all taxa have the same number of tarsals and the same articulations between the tarsals. Features such as muscle attachment sites and grooves for tendons or ligaments are much more variable, both intraspecifically and also interspecifically. Devising landmarks for such structures is problematic because they are not repeatable, and are often not equivalent. Equivalence might refer to developmental or evolutionary equivalence of form or process, and in this case it is often termed “homology”. Alternatively, equivalence might be functional or biomechanical, e.g. the end of a lever arm. In this study, landmarks are chosen to be homologous in an evolutionary-developmental sense. A system has been devised to classify the relative homology of such anatomical landmarks (Bookstein, 1991; Marcus *et al.*, 1996; O'Higgins, 2000):

Type I Landmarks

Homology is supported by strong local evidence (often histological), where two or more structures meet. An example would be the meeting of the coronal and sagittal sutures on the skull.

Type II Landmarks

Homology is supported by geometric evidence. An example would be the point at either end of a distinct margin between two articular facets.

Type III Landmarks

Homology is only supported by a relative position on a feature, rather than a specific location. An example would be the most inferior point on the femoral head.

Table 2.2 Cuboid Landmarks*Distal facet*

Number	Type	Description
1	II	Most dorso-medial point, i.e. where medial and dorsal facet margins meet
2	II	Most medio-plantar point, i.e. where medial and plantar facet margins meet
3	III	The most medial point of the medial margin
4	II	Most dorsal point of the facet margin between the articular surfaces for 4 th and 5 th metatarsals
5	II	Most dorsal point of the facet margin between the articular surfaces for 4 th and 5 th metatarsals
6	III	Most lateral point of facet
7	III	Deepest point of indentation on facet for 4 th metatarsal
8	III	Deepest point of indentation on facet for 5 th metatarsal

Medial facet

9	III	Most distal point of facet margin
10	II	Most disto-plantar point of facet margin
11	III	Most proximal point of facet margin
12	II	Most proximo-plantar point of facet margin
13	III	Most dorsal point of facet margin

Proximal facet

14	I / II	Point where dorsal surface, proximal facet and medial facet meet
15	III	Most dorsal point of dorsal facet margin
16	III	Most dorso-lateral point of facet margin
17	III	Most plantar-lateral point of facet margin
18	II	Most proximal point of plantar "beak".
19	III	Most plantar-medial point of facet margin
20	III	Deepest/most distal point of facet

Lateral side

21	II	Between distal and proximal facets, lateral side, the most medial point of the indentation
----	----	--

Table 2.3 Talar landmarks
Trochlea

Number	Type	Description
1	III	Most distal point of the trochlear groove
2	II	Most distal point of contact between the medial malleolar facet and the trochlear surface
3	III	Most dorsal point on the medial facet margin
4	II	Most proximal point of contact between the medial malleolar facet and the trochlear surface
5	III	Most proximal point of the trochlear groove
6	II	Most proximal point of contact between the lateral malleolar facet and the trochlear surface
7	III	Most dorsal point on the lateral facet margin
8	II	Most distal point of contact between the lateral malleolar facet and the trochlear surface
9	III	Most dorsal point on the trochlear groove
10	III	Most distal point on medial malleolar facet
11	III	Most plantar point on medial malleolar facet
12	III	Most distal point on lateral malleolar facet
13	III	Most plantar point on lateral malleolar facet
14	III	Deepest (most medial) point on lateral malleolar facet, between landmarks 14 and 7
<i>Proximal calcaneal facet</i>		
15	II	Most disto-lateral point
16	III	Most lateral point
17	II	Most proximo-lateral point
18	III	Deepest (most dorsal) point on the proximal facet margin
19	II	Most proximo-medial point
20	III	Most medial point
21	II	Most disto-medial point
22	III	Deepest (most dorsal) point on the distal facet margin
23	III	Deepest (most dorsal) point of the facet
<i>Head/navicular facet</i>		
24	III	Most dorsal point
25	III	Most plantar point
26	III	Most medial point

27	III	Most lateral point
28	III	Most distal point
29	II	Most lateral point of contact between the navicular facet and the distal calcaneal facet

Table 2.4 Navicular landmarks

Proximal (talar) facet

Number	Type	Description
1	III	Most medial point
2	III	Most plantar point
3	III	Most lateral point
4	III	Most dorsal point
5	III	Deepest (most distal) point of facet

Distal (cuneiform) facets

6	II	Most dorso-medial point
7	III	Most medial point
8	II	Most dorso-plantar point
9	II	Most dorsal point of margin separating facets for medial and intermediate cuneiforms
10	II	Most plantar point of margin separating facets for medial and intermediate cuneiforms
11	II	Most dorsal point of margin separating facets for intermediate and lateral cuneiforms
12	II	Most plantar point of margin separating facets for medial and intermediate cuneiforms
13	II	Most dorso-lateral point
14	III	Most lateral point
15	II	Most plantar-lateral point.
16	III	Mid-point on lateral cuneiform facet
17	III	Mid-point on intermediate cuneiform facet
18	III	Mid-point on medial cuneiform facet

Medial tuberosity

19	III	Most proximal point
20	III	Most medial point
21	III	Most plantar point

Table 2.5 Calcaneus landmarks*Posterior talar facet*

Number	Type	Description
1	III	Most proximal point
2	III	Most distal point
3	III	Most medial point
4	III	Most lateral point

Anterior talar facet

5	III	Most proximal point
6	III	Most lateral point
7	III	Most distal point
8	III	Most medial point

Posterior surface

9	III	Most dorsal point
10	III	Most dorso-medial point
11	III	Most dorso-lateral point
12	III	Most posterior point
13	III	Most plantar point
14	III	Most plantar-medial point
15	III	Most plantar-lateral point
16	II	Most distal point on medial tubercle

Cuboid facet

17	II	Most proximal point of “beak” articulation
18	III	Most lateral point
19	III	Most dorsal point
20	III	Most medial point

Table 2.6 Medial Cuneiform Landmarks*Distal (hallucial) facet*

1.	III	Most dorsal point
2	III	Most plantar point
3	III	Dorsal section: most medial point
4	III	Dorsal section: most lateral point
5	III	Plantar section: most medial point
6	III	Plantar section: most lateral point
7	III	Dorsal section: most distal point
8	III	Plantar section: most distal point

Proximal (navicular) facet

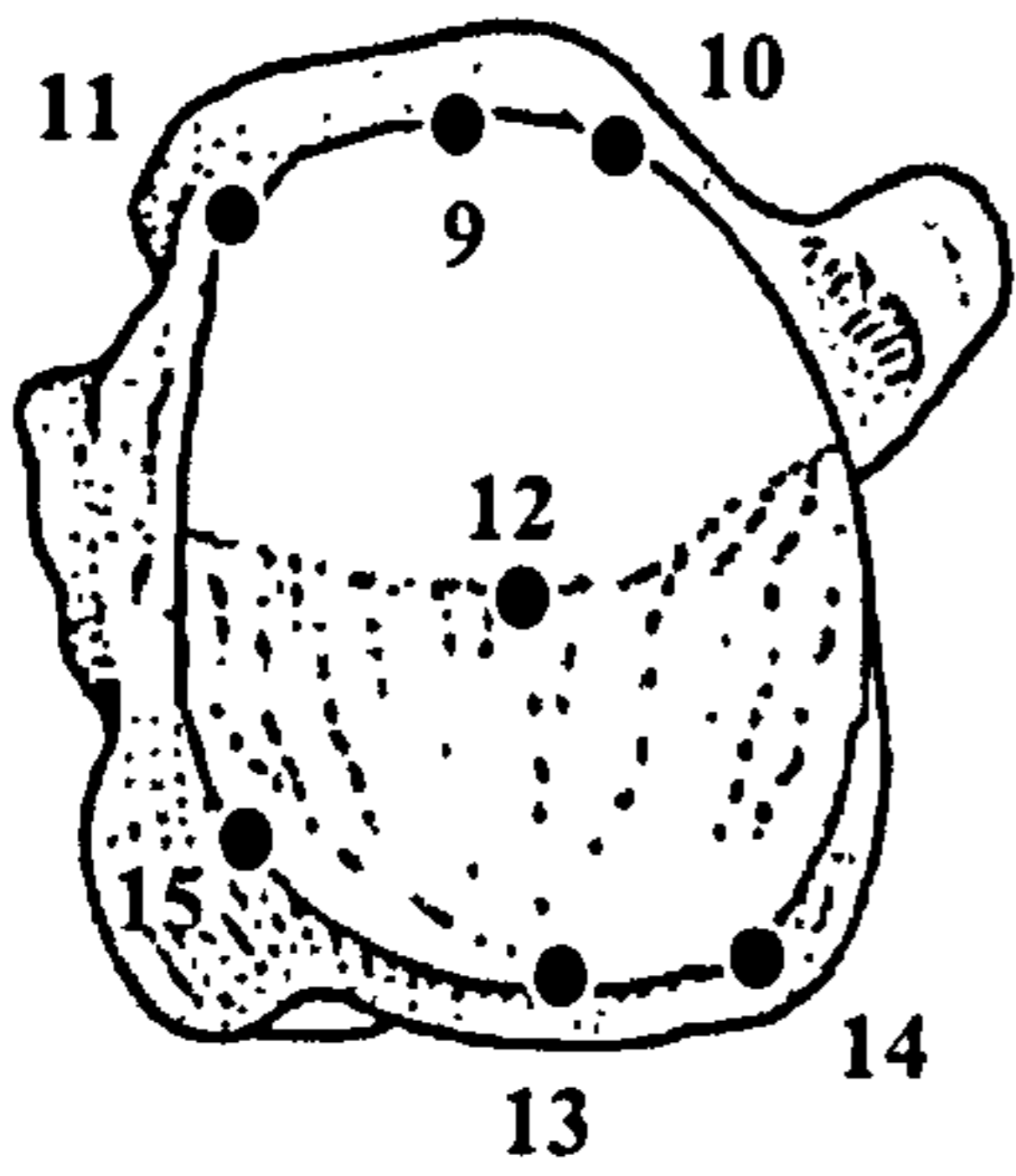
9	II	Most dorsal point
10	II	Most plantar point
11	II	Most lateral point
12	II	Most medial point
13	III	Deepest point

Lateral (intermediate cuneiform) facet

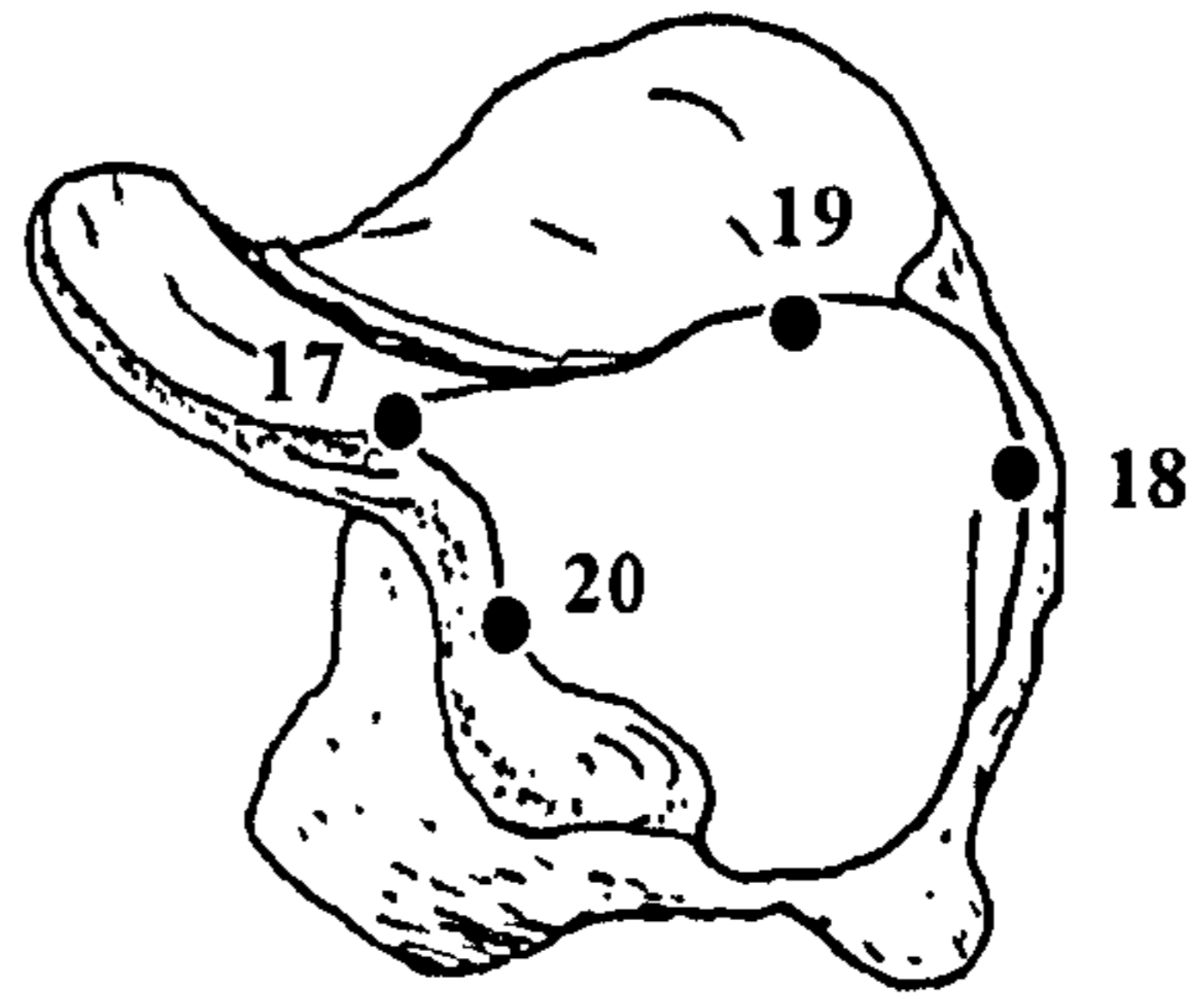
14	II	Most distal point
15	III	Most dorsal point
16	III	Most proximal point
17	III	Most plantar point

Below Figure 2.1 illustrates the landmarks used for each bone. Figure 2.2 shows different views of constructed wireframe models using triangles.

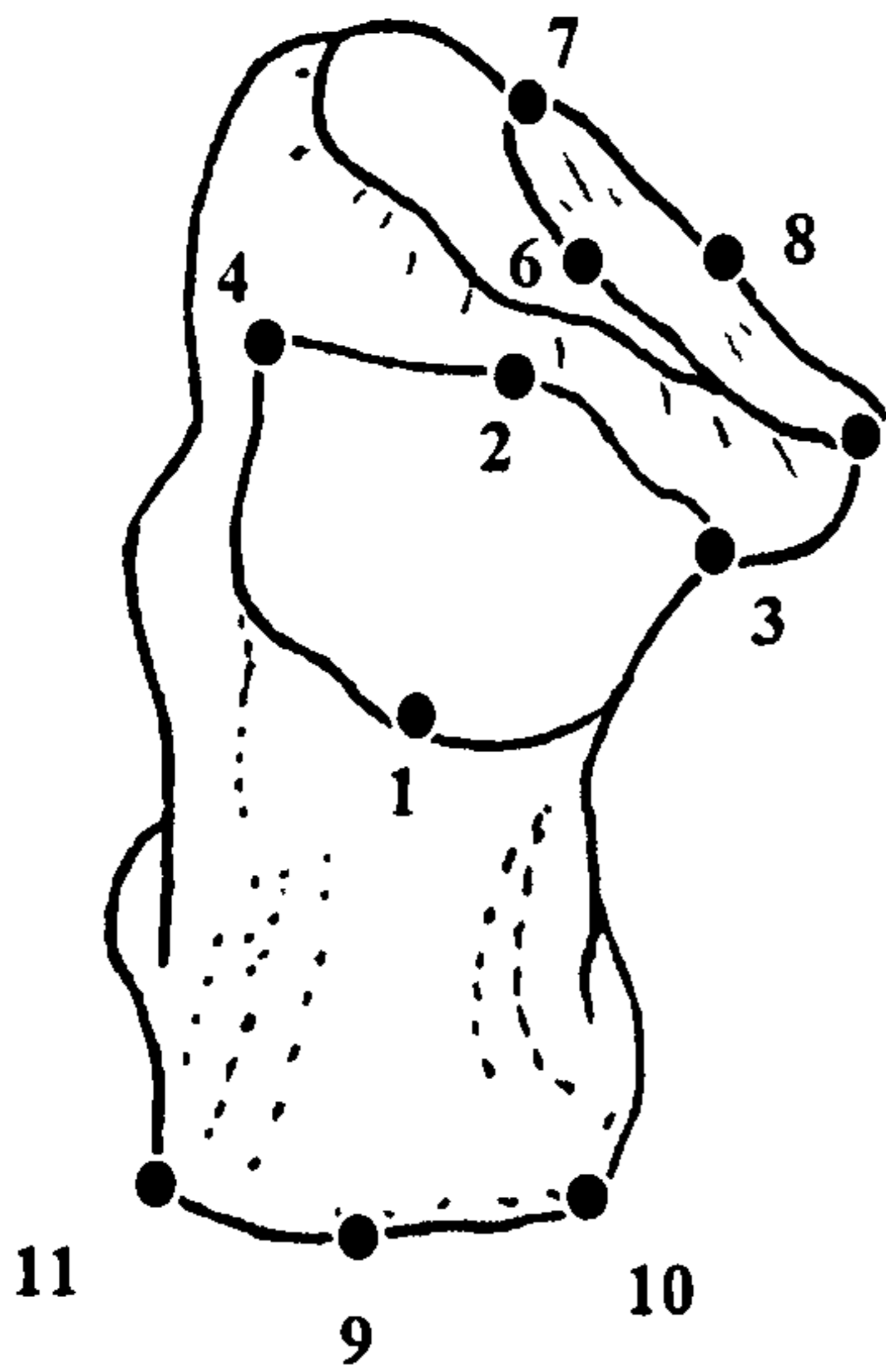
Figure 2.1 Diagrams of Landmarks



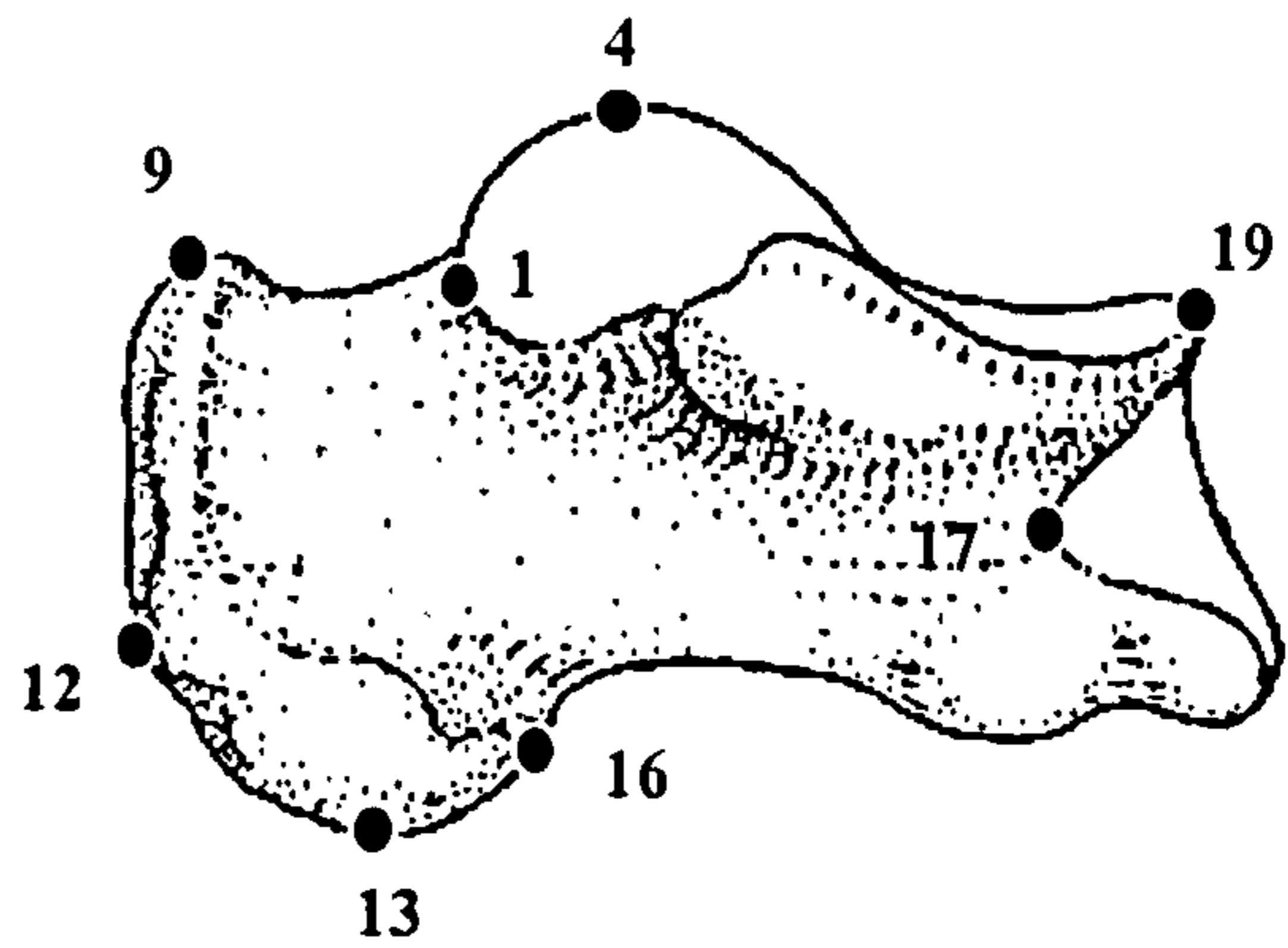
**Calcaneus:
Proximal aspect**



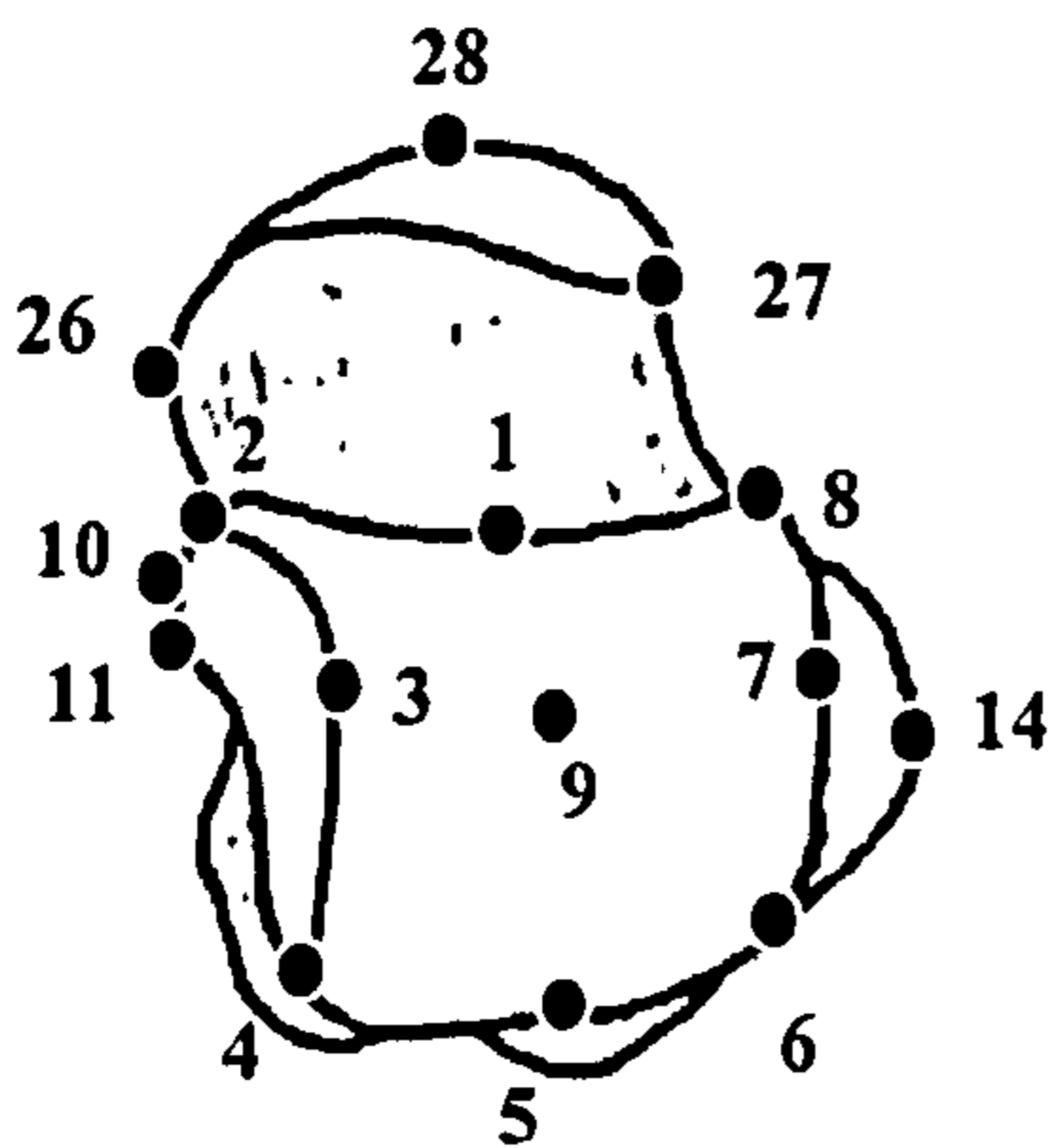
**Calcaneus:
Distal aspect showing cuboid facet**



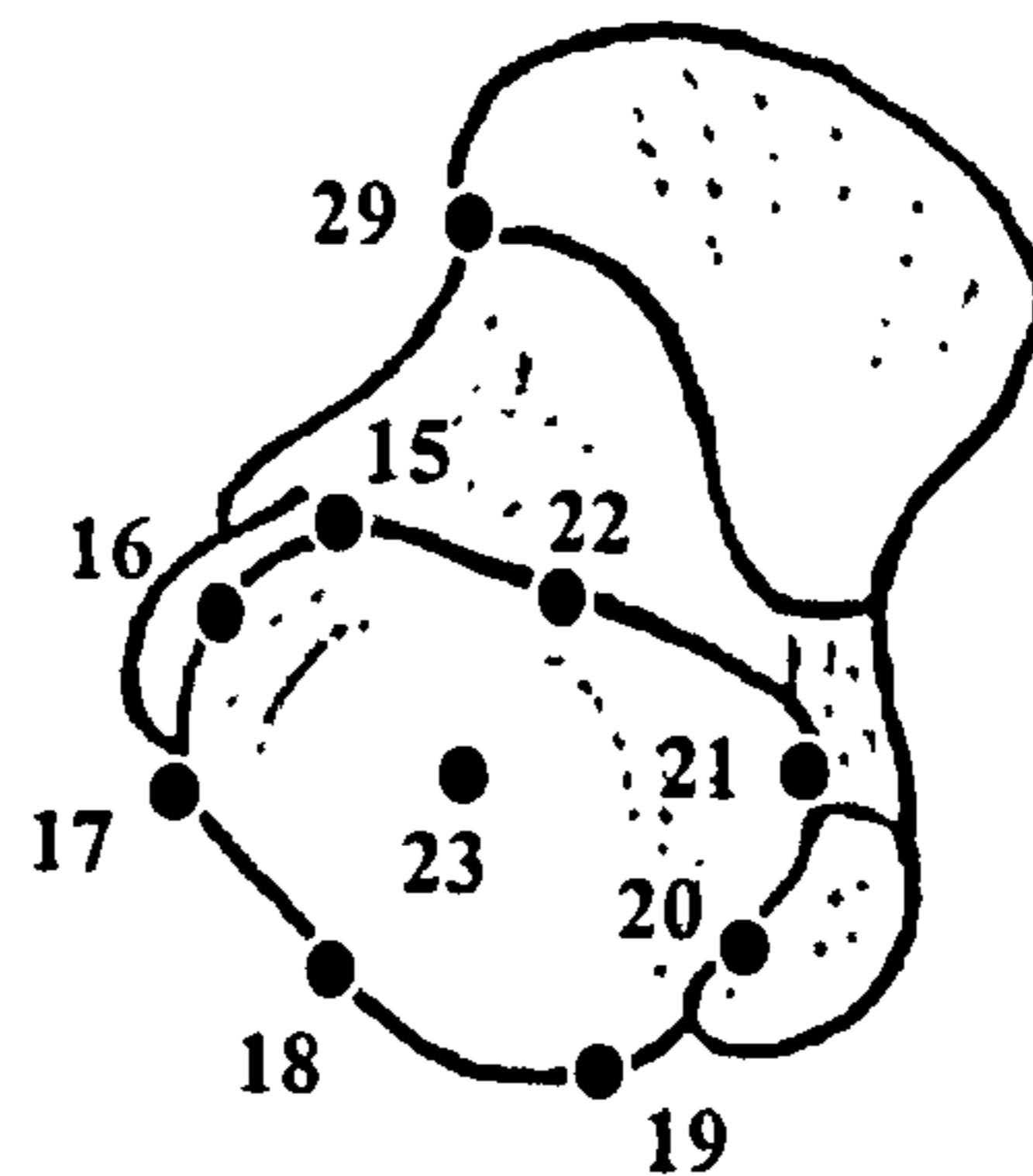
**Calcaneus:
Dorsal aspect showing talar facets**



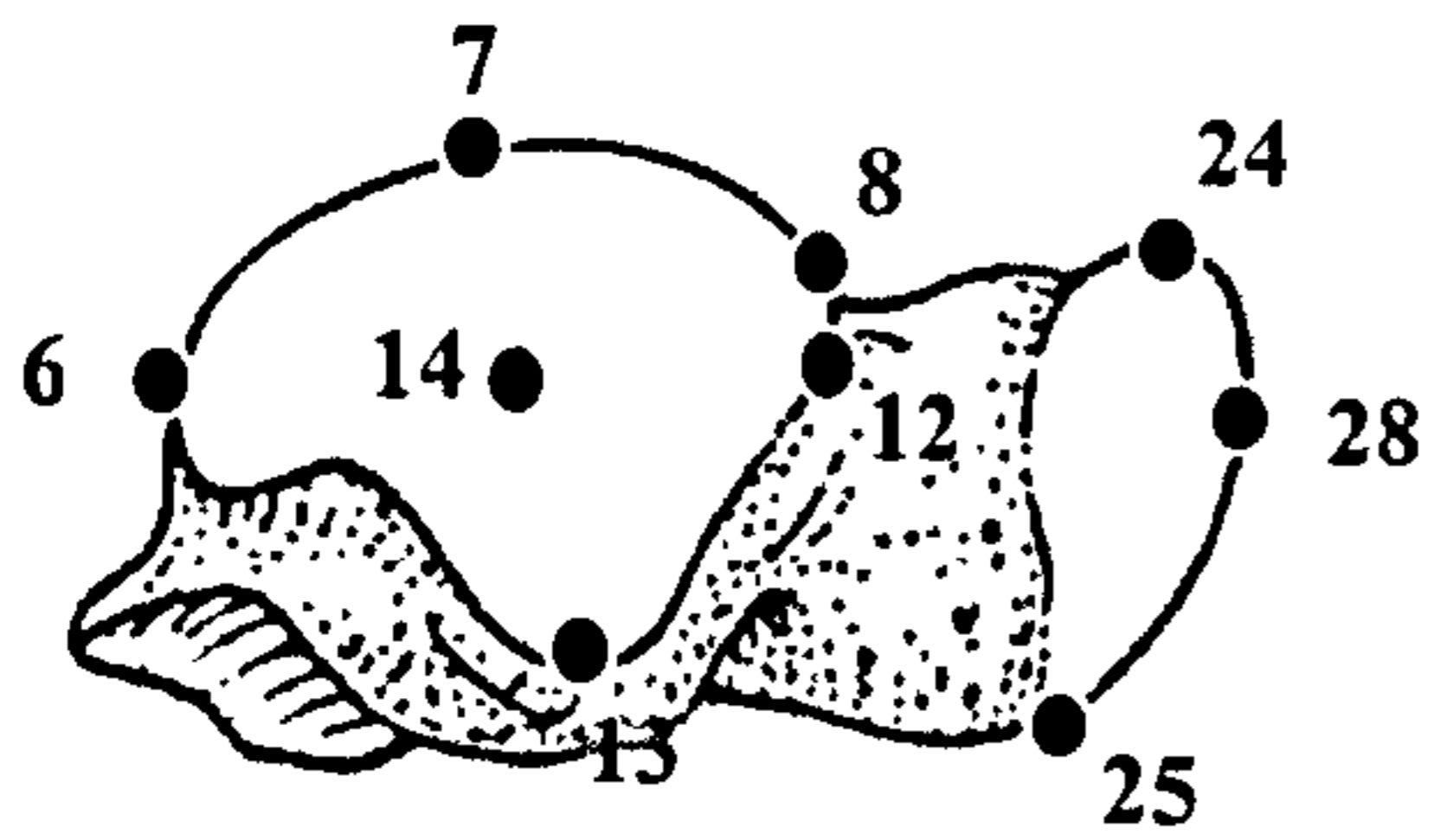
**Calcaneus:
Medial aspect**



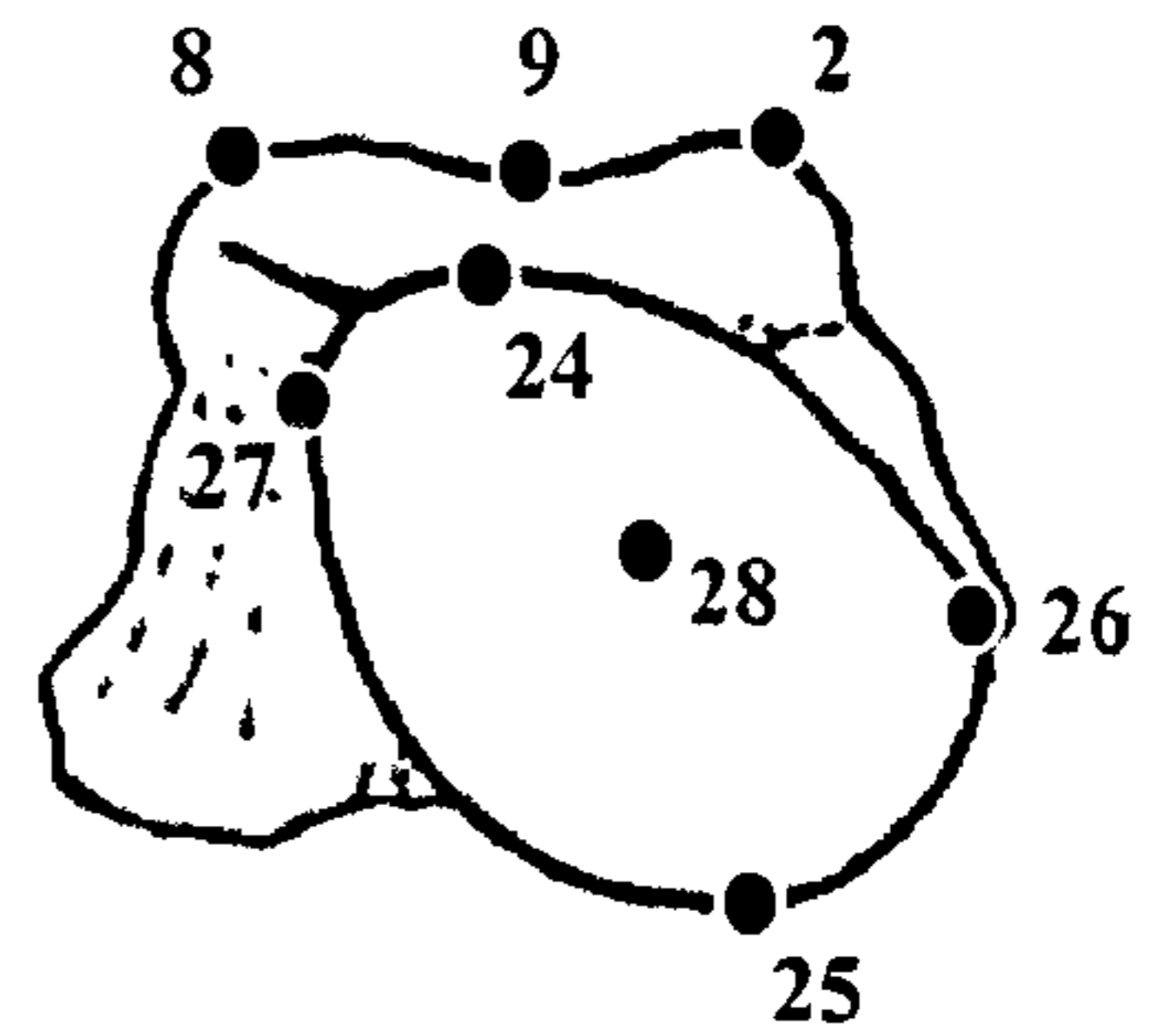
**Talus:
Dorsal aspect showing trochlea**



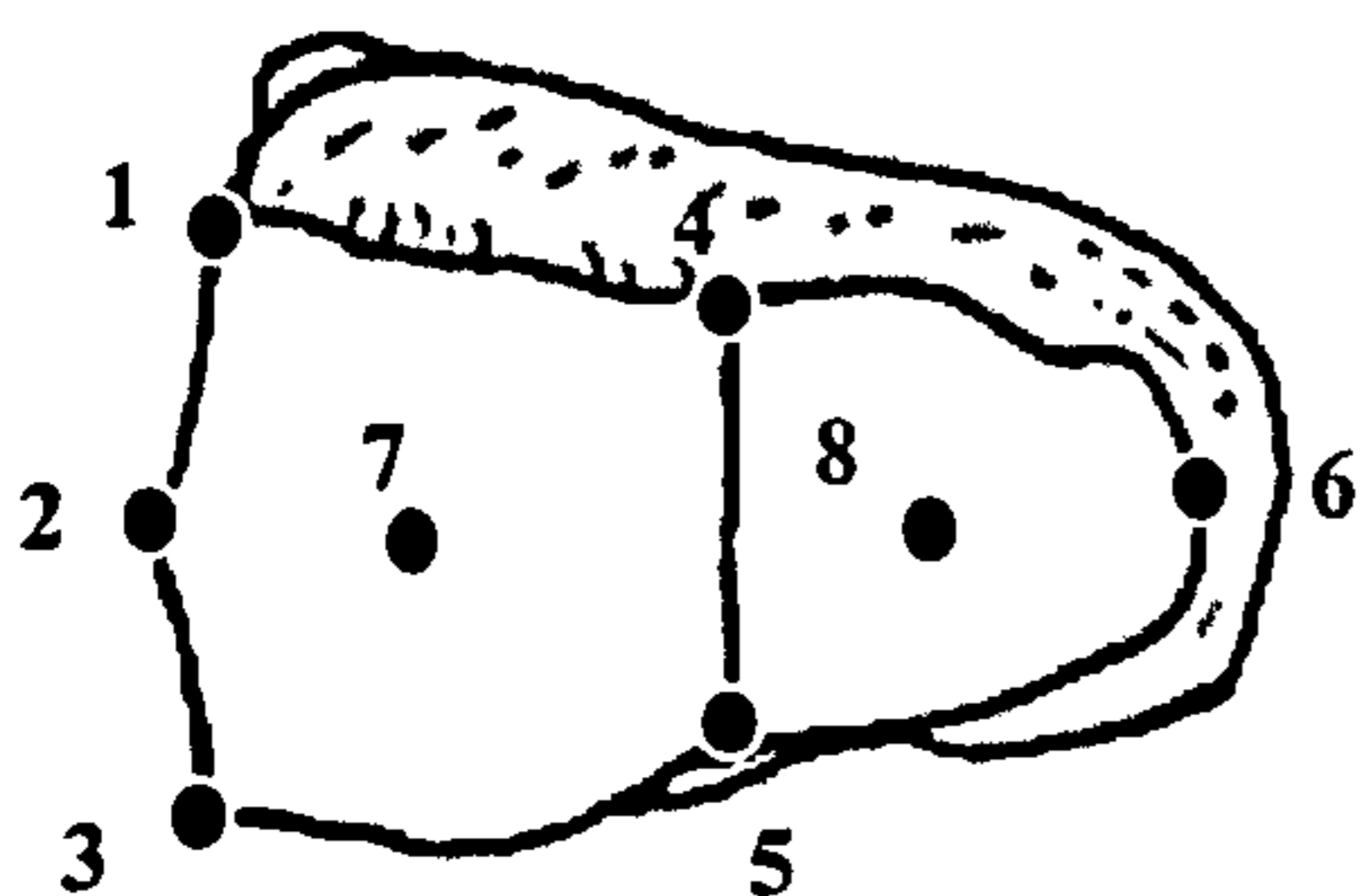
**Talus:
Plantar aspect showing anterior
calcaneal facet**



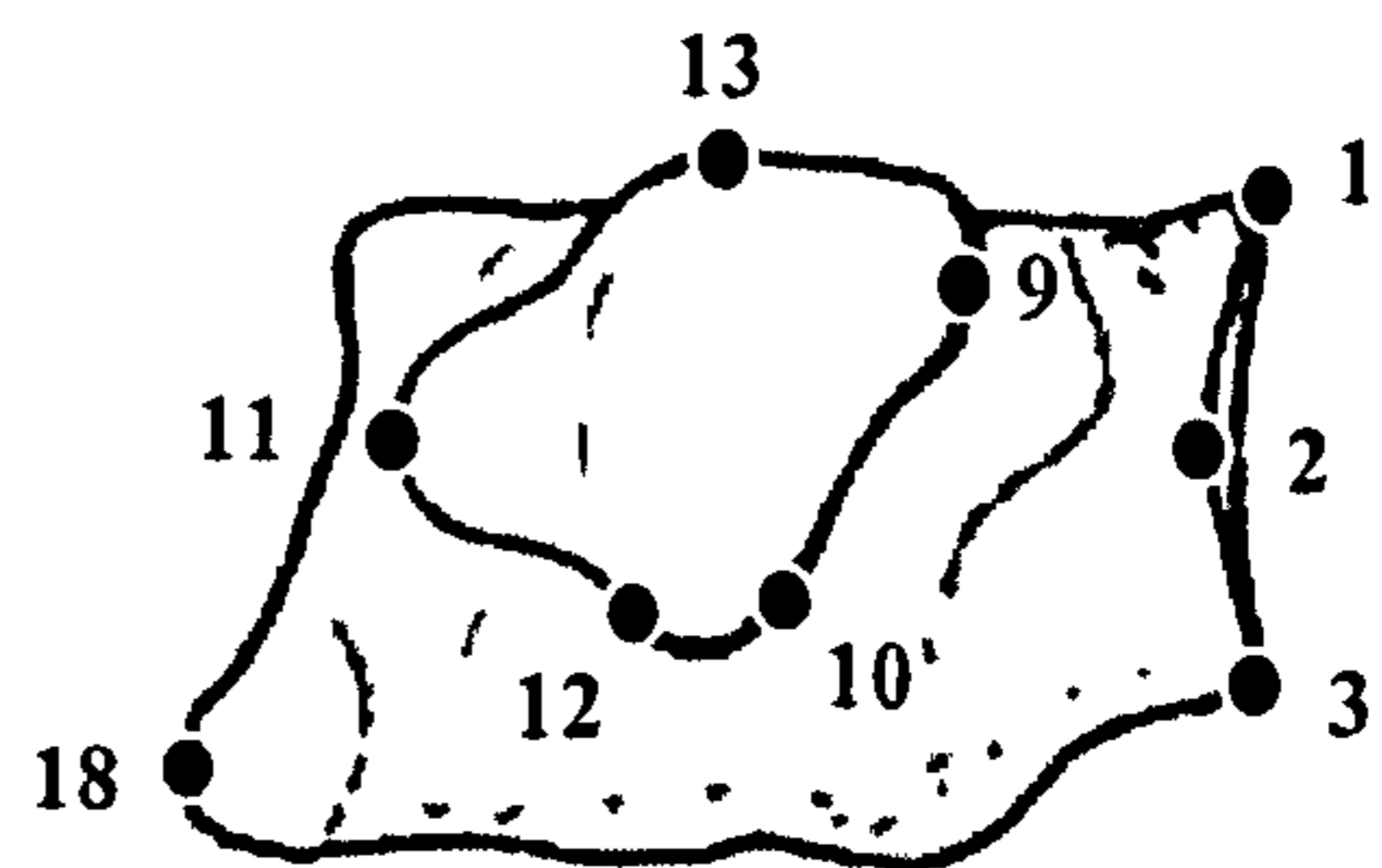
Talus:
Lateral aspect showing lateral malleolar facet



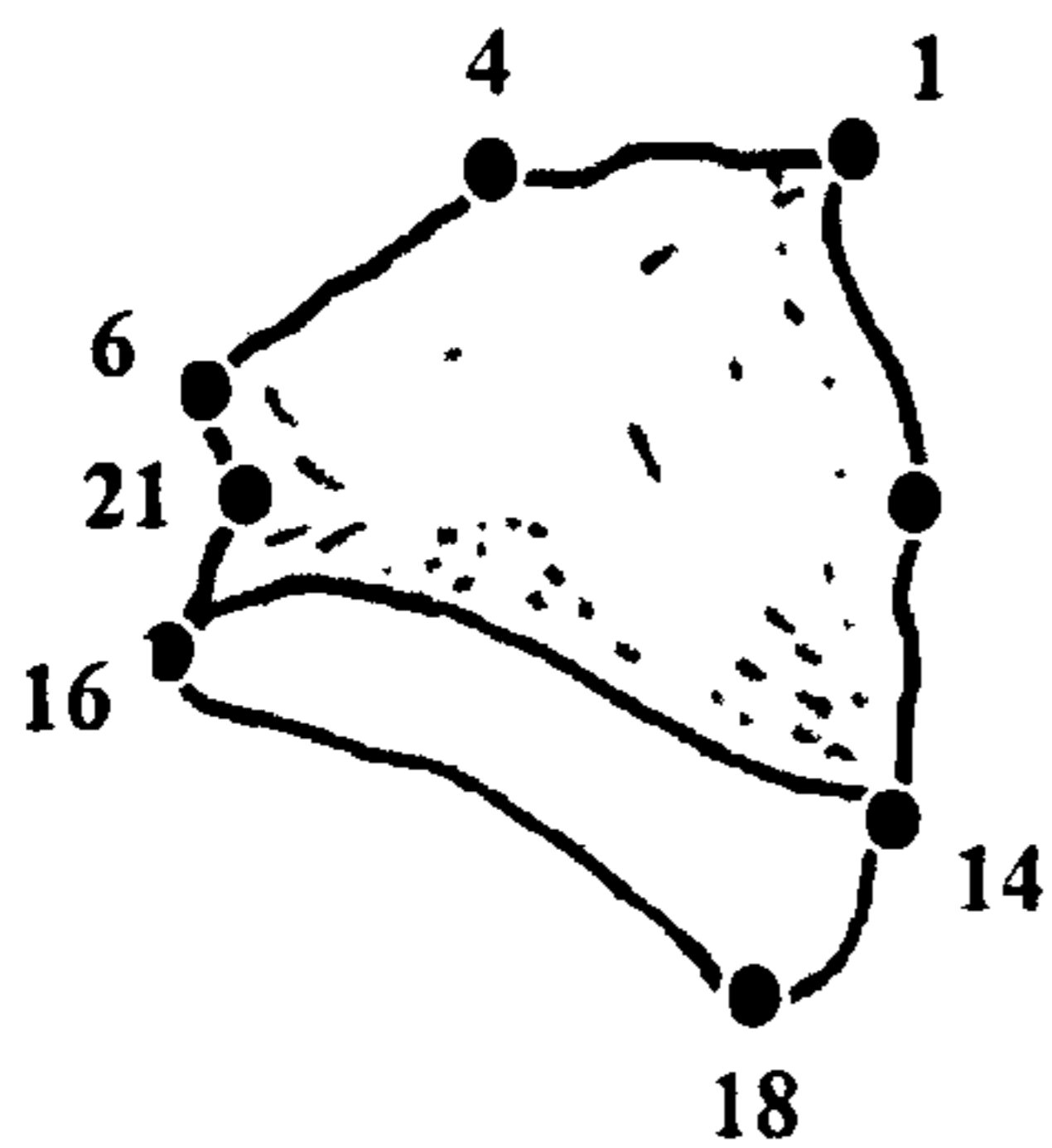
Talus:
Distal aspect showing navicular facet



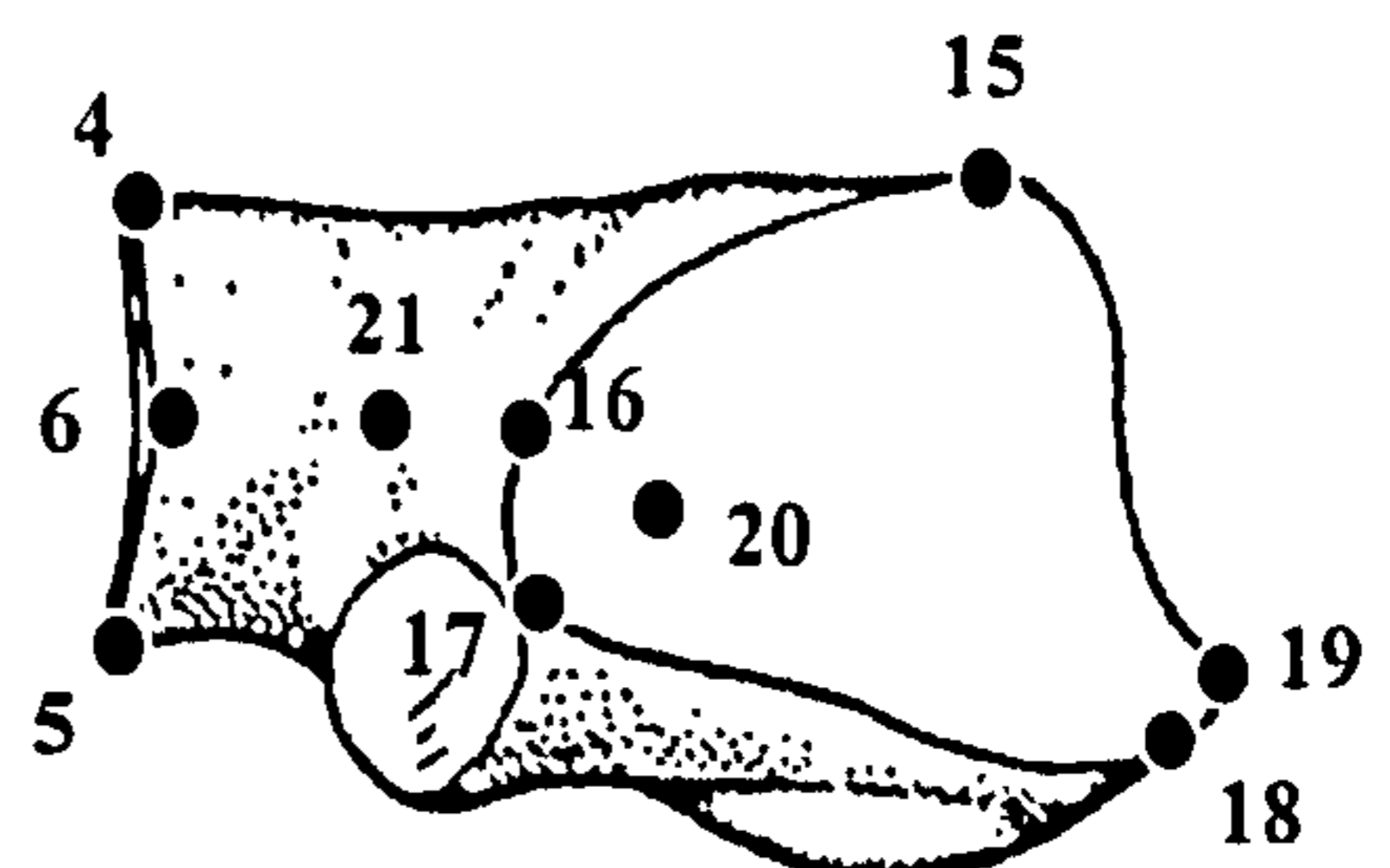
Cuboid:
Distal aspect showing metatarsal facets



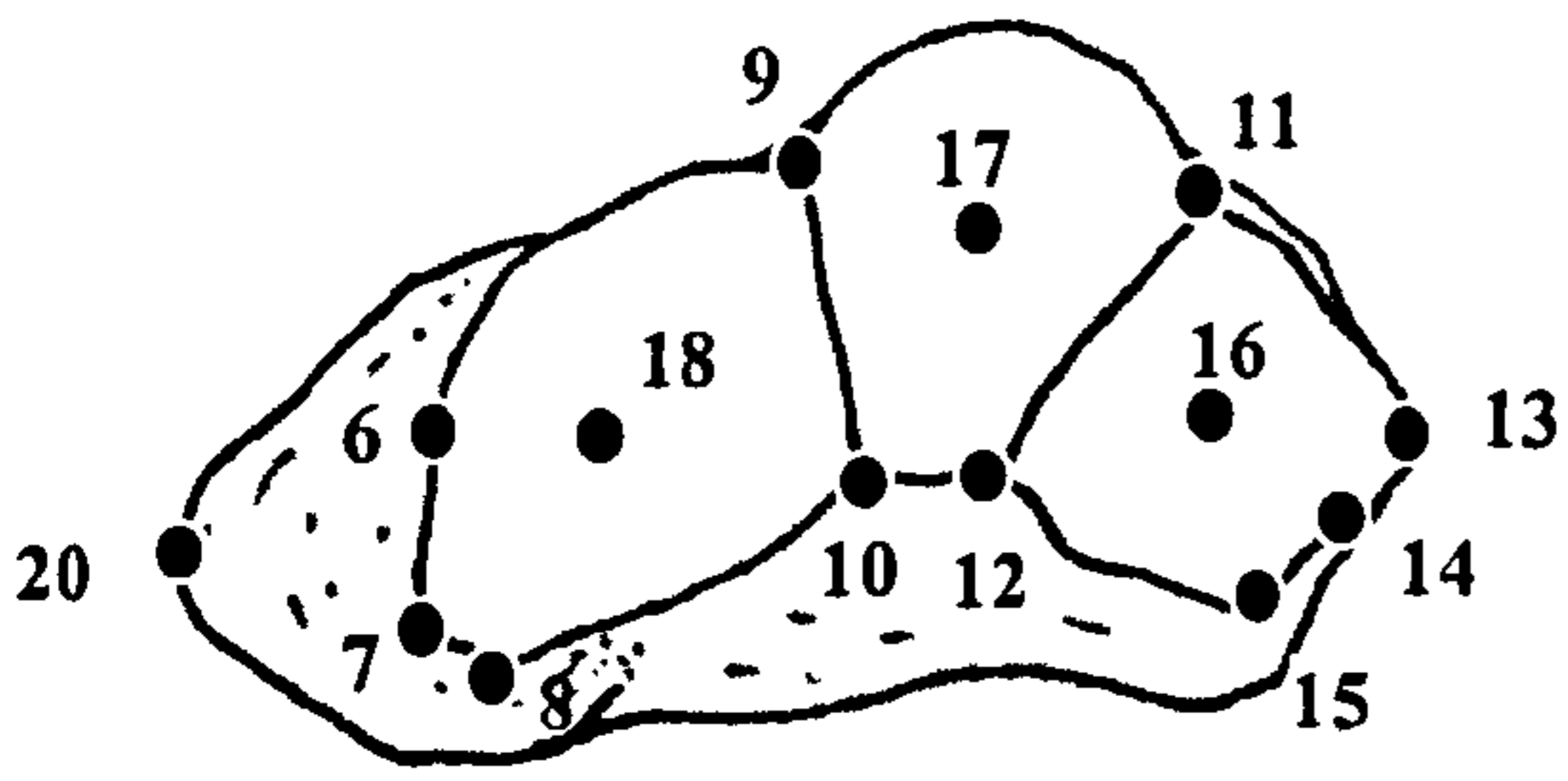
Cuboid:
Medial aspect showing medial facet



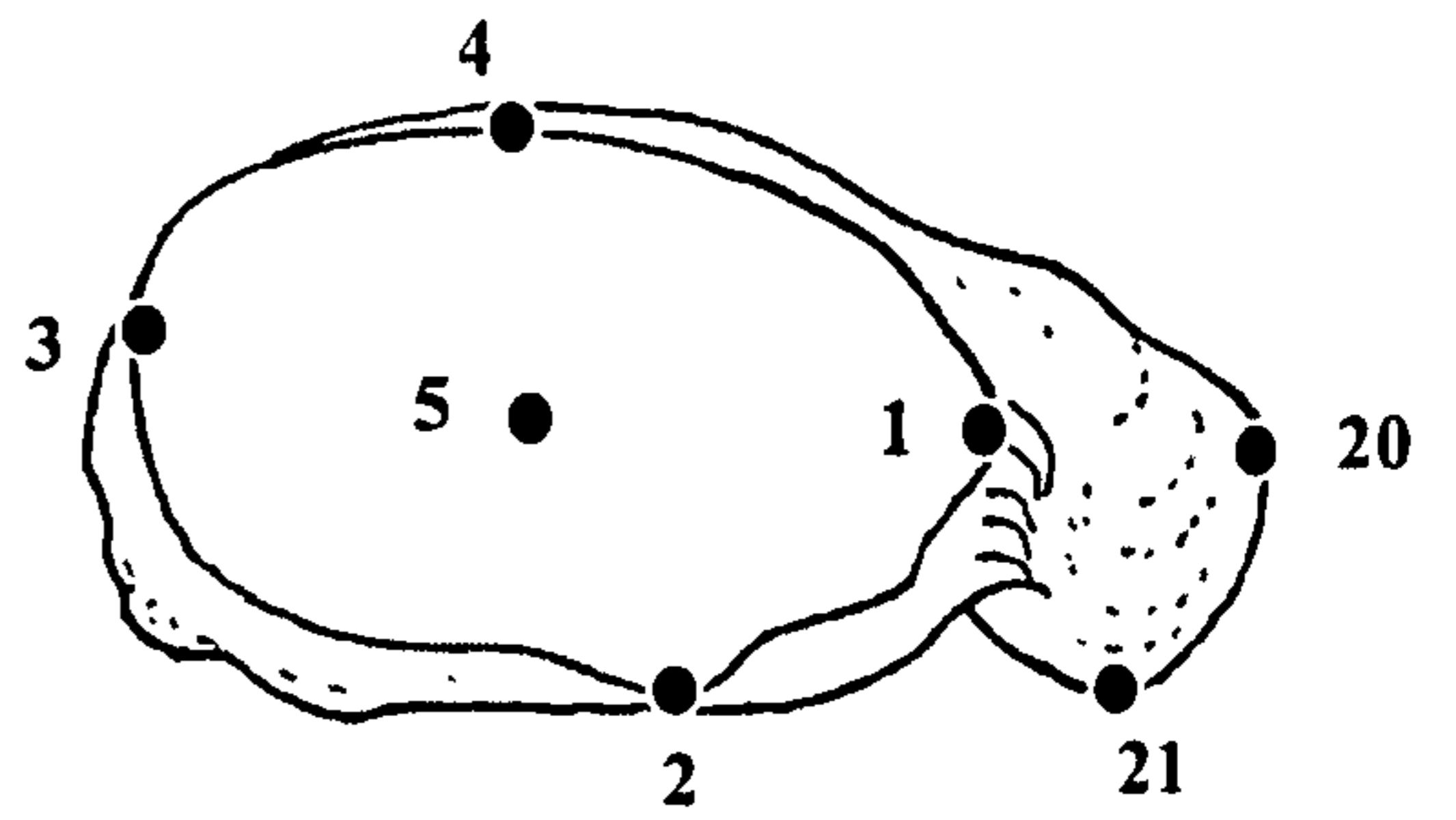
Cuboid:
Dorsal aspect



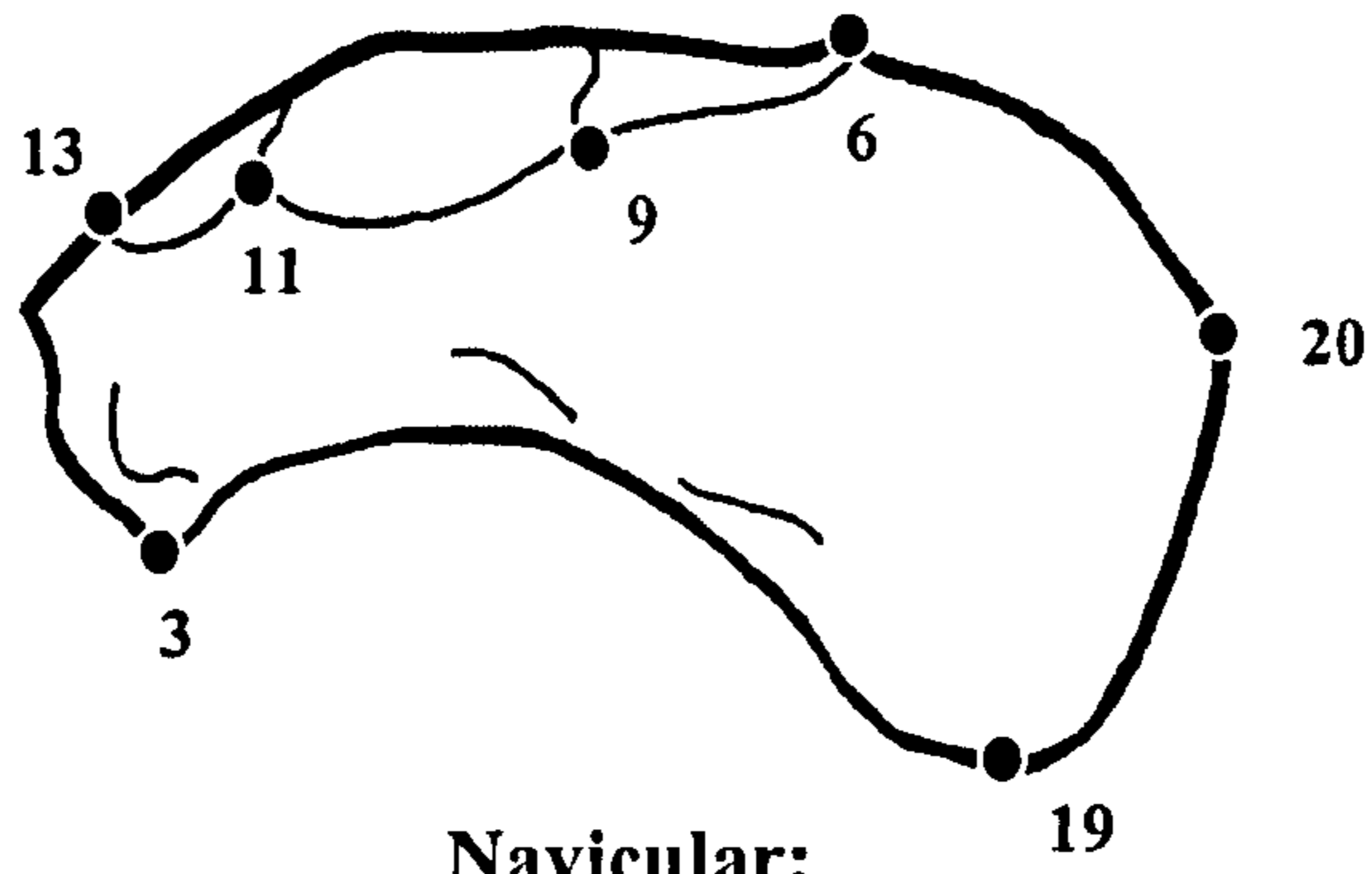
Cuboid:
Proximal aspect



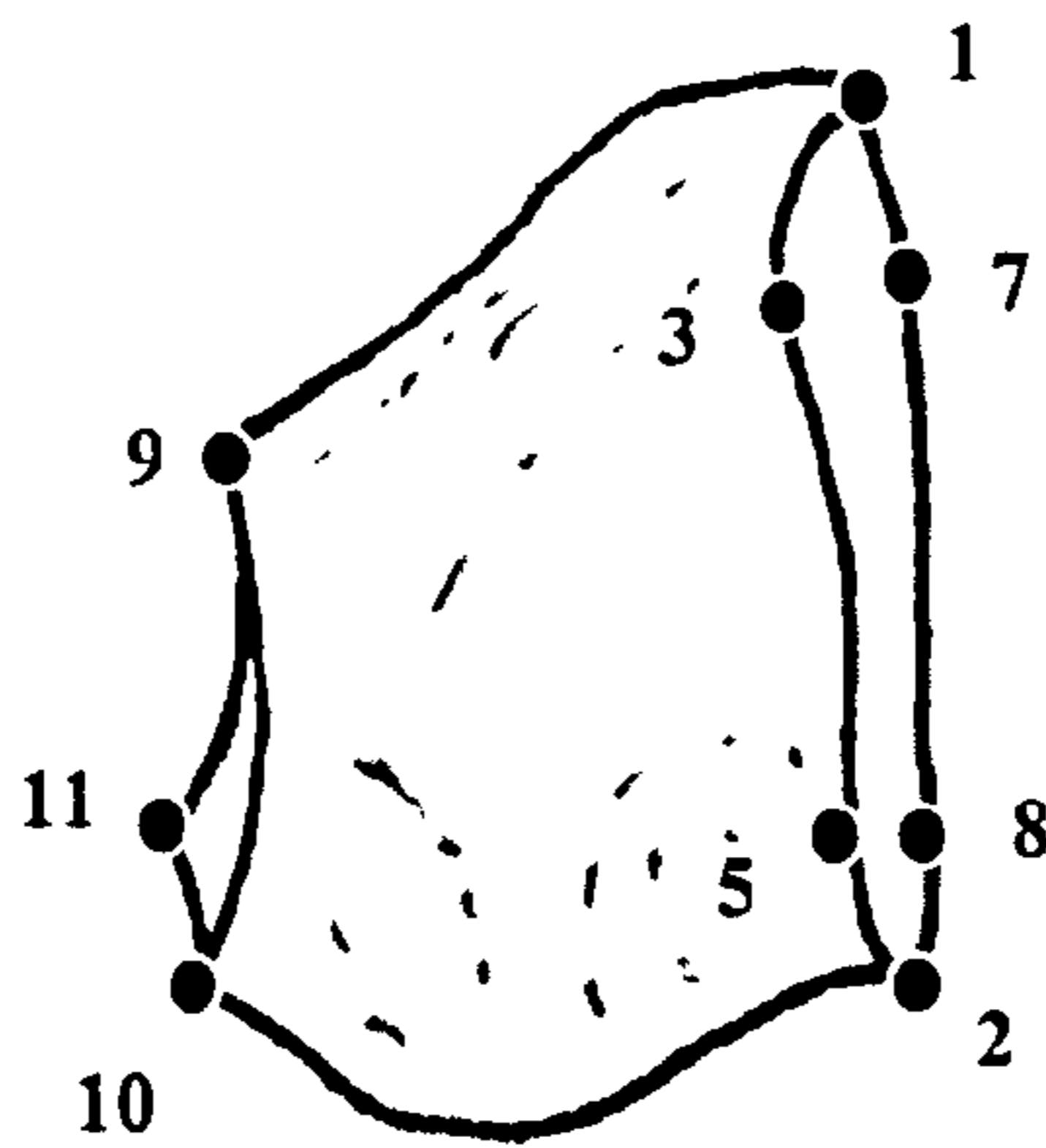
**Navicular:
Distal aspect showing
cuneiform facets**



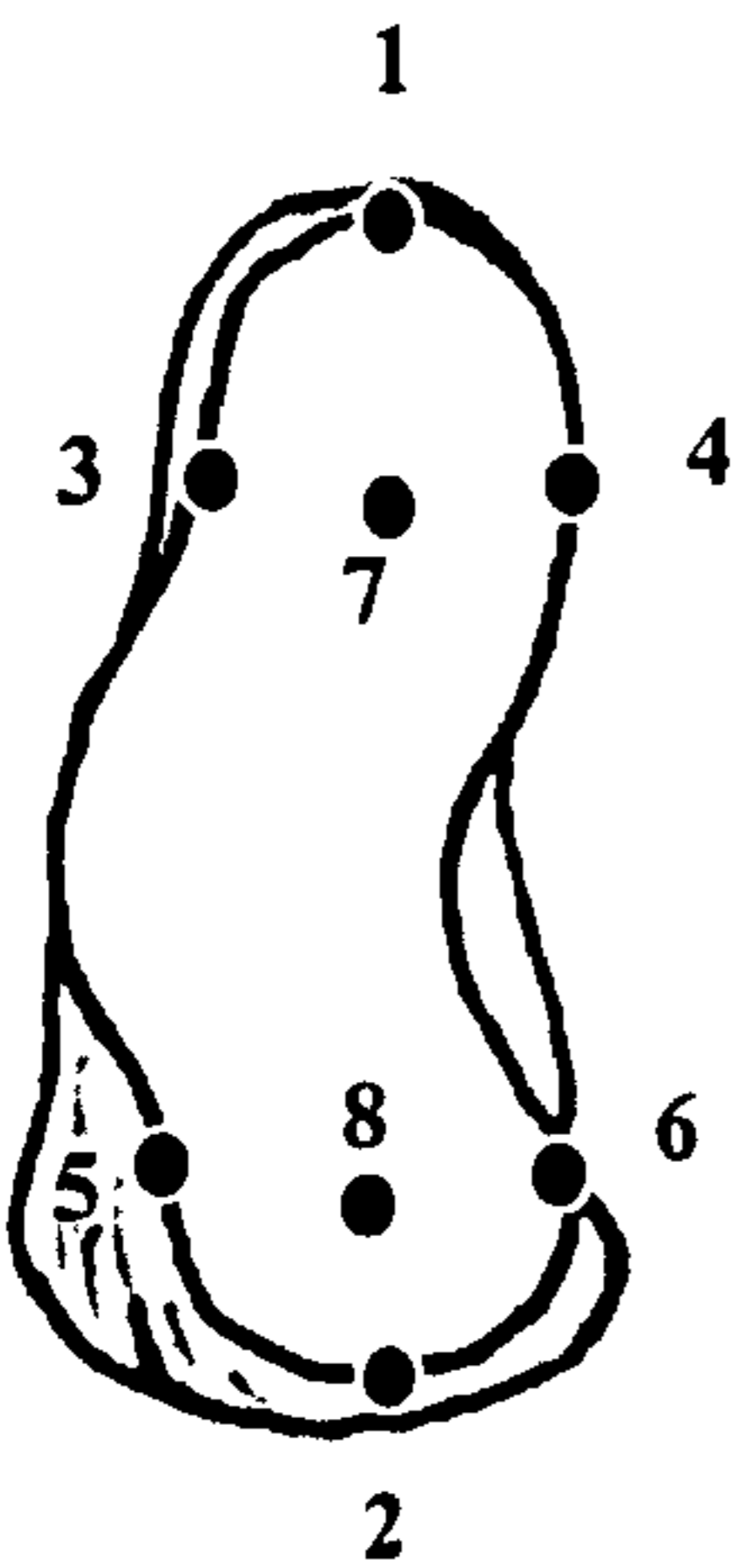
**Navicular:
Proximal aspect showing
talar facet**



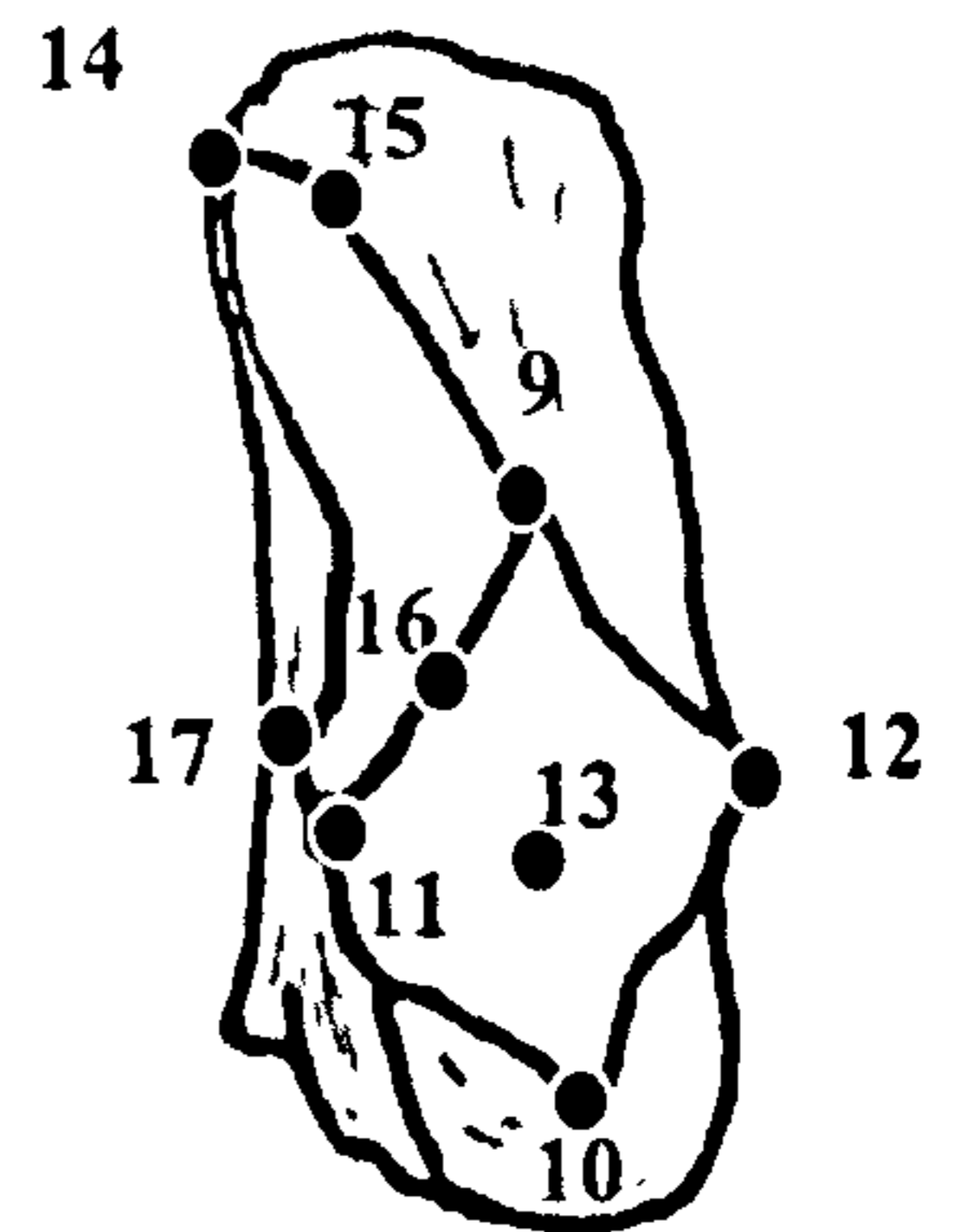
**Navicular:
Dorsal aspect**



**Medial Cuneiform:
Medial aspect**

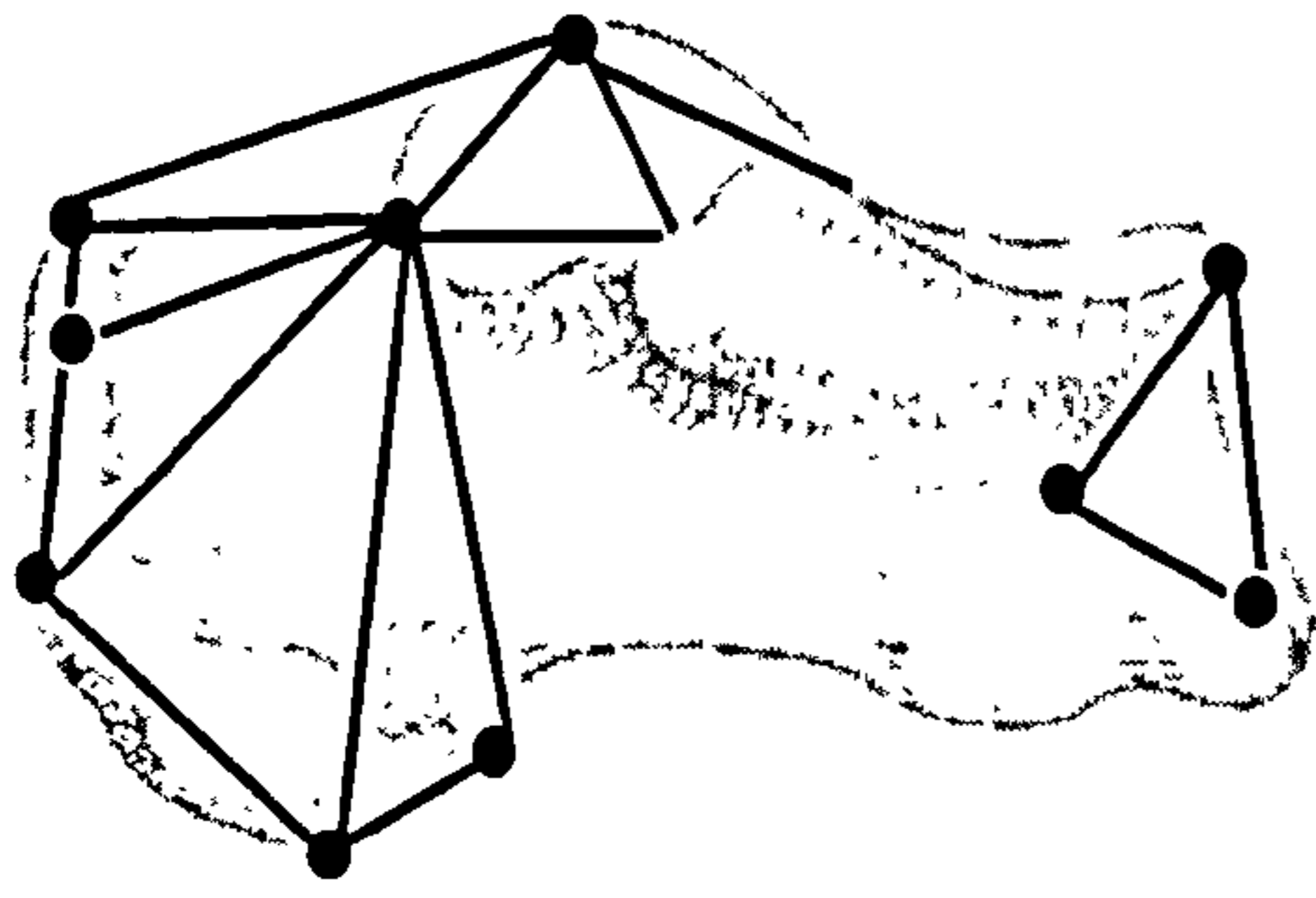


**Medial Cuneiform:
Distal aspect showing
hallucial facet**

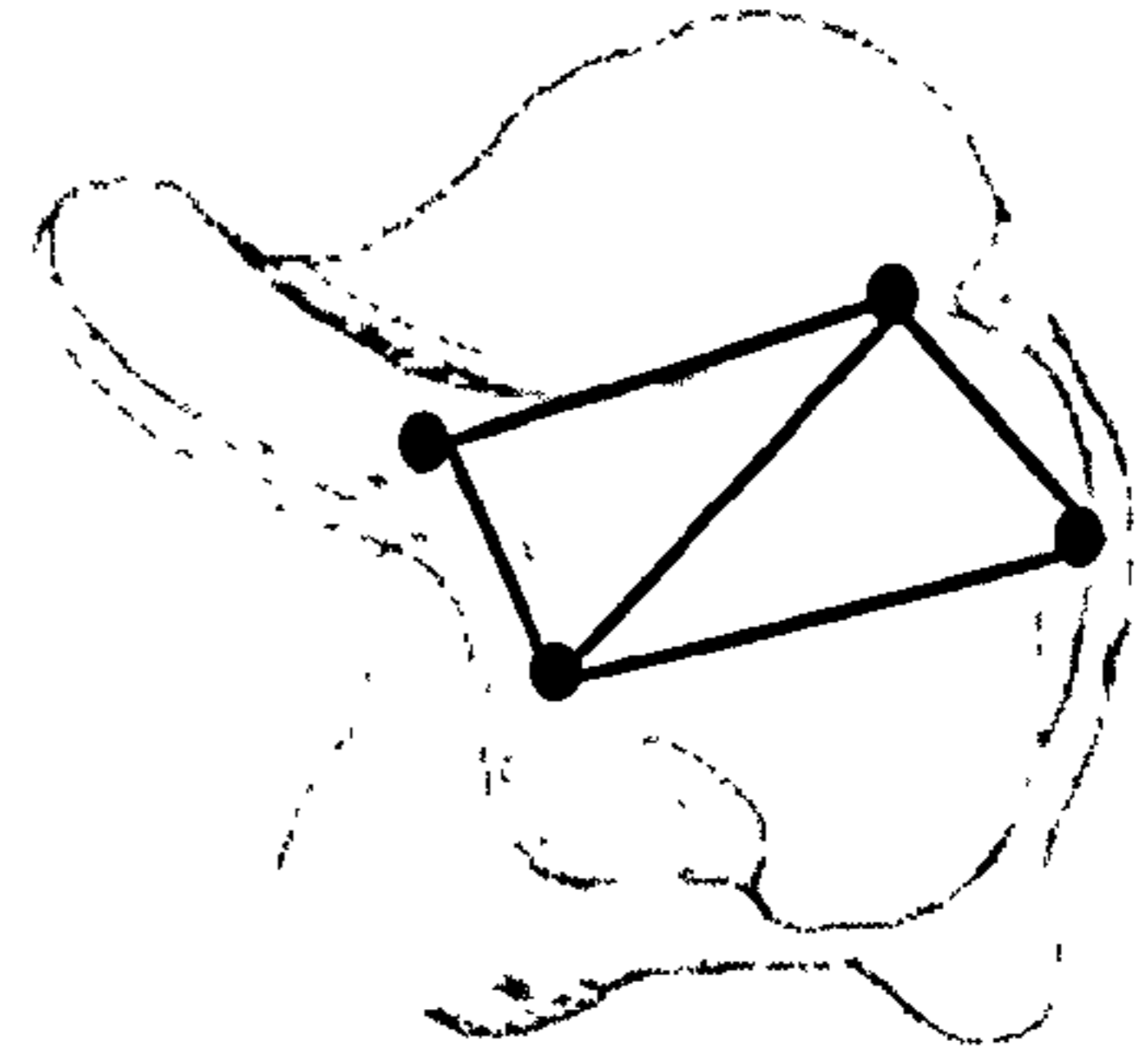


**Medial Cuneiform:
Proximal aspect showing
navicular and intermediate
cuneiform facets**

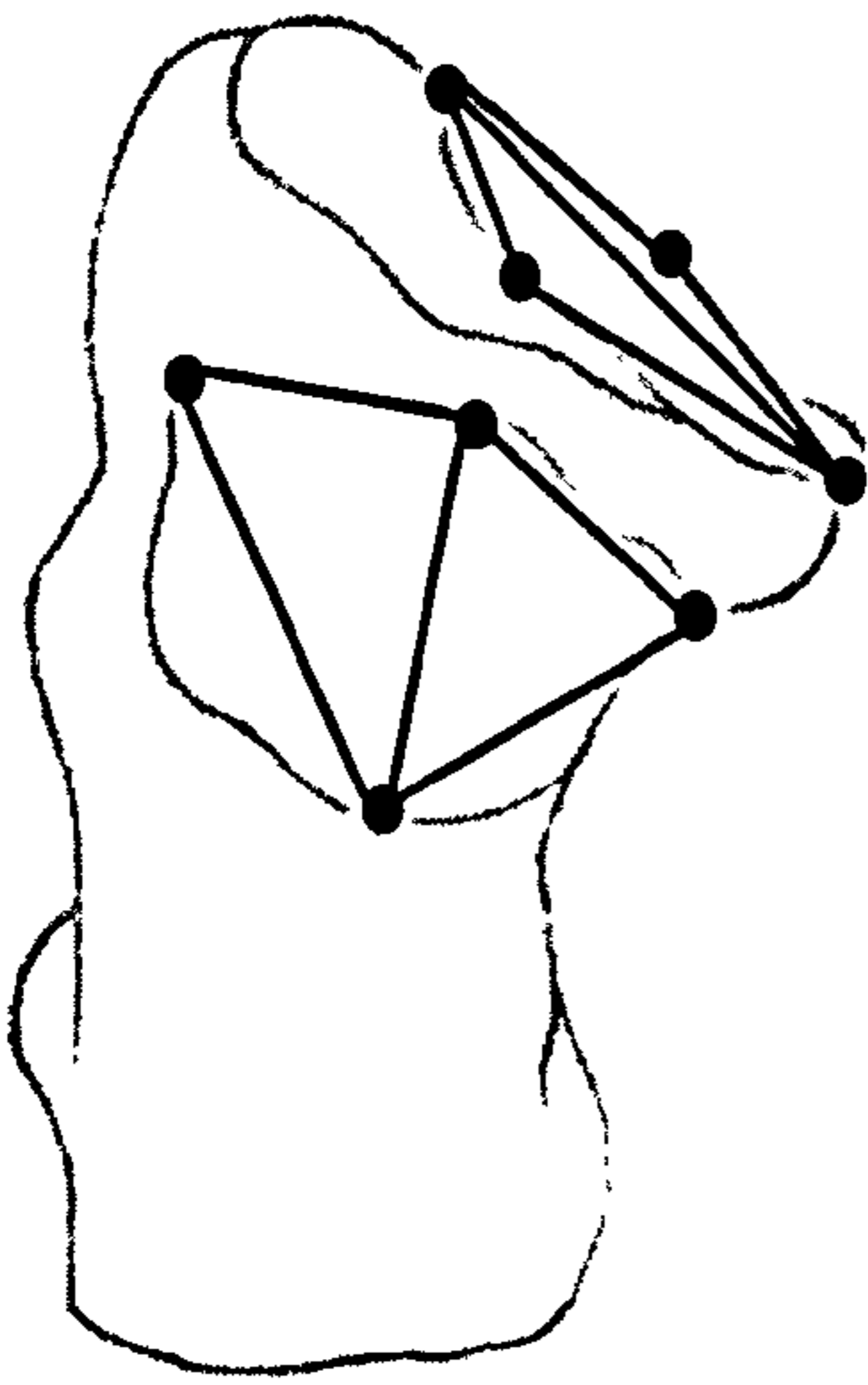
Figure 2.2 Wireframe models



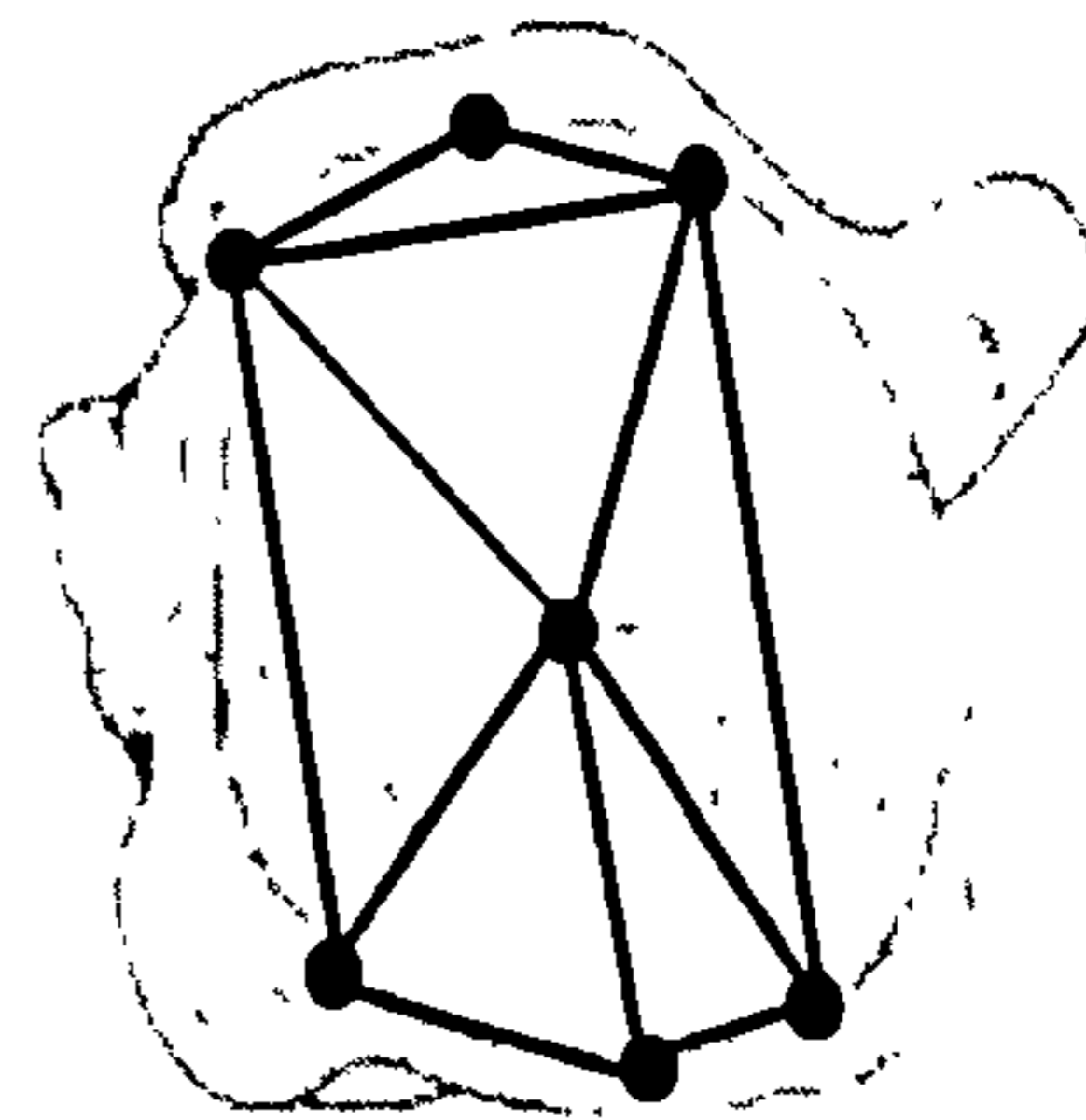
Calcaneus: Medial aspect



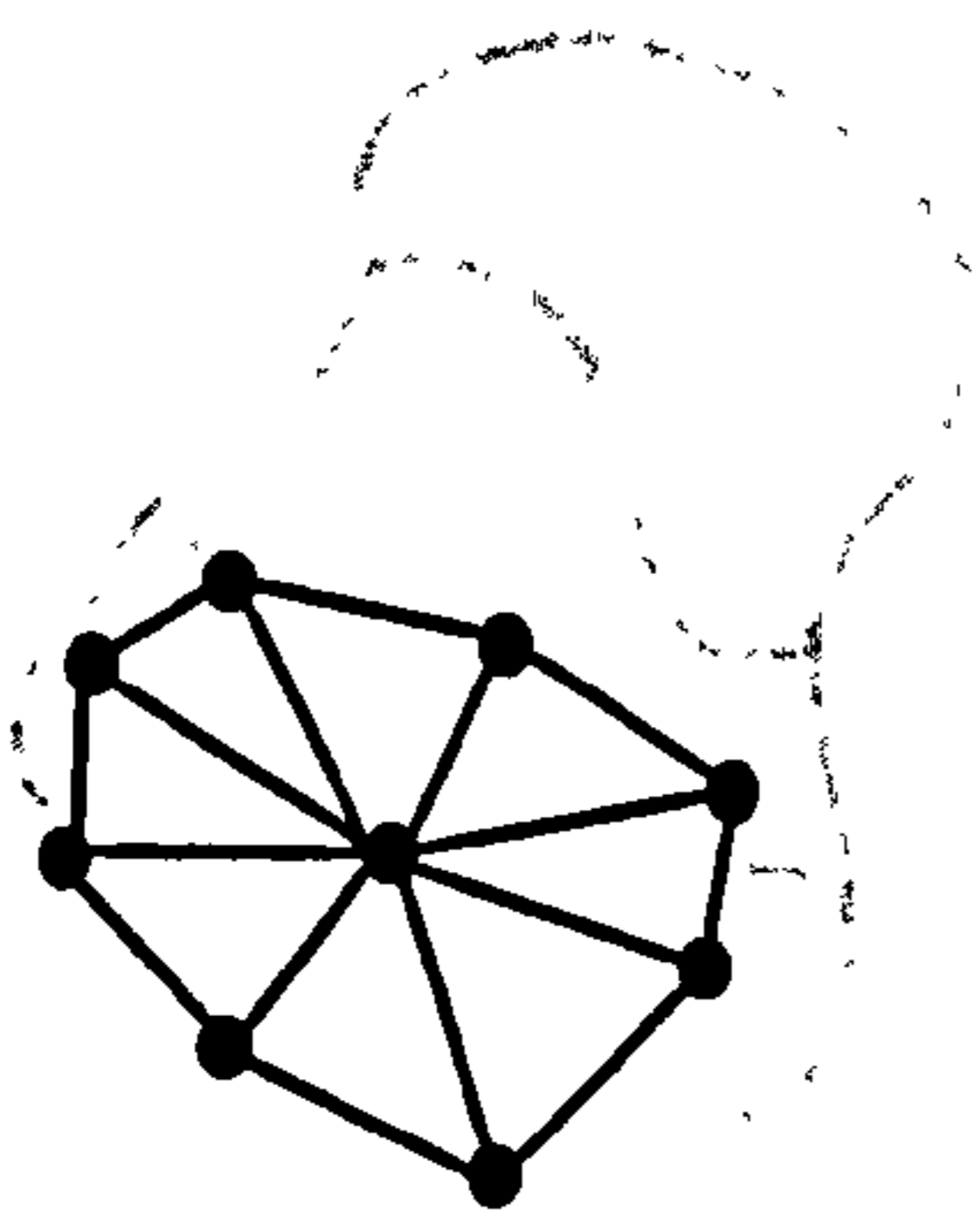
Calcaneus: Cuboid facet



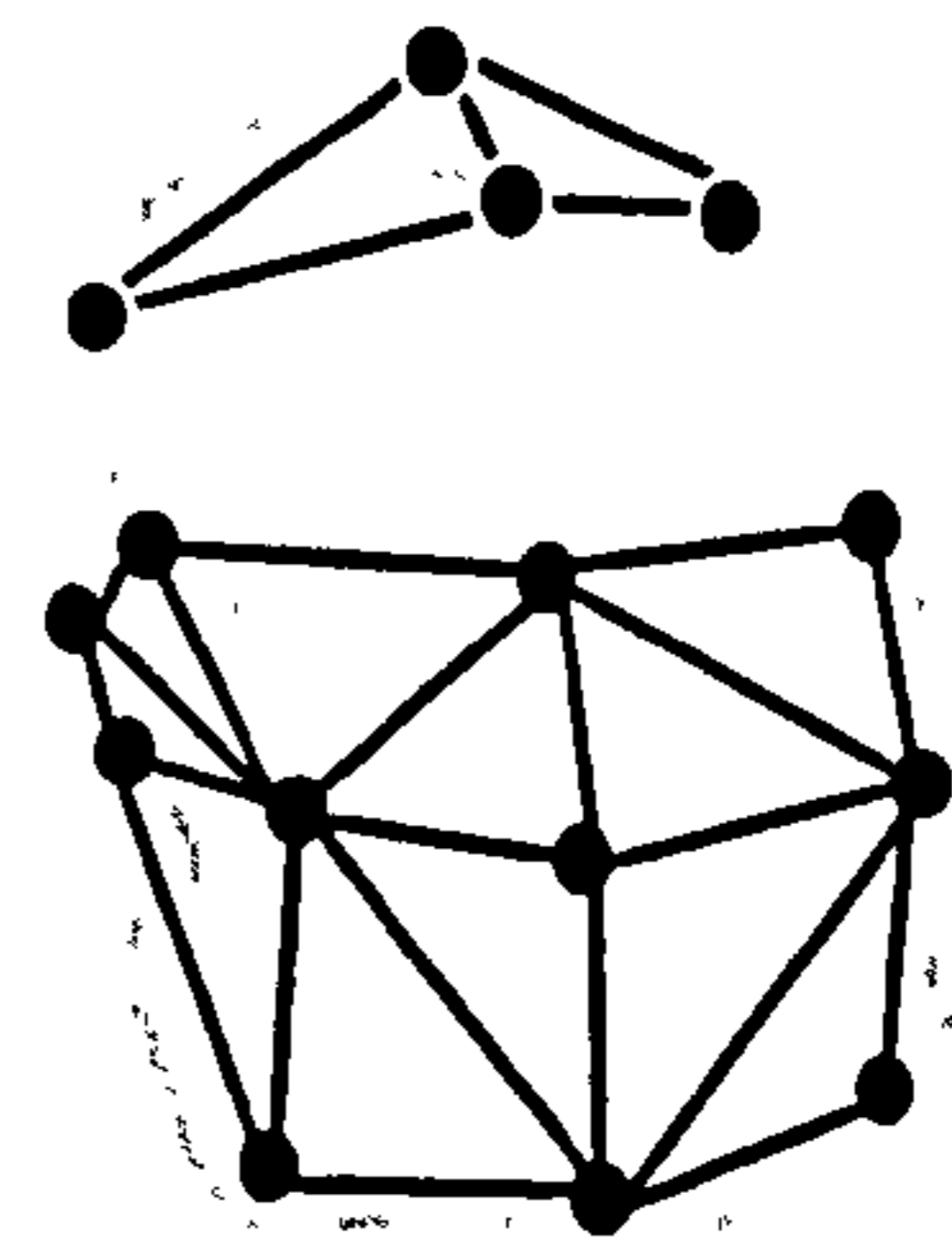
Calcaneus: Talar facets



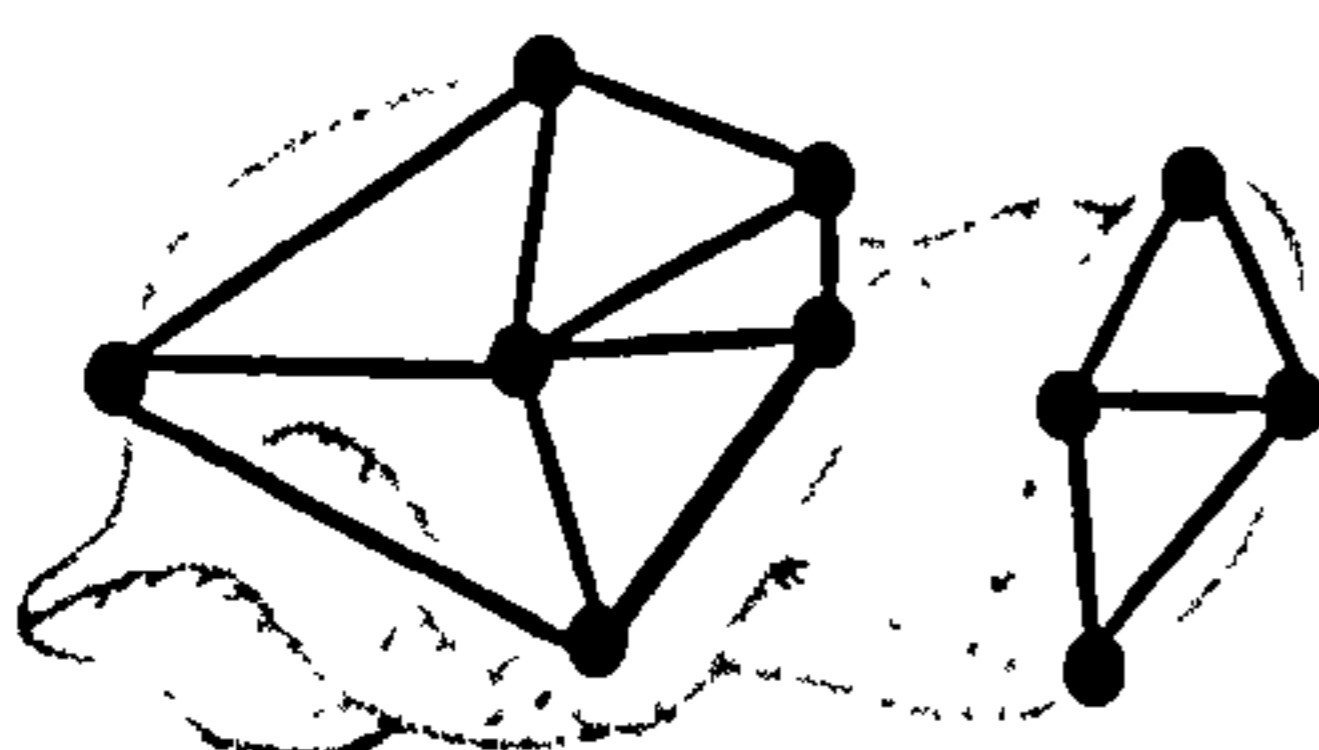
Calcaneus: Proximal aspect



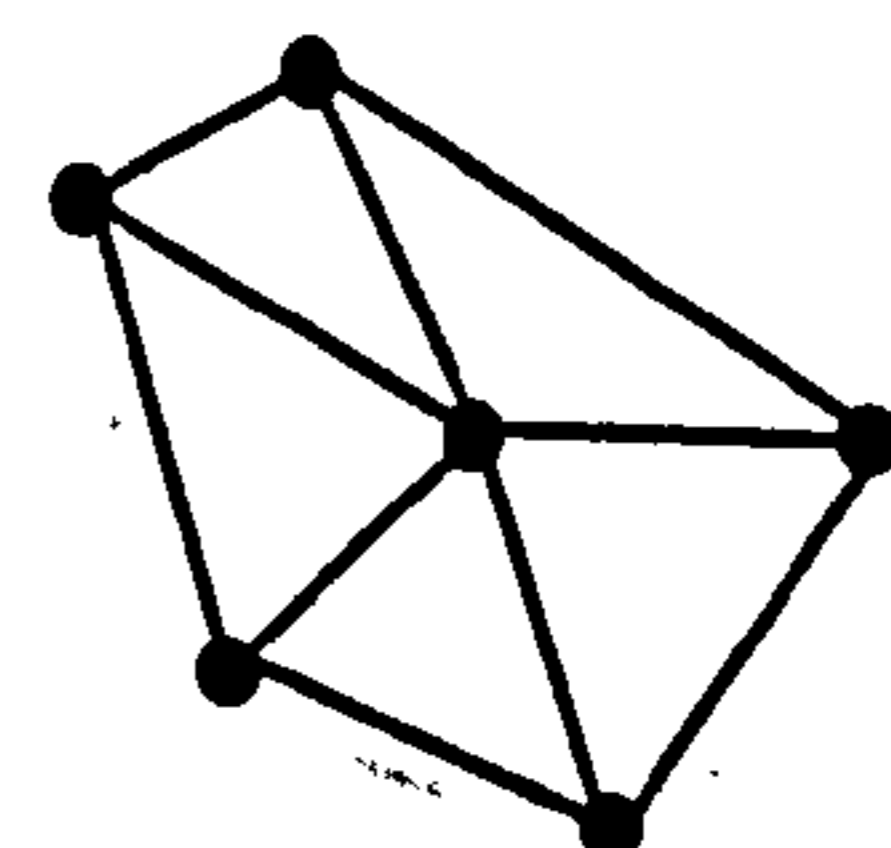
Talus: Calcaneal facet



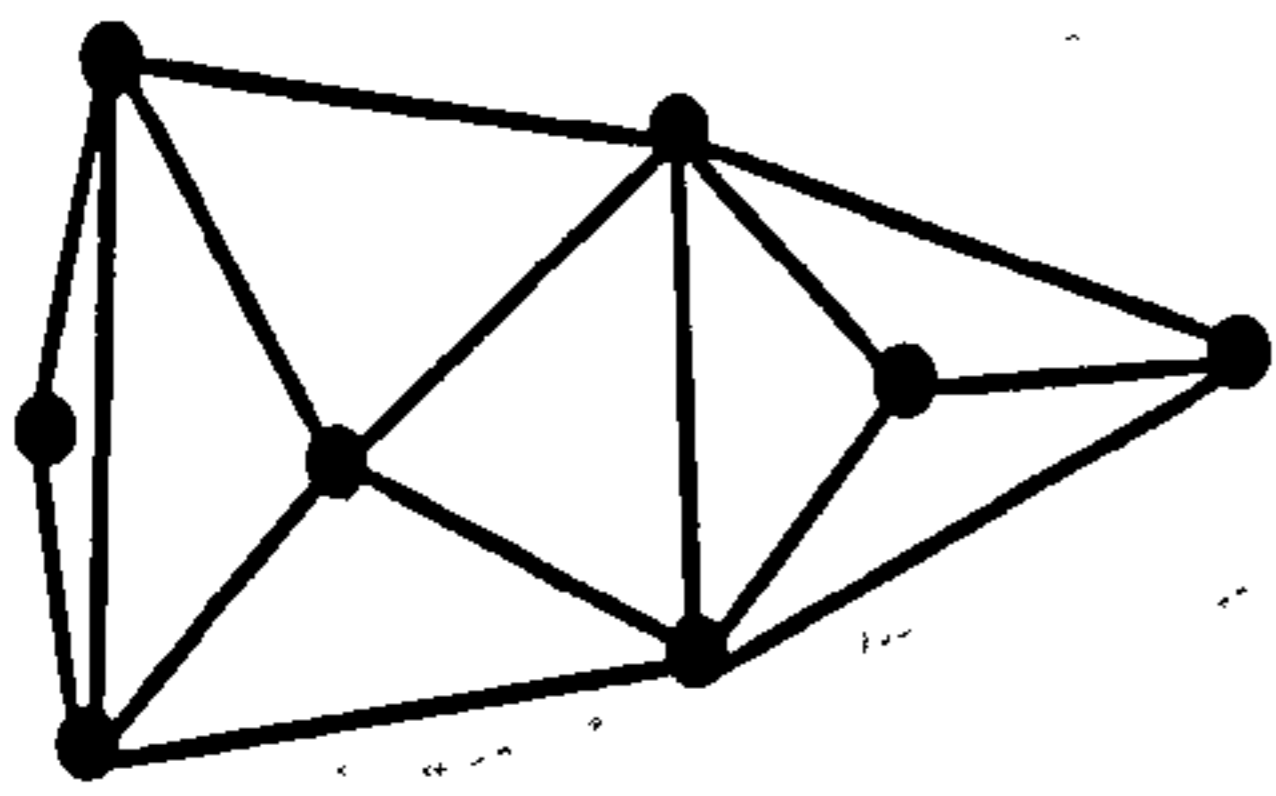
Talus: Trochlea & head



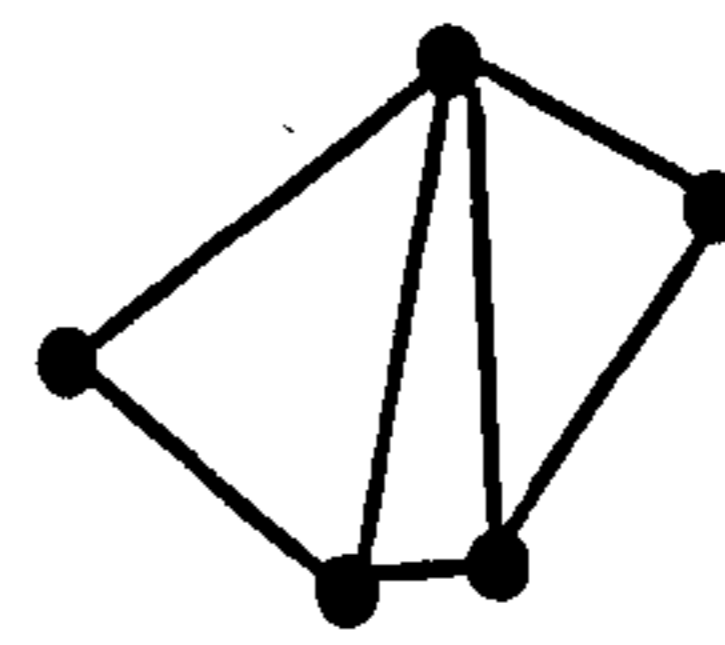
Talus: Lateral aspect



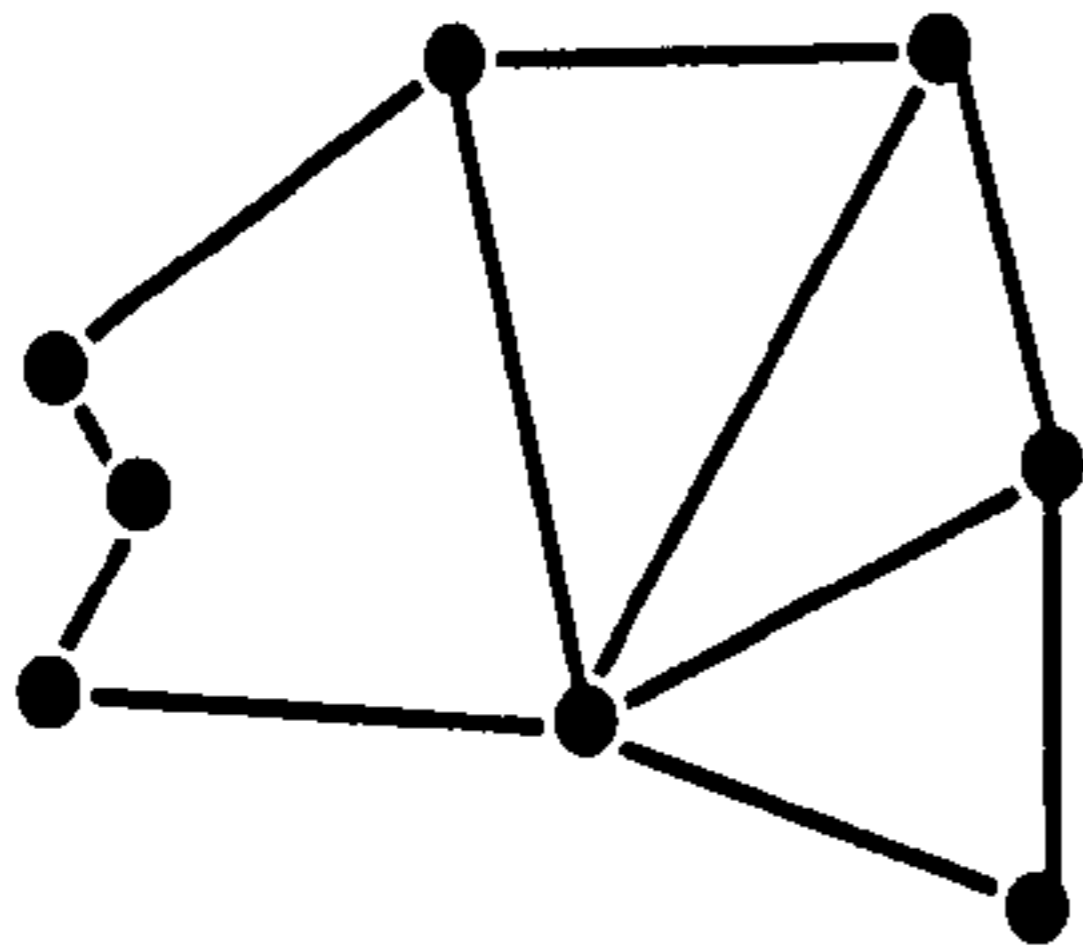
Talus: Head



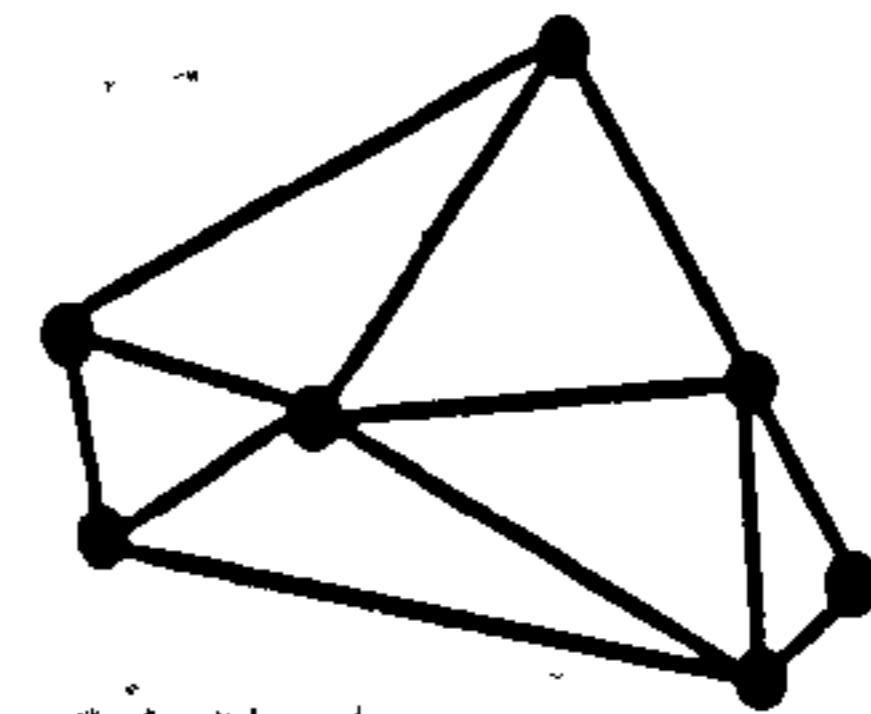
Cuboid: Metatarsal facets



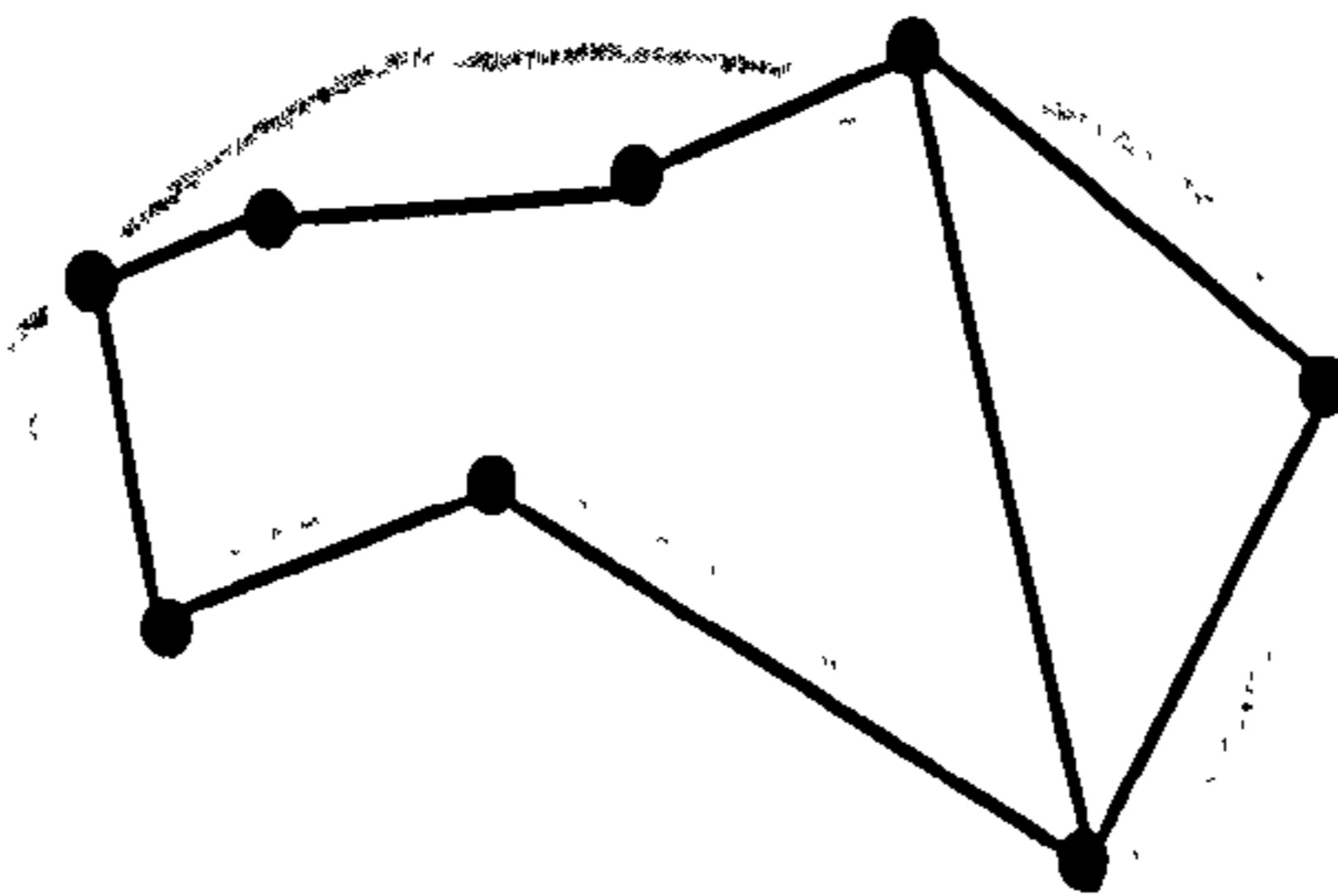
Cuboid: Medial facet



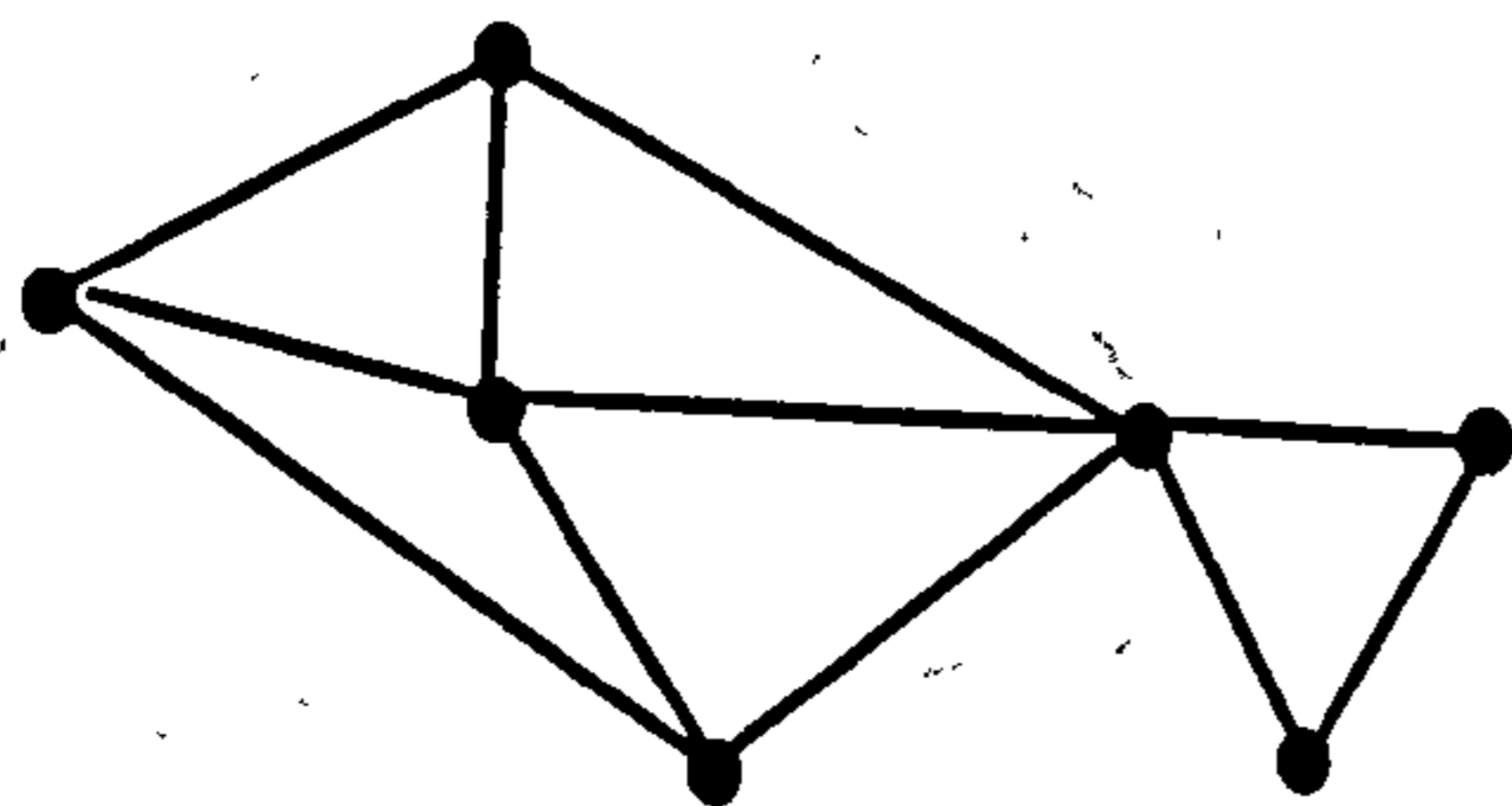
Cuboid: Dorsal aspect



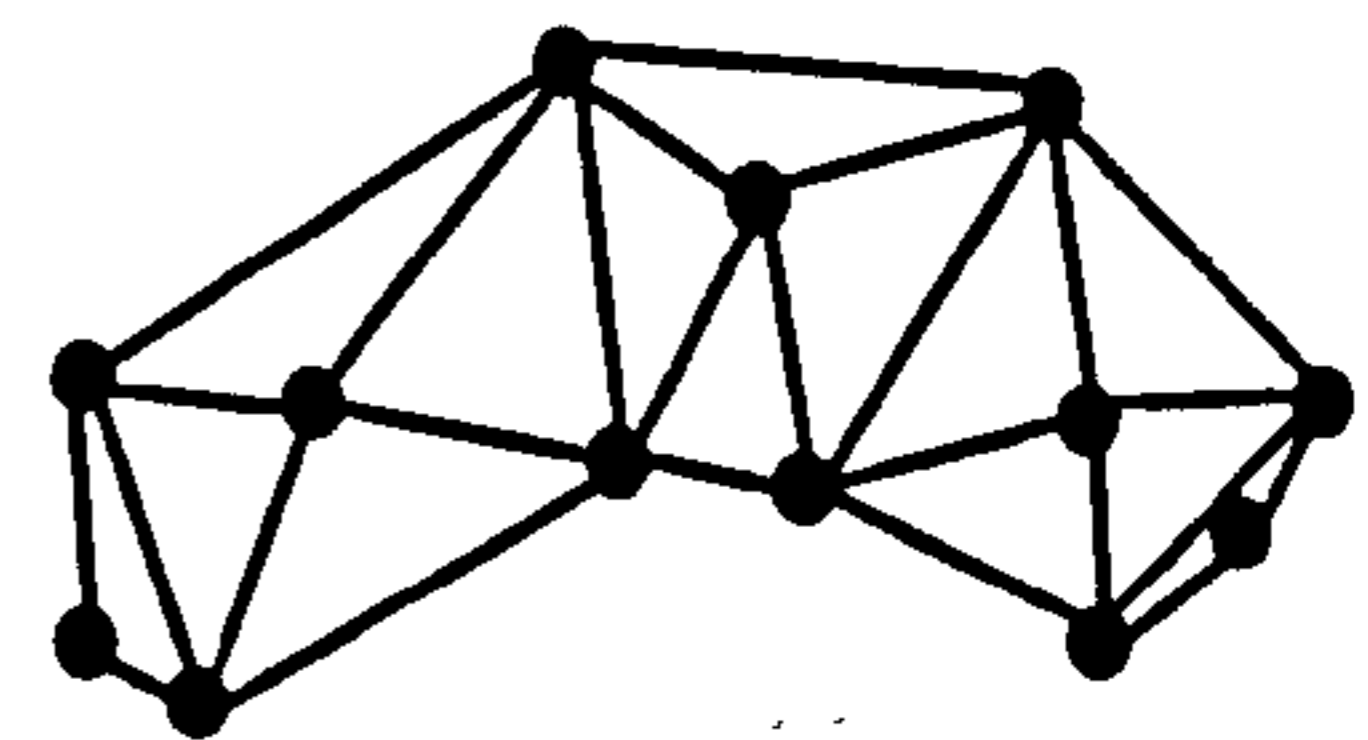
Cuboid: Calcaneal facet



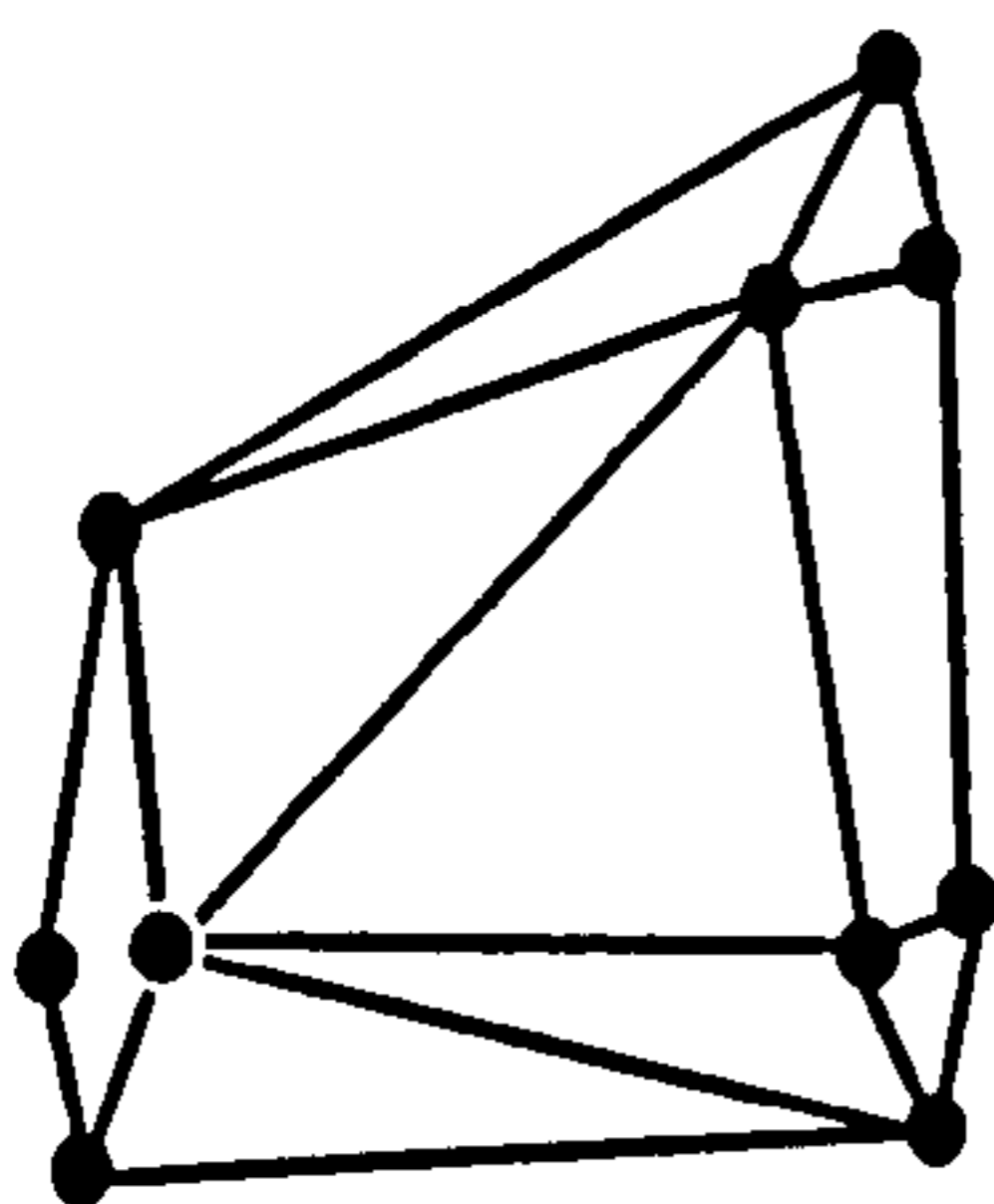
Navicular: Dorsal aspect



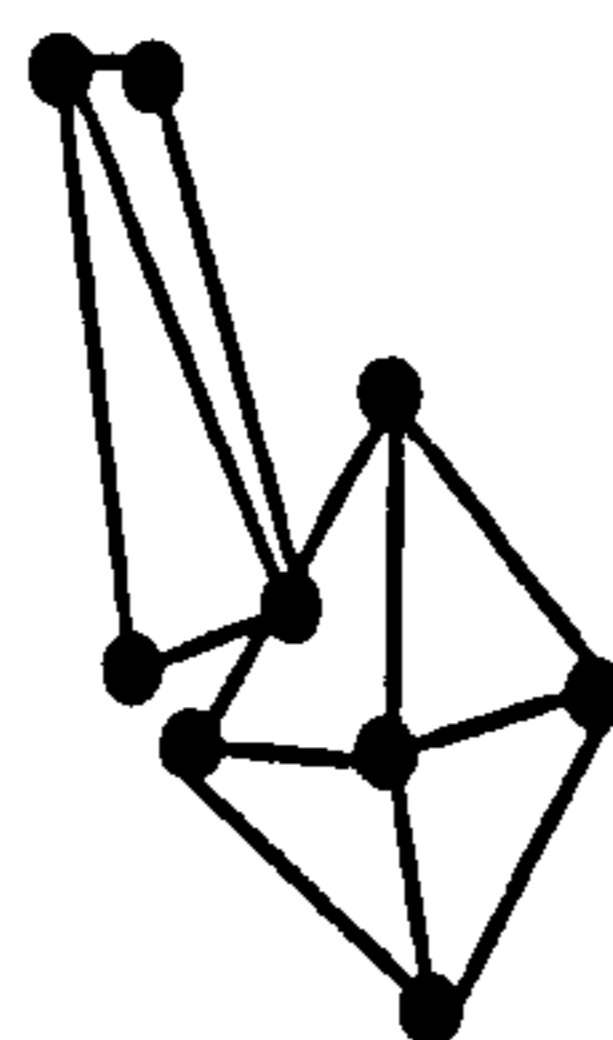
Navicular: Talar facet



Navicular: Cuneiform facets



**Medial Cuneiform:
Medial aspect**



**Medial Cuneiform:
Proximal aspect**



**Medial Cuneiform:
Hallucial facet**

2.2.2 Data collection

3D landmarks were collected using a Microscribe 3DX digitiser (Immersion Corporation, 801 Fox Lane, California 95131, USA). The Microscribe is a digitising arm with five, separate rotating joints. Each joint contains a digital optical sensor, and it is important to note, that unlike earlier digitising systems, these sensors are not affected by external environmental factors such as magnetic fields.

Each bone was placed in a secure device that was clamped to the workbench surface so that it could not move. The device consisted of two horizontal metal arms with rubber cushioned ends (so as to not damage any specimen). The arms were attached to fixed vertical anchors, and could be rotated so as to move towards or away from each other. The arms sat about four inches above the work surface, so that they could secure the specimen away from the work surface so that all sides could be accessed with the digitiser's stylus. The device also ensured that the specimen could not move during measuring. The digitiser was attached to a foot pedal and also to a laptop computer via a serial cable. Each depression of the foot pedal delivered the x, y, z coordinates of the landmark in question to an Excel spreadsheet (© Microsoft corporation), where the data was archived for later analysis.

Error was investigated by the author measuring one dissecting room specimen (a human navicular) ten times, and then combining those ten shapes with forty randomly selected Zulu naviculars from the Dart Collection, South Africa. The combined sample was Procrustes registered, and the PCA of those registered shapes is presented below in Figure 2.3. It can be seen from PC 1 (24.2% of variance) versus PC 2 (11.0% of variance) that the ten repeats form a very tight grouping with each other on both PC axes. The same is the case for the remaining PC axes. It can also be seen that the spread of the ten repeats is considerably smaller than that for the Zulu sample. It can thus be concluded that any error between specimens is considerably smaller than intraspecific differences observed.

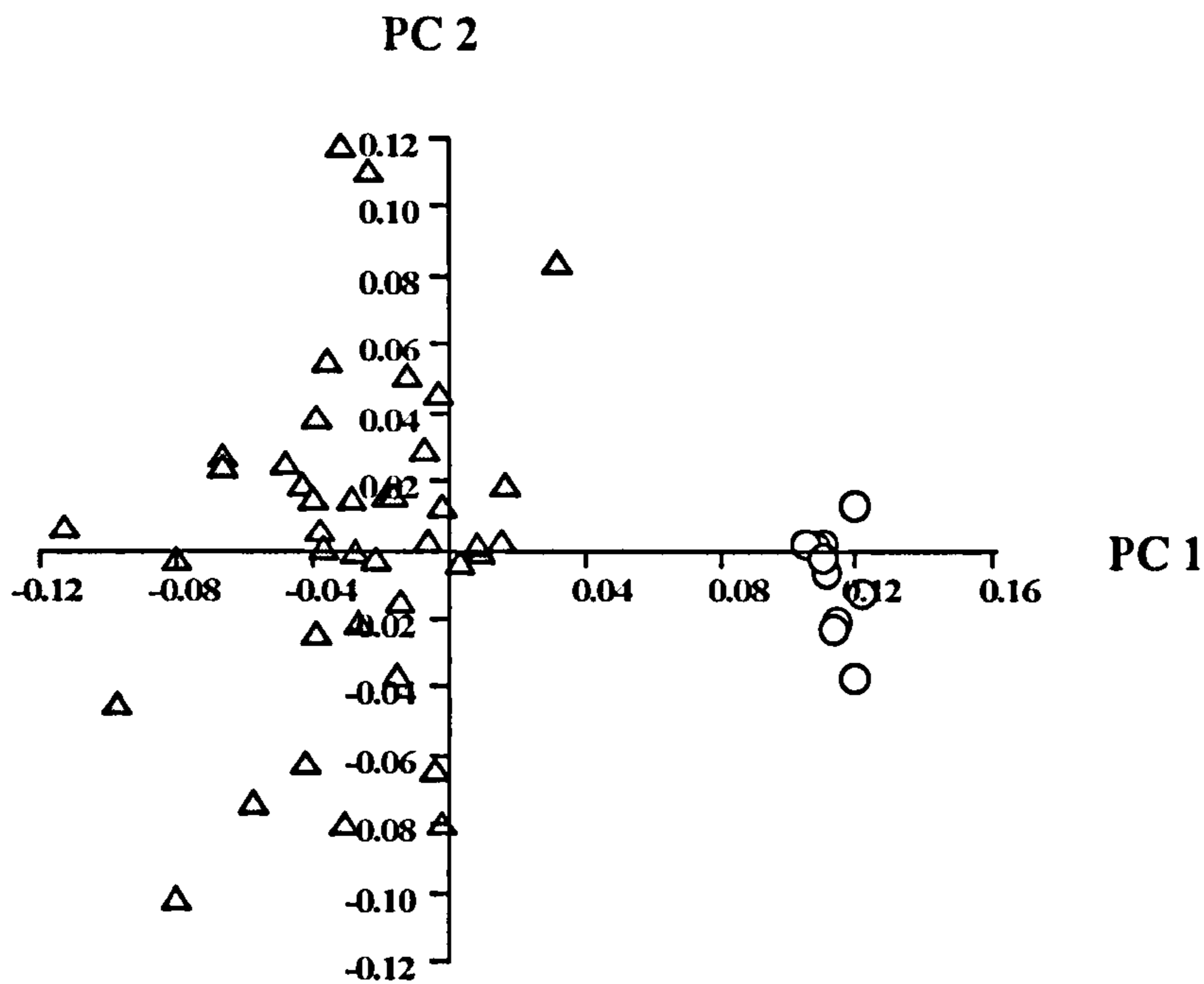


Figure 2.3 Zulu naviculars versus repeats for one dissecting room human navicular. Circles = Dissecting room specimen. Triangles = Zulus.

2.2.3 The issue of size

There is considerable debate over the relationship between body-size and shape in the hominoids. The problem is several fold. There is ambiguity about what “body size” actually refers to, although most studies assume it means body mass (Smith & Jungers, 1997). There is also much debate about what proxies can be used for body size when only skeletal remains exist, as in the fossil record (e.g. McHenry, 1992). Finally there is disagreement about whether body-size proxies should be functionally related to body mass itself, e.g. taken from a weight-bearing limb (Ruff *et al.*, 1997) or independent of it (Smith, 1993).

An alternative is to examine the relationship between actual bone size and bone shape. Parts of this study *are* concerned with exploring the relationship between bone size and shape, since if size related shape-change can be ruled out, then other factors, such as function, can be used to explain shape differences between taxa. When studying form based on landmark data, *centroid size* is considered to be the only measure of size that is independent of shape (Dryden & Mardia, 1998), and it also has the added benefit of being directly computed from the landmark configuration being analysed rather than more arbitrary proxies for size (e.g. body mass or femoral head breadth).

As such, centroid size is used in this study to explore the relationship between size and shape (as determined by PC axes). Further discussion of centroid size is presented below.

2.2.4 Analysis of landmark data

2.2.4.1 Background

As discussed at the start of Chapter 1, the commonest way of quantifying form in physical anthropology has been to use interlandmark distances (*ilds*) and angles. However, these are two dimensional measurements being used to quantify three-dimensional form. If one wants to comment on the differences between taxa based on specific measurements, such as the relative flexion of the cranial base, then using these sorts of two-dimensional measurements is reasonable and entirely appropriate. However, if one is interested in commenting on the overall form (i.e. size and shape) differences between taxa, or the relationship between overall size and overall shape, then three dimensional approaches greatly increase the resolution of any analysis. The only way that ilds can truly provide full information on 3D geometry is if all possible combination of distances are measured for the landmarks chosen. This is essentially the approach that Euclidian Distance Matrix Analysis (EDMA) uses. However, there are a number of problems with EDMA that are discussed in the next section

2.2.4.2 Recent approaches

2.2.4.2.1 EDMA

EDMA (Lele, 1993) uses interlandmark distances to describe form. As discussed above, the technique is based on all possible combinations of interlandmark distances taken on an object. As such, the resultant matrix (known as the *form matrix*) will accurately reflect that object's 3D form (Lele & Richtsmeier, 1991; Lele, 1993). The number of ilds required to satisfy this is $(k(k-1)/2)$ for k landmarks. With complex biological structures, this can result in very large matrices of interlandmark distances. Form difference between two specimens is calculated by computing the ratio between each equivalent interlandmark distance. If two groups are to be compared, then mean form matrices for each group are computed from each set of individual matrices, and these are then compared pairwise through a separate matrix of ratios (called the *form difference matrix*). One of the limitations of EDMA is that comparisons between

individuals or group means can only be pairwise. It is argued that one of the major benefits of the technique is that it avoids the problems of registration (i.e. translational and rotational differences are not “nuisance” factors) (Richtsmeier et al., 1992). However, it has been noted that it is extremely difficult to visualise shape-change using EDMA, and that the form difference matrix is hard to interpret (Dryden & Mardia, 1998; O'Higgins, 2000; Cobb, 2001). There is considerable debate about the relative merits of superimposition techniques versus distance-based techniques (such as EDMA), and this debate has been furthered by recent studies showing that EDMA has a higher level of error than other forms of shape analysis (Rholff, 2000, 2002). When estimating means and in detecting significant differences, perhaps the best conclusion about EDMA is that it is a suitable technique if a researcher is interested in the differences between two individuals or two group means estimated using large sample sizes, where a few, specific interlandmark distances are used, but is less suitable if one is concerned with patterns of overall form variation within or between moderate sample sizes taken from one or more populations (Dryden & Mardia, 1998).

2.2.4.2.2 Superimposition

An alternative method of analysing form is to superimpose landmark configurations, and then explore the relative deviation of equivalent landmarks to explain changes in shape. There are two major problems that arise if objects are to be superimposed in an appropriate fashion. The first is how to remove “nuisance” factors. These are rotational and translational differences between each landmark configuration that arise out of differing positions between each object measured and the base position on the digitiser. In order to efficiently observe shape-change, it is imperative that these factors are removed. The process of this removal is known as *registration*. If one is concerned with strictly analysing shape, rather than form (size *and* shape) then size can also be considered as a “nuisance” factor.

The second problem is how to actually superimpose landmark configurations. A recent review of the various approaches to this (O'Higgins *et al.*, 2001) concludes that there are three predominant methods: 1). Registering shapes to a common baseline, such as Bookstein's 2-point registration (Bookstein, 1984). 2). Using a resistant or robust fit, where the majority of landmarks are used, but those that cause relatively large scale deviation are omitted (Siegal & Benson, 1982). 3). Registration by

minimising the sum of the squared distances between equivalent landmarks for all forms. This last technique is known as Generalised Procrustes Analysis (GPA) (Gower, 1975; Rohlf & Slice, 1990; Goodall, 1991).

GPA has a number of advantages, but its principal benefits are twofold. Firstly, following GPA registration, the landmark configurations are represented in a shape space that is statistically well understood (O'Higgins *et al.*, 2001; Rohlf, 2002). This is known as Kendall's shape space (Kendall, 1984) and is described later on in this chapter. Secondly, all landmarks are considered equal to each other in terms of registration. That is to say, all landmarks are used in the registration process. If, as an alternative, one were to superimpose two objects using a particular region of those objects, then the points in that region will inevitably deviate less from each other than would be the case for points further away from that region. The major assumption here is that the region of registration is somehow less subject to change than other regions. In terms of biology, this assumption need not hold. GPA avoids such assumptions in a way that the other techniques do not (O'Higgins *et al.*, 2001), and it is thus the method of registration that is used in this study. Further benefits of GPA are that it estimates means well, even with small to moderate sample sizes, and leads to statistical approaches that are powerful in testing for shape differences.

2.2.4.3 How GPA works

GPA works in a number of steps. Firstly size is removed, and this is followed by the removal of rotational and translational differences. Size is eliminated in two steps. First of all centroid size, which is statistically independent of the shape of a landmark configuration (Dryden & Mardia, 1998; O'Higgins & Jones, 1998), is calculated. Centroid size is the square root of the sum of the squared Euclidian distances from each landmark to the centroid. Squaring and then square rooting eliminates any negative values. The centroid is described as being the mean of all landmark coordinates for a shape, i.e. it is $(\bar{x}, \bar{y}, \bar{z})$ (O'Higgins & Jones, 1998). The x , y and z values for each co-ordinate are then, separately, divided by centroid size. This leads to new x , y and z values where size has been removed, and each shape is at unit size (i.e. centroid size = 1). The following equation summarises this process:

$$S(X) = \sqrt{\sum_{i=1}^k \sum_{j=1}^m (X_{ij} - \bar{X}_j)^2}$$

$S(X)$ is centroid size. X is a matrix of $k \times m$ Cartesian coordinates, with k landmarks and m real dimensions. X has i, j th elements X_{ij} , and \bar{X} is an $m \times 1$ matrix of mean coordinates representing the centroid, and has j th element \bar{X}_j . The centroids for all the shapes are then superimposed onto that of the first specimen, and this is then followed by each configuration of landmarks undergoing repeated least squares fitting of shapes to estimates of the mean until the fit can no longer be improved, so that the distances between them are minimised. This removes translational and rotational differences respectively. The distance between each equivalent landmark (i.e. that that is minimised) is known as the Procrustes chord distance (d^2). The following equation summarises how this distance is calculated:

$$d^2 = \sum_{i=1}^n \sum_{j=i+1}^n (X'_i - X'_j)^2$$

The number of individuals is represented by n . Each individual is represented by a $k \times m$ matrix (where k is the number of landmarks and m the number of real dimensions), of landmark coordinates, X_i , where $i = 1, \dots, n$. X'_i represents the registered landmark coordinates.

2.2.4.4 Statistical analysis of registered forms

GPA results in each set of landmarks being represented as points in a shape space known as Kendall's shape space (Kendall, 1984), which has a reduced dimensionality. Thus GPA removes translational (m), rotational ($m(m-1)/2$) and scaling (1 dimension) differences, resulting in a shape space of $km - m - (m(m-1)/2) - 1$ dimensions. The problem with this space is that it is non-Euclidean (it is curved), which makes it difficult to statistically analyse. However, it is possible, if there is little variation in relation to all possible configurations of the landmarks, to project the data points from Kendall's shape space into a linear tangent space (Dryden & Mardia, 1998; O'Higgins & Jones, 1998). The assumption about there being a relatively small amount of variation is usually acceptable when dealing with biological specimens,

since the space takes into account all possible landmark combinations, and biological specimens are likely to only occupy a highly restricted part of that shape space. The tangent space projection then makes it possible to explore the statistical relationship between different specimens using standard multivariate techniques such as principal components analysis.

2.2.4.5 Principal Components Analysis

Principal components analysis (PCA) is a multivariate statistical technique designed to represent relationships among sets of variables in as parsimonious a way as possible. If one were to imagine, for a given set of variables, the sample of specimens forming a cloud of points in a multidimensional space, then information about the relative relationships between specimens in the cloud would be extremely useful, since it would help to show how the different specimens are related to each other. PCA effectively summarises this information by producing factors, or “principal components”, which can be considered as classificatory axes. The first component, or axis, usually provides the majority of the information concerning the distribution of specimens (i.e. it accounts for the largest amount of variance). The second component provides the next largest amount, the third component, and so on. The second and subsequent principal components are orthogonal (at right angles) to the first and each other. Although there are as many principal components as there are variables when the number of specimens exceed the number of variables, the benefit of this statistical technique is that the majority of the information about the different biological groups can usually be summarised by the first few components (Norušis, 1994; Kinnear & Gray, 1995).

2.2.4.6 Thin Plate Splines

One way of exploring the relative positions of landmarks between individuals or groups is to use thin plate splines (TPS). The TPS is essentially a version of the Cartesian transformation grid as first described by Thompson (1917). The concept behind such an approach is that the difference in shape between two objects can be explored by superimposing a rectangular grid over one object (the reference shape) and then distorting that object until it is the shape of the second object (the target shape) and seeing how the grid becomes deformed. This deformation is registration free, and provides information about both size and shape change (Bookstein, 1989).

2.2.4.7 Visualisation

One useful way to study shape change is through visualisation. GPA preserves the landmark geometry of a shape, so, theoretically, the mean shape can be constructed (i.e. the shape at the centroid) and this corresponds to the zero point on the x and y axes. A hypothetical shape at any point along a PC axis can then be constructed using the following equation:

$$X_h = X_{\text{mean}} + c\gamma$$

Where X_h is the hypothetical shape, X_{mean} the mean shape, c the PC score of the hypothetical shape in question on the relevant axis, and γ the eigenvector of the PC of interest. This warping of the mean shape can be visualised by constructing triangular polygons between sets of landmarks, so as to build up a wireframe model (see Figure 2.3) of the landmark configuration. Observation of how the wireframe deforms along each PC axis provides important visual information on how shape change between specimens occurs.

2.2.4.8 Implementation of methods for this study

The methods used in this study were conducted using a specially designed software suite called *morphologika*© (O'Higgins & Jones, 1998). As discussed above, the program takes sets of Cartesian coordinate data, rotates, translates and scales it, using Generalised Procrustes Analysis, and carries out a principal components analysis in the tangent plane. The software displays the following: a graphical plot capable of pairing any two PCs or any one PC and centroid size, a 3 dimensional viewer window, which allows visualisation of mean landmark configurations, either as a series of points, a wireframe model, or a surface rendered object, and a control window. This makes it possible to investigate the variability displayed in the PC plots by "walking" along the PC axes and at the same time observing any warping of the mean landmark configuration in the 3D viewer window. There is also the facility to view the shape represented by any point on the PC graph. The control window also contains the options to use TPS deformation grids to warp between different groups or group means. The software has been used successfully in a wide number of peer reviewed

studies (e.g. O'Higgins & Jones, 1998; Cobb, 2001; Niewoehner, 2001; O'Higgins et al., 2001; Collard & O'Higgins, 2002; Singleton, 2002).

2.2.4.9 Procrustes distances

In some cases, the absolute Procrustes distances between each and every individual in a sample needs to be calculated. In house software (O'Higgins, University College London) calculates each distance in a pairwise fashion. This way, a frequency histogram of the distribution of Procrustes chord distances *within* and *between* groups can be plotted. This technique is especially important when considering the relationship between two isolated fossil specimens. If the Procrustes distance between them, say, can be shown to be well outside the range of within group variation of extant taxa, then it can be said with some confidence that they may come from different taxa themselves.

2.2.4.10 Procrustes distances between means

In many cases it was necessary in this study to compare the mean shape of one group with the mean shape of another. For instance, if a particular tarsal bone was found to show significant sexual dimorphism in terms of centroid size, then the mean male and female shape were separately analysed using *morphologika*© in order to visualize what that difference means in anatomical terms. All male specimens for that species and bone are Procrustes registered. The program *morphologika*© automatically calculates the mean Procrustes registered coordinates for any analysis done. Male and female means are combined into a single data file and then Procrustes registered again in order to put them both into the same shape space. The Procrustes chord distance between the mean male shape and the mean female shape is calculated using in house software (O'Higgins & Jones, University College London). This technique can be used to calculate the Procrustes chord distance between any two group means.

2.2.4.11 Permutation Tests

In house software also made it possible to use permutation tests (Good, 1993) to calculate the significance of a Procrustes chord distance. The real Procrustes chord distance between two group means was calculated, and then individuals were randomly allocated to each group and a mean calculated. The original distance was compared to the distribution of permuted distances to see if it could be considered

significant. If it fell outside the 95% range of variation, then it was considered as significantly different. The elegance of this technique is that it does not assume normal distribution, but, rather, creates its own distribution from which p values are subsequently calculated. The tests were done 3000 times in each case. The reason for this was that when repeated tests were run using only 1000 permutations, it was found that there was some variation in the final p values. In some cases this resulted in p values that could be either significant or not significant for the same test. With 3000 permutations repetition of the same test resulted in the p values being consistently the same.

2.2.4.12 UPGMA phenograms

Phenograms provide a convenient way of visualising the relationship between individuals or group means as summarised by a distance matrix. In the case of distances used in this study Procrustes distances are used, whether between individuals, group means or between group means and individuals (i.e. a fossil versus an extant taxa mean). UPGMA stands for *unweighted pair-group method using arithmetic averages*. For this study, UPGMA phenograms were calculated using the program NT-SYS (© Exeter Software, 47 Route 25A, Suite 2, Setauket, NY 11733-2870, USA).

2.2.4.13 Maximum Likelihood trees

Maximum likelihood is a form of analysis that can estimate phylogenies using continuous morphological data (Felsenstein, 1973; Lewis, 2001). It has an advantage over UPGMA analysis, in that it does not assume that the divergence of morphologies from a branching point occurs at a constant rate. However, a limitation of the procedure is that an outgroup has to be predetermined, thus adding an element of subjectivity to the analysis. For this study, trees were calculated using the PC scores from the PCA of GPA rotated extant taxon means with and without individual fossils. These PC scores are considered as the continuous traits that this form of analysis requires. These trees were calculated using the program CONTML (Felsenstein, 1981).

Chapter 3

3.1 Introduction

This chapter is concerned with exploring extant hominoid adult intra-specific variation in the tarsals. When looking at such variation, one of the principal sources of variation is often sexual dimorphism. One of the reasons that addressing the issue of sexual dimorphism is important, is in the context of trying to explain shape differences between fossil specimens. If sexual dimorphism can be ruled out, on the basis of a study of extant groups, then other avenues of reasoning can be explored to explain these apparent morphological differences.

When dealing with adult intra-specific variation, such as sexual dimorphism, there are a number of ways it can be explained. Differences can be due to differing ontogenetic growth trajectories, allometric relationships between size and shape, or function. There is very little research and few findings relating to intra-specific shape variation in the hominoid tarsal complex. Those studies that do exist deal exclusively with modern humans. A recent study has suggested, from 3D scanning of the hallucial facet of the medial cuneiform of cadaver specimens, that females have a slightly more curved joint surface than males do (Dykyj *et al.*, 2001). Why this is the case has yet to be explained, and epigenetic factors, such as differences in footwear choice, cannot be ruled out as being a possible explanation, especially as cadaver specimens tend to be from individuals of advanced age where such factors would have had a lifetime to have taken effect. Studies by Kidd (1995, 2002), who conducted a multivariate analysis of interlandmark distances for the calcaneus, cuboid, talus and navicular, found that for four different modern human populations (South African Zulus, Romano-British, Southern Chinese and Victorian English) there are significant differences between males and females over several canonical axes (the most consistent and marked differences were on the first axis, and these were considered to be exclusively size related). However, size was not removed from any of the analyses, so the study must be considered cautiously when considering any shape differences between the sexes, since there are varying degrees of body-mass dimorphism between males and females (and so presumably pedal size dimorphism)

in not only all modern human populations, but also all extant hominoid taxa. Not only is there body mass dimorphism, but also there are known differences, for *Pan*, *Gorilla* and *Pongo*, between adult males and females in terms of locomotor repertoire.

3.1.1 Sex differences in Locomotor repertoires

Pan

There are considerable amounts of data from field observations that show that female chimpanzees have a more arboreal locomotor repertoire than males (Doran, 1992; Hunt, 1993). Adult males, and in particular the larger ones, arm-hang less than females, and sit and walk more terrestrially. Females have been observed to spend more time in trees, and to climb and walk arboreally more than males (Hunt, 1993). There are several main explanations in the literature as to why this is so. Doran (1993) argues that the determining factor is body size, and hypothesises that the larger a chimpanzee gets the less arboreal it is likely to be. Hunt (1993) argues that this is not the case, and that males simply monopolise more easily processable food resources, meaning that the females have to range further into the trees to get sufficient amounts of food. To add to this, Wrangham (1979) has shown that chimpanzee travelling, as opposed to feeding or socializing, is almost exclusively terrestrial, and that since male chimpanzees have larger home ranges than females they tend to spend more time on the ground. Wrangham (1979) also noted that males travelled faster on the ground than females. In general it can be concluded that female chimpanzees are more arboreal than males, but that the reasons why remain unclear.

Gorilla

The case is similar for gorillas. Field observations on the Western and Eastern lowland gorilla have shown that adult males tend to be more terrestrial than females, with the females using more suspensory and arboreal climbing behaviour (Remis, 1995; Remis, 1996, 1997a). It was observed that the larger an individual became, the less likely it was to engage in arboreal behaviour. This is borne out by data showing that the larger mountain gorillas are less arboreal than either sub-species of lowland gorilla (Remis *in* Doran, 1997). However, it is important to note that in absolute terms adult male gorillas still spend a considerable amount of time in trees, although they do tend to stay very near the main trunk, and do not climb to the peripheries as do the females (Remis, 1995). As for the chimpanzees, it possible that body size is

the overriding factor governing this, or, as Remis (1995) argues, that the males are monopolising the more easily available food resources, the evidence for this being that females occupy parts of the tree requiring less precipitous climbing behaviour (i.e. suspensory and arboreal climbing on peripheral branches) when males are elsewhere.

Pongo

Compared to *Pan* and *Gorilla* there is far less field data on male versus female orangutan locomotor behaviour. From what data that do exist, there are a few tentative conclusions that can be made. Studies from Ketamba, Sumatra (Sugardjito & Cant, 1994), Kutai National Park, Kalimantan (Cant, 1987) and Tanjung Puting Reserve, Kalimantan (Galdikas & Teleki, 1981) have shown that adult females of both sub-species of *Pongo* are almost exclusively arboreal in their locomotor repertoires. It is important to note, however, that although the number of actual observations in these studies is high (typically in the thousands) the number of individuals studied is usually very low indeed. For instance, 4 females were observed in the first study cited and 2 in the second. For the males, the data available (Galdikas and Teleki, 1981; Cant, 1987; Cant, pers.comm.) suggests that adult males, in particular the larger ones, do travel more frequently on the ground than females. Galdikas and Teleki (1981) have shown that males spend over 20 times more time on the ground per day than females do. However, this is only thought to be the case for the Bornean Orangutan, *Pongo pygmaeus pygmaeus*, since the presence of tigers on Sumatra results in the orangutans from that island hardly ever leaving the trees (Sugardjito and Cant, 1994).

Homo sapiens

It is well known that males and female modern humans are habitual, obligate bipeds. There are no data to suggest that there is any significant locomotor differences between modern human males and females.

To summarise, field observations have shown that adult females for both *Pan* and *Gorilla* are significantly more arboreal than adult males. The case may be so for *Pongo* as well, but in that case field observations used small sample sizes, and so make that finding tentative at best. These locomotor differences could occur for a

number of reasons. They could be purely behavioural, such as male gorillas monopolising easily available food resources (Remis, 1997b), or they could be linked back to body-size/mass constraints. The likely answer is probably a combination of such factors, but what is relevant, in the context of this thesis, is if these differences are reflected in tarsal morphology. That is to say, are any sex-based differences in extant great ape tarsal morphology correlated with locomotor differences and /or body mass dimorphism? One of the ways that this can be explored is to look at the forefoot and the hindfoot as discreet units. As discussed in Chapter 1, the forefoot (navicular, cuboid, cuneiforms and all five rays) is primarily involved in grasping in the great apes. The hindfoot (talus and calcaneus), as for modern humans, is involved mainly in the absorption and transference of force through the foot during locomotion (particularly terrestrial locomotion). In species where males are observed to be more terrestrial than females, one might, therefore, expect to see shape dimorphism in the hindfoot. Likewise, one might expect to see subtle differences in the female forefoot reflecting increased arboreality.

3.1.2 Hypotheses

The main purpose of this chapter is to explore intra-specific tarsal shape variation in *Homo*, *Pan*, *Gorilla* and *Pongo*. The implications of any results are will be discussed in Chapter 6. The main question that naturally arises for such an analysis is:

“What is the degree, if any, of sexual dimorphism seen in the tarsal bones of these species, and how does this relate to known locomotor and body mass differences between the sexes?” For each species the a null hypothesis (H_0) and resultant hypothesis (H_1) are constructed:

H_0 “There is no shape difference between male and female tarsal bones”

H_0 is tested by calculating the significance of the difference (see Methods section) between the mean male and mean female shape for each taxon. If there is a significant difference, then the nature of that shape difference is explored further.

H_1 “If H_0 is falsified, then that shape difference is due to differences in size”

H_1 is tested by examining the correlation between centroid size and PC scores. Centroid size is an accurate reflection of the size of a bone, and so, indirectly, is a very approximate proxy for body size when considering an intraspecific sample. Association between centroid size and PC scores is considered statistically strong if the r values are high (above 0.7) and the $p < 0.05$.

These hypotheses are tested for the calcaneus, the talus, the cuboid, the navicular and the medial cuneiform, and if any of these hypotheses are refuted, then the study explores the nature of the differences and what they might mean in functional terms.

3.2 Materials

The materials used in this study represent two populations of modern humans, Zulus and Xhosa, and four species of extant great apes, *Pan troglodytes troglodytes*, *Pan paniscus*, *Gorilla gorilla gorilla*, and *Pongo pygmaeus*. All individuals used in this study are full adults. Further details of the provenance of these specimens, criteria for measurement, and determination of maturation can be found in the materials section of Chapter 2.

3.2.1 Sample Sizes for Intra-Specific Study

The number of tarsals measured for each sex of each species is summarized in Table 3.1. The table shows that for each taxon, sample size slightly varies according to the bone examined. This is due to not all foot bones being present for every specimen.

Table 3.1 Sample sizes for each bone and species, separated by sex.

		Medial Cuneiform	Navicular	Cuboid	Talus	Calcaneus
<i>Pongo pygmaeus</i>	Males	11	9	19	19	11
	Females	18	17	24	22	21
<i>Pan troglodytes</i>	Males	21	21	23	23	21
	Females	19	19	19	21	19
<i>Pan paniscus</i>	Males	7	7	7	6	7
	Females	8	8	9	10	9
<i>Gorilla gorilla gorilla</i>	Males	20	20	21	20	19
	Females	21	21	21	21	21
<i>Homo sapiens</i> (Zulu)	Males	38	39	39	39	40
	Females	39	41	41	41	41
<i>Homo sapiens</i> (Xhosa)	Males	16	17	17	16	17
	Females	17	17	17	17	17

3.3 Methods

Detailed descriptions and discussion of these methods are discussed in Chapter 2.

Determination of sexual dimorphism.

For each bone of each species, the significance of the Procrustes distance between the average male and average female Procrustes registered shape was calculated using the in-house program *Perm PCA* (Paul O'Higgins). 3000 permutations were run in each case, and a distance was deemed to be significant if p was less than 0.05.

Correlation between centroid size and shape

This is tested by calculating the correlation coefficient (Pearson's) between PC scores and centroid size. If two criteria of satisfaction are met, then the relationship between a set of PC scores and centroid size is considered to be statistically strong. Firstly, if there is a statistically significant p value for the correlation ($p < .05$). Secondly, if the r value is higher than 0.7.

In subsequent tables and discussion the following terminology is used to refer to significance levels of results:

p value	Degree of Significance
$p .05$	Significant
$p .01$	Very Significant
$p .001$	Highly Significant

Exploration of sexual dimorphism.

If a particular bone was found to show significant sexual dimorphism, then the mean male and female shapes were separately analysed in order to visualize what that difference meant in anatomical terms. The average male and average female Procrustes registered shapes were Procrustes registered together, in order to put them into the same shape space. Tangent projection and principal components analysis of these registered shapes was then performed, and finally shape differences between mean male and mean female shape were visualised.

	Medial Cuneiform	Navicular	Cuboid	Talus	Calcaneus
<i>Pongo pygmaeus</i>	0.0536	0.0798	0.061	0.048	0.0593
	p=.516	p=.348	p=.124	p=.046	p=.005
<i>Pan troglodytes troglodytes</i>	0.0385	0.0331	0.0312	0.0385	0.035
	p=.580	p=.878	p=.951	p=.076	p=.327
<i>Pan paniscus</i>	0.0592	0.0744	0.0632	0.0548	0.0628
	p=.448	p=.221	p=.532	p=.898	p=.032
<i>Gorilla gorilla gorilla</i>	0.0528	0.0473	0.0491	0.0627	0.0514
	p=.059	p=.127	p=.312	p<.001	p<.001
<i>Homo sapiens (Zulu)</i>	0.0413	0.036	0.0357	0.0288	0.0254
	p<.001	p=.141	p=.076	p=.067	0.248
<i>Homo sapiens (Xhosa)</i>	0.0383	0.0392	0.0441	0.0331	0.0285
	p=.350	p=.770	p=.461	0.784	p=.734

Table 3.2 Procrustes distance and *p* values of significance for permutation tests of mean male versus mean female shape for all five tarsal measured for all extant species analysed. Upper number is the Procrustes distance between the means, and the lower *p* value is the significance of that distance after 3000 permutations. Significant *p* values are highlighted bold.

3.4 Results

As Table 3.2 shows, there is a small number of significant values for mean male versus mean female shape. The format of this section is that shape differences for each taxon are discussed if a significant difference was found between mean male and mean female shape.

3.4.1 Centroid size

In all cases, based on unpaired two sample t-tests, there is a highly significant difference between mean male and mean female centroid size. However, no strong association was found between any PC axis and centroid size, since all r values (Pearson's correlation) were well below 0.7 (Table 3.3), even though the p values in two cases indicated significant correlations (*Pongo* & *Gorilla* calcaneus).

Table 3.3 Correlation between PCs 1 to 3 and Centroid Size for each tarsal. Only those results for where there was significant shape difference between mean male and mean female shape are given.

	Sample Size	r value	p value
<i>Pongo</i> Calcaneus			
PC 1 vs. Centroid Size	32	-0.450	<.05
PC 2 vs. Centroid Size	32	0.332	n.s
<i>Pongo</i> Talus			
PC 1 vs. Centroid Size	41	0.113	n.s
PC 2 vs. Centroid Size	41	-0.271	n.s
<i>P.paniscus</i> Calcaneus			
PC 1 vs. Centroid Size	16	-0.144	n.s
PC 2 vs. Centroid Size	16	-0.005	n.s
<i>Gorilla</i> Calcaneus			
PC 1 vs. Centroid Size	40	0.111	n.s
PC 2 vs. Centroid Size	40	-0.442	<.05
<i>Gorilla</i> Talus			
PC 1 vs. Centroid Size	39	0.309	n.s
PC 2 vs. Centroid Size	39	-0.306	n.s
Zulu Medial Cuneiform			
PC 1 vs. Centroid Size	77	0.038	n.s
PC 2 vs. Centroid Size	77	0.129	n.s

3.4.2 *Pongo pygmaeus*

From Table 3.2 it can be seen that no significant differences are found between males and females for the *Pongo* medial cuneiform, navicular and cuboid. For the talus, $p = .046$, indicating that there is a significant shape difference between male and female tali. For the calcaneus, $p = .005$, making the distance between mean male and female shape very significant.

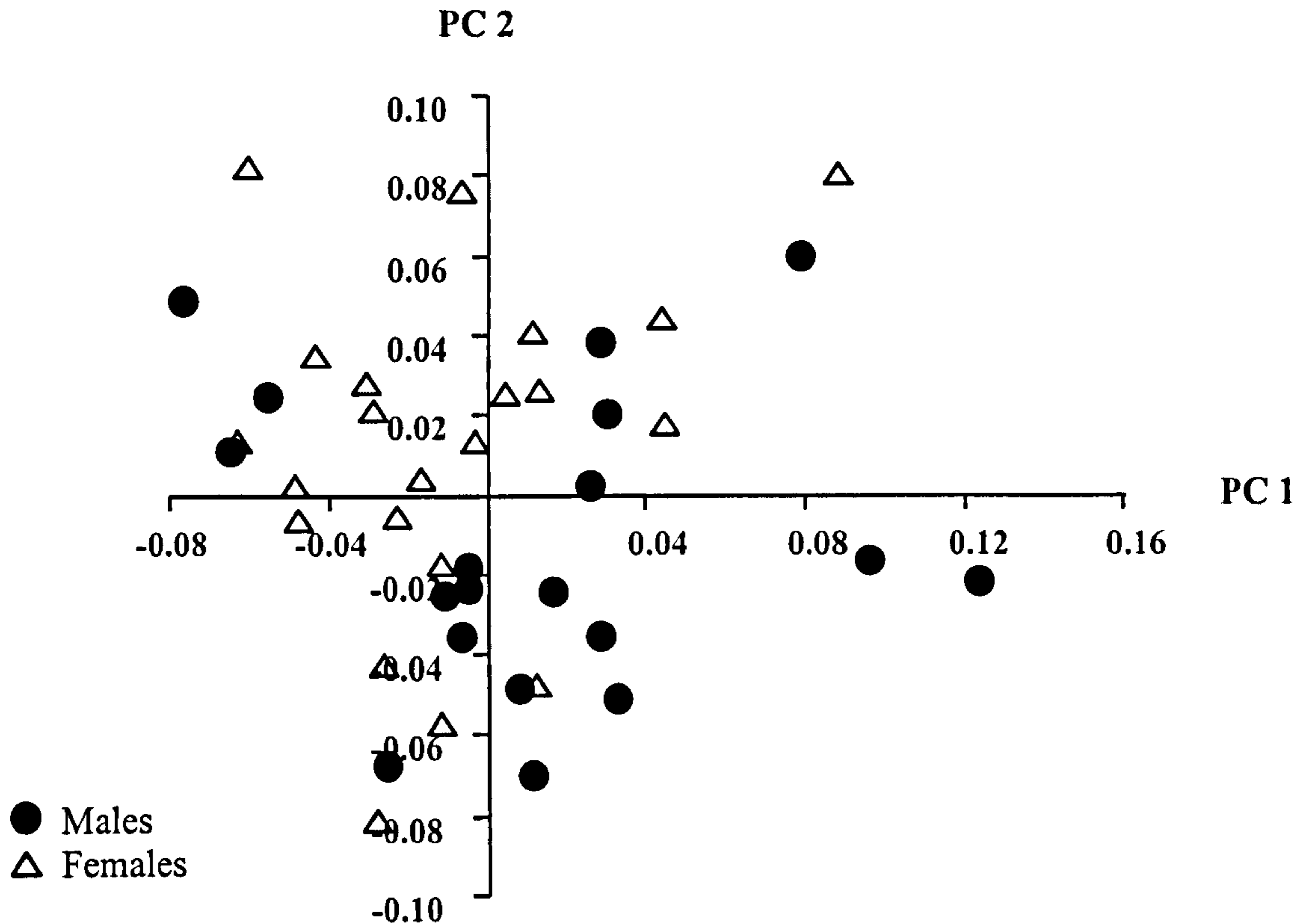


Figure 3.1 Talus: PC 1 versus PC 2 for males and females of *Pongo pygmaeus*.

Looking at the spread of each sex on PC 1 versus PC 2 (Figure 3.1), it can be seen that there is a considerable degree of overlap between males and females, and no distinct clustering of either sex. All those PC axes beyond PC 2 do not separate sex to any degree, and there is no correlation observed between any PC axis and centroid size. Table 3.4 shows that PC 1 and 2 account for roughly similar proportions of total variance.

Table 3.4 Talus: Percentage variance explained by PC 1 to PC 4 for *Pongo*

Principal Component	Percentage variance
1	13.0%
2	11.2%
3	9.6%
4	6.7%

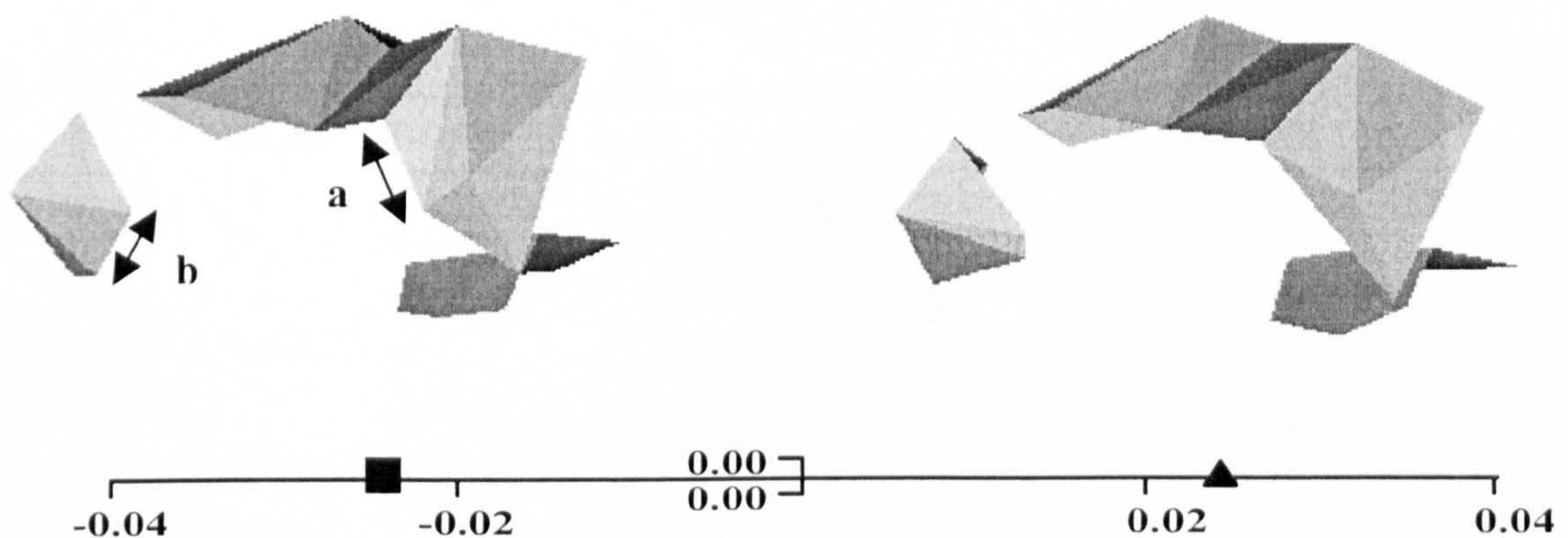


Figure 3.2 Talus (distal/lateral) view: mean *Pongo* male shape (triangle) versus mean *Pongo* female shape (square). Black arrow points to region of shape difference. N.B. Warped images are amplified twice from actual position of means on axis.

To investigate the significant shape difference further, the mean male shape and the mean female shape for the talus of *Pongo* were put through GPA/PCA. Since only two mean shapes were analysed, there was only one principal component for this analysis. For the *Pongo* talus, warping from the mean female shape (left hand side on Figure 3.2) to the mean male shape, several very subtle changes in shape are visible.

Principally, there is relative reduction of the distance between landmarks 8 (most disto-lateral point of trochlear surface) and 12 (most distal projection of lateral malleolar facet). This means that there is a relative reduction dorso-plantarly of the dorsal section of the distal facet margin of the lateral malleolar facet. This effectively leads to a slight reduction in the total area of the facet itself. This change is

highlighted by the arrow “a”. There is also a slight relative increase in the dorsoplantar height of the lateral side of the head, as shown by arrow “b”. Finally, there is also a very slight relative flattening of the trochlear surface in the medio-lateral direction, and a very slight increase in the relative distance between the posterior calcaneal facet and the trochlear surface.

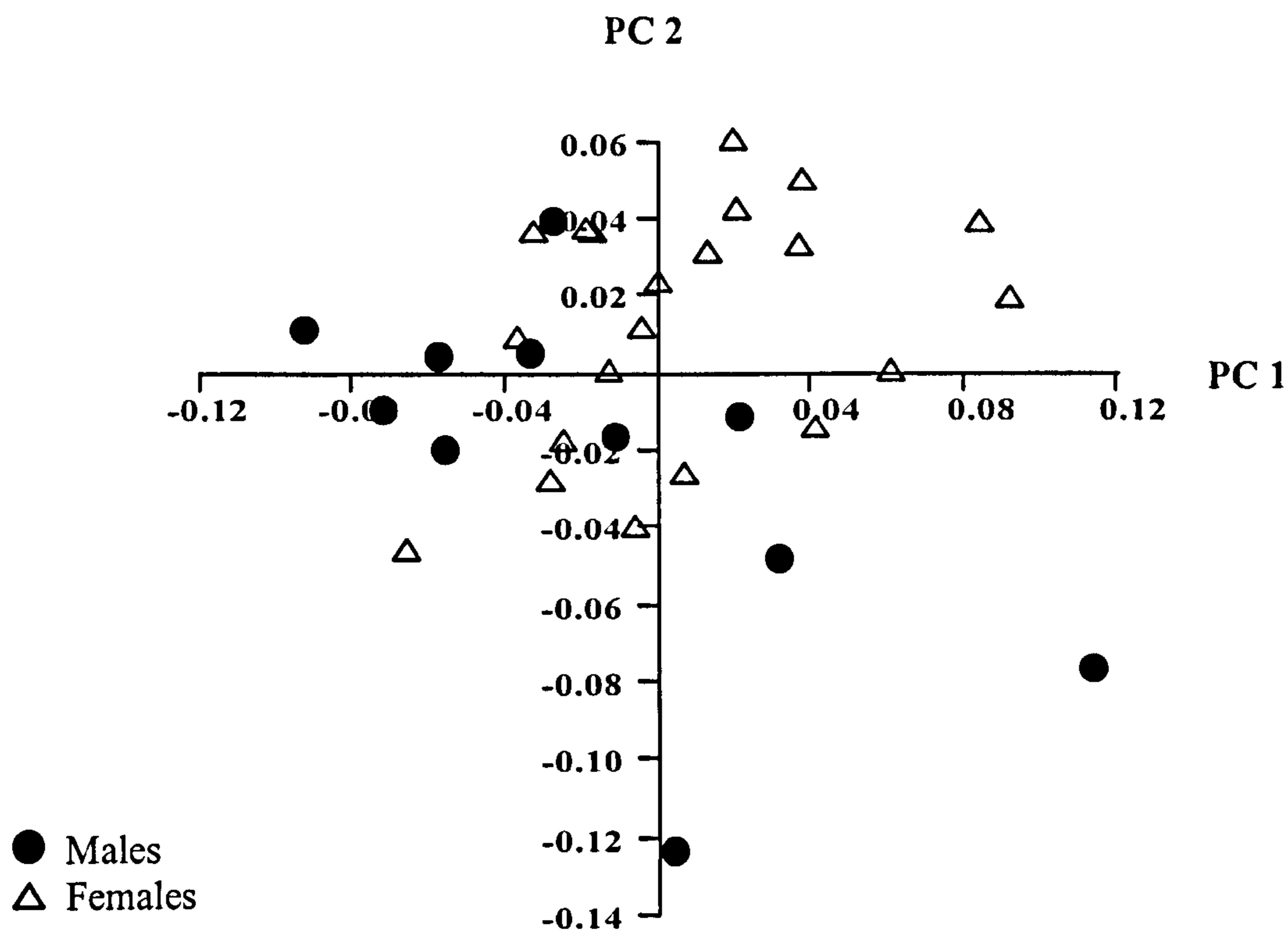


Figure 3.3 Calcaneus: PC 1 versus PC 2 for males and females of *Pongo pygmaeus*.

PC 1 versus PC 2 for the Procrustes registered male and female *Pongo* calcanei (Figure 3.3), shows that there is some separation between males and females, although there is also a degree of overlap as well. Over half the females sit in the upper right quadrant of the plot, outside the male range of variation. However, only three males fall outside the female range of variation. No other combination of PC axes resulted in any degree of separation. Likewise, there was no strong association between any PC axes and centroid size.

Table 3.5 Calcaneus: Percentage of total variance explained by PC 1 to PC 4 for *Pongo*.

Principal Component	Percentage variance
1	17.6%
2	12.1%
3	10.1%
4	8.6%

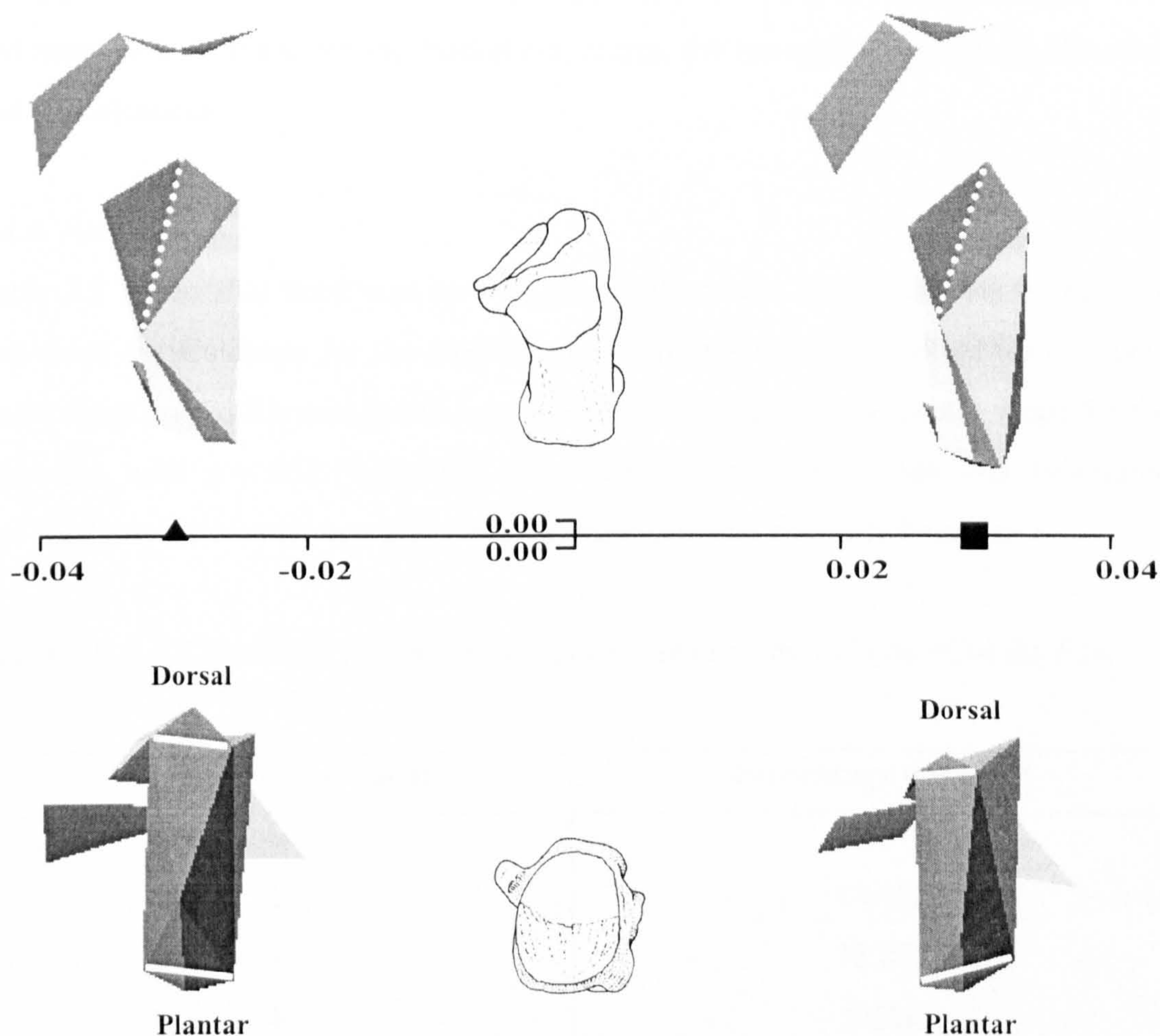


Figure 3.4 Calcaneus: Mean *Pongo* male shape (triangle) versus Mean *Pongo* female shape (square). Above: dorsal view. Below: posterior view. N.B. Warping of images is amplified twice from actual position of means on axis to make differences more obvious.

Warping from the mean male shape to the mean female shape along the PC 1 axis (Figure 3.4) causes several subtle changes. To amplify these changes, the warping of images is multiplied by a factor of two so as to aid visualisation. Firstly, there is a relative increase in the proximo-distal length of the posterior talar facet. This is

highlighted by the white lines in the upper (dorsal) views (Figure 3.4). Secondly, on the posterior surface of the tuberosity, there is a relative increase in dorso-plantar height, and a relative increase in the medio-lateral width of the dorsal section, and a relative decrease in the medio-lateral width of the plantar section. These latter two shape differences are referred to with white bars on the lower (proximal) views.

3.4.3 *Pan troglodytes troglodytes*

Table 3.2 shows that there were no significant differences found between mean male and mean female shape for the medial cuneiform, the navicular, the cuboid, the talus and the calcaneus.

3.4.4 *Pan paniscus*

Table 3.2 shows that there was no significant differences found between mean male and mean female shape for the medial cuneiform, navicular, cuboid or talus. There was a significant difference found between mean male and mean female shape for the calcaneus, with $p = .032$ (Table 2.2). However it is important to note that the sample size for *Pan paniscus* is very low, with 9 female calcanei and only 7 males.

Table 3.6 Calcaneus: Percentage variance explained by PC 1 to PC 4 for *Pan paniscus*.

Principal Component	Percentage variance
1	21.8%
2	14.8%
3	13.6%
4	9.5%

On PC 1 versus PC2 (Figure 3.6), PC 1 is responsible for some degree of separation between the sexes, with all the females occupying the positive end of the x-axis, and four of the seven males situated more towards the negative end. PC 2 does not separate the sexes at all, and this is the same for all other PCs. As for *Pongo*, comparison of the mean male and mean female shapes is the best way to explore the any shape dimorphism in the *P.paniscus* calcaneus. The main discernable differences between mean male shape and mean female shape are shown in Figure 3.6.

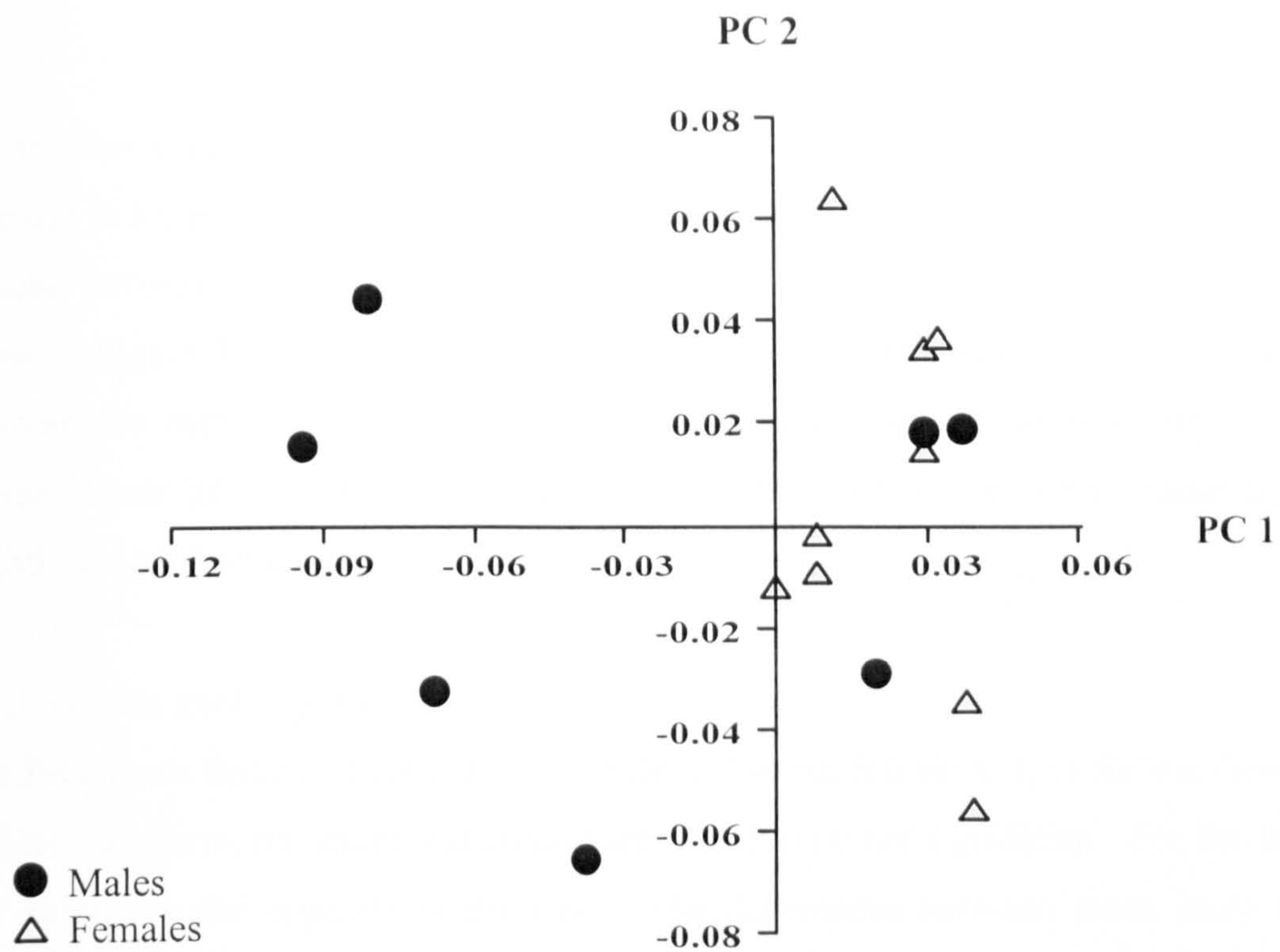


Figure 3.5 Calcaneus: PC 1 versus PC 2 for males versus females of *Pan paniscus*.

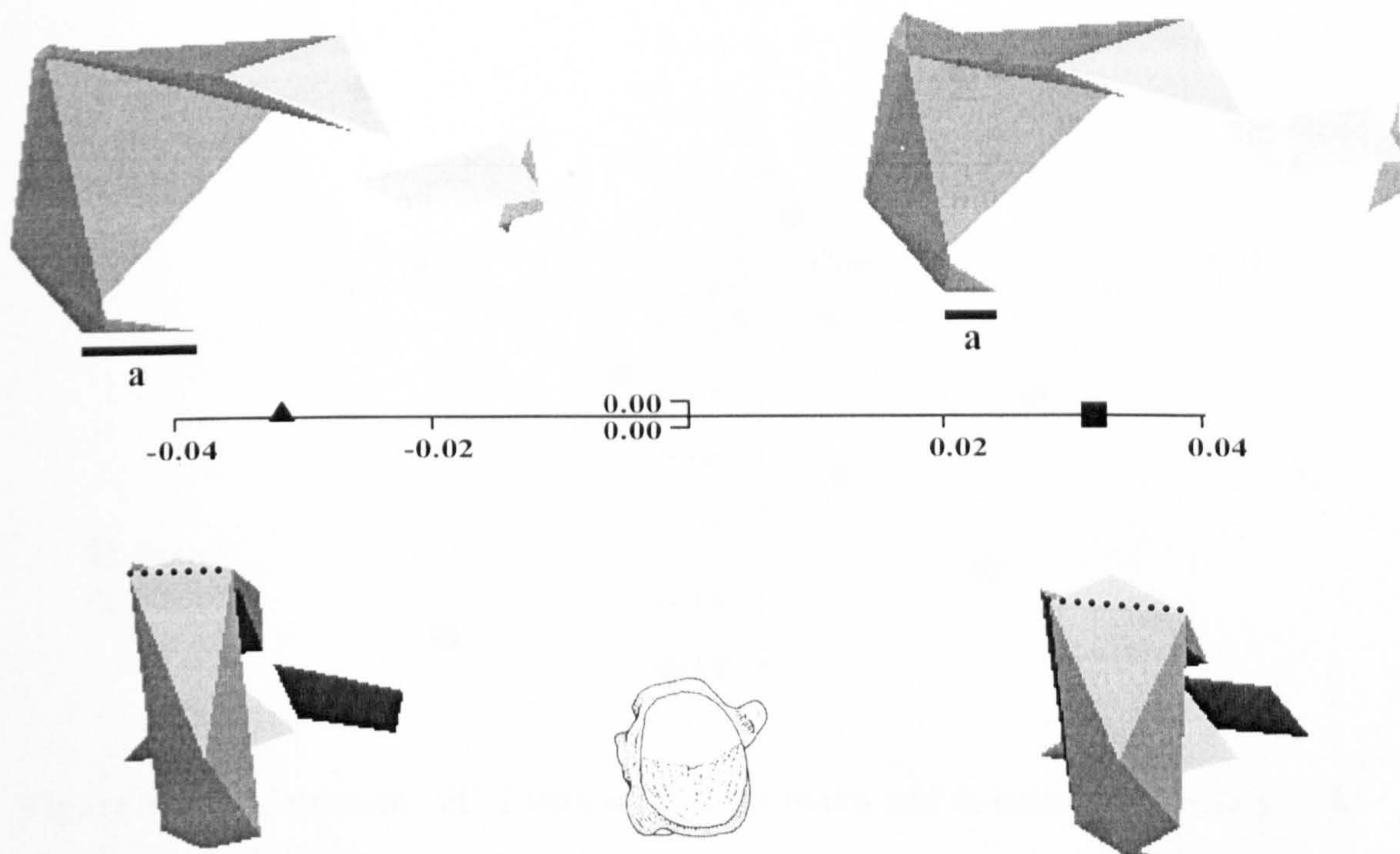


Figure 3.6 Calcaneus, *Pan paniscus*. Mean males shape (triangle) versus mean female shape (square). Above: medial view. Below: posterior view. N.B. Warping of images is amplified twice from actual position of means on axis to make differences more obvious.

For the *Pan paniscus* female mean, warping along the axis resulted in a slight relative increase in the medio-lateral width of the dorsal section of the posterior surface for the bonobo females. This is marked by the dotted black line on the lower (proximal) views in Figure 3.6. The mean male shape also has a slightly longer relative distance between the dorsal margin of the posterior surface and the distal extremity of the lateral plantar tubercle (black bars on upper, medial, views). i.e. it has, relatively, a slightly longer lateral tubercle.

3.4.5 *Gorilla gorilla gorilla*

The Procrustes distance between mean male and mean female shapes for the *Gorilla* medial cuneiform, navicular and cuboid are found to be not significant. For the talus and calcaneus the opposite is the case. The differences between mean male and female shape were found to be highly significant, with a $p < .001$ in both cases.

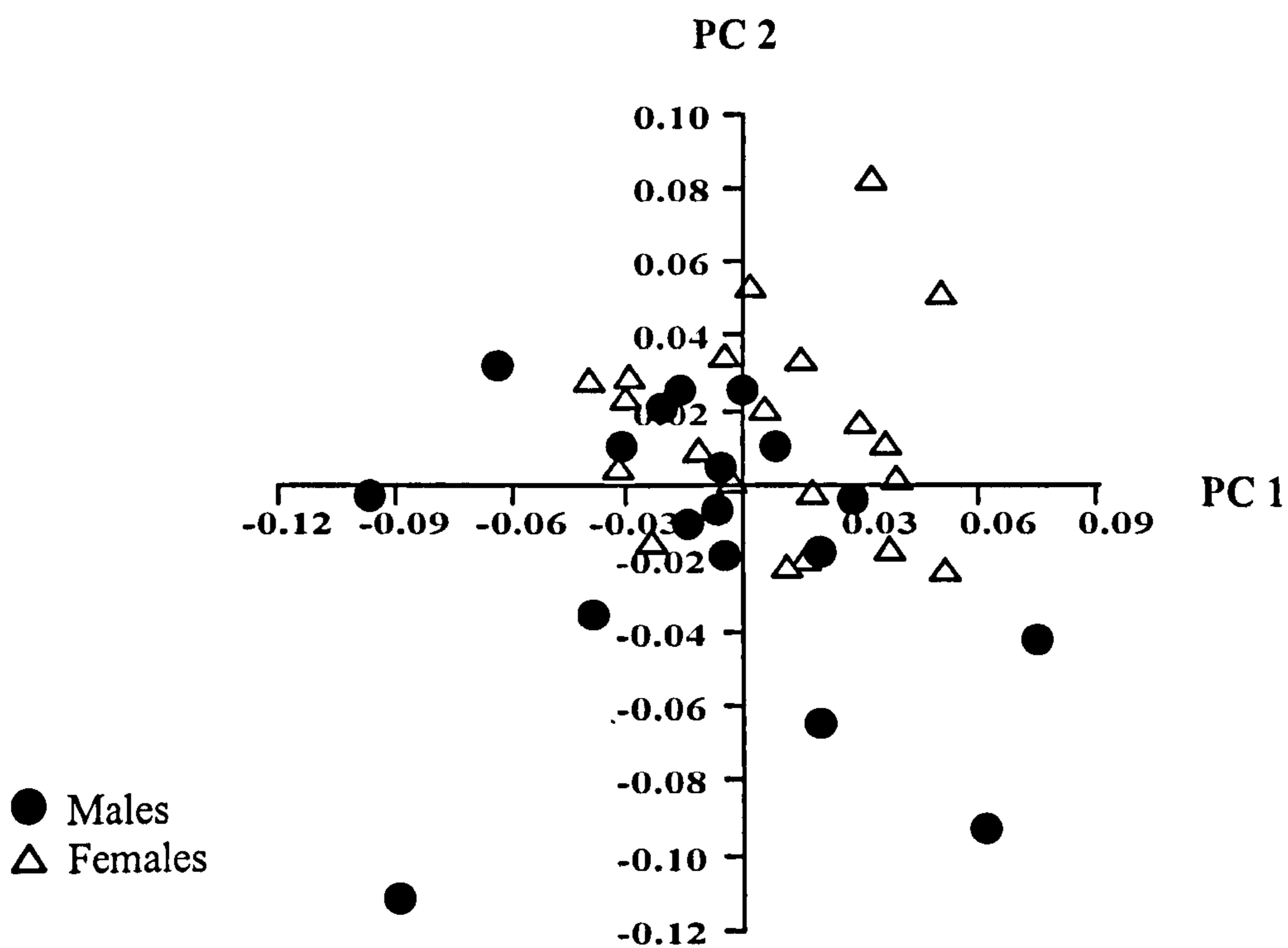


Figure 3.7 Calcaneus: PC 1 versus PC 2 for males and females of *Gorilla gorilla gorilla*.

For the *Gorilla* calcaneus, there is little separation between male and female individuals on PC1 versus PC 2 (Figure 3.7). Seven females do fall outside the male range of variation, and occupy the top right quadrant of the PC plot. Likewise, six

males fall outside the female range of variation, mainly on having lower PC 2 scores, although one male outlier has very low scores for both PC 1 and PC 2.

Table 3.7 Calcaneus: Percentage variance explained by PC 1 to PC 4 for *Gorilla*.

Principal Component	Percentage variance
1	13.2%
2	12.7%
3	10.2%
4	8.4%

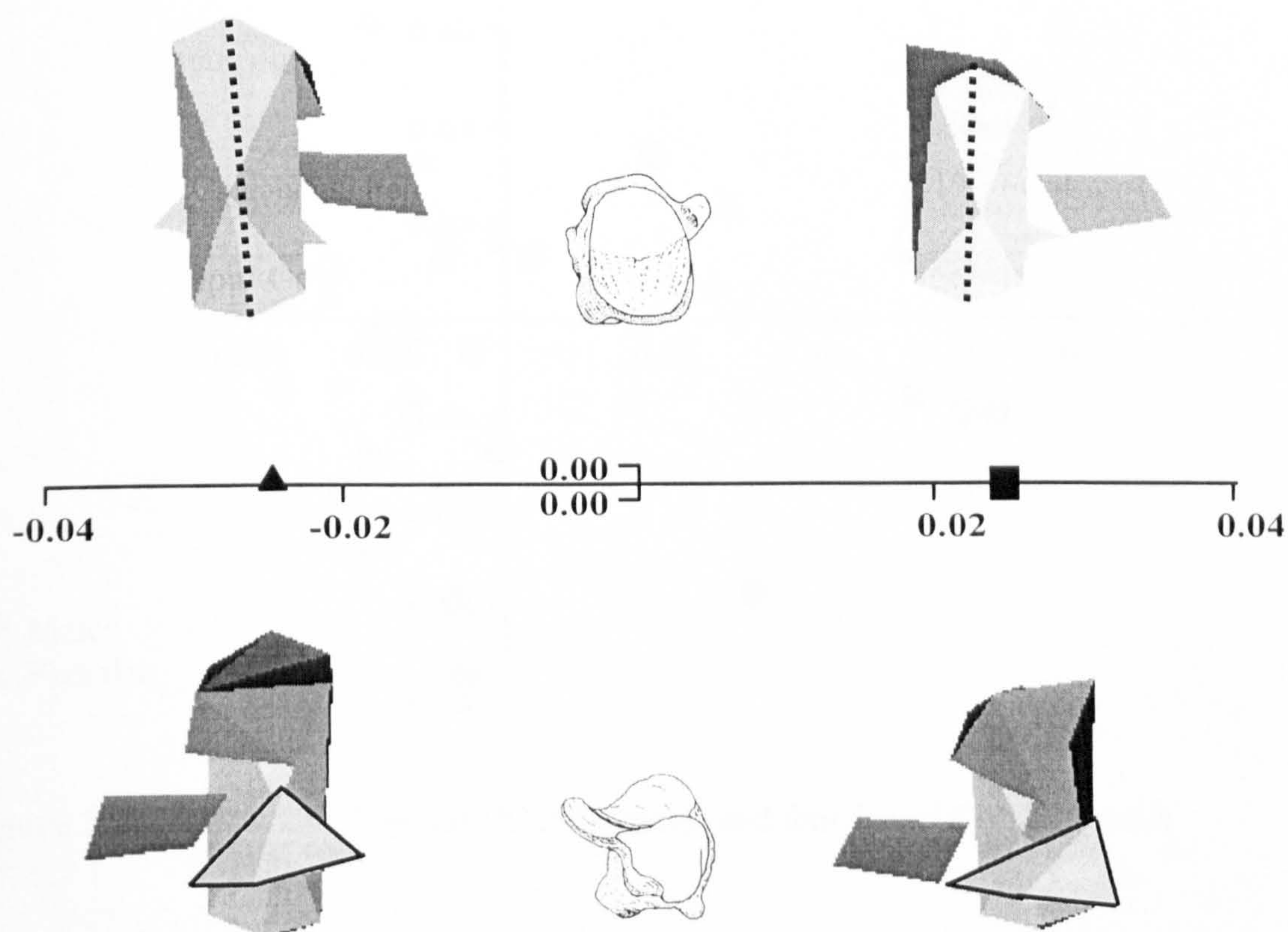


Figure 3.8 Calcaneus: Mean *Gorilla* male shape (triangle) versus mean female shape (square). Above: posterior view. Below: anterior view. N.B. Warping of images is amplified twice from actual position of means on axis to make differences more obvious.

Warping from the mean female shape to the mean male shape reveals several subtle shape differences (Figure 3.8). Principally there is a slight relative increase in the dorso-plantar height of the posterior surface of the tuberosity (depicted by black dotted line in upper, proximal views). There is also a slight relative increase in the medio-lateral width of the dorsal section of the posterior surface of the tuberosity, and a slight rotation medially and dorsally of the cuboid facet (bordered by black lines in the lower, distal views). This is due to relative dorsal movement of landmark 18 (most lateral point of facet) and medial movement of landmark 19 (most dorsal point of facet).

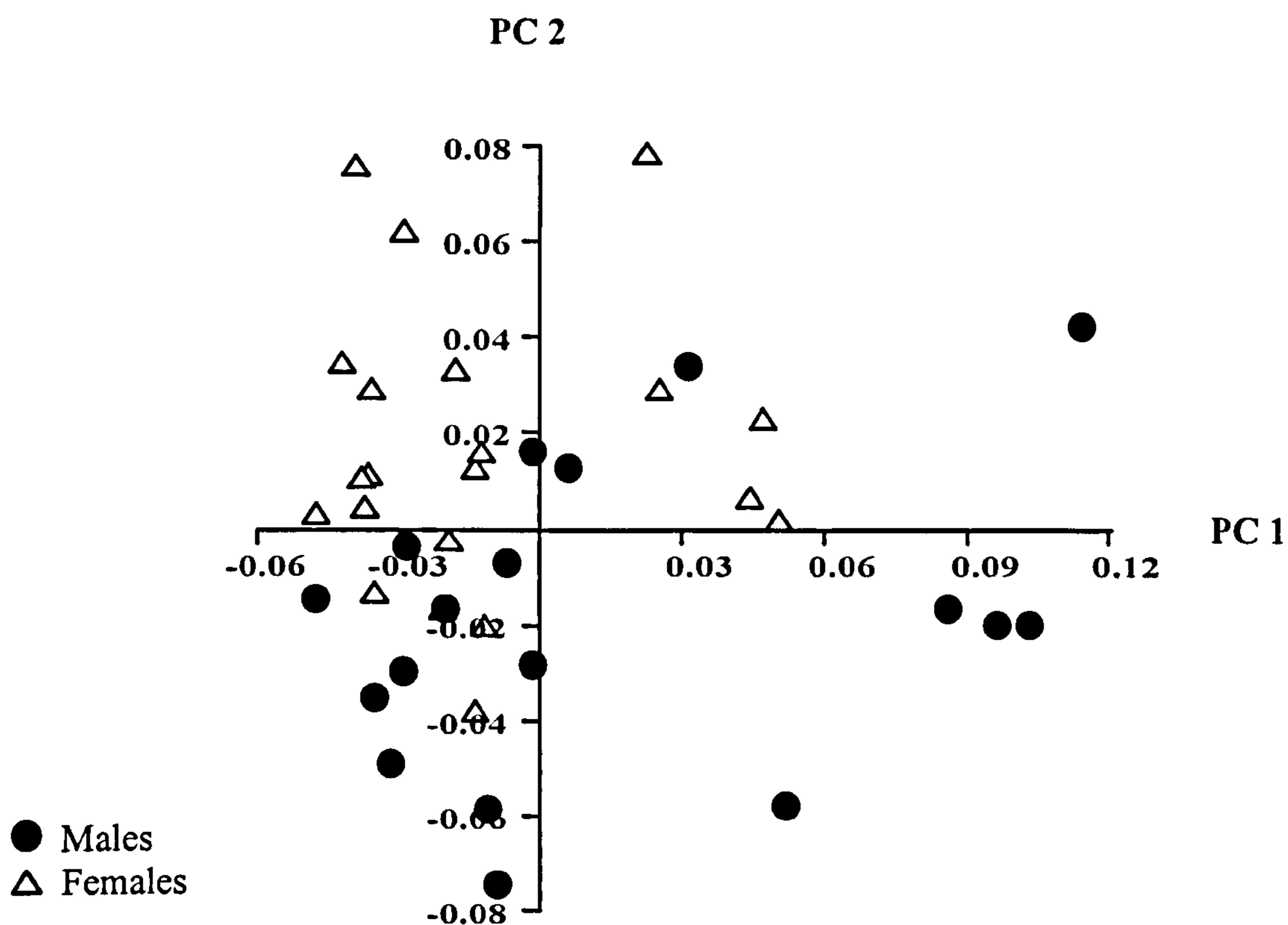


Figure 3.9 Talus: PC 1 versus PC 2 for males and females of *Gorilla gorilla gorilla*.

For PC1 versus PC 2 for *Gorilla*, there is a degree of separation between males and females (Figure 3.9). Females mainly occupy the top portion of the graph and males the bottom, meaning that it is PC 2 that is mainly explaining any separation between the groups. No PC axis was found to correlate with centroid size. As in previous cases in this chapter, significant differences between male and female gorilla talar shape are further explored by comparing their means.

Table 3.8 Talus: Percentage variance explained by PC 1 to PC 4 for *Gorilla*.

Principal Component	Percentage variance
1	16.2%
2	10.0%
3	8.8%
4	7.4%

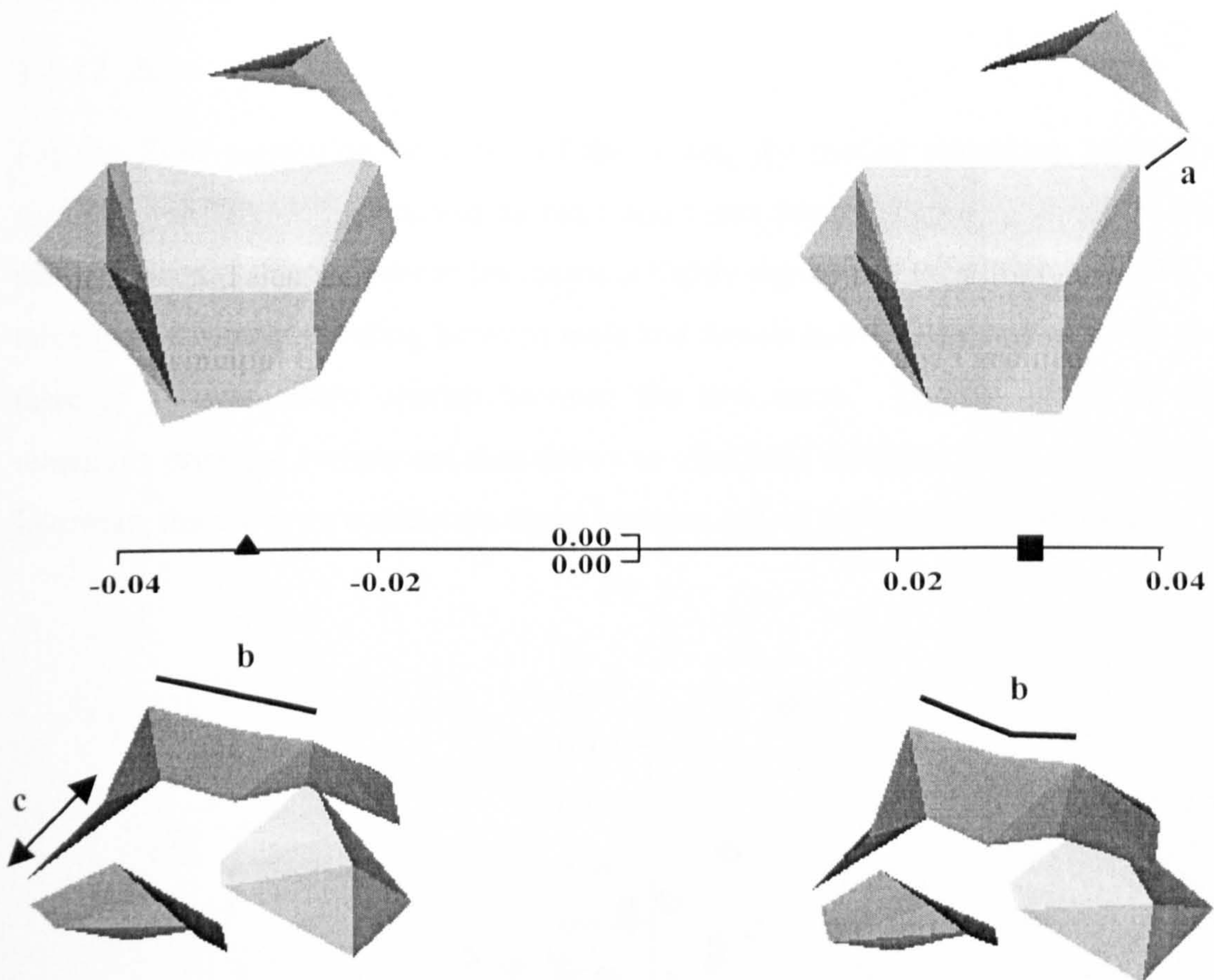


Figure 3.10 Talus: Mean *Gorilla* males (triangle) versus Mean *Gorilla* females (square). Above: dorsal view. Below: proximal view. N.B. Warping of images is amplified twice from actual position of means on axis to make differences more obvious.

Warping from mean female shape to mean male shape results in several subtle shape changes (Figure 3.10). There is a slight relative shortening of the medial side of the talar neck, resulting in medial side of head “swinging” in laterally around landmark 28 (most lateral point of navicular facet margin), which stays relatively static. This

results in the whole head being slightly more medially orientated, relatively, in the male mean shape. This is marked by the black line “a” on the upper (dorsal) view in figure 3.10. There is also a slight flattening of the trochlear surface, i.e. an increase in the angle between the trochlear groove and the lateral and medial trochlear margins. This shown by the black bars “b” in the lower (proximal) views. Finally, there is slight relative lateral flaring of the lateral malleolar facet, as shown by arrow “c” in the lower (proximal) views.

3.4.6 *Homo sapiens*

3.4.6.1 *Zulus*

For the Zulu population only one of the bones, the medial cuneiform showed a significant difference between mean male and mean female shape. With a $p < .001$ the Procrustes distance between the means is highly significant. For PC 1 versus PC 2 there is no distinct clustering between male and female individuals (Figure 3.11), and there is a considerable overlap between the two sexes. Exploration of all the remaining principal component axes shows no other axis separates males and females. Likewise, there was no correlation found between any of the axes and centroid size.

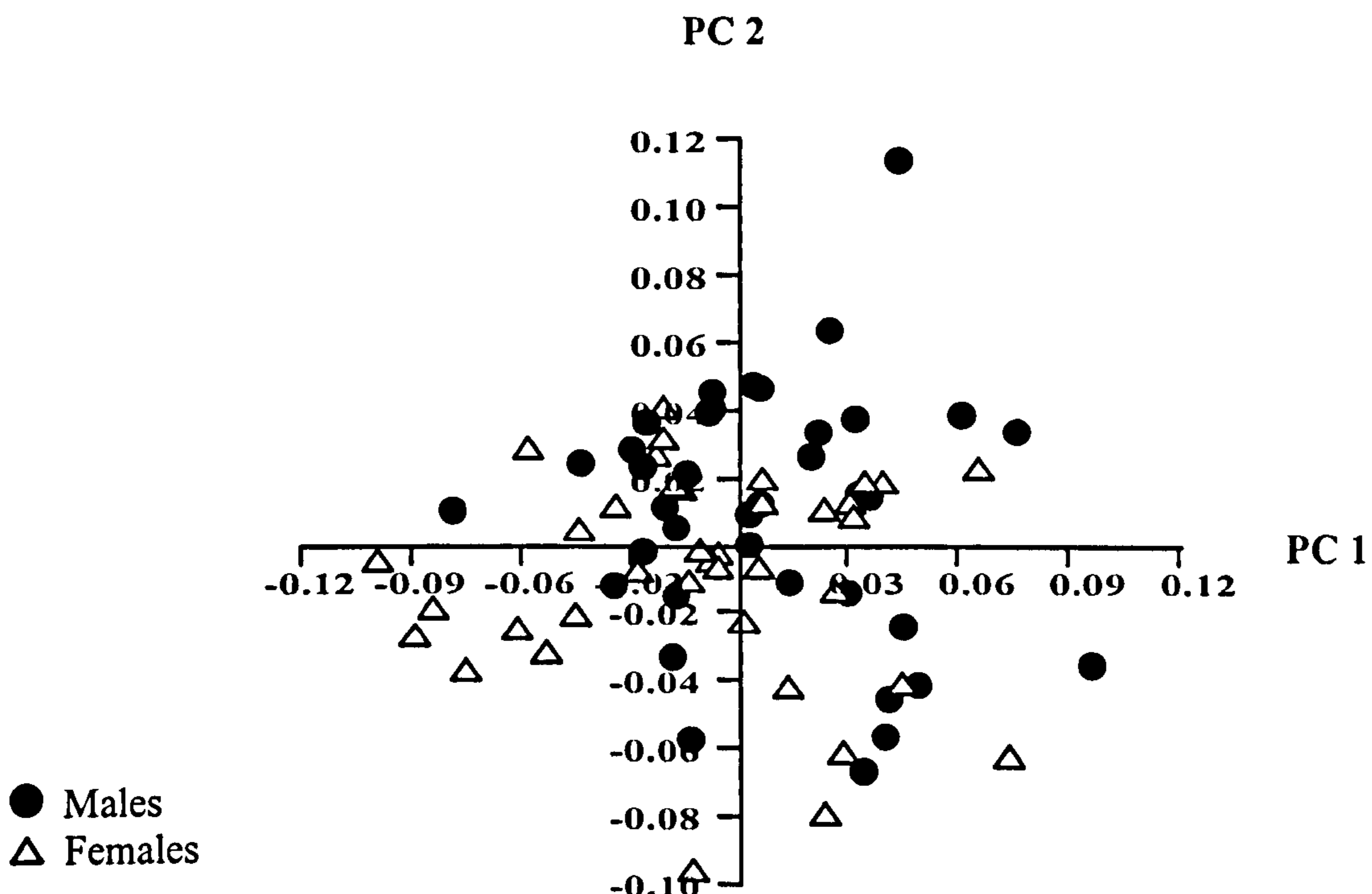


Figure 3.11 Medial Cuneiform: PC 1 versus PC 2 for *Homo sapiens* (Zulus)

Table 3.9 Medial Cuneiform: Percentage variance explained by PC 1 to PC 4 for *Homo sapiens* (Zulus).

Principal Component	Percentage variance
1	14.3%
2	11.4%
3	8.5%
4	9.7%

To further explore the finding of a significant difference mean male and mean female shape in the Zulu medial cuneiform, the plot below (Figure 3.12) shows the result the mean female versus the mean male shape. The visible differences were very subtle, with the most visible difference being that males have, relatively, a slightly dorso-plantarly higher proximal facet margin of the intermediate cuneiform facet (see white arrows on lateral views below).

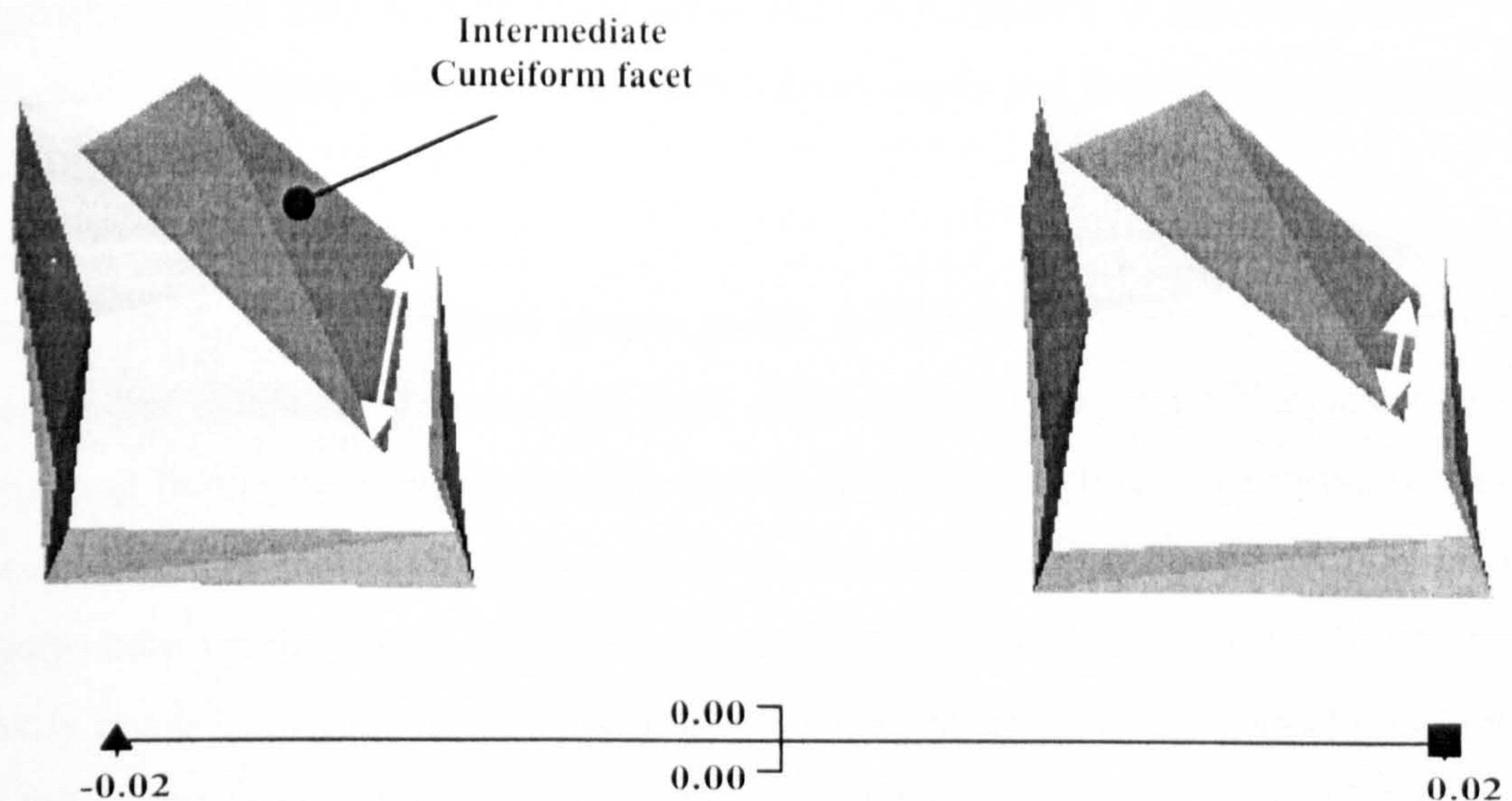


Figure 3.12 Medial Cuneiform: PC 1 of mean Zulu males (triangle) versus females (Square). Above: lateral view. Below: distal view.

3.4.6.2 Xhosa

For the Xhosa population, no significant difference is found between the mean male and female shape for any of the five bones measured.

3.5 Discussion

As the results show, there was no significant shape difference found between sexes in either the navicular or the cuboid for any of the species measured. In this respect, the null hypothesis (H_0) given at the start of this chapter can be **accepted** in all cases for these two bones. In addition, there was no shape dimorphism in the medial cuneiform for all the taxa bar *Homo sapiens*. So in that case as well, bar one human population, hypothesis H_0 can be **accepted** for the medial cuneiform as well. Even in that one unusual case, only one of the two populations measured (the Zulus) showed significant dimorphism, and the actual differences were very subtle indeed, with the male Zulus having slightly larger facet dimensions on the distal and lateral facets of the bone. There was no strong association between these morphological differences (as represented by the PC axes) and centroid size, so the reasons for this unusual finding are not clear. It is possible that the uniqueness of the human “toe-off” part of the stance phase is linked to this finding, but that would not explain the lack of any shape dimorphism found in the Xhosa medial cuneiform. It is more likely that epigenetic factors may well be responsible, such as difference in footwear choice or daily activity patterns, since both modern human males and females are committed, habitual bipeds.

Despite this finding, the overall picture is that the tarsal component of the hominin forefoot (for extant taxa) shows very little shape dimorphism. This is a particularly interesting finding with respect to *Pan*, *Gorilla* and *Pongo*, since the locomotor data discussed in this chapter suggests that there are discernable differences in activity patterns between the sexes. In these species, as discussed in Chapter 1, the forefoot is heavily involved in grasping. The navicular and cuboid form the distal components of the transverse tarsal joint, which is highly flexible in the great apes, resulting in a higher degree of flexion and extension around that joint complex than for humans. This is seen as a direct adaptation to climbing. Likewise, the medial cuneiform, and to a lesser degree, the navicular, as part of the medial column of the foot, form an integral part of the complex responsible for hallux abduction. In species where there are observed differences between male and female activity patterns, with one sex a little more terrestrial than the other, one might expect to see subtle but significant differences in the morphology of that part of the foot responsible for grasping, which

is principally an arboreal adaptation. This is not the case, and lends credence to the suggestion that behavioural differences observed in degrees of arboreality in extant great apes are not reflected in tarsal morphology.

The case for the hindfoot was very different. There was no significant shape dimorphism between males and female tali and calcanei for both populations of *Homo sapiens* and for the *Pan troglodytes* sample. In these cases, the null hypothesis H_0 is **accepted**. However, there was significant shape dimorphism in the talus and calcaneus for both *Pongo* and *Gorilla*, although it was very hard to visualize, since the differences appeared subtle when warping mean shapes on the PCA plots. There was also significant shape dimorphism in the *Pan paniscus* calcaneus, but the sample sizes were much smaller for this taxon. However, in all these cases, the null hypothesis H_0 is **falsified**.

There is no strong correlation between centroid size and any of the PC axes for all five tarsals. According to the criteria needed to accept hypothesis H_1 , this hypothesis is **falsified**. This does not necessarily mean that the size of the tarsals has no influence on their shape, since although having low r values, there were significant correlations (in terms of p values) between centroid size and PC 1 for the *Pongo* calcaneus, and centroid size and PC 2 for the *Gorilla* calcaneus. In these cases it can be summarised that size and shape are weakly associated.

3.5.1 Functional considerations

The talus and calcaneus are the largest bones of the foot. As discussed in Chapter 1, these bones directly transfer weight from the lower leg through the foot itself to the substrate. The chief role of the talus is in the transmission of force from the tibia, through the trochlea and then plantarly and distally through the sub-talar joint, and also distally and slightly medially through the talo-navicular joint. The calcaneus acts as the main absorber of force during heel strike (something that all great apes do in terrestrial locomotion (Gebo, 1992; Sarmiento, 1994)), and then acts as a lever to direct forces distally as the body moves forwards. The heavier an individual the more force there is travelling through the ankle joint, so in those species with a relatively high degree of body mass sexual dimorphism, one would expect very different forces to be transmitted through male and female ankle complexes.

Inspection of primate body mass data in Smith and Jungers (1997) shows that for both *Gorilla* and *Pongo*, adult females typically have a body mass of 42% and 45.6% lower than that of adult males respectively. Likewise, for *Pan troglodytes* and *Pan paniscus*, adult females are, respectively, 73.8% and 78.9% lighter than males. Analysis of data for a suite of different modern human populations shows that adult females are typically between 80% and 90% of the mass of adult males. Overall, *Pongo* and *Gorilla* are significantly more sexually dimorphic in terms of body mass, than is either species of *Pan* or any modern human population. So during locomotion, adult males of both *Pongo* and *Gorilla* experience, compared to females, far more force transmission through their hindfoot than is the case for adult males of *Homo sapiens* or either species of *Pan*.

The data does not exist to prove this, but since force is related to mass (and how the foot is used), the body mass data alone strongly suggest this. Whilst it is not possible to directly correlate the body mass data with the shape data from this study, it is the conclusion of this study that it is possible that the morphologically subtle, but highly statistically significant shape-based sexual dimorphisms seen in the hindfoot of *Gorilla* and *Pongo* are due to the high degree of body mass dimorphism in those species. Furthermore, for both these taxa, the anterior talar facet dimensions on for the male calcaneus is very slightly larger, as is the overall size of the posterior surface of the tuberosity. A relatively larger talar facet is likely to be a reflection of increased loading through that facet. Likewise, slightly larger dimensions for the posterior surface of the tuberosity, indicate a larger attachment site for the *tendo calcaneus*, thus indicating stronger plantar flexion. Stronger plantar flexion would be important in supporting and propelling higher loads during vertical climbing.

The lack of sexual dimorphism in the great ape forefoot (principally involved in grasping rather than force transmission) supports this assertion. Conversely, the relatively low degree of body mass dimorphism in modern humans and both species of *Pan* would explain why there is almost no shape dimorphism in the tarsals of any of those species (the case with the *Pan paniscus* calcaneus is debatable due to the very small sample size).

Chapter 4

4.1 Introduction

This chapter is concerned with exploring adult inter-specific shape differences between the tarsals of *Pongo*, *Pan*, *Gorilla* and *Homo sapiens*. As discussed in detail in Chapter 1, anatomical differences between the tarsals of modern humans and the extant great apes have been well described and discussed in the literature for well over a century. The vast majority of this literature has been concerned with visual anatomical comparison as opposed to metrical comparison, and whilst visual comparison can explain much of what is there, a 3D morphometric approach will increase the resolution of our knowledge about hominoid tarsal shape variation. This is important in terms of explaining the affinities of those specimens currently present in the fossil record. Likewise it is important to corroborate known observable anatomical differences with quantifiable morphometric differences, since if there is a disparity between the two then earlier analyses and interpretations may need to be re-evaluated.

The Introduction section of this chapter is made up of five parts. It starts with a brief summary of, respectively, known anatomical (4.1.1) and locomotor differences (4.1.2) between extant hominoid tarsals. There is then a discussion of factors that could feasibly explain inter-specific shape differences (4.1.3). This is followed by a number of hypotheses related to the relative importance of those factors (4.1.4). Finally there is a summary of how and why the results are organised as they are (4.1.5).

4.1.1 Summary of anatomical differences between extant hominoid tarsals

Calcaneus

There are several principal differences between the great ape and modern human calcaneus (Aiello & Dean, 1990). The tuberosity is considerably more prominent in modern humans, both mediolaterally, and dorsoplantarly. There is debate surrounding

the orientation of the sustentaculum tali, with some researchers suggesting that it is orientated relatively plantarly in the great apes, but others suggest that it is impossible to tell (Elftman & Manter, 1935; Latimer & Lovejoy, 1989; Aiello & Dean, 1990). The morphology of the cuboid facet is very distinct in modern humans, with a sharp proximal depression in the dorso-medial corner of the facet, which corresponds with the “plantar beak” on the calcaneal facet of the cuboid. In the great apes, the depression for the plantar beak is located far more centrally in the facet, and is far less pronounced (Lewis, 1989).

Talus

The main difference between the talus of the great apes and that of modern humans lies in the morphology of the trochlear surface. In humans the medial and lateral margins of the trochlea lie at similar elevations to each other, but in the great apes the medial margin is relatively depressed plantarly, and the lateral margin relatively elevated dorsally. The result is that the human trochlear surface is essentially horizontal and flat, whilst that of the great ape is angled medially. Great apes also have a far more pronounced trochlear groove. The result of all this is, as Latimer and Lovejoy (1987) point out, that in humans the flat horizontal surface facilitates the passing of the tibia over the talus in a straight path. It has also been noted that the degree of curvature of the posterior calcaneal facet is higher in humans than in the great apes, and that this may cause a reduction in the degree of inversion and eversion in the human foot (Aiello & Dean, 1990).

Cuboid

The most obvious difference between the great ape cuboid and that of modern humans is in the morphology of the modern human calcaneal facet. In modern humans there is a pronounced “plantar beak” that is situated plantarly and medially on the facet. In the great apes the plantar beak is markedly less pronounced and is invariably situated more laterally and often a little more dorsally. As discussed in Chapter 1, the result of this is that the great ape calcaneocuboid joint is a very mobile joint, whilst that of modern humans is an efficient locking mechanism that reaches maximum rigidity during the first half of the stance phase (Lewis, 1980a, 1980b; Aiello & Dean, 1990).

Navicular

The most discernable difference between the navicular of the great apes and that of modern humans, is that the tuberosity is relatively enlarged, distoproximally, dorsoplantarly and mediolaterally (i.e. in all directions), in the great apes. The navicular tuberosity is the principal attachment site of the *tibialis posterior*, which is the main muscle responsible for inversion. One possibility is that since great apes lack a medial longitudinal arch, that the relative massiveness of the tuberosity is due to it being weight bearing (Elftman & Manter, 1935; Sarmiento 2000). Combined with this is the relative proximodistal narrowness of the lateral side of the great ape navicular. In humans the lateral side, relative to the medial side, is fairly long distoproximally. The overall result is that when viewed dorsally, the great ape navicular appears very wedge shaped (with the narrow end of the wedge on the lateral side), whilst the modern human navicular is more rectangular.

Medial Cuneiform

The principal observed difference between the medial cuneiform of modern humans and that of the extant great apes lies in the orientation and degree of curvature of the distal, or hallucial facet. In modern humans it is forward facing, and subsequently in line with the remaining tarso-metatarsal joints, as well as being essentially flat. This results in an adducted hallux that is inline with the remaining metatarsals. This is seen as an adaptation for a strong and energy efficient toe-off in modern humans. In the great apes the joint is orientated in a relatively abducted position, and is considerably curved convexly. The reason for this is that hallucial-medial cuneiform joint is highly movable in the great apes, and is a key component of the grasping foot (Morton 1935; Lewis 1980a; Susman, 1983; Aiello & Dean; 1990; Gebo, 1993).

4.1.2 Summary of locomotor differences between extant hominoids

This is a summary of the in depth section on locomotion in Chapter 1. It is well known that modern humans are obligate, habitual bipeds. Their specific adaptations to bipedal locomotion are unique amongst living primates. *Pan* and *Gorilla* can be both classed as mosaic in their locomotor repertoires. They spend significant amounts of time knuckle

walking (terrestrial quadrupedalism), as well as climbing in the trees, standing bipedally and occasionally shuffling bipedally. *Gorilla* is considered to be slightly more terrestrial than *Pan*, and within the *Pan* clade, *Pan paniscus* has been shown to be slightly more arboreal than *Pan troglodytes*. *Pongo* is almost exclusively arboreal, and can be considered to be a suspensory, climbing and arboreal quadrupedalism specialist. Figure 4.1 summarises what is known about extant hominoid locomotion.

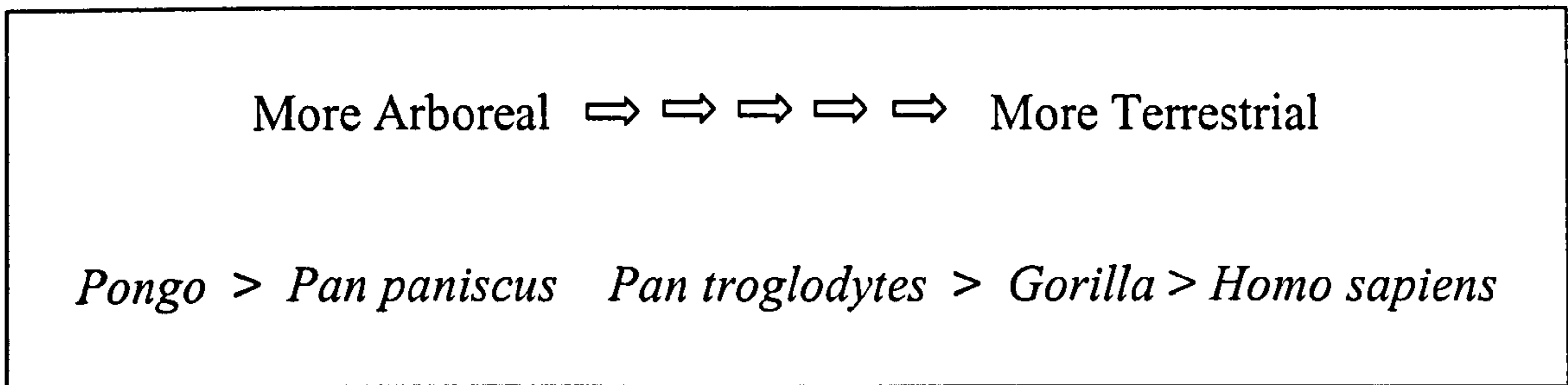


Figure 4.1 Summary of relative degrees of arboreality/terrestriality in the hominoids.

4.1.3 Factors that may account for shape differences between species

Size

Size may play an important role in explaining shape differences between different taxa. Although there is no discussion of this issue in relation to the foot, there is a significant body of literature addressing the relationship between size and shape in the rest of the hominoid skeleton. For instance, Shea (1983) argues that the *Pan paniscus* craniofacial region is a scaled down version of that of *Pan troglodytes*. Recent work by Cobb (2001) refutes this, but it is possibilities such as these that must be ruled out, before explaining morphological differences between taxa by factors such as function or phylogeny.

Function

Shape differences could well be a reflection of functional, and thus possibly locomotor differences. As discussed at length in Chapter 1, the morphology of the tarsal bones in the hominoids is closely related to foot function. Morphologically, tarsal bones are dominated by both muscle attachment sites and joint facets. A case in point is the talus.

If you equate the talus to a structure of six aspects (like a cube), five of those aspects articulate with other bones. Whilst the sixth (posterior) aspect does not articulate with any other bone, it is still functionally important, because it is responsible for channelling the tendon of the *flexor hallucis longus*. The talus is therefore a bone that is functionally important in all of the aspects. The case is similar for the remaining tarsals, and, as such, it would be expected that functional factors should play a key role in explaining the observed morphological separation between taxa.

Phylogenetic propinquity

Shape differences between taxa could also be explained by phylogenetic propinquity. Shape differences observed between taxa could be no more than would be expected as a reflection of phylogenetic relatedness. The current literature on extant hominoid molecular phylogeny is clear that the genetic relationships between the taxa considered in this thesis are relatively well resolved (Ruvolo, 1997; Gagneux & Varki, 2000; Page & Goodman, 2001). Figure 4.2 summarises this relationship.

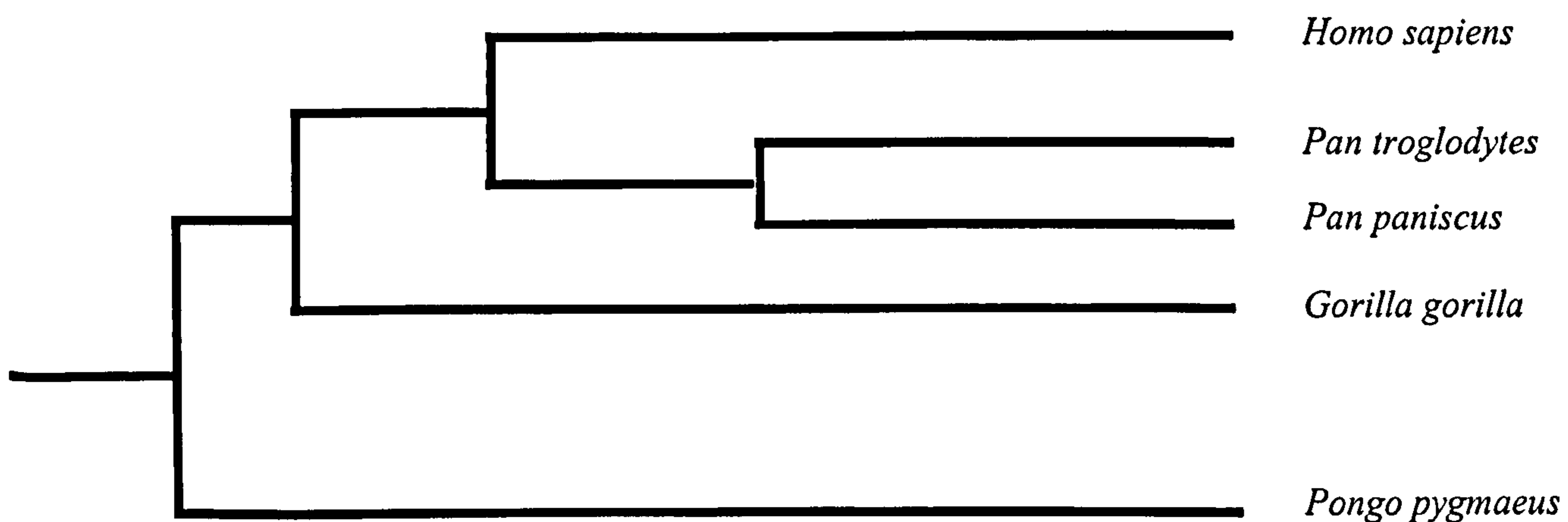


Figure 4.2 Consensus molecular relationships amongst extant hominoidea.

If the molecular phylogeny is taken to be the correct reflection of the relationship between extant hominoids, then it would be interesting to test whether the phenetic similarities between the tarsals of those taxa not only match each other, but also match

the molecular pattern of phylogenetic relatedness. It has recently been shown that there is considerable incompatibility between morphological and molecular phylogenies in primates (Collard & Wood, 2000). Therefore, with the likelihood being high of disparity between the phenetic relationships and the consensus molecular phylogeny, then factors such as function would need to be explored in order to explain the morphological relationships between the tarsals.

4.1.4 Hypotheses

The preceding discussion leads to the formulation of three hypotheses to be tested in this chapter.

H₁ There is a strong and significant relationship between centroid size and shape.

This is tested using Pearson's correlation. H₁ is accepted if two criteria of satisfaction are met. Firstly, if there is a statistically significant p value for the correlation ($p < .05$). Secondly, if the r value is higher than 0.7. If there is no statistically strong and significant relationship between size and shape, then other factors, such as function and behaviour, can be explored to explain shape differences between taxa.

H₂ The phenetic relationships between taxa are consistent for each of the individual tarsals.

This is tested by comparing phenograms of Procrustes means shapes for each bone. If the phenograms are not consistent with each other, then it can be concluded that since some tarsals may be more morphologically distinct than others for particular taxa, then this raises the possibility of those tarsals being more functionally specialised. This has especial importance when considering fossil specimens, where, more often than not, only isolated bones are found. If certain tarsal elements for a taxon are more morphologically distinct than others, then great caution would have to be taken when assigning particular taxonomic affinities to any fossils on the basis of individual bones of the foot.

H₃ The patterns of phenotypic similarity between individual tarsal bones reflects the molecularly determined phylogeny.

This is tested by comparing the phenetic relationships between the Procrustes mean shapes for each bone, and the consensus molecular phylogeny. For H₃ to be accepted, it would have to be shown on the phenograms that the two subspecies of *Pan* cluster together, then both subspecies of *Pan* and *Homo sapiens* clustering together, then *Pan*, *Homo* and *Gorilla*, and then all three plus *Pongo*.

4.1.5 Summary of how results are laid out

Section 4.4.1

The section explores the relationship between the size of each bone (as expressed by centroid size) and its shape (as determined by relevant principal component axes). The significance of the relationship between centroid size and shape is tested using Pearson's correlation.

Section 4.4.2

This section explores the distribution of all the individual specimens relative to each other, how patterns of within group variability relate to between group variability, and whether there are there overlaps in morphology between taxa.

Section 4.4.3

This section describes the actual shape differences between the different taxa. For this, warping from one mean shape to another is demonstrated using TPS grids and screen-captured shots of warped mean shapes.

Section 4.4.4

This section addresses, for each bone, the patterns of distribution of each taxon in relation to each other. For this, tables of Procrustes distances, PCA plots of group means and UPGMA and Maximum Likelihood trees, using mean shapes, are presented and compared.

4.2 Materials

The materials in this study represent one population of modern humans, the Zulus, and four species of extant great apes, *Pan paniscus*, *Pan troglodytes troglodytes*, *Gorilla gorilla gorilla*, and both *Pongo pygmaeus*. The *Pongo* sample consists of approximately equal proportions of both subspecies, *Pongo pygmaeus pygmaeus* and *Pongo pygmaeus abelli*. All samples were half adult males and half adult females. Further details of the provenance of these specimens, criteria for measurement and determination of maturation can be found in the materials section of Chapter 2.

Table 4.1 summarizes the sample sizes for each bone and taxa:

Table 4.1 Sample size for each bone and each taxa

	Medial Cuneiform	Navicular	Cuboid	Talus	Calcaneus
<i>Pongo pygmaeus</i>	32	32	47	43	32
<i>Pan troglodytes troglodytes</i>	40	40	42	44	40
<i>Pan paniscus</i>	15	16	17	15	16
<i>Gorilla gorilla gorilla</i>	41	41	43	42	40
<i>Homo sapiens sapiens</i>	77	79	80	80	78

4.3 Methods

As discussed in Chapter 2, all shapes were Procrustes registered to remove translational, rotational and size differences before being analysed. Principal components analysis was conducted on tangent space projected Procrustes registered coordinates, and shape differences visualised using warped means of wireframe models with flat rendered surfaces. Size related shape-change was investigated by plotting centroid size against each PC axis. The spread of individuals within and between each group was then explored through each PC axis, and then group means were plotted against each other.

Thin Plate Splines (TPS) were also used to more thoroughly explore shape differences between group means.

Correlations

In order to investigate whether there was a correlation between centroid size and any PC axis, Pearson's correlation coefficient (r) was calculated using the statistical software package SPSS. In addition, the program provided p values for each correlation coefficient, which indicate whether an r value is a matter of chance or not.

Permutation tests

For each bone of each taxon, the Procrustes distances between means and the significance of these differences were calculated using the program *Perm PCA*. The program calculates the Procrustes chord distance between two group means, and then randomly permutes distances using the same sample numbers. 3000 permutations were run in each case, and a Procrustes chord distance was deemed to be significant if p was less than 0.05.

Distance Trees

In order to summarise the morphological relationships between taxa for each bone, UPGMA phenograms were constructed using Procrustes distances between the mean shapes of each taxa. This was performed using the program NTSYS (Exeter Software). Maximum Likelihood trees were also constructed as described in Chapter 2.

4.4 Results

4.4.1 Centroid Size

When considering the individual specimens of all taxa together, there was no strong correlation (using Pearson's correlate) found between any PC axis and centroid size. The reason individuals and not group means are used, is that with only five taxa in this analysis (and therefore only five values), it is highly unlikely that significant correlations would be found. As presented in Table 4.2, none of the r values are high enough (>0.7) to suggest a strong association between centroid size and PCs 1, 2 or 3. For any PC axis

beyond PC 3, all r values are very close to zero, and there are no significant p values. The graphs of centroid size versus the PC axes are located in the appendix of this study.

Table 4.2 Correlation between PCs 1 to 3 and Centroid Size for each tarsal

Calcaneus	Sample Size	r value	p value
PC 1 vs. Centroid Size	209	0.452	<0.001
PC 2 vs. Centroid Size	209	0.497	<0.001
PC 3 vs. Centroid Size	209	-0.291	<0.001
Talus			
PC 1 vs. Centroid Size	224	-0.540	<0.001
PC 2 vs. Centroid Size	224	0.166	<0.05
PC 3 vs. Centroid Size	224	-0.100	n.s.
Cuboid			
PC 1 vs. Centroid Size	226	0.587	<0.001
PC 2 vs. Centroid Size	226	0.315	<0.001
PC 3 vs. Centroid Size	226	0.285	<0.001
Navicular			
PC 1 vs. Centroid Size	208	-0.199	<0.01
PC 2 vs. Centroid Size	208	0.577	<0.001
PC 3 vs. Centroid Size	208	-0.073	n.s.
Medial Cuneiform			
PC 1 vs. Centroid Size	205	0.513	<0.001
PC 2 vs. Centroid Size	205	-0.408	<0.001
PC 3 vs. Centroid Size	205	-.414	<0.001

Therefore, for the talus, calcaneus, cuboid, navicular and medial cuneiform, since both criteria of satisfaction are not met in any case, Hypothesis H_1 is rejected for all five tarsals.

4.4.2 Distribution of individual specimens

In this section, only those principal component axes that significantly separate out any of the measured taxa are presented.

4.4.2.1 Calcaneus

As shown in Figure 4.3, PC 1 clearly separates modern humans from the remaining extant great apes. There is no discernable separation between *Pongo*, *Gorilla* or both species of *Pan* on this PC axis. Table 2 shows that PC 1 is responsible for 36.8% of the variance, compared to 10.1% for PC 2, so PC 1 can be considered as the major axis of variation.

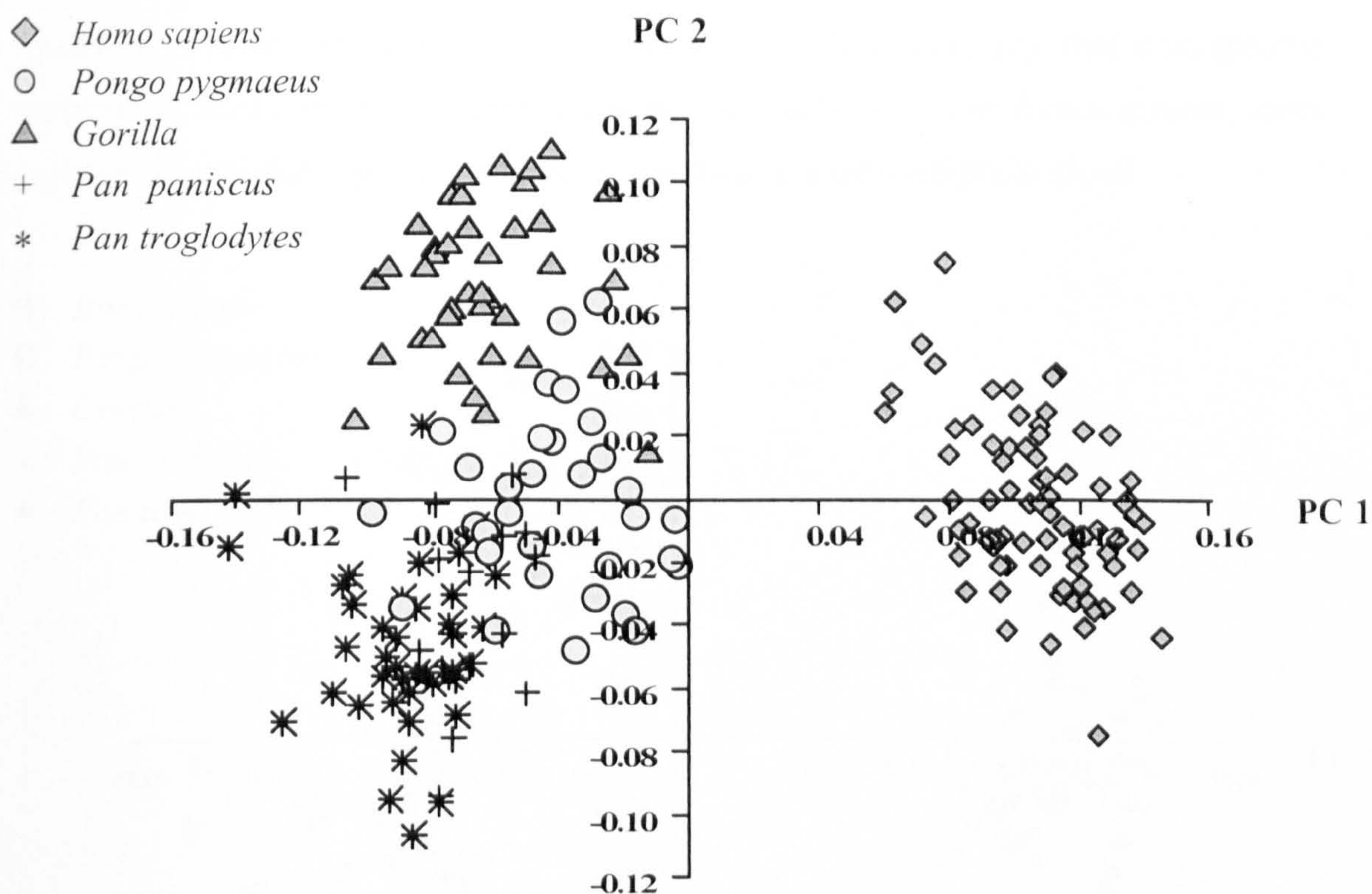


Figure 4.3 Calcaneus: PC 1 versus PC 2.

Table 4.3 Calcaneus: Percentage variance explained by PC 1 to PC 4

Principal Component	Percentage variance
1	36.8%
2	10.1%
3	6.6%
4	4.4%

PC 2 separates the extant great ape taxa from one another, and the separation runs parallel to that axis. *Gorilla* and *Pan*, at the positive and negative ends of the axis respectively, are clearly separated. *Pongo* falls between these two taxa, and overlaps with both. There is no discernable separation between the two species of *Pan* on either PC 1 or PC 2. In terms of distribution of individuals for each taxon, *Pan*, *Pongo* and *Gorilla* all show a relatively circular distribution on PC 1 versus PC 2. That is to say, that intra-specific variation is accounted for, to similar degrees, by each axis. For *Homo sapiens*, more variation is explained by PC 2 than PC 1, resulting in a more elliptical cloud.

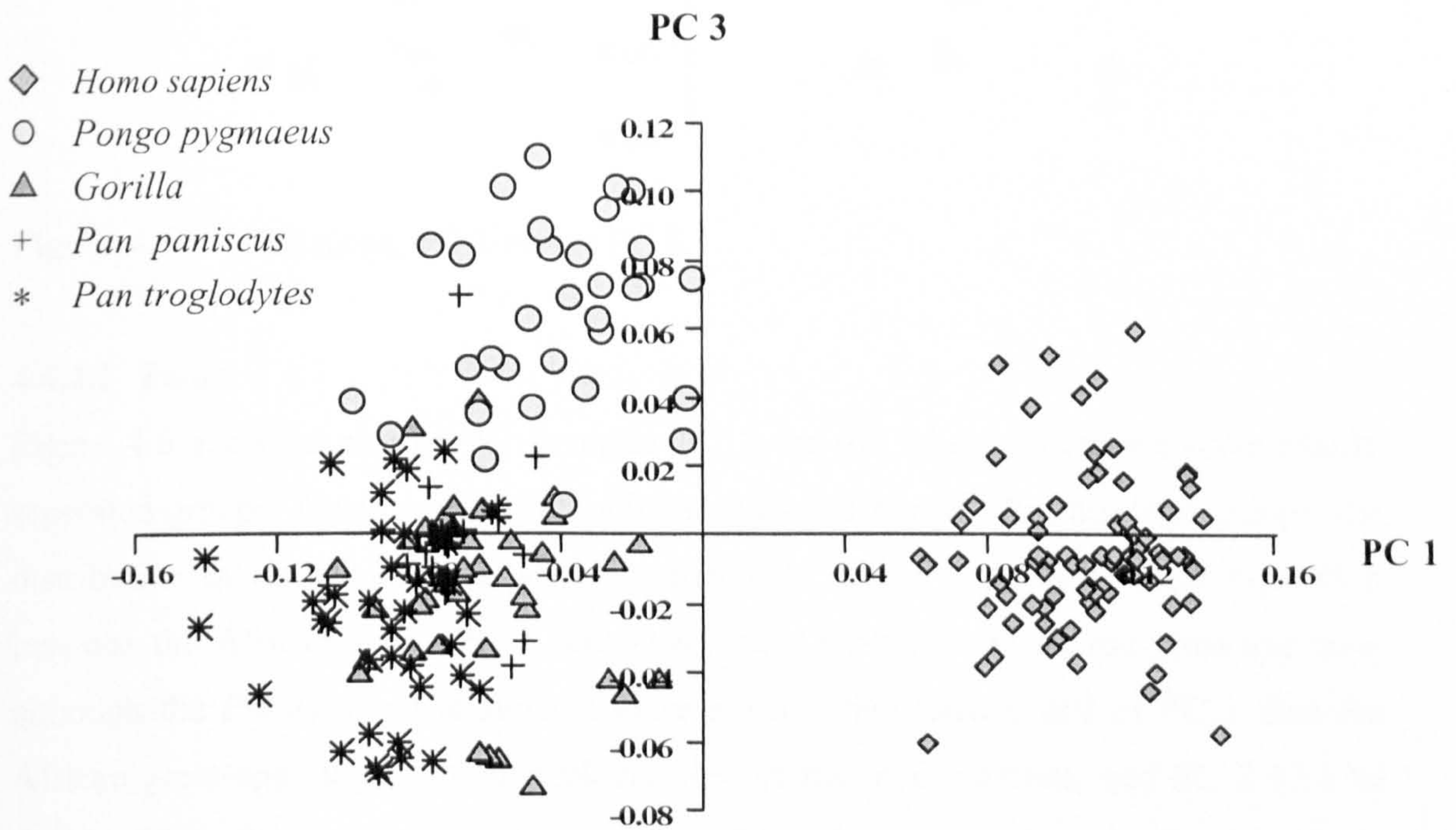


Figure 4.4 Calcaneus: PC 1 versus PC 3.

PC 3 essentially separates *Pongo* from all the other taxa, with *Pongo* lying at the positive end of this axis (Figures 4.4 and 4.5). However, there is a small degree of overlap between *Pongo* and the other taxa.

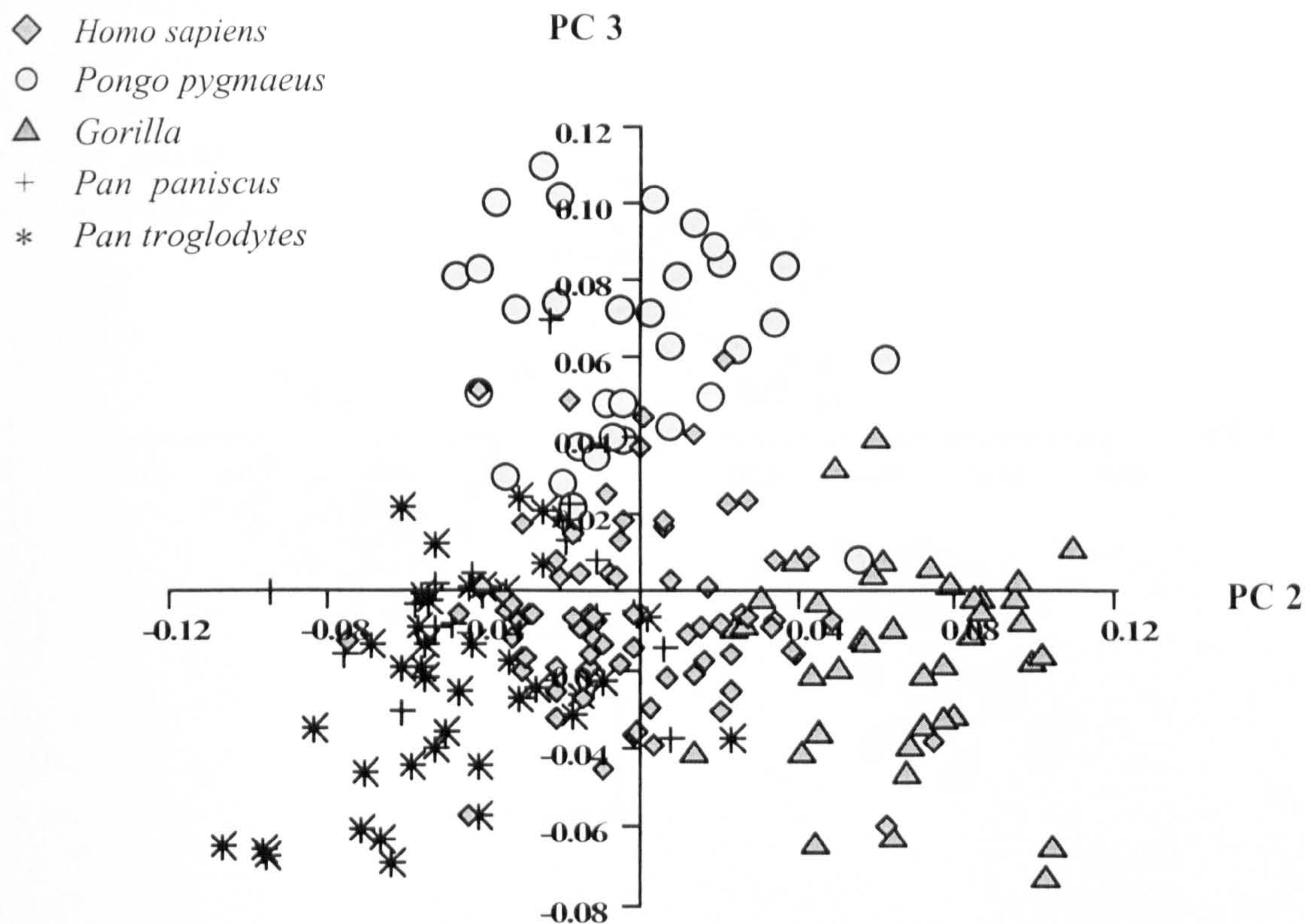


Figure 4.5 Calcaneus, PC 2 versus PC 3.

4.4.2.2 Talus

Figure 4.6 shows a plot of PC 1 versus PC 2 for the talus. There are three clearly separated groups: *Homo sapiens*, the African apes and *Pongo*. For all three groups, the distribution of individuals is relatively spheroidal. There is no discernable separation between the African apes. PC 1 separates *Homo sapiens* from all the great ape taxa, although the *Pongo* cloud is situated more towards the positive end of PC 1 than the African great ape cloud. PC 1 explains 26% of the total variance, and PC 2 13.1 % (Table 4.4). PC 2 clearly separates *Pongo* from the African ape cloud, with *Homo sapiens* falling in between the groups. PC 2 also separates the African ape cloud from

Homo sapiens, although there is a small amount of overlap. There is considerably more overlap between *Pongo* and *Homo sapiens* on this axis.

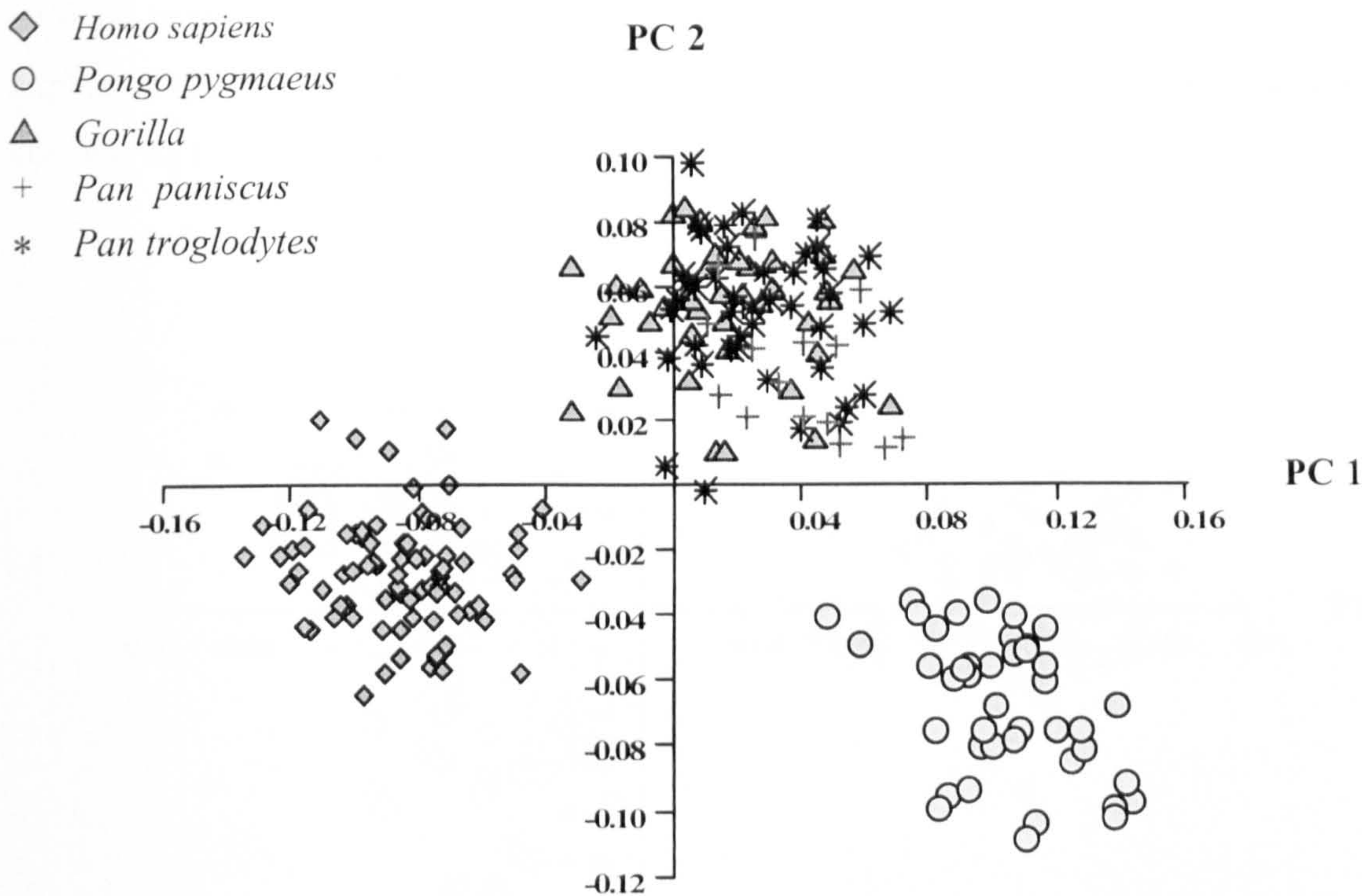


Figure 4.6 Talus, PC 1 versus PC 2.

Table 4.4 Talus: Percentage variance explained by PC 1 to PC 4

Principal Component	Percentage variance
1	26.0%
2	13.1%
3	5.6%
4	4.3%

4.4.2.3 Cuboid

For the cuboid, PC 1 clearly separates *Homo sapiens* from all the great ape taxa (Figure 4.7). However, PC 1 does not separate any of the great ape taxa from each other. PC 2

separates the African apes from *Pongo*, although there is a small degree of overlap. In terms of distribution of individuals, the clouds for *Homo sapiens*, *Pan* and *Gorilla* are all roughly circular, whilst that of *Pongo* is elongated along PC 2, meaning that PC 2 explains more intra-specific variation in *Pongo* than PC 1 does. 37.6% of the variance is explained by PC 1, as opposed to 7.2% for PC 2 (Table 4.5). PC 1 is therefore explaining considerably more variance than PC 2 is.

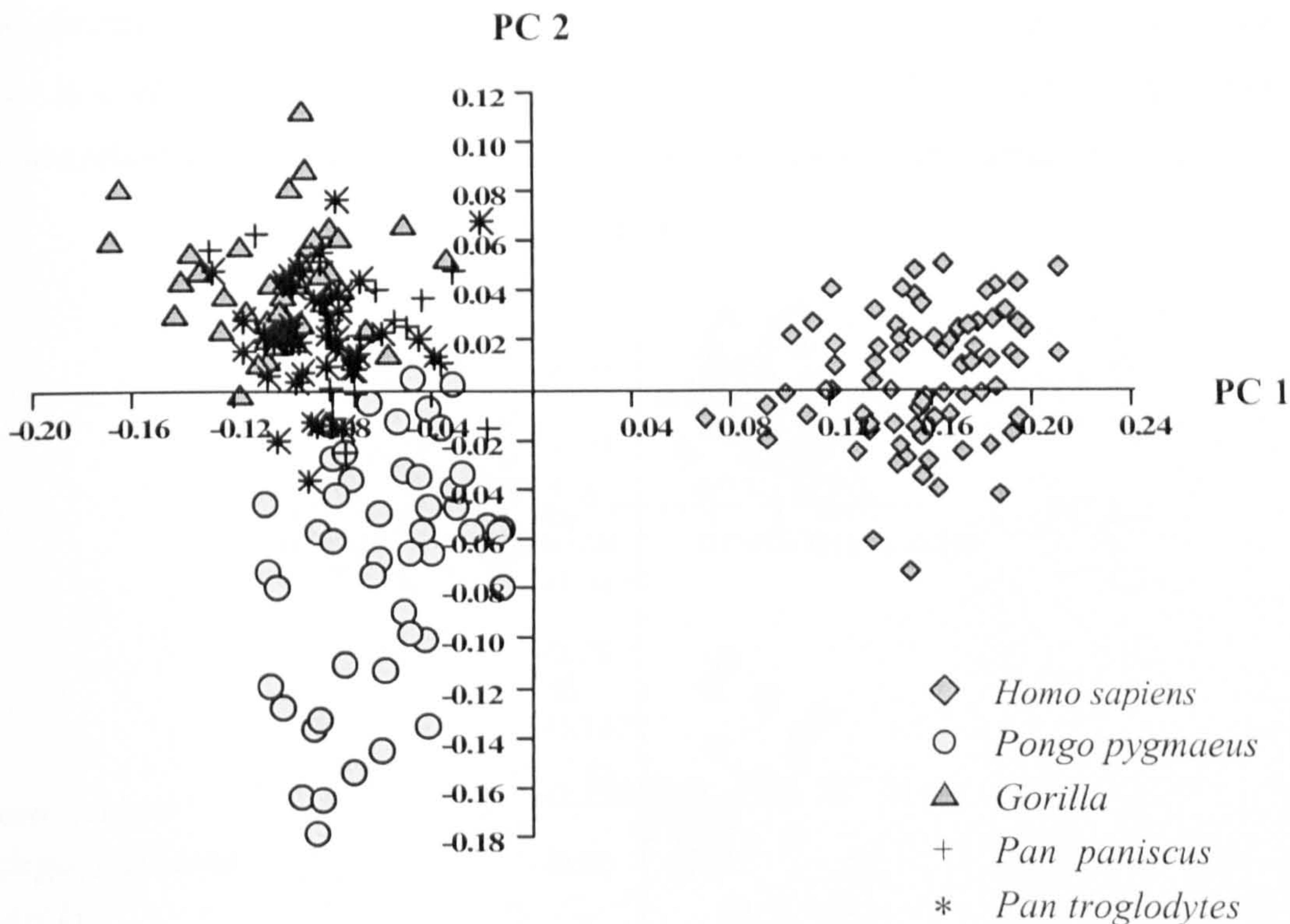


Figure 4.7 Cuboid: PC 1 versus PC 2.

Table 4.5 Cuboid: Percentage variance explained by PC 1 to PC 4

Principal Component	Percentage variance
1	37.6%
2	7.2%
3	5.8%
4	4.3%

4.4.2.4 Navicular

PC 1 versus PC 2 clearly separates *H.sapiens*, the African apes and *Pongo* (Figure 4.8). There is no discernable separation between any of the African ape taxa. Although some *Pongo* outliers overlap with the *H.sapiens* cloud, PC 1 separates the cloud from that of the great apes. PC 2 clearly separates *Pongo* from *H.sapiens* and the African apes, between which there is no discernable difference on this axis. All taxa have fairly circular distributions, but *Pongo* has a greater spread than the other taxa. 25.5% of the variance is explained by PC 1, whilst PC 2 explains 19.1% (Table 4.6). These two figures are relatively close to each other, indicating the relative importance of PC 2.

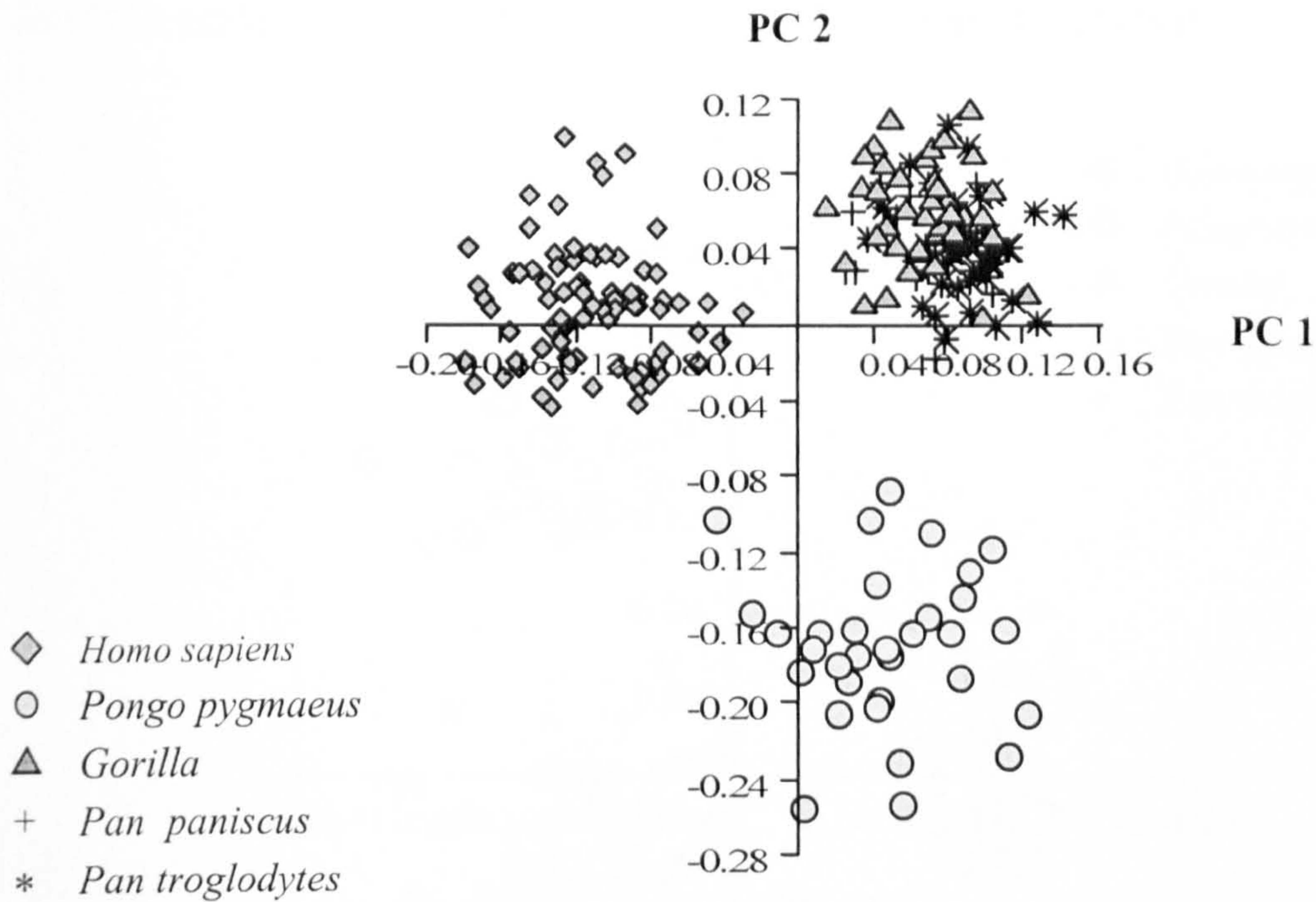


Figure 4.8 Navicular. PC 1 versus PC 2.

Table 4.6 Navicular: Percentage variance explained by PC 1 to PC 4

Principal Component	Percentage variance
1	25.5%
2	19.1%
3	6.8%
4	5.1%

4.4.2.5 Medial Cuneiform

PC 1 versus PC 2 clearly separates three groups: *Homo sapiens*, the African apes and *Pongo* (Figure 4.9). PC 1 separates *H.sapiens* from the remaining great ape taxa. There is no separation between *Pongo* and the African apes on this axis. Within the African ape data cloud, there is a degree of separation between *Pan* and *Gorilla* along PC 1, whilst here is no discernable separation between *Pan paniscus* and *Pan troglodytes*. PC 2 separates *Pongo* from the *H.sapiens* and African ape clouds. In terms of within-species variation, the African ape clouds are relatively circular. The *Pongo* and *H.sapiens* clouds are more elliptical, with PC 1 explaining proportionally more of the variation in *Pongo*, and PC 2 explaining proportionally more of the *Homo sapiens* variation.

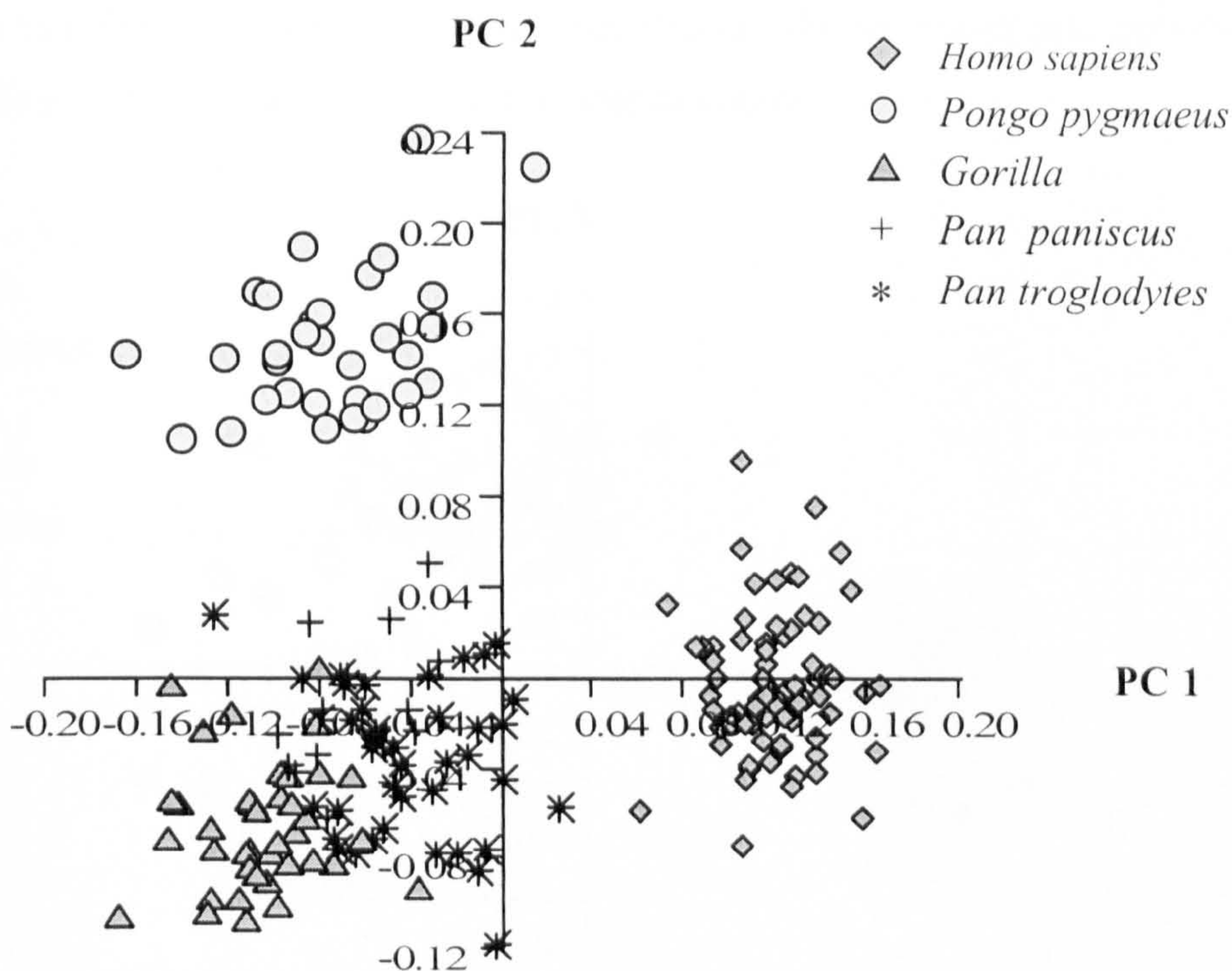


Figure 4.9 Medial Cuneiform. PC 1 versus PC 2.

Table 4.7 Medial Cuneiform: Percentage variance explained by PC 1 to PC 4

Principal Component	Percentage variance
1	33.2%
2	18.4%
3	9.4%
4	4.3%

PC 1 explains 33.2% of the variance, as opposed to 18.4% for PC 2 (Table 4.7). This indicates that a third of the variance is explained by the first principal component. PC 3 separates both species of *Pan* from the *Gorilla* sample (Figure 4.10). *Pongo* and the *Homo sapiens* samples lie between the *Gorilla* and *Pan* clouds, but *Pan* is still essentially distinct, despite a very small amount of overlap due to outliers.

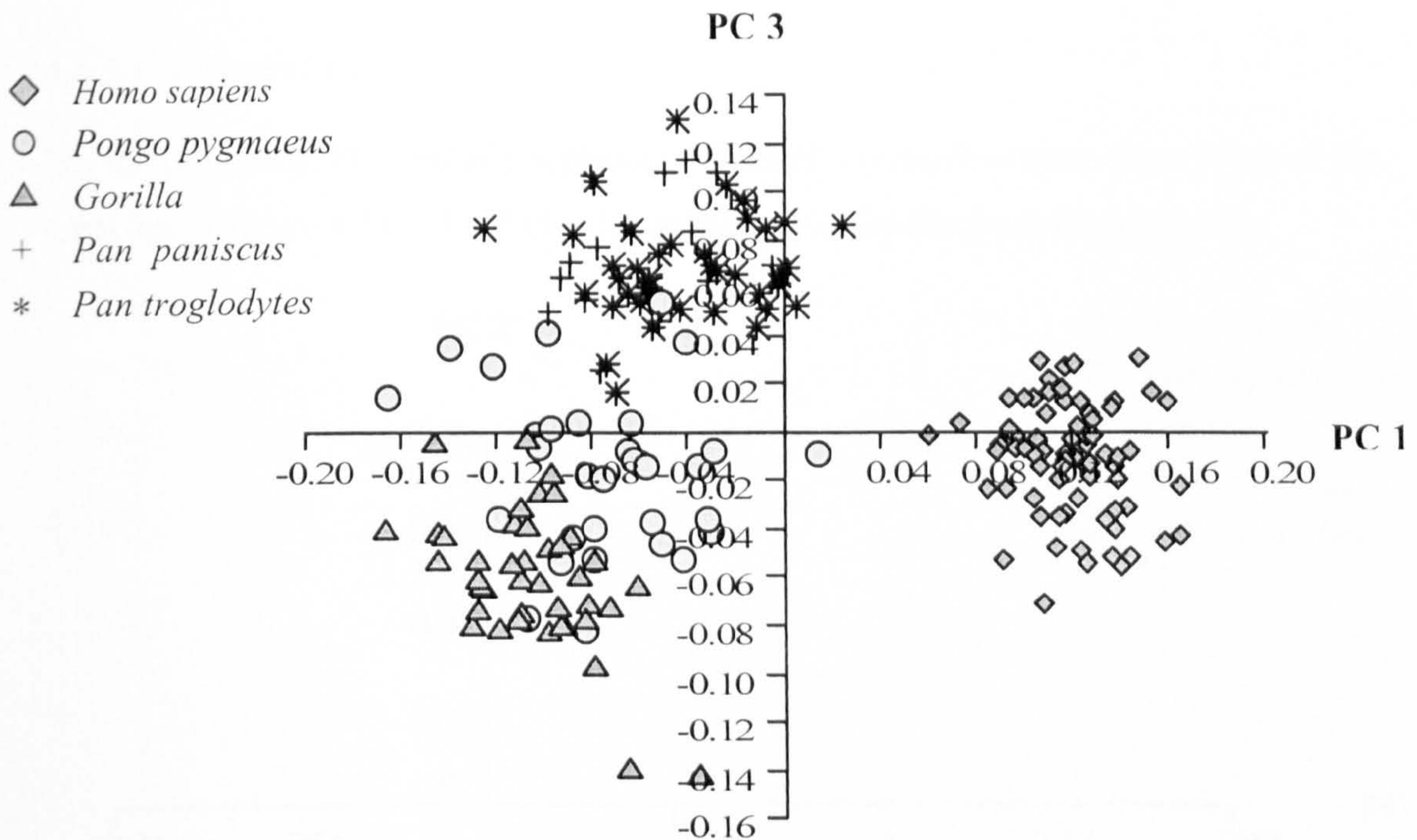


Figure 4.10 Medial Cuneiform: PC 1 versus PC 3.

4.4.3 Shape variation between taxa

This section explores in more depth the shape differences between each taxon. The extent to which size variation explains inter-taxon variation was explored in the previous section through plots of centroid size versus PC axes, and by computation of correlation coefficients between centroid size and various PCs. Although the r values are small, this exploration allows an assessment of the likelihood that size differences alone are sufficient to explain differences between taxa, with residual differences, likely being due to functional causes or phylogenetic propinquity. In this analysis, for each bone, plots are shown using only the mean shape for each taxon. As in the previous section, only those PC axes that separate the taxa are discussed. Furthermore, principal shape differences between taxa, particularly between *Homo sapiens* and the great apes, are described using thin plate spline (TPS) grids. For formatting reasons, these figures are situated at the back of this chapter. Less marked shape differences are described in the text.

4.4.3.1 Calcaneus

For the calcaneus, PC 1 clearly separates out the *Homo sapiens* mean from those of the great apes (Figure 4.11). PC 2 clearly separates out *Gorilla* from the other taxa.

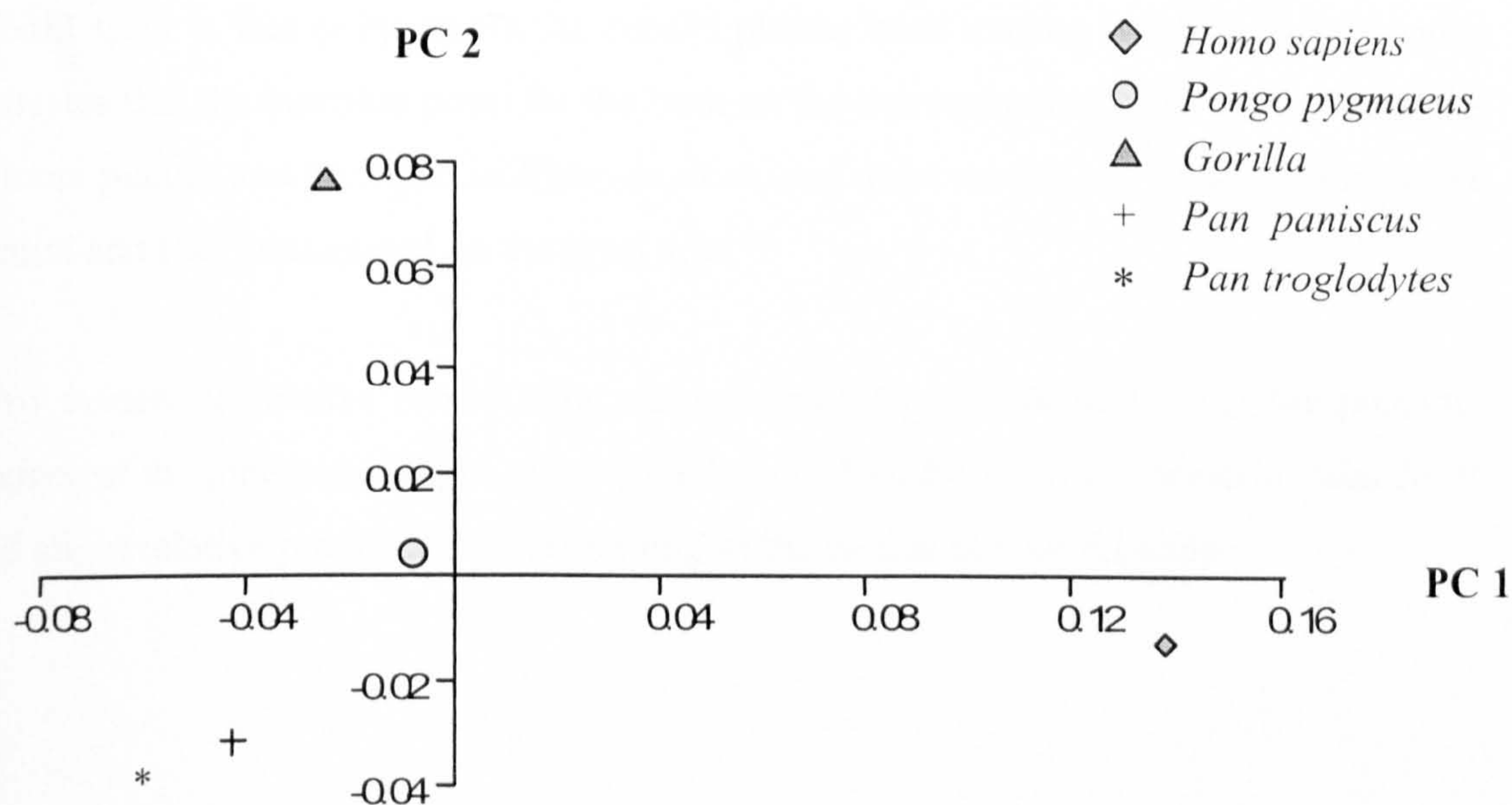


Figure 4.11 Calcaneus Means: PC 1 versus PC 2.

PC 1

The shape variability represented by PC 1 is visualised by warping from the *Homo sapiens* mean to those of the great apes. The distal margin of the anterior talar facet dips plantarly, resulting in a less perpendicular facet to the long axis of the tuberosity. The posterior talar facet also dips slightly dorsally. This is shown in the distal view of the calcaneus in Figure 4.23 at the end of this chapter. The left hand side of the diagram shows shape change that occurs when warping from the *Homo sapiens* to the great ape means, i.e. along PC 1. Note the plane of the horizontal TPS grid above the *Homo sapiens* calcaneus is represented by a line. That is the reference grid, with the target grid being on the ape calcaneus. Arrow “a” indicates the relative movement of the facet when warping along PC 1 from *Homo sapiens* to the great apes. The right hand side of the figure shows what happens when the deformed grid is shifted through the bone plantarly. As can be seen, the medial side of the grid remains plantarly shifted to a distinct degree.

There is also relative lateral and distal shifting of the most proximal point of cuboid facet (upper white arrow for facet “b” in Figure 4.23, and also the back arrow marked “b” on the left hand side of the figure at position 4), combined with relative medial shifting of the most medial point of the facet (lower white arrow). The most proximal point of the cuboid facet is that point where the cuboid plantar beak inserts, and this shape change indicates that the insertion point for the beak on the corresponding facet on the calcaneus is more plantar and proximal in *Homo sapiens*, and more medial and distal, so thus more central and less pronounced, in the great apes.

Also evident is relative mediolateral narrowing of the plantar section of the posterior surface of the tuberosity, slight relative mediolateral widening of the posterior talar facet, and slight relative proximodistal shortening of the medial plantar tubercle.

Table 4.8 Calcaneus means: Percentage variance explained by PC 1 to PC 4

Principal Component	Percentage variance
1	62.7%
2	20.3%
3	13.8%
4	3.2%

PC 2

PC 2 separates *Gorilla* from *Pan*, *Pongo* and *Homo sapiens*. From the negative (*Pan*) end of the axis to the positive (*Gorilla*), there is slight relative narrowing of the plantar section of the posterior surface of the tuberosity, and a relative increase in dorsoplantar length of the posterior surface of the tuberosity. This is mainly due to an increase in relative dorsoplantar length of the attachment area for the *tendo calcaneus*. There is also a marked increase in the proximodistal distance between the tuberosity and the posterior talar facet, relative lateral movement of the dorsal most point of the cuboid facet, and a decrease in the relative distance between the anterior and posterior talar facets.

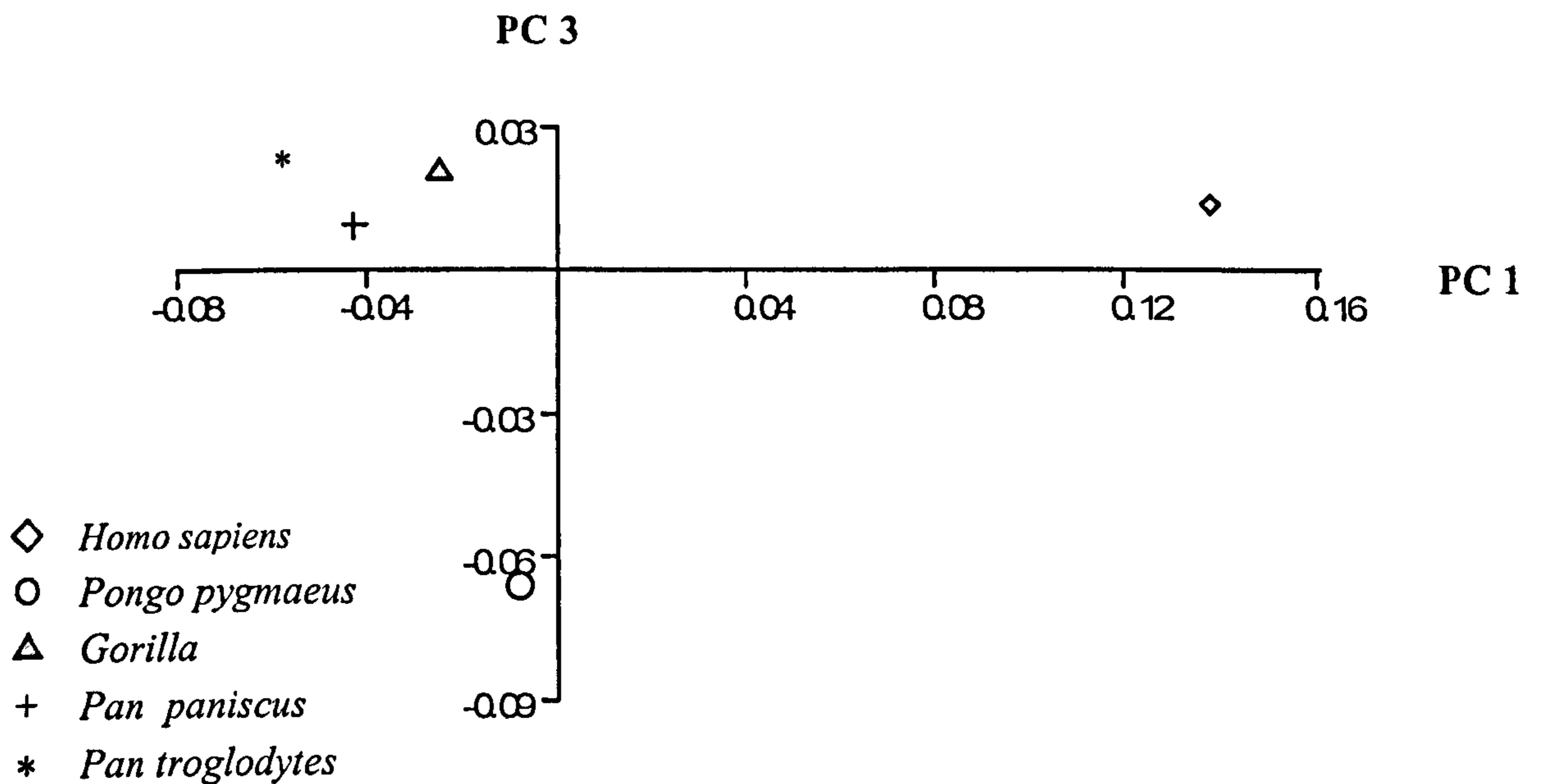


Figure 4.12 Calcaneus Means: PC 1 versus PC 3.

PC 3

PC 3 clearly separates the *Pongo* mean from those of the other taxa, with *Pongo* having a highly negative score on the y-axis (Figure 4.12). Warping from the negative to the positive end of the axis results in marked narrowing of the dorsal section of the posterior surface of the tuberosity, and an increase in the relative dorsoplantar length of the dorsal section (i.e. where *tendo calcaneus* attaches) of the posterior surface.

4.4.3.2 Talus

PC 1 clearly separates the *Homo sapiens* mean from those of the great apes (Figure 4.13). There is also clear separation between the African great apes (which all cluster very tightly) and *Pongo*. Along PC 1, the African apes lie in a position intermediate to *Pongo* and *Homo sapiens*. PC 2 separates African apes from both the *Pongo* and *Homo sapiens* means. The three African ape means cluster very close together on PC 2. The overall result of PC 1 versus PC 2 is that there are three distinct groups: *Homo sapiens*, the African great apes, and *Pongo*.

Table 4.9 Talus means: Percentage variance explained by PC 1 to PC 4

Principal Component	Percentage variance
1	53.5%
2	32.9%
3	9.3%
4	4.2%

PC 1

Warping along PC 1, from *Homo sapiens*, through the great apes, to *Pongo*, a number of shape changes occur. There is a lowering of the medial margin of trochlear surface, relative to the lateral margin. There is also relative elevation of the lateral margin. This can be visualised in both Figures 4.24 and 4.25 at the end of this chapter. In Figure 4.24, the horizontal grid, when warped from *Homo sapiens* to the great apes (i.e. along PC 1) is relatively elevated on the lateral side and dipped on the medial side. The arrows

indicating movement “a” show this on the figure. This can also be seen when looking at the vertical grid in Figure 4.25, where arrows marked “a” indicate dipping of the medial trochlear facet margin, and elevation of the lateral facet margin. There is also increased flattening of the lateral malleolar facet, and an increase in the length of the medial malleolar facet, which is markedly long in *Pongo*.

There is also a relative reduction in the size of the head (navicular facet). This is mainly due to a relative reduction in the dorsoplantar height of the medial side of the head. This is indicated by movement “b” on figures 4.24 and 4.25. The reduction is clearly visible on Figure 4.24, and on grid 5 in Figure 4.25, which sections through the talar head, arrow “b” shows the warping of the grid dorsally. The talar head of *Pongo* is markedly small compared to the other taxa. Warping along PC 1 to *Pongo* also results in an increase in the relative length of the talar neck, particularly on the lateral side, and an increased medial deviation of the talar head. The relative distance between the most distal point of the medial malleolar facet and the talar head does not appear to change, and so it is the increase in the relative length of the medial malleolar facet that is driving the medial deviation of the head. There is also a relative increase in the prominence of the trochlear groove. In Figure 4.26, TPS grids 3 and 4, which correspond to the trochlear groove, show relative plantar deformation, particularly distally. Thus the trochlear groove deepens more distally than proximally in the great apes. Finally, there is a relative decrease in the curvature of the posterior calcaneal facet, with *Homo sapiens* having the most curved facet, and *Pongo*, the least curved.

PC 2

Warping along PC 2, from the *Homo sapiens* and *Pongo* means on the axis to the African ape means, a number of shape changes are observable. Firstly there is relative to the medial margin, marked lengthening of the lateral margin of the trochlear surface. The distal section of the lateral margin is the section that lengthens most dramatically, relative to the proximal section. There is also a relative increase in the degree of convexity of the lateral malleolar facet (i.e. it gets less flat), and relative mediolateral shortening of the proximal section of the trochlear surface. Finally there is decrease in the relative height

of the lateral side of the navicular facet (head). This is essentially a reduction in the distance between the most lateral point of contact between the navicular facet and the anterior calcaneal facet, and the most lateral point of the navicular facet. The result is that in the African apes, the anterior calcaneal facet curls dorsally onto the head far more than it does in either *Pongo* and *Homo sapiens*.

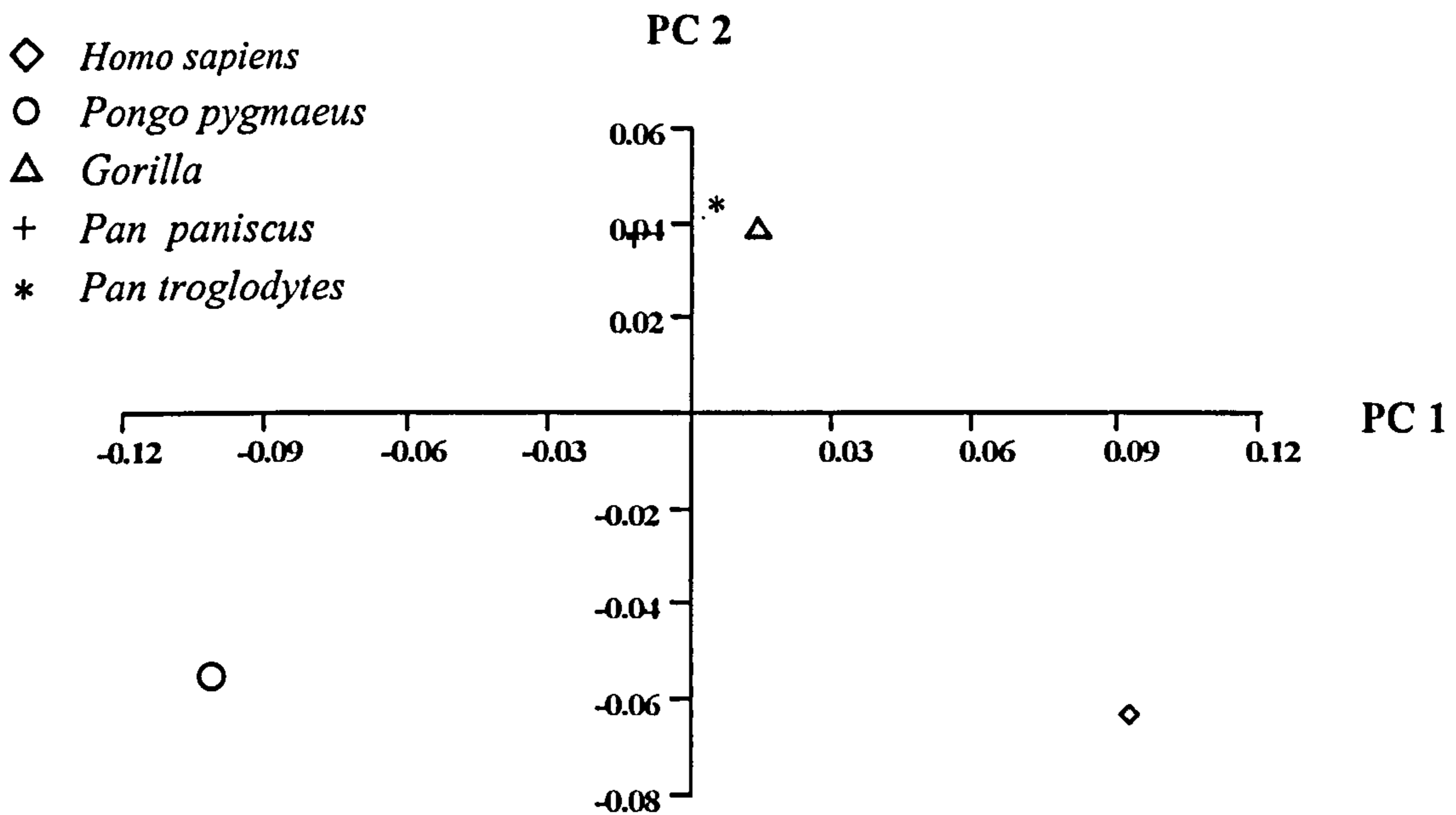


Figure 4.13 Talus Means: PC 1 versus PC 2.

4.4.3.3 Cuboid

PC1 clearly separates the *Homo sapiens* means and those of the great apes (Figure 4.14). There is little difference between the four ape means on PC 1. PC 2 separates the mean for *Pongo* from those of *Homo sapiens* and the African great apes. It must be noted that for both PC 1 and PC2 combined, the African ape means all cluster together very closely.

PC 1

In terms of shape differences, the most striking difference warping from the great apes to *H.sapiens* is the relatively more marked and medio-plantarly orientated plantar beak. Conversely, it can be seen that it is far less pronounced and more medially orientated in the great apes (arrows “a” in Figure 4.27). There are also changes observed in the overall

dimensions of the bone, with the *H.sapiens* cuboid being longer proximo-distally, relative to its medio-lateral breadth, than for any of the great ape taxa (arrows “b” in Figure 4.27). For the distal facet, the 4th metatarsal facet, relative to the 5th metatarsal facet, becomes smaller in overall area. Both facets also become less concave (i.e. they become flatter).

Table 4.10 Cuboid means: percentage variance for Principal components 1 to 4

Principal Component	Percentage variance
1	73.4%
2	14.1%
3	8.6%
4	3.8%

PC2

PC 2 separates *Pongo* from the African apes and *H.sapiens*. There are two principal shape changes that occur when warping from *H.sapiens* and the great apes to *Pongo*. Firstly, the lateral side of the *Pongo* cuboid becomes longer proximo-distally, relative to the medial side. This essentially reduces the “keystone” shape of the cuboid when viewed dorsally. Secondly, the lateral part of the *Pongo* proximal facet dips plantarly, relative to the medial side. This creates a more “crescent” shaped facet in the dorso-plantar plane.

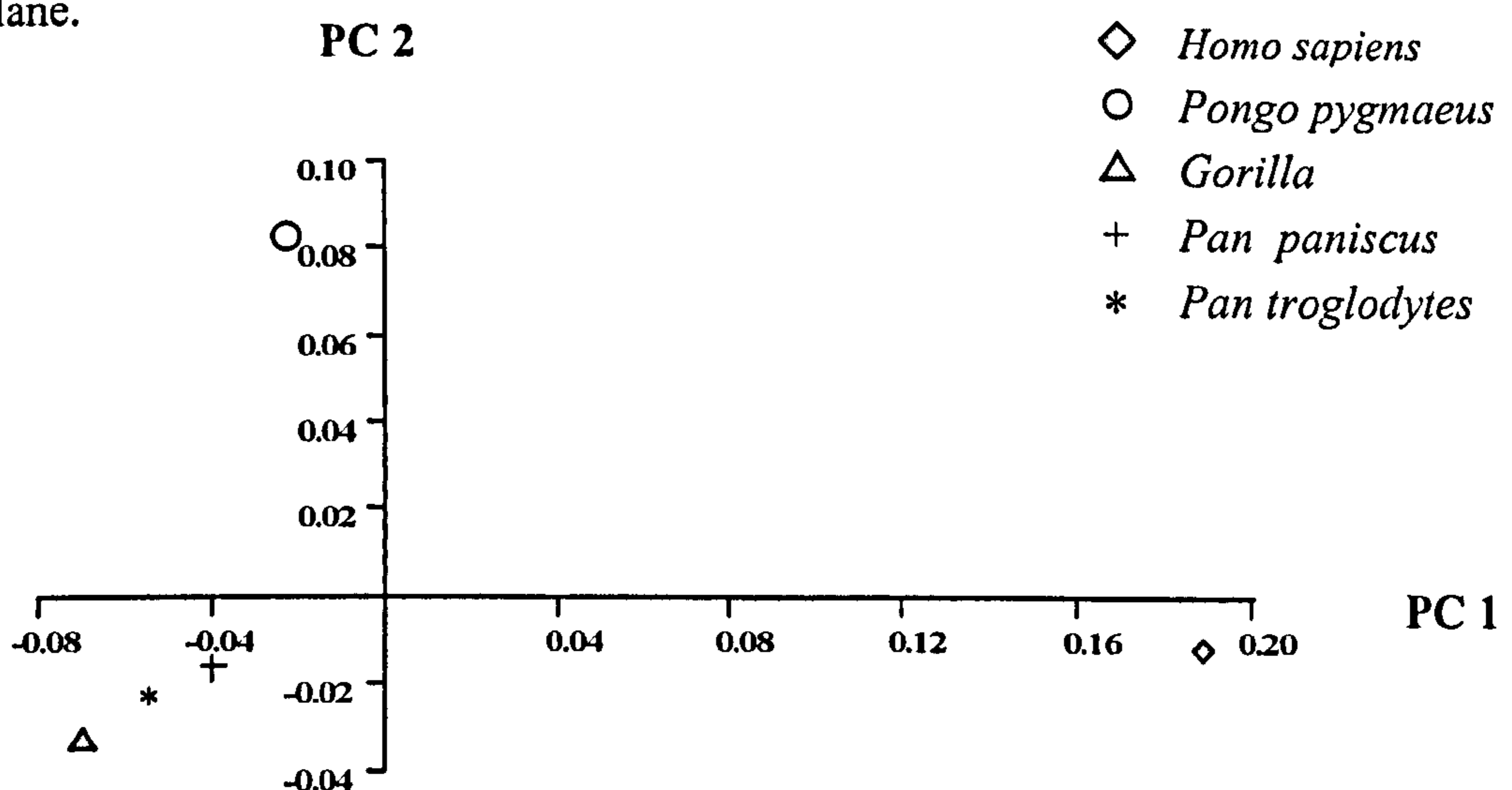


Figure 4.14 Cuboid Means: PC 1 versus PC 2.

4.4.3.4 Navicular

For the navicular the three African ape taxa all group very tightly on PC 1 (Figure 4.15). The *Homo sapiens* mean is relatively close to those of the African apes, but it is the *Pongo* mean that so clearly separates from the other taxa. Therefore, warping along PC 1, from positive to negative, is warping from the African apes and *Homo sapiens*, to *Pongo*. PC 2 clearly separates the *Homo sapiens* from the great ape taxa.

PC 1

Warping from positive (African apes and *Homo sapiens*) to negative (*Pongo*) results in two main shape changes. Most prominently, there is a very marked decrease in size of tuberosity relative to the rest of the bone, particularly mediolaterally. This acts to bring the distal (cuneiform) and proximal (talar) facets more parallel to each other. The tuberosity in *Pongo* appears greatly reduced relative to the African apes and even *Homo sapiens*. There is also a relative increase in the size of the lateral and intermediate cuneiform facets, and a relative decrease in the size of the medial cuneiform facet.

Table 4.11 Navicular means: Percentage variance explained by PC 1 to PC 4

Principal Component	Percentage variance
1	52.8%
2	37.5%
3	6.7%
4	3.1%

PC 2

Warping from the *Homo sapiens* mean to the great apes means, results in a number of shape changes. There is a decrease in the size of the tuberosity, particularly in the mediolateral dimension. There is also an increase in the proximodistal distance between the lateral most points of the distal and proximal facets, relative to the medial side of the bone. This results in the distal and proximal facets being relatively more parallel to each other in *Homo sapiens*, resulting in the human navicular, when viewed dorsally, being

more rectangular, and less wedge-shaped, as in the apes. This shape change can be viewed in Figure 4.28 and 4.29. The black arrows in both Figures 4.28 and 4.29 indicate the relative narrowing of the lateral side of the great ape navicular, and the relative enlargement of the tuberosity. It can be seen that this narrowing is constant through the bone from the dorsal to the plantar surfaces. There is also an increase in the relative dorsoplantar length of the facet margin between the intermediate and lateral cuneiform facets.

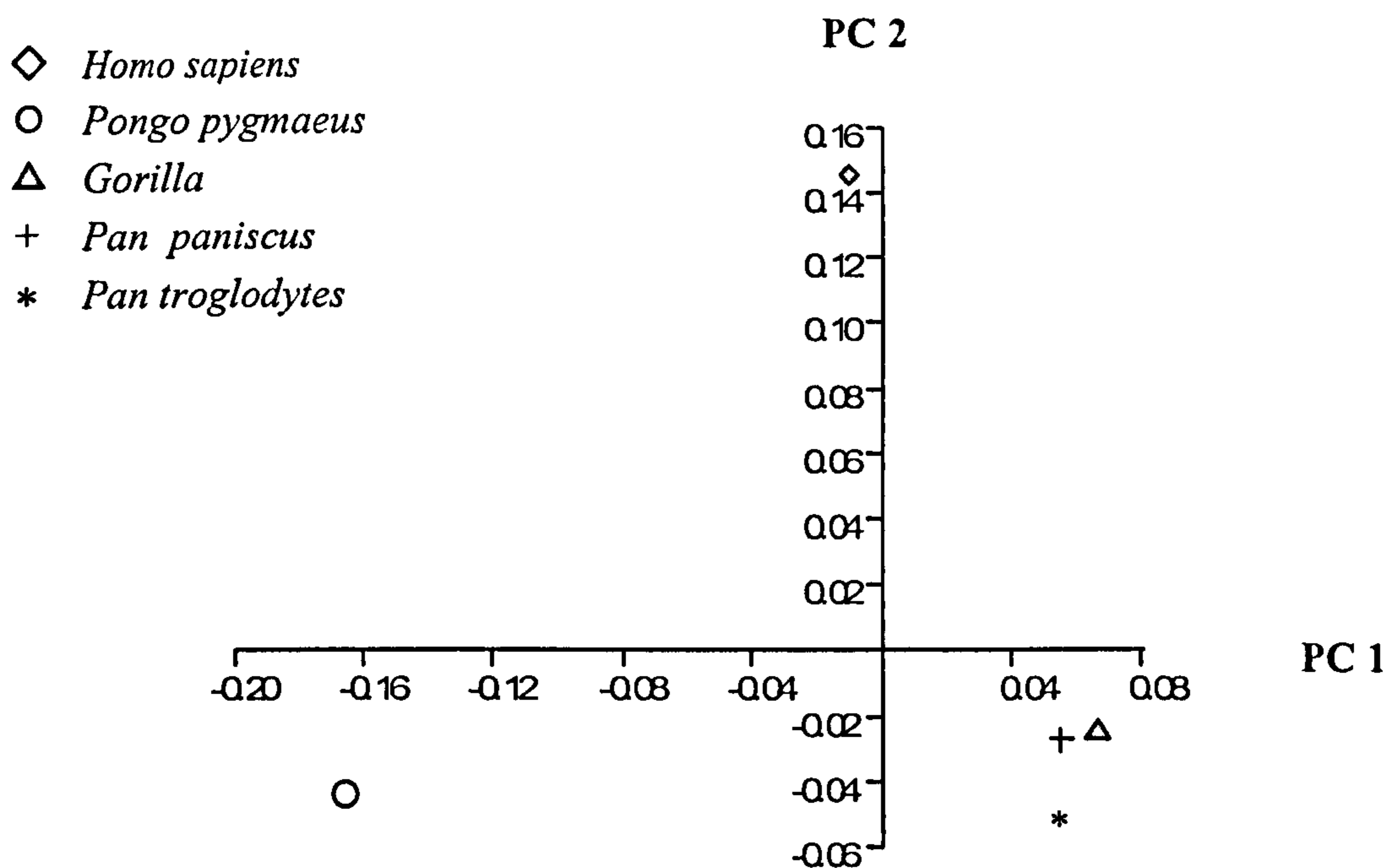


Figure 4.15 Navicular Means: PC 1 versus PC 2.

4.4.3.5 Medial Cuneiform

For the medial cuneiform, there are three approximate groupings on PC 1 versus PC 2: African apes, *Homo sapiens* and *Pongo* (Figure 4.16). PC 1 separates the great ape means from that of *Homo sapiens*, although the *Pongo* mean is situated a little more extremely towards the negative end of the x-axis than the African ape means are. PC 2 is responsible for clear separation between the *Pongo* means and those of the African apes. The *Homo sapiens* mean falls between those two groups. On both PC 1 and 2, the two

subspecies of *Pan* are very similar to each other. On Figure 4.17, PC 1 versus PC 3, there is clear separation between the means of *Pan* and that of *Gorilla*. Both *Pongo* and *Homo sapiens* are intermediate between the groups.

Table 4.12 Medial Cuneiform means: Percentage variance explained by PC 1 to PC 4

Principal Component	Percentage variance
1	42.2%
2	36.9%
3	18.3%
4	2.6%

PC 1

Warping of the overall mean from *Homo sapiens* (positive) to the great ape (negative) ends of PC 1 results in a number of shape changes. There is marked curving of the hallucial facet, with the medial margin of the hallucial facet moving relatively proximally and medially, resulting in relative proximodistal reduction of the medial surface. This shifting of the medial margin is demonstrated with the use of warped TPS grids in Figure 4.30. The white arrows in the upper diagram indicate the relative movement of the medial facet margin of the hallucial facet. Likewise, in the lower schematic on Figure 4.30, grid 5, which corresponds to the position of the facet, shows the greatest degree of distortion, with the medial end of the grid warped proximally, and its centre bulging out distally, as signified by the black arrows. Figure 4.31 also shows this if the grid is shown in a different orientation. Note the marked proximodistal narrowing of the grid on the medial side of the bone, as signified by the black arrows. This is particularly evident on distal end of the grid, which is a result of the proximal shifting of the hallucial medial facet margin. The shift from the human flat facet to the great ape convex facet can be easily seen by viewing the bone dorsally, as in Figure 4.32. The warped TPS grids 1 to 4, show that from dorsal to plantar ends of the bone, the most warping occurs in the region of the hallucial facet. The black arrows indicate the direction of the warping, and it can be seen that the great ape hallucial facet becomes markedly convex. This is particularly apparent on the plantar section of the facet, as shown in TPS grid 4. It can also be seen

from Figure 4.32 that warping from *Homo sapiens* to the great apes results in the hallucial facet undergoing medial rotation (relative to navicular facet) so that it is essentially more medial facing, or abducted.

PC 2

Warping from the African apes and *Homo sapiens* (positive) to *Pongo* (negative) results in a number of subtle changes. The most marked change is on the proximal (navicular) facet, where there is marked dorsoplantar shortening (relatively) when warping from *Homo sapiens* and African great apes to *Pongo*. There is also increased angulation of the dorsal section of the hallucial facet (i.e. the facet gets more convex), a relative reduction of the dorso-plantar height and medio-lateral width of the hallucial facet (i.e. it gets relatively smaller), a slight relative increase in the distance between the hallucial and navicular facets, and a slight relative increase in the length of the lateral facet, which becomes relatively longer and thinner.

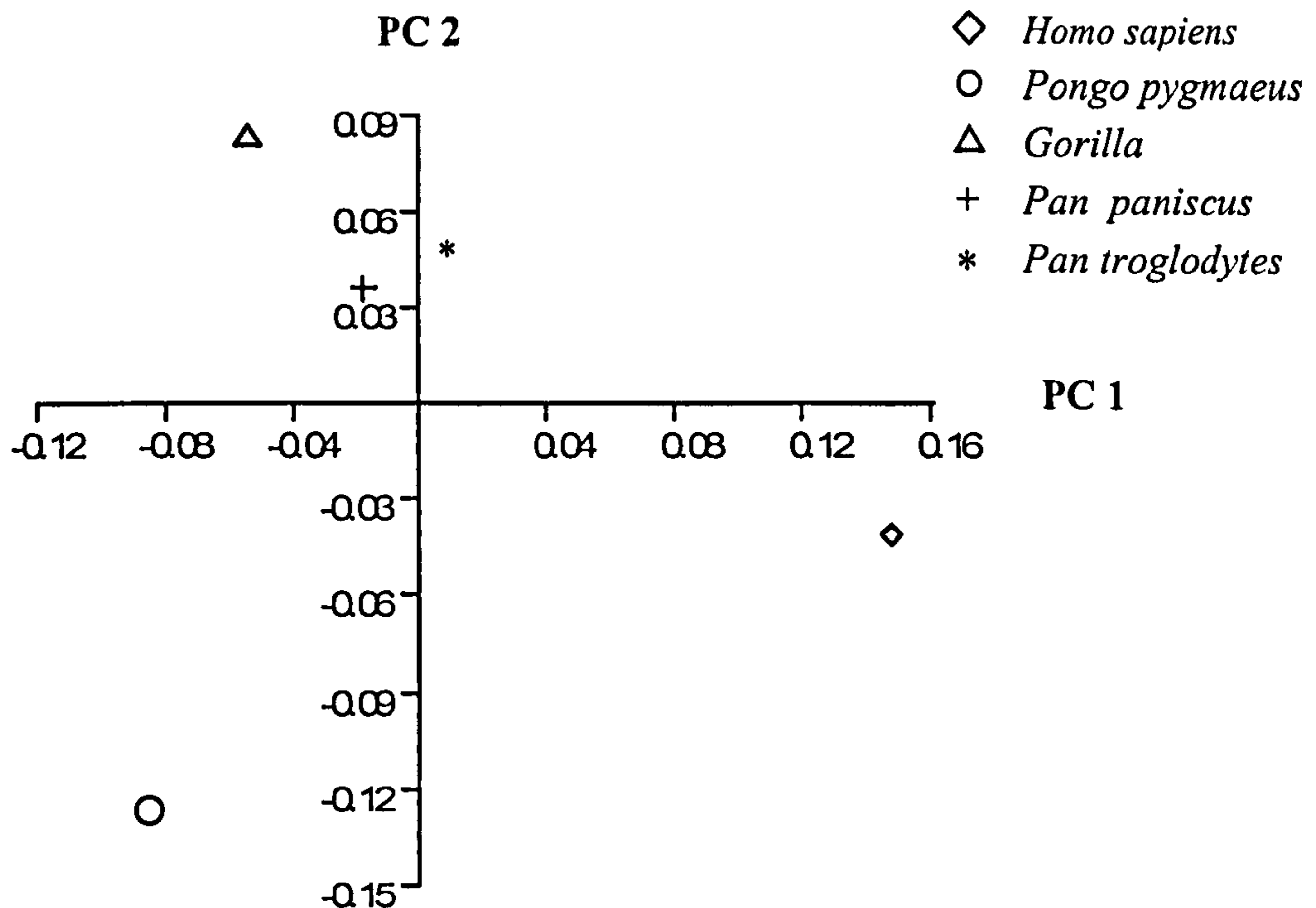


Figure 4.16 Medial Cuneiform means: PC 1 versus PC 2.

PC 3

Warping from the positive end of PC 3 (*Pan*) to the negative (*Gorilla*) results in a slight flattening and distolateral shifting of the hallucial facet. This is an indication of a less opposable hallux in *Gorilla*, when compared to *Pan*, but the difference is only slight.

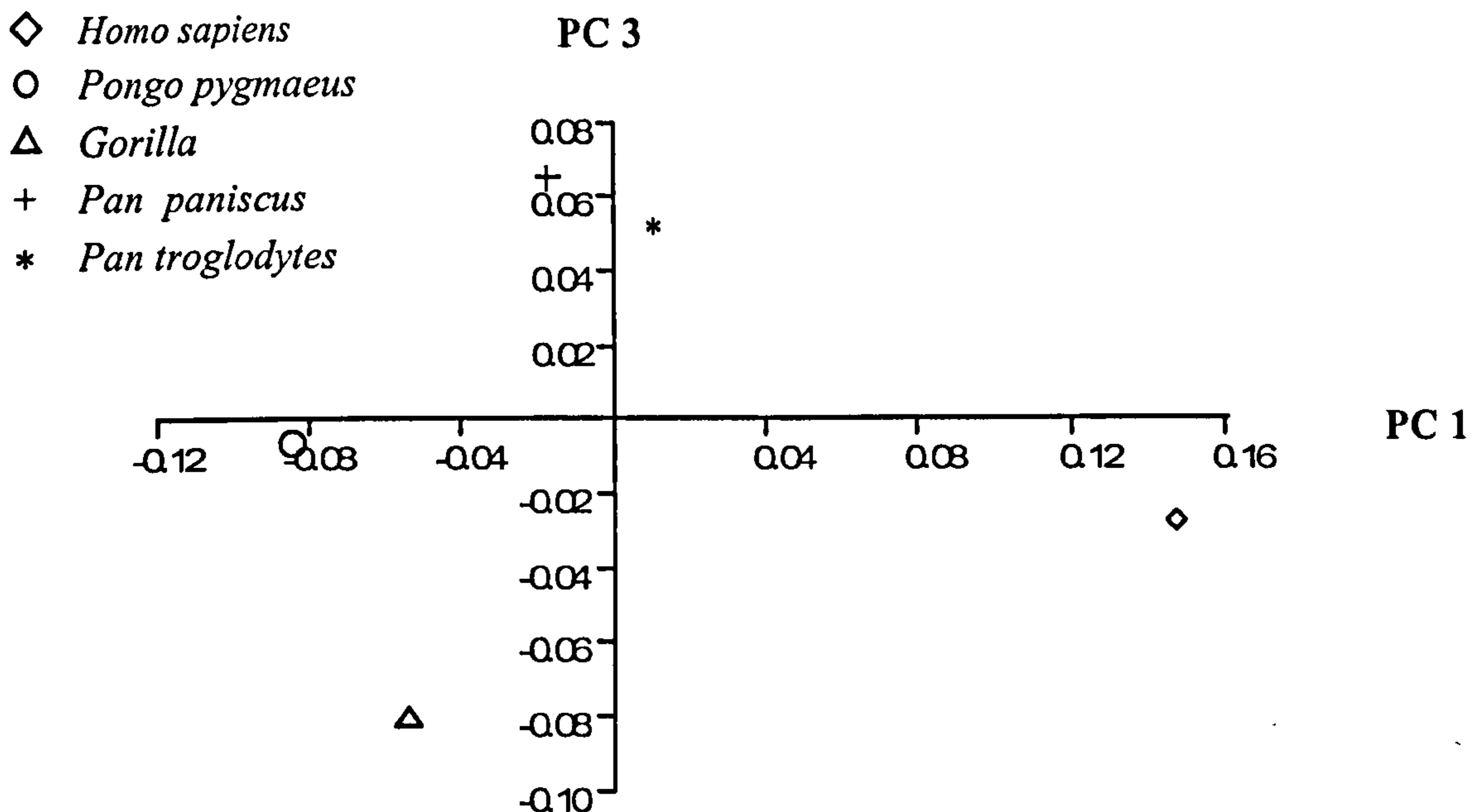


Figure 4.17 Medial Cuneiform means: PC 1 versus PC 3.

4.4.4 Statistical relationships between taxa

This section looks, per tarsal, at the Procrustes distances and their significance, between mean shapes for each taxon. The relative relationships between taxa for each bone, are then explored using distance trees.

Tables 4.13 to 4.7 show the pairwise Procrustes distances between means, and the significance of those distances after 3000 permutations. It can be seen that for every bone, all taxa were significantly different in shape from each other, with $p < .0003$ in each and every case (when running 3000 permutations, .0003 is the lowest possible p value the software can give). So, all the mean shapes for the taxa are highly significantly

different from each other. However, observation of the tables shows that whilst all means are significantly different to each other, the absolute Procrustes distances between mean shapes are very varied. This indicates that some taxa, whilst significantly different in shape, are morphologically more similar to each other than to other taxa. The relationship between taxa, for each bone, is illustrated by UPGMA phenograms, based on the Procrustes distances between means.

Table 4.13 Calcaneus: Procrustes distances and significance of those distances from pairwise permutation tests of each mean species shape versus all other mean species shapes. Upper number is the Procrustes distance between means and the lower one is the *p* value.

	<i>Pongo</i>	<i>Pan troglodytes</i>	<i>Pan paniscus</i>	<i>Gorilla</i>
<i>Pan troglodytes</i>	0.1127 p<.0003			
<i>Pan paniscus</i>	0.0954 p<.0003	0.0555 p<.0003		
<i>Gorilla gorilla gorilla</i>	0.1132 p<.0003	0.1198 p<.0003	0.1124 p<.0003	
<i>Homo sapiens</i>	0.1649 p<.0003	0.2011 p<.0003	0.1822 p<.0003	0.1834 p<.0003

Table 4.14 Talus: Procrustes distances and ratings of significance for pairwise permutation tests of each mean species shape versus all other mean species shapes. Upper number is the Procrustes distance between means and the lower one is the *p* value.

	<i>Pongo</i>	<i>Pan troglodytes</i>	<i>Pan paniscus</i>	<i>Gorilla</i>
<i>Pan troglodytes</i>	0.1466 p<.0003			
<i>Pan paniscus</i>	0.1368 p<.0003	0.0631 p<.0003		
<i>Gorilla gorilla gorilla</i>	0.1523 p<.0003	0.0646 p<.0003	0.0845 p<.0003	
<i>Homo sapiens</i>	0.1926 p<.0003	0.1407 p<.0003	0.1496 p<.0003	0.1367 p<.0003

Table 4.15 Cuboid: Procrustes distances and ratings of significance for pairwise permutation tests of each mean species shape versus all other mean species shapes. Upper number is the Procrustes distance between means and the lower one is the *p* value.

	<i>Pongo</i>	<i>Pan troglodytes</i>	<i>Pan paniscus</i>	<i>Gorilla</i>
<i>Pan troglodytes</i>	0.1194 p<.0003			
<i>Pan paniscus</i>	0.1136 p<.0003	0.0703 p<.0003		
<i>Gorilla gorilla gorilla</i>	0.1321 p<.0003	0.0956 p<.0003	0.1009 p<.0003	
<i>Homo sapiens</i>	0.2288 p<.0003	0.2466 p<.0003	0.2329 p<.0003	0.2616 p<.0003

Table 4.16 Navicular: Procrustes distances and ratings of significance for pairwise permutation tests of each mean species shape versus all other mean species shapes. Upper number is the Procrustes distance between means and the lower one is the *p* value.

	<i>Pongo</i>	<i>Pan troglodytes</i>	<i>Pan paniscus</i>	<i>Gorilla</i>
<i>Pan troglodytes</i>	0.2222 p<.0003			
<i>Pan paniscus</i>	0.2262 p<.0003	0.0945 p<.0003		
<i>Gorilla</i>	0.2325 p<.0003	0.0725 p<.0003	0.0819 p<.0003	
<i>Homo</i>	0.2403 p<.0003	0.2062 p<.0003	0.1907 p<.0003	0.1888 p<.0003

Table 4.17 Medial Cuneiform: Procrustes distances and ratings of significance for pairwise permutation tests of each mean species shape versus all other mean species shapes. Upper number is the Procrustes distance between means and the lower one is the p value.

	<i>Pongo</i>	<i>Pan troglodytes</i>	<i>Pan paniscus</i>	<i>Gorilla</i>
<i>Pan troglodytes</i>	0.2059 p<.0003			
<i>Pan paniscus</i>	0.191 p<.0003	0.0699 p<.0006		
<i>Gorilla gorilla gorilla</i>	0.2218 p<.0003	0.1512 p<.0003	0.1583 p<.0003	
<i>Homo sapiens</i>	0.2461 p<.0003	0.185 p<.0003	0.2049 p<.0003	0.24 p<.0003

4.4.4.1 Phenograms

For each table of Procrustes distances between the species mean shapes (i.e. per bone) a UPGMA phenogram is constructed (see methods section of this chapter plus Chapter 2).

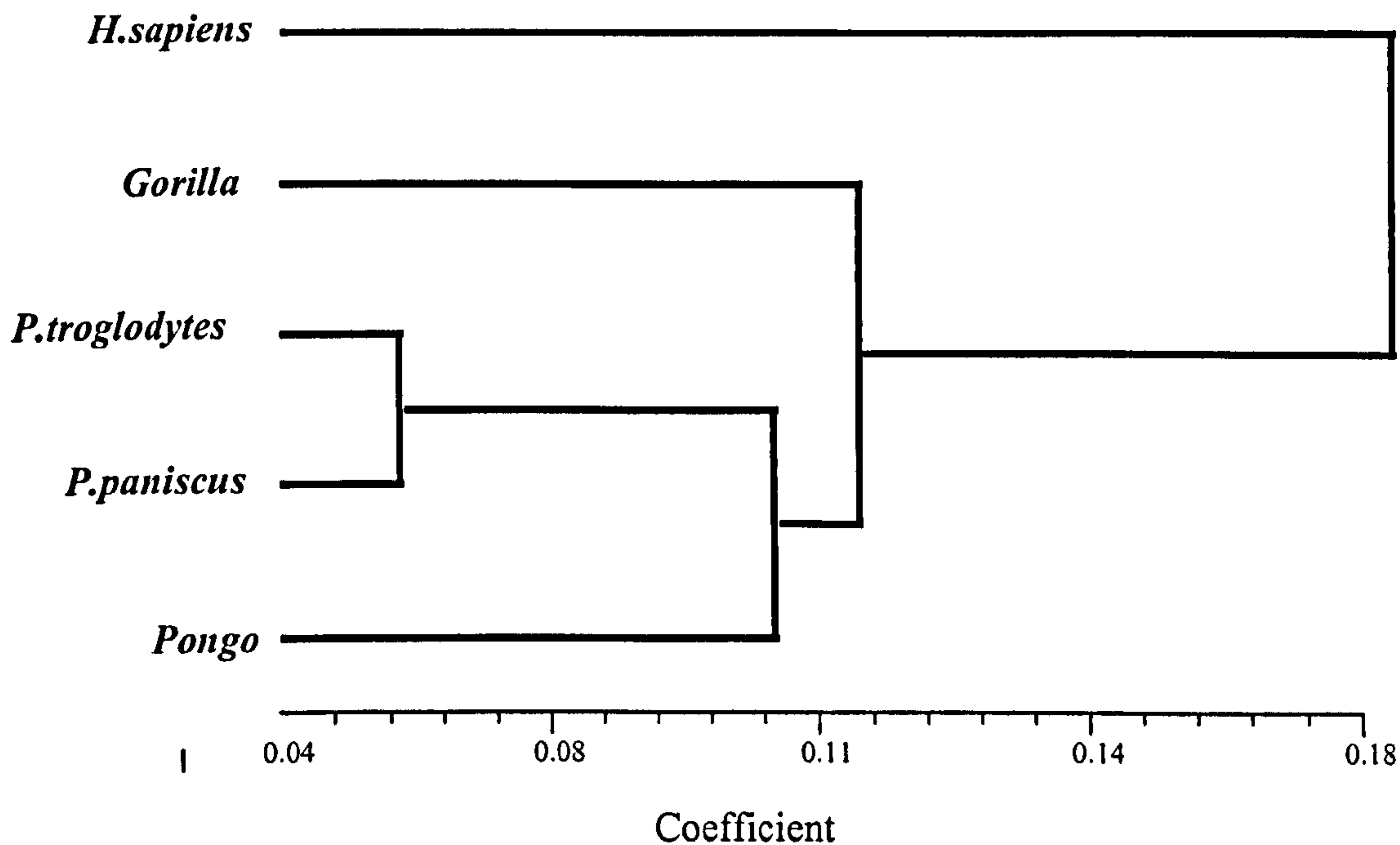


Figure 4.18 Calcaneus: UPGMA phenogram using Procrustes distances between means.

For the calcaneus, the great apes are all closer to each other than any are to *Homo sapiens* (Figure 4.18). Within the ape grouping, *Pan paniscus* and *Pan troglodytes* group to the exclusion of *Pongo* and *Gorilla*. The two species of *Pan* group with *Pongo* to the exclusion of *Gorilla*, although it must be noted that the distances between *Gorilla* to *Pan*, and *Pongo* to *Pan*, are very similar to each other.

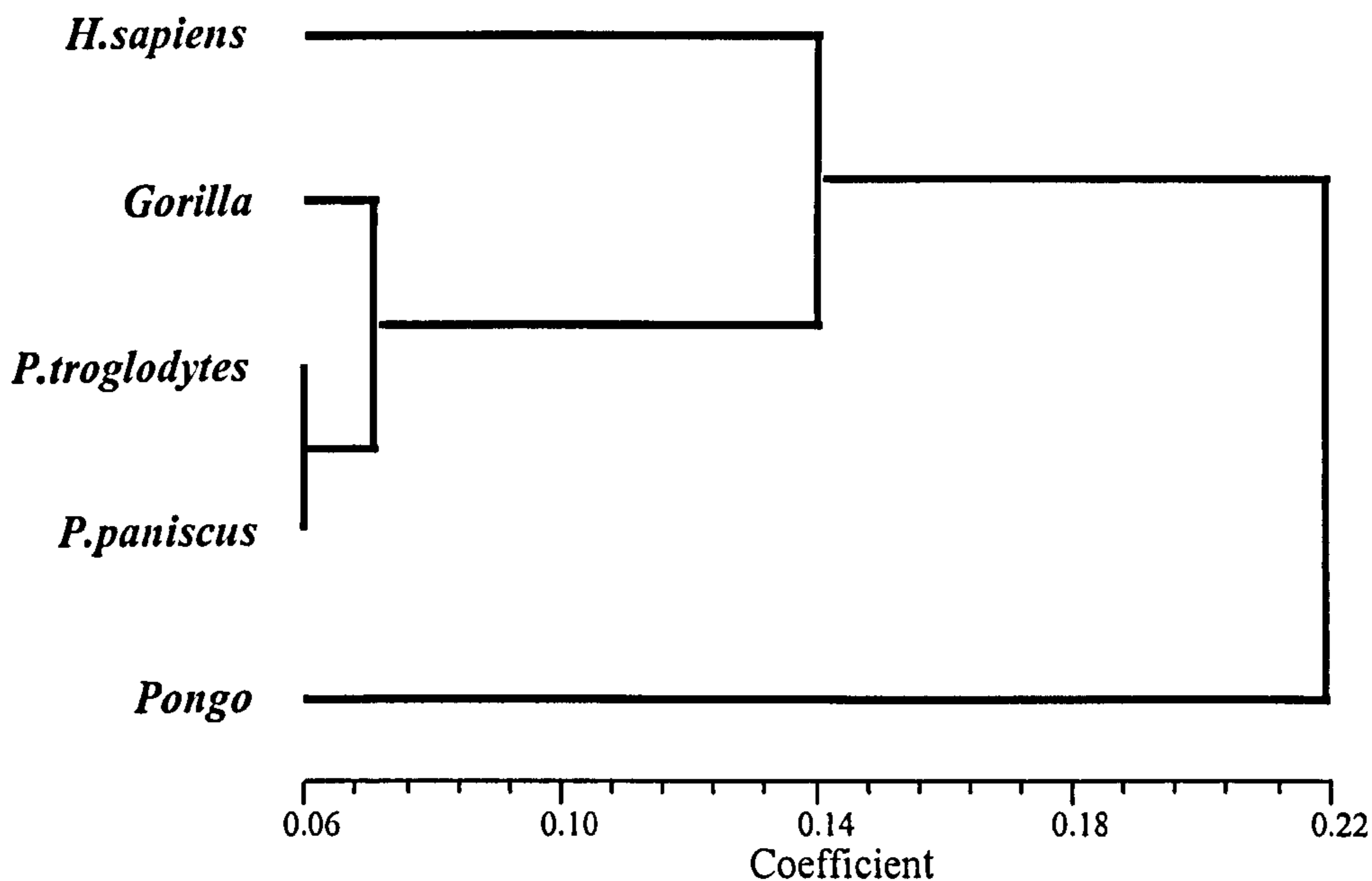


Figure 4.19 Talus: UPGMA phenogram using Procrustes distances between means.

The UPGMA phenogram for the mean talar shapes, shows that *Pongo* separates to the exclusion of all the other taxa (Figure 4.19). The African apes all cluster together to the exclusion of *Homo sapiens*, and the two species of *Pan* group together to the exclusion of *Gorilla*. All the African apes are very close to each other in terms of absolute Procrustes distance.

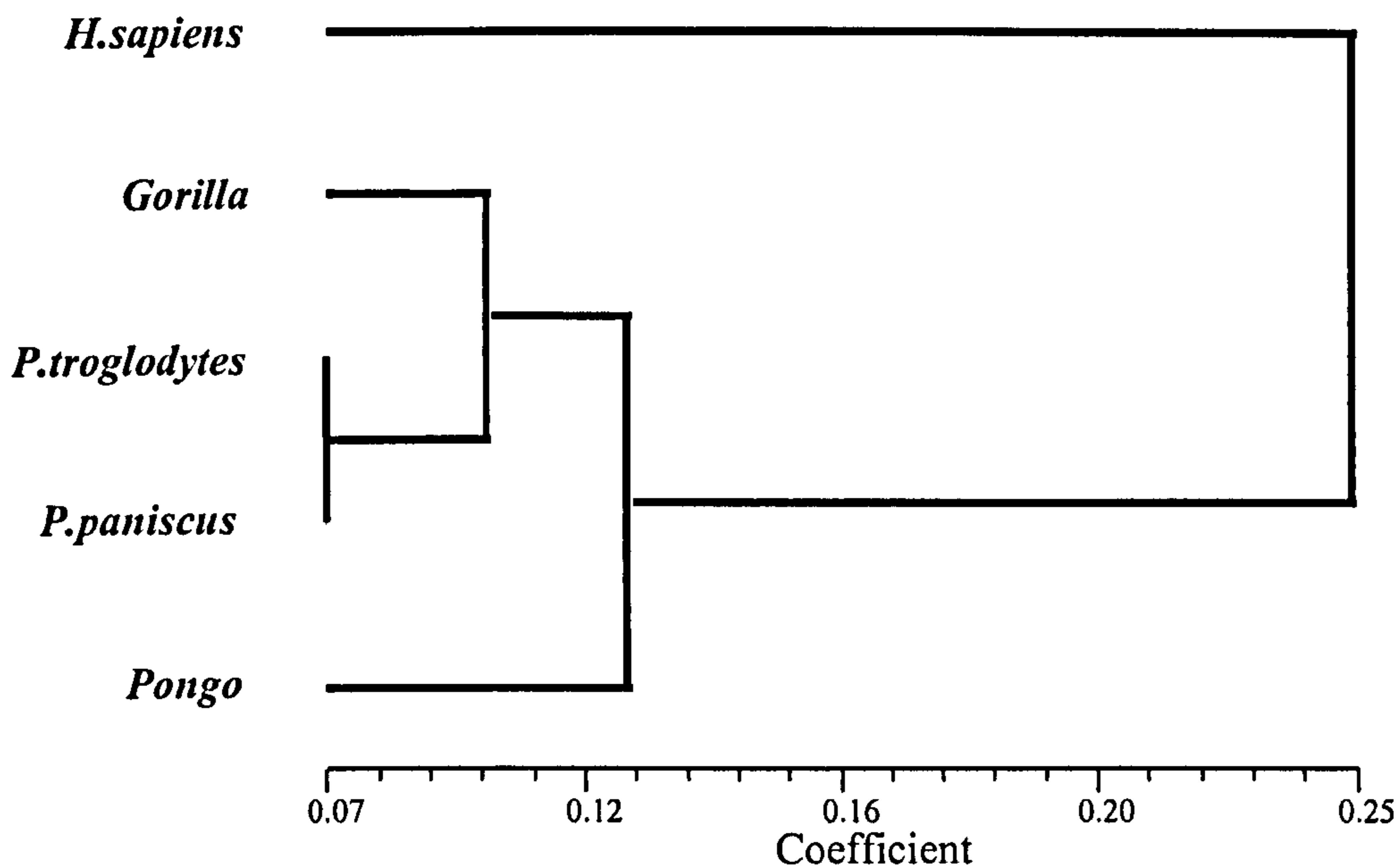


Figure 4.20 Cuboid: UPGMA phenogram using Procrustes distances between means.

For the cuboid means, *Homo sapiens* separates to the exclusion of all the remaining ape taxa (Figure 4.20). The great ape taxa are all relatively close to each other, and relatively distant from *Homo sapiens*. Within the ape cluster, the African apes and *Pongo* separate out from each other, and the two species of *Pan* separate out to the exclusion of *Gorilla*.

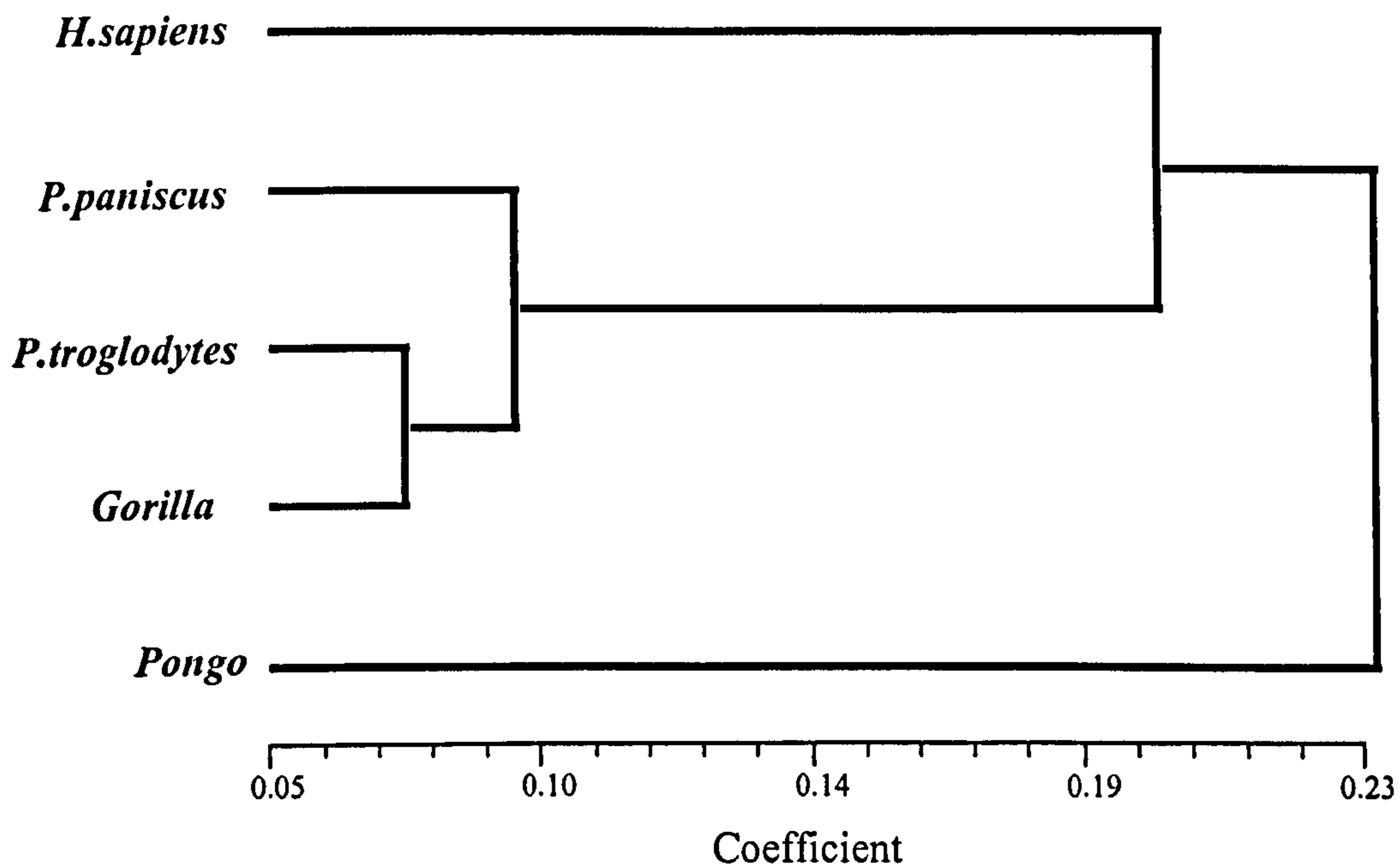


Figure 4.21 Navicular: UPGMA phenogram using Procrustes distances between means.

For the navicular UPGMA phenogram *Pongo* separates to the exclusion of the African apes and *Homo sapiens* (Figure 4.21). Within that later group, the African apes cluster closely together to the exclusion of *Homo sapiens*. Within the African ape cluster, *Pan troglodytes* and *Gorilla* cluster to the exclusion of *Pan paniscus*.

The UPGMA distance tree for the medial cuneiform, *Homo sapiens* separate to the exclusion of both *Pongo* and the African apes (Figure 4.22). The African apes separate to the exclusion of *Pongo*. *Pongo* is relatively distant from the African apes, as *Homo sapiens* is. Within the African ape cluster, the two species of *Pan* separate to the exclusion of *Gorilla*.

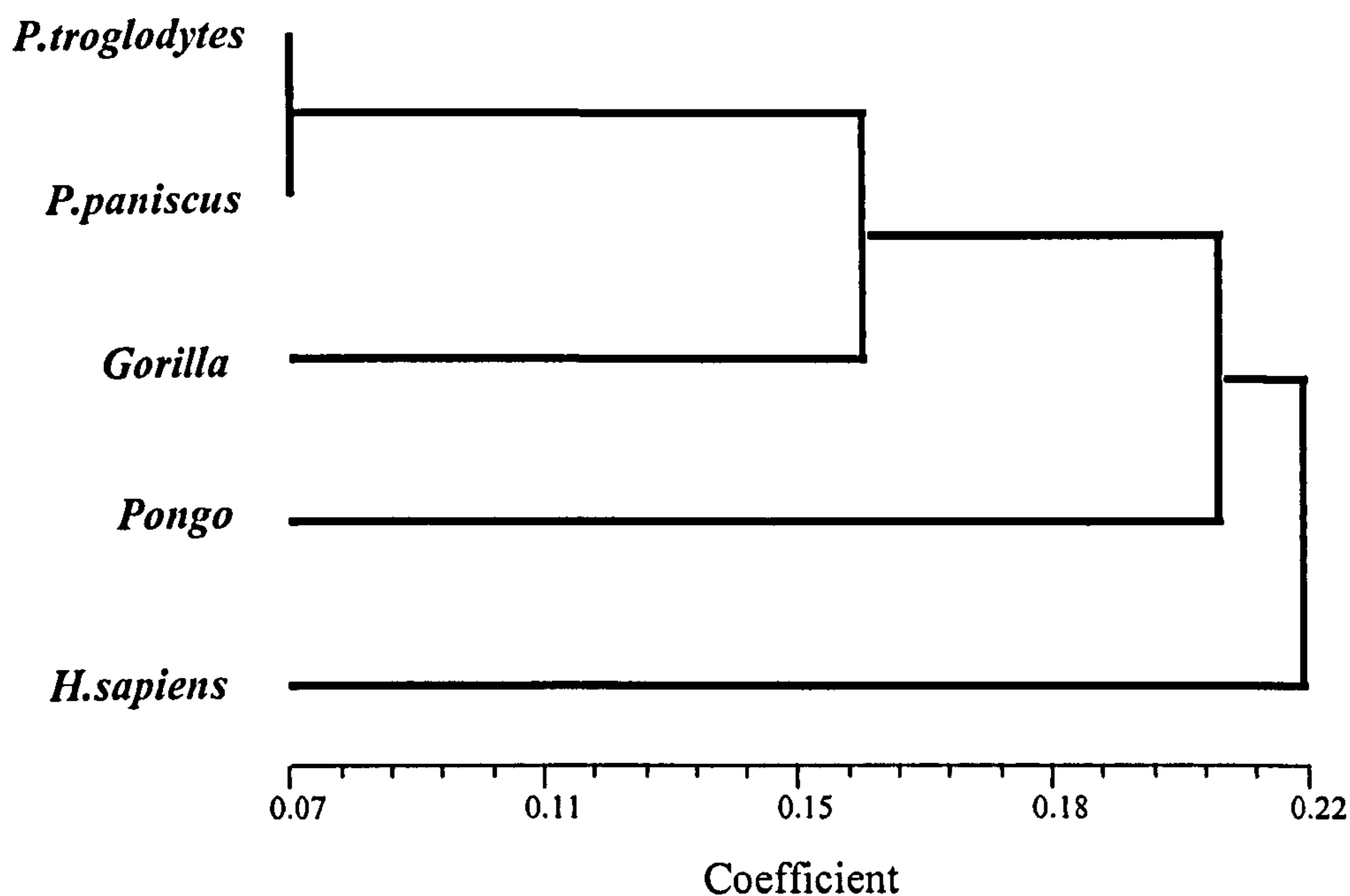


Figure 4.22 Medial Cuneiform: UPGMA phenogram using Procrustes distances between means.

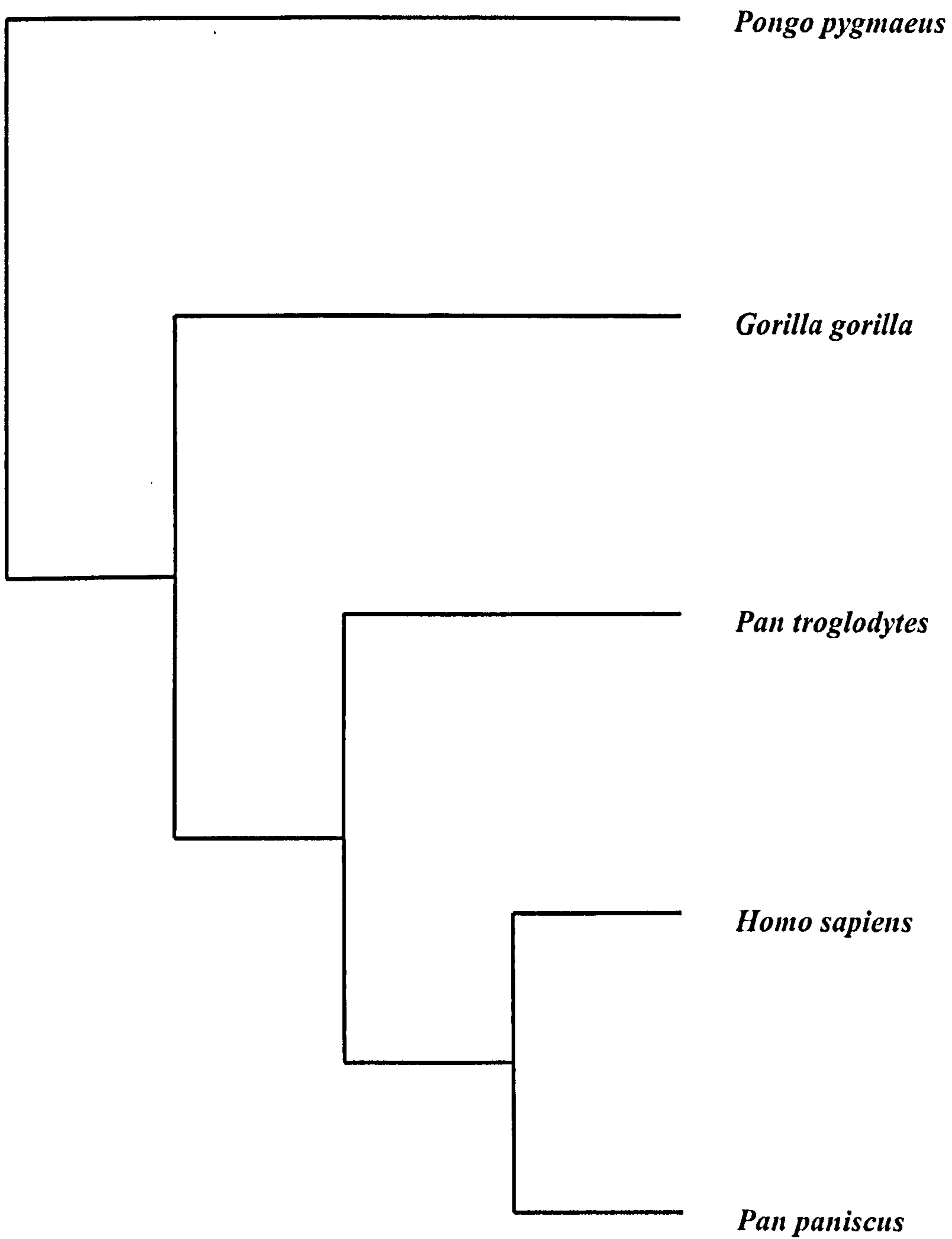


Figure 4.33 Calcaneus: Maximum likelihood tree for extant taxon means.

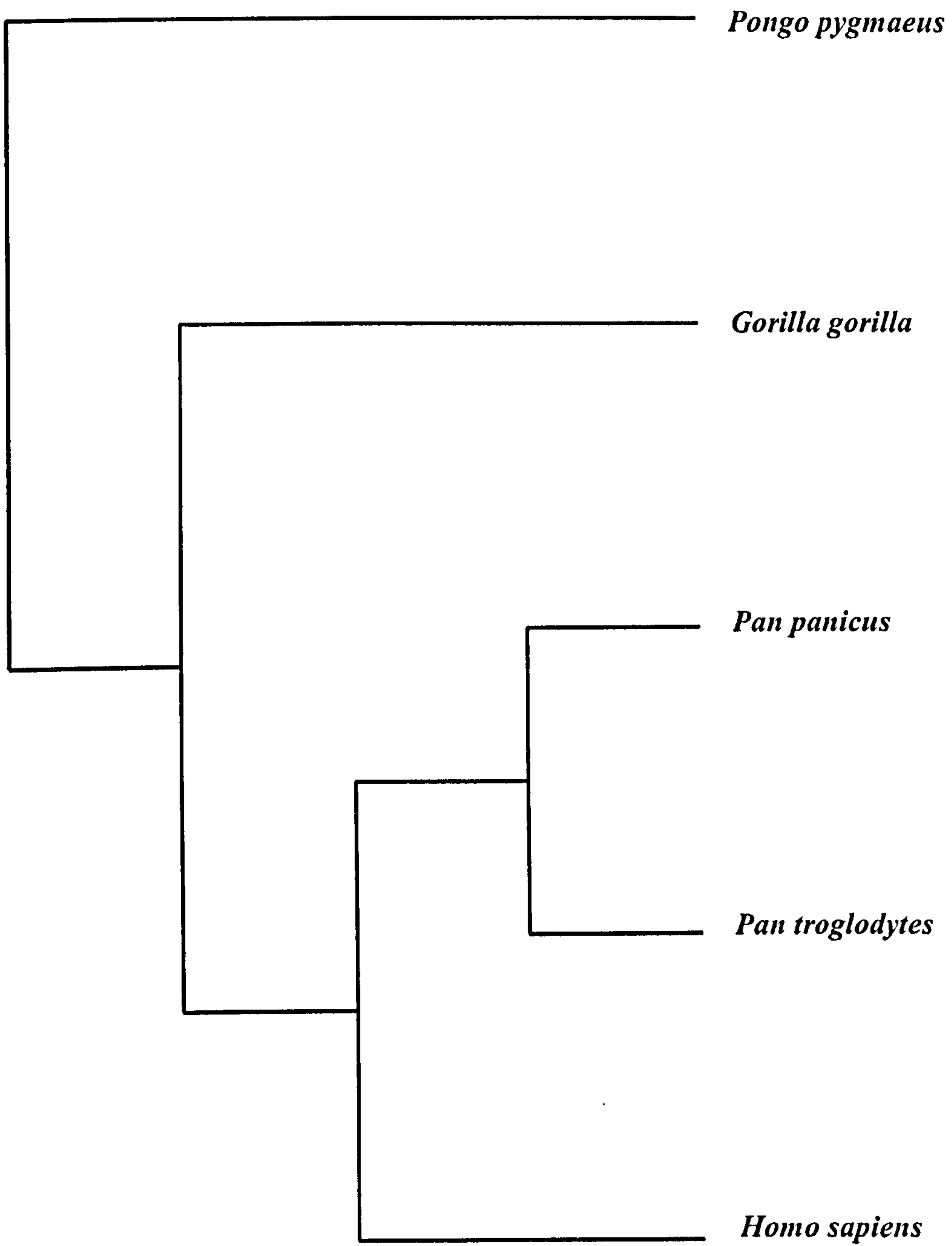


Figure 4.34 Talus: Maximum likelihood tree for extant taxon means.

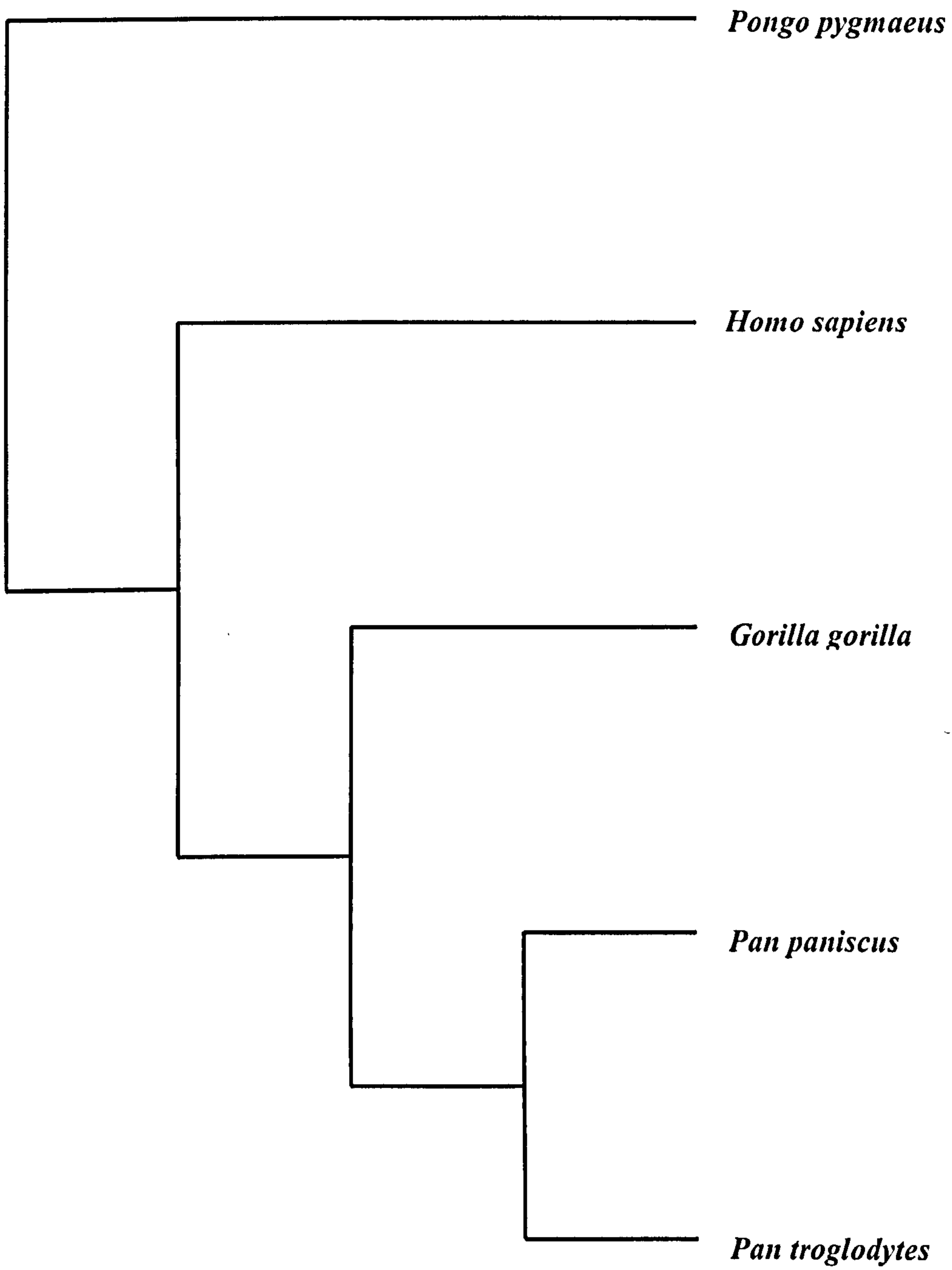


Figure 4.35 Cuboid: Maximum likelihood tree for extant taxon means.

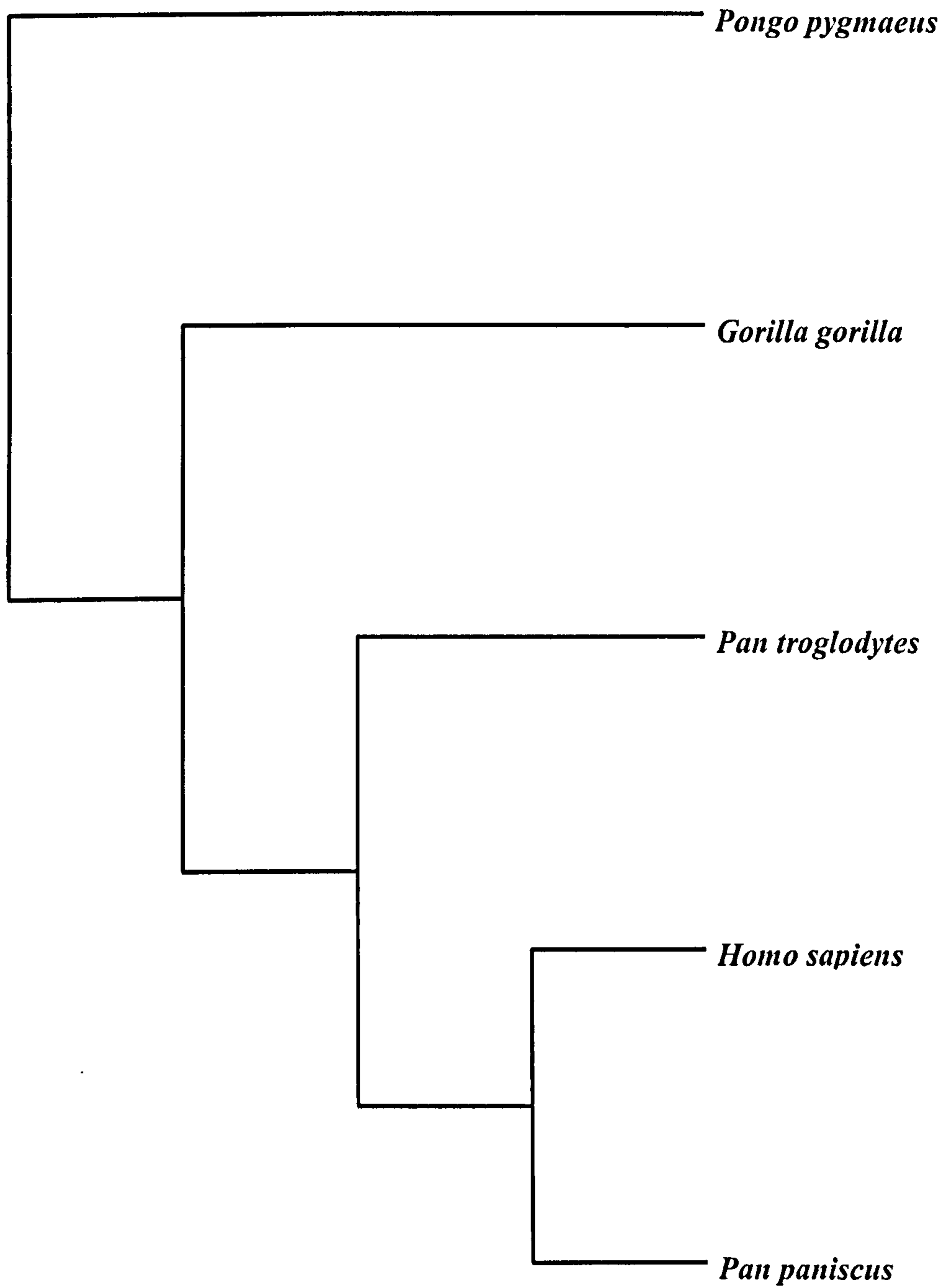


Figure 4.36 Navicular: Maximum likelihood tree for extant taxon means.

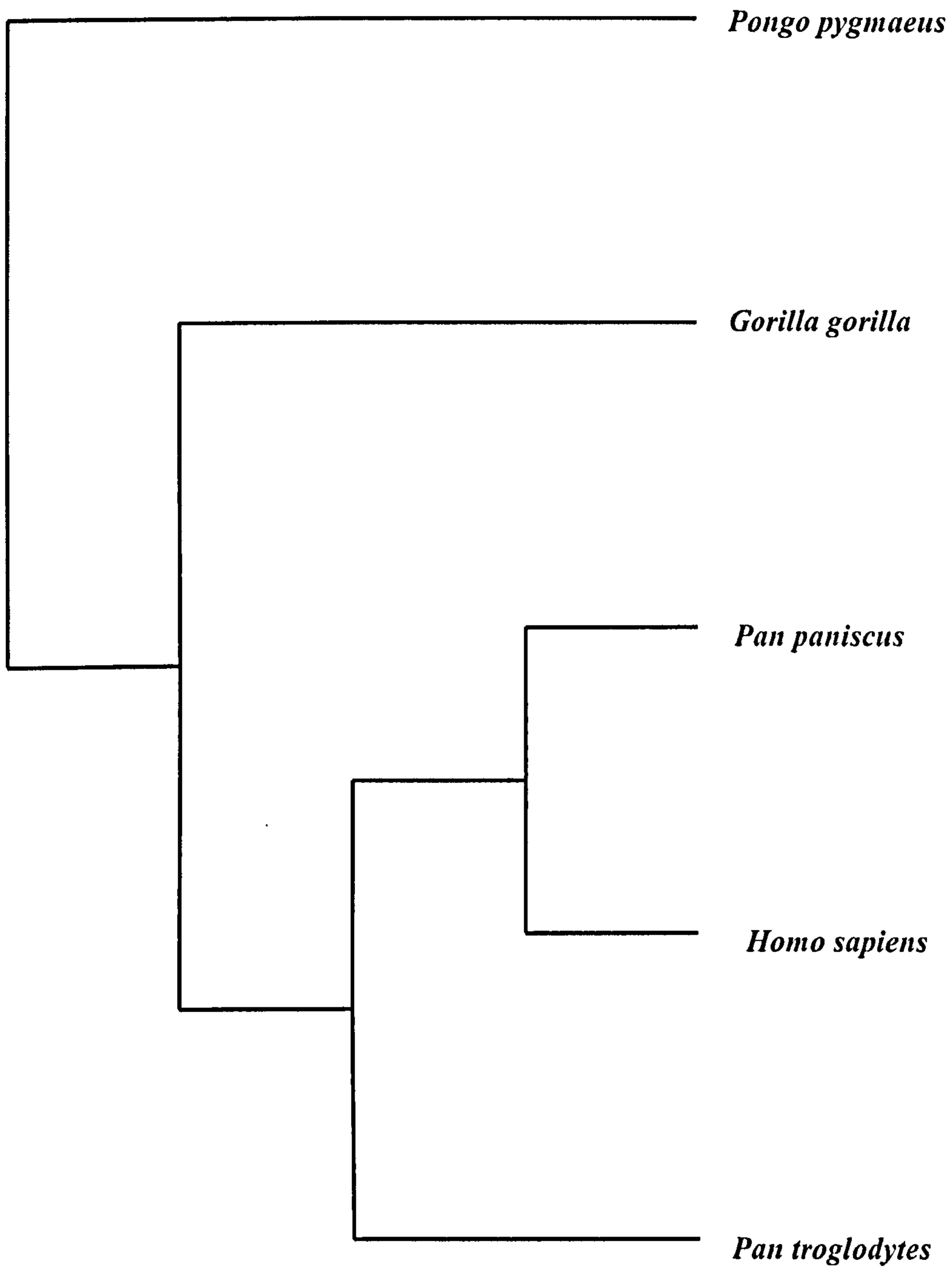


Figure 4.37 Medial Cuneiform: Maximum likelihood tree for extant taxon means.

4.4.4.2 Maximum Likelihood

For the Maximum Likelihood trees (Figures 4.33 - 4.37), *Pongo* is predetermined as the outgroup (based on known genetic phylogenies discussed earlier in this chapter), and so all other taxa obviously cluster to the exclusion of that taxon. For all bones but the cuboid, both species of *Pan* and *Homo sapiens* group together to the exclusion of *Gorilla*. In the case of the cuboid, the African apes group together to the exclusion of *Homo sapiens*. Within the *Pan-Homo* grouping for the other four bones, *Homo sapiens* and *Pan paniscus* group together for the navicular, calcaneus and medial cuneiform, and *Pan paniscus* and *Pan troglodytes* group together for the talus. These two taxa also group together for the cuboid.

4.5 Discussion

4.5.1 Size versus Shape

Using Pearson's correlation, although most of the p values are significant, there is no strong statistical association between centroid size and any PC axis for all five tarsals. Furthermore, the two criteria of satisfaction are not both met for Hypothesis H₁, and therefore **Hypothesis H₁ cannot be accepted**. Morphological differences between the taxa are therefore most likely due to functional differences that are not related to size. This is important when considering morphological differences between fossil specimens, since significant shape differences between fossil hominin tarsals would subsequently, in the absence of size as an explanatory factor, rather imply distinct functional differences.

4.5.2 Comparative anatomy

4.5.2.1 Calcaneus

The findings for the calcaneus strongly support previously observed differences reported for *Homo sapiens* and great ape calcanei. The most striking difference between *Homo sapiens* and the great apes is in the relative position of the anterior talar facet, and thus also, the sustentaculum tali. For *Homo sapiens*, this study shows that the anterior talar facet is essentially perpendicular to the long axis of the bone. This is not the case in the great apes, where it significantly dips plantarly and also medially. There has been much debate over the orientation of the sustentaculum tali (Aiello & Dean, 1990) and ultimately the problem lies with the overall orientation of the calcaneus not only relative to the rest of the foot but also to the substrate. When the great ape and *Homo sapiens* calcaneus is positioned along its long axis, then the great ape's sustentaculum tali is far less elevated than for *Homo sapiens*, resulting in an altered set of the talonavicular joint, making it relatively medial and plantar. However, it has been argued (Elftman & Manter, 1935b; Latimer & Lovejoy, 1989) that the calcaneus as a whole is orientated differently in the great apes, compensating for the lack of sustentaculum elevation.

The more likely explanation is that the relatively elevated sustentaculum tali in *Homo sapiens* is a reflection of the marked medial longitudinal arch, which, as discussed in

Chapter 1, great apes lack. The modern human orientation of the sustentaculum tali, as shown in this study to be distinctly different to that of the great apes, results in a far more elevated position for the talus, the talar head, and the talonavicular joint. This means that the navicular and medial cuneiform are also more elevated, and do not come into contact with the ground. This helps to maintain the structure of the arch.

The other main result from PC 1, is that the *Homo sapiens* cuboid facet is different in morphology to that of the great apes. The main difference was in the positioning of the reciprocal point on the calcaneus where the cuboid's plantar beak articulates. It is far deeper and more medially and plantarly orientated in *Homo sapiens*, and this reflects the strong locking mechanism of the *H.sapiens* calcaneocuboid joint (Lewis, 1989). The wider plantar section of the *Homo sapiens* calcaneal tuberosity indicates an increased requirement for weight-bearing, both in walking and in the stationary position.

4.5.2.2 Talus

The findings for the talus provide strong support for several previously published results. As discussed in Chapter 1 modern humans have lateral and medial trochlear margins that are at the same elevation as each other (Elftman & Manter, 1935b; Latimer *et al.*, 1987). This is not the case in the great apes, where the lateral margin is relatively superior, and the medial margin relatively inferior, resulting in a sloping trochlea (mediolaterally). This means that the leg can only pass over the foot in an arcuate path. The findings of this study strongly support this observation. *Pongo*, has the most sloping trochlea, and this is likely to be a reflection of an increased range of motion at the ankle joint. The increased length of the *Pongo* medial trochlear margin is found to be due to an increase in the length of the medial malleolar facet. This implies that there is a larger range of dorsiflexion and plantar flexion in the *Pongo* ankle joint than in the African great apes or *Homo sapiens*, and this indicates a greater mobility of the foot around the axis of the tibia

The reduction in talar head size from *Homo sapiens*, through the African great apes, to *Pongo* (as shown along PC 1), is most likely to be a reflection of the strong toe-off of modern humans at the end of the stance phase of walking (Elftman & Manter, 1935a;

Czerniecki, 1988). A strong toe-off means that there is increased loading through the talo-navicular joint, and a relatively larger navicular facet on the talus (and therefore a larger talar head size) would be a necessary requirement for this increase in loading. The *Pongo* talar head was markedly reduced in size, and this is a reflection of the fact that of its almost exclusive arboreality. As has been discussed, *Pongo* spends the majority of the time climbing or in a suspensory position (Tuttle 1968), and so has a greater need for manoeuvrability of the foot, rather than the efficient transmission of force to the substrate.

The finding that the great ape posterior calcaneal articular facet is less curved than that of *H.sapiens* supports a similar finding by Lewis (1980a), who based his conclusion on visual inspection of the facet. Lewis (1980a) suggested that the decrease in curvature in the great ape facet was an indication of a heightened degree of inversion and eversion at the subtalar joint, but does not elucidate why this would be the case.

The separation of the African apes from *Pongo* and the *Homo sapiens* was mainly due to the dimensions of the lateral malleolar facet, which is more curved dorsoplantarly (so that the plantar section of the facet flares out more laterally), and also longer along its dorsal margin (i.e. that that borders the trochlear). This larger, more curved facet could be an adaptation to a mosaic locomotor repertoire. The African apes climb and grasp in the trees, but also spend considerable amounts of time on the ground. Since the great ape foot is more inverted than that of *Homo sapiens* during terrestrial locomotion (Elftman & Manter, 1935a, 1935b; Morton, 1936; Tuttle 1970), the lateral malleolus of the fibula is subjected to downward forces that cause it to shear away plantarly and laterally from the lateral malleolar facet of the talus. Although not discussed in the literature, a more convex lateral malleolar facet with increased plantar-lateral flaring, could possibly act as a type of “shelf” that would help to prevent the distal fibular slipping away and destabilising the ankle joint.

4.5.2.3 Cuboid

The findings for the cuboid strongly support known differences between *Homo sapiens* and the great apes. For the group means, PC 1 clearly shows that the human cuboid is very distinct in its morphology. The presence of a marked plantarly orientated beak on the calcaneal facet in modern humans has been well documented, and has been shown by many to be a vital part of the locking mechanism of the lateral column during the mid-stance phase (Bojson-Møller, 1979; Lewis 1980, 1981; Susman, 1982; Aiello & Dean, 1990; Kidd et al., 1996). This study shows that, quantifiably, the modern human plantar beak is more pronounced and is more medially and plantarly orientated than that of the great apes, where it is more laterally orientated and less pronounced.

The finding that the *Homo sapiens* cuboid is relatively longer (in the proximal-distal direction) than that of the great apes supports the findings of other researchers who have shown that modern humans have relatively long tarsals, which increases the levering efficiency of the foot (Morton, 1922; Keith, 1928; Schultz, 1963; Stern & Susman, 1983; Aiello & Dean, 1990).

The finding that on the cuboid distal articular facet, *H.sapiens*, in relation to the great apes, have a relatively smaller 4th metatarsal facet compared to the 5th metatarsal, is most likely a reflection of weight distribution through the foot during the stance phase. Another way of looking at it is to state that the great ape 4th metatarsal facet is relatively large. As discussed earlier in Chapter 1, in modern humans weight transmits through the lateral side of the foot during the first part of the stance phase. Force then rapidly passes across to the medial side of the foot. This is reflected in the metatarsal robusticity pattern of *Homo sapiens*, where the 5th metatarsal is the most robust after the 1st (Archibald, 1972). In the great apes the whole foot takes the weight of the body, and the 2nd 3rd and 4th metatarsals take a relatively increased amount of loading (Elftman & Manter, 1935a). This is also reflected in the metatarsal robusticity pattern, where the 2nd 3rd and 4th metatarsals are more robust in the great apes. As such, the great ape foot is subject to more loading through the 4th metatarsal than that of *Homo sapiens*. The finding of this study that the great ape 4th metatarsal facet is relatively large, and that the modern human

one is relatively small, indicates that these differences are both adaptations to increased and decreased degrees of loading respectively. The increased curvature of the great ape 4th and 5th metatarsal facets is likely a reflection of a requirement for increased movement at those joints. This would help to make the tarso-metatarsal junction more flexible in the great apes, which is concordant with a grasping foot.

The difference between, on the one hand *Pongo*, and on the other hand the African apes and *Homo sapiens*, is a reflection of increased arboreality in *Pongo*. The decrease in the “keystone” shape of the *Pongo* cuboid means that the degree of arching of the lateral column is likely to be further reduced (i.e. more than it is already in the African great apes). This is most likely a reflection of the increased need for the *Pongo* tarsus to grasp, and cope with tensile stresses, and the reduced need for compressive weight bearing.

4.5.2.4 Navicular

For the means of each taxon, PC 1 showed that *Pongo* is as different from the African apes as is *Homo sapiens*. The most striking feature of the African apes is the relatively massive medial tuberosity. It has been argued that since the great ape foot lacks longitudinal arches, the navicular and medial cuneiform would be fully weight-bearing during plantigrade posture or locomotion (Elftman & Manter, 1935a; Kidd, 1999; Sarmiento, 2000). *Pongo* is almost exclusively arboreal, where as both *Pan* and *Gorilla* spend a considerable amount of time engaged in terrestrial locomotion. There is thus an increased demand in the African great apes for terrestrial weight bearing in the foot. The relatively large navicular tuberosity found in the African great apes in this study support that assertion.

Pongo has a highly reduced tuberosity. The taxon also has a relatively small medial cuneiform facet, but relatively larger intermediate and lateral cuneiform facets. The reduced tuberosity is most likely a reflection of the fact that *Pongo* is almost exclusively arboreal, and so has little need for a foot adapted to cope with large compressive forces dorsoplantarly (as in a plantigrade terrestrial foot). The small medial cuneiform facet is a reflection of the significantly reduced hallux in *Pongo* (Tuttle, 1968). It has been shown

that *Pongo* has a specialised four-digit grasp, that does not use the hallux (Tuttle & Rogers, 1966). During arboreal locomotion in *Pongo*, there is thus increased loading (both compressive and tensile) along rays II to V, and reduced loading in the first ray. The relatively large intermediate and lateral cuneiform facets are most likely a reflection of this requirement for increased loading.

4.5.2.5 Medial Cuneiform

The principal findings support what is well known about the comparative anatomy of the extant hominoid medial cuneiform. For the means of each taxon, PC 1 clearly shows that the hallucial facet is curved and in an abducted position in the great apes, and is flat and more forward facing in modern humans. The clear separation between *Homo sapiens* and the great ape is mainly driven by this feature, and the findings strongly support the well known view that the joint is a reflection for the requirement of arboreal grasping in the great apes, and obligate bipedalism in modern humans (Morton 1922, 1924, 1927, 1935; Schultz, 1930; Lewis 1980a, 1980b; Szalay & Langdon 1986; Aiello & Dean, 1990).

The findings from PC 2 clearly show that the medial cuneiform is also very distinct in *Pongo*, relative to the African great apes and also *Homo sapiens*. Both the navicular and hallucial facets are relatively smaller in *Pongo*, and the hallucial facet is more convex. These findings suggest two things. Firstly, the more curved hallux of *Pongo* indicates a greater degree of opposability. Secondly, the reduced size of the articular facets implies that there is less of a need for loading through those joints. As discussed in the previous section (and also in Chapter 1), *Pongo* is by far the most arboreal of the great apes (Tuttle, 1968; Cant, 1987). An increased ability to oppose the hallux would be an ideal arboreal adaptation, where a grasping foot is essential. However, it has also been shown that the hallux is markedly reduced in *Pongo*, and that this is a result of an adaptation for a four digit grasp when climbing. As a result, the hallux is thought to play a role in fine manipulation of branches rather than in a weight bearing capacity (Tuttle & Rogers, 1966). Although it cannot be directly tested, smaller articular facets on the medial cuneiform of *Pongo* are likely to be a result of a lessened requirement for loading (whether tensile or compressive) through those joints.

4.5.3 Relationships between taxa

The most notable result from the permutation tests, UPGMA phenograms is that, whilst all the bones are distinct from each other, the pattern of the phenetic relationship between the different taxa varies from tarsal to tarsal. Hypothesis H₂ stated: “The phenetic relationships between taxa are consistent for each of the individual tarsals”. On this finding alone, Hypothesis H₂ cannot be accepted.

However, before discussing those relationships further, there are a number of evident trends. For all bones except the calcaneus, the African apes cluster together to the exclusion of both *Homo sapiens* and *Pongo*. For the calcaneus, the differences between *Gorilla* and *Pan*, and *Pongo* and *Pan* are relatively small, and could be explained by factors such as landmark choice. The important thing for that bone is that all apes cluster together to the exclusion of *Homo sapiens*. In the calcaneus, talus, cuboid and medial cuneiform, both species of *Pan* group together. In the case of the navicular, *Gorilla* clusters with *Pan troglodytes* to the exclusion of *Pan paniscus*, but the absolute differences in distance in this case are very small. The *Homo sapiens* medial cuneiform, cuboid and calcaneus all separate to the exclusion of the great apes. That is to say that the *Homo sapiens* medial cuneiform, cuboid and calcaneus are more distinctly different from those of the great apes than are the navicular and talus. This evidence therefore suggests that these bones are more specialised and modified in humans than are the talus and navicular. Conversely, in terms of functional complexes, it is the talo-navicular joint in modern humans that is relatively conservative. This is supported by studies that argue that it is the calcaneocuboid joint, with its ability to lock into a rigid joint during the stance phase, that is the most specialised component of the *Homo sapiens* transverse tarsal joint (Elftman, 1960; Lewis, 1980a).

Based on the phenograms, the *Homo sapiens* talus seems to be the least distinctive bone of the five tarsals measured. This is an important finding when considering isolated fossil specimens. What it highlights is that since some tarsals are likely to be more diagnostic of human-like foot function than others, that great caution should be taken when considering isolated pedal elements. The talus is a case in point. Compared to the

other tarsals, this bone happens to be relatively prominent in the hominin fossil record, and, as discussed in Chapter 1, has been much discussed in the literature. There has been considerable debate about the affinities of the OH 8 talus (e.g. Lisowski, 1967; Day & Wood, 1968; Oxnard, 1973; Lewis, 1980b; Kidd et al., 1996; Berillon, 2000), that of Kromdraai (Le Gros Clark, 1947; Robinson, 1972; Lisowski *et al.*, 1974; Wood, 1974) and that of *A. afarensis* (Susman, 1983; Latimer et al., 1987). The findings of this study suggest that one of the reasons for this may be that as the bone is relatively conservative in the hominins, and so it is likely that tali from the Plio-Pleistocene are going to be more similar to each other than bones that are considerably more remodelled in modern humans, such as the cuboid or medial cuneiform.

Conversely, the talus and navicular of *Pongo* are particularly distinctive, and branch separately from other taxa. Therefore, it is argued that the *Pongo* talo-navicular complex is particularly remodelled and specialised relative to *Homo sapiens* and the African apes.

Not one of the five phenograms reflects the current (and well resolved) genetic distance trees for the great apes (see Figure 4.2 at the start of this chapter). For that to be so, *Pan* and *Homo sapiens* would have to cluster together to the exclusion of all other taxa. This is not the case for any of the tarsals measured. Subsequently, the relationship between taxa is unlikely to be explained simply in terms of phylogenetic propinquity. Hypothesis H₃ stated: “The patterns of phenotypic similarity between individual tarsal bones reflects the molecularly determined phylogeny”. So, **Hypothesis H₃ cannot be accepted**. It is therefore postulated that function is a more likely explanation for the relationships between the taxa. This explains why the African ape taxa nearly always cluster together, whether on the PCA plots, or in the distance trees. It also explains why both *Pongo* and *Homo sapiens* are so specifically distinct. The locomotor literature shows that the African apes are all relatively similar in their mosaic locomotor repertoires, whilst both *Pongo* and *Homo sapiens* are specialist arborealists and bipeds respectively. Combined with this is the evidence from the different degrees of specialisation in the tarsals. It is well known that the most distinctive features of the human foot are its lever like rigidity during the stance phase, and the loss of an abductable hallux. The former is mainly due

to the “lock and key” morphology of the calcaneocuboid joint, whilst the latter is mainly due to the morphology of the medial cuneiform. The results from the distance trees show that it is these three bones (calcaneus, cuboid and medial cuneiform) that are most specialised in modern humans.

For the Maximum Likelihood trees, the situation is similar to that with the UPGMA phenograms. The topology of the trees are not consistent for all five bones, even though *Pongo* is predetermined as the outgroup. The African apes only cluster together for the cuboid, and this may only be due to the fact that that bone is so highly derived and specialised in its morphology in *Homo sapiens*. So, even inserting a degree of phylogenetic bias into the tree design does not alter the fact that the relationships between taxa depend on the bone being analysed.

Finally, if we are to believe the genetic phylogeny of the extant hominoids as being the correct one, with *Pan* being closer to *Homo sapiens* than to *Gorilla*, then the morphological similarities between *Pan* and *Gorilla* can be assumed to have been a result of independent modification of already similar structures, and are thus evidence of homoplasy, and more specifically, parallelism. This is an important finding in terms of explaining morphological similarities in the fossil record, as presented and discussed in the next chapter.

4.5.4 Summary

The wider functional and evolutionary implications of the results for this chapter are discussed in Chapter 6. Below is a summary of the findings of this chapter.

- 1). For all five tarsals, the results from the permutation tests show that there were highly significant differences in shape between *Homo sapiens*, *Pongo*, *Pan troglodytes*, *Pan paniscus* and *Gorilla*.

- 2). Warping along PC axes and analysis of thin plate splines show that 3D morphometric differences between taxa mirror closely those observed anatomical differences described

in the literature. *Pongo's* tarsals are specialised for almost exclusive arboreal locomotion, whilst those of the African great apes reflect adaptations that are a result of a need for a mosaic of arboreal and terrestrial locomotion. The tarsals of *Homo sapiens* reflect those of full, obligate bipeds.

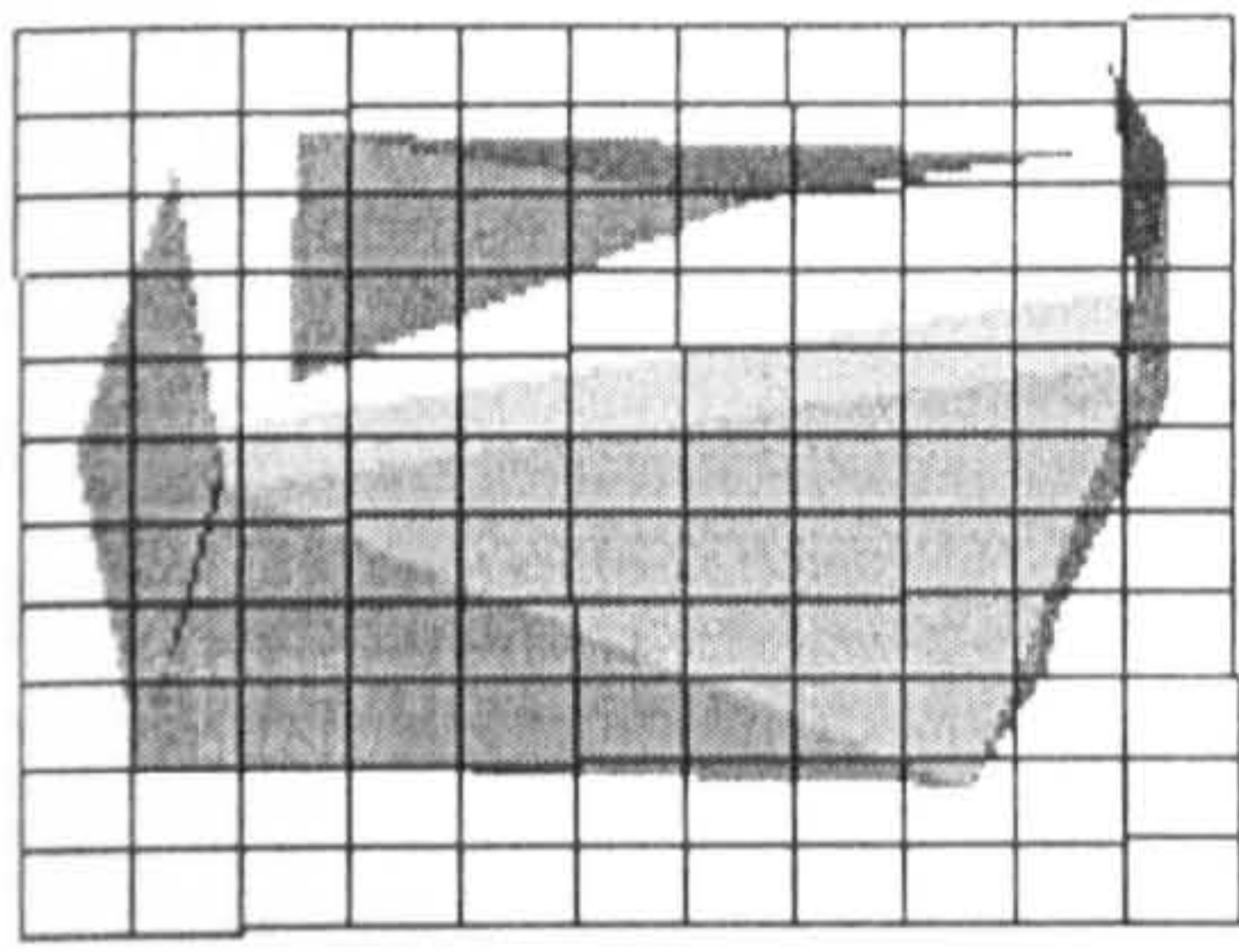
3). For all five tarsals measured, there is no strong statistical association between any PC axis and centroid size. Hypothesis H₁ stated: "There is a strong and significant relationship between centroid size and shape". Therefore, **Hypothesis H₁ cannot be accepted.**

4). The relationships between taxa differ from tarsal to tarsal. Hypothesis H₂ stated: "The phenetic relationships between taxa are consistent for each of the individual tarsals". Therefore, **Hypothesis H₂ cannot be accepted.**

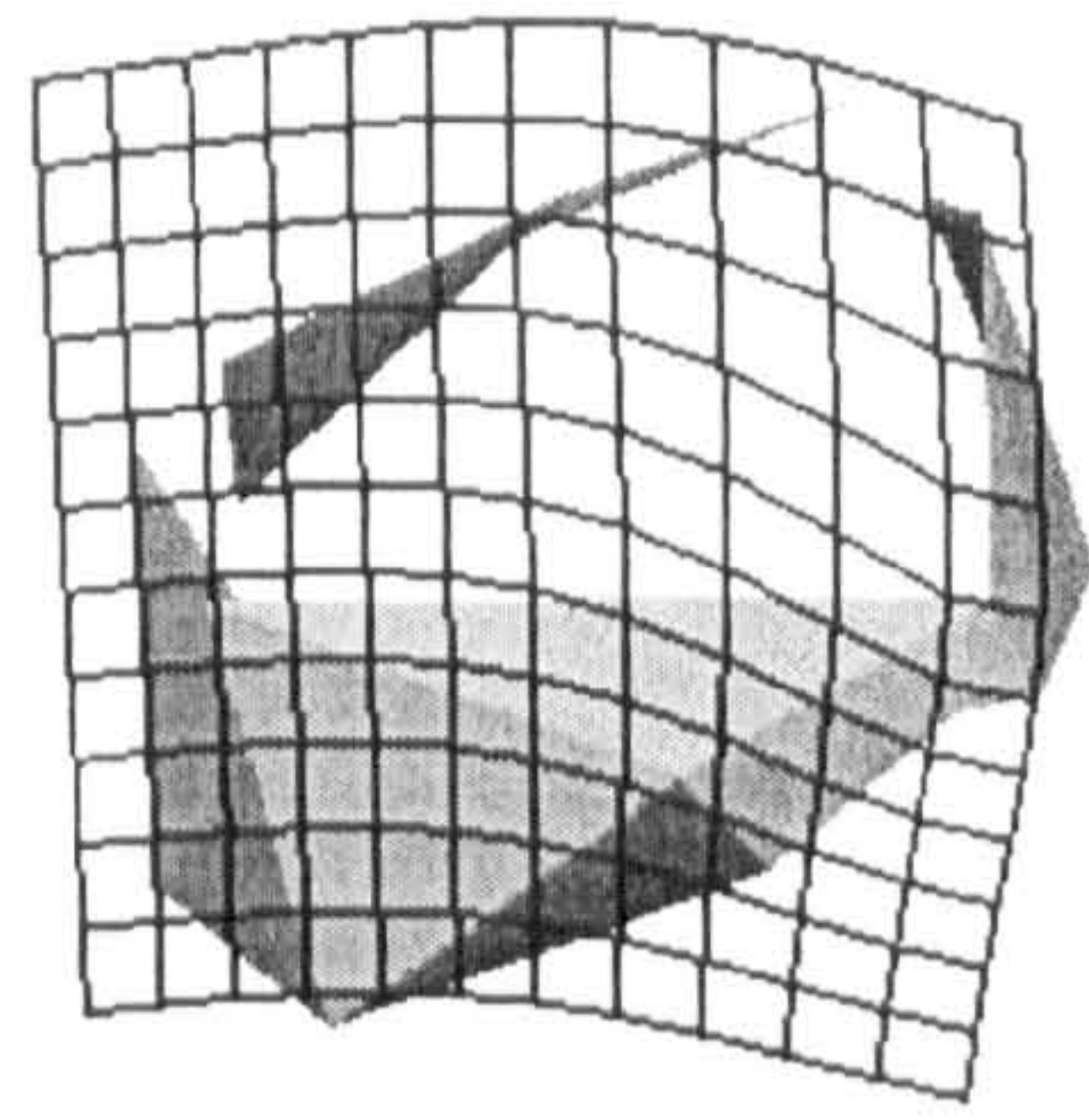
5). The phenetic relationship between extant hominoids, for the tarsals, does not reflect the consensus molecular phylogeny. H₃ stated: "The patterns of phenotypic similarity between individual tarsal bones reflects the molecularly determined phylogeny". Therefore, **Hypothesis H₃ cannot be accepted.**

6). Although significantly different to each other, *Pan paniscus* and *Pan troglodytes* were, for all but the navicular, morphologically closer to each other than any other taxa.

7). Morphological similarities between *Pan* and *Gorilla* are most likely due to homoplasy, and more specifically, parallelism.



Homo sapiens



Great apes

Dorsal view of Medial Cuneiform. The left hand shape is the overall mean warped along PC 1 to the human mean. The reference grid is situated dorsal to it. The left hand shape is the result of warping along PC 1 to the great ape means. The deformed target grid for the great ape mean shape is shown at the most dorsal position. Numbers 1 – 4 represent different planes at which screen captures of the deformed grid are presented.

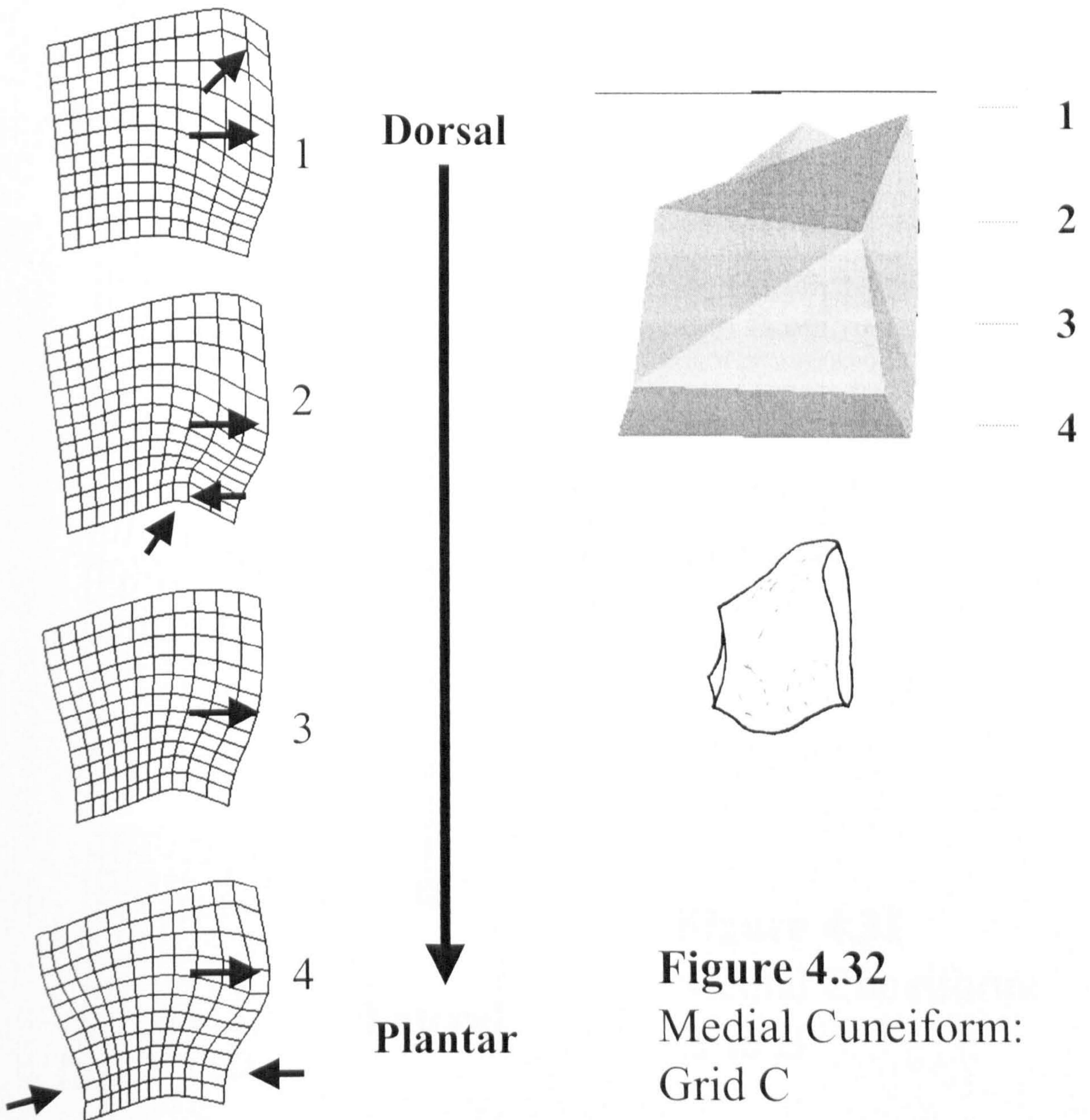
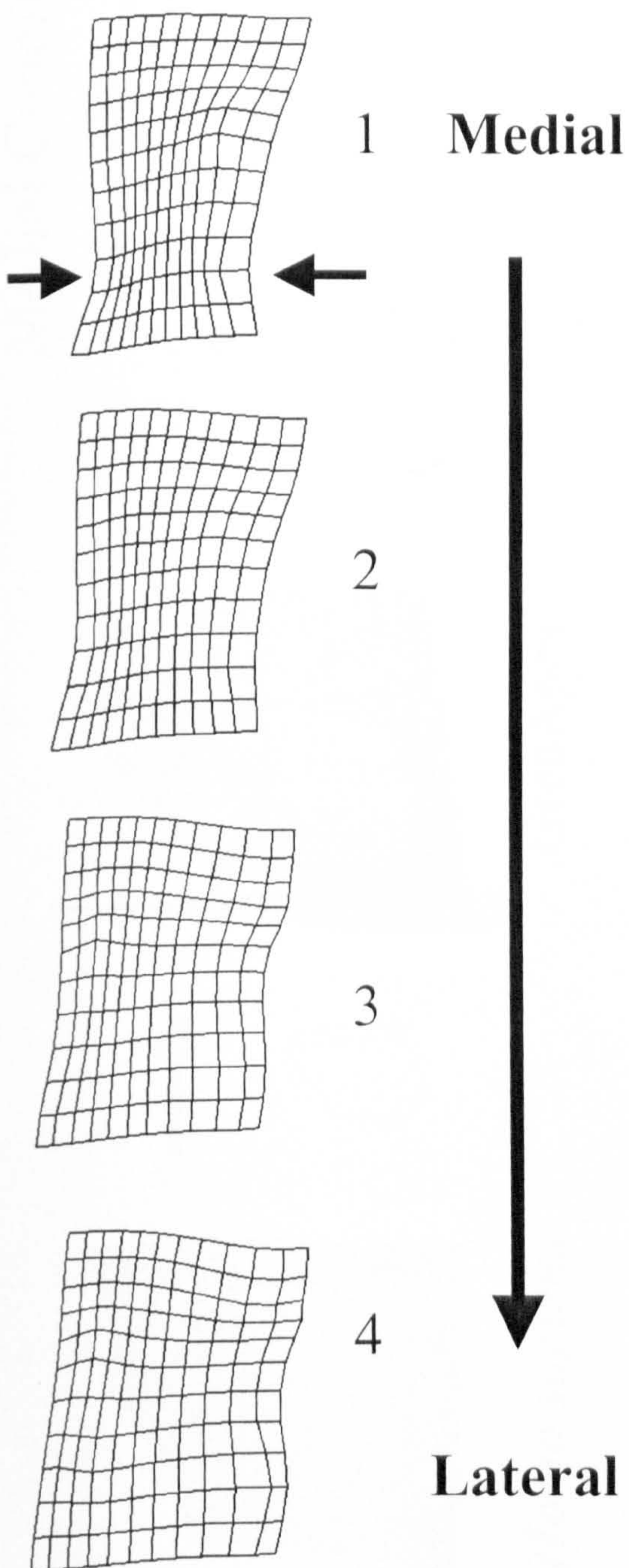
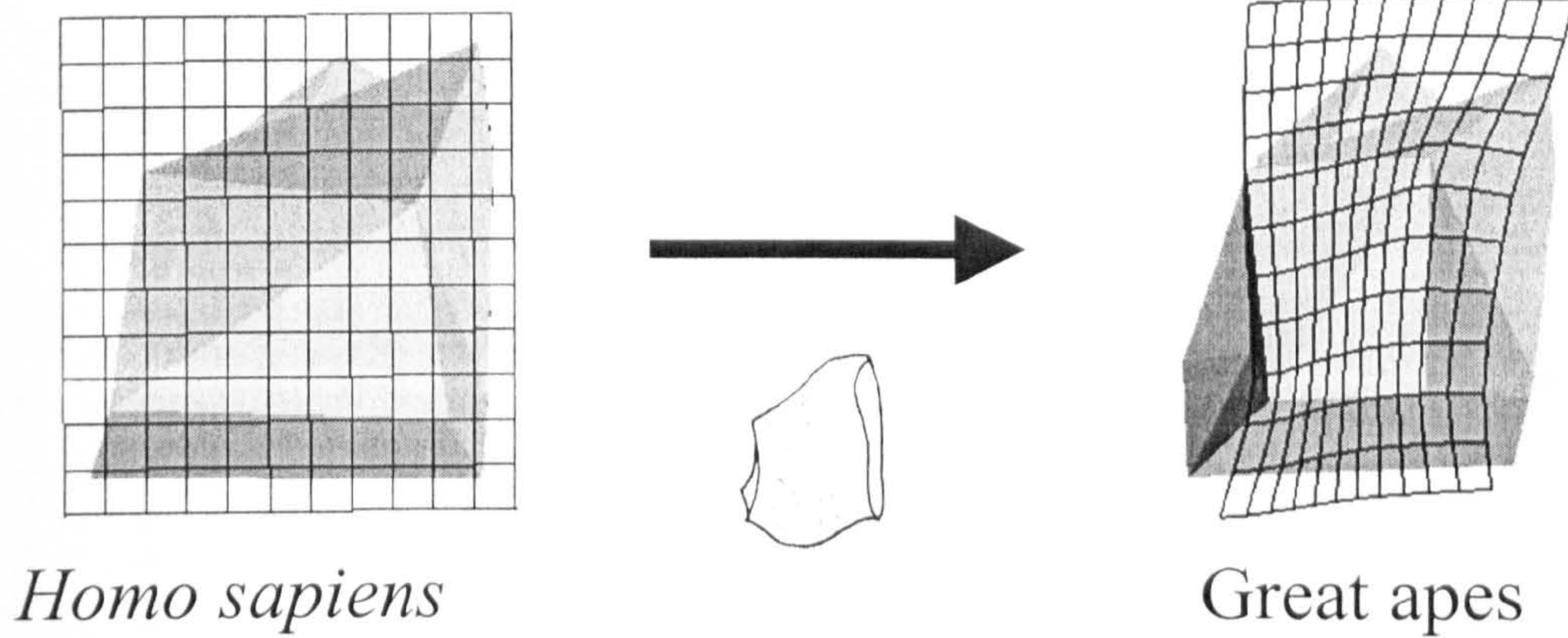


Figure 4.32
Medial Cuneiform:
Grid C



Medial view of Medial Cuneiform.
Above: The left hand shape is the overall mean warped along PC 1 to the human mean. The reference grid is situated medial to it. The left hand shape is the result of warping along PC 1 to the great ape means. The deformed target grid for the great ape mean shape is shown at the most medial position. *Below:* Numbers 1 – 4 represent different planes at which screen captures of the deformed grid are presented (viewed dorsally).

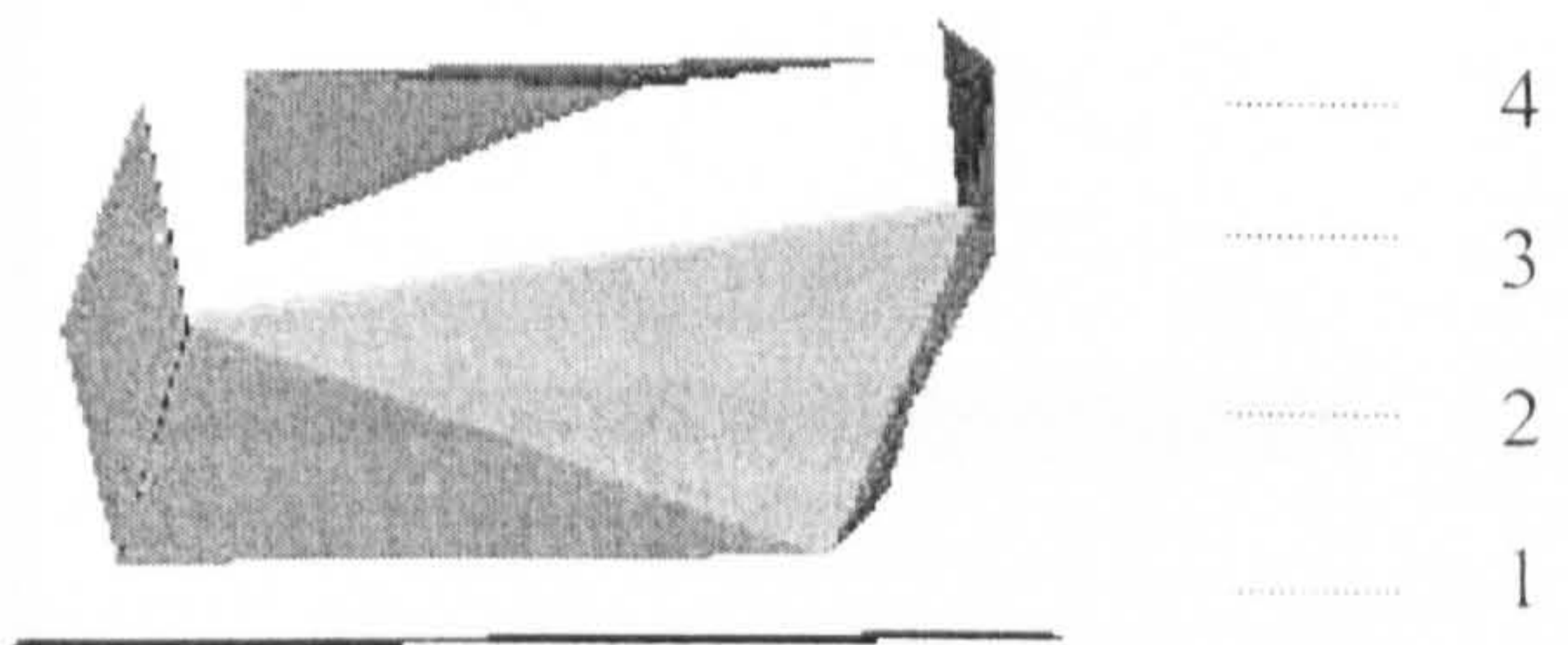
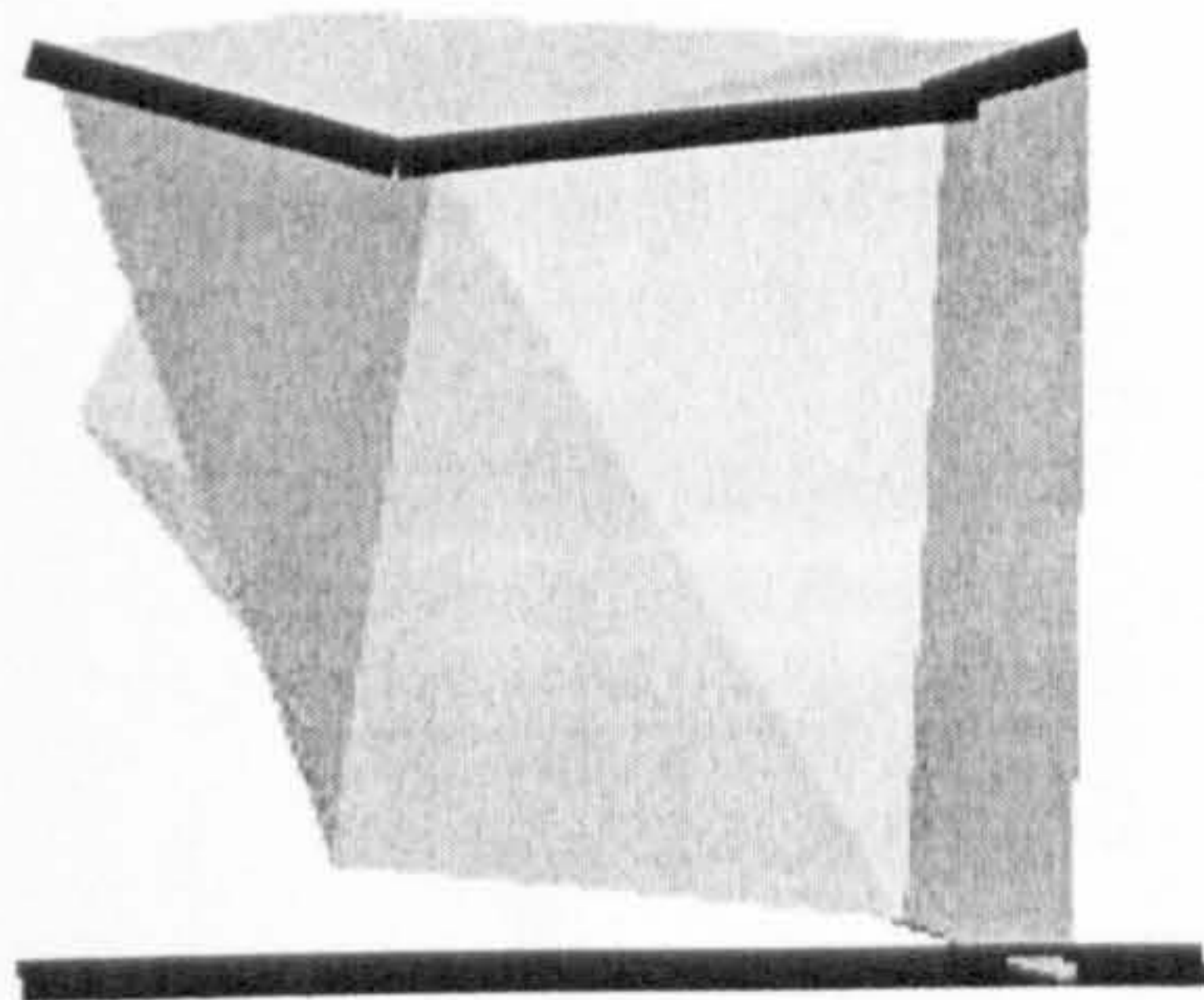
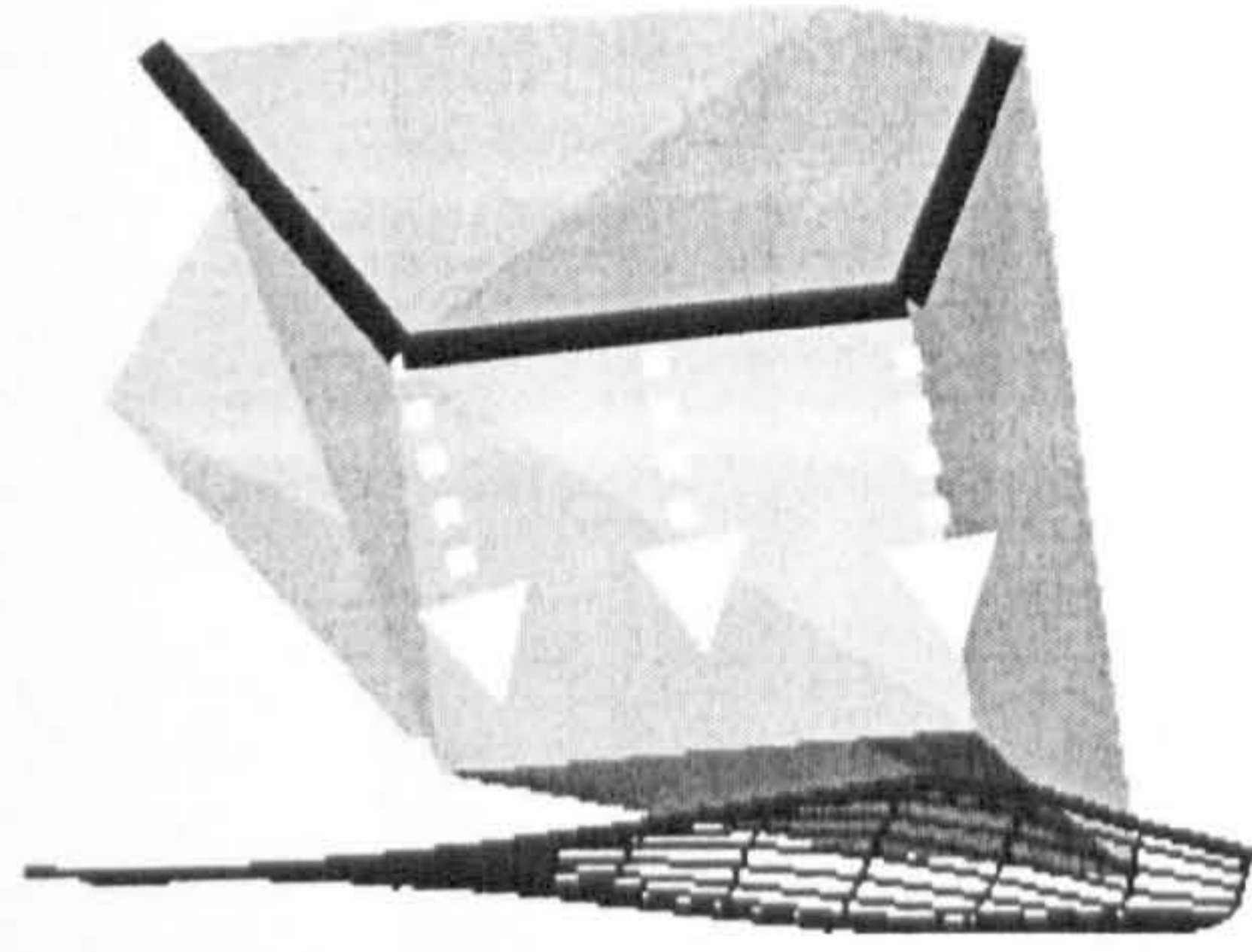


Figure 4.31
 Medial Cuneiform:
 Grid B

1 2 3 4 5 6



Homo sapiens



GreaApes

Figure 4.30

Medial Cuneiform: Grid A

Medial view of Medial Cuneiform. Black bars represent the medial margin of the hallux facet. White dotted arrows indicate movement of that facet when warping from humans to apes. The left hand shape is the overall mean warped along PC 1 to the *Homo sapiens* mean. The reference grid is situated proximal to it. The left hand shape is the result of warping along PC 1 to the great ape mean shape. The deformed target grid for the great ape mean shape is shown at the most proximal position. Numbers 1 – 6 represent different planes at which screen captures of the deformed grid are presented.

Proximal

Distal



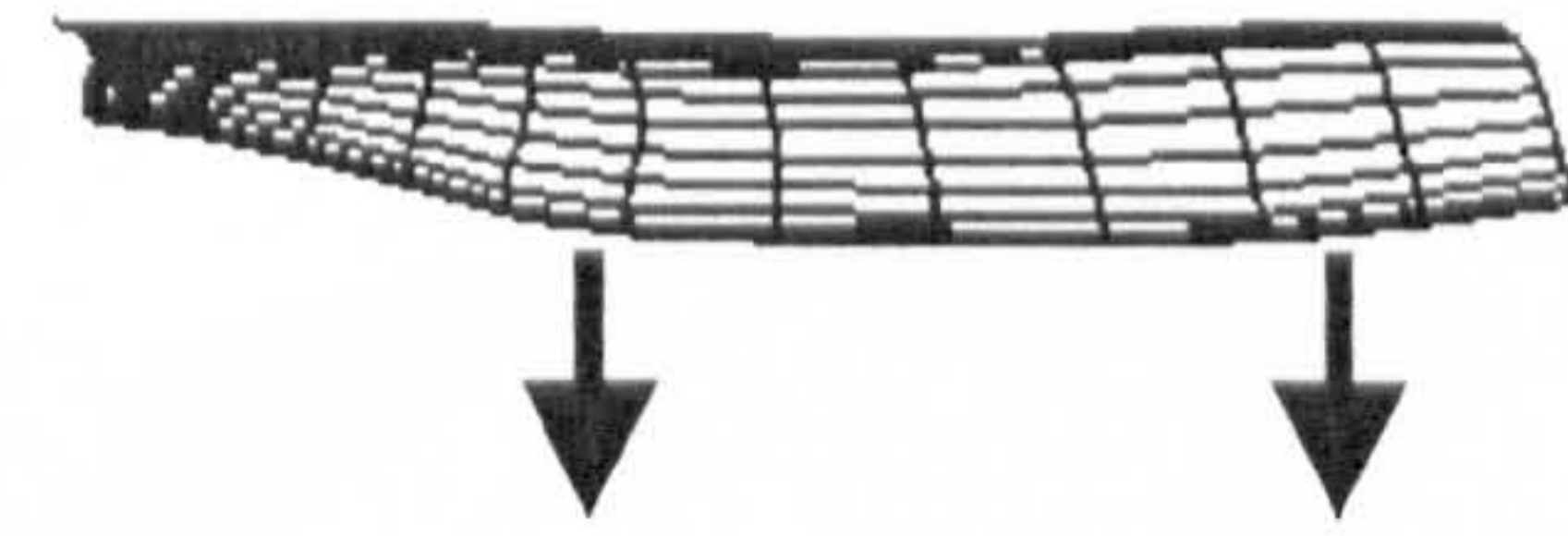
1



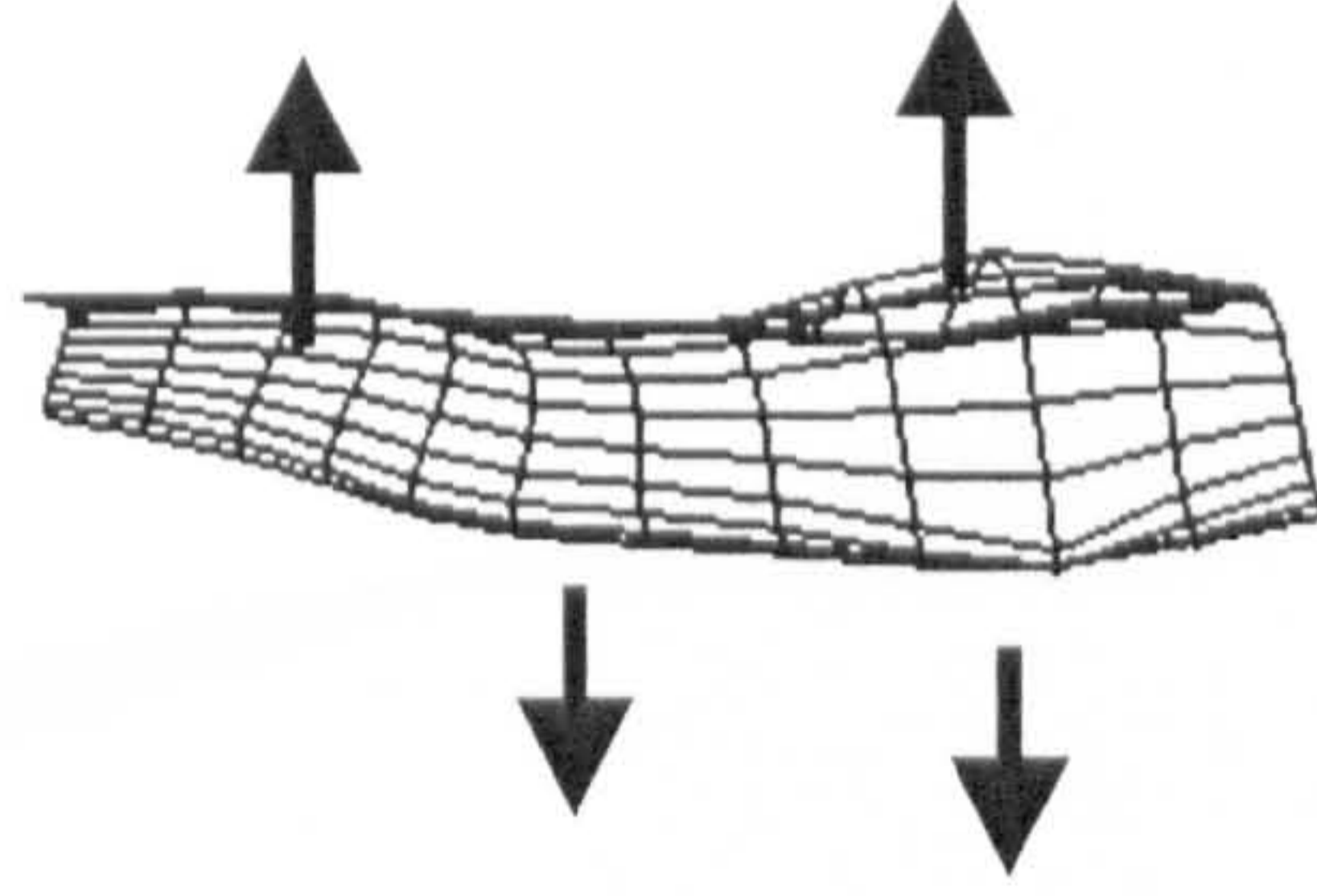
2



3



4



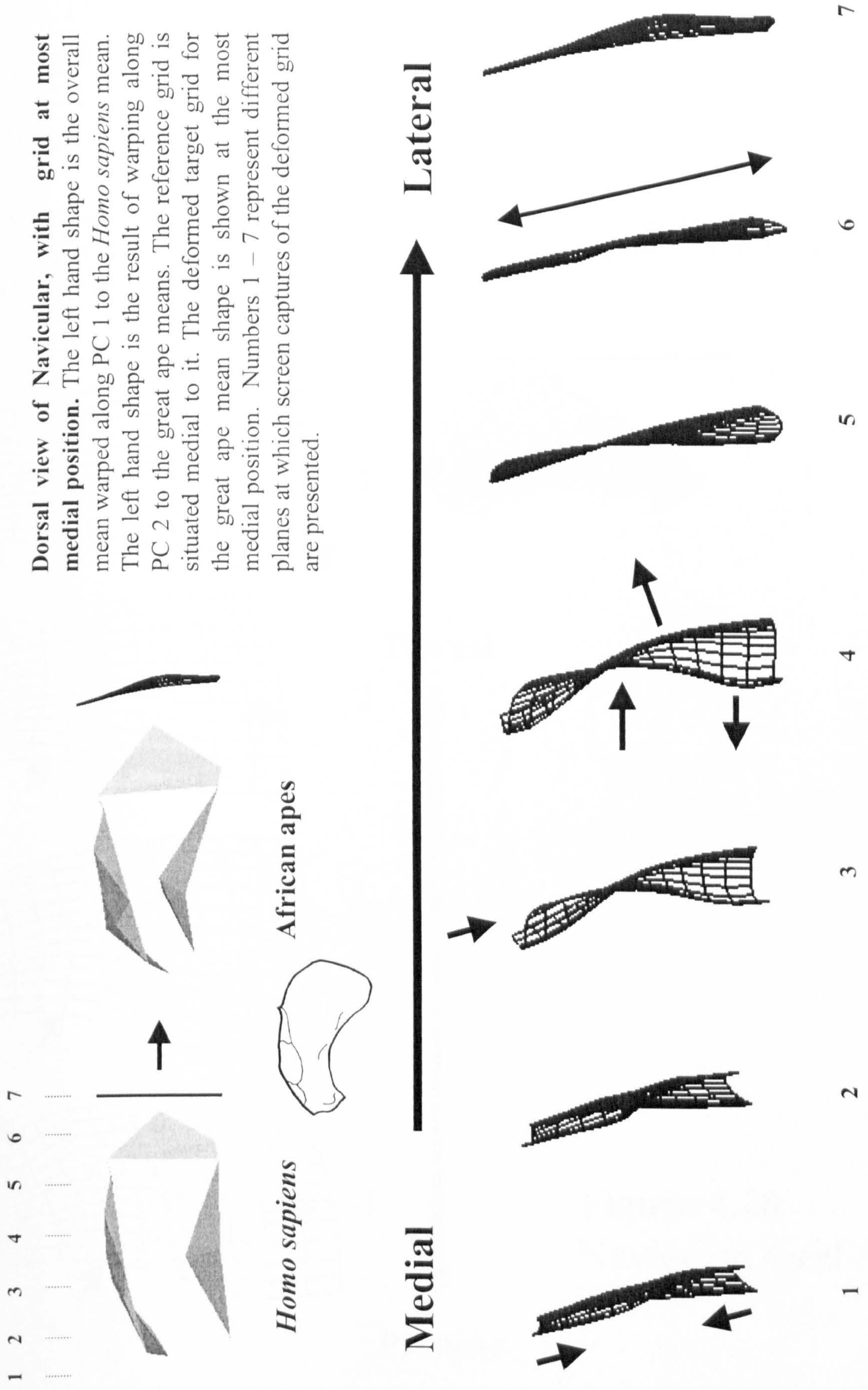
5

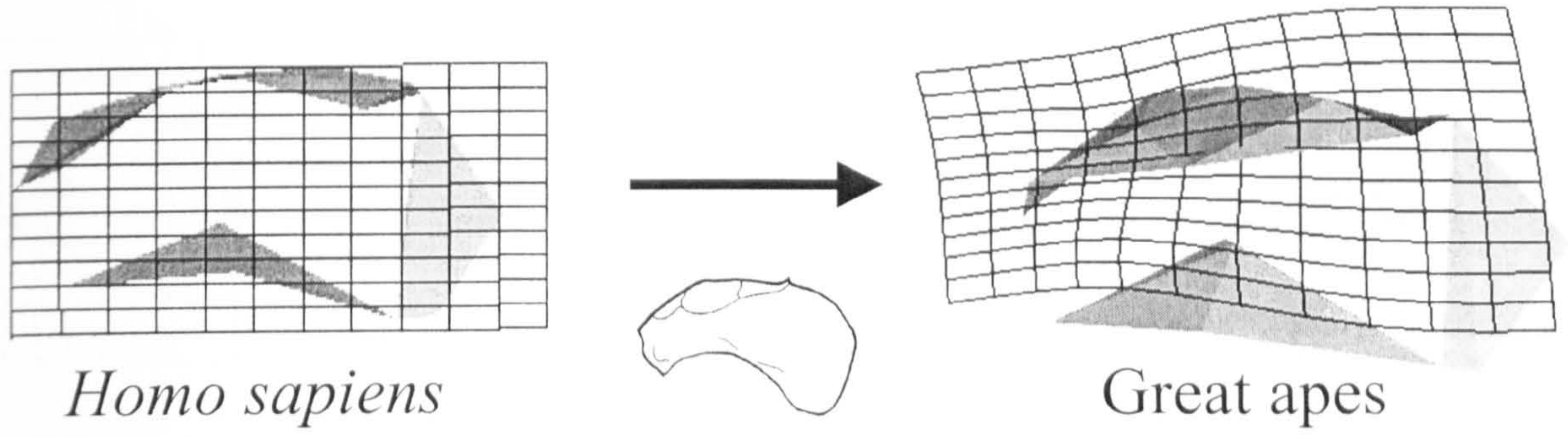


6

Figure 4.29
Navicular: Grid B

Dorsal view of Navicular, with grid at most medial position. The left hand shape is the overall mean warped along PC 1 to the *Homo sapiens* mean. The left hand shape is the result of warping along PC 2 to the great ape means. The reference grid is situated medial to it. The deformed target grid for the great ape mean shape is shown at the most medial position. Numbers 1 – 7 represent different planes at which screen captures of the deformed grid are presented.





Above: Dorsal view of navicular with warping from humans (reference grid) to apes (target). Below right: proximal view showing position of TPS grids 1 – 4. Below left: warped TPS grids in dorsal view.

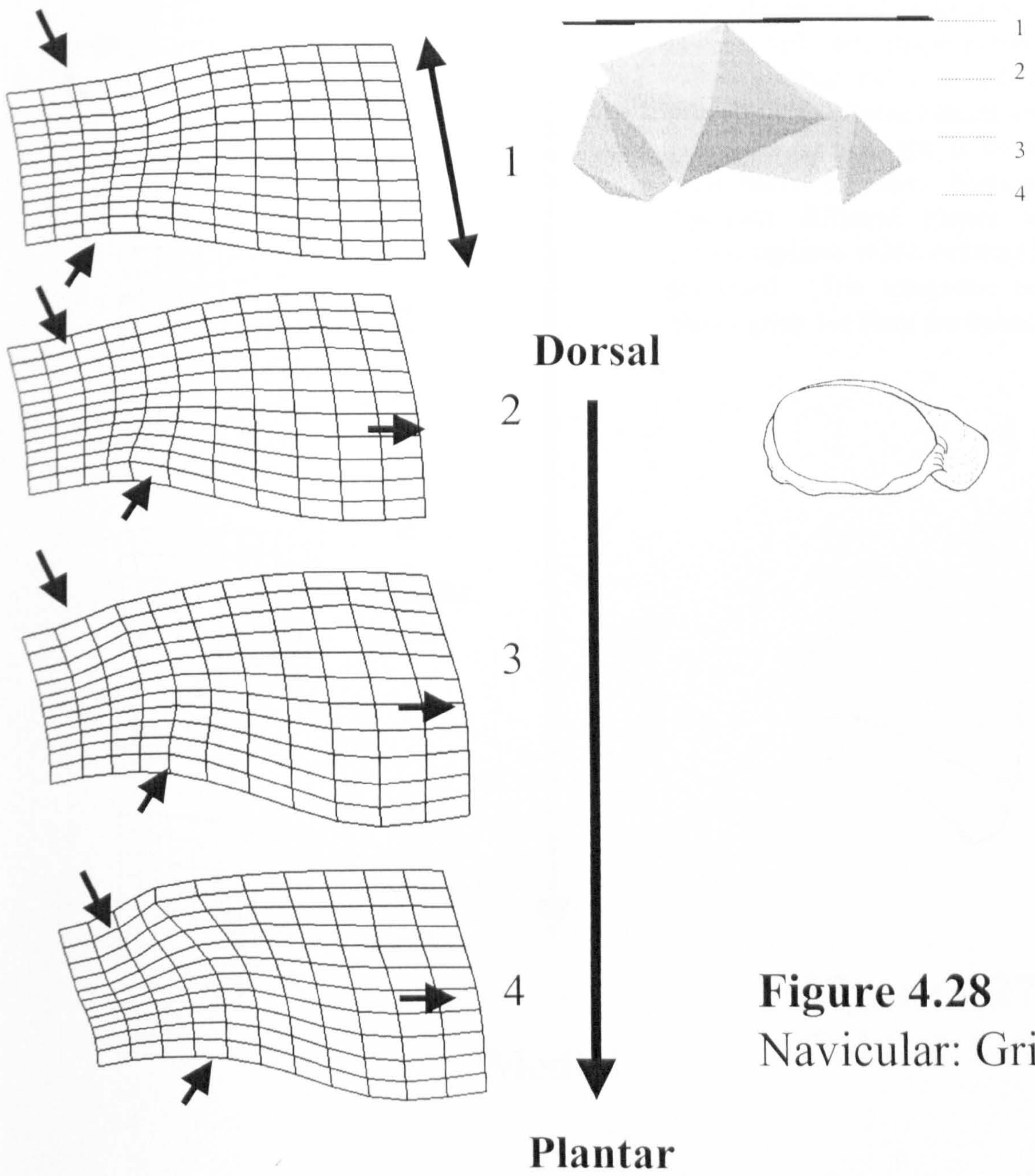
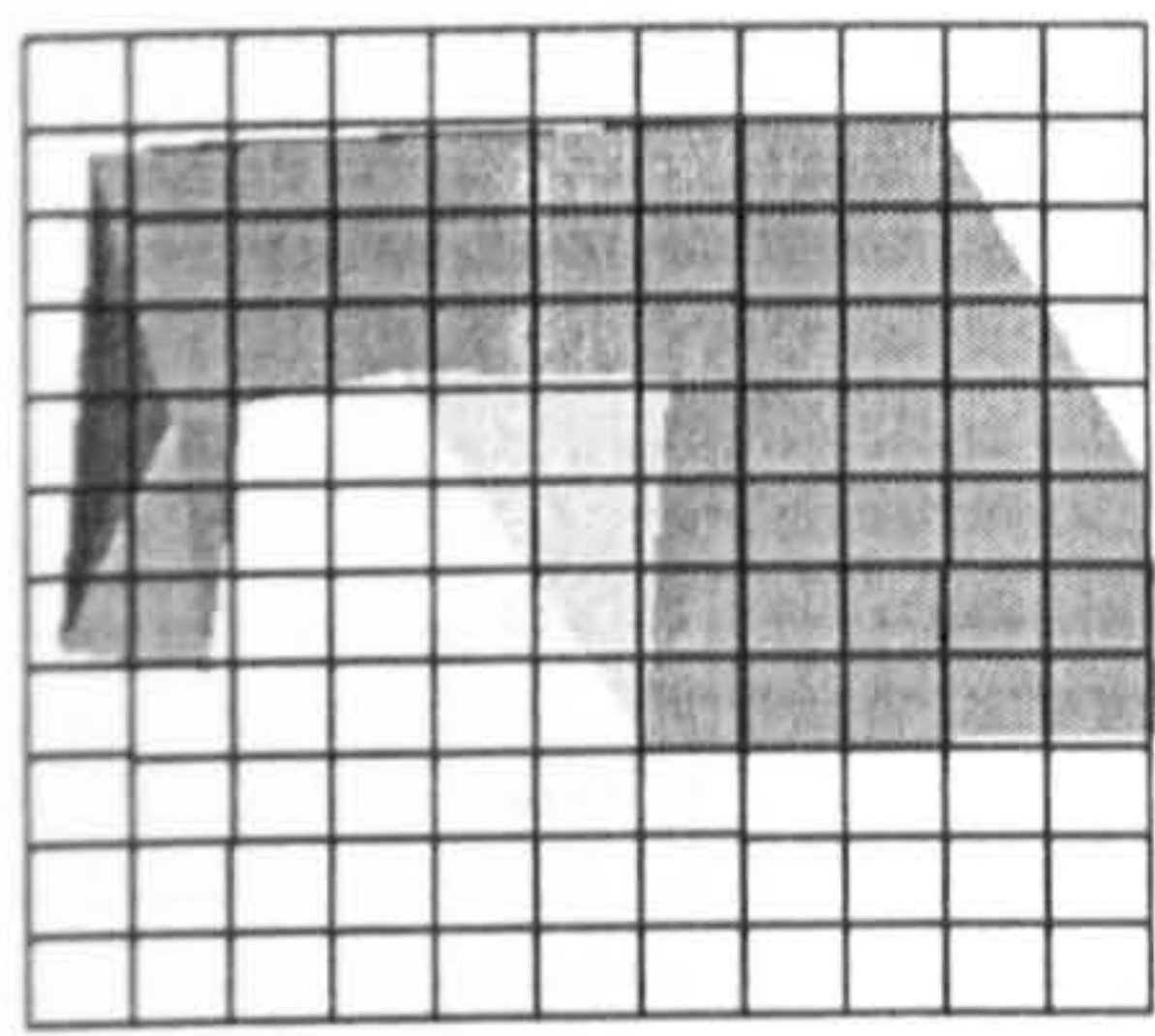
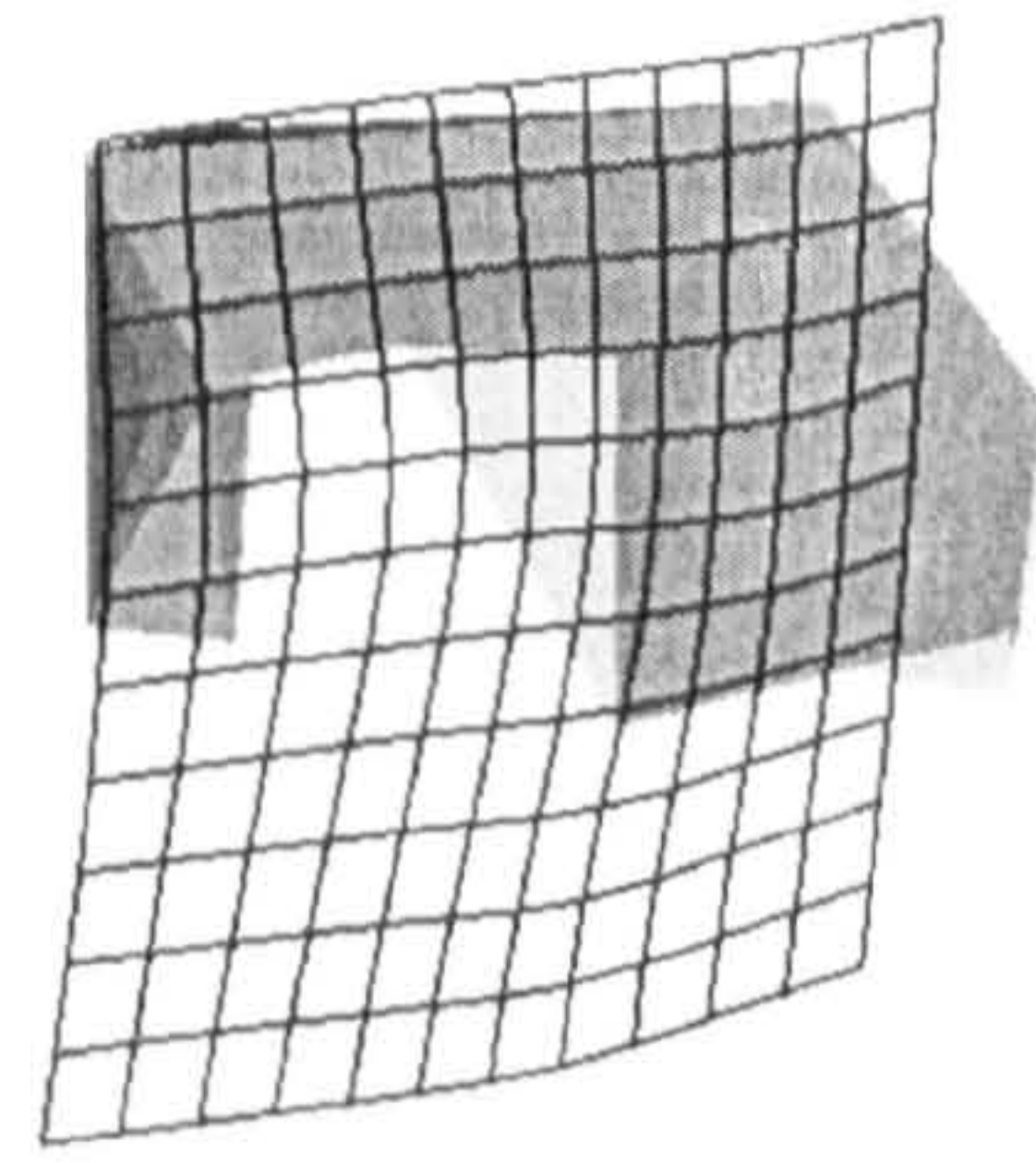
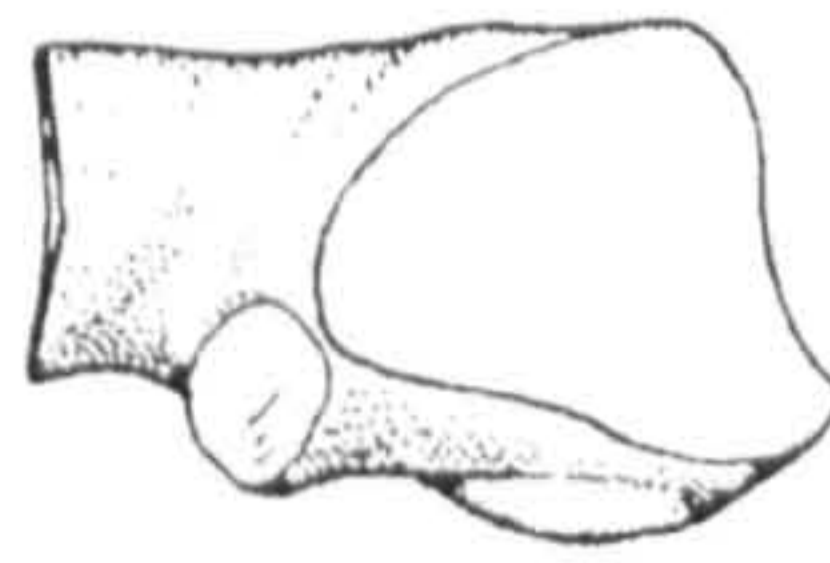


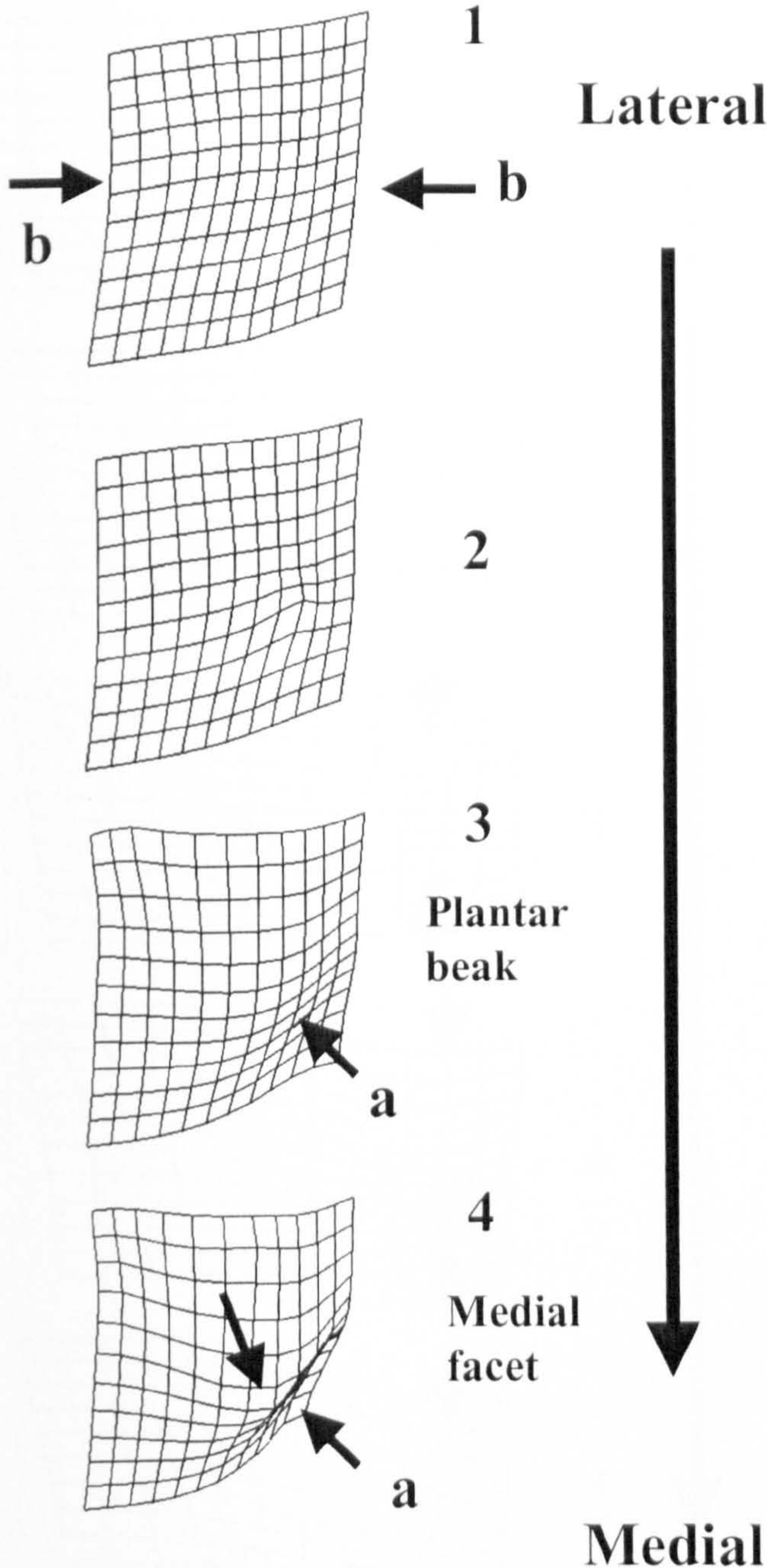
Figure 4.28
Navicular: Grid A



Homo sapiens



Great apes

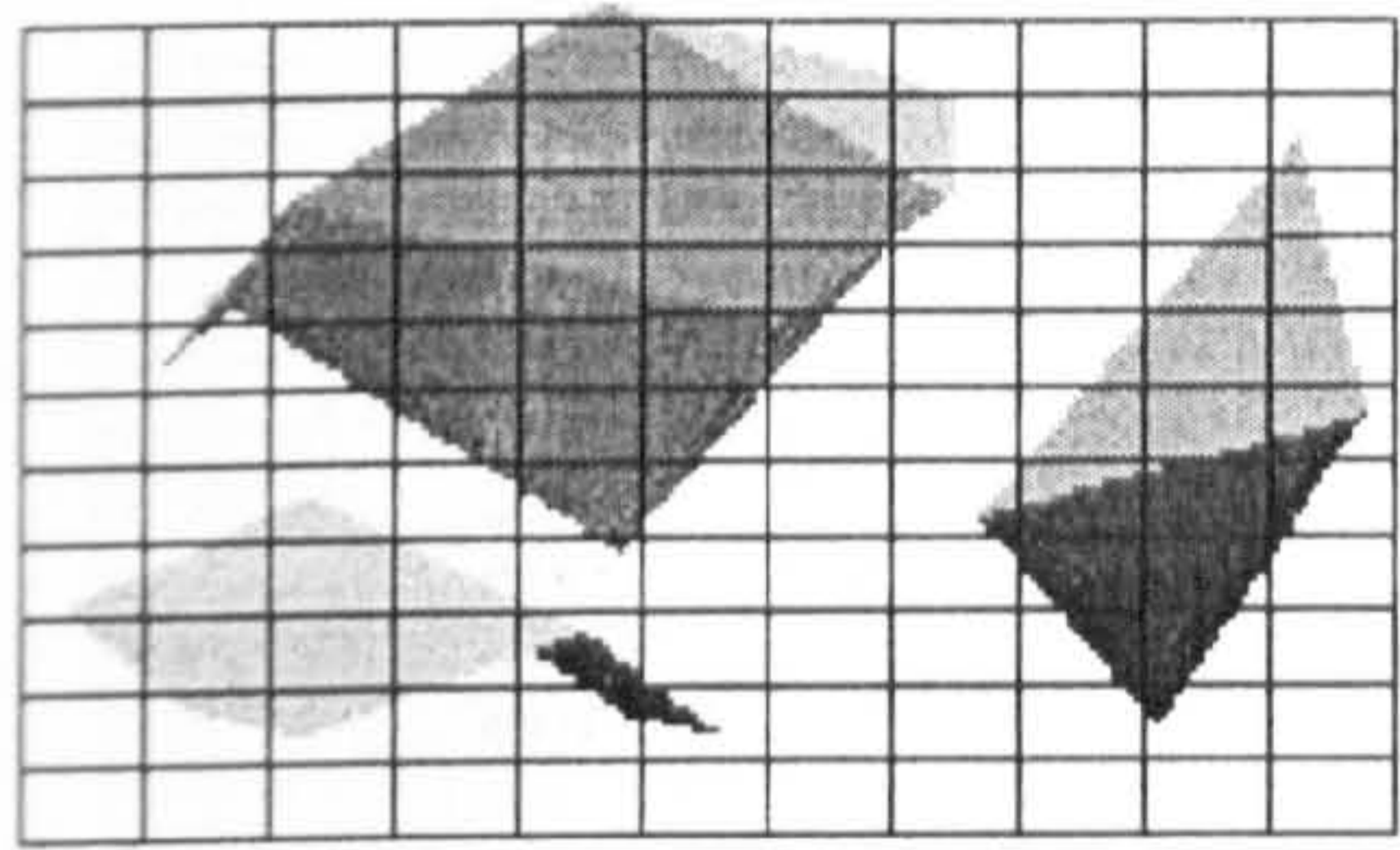


Lateral view of Cuboid Above: The right hand shape is the overall mean warped along PC 1 to the human mean. The reference grid is situated lateral to it. The left hand shape is the result of warping along PC 1 to the great ape means. The deformed target grid for the great ape mean shape is shown at the most lateral position. Numbers 1 – 4 represent different planes at which screen captures of the deformed grid are presented. The schematic below left shows grids 1-4 from the dorsal view.

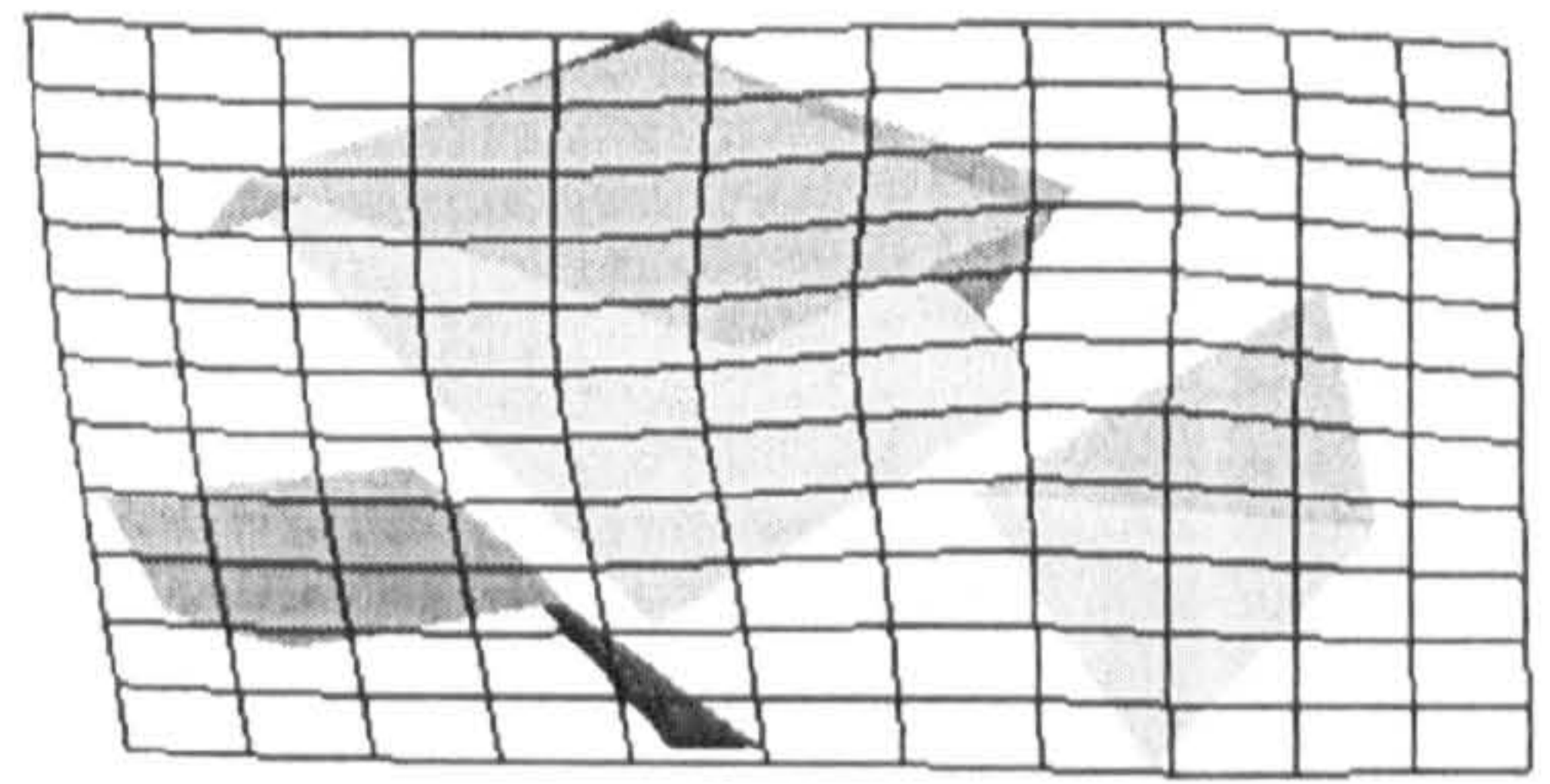
1 2 3 4



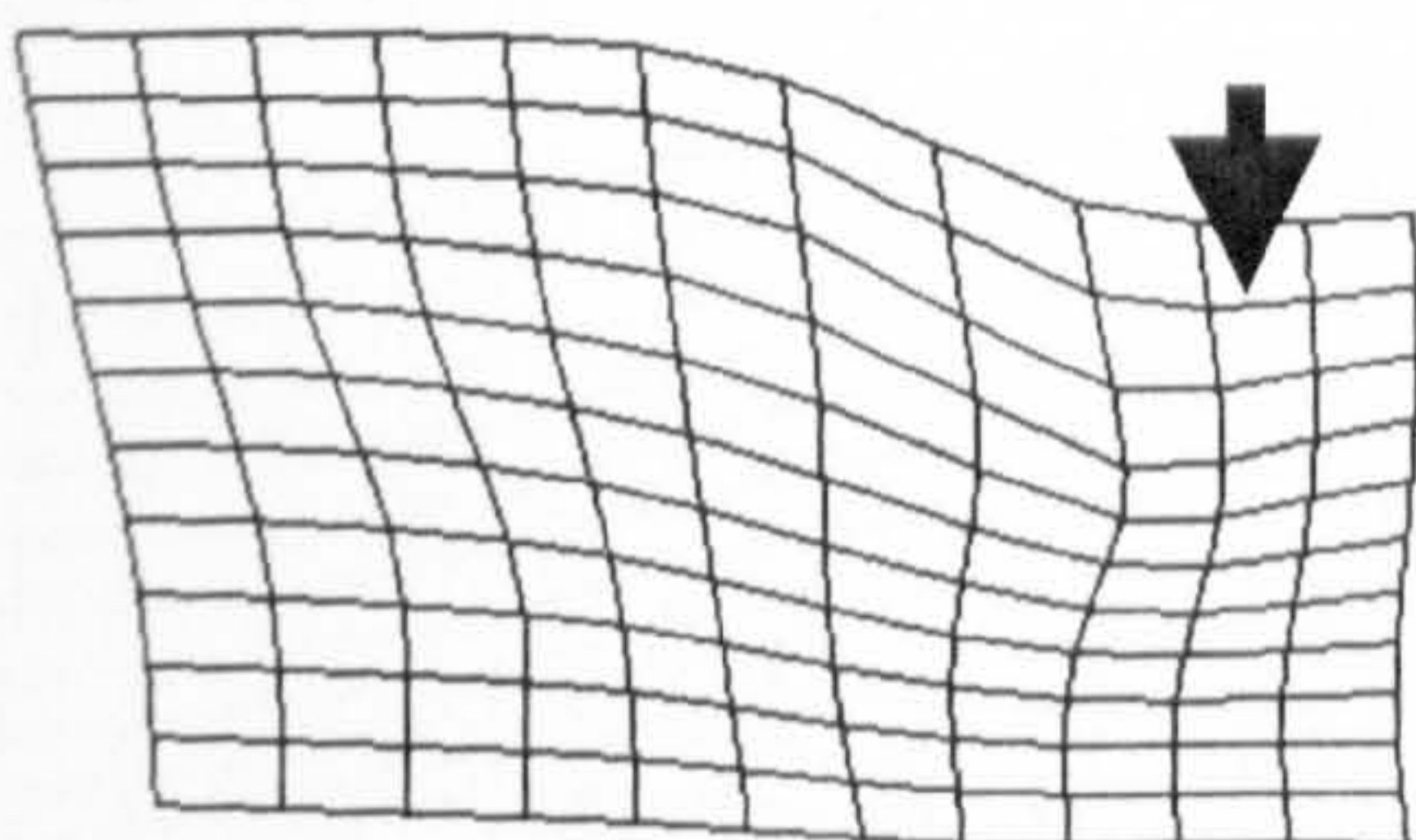
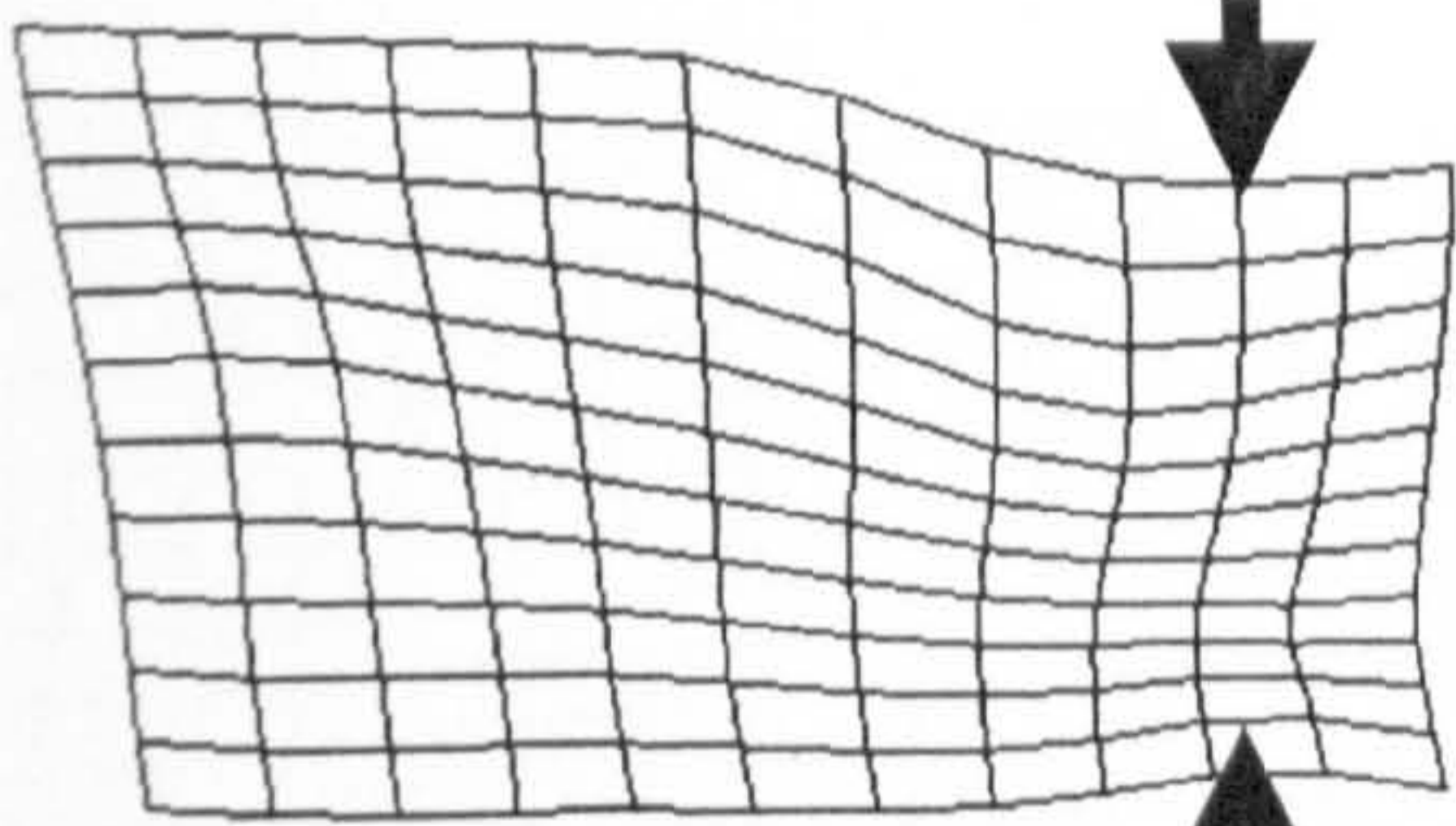
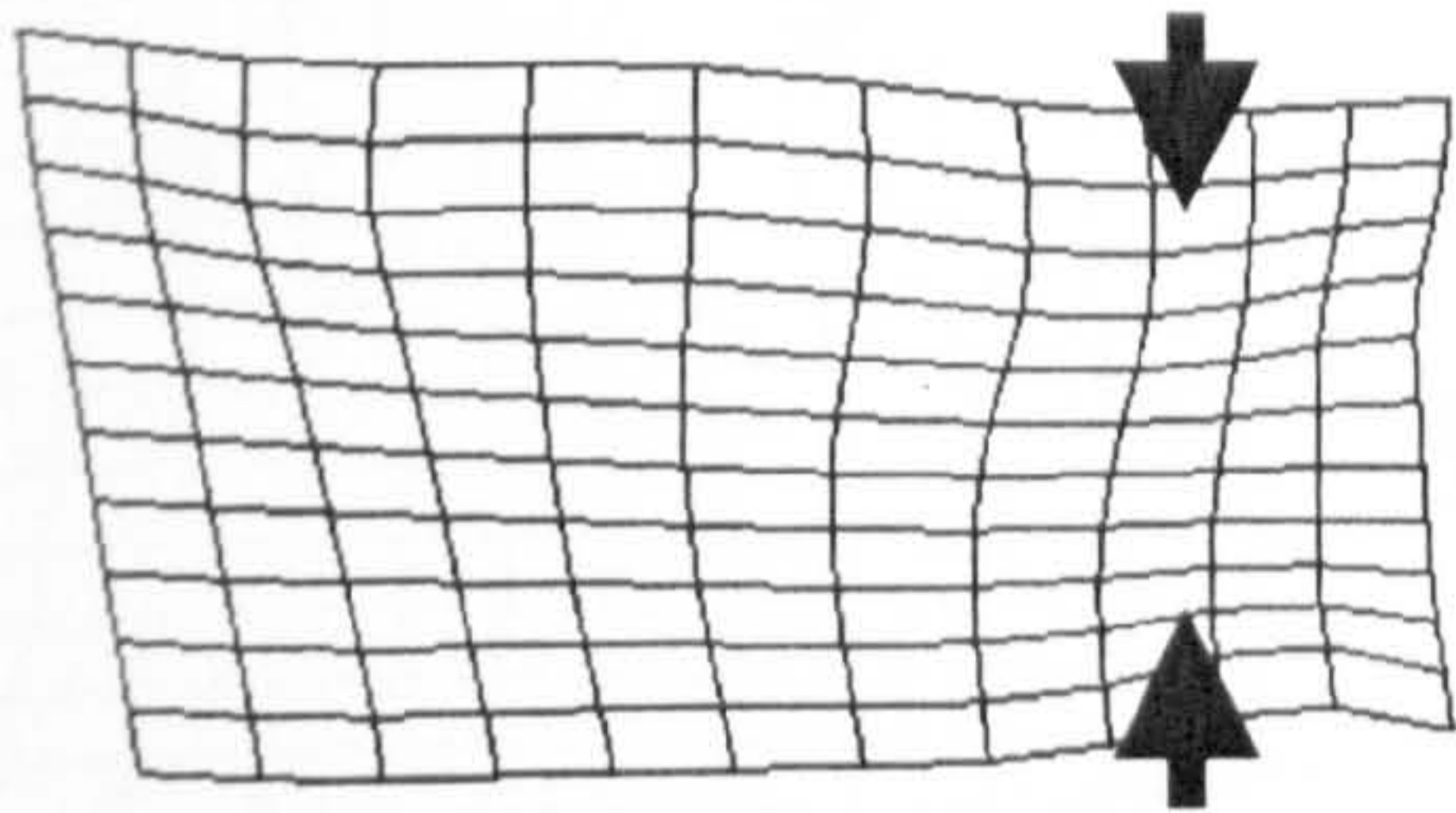
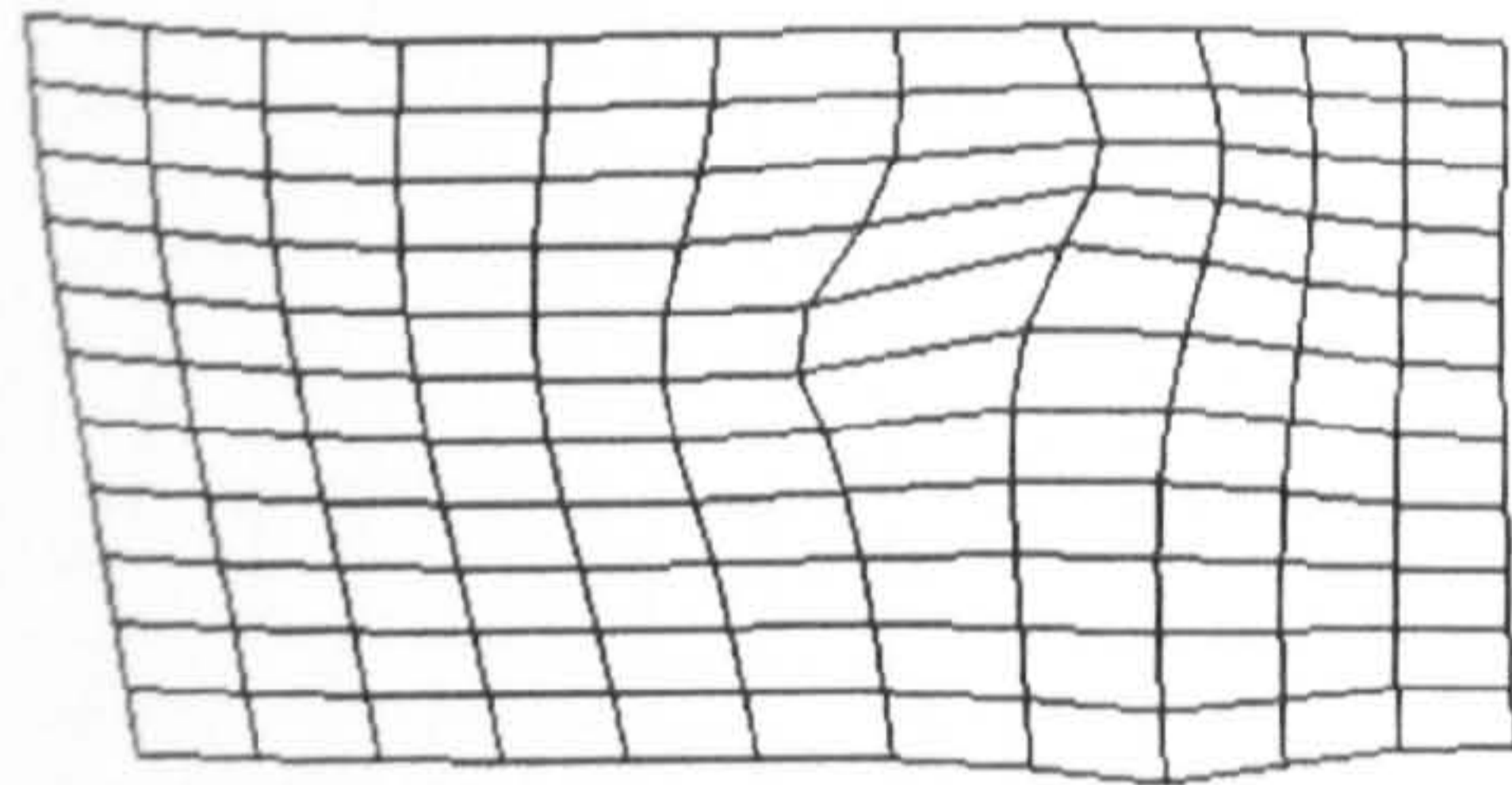
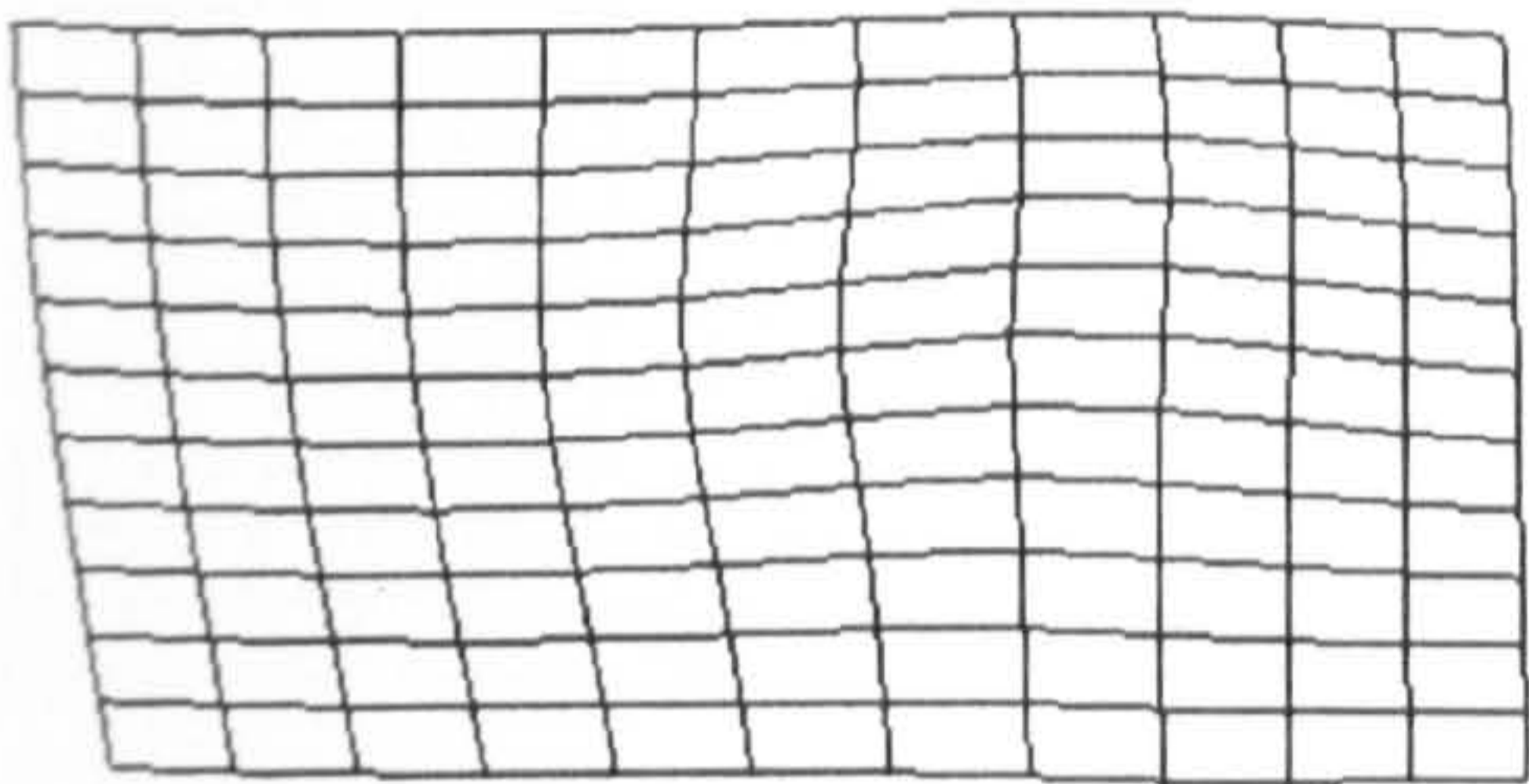
Figure 4.27
Cuboid: Grid A



Homo sapiens



Great apes



Medial

1

2

3

4

5

Proximal

Medial view of Talus Above: The right hand shape is the overall mean warped along PC 1 to the human mean. The reference grid is situated medial to it. The left hand shape is the result of warping along PC 1 to the great ape means. The deformed target grid for the great ape mean shape is shown at the most medial position. Numbers 1 – 5 represent different planes at which screen captures of the deformed grid are presented. The schematic to the lower left shows grids 1-5 from the medial view.

5 4 3 2 1

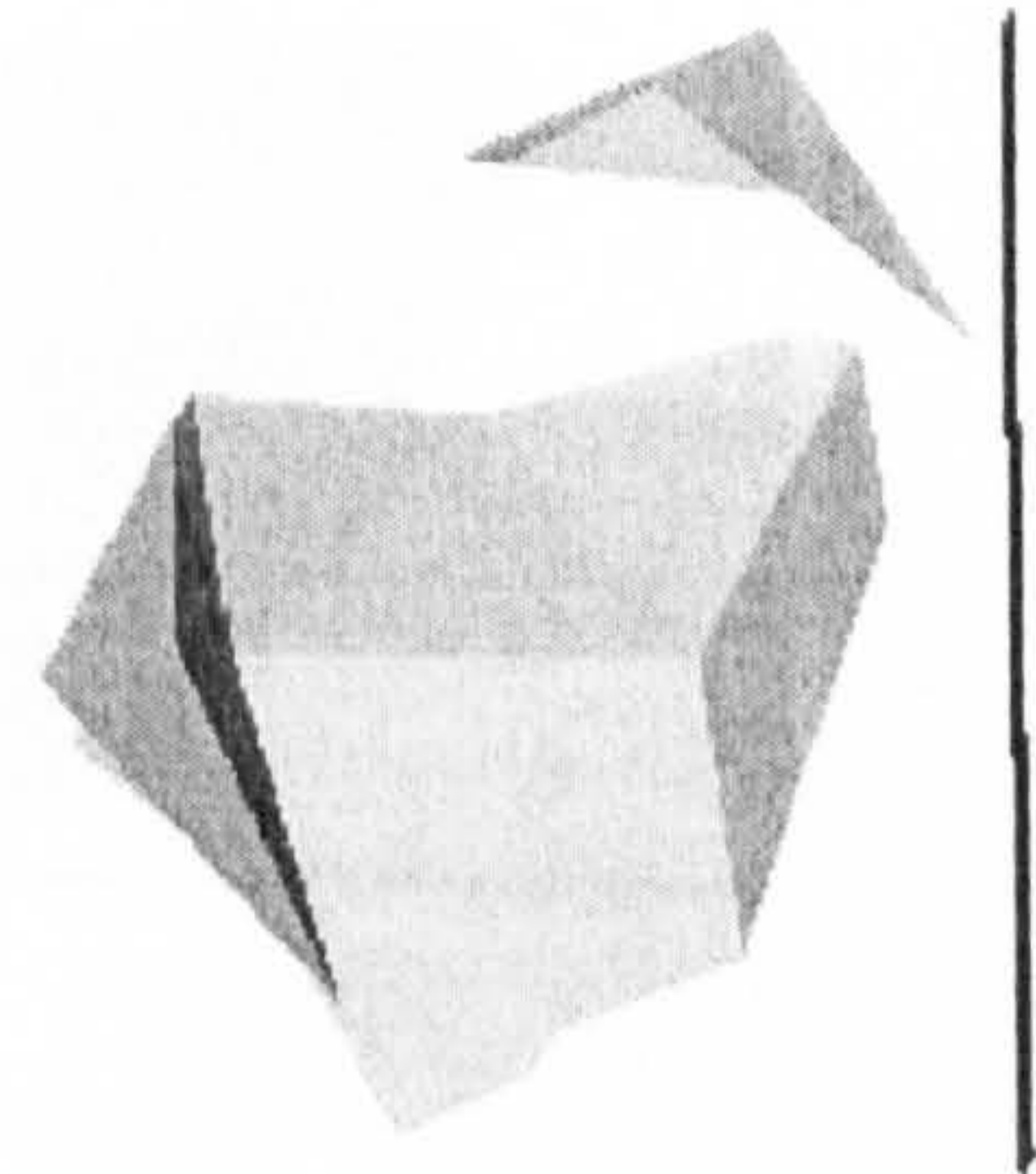
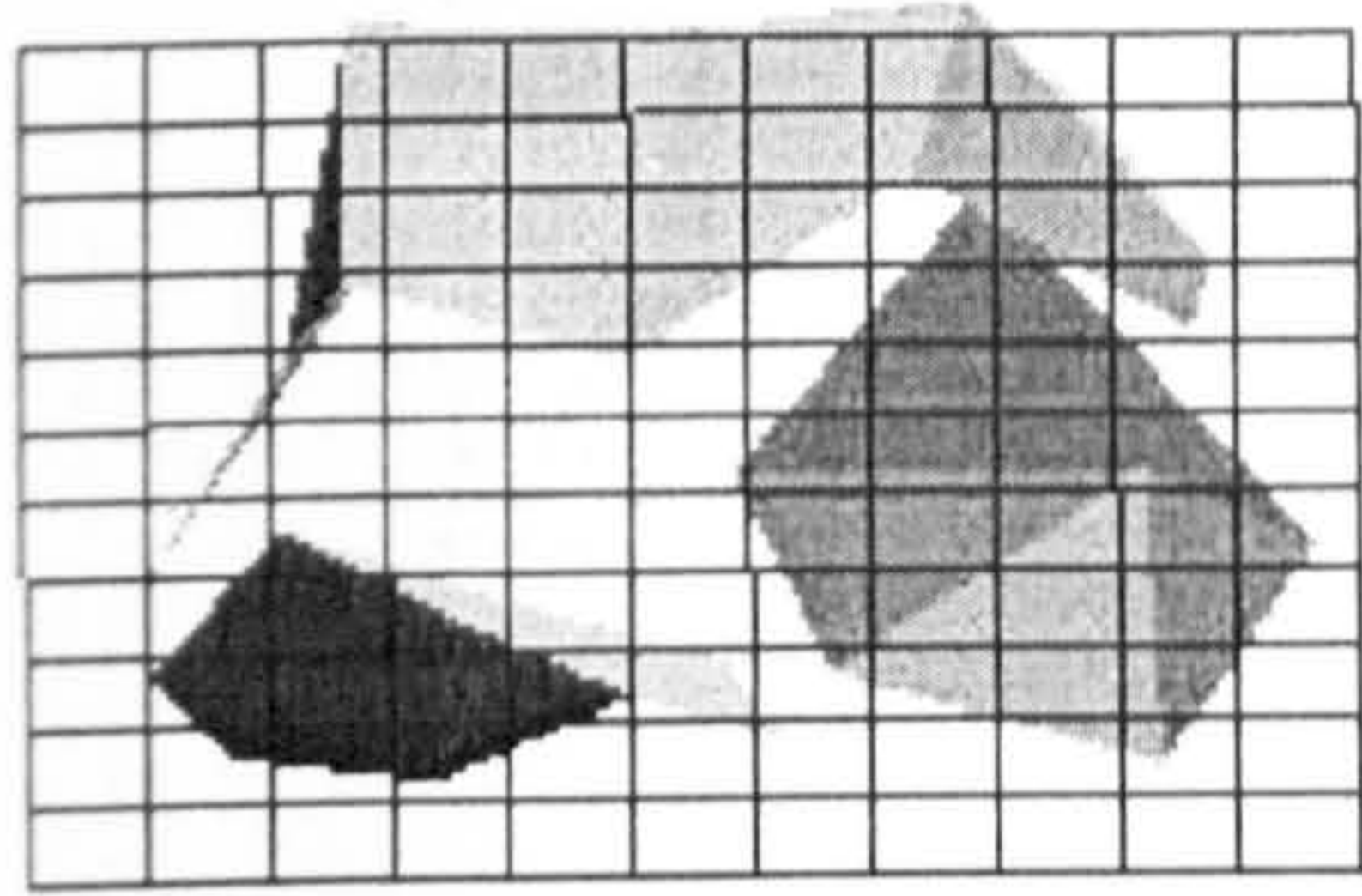
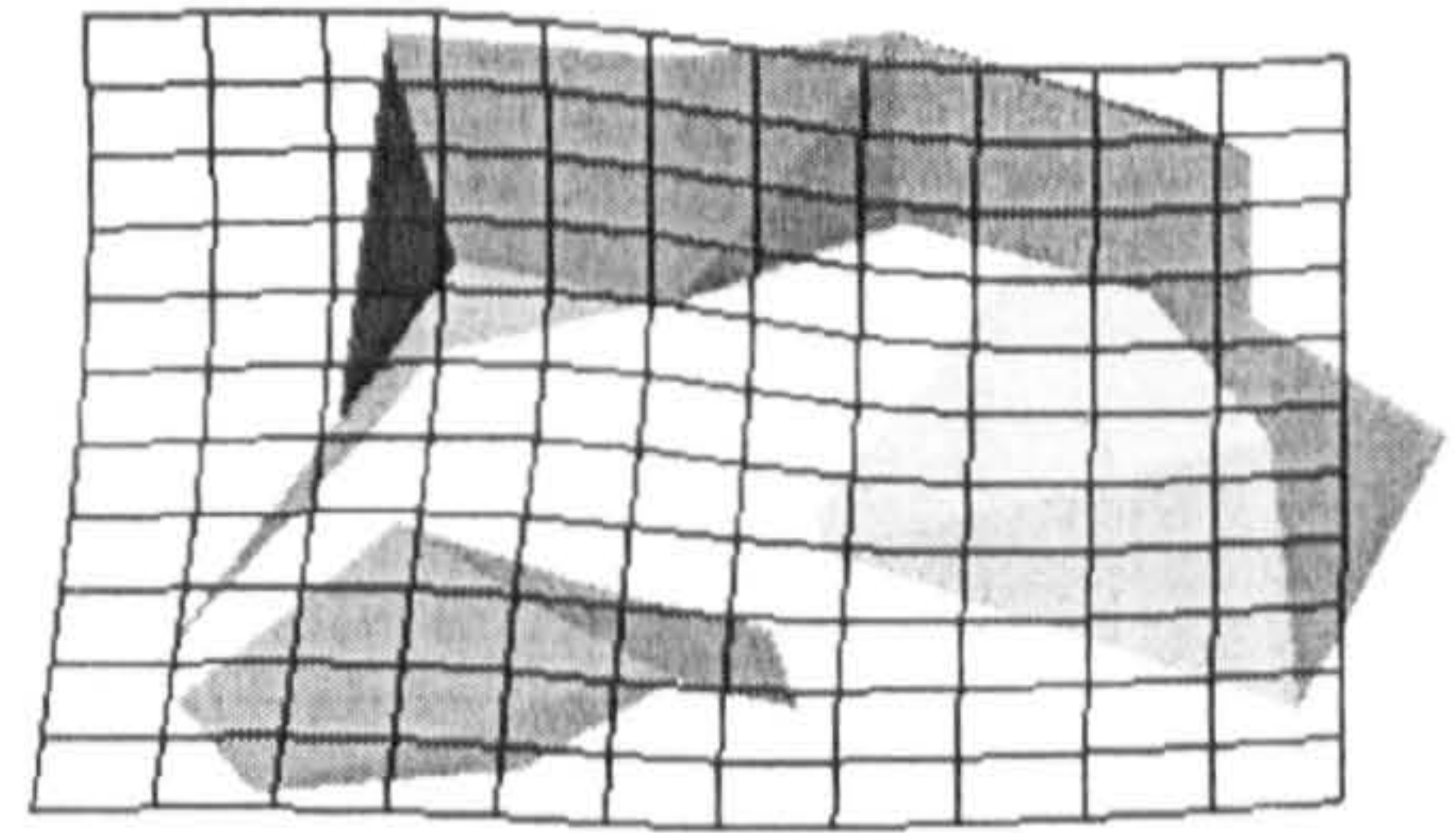


Figure 4.26

Talus: Grid C



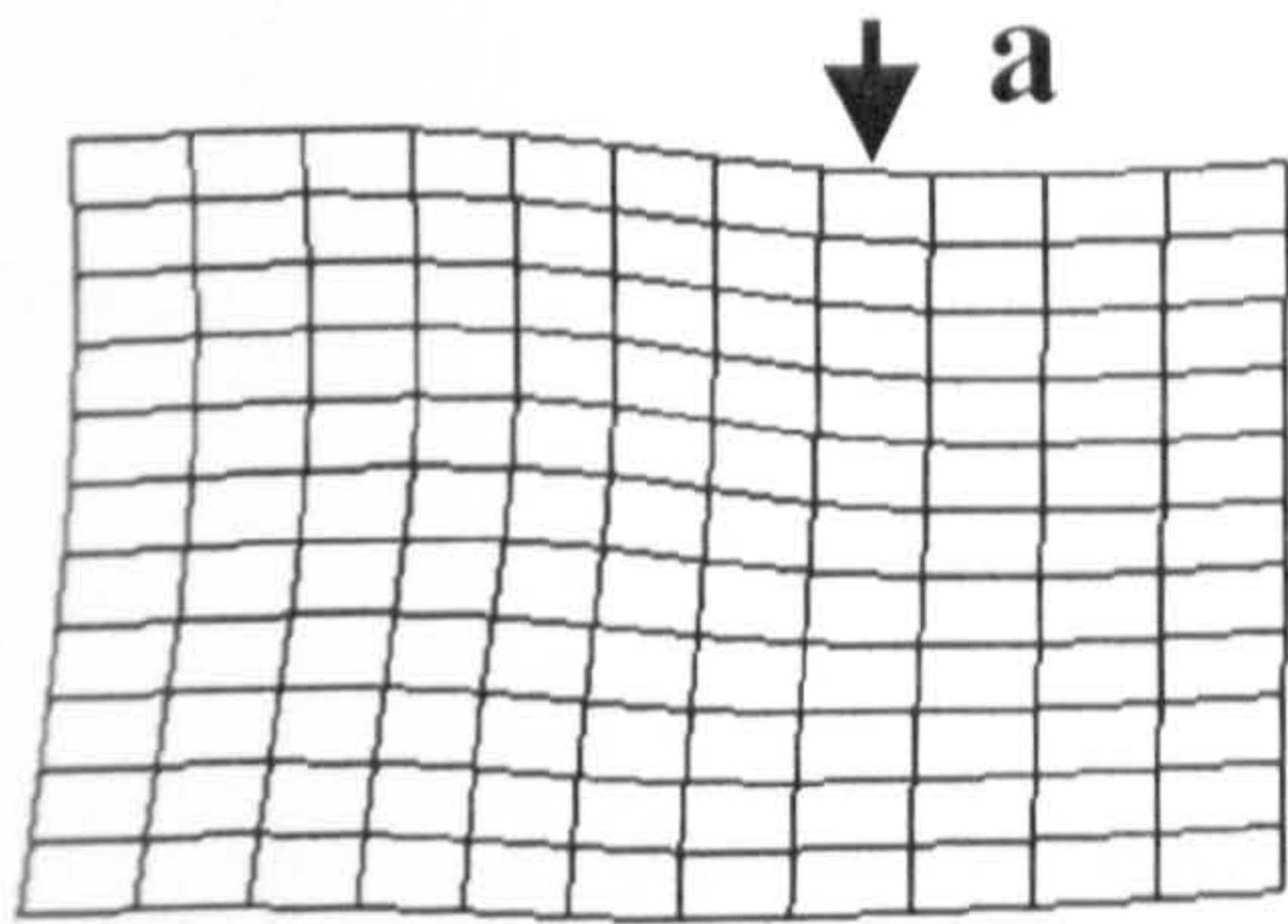
Homo sapiens



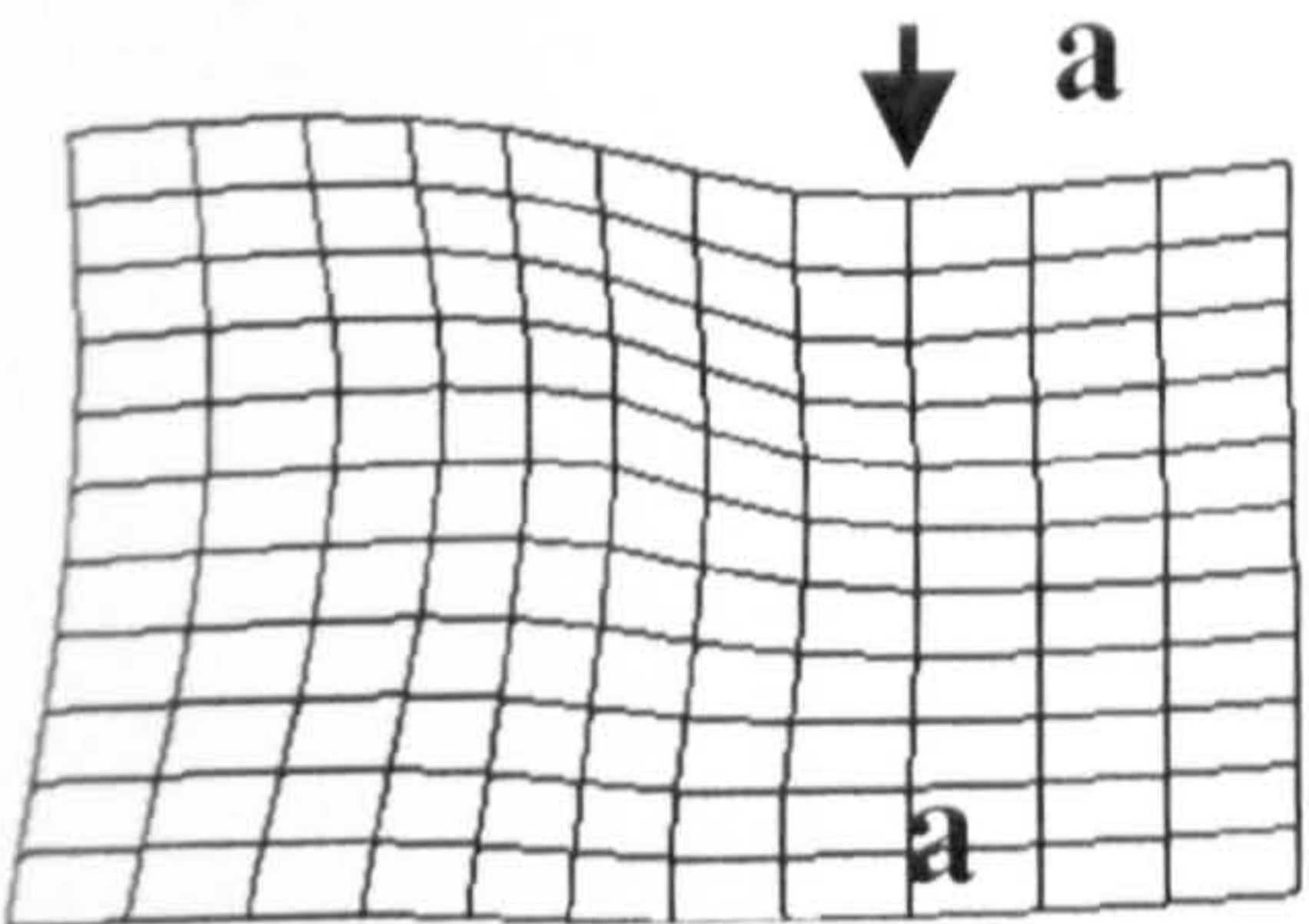
Great apes

Proximal

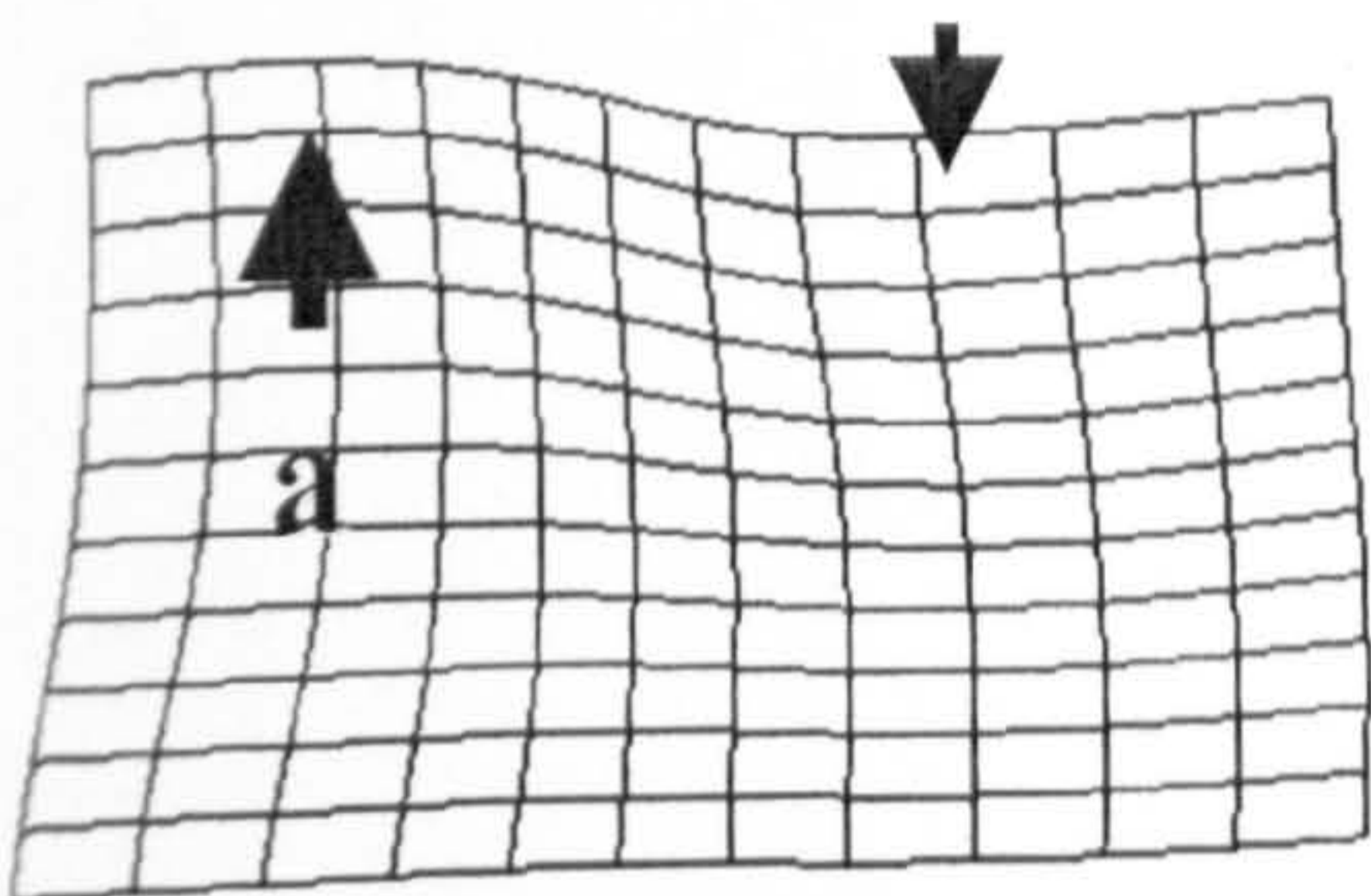
1



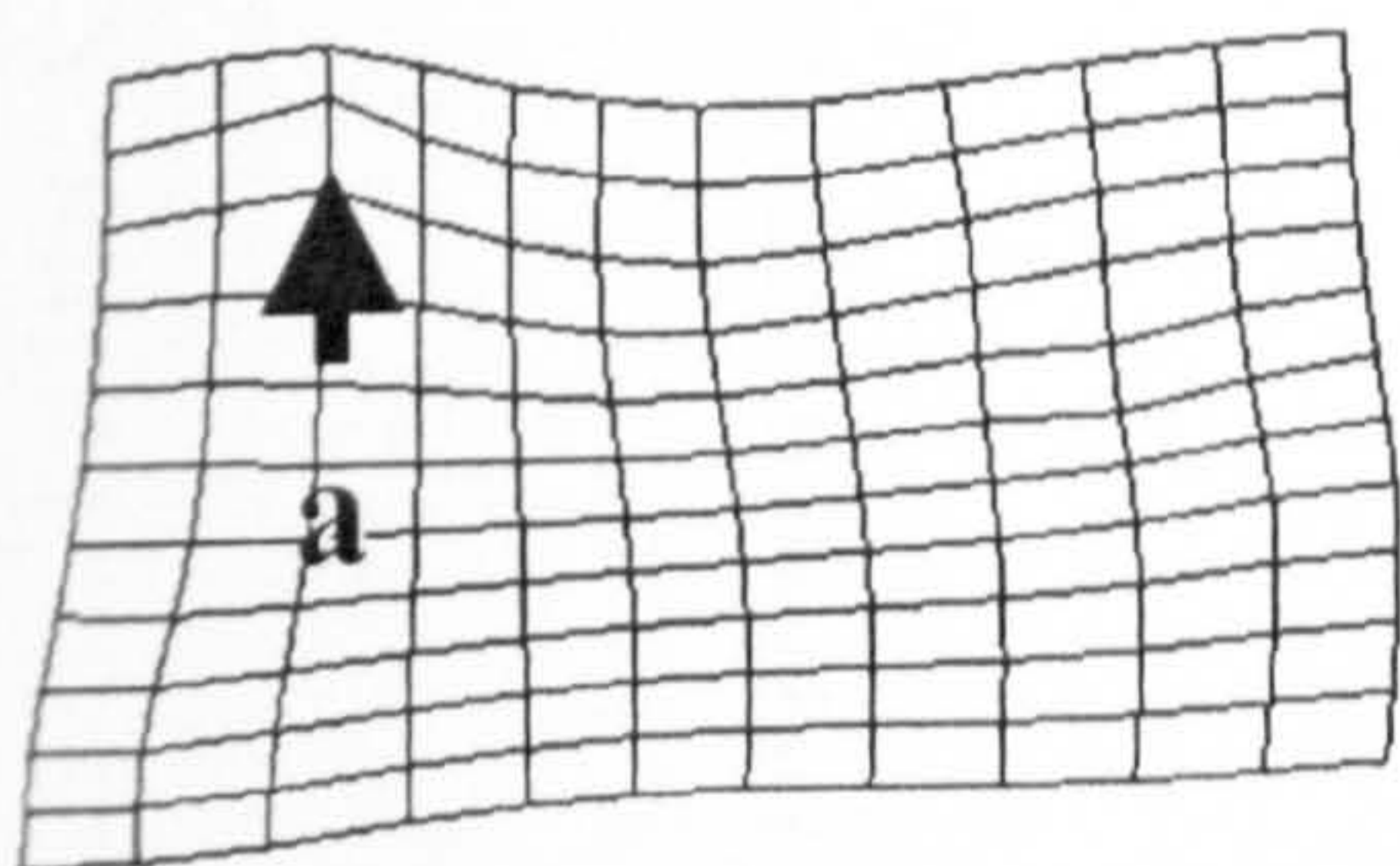
2



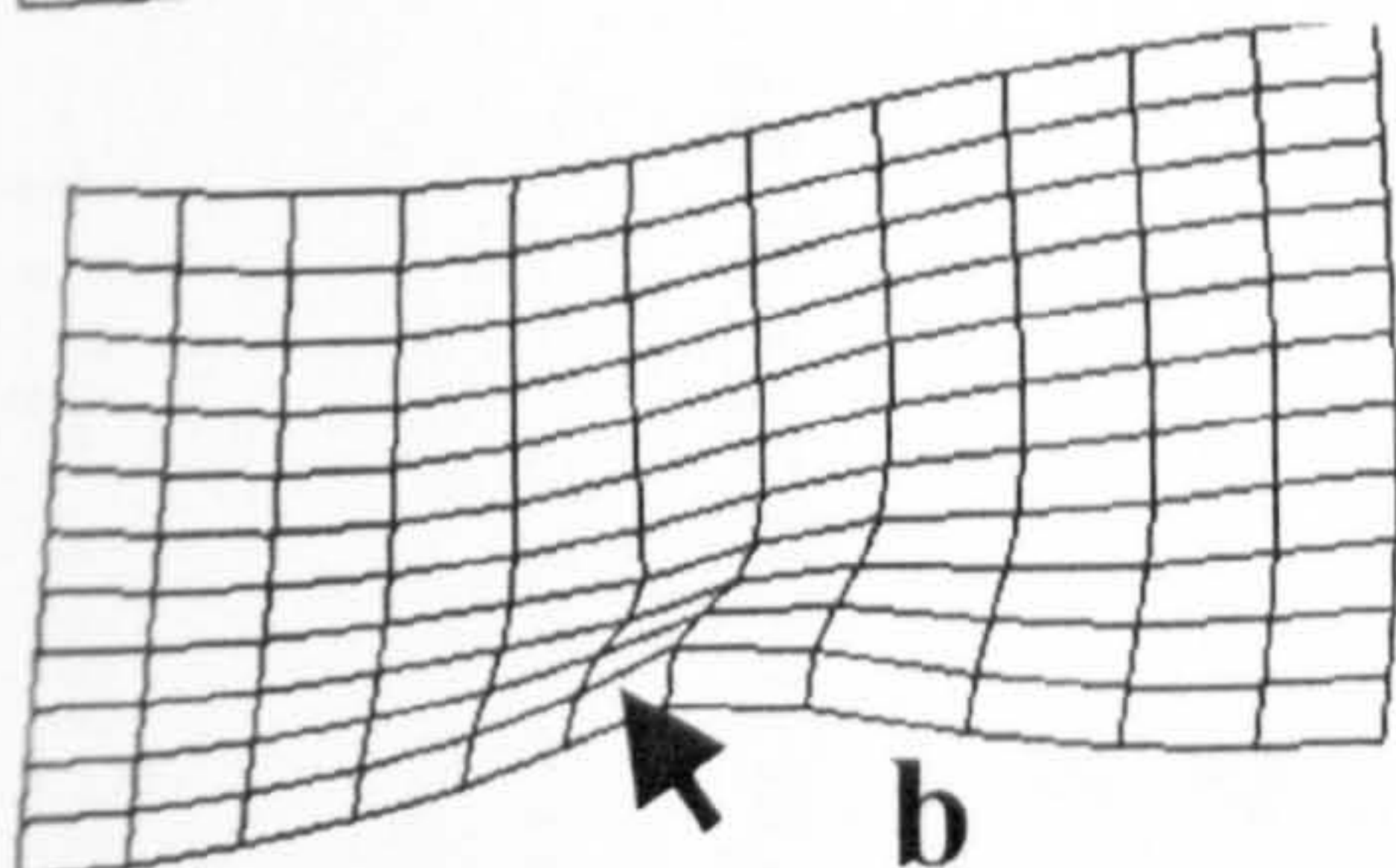
3



4



5



Distal

Proximal view of Talus The right hand shape is the overall mean warped along PC 1 to the human mean. The reference grid is situated in front of it, i.e. The left hand shape is the result of warping along PC 1 to the great ape means. The deformed target grid for the great ape mean shape is shown at the most dorsal position. Numbers 1 – 5 represent different planes at which screen captures of the deformed grid are presented (right hand side of this figure). The schematic to the lower right shows grids 1-5 from the dorsal view.

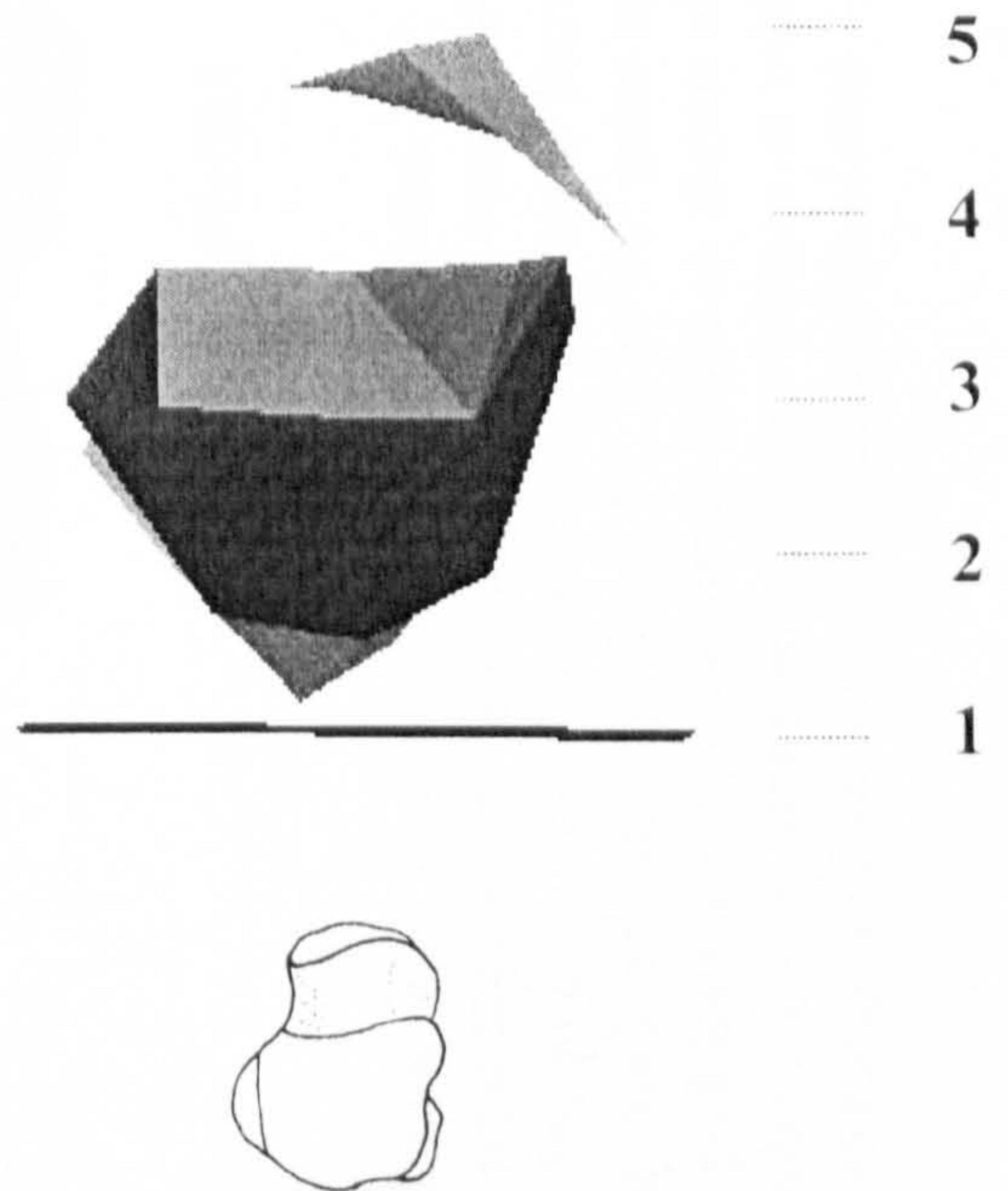
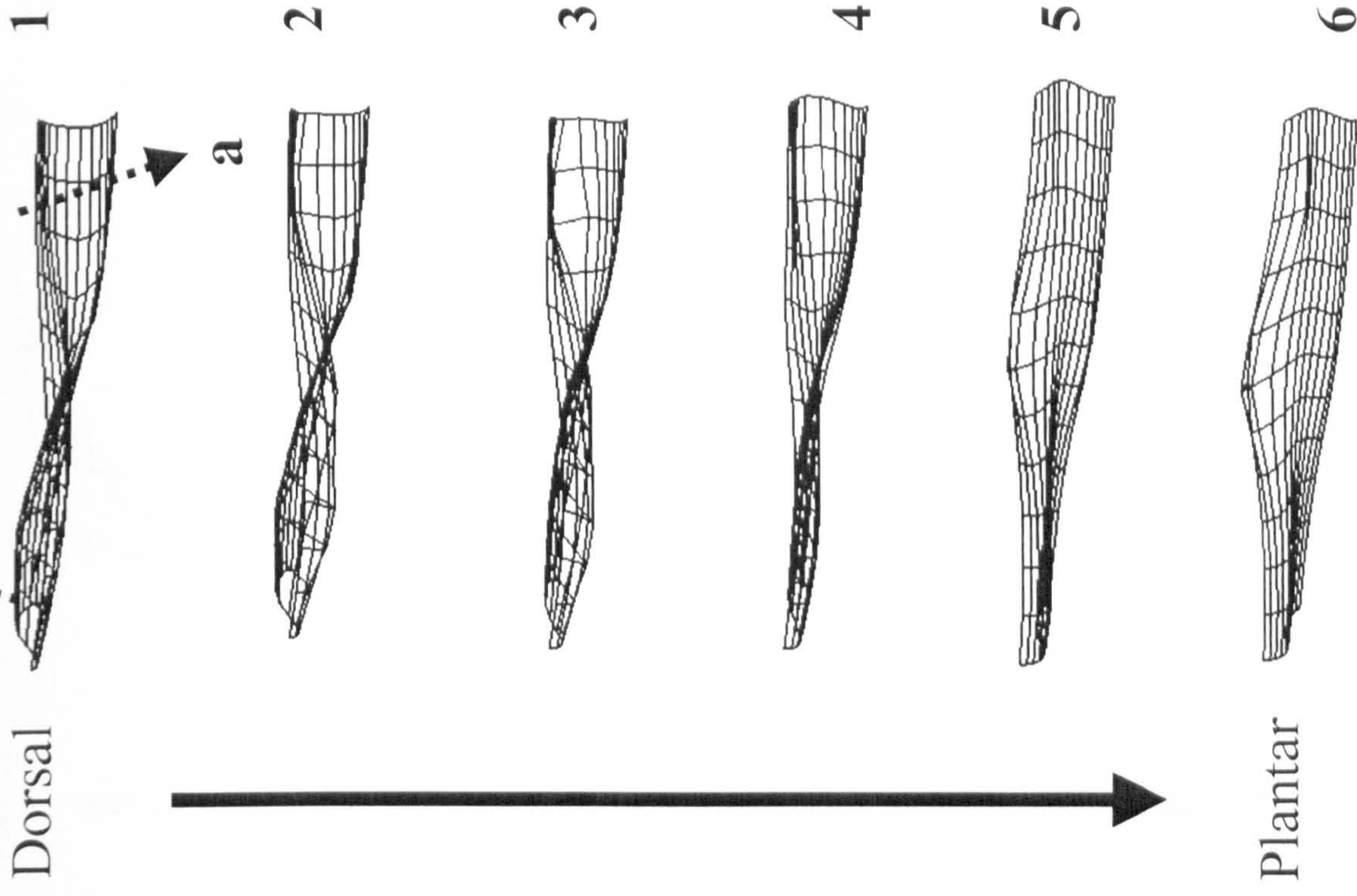


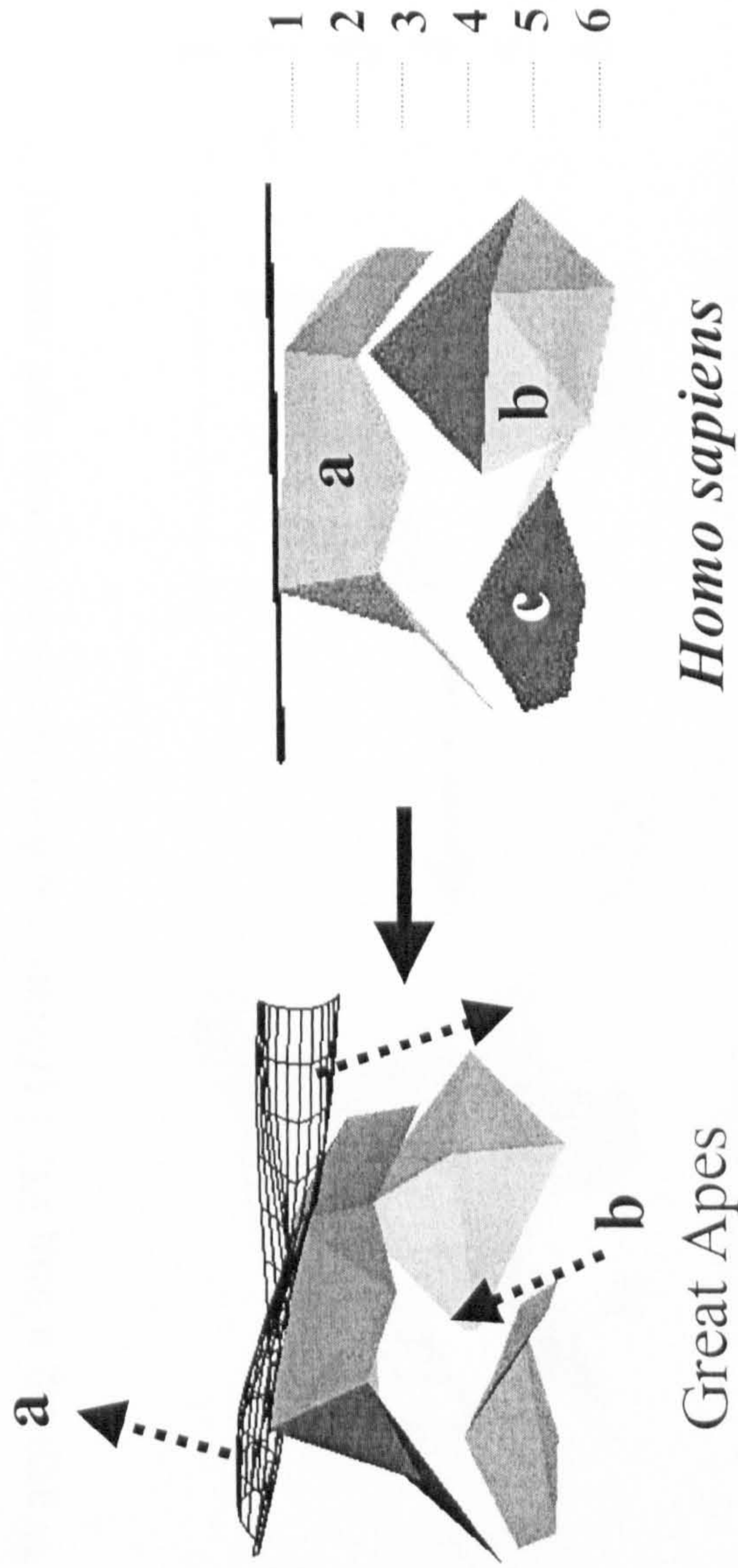
Figure 4.25
Talus: Grid B

Figure 4.24

Talus: Grid A



Warping along PC 1 (*Homo sapiens* mean to great ape means)

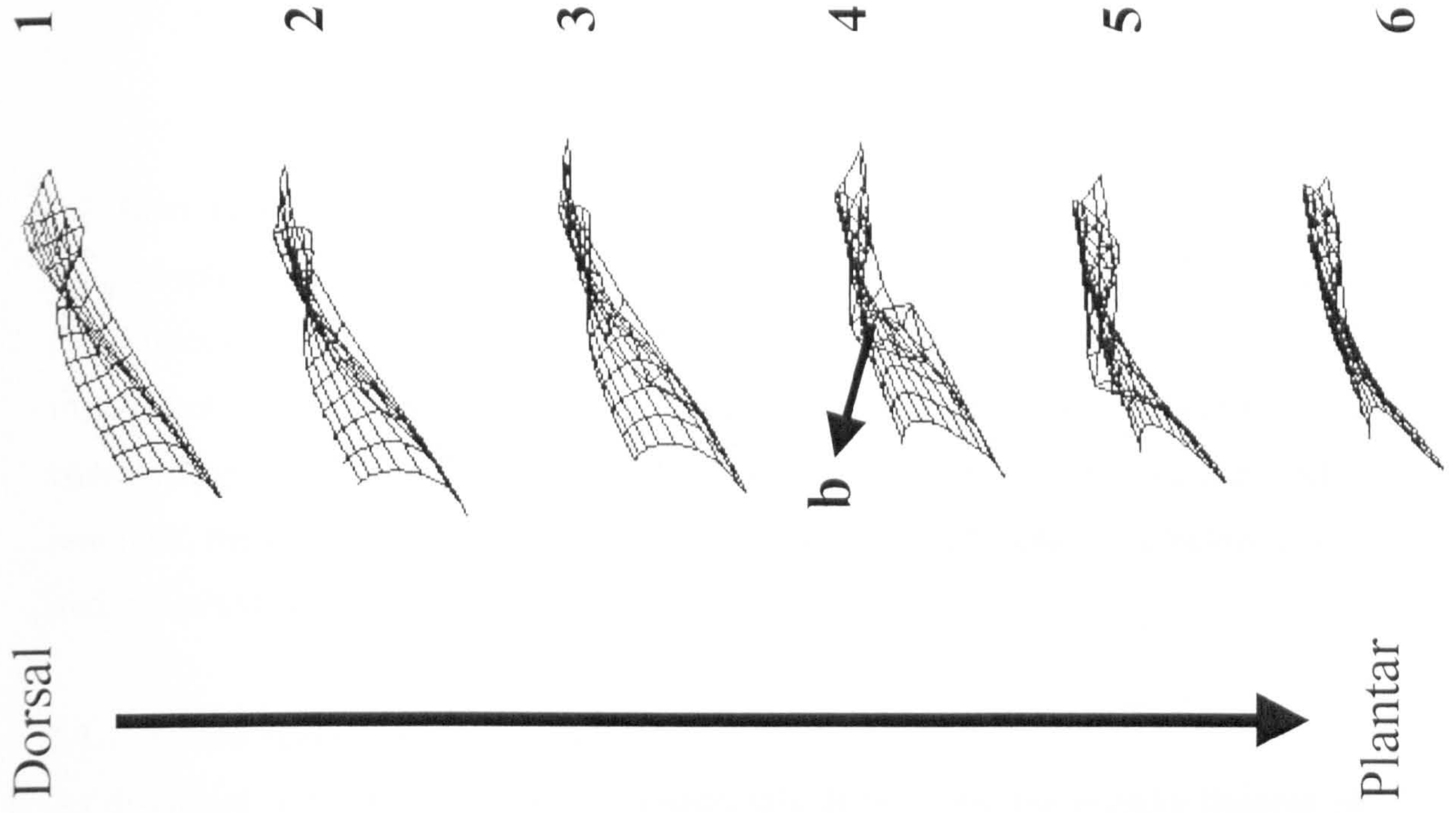


Great Apes

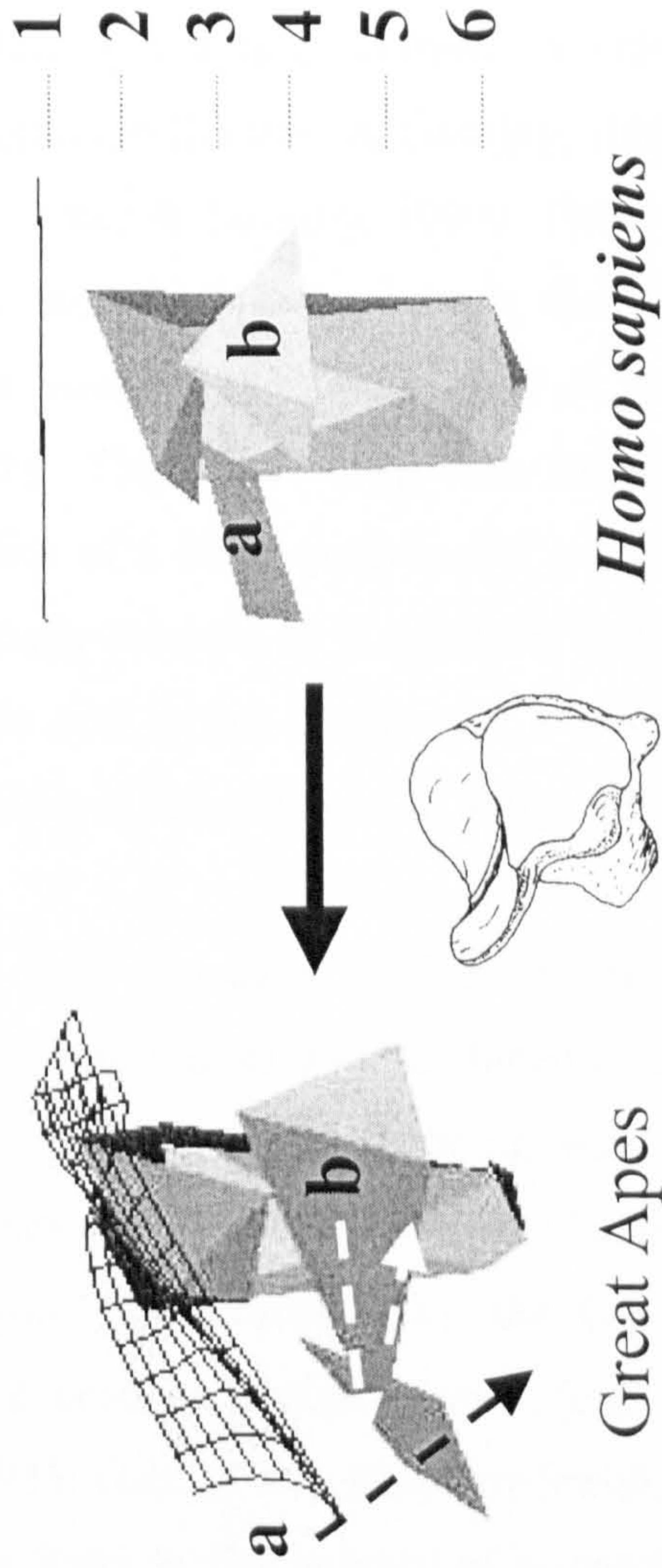
Homo sapiens

Proximal view of Talus, a = trochlear surface, **b** = head, **c** = proximal calcaneal facet. The right hand shape is the overall mean warped along PC 1 to the human mean. The plane of the reference grid is situated above it. The left hand shape is the result of warping along PC 1 to the great ape means. The deformed target grid for the great ape mean shape is shown at the most dorsal position. Numbers 1 – 6 represent different planes at which screen captures of the deformed grid are presented (right hand side of this figure).

Figure 4.23 Calcaneus: Grid A



Warping along PC 1 (*Homo sapiens* mean to great ape means)



Distal view of Calcaneus. **a** = distal talar facet, **b** = cuboid facet. The right hand shape is the overall mean warped along PC 1 to the human mean. The reference grid is situated above it. The left hand shape is the result of warping along PC 1 to the great ape means. The deformed target grid for the great ape mean shape is shown at the most dorsal position. Numbers 1 – 6 represent different planes at which screen captures of the deformed grid are presented (right hand side of this figure).

Chapter 5

5.1 Introduction

This chapter is concerned with exploring the relationship between fossil hominin tarsal bones and those of the extant taxa analysed in Chapters 3 and 4. As discussed in Chapter 1, there are a number of issues surrounding these fossils, and there is considerable debate over both their taxonomic affinities and inferred function. As a reminder, these issues, and the questions they raise, are briefly presented below, and a number of hypotheses are then proposed.

5.1.1 Which species were fully bipedal?

As discussed in Chapter 1, there is considerable debate over the relative degrees of bipedality of different Plio-Pleistocene hominin taxa. *Australopithecus afarensis* has been described by some as having a suite of derived postcranial traits that indicate habitual, obligate bipedal locomotion (Latimer & Lovejoy, 1982; Latimer *et al.*, 1987; Latimer & Lovejoy, 1989; Latimer & Lovejoy, 1990a, 1990b). Others have shown that *A. afarensis* has equally numerous skeletal traits that indicate adaptations to arboreal locomotion (Stern & Susman, 1983; Susman *et al.*, 1985; Stern & Susman, 1991; Susman & Stern, 1991). There have even been suggestions that *A. afarensis* retained certain traits indicative of a more quadrupedal locomotor heritage, but that these traits were not functionally relevant in *A. afarensis* itself (Richmond & Strait, 2000). The best summary to date is that *A. afarensis* was mosaic in its locomotor repertoire, and cannot be considered to have been an obligate biped.

The *Homo habilis* remains have provoked similar debate, and there is no real consensus over whether that taxon was an obligate biped or not. In terms of pedal morphology, the original criteria for a specimen being assigned to that taxon were well-marked longitudinal arches and an adducted hallux (Leakey *et al.*, 1964). Many studies have concluded, mainly from research on the OH 8 foot complex, that *H. habilis* was likely to have been an obligate biped (e.g. Day & Napier, 1964; Preuschoft, 1971; Susman, 1983; Gebo, 1996; Harcourt-Smith, 1999, 2002; Berillon, 1998, 1999, 2000). However, there is also a body of research pointing to *H. habilis*

being a taxon that retained an arboreal component to its locomotor repertoire. The ankle joint it described as some as being a combination of ape-like and unique in its morphology and associated function (Lisowski, 1968; Oxnard 1972; Lisowski *et al.*, 1974, 1976; Lewis, 1980b; Kidd *et al.*, 1996) and, at various times, it has been suggested that the hallux of OH 8 was, at least in part, opposable and therefore indicative of a degree of arboreal grasping behaviour (Lewis, 1980b, 1981; Kidd *et al.*, 1996). The more recent find of the partial *H.habilis* skeleton OH 62 (Johanson *et al.*, 1987; McHenry & Berger, 1998) has shown that *H.habilis* had limb proportions that were more ape-like than human-like, with a relatively long arms, and relatively short legs. This suggests that *H.habilis* could well have been a capable climber (Wood & Collard, 1999). However, if, as some researchers suggest, OH 8 is very human-like in its morphology and function, the question arises, do OH 62 and OH 8 actually represent the same species? To summarise, research to date indicates that *Homo habilis* certainly had a number of adaptations in its foot to suggest that it was an efficient biped, but there is also research that shows that it probably was not an *exclusive* biped, and still retained some arboreal locomotor behaviours.

As discussed in Chapter 1, there is only one piece of published work on the foot bones of *Australopithecus africanus*. The foot was described as being mosaic in its affinities, with a human-like ankle joint but and ape-like retention of the ability to (at least partially) oppose the hallux, inferring at least some degree of arboreality and therefore grasping potential (Clarke & Tobias, 1995). This possible arboreal component of *A.africanus*' locomotor repertoire has been supported by the finding that the morphology of the semicircular canals of the inner ear (the organ of balance) is very ape-like in both *A.africanus* and *P.robustus* (Spoor *et al.*, 1994).

5.1.2 *H.habilis* versus *A.africanus*

There have been a number of suggestions that, in general, *Homo habilis* specimens do not show enough morphological traits to warrant being placed in the genus *Homo*, and are, in fact, far more *Australopithecus*-like in many ways (Wood, 1974; McHenry & Berger, 1998; Wood & Collard, 1999). This problem has been highlighted by the reports of OH 62's more ape-like limb proportions, which are described as being very similar to those of *A.africanus* (Johanson *et al.*, 1987; McHenry & Berger, 1998). If the *H.habilis* specimens were reassigned to the genus *Australopithecus*, the question

is, what specific taxa would they be assigned to? Based on limb proportions, *A.africanus* might be a reasonable choice. It is also perfectly possible that any similarities between *A.africanus* and *H.habilis* may simply be plesiomorphies, and thus a result of parallelism rather than recent common ancestry.

However, Clarke and Tobias (1995) argue that the foot of *A.africanus* is different to that of *H.habilis*, in that *A.africanus* still had an opposable hallux and a mobile mid-tarsal joint. The issue remains an open one until more comparative analyses are conducted. It is the hope of this study to add to that debate by statistically comparing homologous 3D data sets from the tarsals of both taxa.

5.1.3 Did the feet of different fossil taxa adapt to bipedalism in different ways?

With respect to the foot, this is a question that has not really been addressed in the literature to date. One of the reasons for this is that studies have mainly rested on isolated pedal elements, often because certain specimens had either not been discovered yet, or were not available for analysis. Furthermore, debate on the origins of bipedalism has rested on issues surrounding the likely locomotor repertoire that *preceded* bipedalism (e.g. Richmond & Strait, 2000; Dainton, 2001; Richmond *et al.*, 2002), the ecological/behavioural reasons as to *why* bipedalism evolved (e.g. Wheeler, 1988, 1994; Wood, 1993; Chaplin *et al.*, 1994; Hunt, 1994), or the *degree* to which certain taxa were bipedal or not (e.g. Le Gros Clark, 1947; Leakey & Hay, 1979; Susman & Stern, 1982; Stern & Susman, 1983; Senut & Tardieu, 1985; Susman *et al.*, 1985; Latimer *et al.*, 1987; White & Suwa, 1987; Latimer & Lovejoy, 1989; Susman & Stern, 1991; Gebo, 1992; Spoor *et al.*, 1994; Clarke & Tobias, 1995).

Based on current geological dates (Walter, 1994; Partridge *et al.*, 1999), the *A.afarensis* remains from Hadar and the Member 2 *A.africanus* remains from Sterkfontein (which include Stw 573) are approximately contemporaneous. As discussed above and also in Chapter 1, both are likely to have been mosaic in their affinities, but it has not been postulated that they may have been mosaic in different ways, thus representing at least two discrete ways of adapting the foot to bipedal locomotion. Based on analysis of pelvic and femoral fossil remains from South Africa, Napier (Napier, 1964) suggested that *P.robustus* and *A.africanus* had “striking differences” (p.701) in their morphology that reflected different types of bipedal

locomotion, with that of *A.africanus* being more similar to the locomotion of modern humans. The *A.africanus* specimens Napier was referring to are of a younger geological age than the Stw 573 remains analysed in this study, and so are closer in age to the *P.robustus* remains. So, it is certainly conceivable that geologically contemporary hominin taxa had differing forms of bipedal locomotion.

5.2 Hypotheses

As a result of the above discussion, the following hypotheses are proposed:

H₁ That, for each tarsal, the fossil specimens are morphologically similar enough to each other to represent a single species.

H₂ That the tarsals of *Homo habilis* and *Australopithecus africanus* are morphologically similar enough to each other to represent a single species.

H₃ That *A.afarensis* tarsals are morphologically distinct from either *H.habilis* or *A.africanus* so as to fall outside extant intraspecific ranges of variation.

5.3 Materials

Extant taxa

The extant taxa used in this analysis are comprised of exactly the same individuals as were used in the interspecific analyses in Chapter 4.

Fossil taxa

The geographical location of the fossil localities is illustrated in a map (Figure 5.1) at the end of this section.

Hadar material

The pedal material from the Hadar formation in Ethiopia comes from the AI 288 partial skeleton (“Lucy”) and the AI 333 assemblage (“The First Family”). The only tarsal belonging to AI 288 is a complete right talus (AI 288-1as). For AI 333, there are a number of specimens, including two complete right naviculars (AI 333-36 and AI 333-47), a partial medial cuneiform and some fragmentary parts of calcanei, tali

and a lateral cuneiform (Latimer et al., 1982). Only the two naviculars are used in this analysis. The most recent dating of the Hadar formation, using $^{40}\text{Ar}/^{39}\text{Ar}$ single-crystal laser-fusion analysis of volcanic tuffs, has established relatively precise dates of 3.18 mya and 3.20 mya for Al 288 and Al 333 respectively (Walter, 1994).

Sterkfontein material

Stw 573

This fossil, also known as “Littlefoot”, was discovered in 1994 among bags of mammalian remains excavated in 1980 from the Sterkfontein cave system, South Africa. The bones were known to have come from the Silberberg Grotto, which is one of the deeper parts of the system, and is dominated by Member 2 of the Sterkfontein formation. The initial discovery consisted of four left-hand hominin foot bones: the talus, navicular, medial cuneiform and the proximal half of the first metatarsal, and were tentatively assigned to the taxon *Australopithecus africanus* (Clarke & Tobias, 1995). They articulated well enough to be considered to have come from the same individual. In 1997 a number of extra foot bones and fragments of the left distal tibia were discovered in further bags, and in 1998 the remaining skeleton was discovered still embedded in the rock of Member 2 (Clarke, 1998). To date the skeleton consists of both lower limbs, a complete arm and articulated hand, ribs, and a complete skull with the mandible in occlusion (Clarke, 1998, 1999). The skeleton promises to be more complete than that of Al 288 (“Lucy”), and is currently being excavated from the rock.

In the foot’s original description the authors suggested that the bones may have come from layers in Member 2 as old as 3.5 mya, and that the youngest age they could be is 3.0 mya. However, this has been disputed by McKee (McKee, 1996) who argued that the faunal remains from Member 2 were similar to those from Member 4, and also younger than the 3 million year old assemblage from Member 3 at Makapansgat. McKee concluded that the foot bones could not be older than 3.0mya. A more recent study (Partridge *et al.*, 1999), using analysis of palaeomagnetic signatures within Member 2, and also interpolation of sedimentation rates, concluded that the likely dates of the skeleton and associated foot bones was 3.30–3.33 mya.

Stw 88

This complete right talus is currently undescribed and was measured courtesy of the Department of Anatomical Sciences, University of the Witwatersrand, South Africa.

Stw 363

This incomplete complete right talus is currently undescribed and was measured courtesy of the Department of Anatomical Sciences, University of the Witwatersrand, South Africa.

Kromdraai material

TM 1517, the right partial talus from Kromdraai, South Africa, was found in 1938 and is assigned to the taxon *Paranthropus robustus* (Broom & Schepers, 1946). The talus is missing both calcaneal facets, and thus only the head and trochlea are available for measurement. It was found in Member 3 of the area Kromdraai B East, which to date is the only hominin fossil bearing layer in the whole site. There is a degree of uncertainty over the precise age of Member 3 (Day, 1988). It has been suggested that it accumulated around 2.0 mya (Vrba & Panagos, 1982), but it has also been suggested that Member 3 is more likely to be aged at between 1.0 and 1.2 mya. The best estimate is that the layer is dated at between 1.0 and 2.0 mya.

Olduvai material

In 1960, whilst excavating site FLKNN I, L.S.B. Leakey reported the discovery of 12 fossilised hominid foot bones from a living floor approximately 20 feet below the upper limit of Bed 1, Olduvai Gorge, Tanzania (Leakey, 1960). Potassium-argon dating of the bone-bearing layer indicated an age of approximately 1.75 mya (Leakey *et al.*, 1961; Hay, 1971). The bones were well mineralised and appeared not to have been crushed or distorted. The bones found were: the talus, the calcaneus, the navicular, the cuboid, the lateral, intermediate and medial cuneiforms, and all five metatarsals. The calcaneus was damaged, and only the anterior half remained. The talus was damaged at the posterior end, and appeared to have teeth marks of a predator on the trochlear surface; all the metatarsals were missing their proximal heads, which appeared to have been broken off, and the styloid process of the fifth metatarsal was also broken off. All the bones came from a left foot, and articulated so well with each other that they were assumed to be from the same individual (Leakey,

1960; Day & Napier, 1964). Leakey, Tobias & Napier (1964) catalogued the foot as Olduvai Hominid 8 (OH 8), and described it as a paratype of their new taxa *Homo habilis*, on the basis of its proximity to the type specimen, OH 7, and their observation that it possessed “most of the specialisations associated with the plantigrade propulsive feet of modern man”. The details of the debate surrounding these specialisations have been addressed in Chapter 1.

Koobi Fora material

Three hominin fossil tali from the site of Koobi Fora, Kenya, are used in this analysis. They are the right talus KNM-ER 813A, the right talus KNM-ER 1464, and the left talus KNM-ER 1476A. All were discovered between 1971 and 1972 (Leakey *et al.*, 1978), and have been dated to between 1.6 and 1.8 mya (Day, 1988), making them roughly contemporary to OH 8.

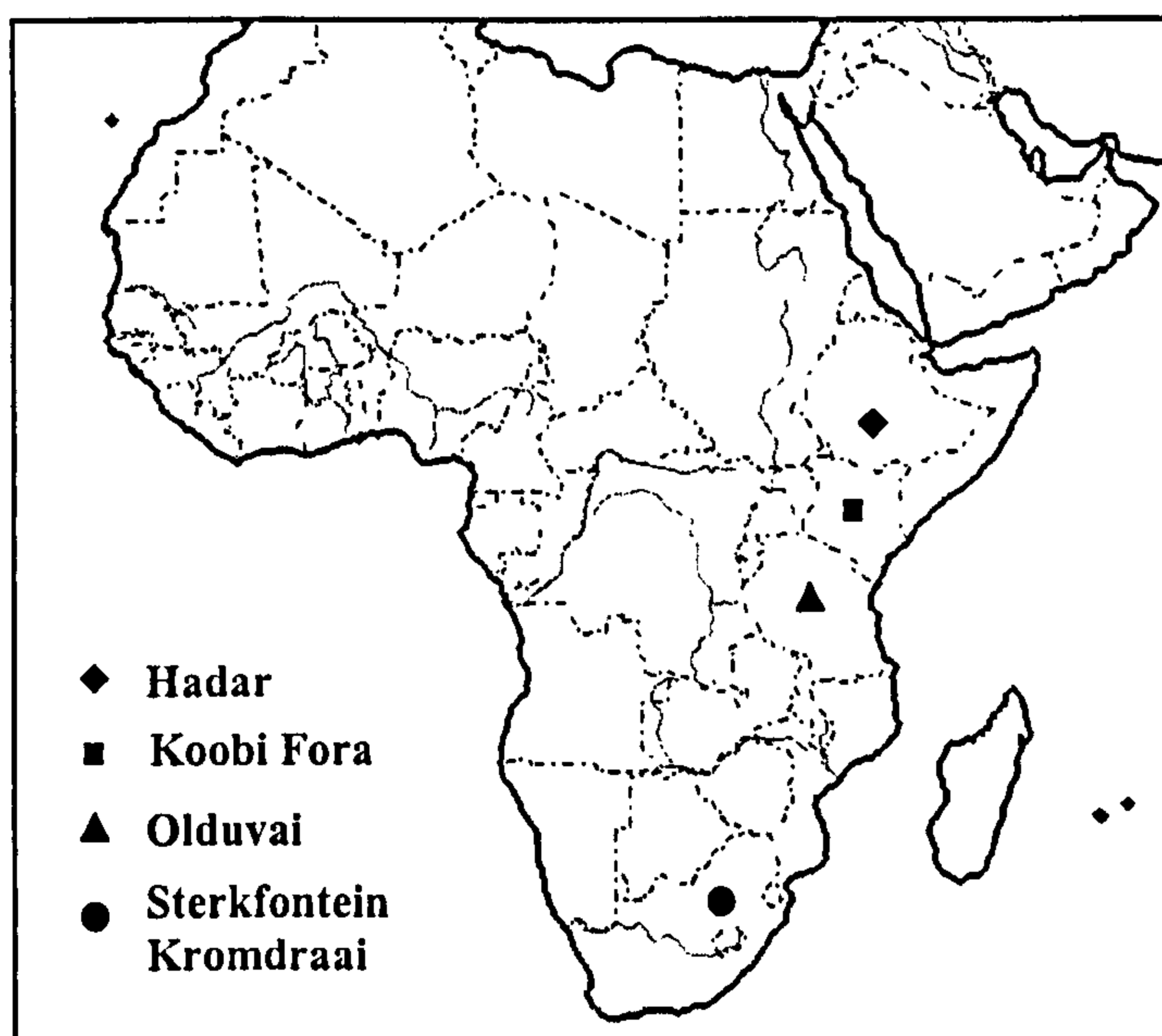


Figure 5.1 Map of Africa showing fossil localities.

5.4 Methods

PCA of individuals and fossils

The methods in this chapter are essentially the same as those used in Chapter 4. For each tarsal, there is a plot of the relevant PC axes for all extant individuals and fossils. In order to more clearly visualise the relationship between the fossils and the clouds of individuals for each taxon, outer limits of each distinct group are signified with a

linear border. This facilitates the task of observing whether a fossil does or does not fall with a taxon's or group's range of variation for any particular PC plot. In this chapter, three groupings are designated borders in each case: *Pongo*, *Homo sapiens* and the three African ape taxa. The reason the African ape taxa are grouped together is the fact that they predominantly fall together in nearly all cases. In instances where this is not the case, taxa are individually designated borders.

PCA of means and fossils

Separate analyses incorporating the fossils and the Procrustes mean shapes are also given. The advantage of plotting the means is that interspecific variation is explained in the first few principal components, making it easier to understand what shape differences exist between extant and fossil taxa.

Procrustes distances between means and fossils

Distance matrices and UPGMA phenograms are also presented, using the extant taxon means and the fossils. This is done to further understand and visualise the relationships between the extant taxa and the fossils. The advantage of this technique is that in using Procrustes distances, variables over the whole shape space are taken into account (i.e. the differences over all PC axes are taken into account).

Procrustes distances between individuals

Finally, frequency histograms of pairwise interspecific and intraspecific Procrustes distances between individuals are plotted. Once this is done, it is easy to calculate 5% and 95% confidence limits for both interspecific and intraspecific ranges, and then plot the pairwise Procrustes distances between each of the fossils in question. This is essentially a robust method of seeing whether or not two fossils are morphologically distinct enough, based on extant taxa, to be from the same species.

For the intraspecific distances, *Homo sapiens* and *Pan troglodytes* are combined. The interspecific distances are *H.sapiens* versus *P.troglodytes*. The reason these two taxa are used is that *P.troglodytes* is, genetically, our closest living relative. In evolutionary terms, fossil hominin taxa fall between *H.sapiens* and the *H.sapiens* -

P.troglodytes common ancestor, so, when considering their affinities, it is pertinent to use the most cladistically proximate extant taxon to the fossils.

5.5 Results

The results for this chapter are laid out in four sections, with one section per tarsal. The order in which they are presented is: talus, cuboid, navicular, medial cuneiform. Within each section, PCA plots of all extant individuals and the fossils are presented. This is followed by PCA plots of the Procrustes means for the extant taxa, and warped rendered images showing shape differences represented by certain axes. Procrustes matrices of distances between extant means and the fossils are given, as are UPGMA phenograms based on these, showing the relationships between extant means and fossils. Finally, frequency histograms of pairwise Procrustes distances between individuals are given.

5.5.1 Talus

It can be seen (Figure 5.2), that the relative grouping of the extant taxa, as presented in Chapter 4, does not change when the fossil tali are included. *Homo sapiens*, the African apes and *Pongo* all form distinct clusters of individuals. The two Koobi Fora tali KNM-ER 813A and 1464, and the AI 288 talus all fall just within the *Homo sapiens* range of variation. KNM-ER 1476A falls just outside the modern human range. Stw 88 falls well outside the modern human range, and well within the African ape range of variation. OH 8 falls between the African ape and modern human clusters, but is closer to the chimpanzee cluster than to the modern human cluster. Relative to other taxa, no fossil is close to the *Pongo* cluster.

Table 5.1 Talus: percentage variance for principal components 1 to 4.

Principal Component	Percentage variance
1	26.1%
2	13.0%
3	5.7%
4	4.4%

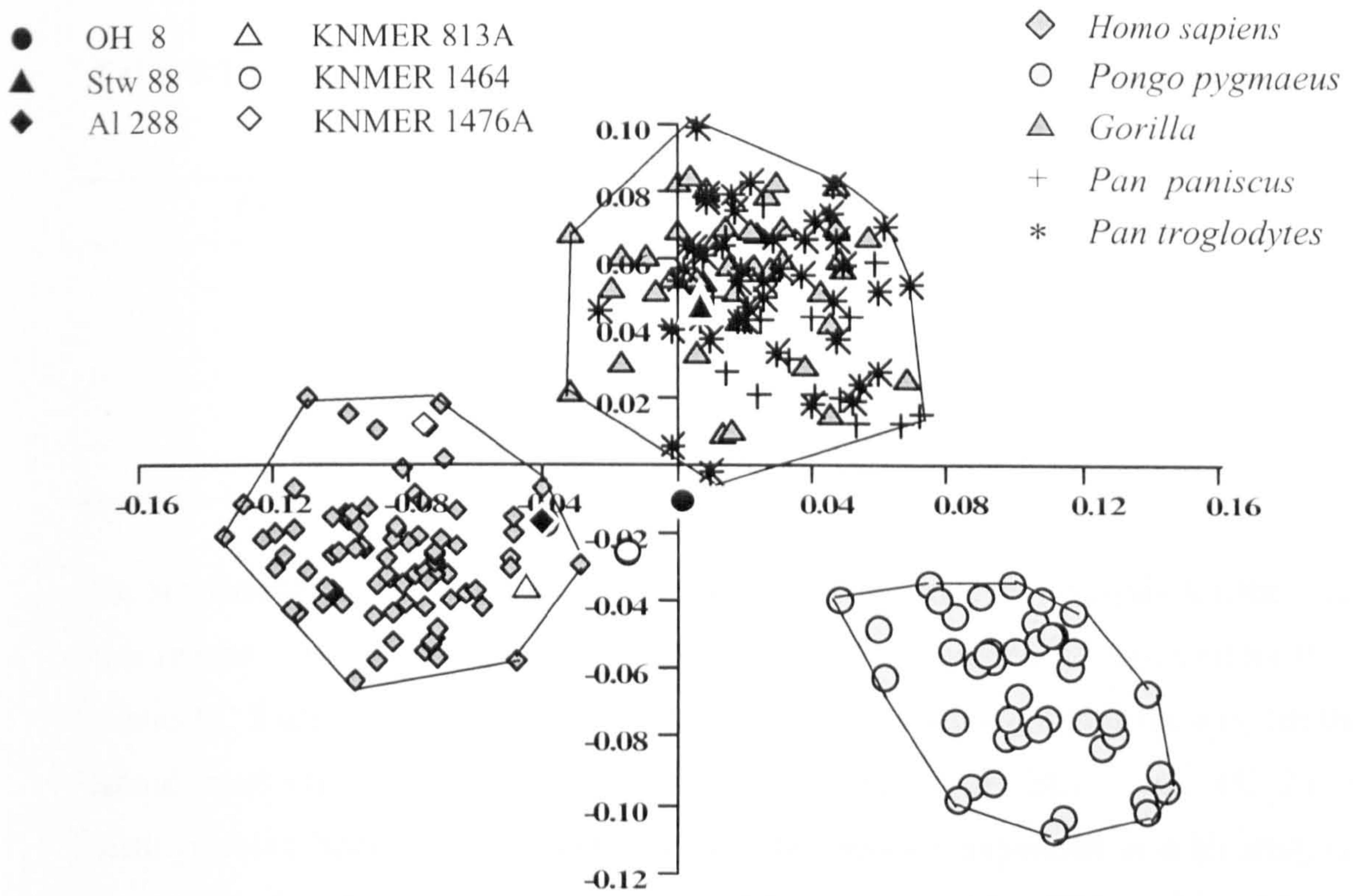


Figure 5.2 Talus (with lateral malleolar facet): PC 1 versus PC 2.

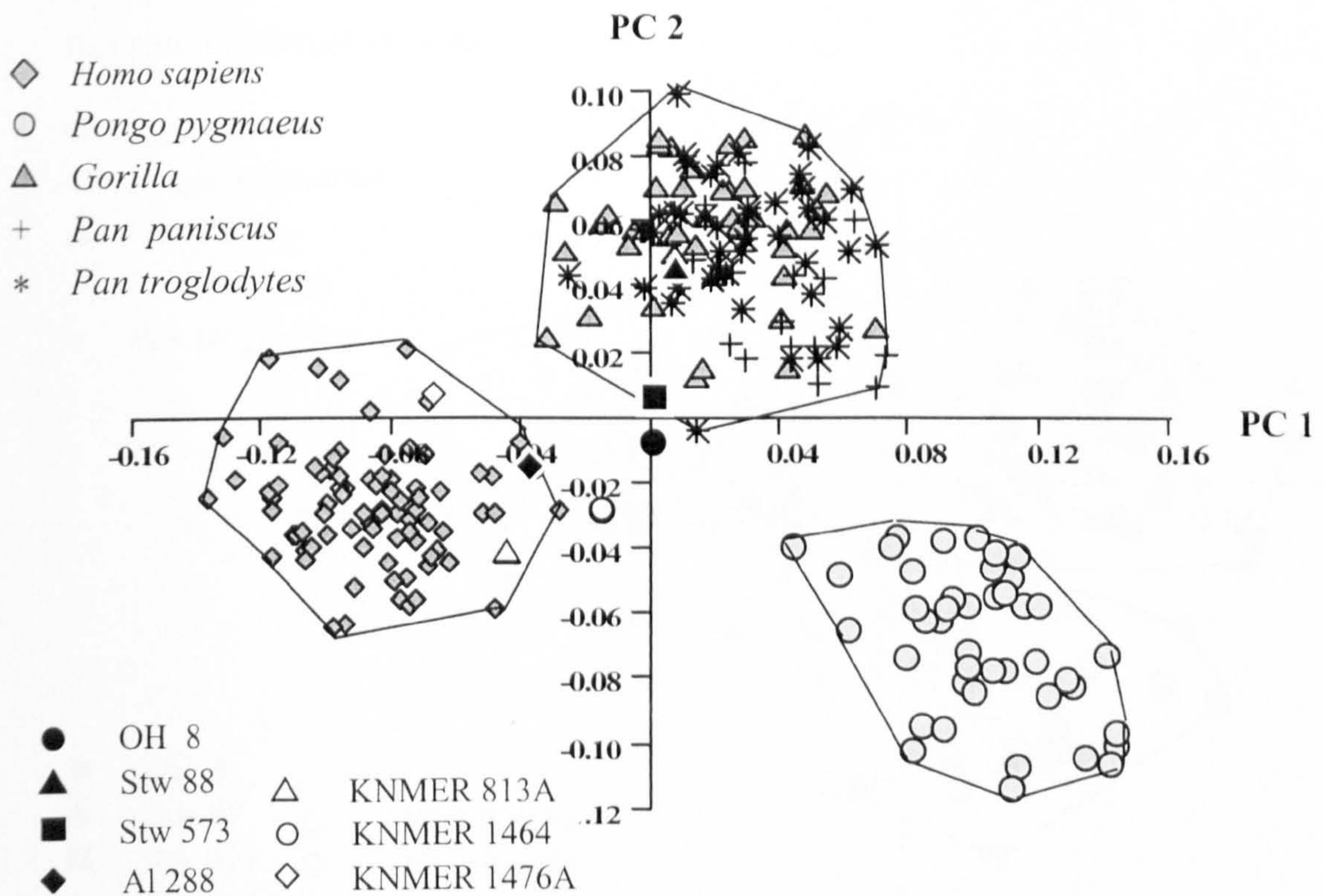


Figure 5.3 Talus (without lateral malleolar facet): PC 1 versus PC 2.

Table 5.2 Talus without lateral malleolar facet: percentage variance for principal components 1 to 4

Principal Component	Percentage variance
1	26.1%
2	13.3%
3	5.9%
4	4.4%

On account of Stw 573 having no lateral malleolar facet, the analysis for the talus was redone with the landmarks for that facet removed (Figure 5.3). The plot for PC 1 versus PC 2 appears virtually identical to Figure 5.2, which highlights the fact that the lateral malleolar facet is not important (with regard to PC 1 and PC 2) in distinguishing hominoid tali. Furthermore, the variance explained in both analyses for the first four PCs is virtually identical (Tables 5.1 and 5.2). The relative positions of the fossil specimens does not appear to change, and the inclusion of Stw 573 shows that it is situated well outside the modern human range of variation, and just inside that of the African apes. Stw 573 and OH 8 are also extremely close to each other for this combination of PC axes.

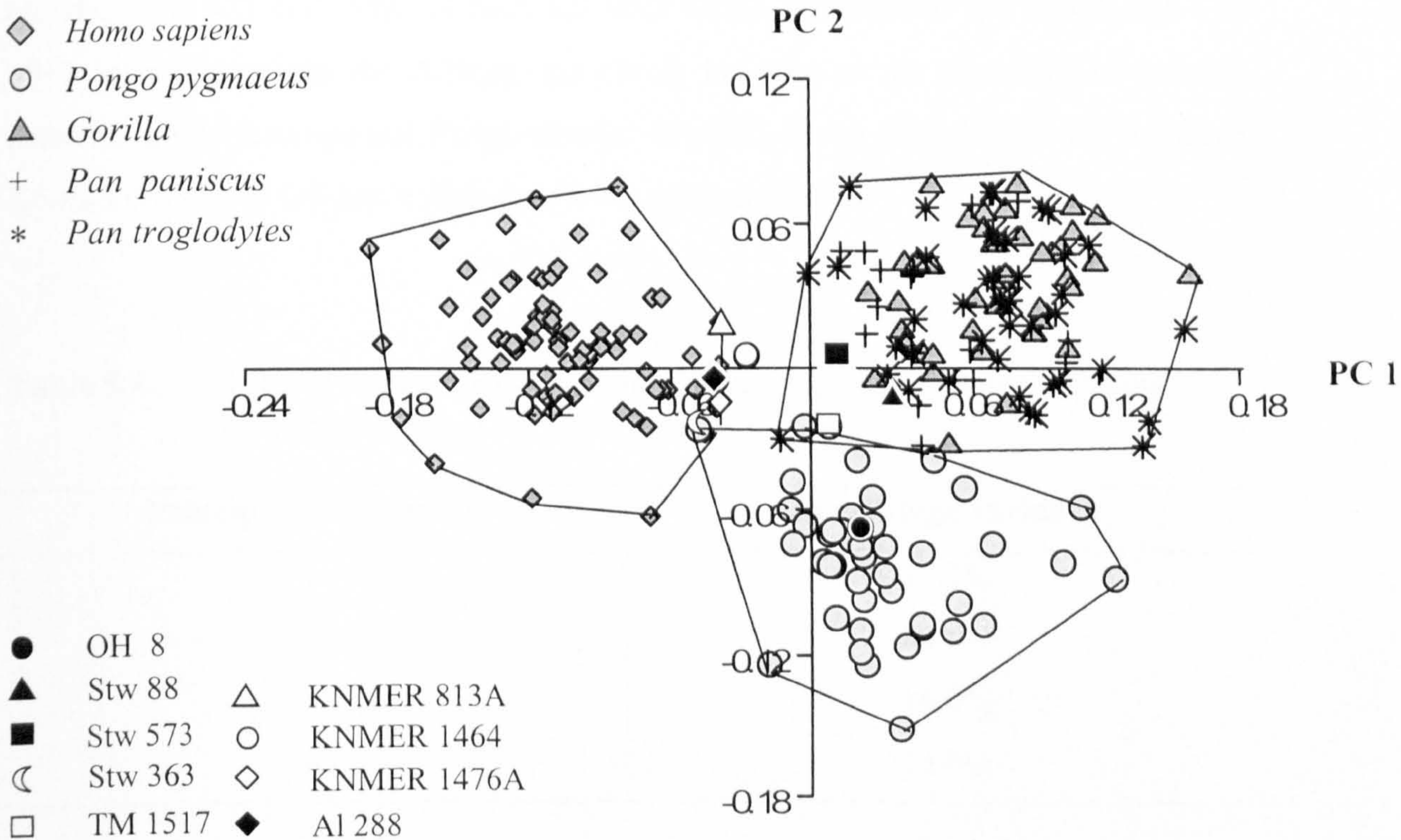


Figure 5.4 Talus: trochlea and medial malleolar facet only. PC 1 versus PC 2.

Table 5.3 Talus with trochlea and medial malleolar facet only: Percentage variance for principal components 1 to 4

Principal Component	Percentage variance
1	35.8%
2	11.5%
3	7.8%
4	6.0%

Two further fossils, TM 1517 from Kromdraai and Stw 363 from Sterkfontein can be included in the analysis of only the trochlear surface and the medial malleolar facet are used. Figure 5.4 shows that there is still distinct separation between the modern humans, the African apes and *Pongo*, even though the talar head and posterior subtalar facet are removed from the analysis. As opposed to the two analyses of the more complete talus, Table 5.3 shows that for this analysis, PC 1, at 35.8%, accounts for a far greater degree of the total variance.

The most interesting change in this analysis is the position of OH 8, which now falls well within the *Pongo* cloud, and well outside the modern human and African ape clouds. Stw 573 and Stw 88 both fall well within the African ape cloud, and TM 1517 falls just within the African ape cloud, but also at the boundary of overlap between the African ape and *Pongo* clouds. Stw 363, along with Al 288 and the three Koobi Fora tali all fall just within the *Homo sapiens* cluster.

Table 5.4 Talus (Fossils & Extant means): percentage variance for Principal components 1 to 4

Principal Component	Percentage variance
1	28.1%
2	20.6%
3	18.0%
4	13.8%

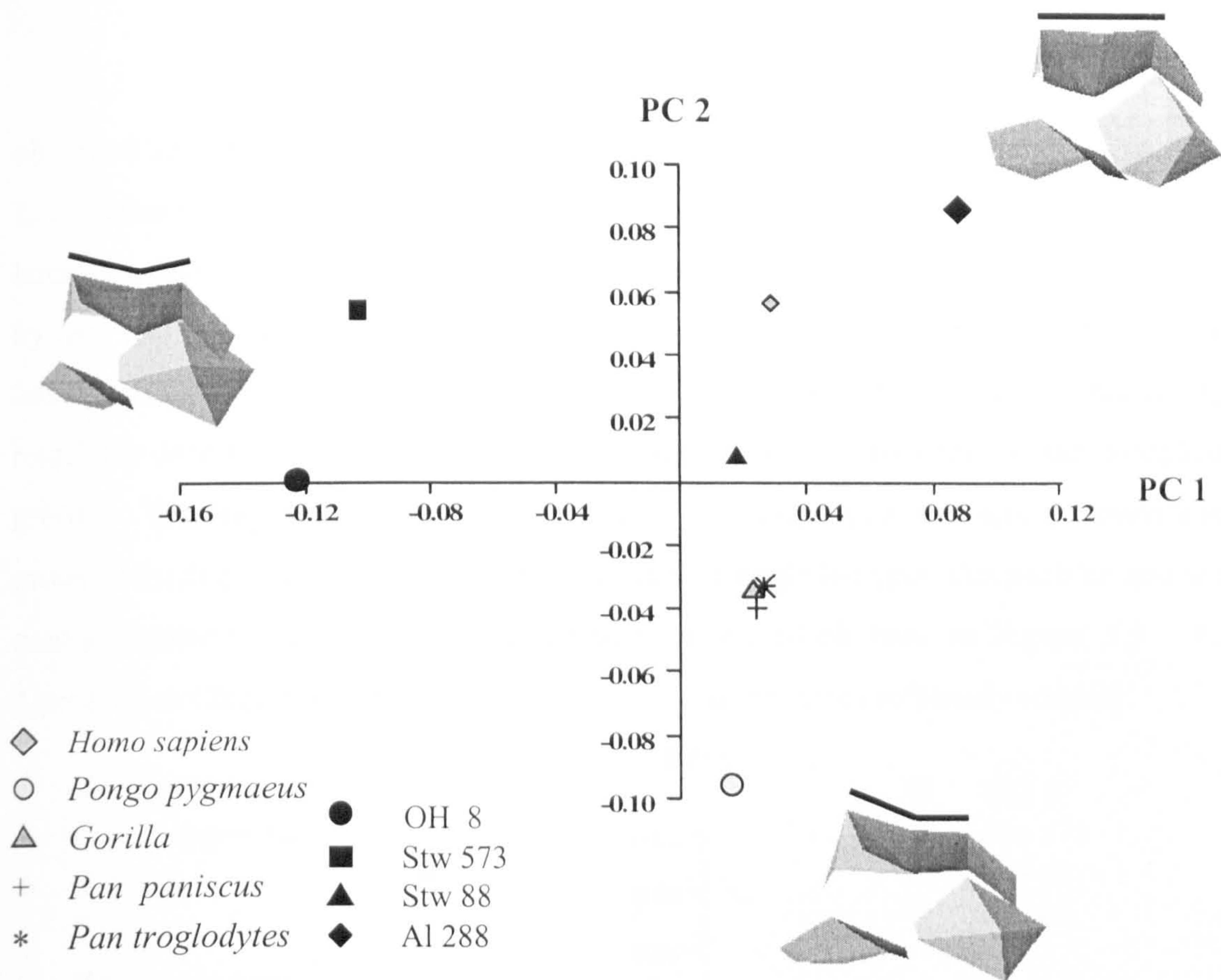


Figure 5.5 Talus (without lateral malleolar facet): Fossils and Extant means, PC 1 versus PC 2. Images are the talus viewed proximally.

Figure 5.5 shows PC 1 versus PC 2 when the extant species Procrustes mean shapes and the fossil shapes are subjected to GPA followed by PCA. As with the analysis shown in Figure 5.2, the lateral malleolar facet is omitted so that Stw 573 can be included. TM 1517 and Stw 363 are not included because they are too incomplete. The same applies to the three Koobi Fora tali, which all had to undergo differing degrees of reconstruction to render them complete. For PC 1, which accounts for 28% of the variance (see Table 5.4), there is a negligible degree of separation between the Procrustes mean shapes for the extant species, namely the African apes, *Pongo* and *Homo sapiens*. The unassigned Stw 88 also falls with the extant mean shapes. The main separation on this axis is between Stw 573 and OH 8 on the negative end, and A1 288 on the positive end. The result here is that on PC 1 there is a high degree of separation between the fossils. PC 2 separates the mean shapes of the African apes, *Pongo* and *Homo sapiens*. Stw 573 is similar to the *Homo sapiens* mean, whilst OH 8 and Stw 88 fall between the *H.sapiens* and the African ape means. Overall, when looking at PC 1 versus PC 2, it can be seen that there is a very tight clustering of the means for *Pan paniscus*, *Pan troglodytes*, and *Gorilla gorilla*, i.e. the African apes. In terms of shape change for PC 1 versus PC 2, the principal differences

observed lie in the morphology of the trochlear surface. High values for PC 1 and PC 2, i.e. where Al 288 and the *H.sapiens* mean lie, show a flat trochlea with medial and lateral margins of a similar elevation to each other. Warping to the positions occupied by Stw 573 and OH 8, results in the trochlea becoming considerably sloped, with the lateral margin becoming relatively elevated, and the medial margin becoming relatively lowered. There is also an increase in the prominence of the trochlear groove. Warping to the *Pongo* mean results in a shape that still has a sloped and grooved trochlea, but in addition there is a smaller angle between the trochlea and the medial malleolar facet. This is illustrated by the black bars in Figure 5.5. As discussed in Chapter 4, the talar head of *Pongo* also becomes relatively smaller.

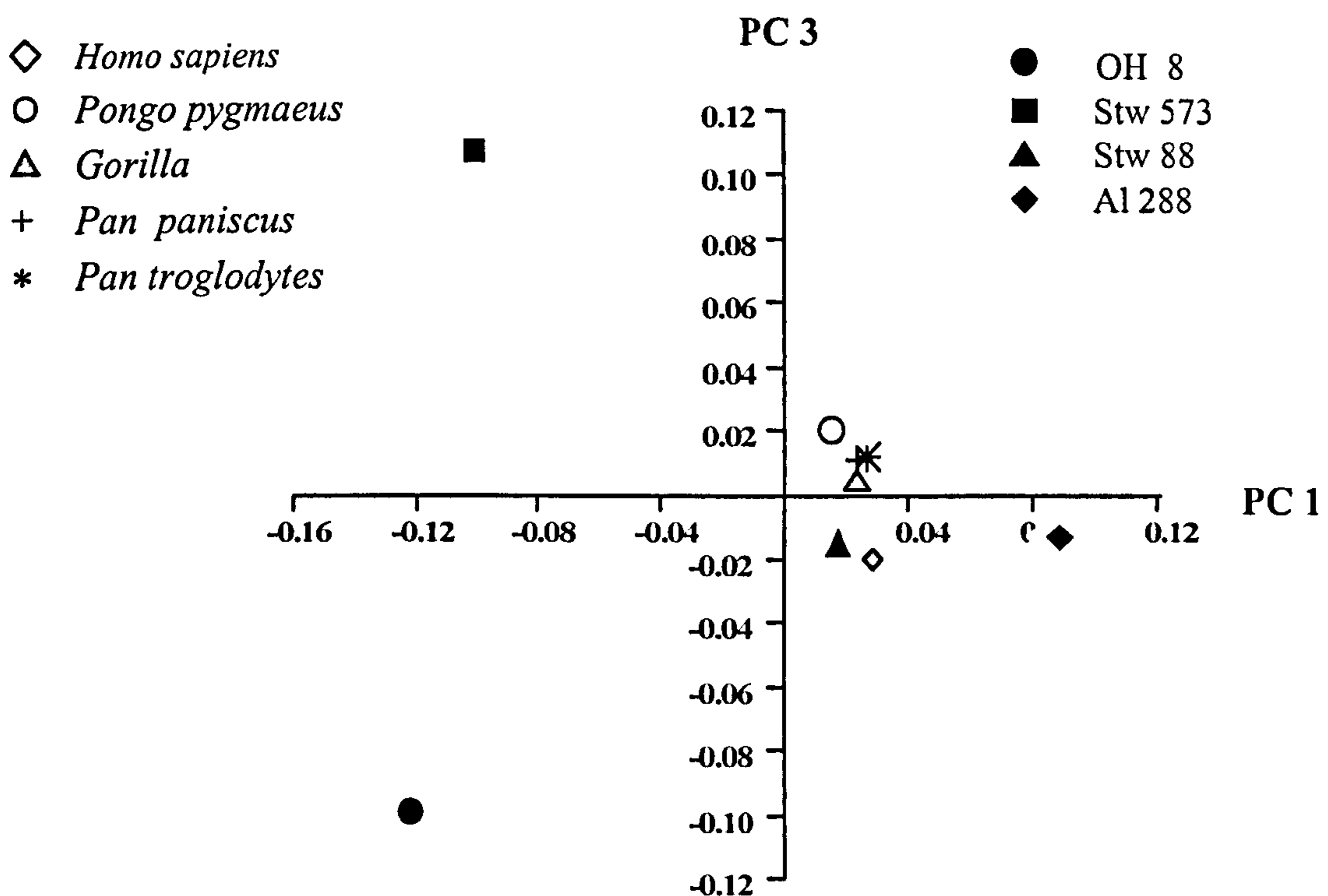


Figure 5.6 Talus (without lateral malleolar facet): Fossils and Extant means, PC 1 versus PC 3.

For PC 1 versus PC 3 (Figure 5.5), it can be seen that there is very little separation between any of the extant species Procrustes means, Stw 573 and Al 288. The main separation on PC 3 is between OH 8 and Stw 573. Plotting PC 2 versus PC 3 (Figure 5.6) also highlights the separation between these two fossil tali on PC 3.

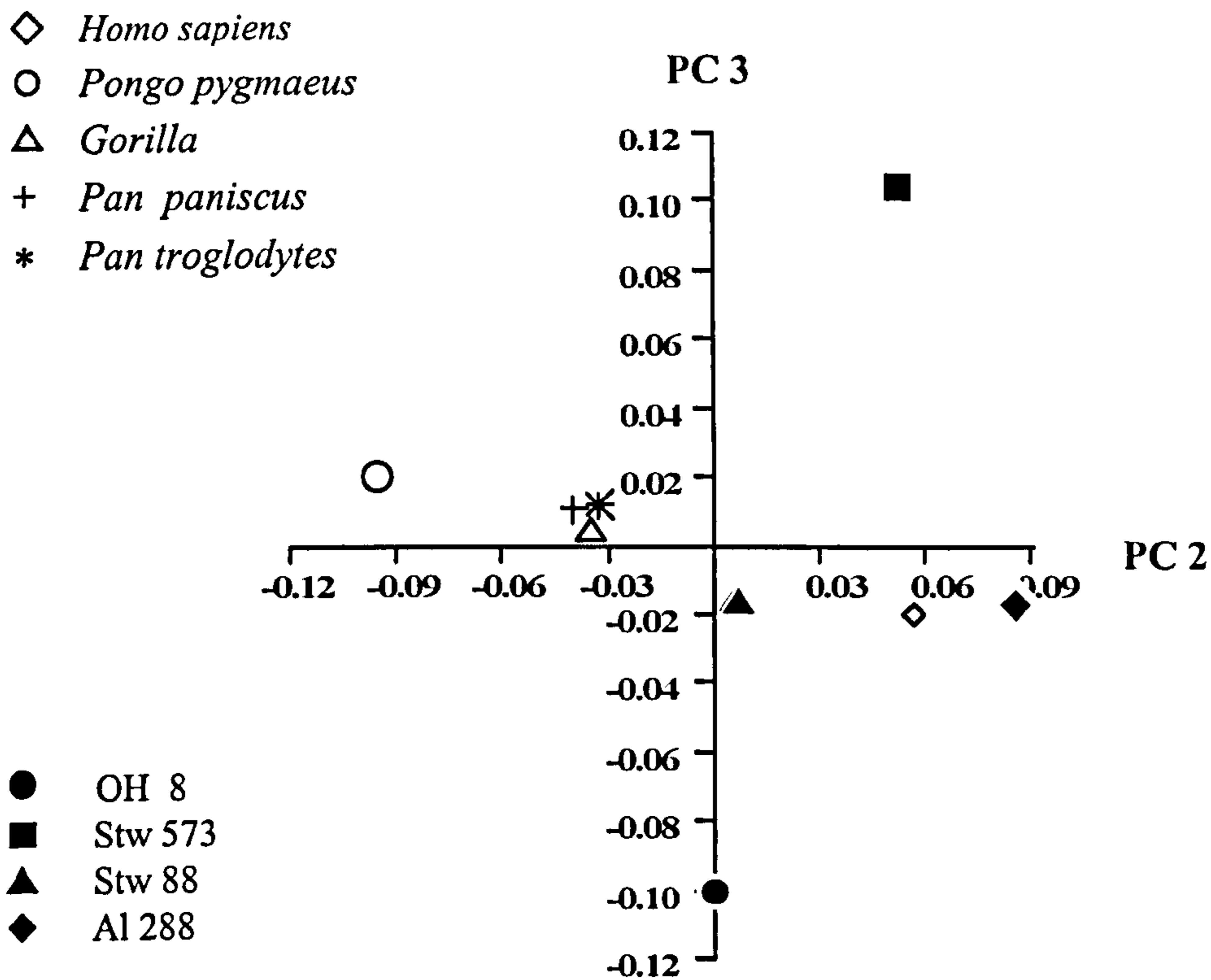


Figure 5.7 Talus (without lateral malleolar facet): Fossils and extant means, PC 2 versus PC 3.

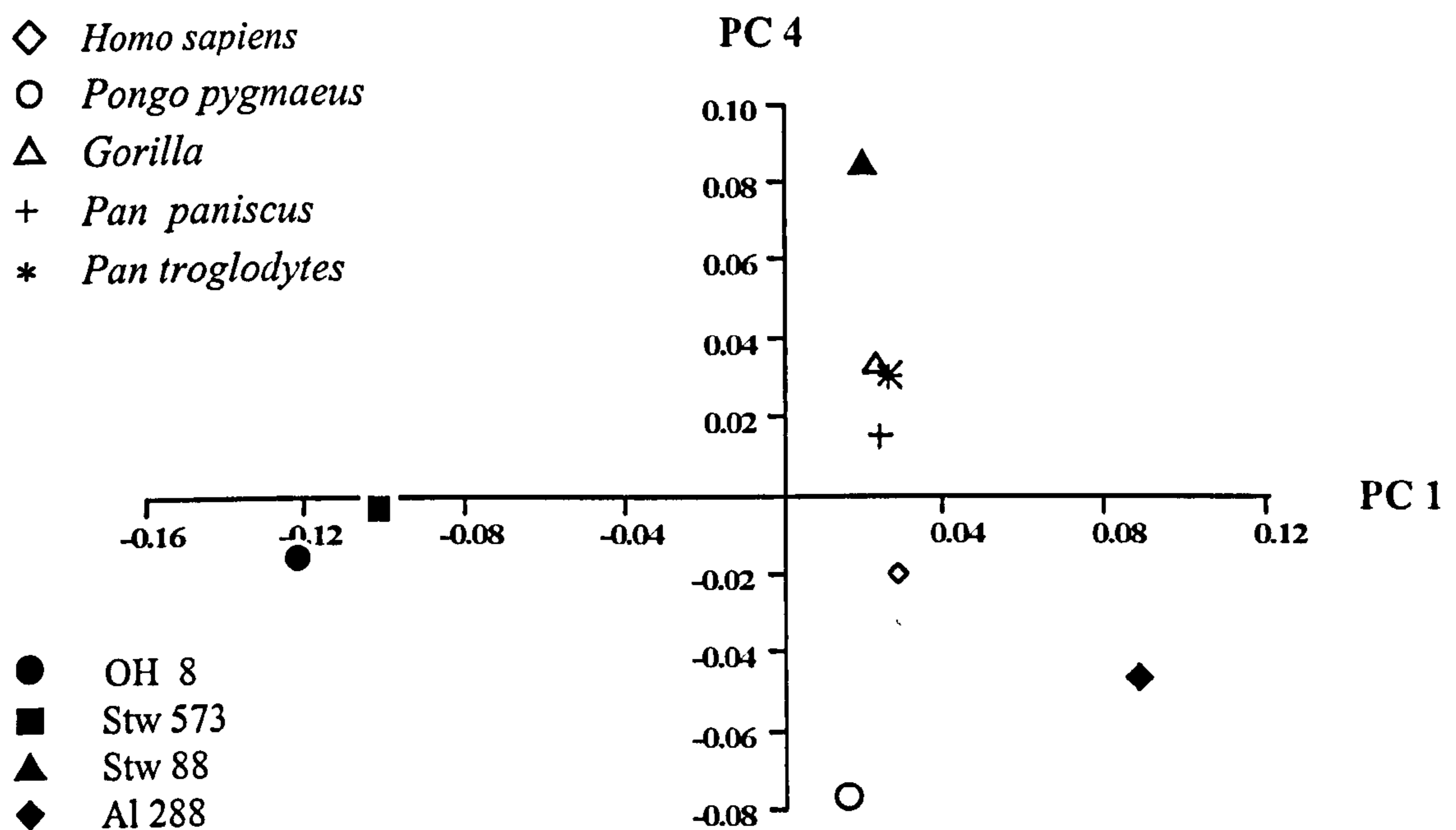


Figure 5.8 Talus (without lateral malleolar facet): Fossils and Extant means, PC 1 versus PC 4.

Figure 5.8 shows PC 1 versus PC 4, and it can be seen that PC 4 separates the African ape means from those of *Pongo* and *Homo sapiens*. Stw 573 and OH 8 both appear similar to each other on PC 4, and fall between the *H.sapiens* mean and those of the

African apes. Al 288 falls between the *H.sapiens* mean and that of *Pongo*. PC 4 also separates Stw 88 from all the other fossils and also the extant species means.

Table 5.5 Talus: Pairwise Procrustes distances between fossils and extant species Procrustes means

	<i>H.sapiens</i>	<i>Gorilla</i>	<i>P.trog</i>	<i>Pongo</i>	<i>P.paniscus</i>	OH 8	Al 288	Stw 573
<i>Gorilla</i>	0.1392							
<i>P.trog</i>	0.1438	0.0648						
<i>Pongo</i>	0.1953	0.1563	0.1483					
<i>P.paniscus</i>	0.1531	0.0813	0.0624	0.1357				
OH 8	0.2060	0.1982	0.1989	0.2212	0.1953			
Al 288	0.1562	0.1829	0.1715	0.2125	0.1685	0.2475		
Stw 573	0.2052	0.1979	0.1903	0.2234	0.1904	0.2156	0.2374	
Stw 88	0.1708	0.1396	0.1294	0.1963	0.1337	0.2051	0.1834	0.2085

Table 5.5 shows the Procrustes distances between the extant species Procrustes means and the fossils. The UPGMA phenogram based on these distances is presented in Figure 5.9. It can be seen that all three African ape means cluster together to the exclusion of all other means and fossils. Stw 88 groups with the African apes to the exclusion of all others. The *H.sapiens* mean then groups with the African ape means and Stw 88. And together these all group with *Pongo*. The most striking result is that the three fossils, Al 288, Stw 573 and OH 8, are all very distinct from the extant means as well as each other. The exception is AL 288, where it can be seen from Table 5.5 that it is considerably closer to the *H.sapiens* mean than either Stw 573 or OH 8 is (which both have very similar distances from the *H.sapiens* mean). Al 288 is also closer to the *H.sapiens* mean than it is to any other extant species mean, which is also not the case for either Stw 573 or OH 8. Given this, it would be expected that Al 288 would link more closely with the *H.sapiens* mean in the phenogram. The reason that it does not is that the *Pongo* mean has closer Procrustes distances to the African ape means than Al 288 does.

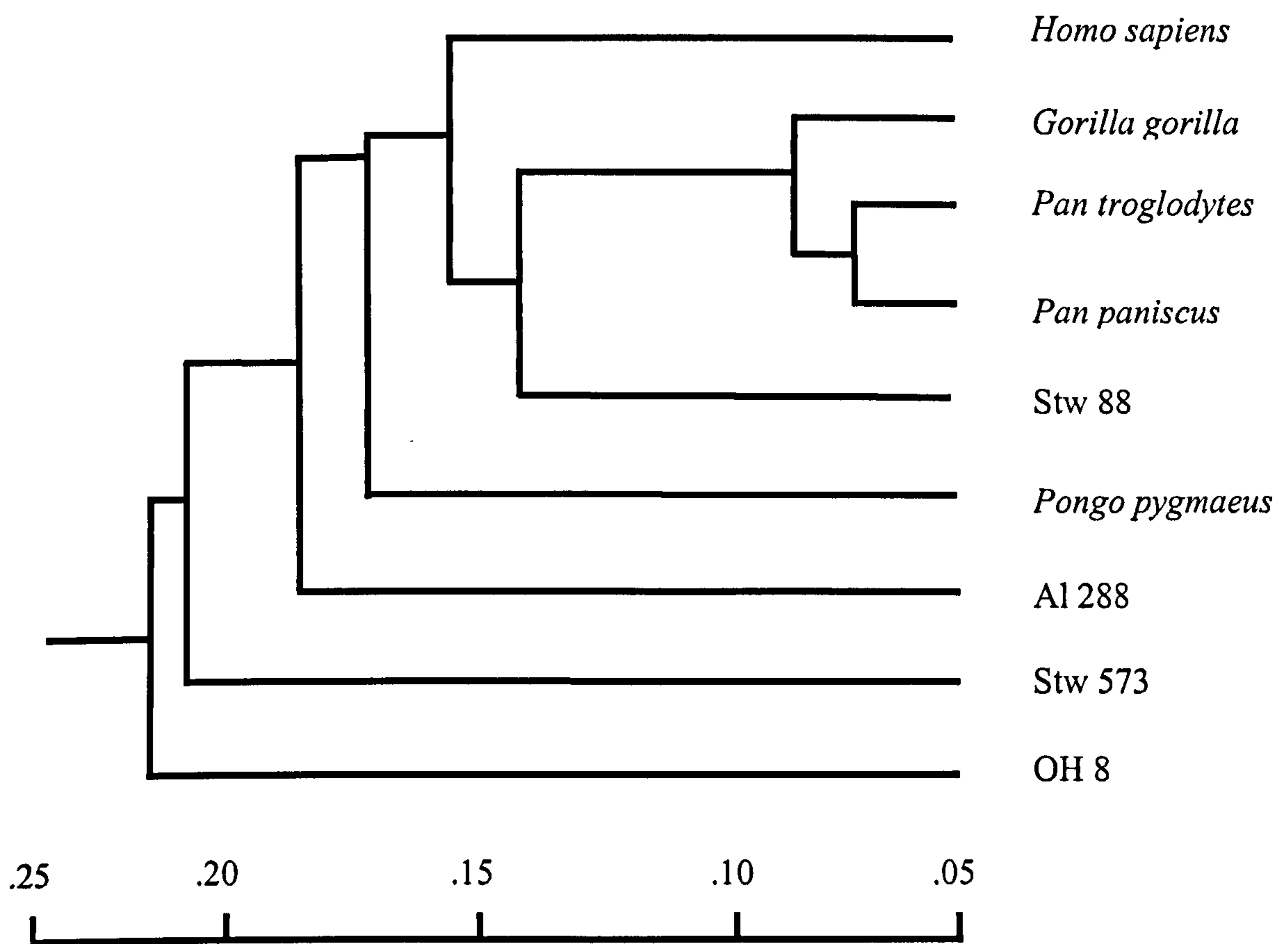


Figure 5.9 Talus: Phenogram of fossils and Procrustes mean shapes for extant taxa. NB. Lateral malleolar facet is not included.

Figure 5.10 shows the distribution of pairwise Procrustes distances for individuals of *Homo sapiens* and *Pan troglodytes*. When considering the fossils, the most striking finding is for the distances between Al 288 and both Stw 573 and OH 8. Al 288 is so distant from either of the other two fossils, that the values fall way outside the range of variation of the intraspecific range of variation for *H.sapiens* and *P.troglodytes*. In fact, the values fall towards the higher end of the interspecific range of variation for *H.sapiens* versus *P.troglodytes*. Stw 573 also has a Procrustes distance between itself and OH 8 that falls beyond the 95% confidence limit of the intraspecific range of variation, and well within the 5% confidence limit of the interspecific range. However, the Stw 573 – OH 8 distance does not fall beyond the absolute intraspecific range. Therefore, based on extant species ranges of variation, whilst it is more likely that OH 8 and Stw 573 are morphologically distinct enough to be from different species, it cannot be asserted absolutely. Stw 88 has Procrustes distances between OH 8 and Stw 573 that are similar to the Stw 573 – OH 8 distance. Stw 88 is slightly closer to Al 288, and falls within the 95% confidence limit of the intraspecific range,

and within the 5% confidence limit of the interspecific range. It is thus difficult to conclude about the relationship between those two fossils.

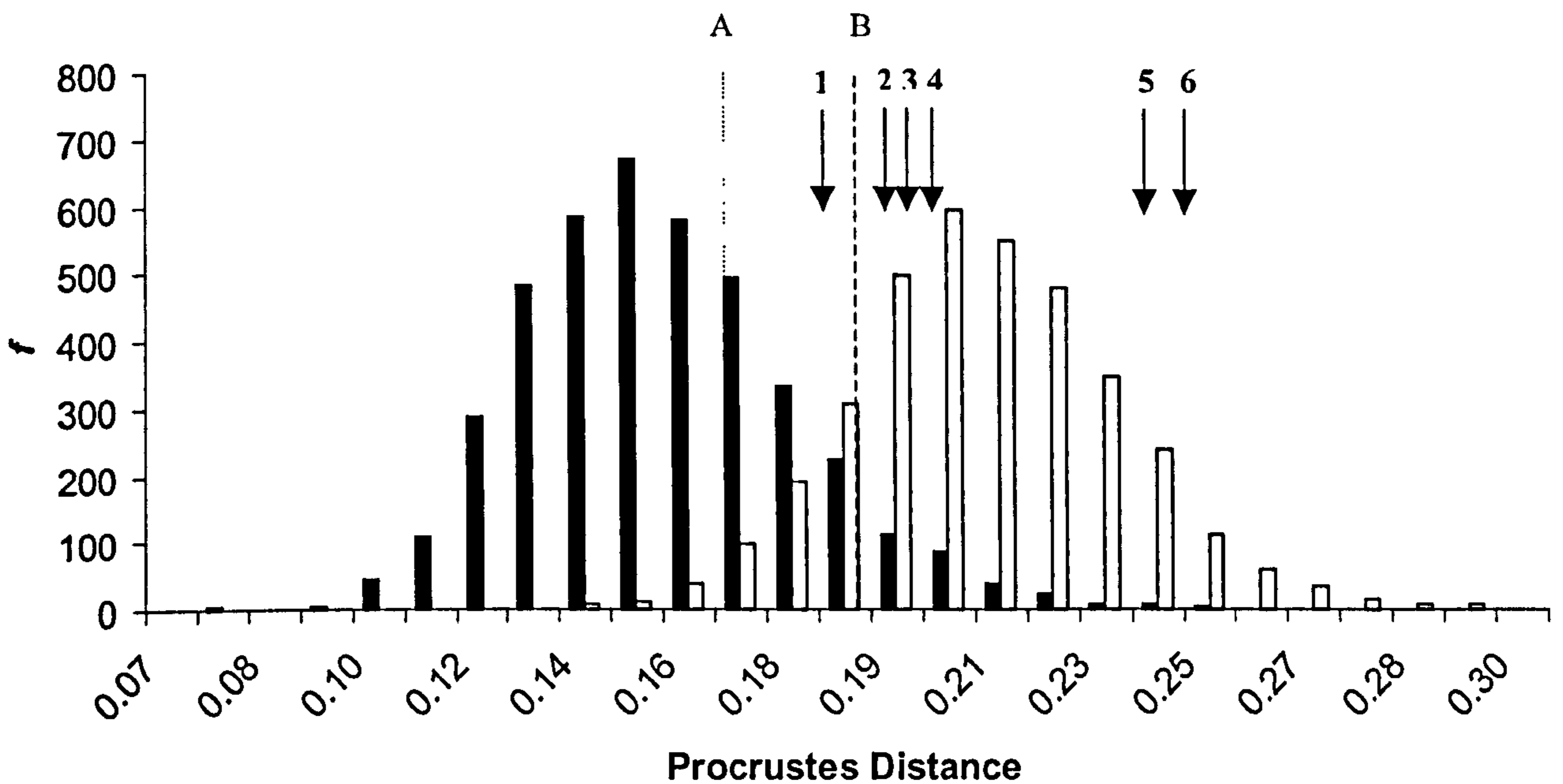


Figure 5.10 Talus: Frequency histogram of pairwise Procrustes distances between individuals. Solid black bars are intraspecific distances for *Homo sapiens* and *Pan troglodytes*. White bars are interspecific distances for *H.sapiens* versus *P.troglodytes*. Dotted line “A” is the 5% confidence limit for the interspecific range, and dashed line “B” is the 95% confidence limit for the intraspecific range. Black arrows signify pairwise Procrustes distances between fossils: 1 = Al 288 vs. Stw 88, 2 = Stw 88 vs. OH 8, 3 = Stw 88 vs. Stw 573, 4 = Stw 573 vs. OH 8, 5 = Al 288 vs. Stw 573, 6 = Al 288 vs. OH 8.

5.5.2 Cuboid

Figure 5.11 shows, as for the analysis without OH 8 in Chapter 4, that there is clear separation between the modern humans and the great apes along PC 1. The OH 8 cuboid clearly falls with the humans on this axis, and from Table 5.6 it can be seen that PC 1 accounts for a far larger proportion of the variance between specimens (39.0%) than the subsequent PC axes. PC 2 separates *Pongo* from the remaining taxa, and OH 8 falls just above the modern human cloud on that axis. Overall, OH 8 falls just outside the modern human range of variation, but only due to its PC 2 score, and is far closer to the modern human cloud than to that of any other taxon.

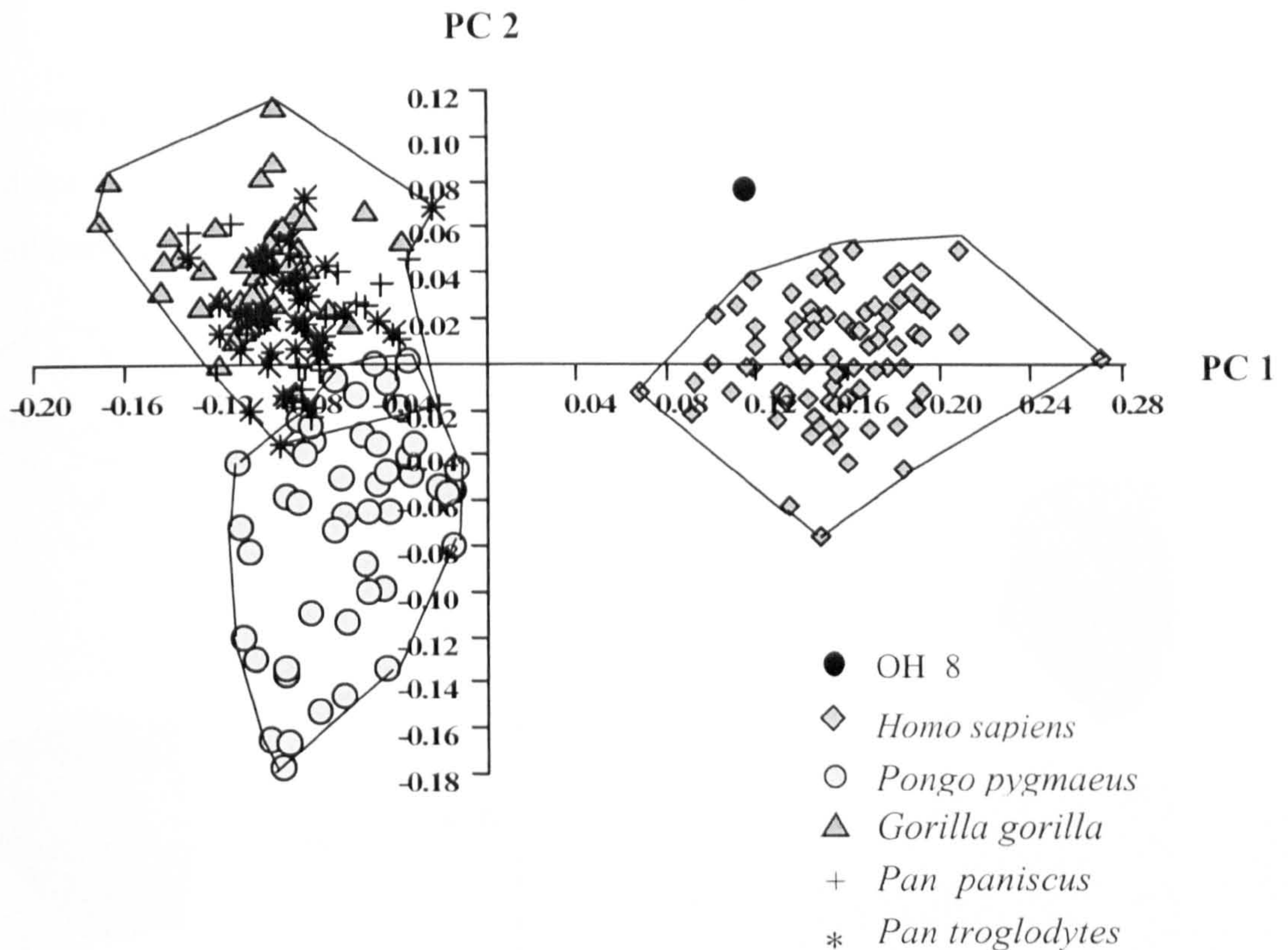


Figure 5.11 Cuboid: PC 1 versus PC 2.

Table 5.6 Cuboid: percentage variance for Principal components 1 to 4

Principal Component	Percentage variance
1	39.0%
2	7.1%
3	6.0%
4	4.2%

When the OH 8 cuboid is included with the extant species Procrustes means, there is a similar pattern. In Figure 5.12, it can be seen that PC 1 clearly separates OH 8 and the *Homo sapiens* mean from those of the great apes. Table 5.7 shows that PC 1 accounts for 69.6% of the variance, which is an unusually high amount for even PC 1. On PC 2 there is more separation between OH 8 and the modern human mean than there is between any of the great ape means. This shows that although the OH 8 cuboid is predominantly human-like (especially so since PC 1 accounts for so much of the variance), it also has some features that are not human-like. In terms of shape differences, PC 1 mainly explains the position and prominence of the “plantar beak” on the calcaneal facet. For the modern human mean and OH 8 the beak is prominent and more medially and plantarly orientated (see warped means on Figure 5.12). In the

great apes it is less pronounced and more lateral and dorsal. The *H.sapiens* mean and OH 8 are also relatively longer in the proximal-distal direction, and narrower in the mediolateral direction.

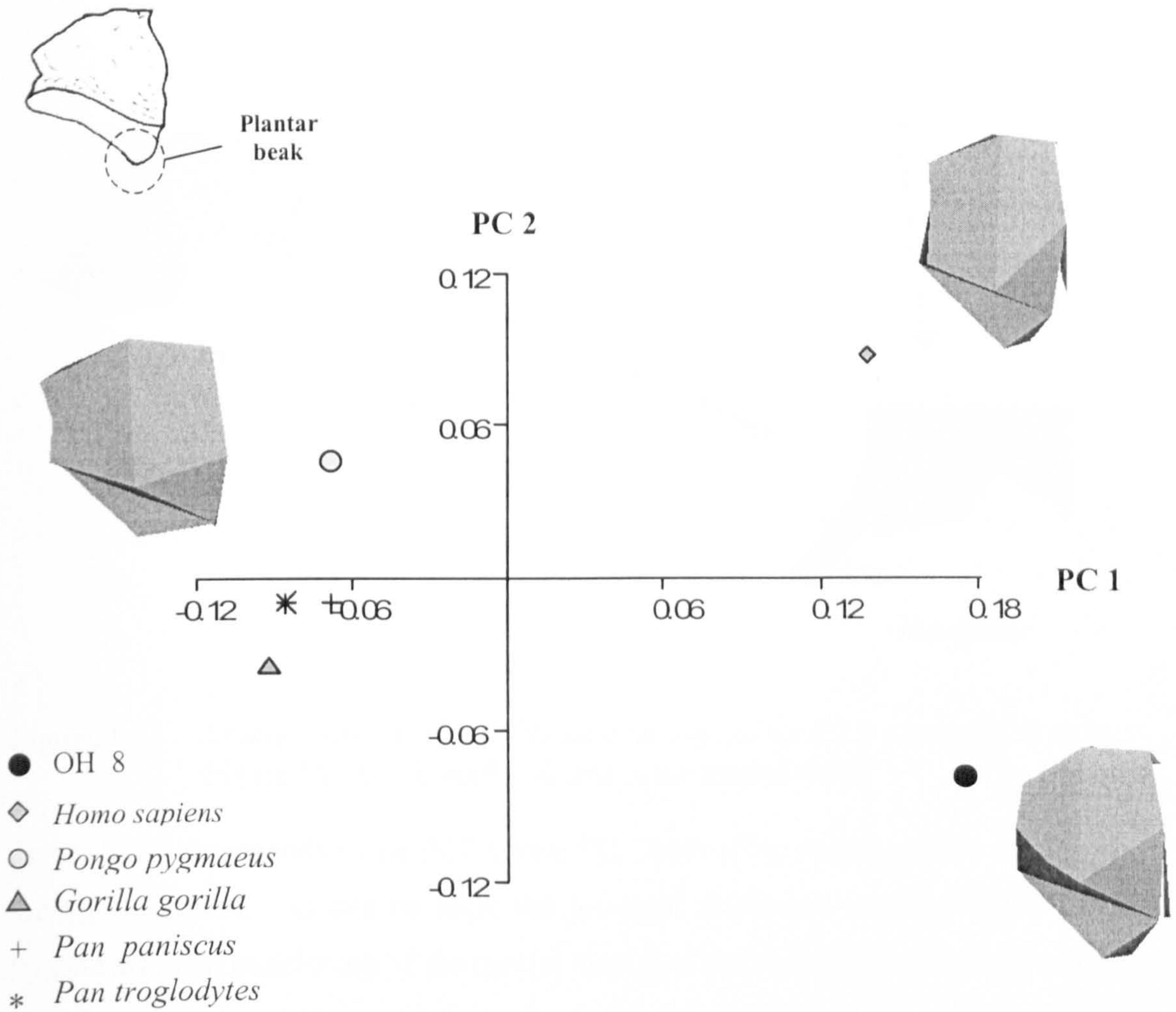


Figure 5.12 Cuboid: PC 1 versus PC 2 for OH 8 and extant species Procrustes means.

Table 5.7 Cuboid (OH 8 & extant means): percentage variance for Principal components 1 to 4

Principal Component	Percentage variance
1	69.6%
2	16.3%
3	7.0%
4	4.9%

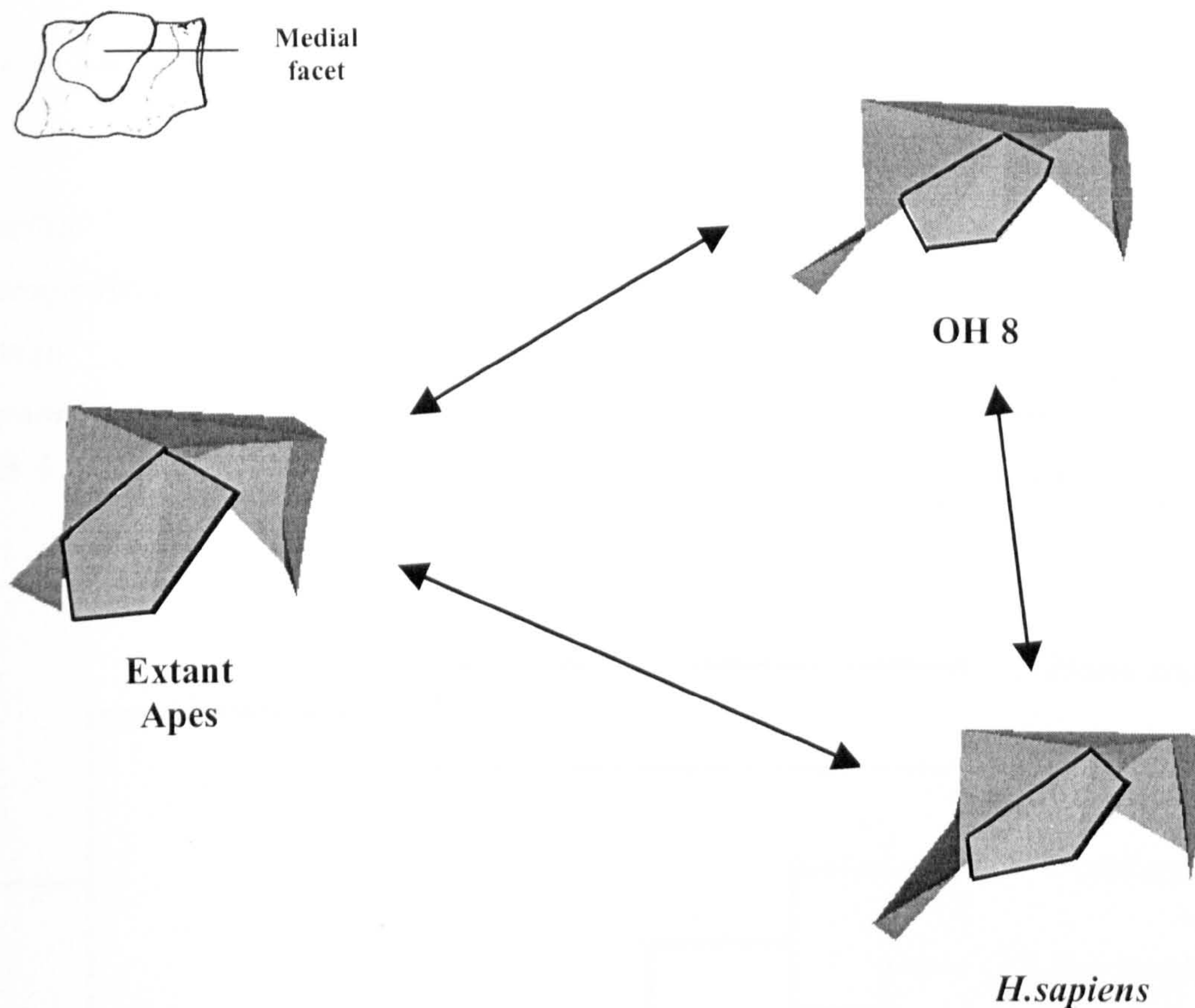


Figure 5.13 Medial view of cuboid. Shape changes are for PC 1 versus PC 2 as in Figure 11. Black bordered area is the medial facet.

Figure 5.13 corresponds to the PC1 versus PC 2 plot of the extant species means plus the OH 8 cuboid. As can be seen, the principal difference in this view is in the relative size and positioning of the medial facet (i.e. that facet that articulates with the lateral cuneiform and the navicular). It can be seen that the mean great ape medial facets are relatively large, and are relatively longer in both the dorsoplantar and proximo-distal directions. The OH 8 medial facet is relatively small, and is more confined to the dorsal part of the medial surface. The *H.sapiens* mean medial facet, like that of OH 8, is relatively shorter dorsoplantarly than is the case for the great apes, but it is also relatively longer proximodistally than the OH 8 facet. The overall impression is that the OH 8 facet is markedly small.

Table 5.8 Cuboid: Pairwise distances between OH 8 and extant species means

	<i>H.sapiens</i>	<i>Gorilla</i>	<i>P.troglodytes</i>	<i>Pongo</i>	<i>P.paniscus</i>
<i>Gorilla</i>	0.2652				
<i>P.troglodytes</i>	0.2496	0.0966			
<i>Pongo</i>	0.2326	0.1341	0.1208		
<i>P.paniscus</i>	0.2359	0.1020	0.0710	0.1149	
OH 8	0.1791	0.2802	0.2770	0.2776	0.2605

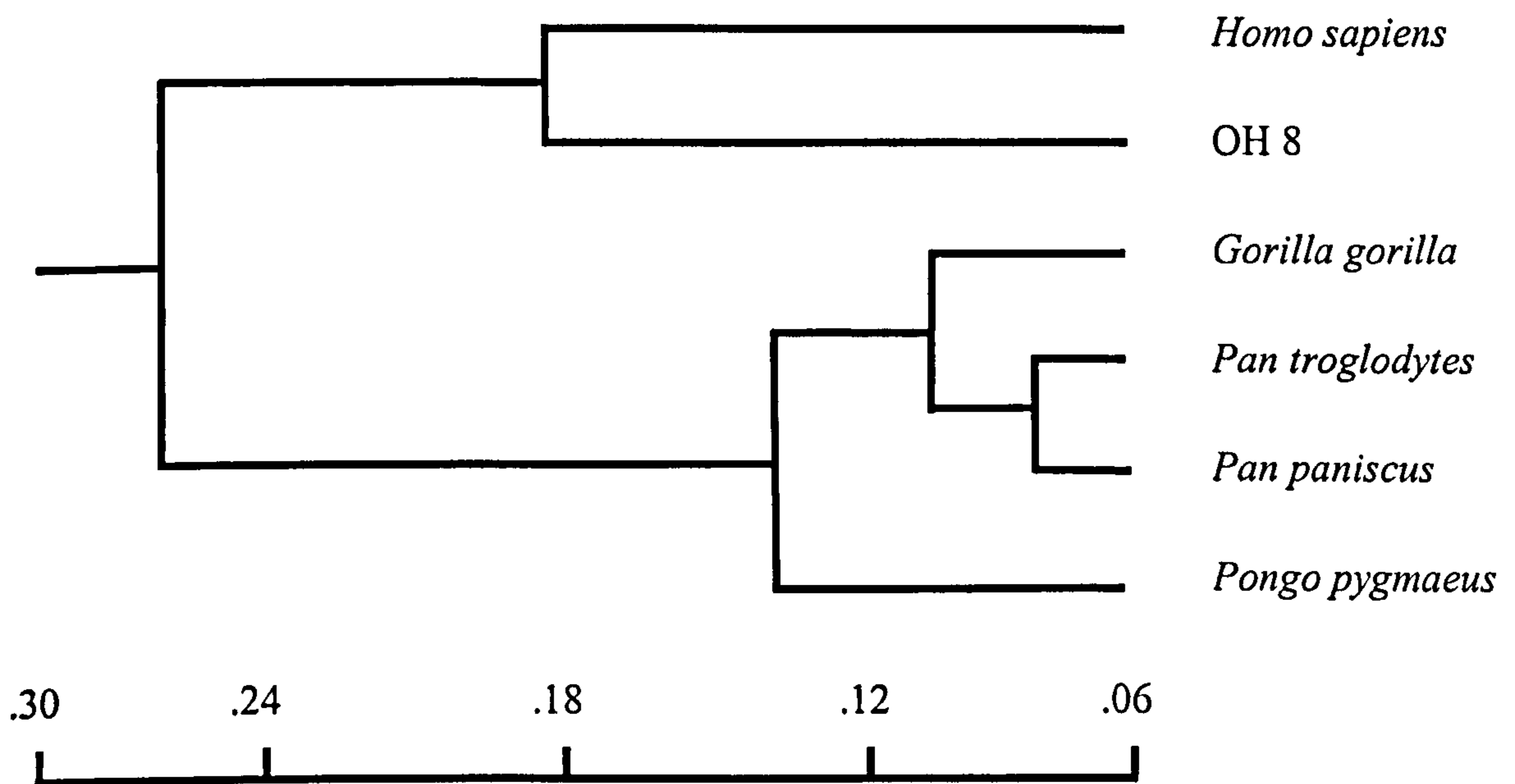


Figure 5.14 Cuboid: Phenogram of OH 8 and Procrustes means of extant taxa

The phenogram (Figure 5.14) reflects the distribution of extant taxon means and OH 8 on PC 1 versus PC 2. OH 8 is distinct from *Homo sapiens*, but still groups with that taxon to the exclusion of the great ape means. That is to say, that over all PCs, although distinct from the *H.sapiens* mean, OH 8 is still far more human-like than it is ape-like. The African great apes all cluster together to the exclusion of *Pongo*, and the two species of *Pan* group together to the exclusion of *Gorilla*. This phenogram also supports the finding in Chapter 4 that the *Homo sapiens* cuboid is highly remodelled, whilst those of the extant great apes are relatively conservative. The proximity of the OH 8 cuboid to that of *Homo sapiens*, highlights the fact that that this remodelling was already considerably advanced in *H.habilis* by the late Pliocene.

5.5.3 Navicular

Figure 5.15 clearly shows that the hominin fossil naviculars fall between the African apes and modern humans on PC 1 versus PC 2. OH 8 appears to be the most human-like, falling just within the modern human range of variation. Stw 573 is the least human-like, and falls just within the African ape range of variation. The two Hadar naviculars fall between the African ape and modern human clouds. Al 333-47 is closer to the African ape cloud than Al 333-36. None of the fossils specimens appear close to the *Pongo* cloud. Table 5.9 shows that at 25.7% and 19.4% respectively, PC 1 and PC 2 account for relatively similar proportions of variance.

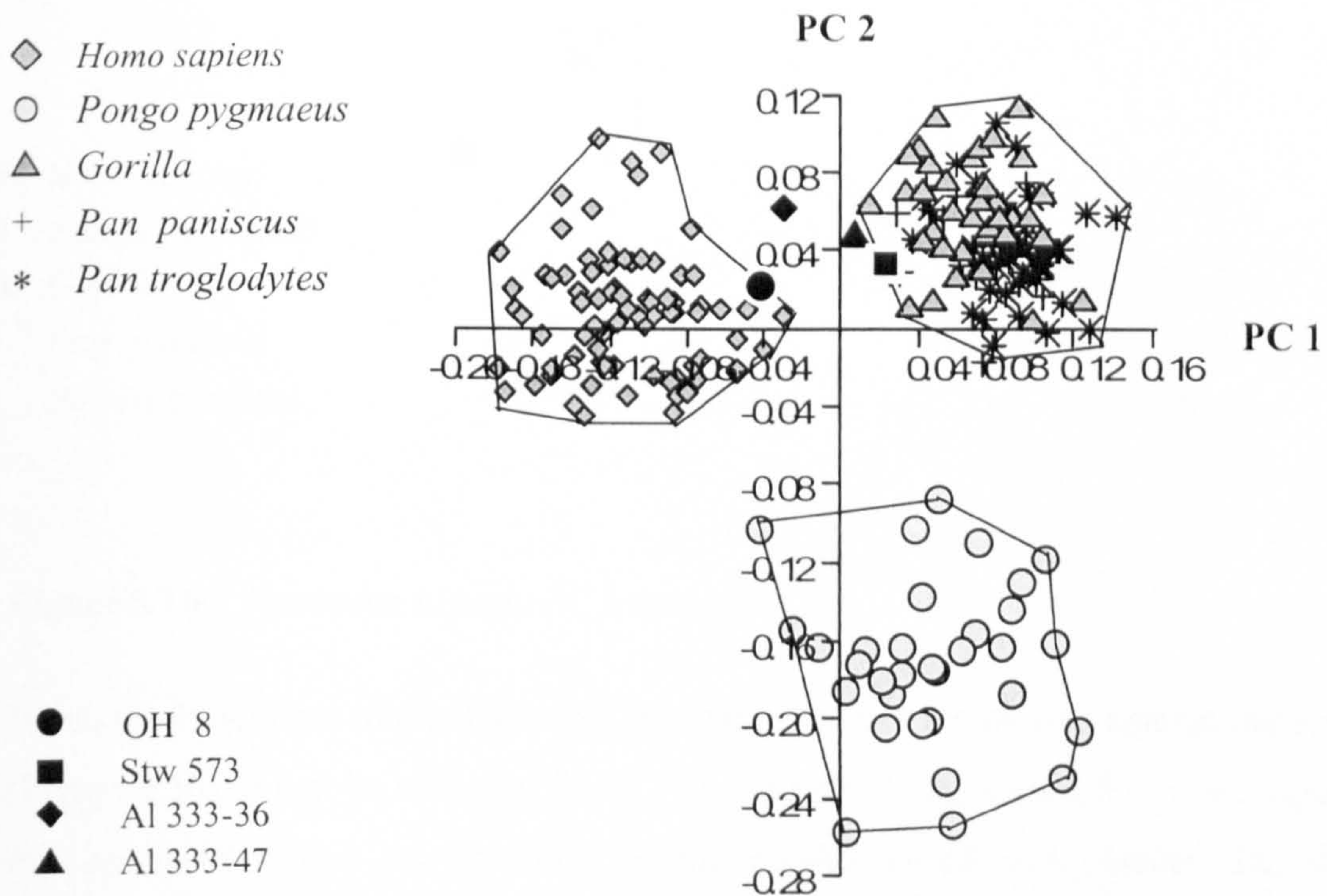


Figure 5.15 Navicular: PC 1 versus PC 2.

Table 5.9 Navicular: Percentage variance for PCs 1 to 4

Principal Component	Percentage variance
1	25.7%
2	19.4%
3	7.1%
4	5.0%

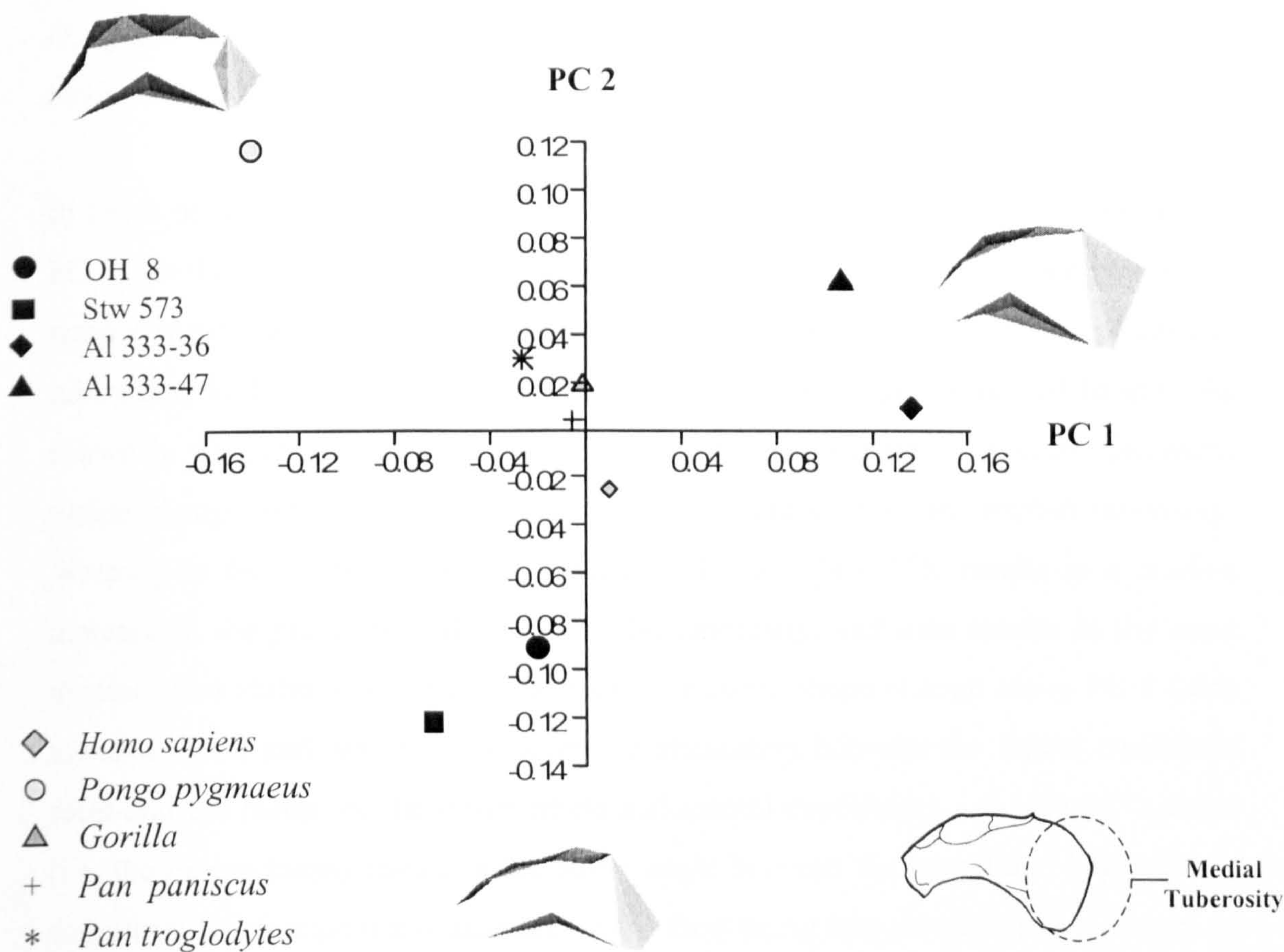


Figure 5.16 Navicular Means: PC 1 versus PC 2.

When the Procrustes mean shapes for the extant species are plotted against the fossils (Figure 5.16), it can be seen that for PC 1 versus PC 2, the means for *Homo sapiens*, *Pan troglodytes*, *Pan paniscus* and *Gorilla gorilla* are all very similar. The mean *Pongo* shape is distinctly separated from the other extant species means as well as the fossil, on account of its very low PC 1 score and very high PC 2 score. It can be seen from Table 5.10 that PC 1 and PC 2 explain relatively similar degrees of variance. The OH 8 and Stw 573 naviculars are relatively similar to each other for both PC 1 and PC 2, and distinct from the *H.sapiens*, *Pongo* and African ape means on account of their very low PC 2 scores. The two Hadar naviculars are also very similar to each other, but appear distinctly different to either OH 8 or Stw 573, on account of their higher PC 1 and PC 2 scores. The two Hadar naviculars are also distinct from the *H.sapiens* and African ape means, on account of having higher PC 1 scores. The overall distribution on Figure 5.14 is of four distinct groupings on the graph:

H.sapiens and the African apes; *Pongo*; OH 8 and Stw 573; and the two Hadar naviculars.

In terms of shape differences, the principal aspects of shape variation represented by PC 1 involve the prominence of the medial tuberosity. As can be seen from the warped means in Figure 5.15, the two Hadar naviculars have an extremely prominent tuberosity, both in terms of its mediolateral width, and its proximodistal length. As shown in Chapter 4, the navicular of *Pongo* has a considerably reduced tuberosity. Shape change along PC 2 also involves the prominence of the medial tuberosity. Warping to the negative end, i.e. towards OH 8 and Stw 573, results in a relative increase in the proximodistal length of the tuberosity, and also results in the most medial point shifting relatively proximally. Further shape change along PC 2 (also towards OH 8 and Stw 573) involves the orientation between the lateral cuneiform facet and the facets for the intermediate and medial cuneiforms. A high PC 2 value (i.e. the *Pongo* mean) results in the larger angle between the lateral and intermediate cuneiform facets, essentially resulting in the facet being less anterior facing, and more in line with the long axis of the foot. Warping down PC 2 to the negative end results in that angle reducing, meaning that the lateral cuneiform facet is more in line (i.e. forward facing) with the intermediate and medial cuneiform facets.

Table 5.10 Navicular (fossils and extant means): Percentage variance for PC 1 to PC 4

Principal Component	Percentage variance
1	31.0%
2	24.3%
3	20.2%
4	11.3%

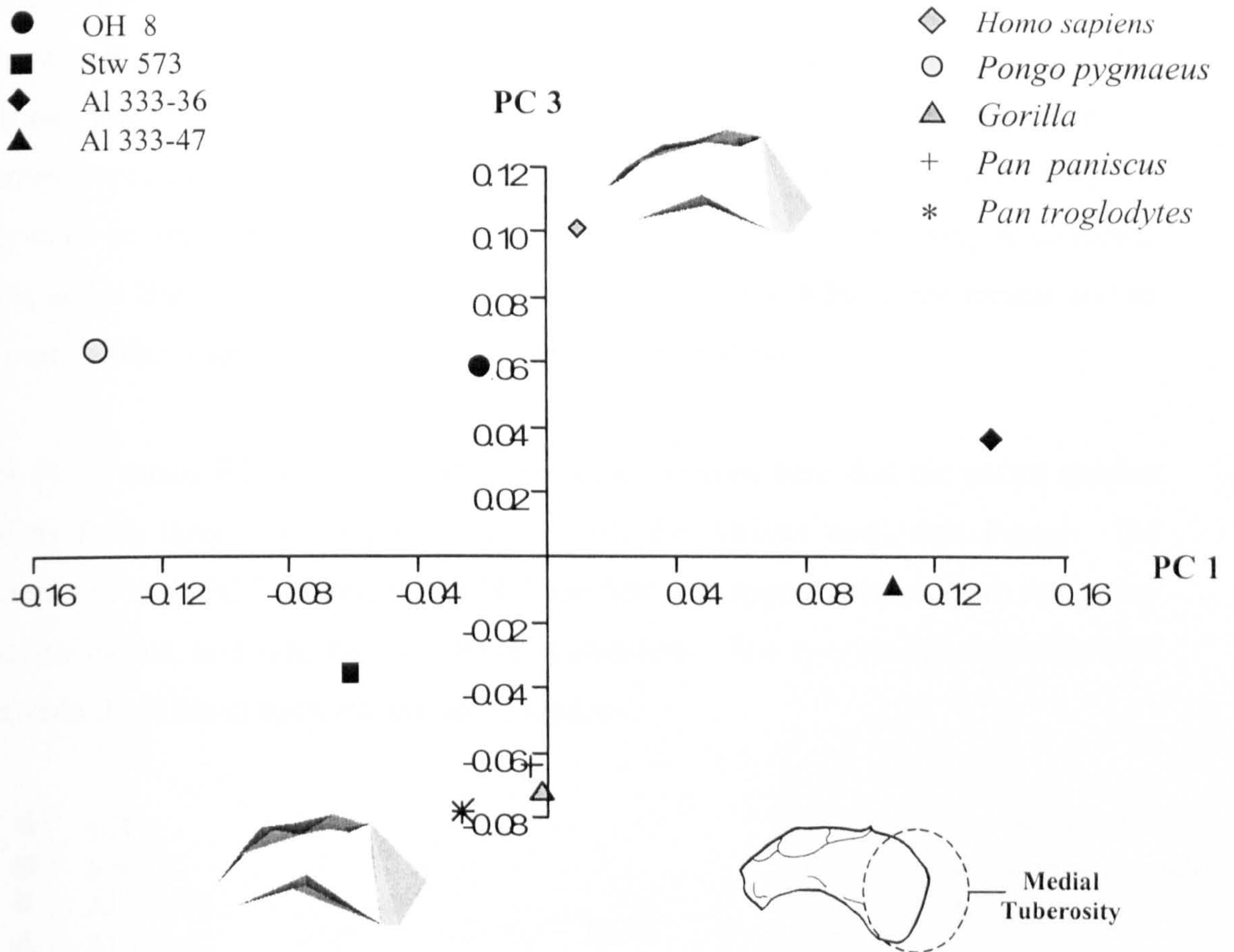


Figure 5.17 Navicular Means: PC 1 versus PC 3.

It can be seen from Figure 5.17 that PC 3 separates the African ape means from that of *Homo sapiens*. It is important to note (see Table 5.10) that PC 3 (20.2%) describes only a little less of the variance than PC 2 (24.3%). The *Pongo* mean shape falls between the *H.sapiens* and African ape means, but is closer to the *H.sapiens* mean. The African ape means are all very similar to each other on PC 3. Stw 573 and OH 8 are more separated on PC 3 than for PC 2 or PC 1, with OH 8 being similar to the *Pongo* and *H.sapiens* means, and Stw 573 being closer to the African ape means. The two Hadar naviculars fall between OH 8 and Stw 573, and are closer to each other on PC 3 than OH 8 is to Stw 573.

There are two aspects of variation represented by PC 3. The first involves the prominence of the medial tuberosity, as for PC 1 and 2. Moving from the positive end of the y-axis (i.e. *H.sapiens* mean) to the negative end (African ape means) results in an increase in the medial projection of the tuberosity, and, on the lateral side of the

bone, a decrease in the proximodistal distance between the cuneiform and talar facets. The overall effect, viewed dorsally, is that warping from the *H.sapiens* mean to the African ape means, results in the bone becoming more “wedge shaped”, with the narrow part of the wedge being on the lateral side. In this respect, since the OH 8 navicular is considerably closer to the *H.sapiens* mean, it has a relatively wide lateral side, and is less wedge shaped. Stw 573 is far closer to the African ape means, and so is more wedge shaped, with a relatively narrower lateral side.

For PC 2 versus PC 3 (Figure 5.18), and it can be seen here that the extant species means form three distinct groups: *H.sapiens*, the African apes, and *Pongo*. On account of their PC 2 scores, both OH 8 and Stw 573 appear distinct from the extant species means, and also the two Hadar naviculars. The two Hadar naviculars fall between the African apes, *Pongo* and *H.sapiens*.

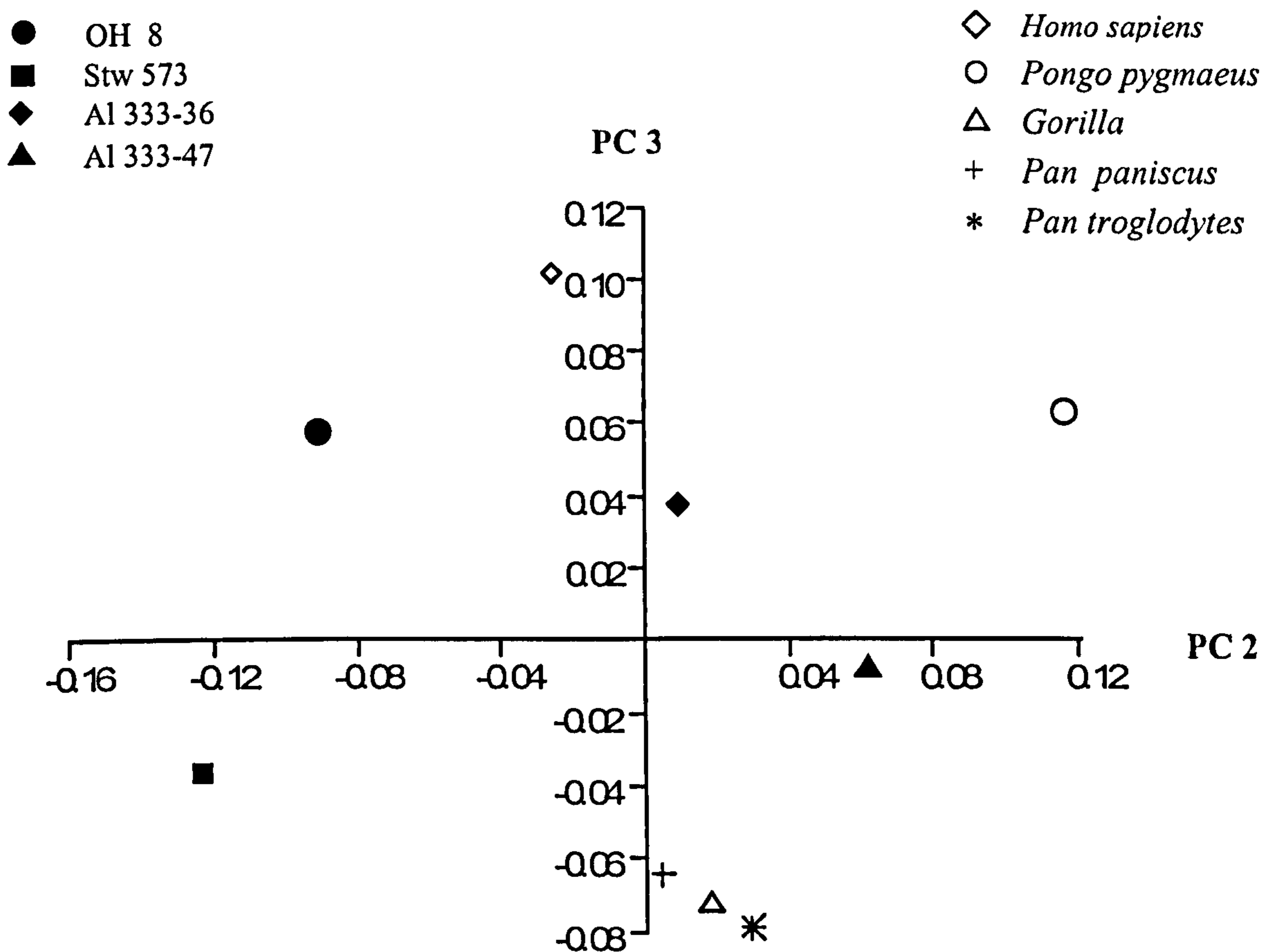


Figure 5.18 Navicular Means: PC 2 versus PC 3.

Table 5.11 Navicular: Pairwise Procrustes distances between fossils and extant species Procrustes means.

	<i>H.sapiens</i>	<i>P.paniscus</i>	<i>P.trog</i>	<i>Pongo</i>	<i>Gorilla</i>	OH 8	Stw 573	AI 333-36
<i>P.paniscus</i>	0.1944							
<i>P.trog</i>	0.2091	0.0978						
<i>Pongo</i>	0.2453	0.2288	0.2257					
<i>Gorilla</i>	0.1919	0.0853	0.0732	0.2359				
OH 8	0.1537	0.1806	0.1933	0.2581	0.1933			
Stw 573	0.2345	0.1802	0.2155	0.2775	0.2019	0.1798		
AI 333-36	0.2055	0.1942	0.2297	0.3031	0.2047	0.2172	0.2669	
AI 333-47	0.2139	0.1768	0.1963	0.2745	0.1772	0.2386	0.2637	0.1500

Table 5.11 shows the Procrustes distances between all the extant species means and the fossils as well. Figure 5.19 summarises this distance matrix in the form of a UPGMA phenogram. In terms of the extant species Procrustes means, the African apes all cluster together to the exclusion of either *Pongo* or *Homo sapiens*. The Procrustes distances between the three African ape taxa are relatively small. The African apes and *Homo sapiens* cluster together to the exclusion of *Pongo*. In terms of the fossils, OH 8 clusters with *Homo sapiens* to the exclusion of all other extant means and fossils. Stw 573 groups with the African apes, *Homo sapiens* and OH 8. OH 8 is considerably closer to the *H.sapiens* mean than is Stw 573. Table 5.10 shows that Stw 573 is closest to OH 8, and most distant from the two Hadar naviculars. The two Hadar naviculars cluster together to the exclusion of everything else (being considerably closer to each other than to anything else). They then cluster with the African apes, *Homo sapiens*, Stw 573 and OH 8, to the exclusion of *Pongo*. However, both Hadar naviculars are further from either OH 8 or Stw 573, than they are from the *Homo sapiens*, *Pan paniscus*, *Pan troglodytes* and *Gorilla gorilla* means.

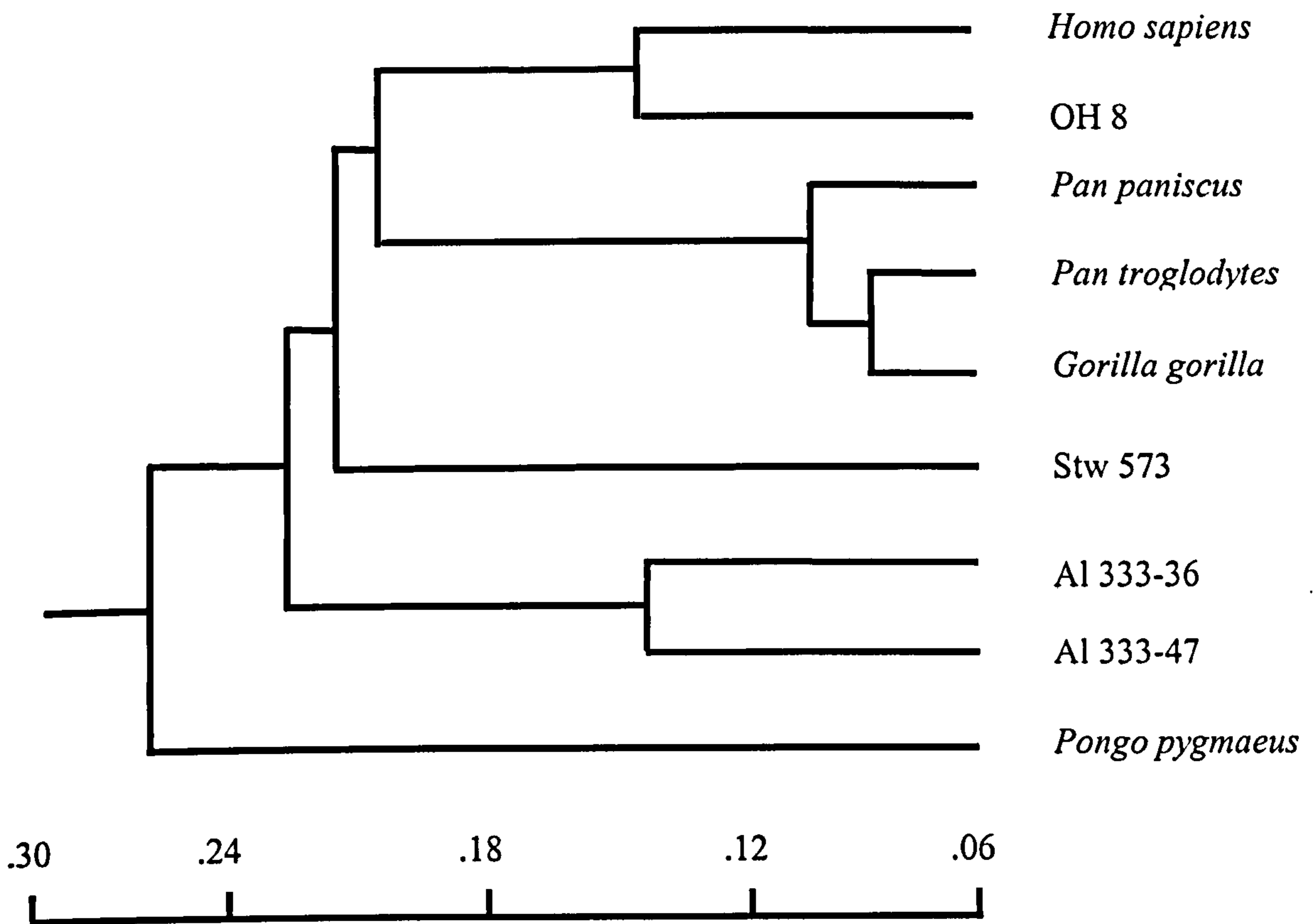


Figure 5.19 Navicular: UPGMA Phenogram using Procrustes distances

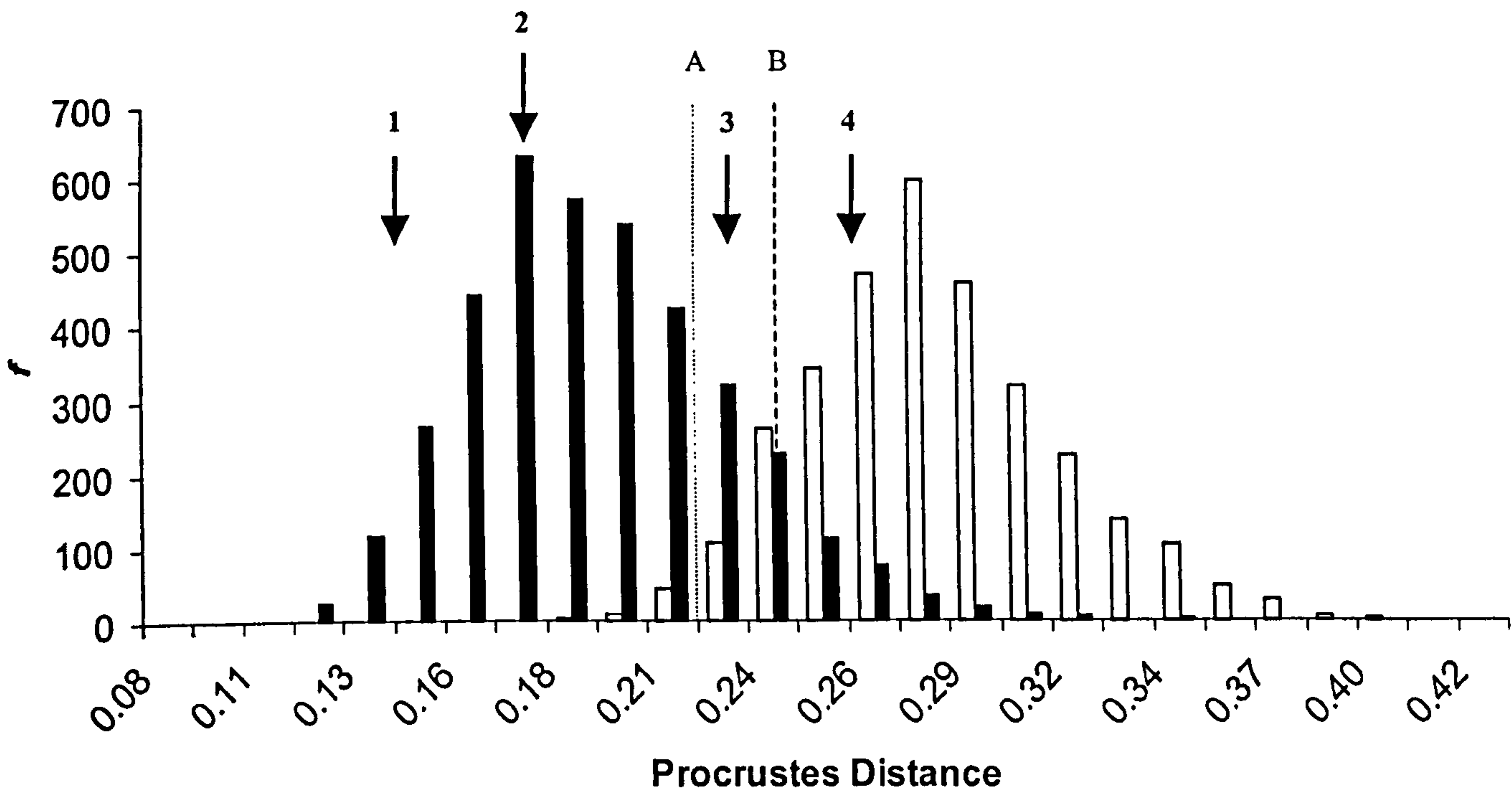


Figure 5.20 Navicular: Frequency histogram of pairwise Procrustes distances between individuals. Solid black bars are intraspecific distances for *Homo sapiens* and *Pan troglodytes*. White bars are interspecific distances for *H.sapiens* versus *P.troglodytes*. Dotted line "A" is the 5% confidence limit for the interspecific range, and dashed line "B" is the 95% confidence limit for the intraspecific range. Black arrows signify pairwise Procrustes distances between fossils: 1 = Al 333-36 vs. Al 333-47, 2 = Stw 573 vs. OH 8, 3 = OH 8 vs. Hadar mean, 4 = Stw 573 vs. Hadar mean.

Figure 5.20 shows the frequency histogram of pairwise Procrustes distances between individuals for *Homo sapiens* and *Pan troglodytes*. It can be seen that the Procrustes distance between the two Hadar naviculars falls well within the intraspecific ranges of variation for *H.sapiens* and *P.troglodytes*, and well beyond the interspecific range for distances between individuals of those two taxa. So based on the ranges of variation of two extant hominoid species, the data suggests that the two Hadar specimens are likely to have been from the same species. Both are assigned to *A.afarensis* (Latimer & Lovejoy, 1982), and this finding supports that assertion. OH 8 and Stw 573 are also close enough to each other to fall within intraspecific ranges, and well beyond even the outer limit of variation of interspecific values. So, despite being separated out on the UPGMA phenogram in Figure 5.19, they are still morphologically similar enough to be from the same species based on extant values. In terms of comparing the two Hadar naviculars to OH 8, the value falls between the 95% confidence limit for the intraspecific range of variation, and the 5% confidence limit of the interspecific range. It is therefore difficult to say whether the OH 8 and Hadar naviculars, are similar enough or not to be from the same species based on extant values. Stw 573, however, is sufficiently distinct from the Hadar naviculars, for the Procrustes distance between them to fall well beyond the 95% confidence limit of the intraspecific range of variation. This makes it likely, but not absolutely certain, that Stw 573 and the Hadar naviculars, based on extant values, are sufficiently morphologically distinct enough to come from different species.

5.5.4 Medial Cuneiform

Figure 5.21 shows that for the medial cuneiform, PC 1 clearly separates modern humans from the great apes. Table 5.12 shows that PC 1 accounts for 33.1% of the variance, as opposed to 18.3% for PC 2 and 9.3% for PC 3. On PC 1, the two fossils OH 8 and Stw 573 fall just on the edge of the modern human range of variation, and well outside the great ape ranges of variation. They both have a similar PC 1 score to one of the modern human outliers. In fact, if one considers that outlier, then the OH 8 and Stw 573 scores fall just within the modern human range of variation. PC 2 separates *Pongo* from both the African apes and modern humans, and on that axis, both fossils fall within the modern human and African ape clouds.

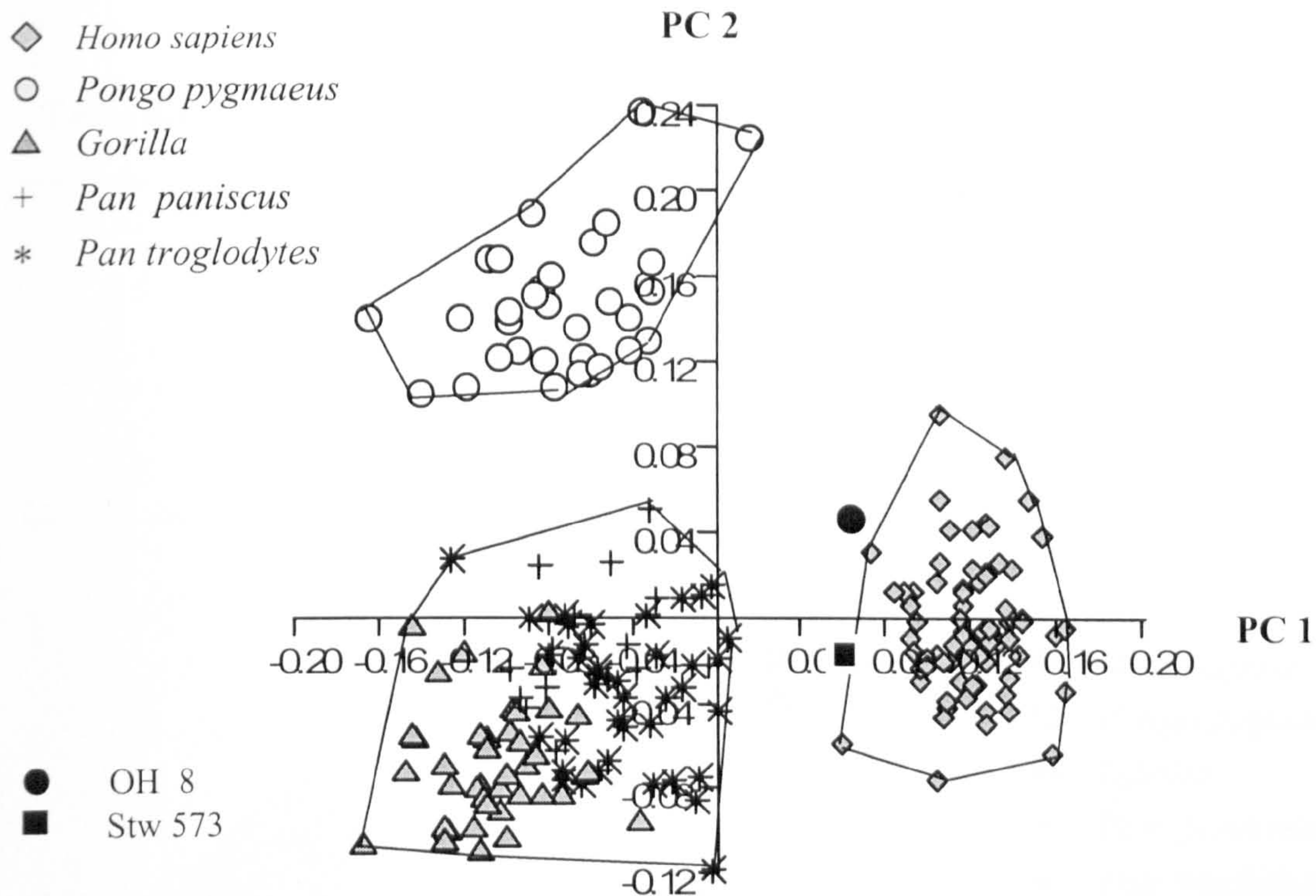


Figure 5.21 Medial Cuneiform: PC 1 versus PC 2.

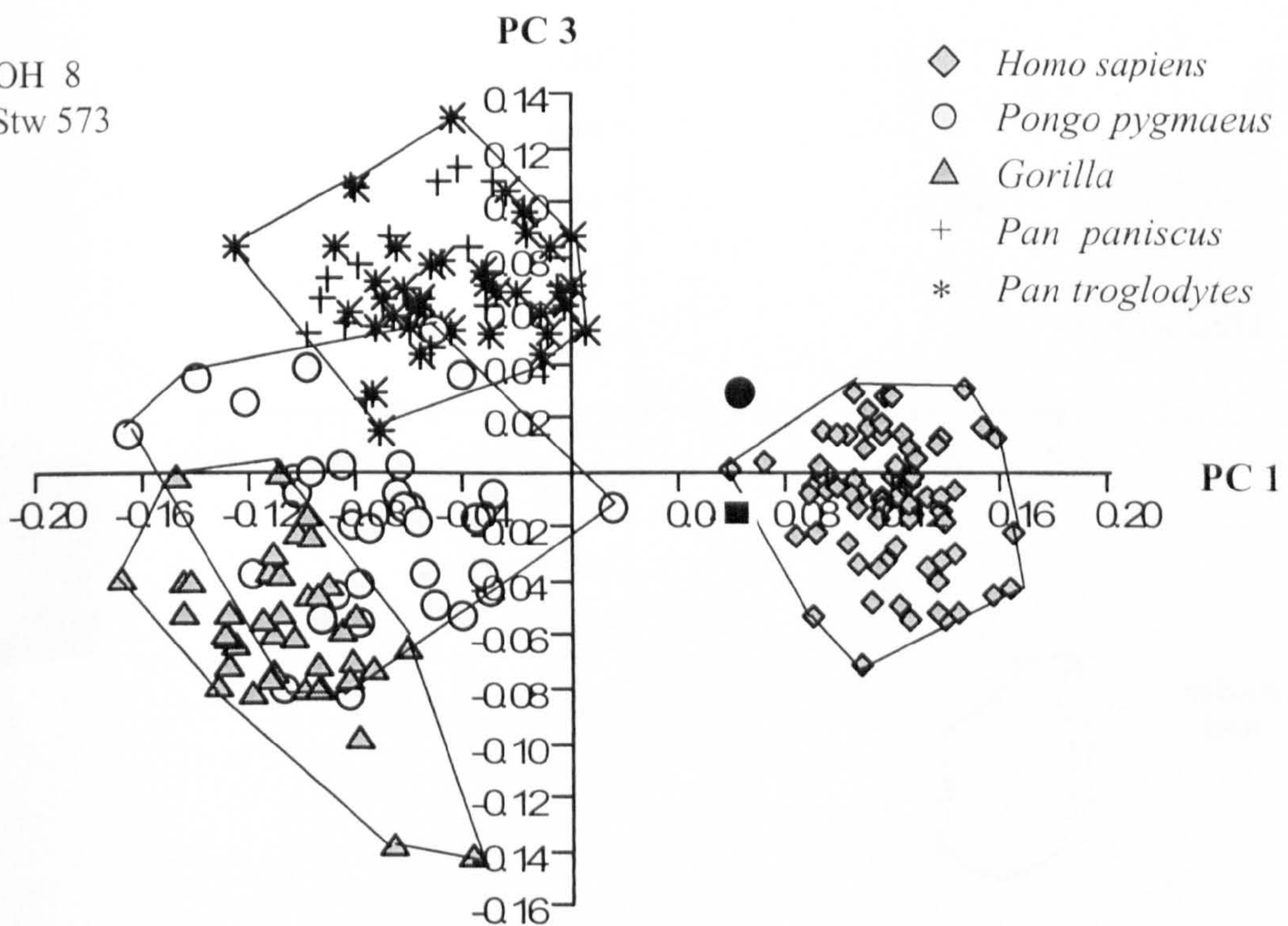


Figure 5.22 Medial Cuneiform: PC 1 versus PC 3.

Figure 5.22 shows that PC 3 separates the two species of *Pan* from the remaining taxa. On this axis modern humans occupy a similar range of scores to *Pongo* and much of *Gorilla*, and both fossils fall within these ranges, and effectively outside the range of variation of the two species of *Pan*.

Table 5.12 Medial Cuneiform: Percentage variance for PC s 1 to 4

Principal Component	Percentage variance
1	33.1%
2	18.3%
3	9.3%
4	4.2%

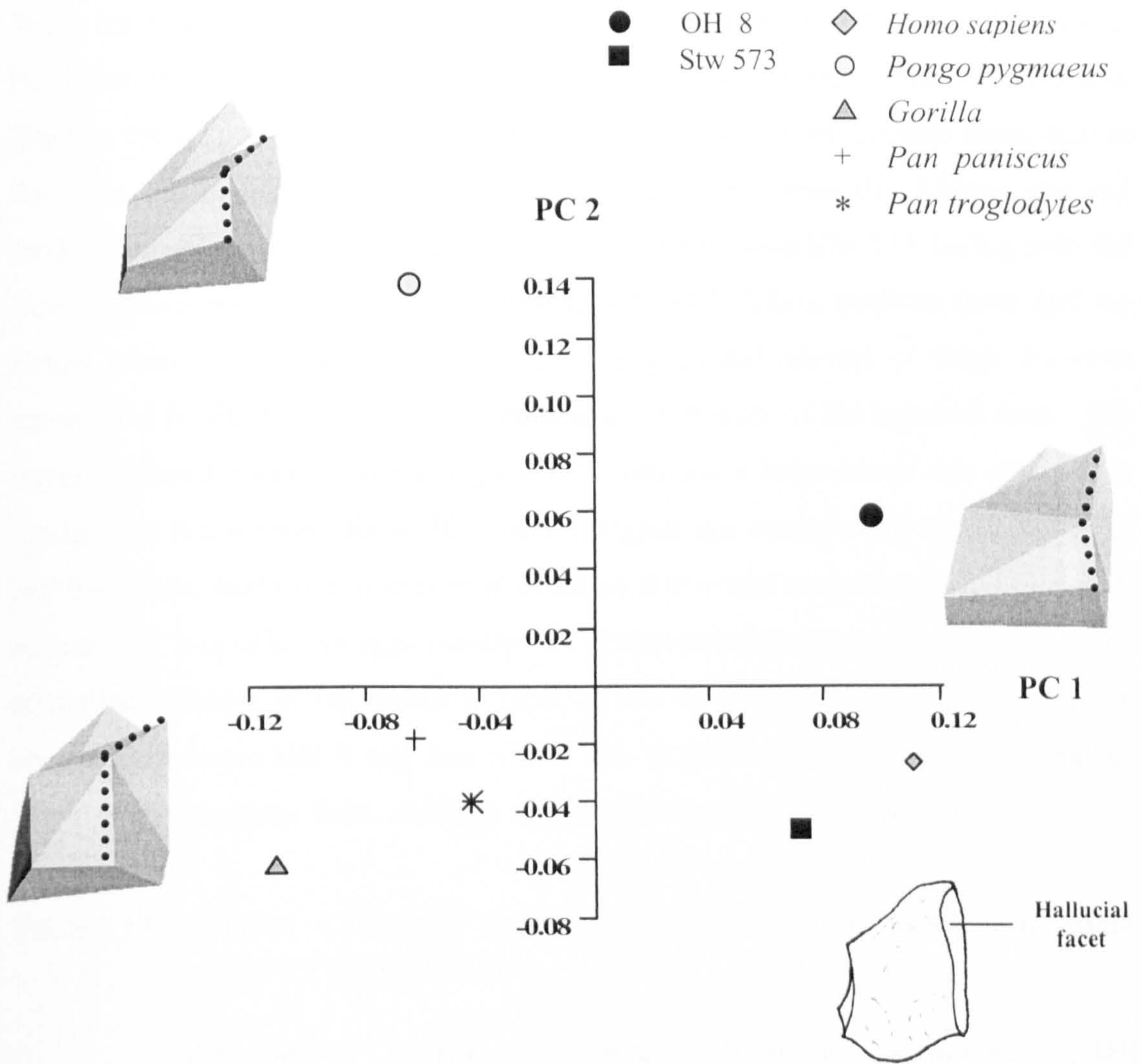


Figure 5.23 Medial Cuneiform (fossils and extant species means): PC 1 versus PC 2. Screen captured images are of the medial cuneiform in medial view. Dotted line represents medial margin of hallucial facet.

Table 5.13 Medial Cuneiform (fossils and extant means): percentage variance for PC 1 to PC 4

Principal Component	Percentage variance
1	41.2%
2	26.8%
3	15.1%
4	9.7%

When the mean shapes for the extant taxa are submitted to GPA/PCA with the fossils, PC 1 separates the *Homo sapiens* mean from those of the great apes (Figure 5.23). The two fossil specimens fall far closer on this axis to the *Homo sapiens* mean than to the great ape means. PC 2 separates the *Pongo* mean from the African ape and modern human means. PC 2 separates the two fossils, with Stw 573 falling with the *Homo sapiens* and extant great ape means, and OH 8 falling between these and the *Pongo* mean. As discussed in Chapter 4, the principal aspects of shape variation represented by PC 1 involves the orientation and curvature of the hallucial facet. The screen captured warped images (Figure 5.23) provide a reminder of this change. It can be seen that warping along PC 1 from the great ape means to the *H.sapiens* mean and the fossils, that the hallucial facet becomes flatter and more anteriorly orientated, indicating a loss of hallux opposability. PC 2 accounted for a relative decrease in the dorsoplantar height of the navicular facet, as can be seen for the *Pongo* mean. The separation between OH 8 and Stw 573 is due to OH 8 having a relatively smaller height of the navicular facet, although the actual difference observed is small.

Table 5.14 Medial Cuneiform: Pairwise distances between fossils and extant species Procrustes means.

	<i>P.troglodytes</i>	<i>Pongo</i>	<i>Gorilla</i>	<i>H.sapiens</i>	<i>P.paniscus</i>	OH 8
<i>Pongo</i>	0.2080					
<i>Gorilla</i>	0.1526	0.2243				
<i>H.sapiens</i>	0.1863	0.2485	0.2421			
<i>P.paniscus</i>	0.0705	0.1929	0.1598	0.2064		
OH 8	0.1944	0.2240	0.2607	0.1580	0.2038	
Stw 573	0.1733	0.2394	0.2166	0.1282	0.1910	0.1906

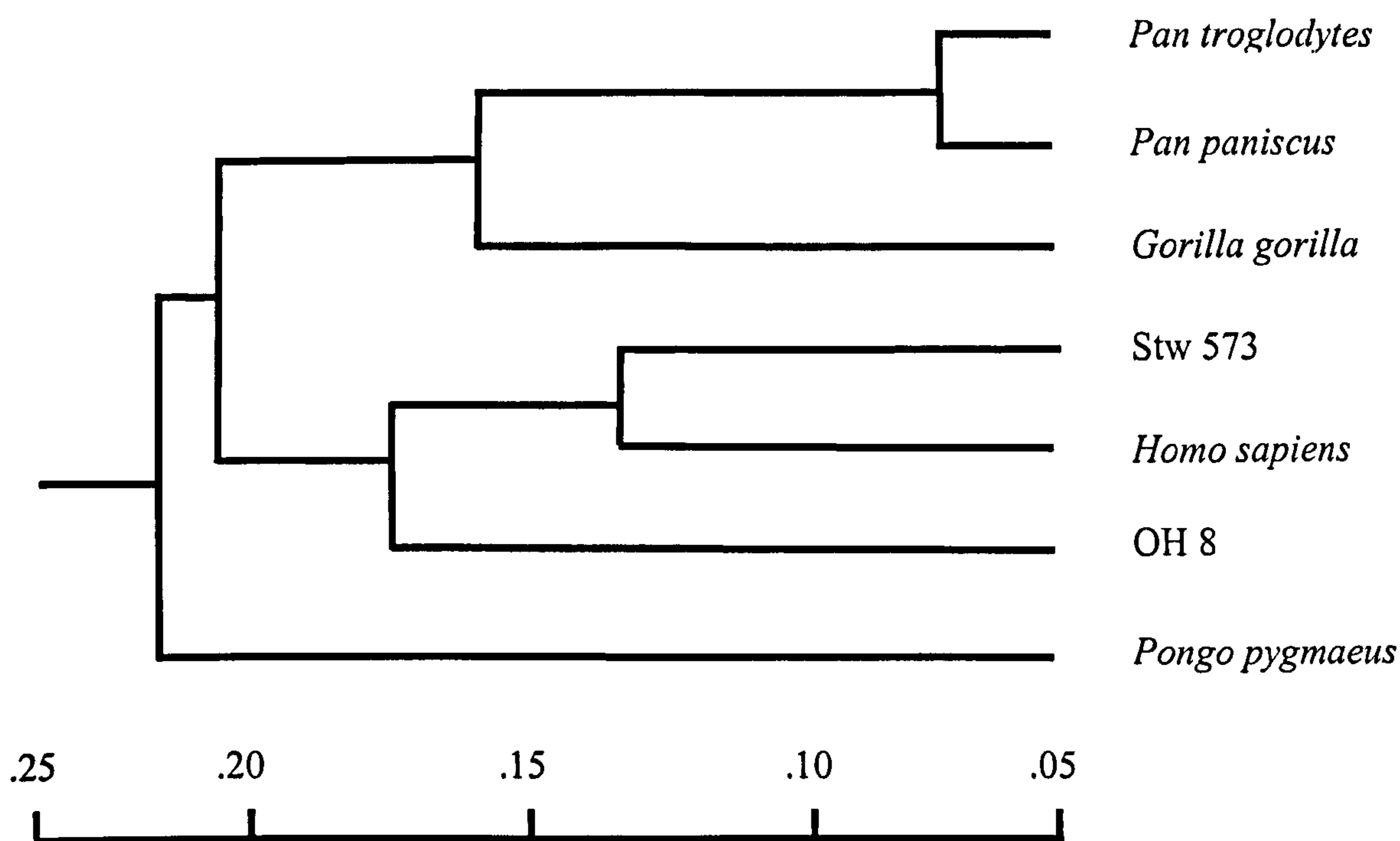


Figure 5.24 Medial Cuneiform: UPGMA phenogram of fossils and Procrustes mean shapes for extant species.

Figure 5.24 shows a UPGMA phenogram for the Procrustes distances between mean medial cuneiform shapes for the extant taxa, and the OH 8 and Stw 573 fossils. There are three distinct groupings on this phenogram. The African ape means group together, both fossils group with the *Homo sapiens* mean, and the *Pongo* mean groups separately to the exclusion of all other taxa. The Stw 573 medial cuneiform groups with the *H.sapiens* mean to the exclusion of OH 8, and is thus closer to the *H.sapiens* mean than is OH 8. However, the differences between the two distances is small, as the absolute Procrustes distance (see Table 5.14) between OH 8 and the *H.sapiens* mean is 0.1580, whilst it is 0.1282 between Stw 573 and the *H.sapiens* mean, which is only a difference of 0.0298.

The frequency histogram in Figure 5.25 shows that for *Homo sapiens* and *Pan troglodytes*, there is some degree of overlap between interspecific and intraspecific ranges of variation for pairwise Procrustes distances. When OH 8 is compared to Stw 573, the Procrustes distance between the two fossils falls beyond the 5% confidence limit for the interspecific range, but well within the 95% confidence limit for the intraspecific range. Whilst this does not completely discount the possibility that the OH 8 and Stw 573 medial cuneiforms are sufficiently morphologically different

enough to warrant being from different taxa, it strongly suggests, based on extant species variation, that the two fossils are morphologically similar enough to each other to have a strong likelihood of being from the same taxon.

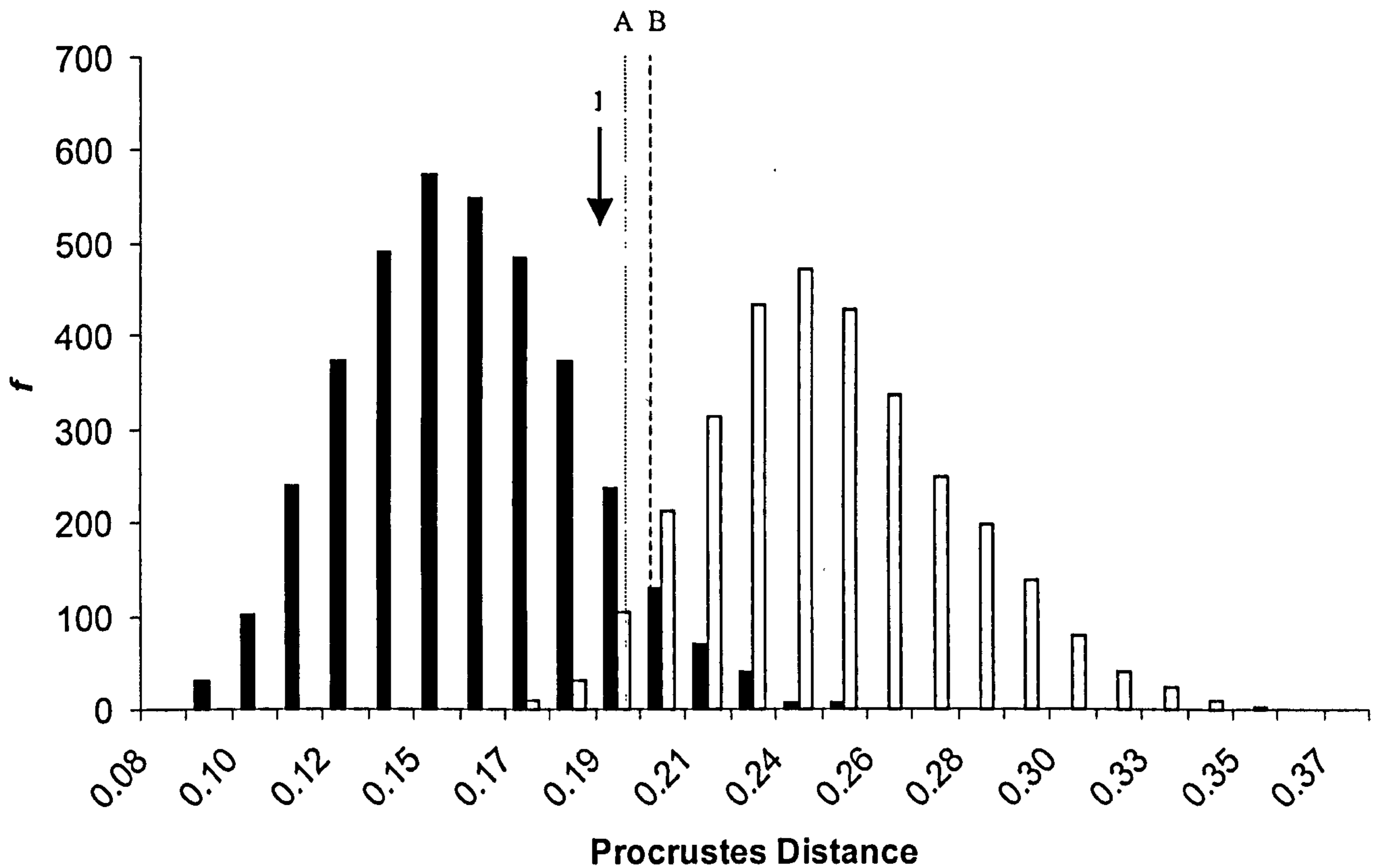


Figure 5.25 Medial Cuneiform: Frequency histogram of pairwise Procrustes distances between individuals. Solid black bars are intraspecific distances for *Homo sapiens* and *Pan troglodytes*. White bars are interspecific distances for *H.sapiens* versus *P.troglodytes*. Dotted line "A" is the 5% confidence limit for the interspecific range, and dashed line "B" is the 95% confidence limit for the intraspecific range. Black arrow 1 signifies the Procrustes distance between OH 8 and Stw 573.

5.6 Discussion

The results for each tarsal are discussed in turn, and then are drawn together and summarised at the end of this section.

5.6.1 Talus

The results of this study show that for the talus, there is considerable morphological variation in the hominin fossil record. The Al 288 talus (Lucy) is so morphologically distinct from both OH 8 and Stw 573, that it is more than likely to come from a different species. This difference is considerably outside modern intraspecific ranges of variation, and towards higher values for interspecific ranges of variation. Al 288 falls just within *H.sapiens* range of variation, and crucially, has the flat trochlear surface of the modern human talus. Al 288 is also far closer to the *H.sapiens* mean than are the other fossils. This finding strongly suggests that the human-like morphology of the *A.afarensis* talus meant that during bipedal locomotion, the leg would pass directly over the talus. As suggested by Latimer *et al.* (1987), this implies that at least at the talo-crural joint, the *A.afarensis* foot was plantar flexing and dorsiflexing in a human-like way, implying that that taxon had an efficient method of transferring weight through the foot to the ground. This implies at least one strong adaptation to efficient bipedal locomotion.

However, the case with OH 8 and Stw 573 is very different. They are somewhat different to each other, as shown in the talus phenogram. However, they are both considerably more different to Al 288. They are more likely than not to be from different taxa based on modern values, but the important issue in terms of their morphology, is that they have both retained an ape-like sloping trochlea. The functional implication for this is that during locomotion, the leg would pass over the foot in a more laterally skewed and arcuate path. This results in a far less efficient transfer of weight from the leg to the foot, and implies that during any form of bipedal locomotion, both *H.habilis* and *A.africanus* would not have had the human-like weight transfer through the talo-crural joint that *A.afarensis* did (Latimer *et al.*, 1987; Aiello & Dean, 1990). This is further corroborated from the analysis using just the trochlea (Figure 3). In that case, for PC 1 versus PC 2, Stw 573 (along with Stw 88) fell well within the African ape range of variation, and outside the *H.sapiens* range.

OH 8 fell well within the *Pongo* range and well outside both the *H.sapiens* range and the African ape range. So both OH 8 and Stw 573 were ape like, but in different ways. This is reflected in the relatively large Procrustes distance between them. The finding that OH 8 falls with *Pongo* for the trochlea is interesting, and helps to resolve some of the considerable debate over the affinities of that talus. As discussed in Chapter 1, a number of studies argued that the affinities of the OH 8 talus lay, in part, with that of *Pongo* (Lisowski *et al.*, 1974; Kidd *et al.*, 1996). Inspection of the measurements used in those studies (interlandmark distances, indices and angles) show that the majority of variables were either direct measurements of the trochlea, or were indirectly related to its dimensions (e.g. total talar length). When the whole talus is considered, as in this study, the OH 8 talus appears more intermediate between the African apes and *H.sapiens*, as would be expected for a fossil hominin.

5.6.2 Cuboid

The results show that the OH 8 cuboid is essentially remodelled to a human-like degree. In Chapter 4 it was shown that the cuboid of *Homo sapiens* is particularly specialised and remodelled when compared to the other tarsals. The principal difference between the cuboid of *Homo sapiens* and that of the great apes is the strong plantar beak on the calcaneal facet, and the fact that the *H.sapiens* cuboid is relatively longer in the proximal-distal direction, and narrower in the medio-lateral direction. When using the Procrustes rotated means for the extant taxa, it is PC 1 that separates the great ape means from that of *H.sapiens*. On PC 1 the OH 8 cuboid clearly falls with the *H.sapiens* mean. So, OH 8 is principally human-like in its functional morphology, and can thus be considered to be considerably remodelled. This is confirmed by the UPGMA phenogram of extant means and OH 8, where OH 8 groups with the *H.sapiens* mean to the exclusion of all other taxa. OH 8 is also a little different from the *H.sapiens* mean in that it has, relative to the 5th metatarsal facet, a slightly larger 4th metatarsal facet. This would imply that the OH 8 lateral column, whilst definitely locking in the stance phase (due to the pronounced plantar beak), transferred a little more weight through the 4th metatarsal than does the foot of *H.sapiens*. This is supported by the metatarsal robusticity pattern of OH 8, which has a slightly more robust 3rd metatarsal than *H.sapiens* (Archibald *et al.*, 1973), also implying slightly more weight transfer through the middle of the foot.

5.6.3 Navicular

For the navicular, the results show that there is a considerable degree of morphological variation in the hominin fossil record. The OH 8 navicular is the most human-like of the four fossil specimens. It falls just within the *H.sapiens* range of variation for PC 1 versus PC 2, it has the smallest Procrustes distance from the *H.sapiens* mean of all the fossil and great ape means. This is reflected in the phenogram, where OH 8 groups with the *H.sapiens* mean to the exclusion of all other shapes. What makes OH 8 more human-like is its relatively reduced tuberosity, and the relatively wide distance between the talar and lateral cuneiform facets on the lateral side of the bone. As discussed in Chapter 1, a reduced tuberosity is likely to be an indication of a reduction in weight bearing on this part of the bone, and thus an increase in elevation of the navicular from the substrate, i.e. an increase in arching of the medial column (Sarmiento, 2000), and so this data strongly suggests that OH 8 had a medial longitudinal arch. Furthermore, a relatively wider lateral side of the navicular (i.e. as in *H.sapiens*), may also be an adaptation to more efficient weight transfer from the lateral side of the foot to the medial side (i.e. the ball of the foot) during the mid to late stance phase (Harcourt-Smith, 1997).

The overall findings for the OH 8 navicular support those of Berillon (1998, 2000) and Sarmiento (2000), which both found, using multivariate analysis of an extensive number of angles and interlandmark distances on the navicular (particularly in Sarmiento's case), that the OH 8 navicular is more human-like than great-ape like, and falls just within the *H.sapiens* range of variation. The study by Sarmiento also produced a phenogram using Mahalanobis' distances, that showed OH 8 grouping with the *H.sapiens* mean to the exclusion of all other extant means and fossils, as is the case with this study. This study does not support the findings by Kidd *et al.* (1996), which found, based on multivariate analysis, that the navicular of OH 8 was closest in its morphological affinities to the African great apes. However, Kidd's study used only 6 measurements to reflect the overall dimensions of the bone. With four separate articular facets and a prominent tuberosity, this is a relatively small number of measurements to reflect the whole bone's morphology.

The Stw 573 navicular is morphologically most similar to OH 8 (in terms of Procrustes distance it is closer to OH 8 than to any other fossil or mean). Both OH 8

and Stw 573b group together on PC 2 of the PCA of the extant means and the fossils. The Procrustes distance between them falls well within the intraspecific range of variation for *H.sapiens* and *P.troglodytes*, and at the same time beyond the interspecific range for those taxa. However, it is also considerably less human-like than OH 8 in some respects (and has a greater Procrustes distance from the *H.sapiens* mean than OH 8), and this is born out on PC 3, where Stw 573 grouped with the African ape means, and OH 8 was closer to the *H.sapiens* mean. As shown, Stw 573 has a larger tuberosity than OH 8. However, it is still not as relatively large as that of the African apes. This implies that the Stw 573 foot is likely to have had a degree of arching in the medial longitudinal column. Viewed dorsally, Stw 573 is also more “wedge shaped” (i.e. like the African apes) than in OH 8. The functional implication is that Stw 573 was slightly less efficient at transferring weight from the mid-foot to the ball of the foot during the mid-late stance phase.

The two Hadar naviculars were markedly similar to each other. The Procrustes distance between them fell well within the intraspecific range of variation for *H.sapiens* and *P.troglodytes*, and well outside the interspecific range for those taxa. Not only that, but on the phenogram for the fossils and the extant Procrustes means, the two fossils grouped closely together to the exclusion of all other fossils and extant means. They also grouped together on the PCA plots (PC 1 versus PC2, and PC 1 versus PC 3) for the extant means and fossils. Sarmiento’s (2000) and Berillon’s (1998, 2000) findings also showed that the two Hadar naviculars strongly grouped together. Both fossils are assigned to *Australopithecus afarensis* (Latimer *et al.*1982), and this study supports that assertion. In terms of the two Hadar specimens relative to OH 8 and Stw 573, the overall conclusion of this study is that the Hadar specimens are markedly different in their morphology. On the phenogram for the navicular, Stw 573 and OH 8 both grouped with the African apes and *H.sapiens* to the exclusion of the Hadar specimens. Furthermore, the virtually identical Procrustes distances between both Hadar specimens and Stw 573 strongly suggest that they are more likely to have come from different species than not, since the distances fall well beyond the intraspecific range for *H.sapiens* and *P.troglodytes*. The case with OH 8 remains a little more ambiguous, and it cannot be concluded either way, based on ranges of variation of extant taxa, whether or not it is different enough from the Hadar specimens to warrant belonging to a different species. However, warping of the mean

shape along the PC axes using the fossils and the extant means, shows that the Hadar specimens are not only very different to OH 8 and Stw 573, but are also different to the extant species means, and so in some respects are unique. The way in which they appear so different is in having a highly pronounced and enlarged medial tuberosity. This is especially so in the proximodistal dimension, where it is very wide. In this respect, this study does not support the case put by Clarke and Tobias (1995). Based on visual appraisal, they stated that the Stw 573 navicular had a medial tuberosity similar in size to those from Hadar.

In Chapter 1 it was discussed that a prominent navicular tuberosity is likely to be indicative of an increased degree of weight-bearing on the medial side of the foot, and would thus be indicative of a medial longitudinal arch *not* being present (Elftman & Manter, 1935a; Sarmiento, 2000). In Chapter 4 it was shown that *Gorilla* has a relatively enlarged tuberosity compared to *Pan* and *Pongo*, and *Gorilla* is known to be considerably more terrestrial than either *Pan* or *Pongo* (Tuttle, 1968) and also to transfer considerable force through the navicular into the ground throughout the stance phase (Elftman & Manter, 1935a; Morton, 1936). So based on these findings, it is the conclusion of this study that the *A. afarensis* foot lacked a human-like medial longitudinal arch, and therefore could not transfer weight as efficiently through the foot during the stance phase. In this respect, this study strongly supports the findings of several other recent studies that reached similar conclusions (Berillon, 1998, 2000; Sarmiento, 2000).

5.6.4 Medial Cuneiform

The results show that the OH 8 and Stw 573 medial cuneiforms have a Procrustes distance between them that is sufficiently small to strongly suggest that they fall well within the intraspecific ranges of variation of both *H.sapiens* and *Pan troglodytes*, and outside the interspecific range of variation for those two taxa. It can thus be concluded, that whilst they cannot definitely be assigned to the same species, they are at least very similar morphologically. This is supported by the PCA of the extant species means and the two fossils. The principal difference (expressed along PC 1) between the great ape means and that of *H.sapiens*, is that the *H.sapiens* medial cuneiform has a flat and forward facing hallucial facet. As discussed in Chapter 1 and Chapter 4, this is a strong indication of the loss of the ability to oppose the hallux in

H.sapiens, an ability all other primates still possess (Huxley, 1863; Owen, 1866; Morton, 1922, 1924, 1927, 1936; Schultz, 1930; Lewis, 1980a, 1980b; Szalay & Langdon, 1986; Aiello & Dean, 1990). The loss of hallux opposability in *H.sapiens* is thus highly specialised, and so a highly derived feature. In this respect this study shows that the medial cuneiforms of both OH 8 and Stw 573 have the human-like flat and forward facing hallucial facet. The feet of both *H.habilis* and *A.africanus*, can therefore be considered to have remodelled so as to have lost the ability to oppose the hallux and therefore operate as a grasping foot.

This study therefore supports previous studies showing that OH 8 did not have an opposable hallux (Day & Napier, 1964; Susman & Stern, 1982; Susman, 1983; Gebo, 1992; Harcourt-Smith, 1997, 1999, 2002; Berillon, 1998, 1999, 2000) and refutes those that suggest it did (Lewis, 1972, 1980b; Kidd *et al.*, 1996). In terms of Stw 573 only one published study exists (Clarke & Tobias, 1995) and that study argued that Stw 574 had a significant degree of hallux opposability and thus grasping potential. This study is the first metrical study of that foot, and it comes to a considerably different conclusion.

5.7 Hypotheses

Below is a reminder of those hypotheses presented at the start of this chapter, followed by a brief summary statement on whether each one can be accepted or not.

H₁ That, for each tarsal, the fossil specimens are morphologically similar enough to each other to represent a single species.

H₁ cannot be accepted, since it has been shown that variation between fossil specimens often exceeds that seen intraspecifically in extant taxa

H₂ That the tarsals of *Homo habilis* and *Australopithecus africanus* are morphologically similar enough to each other to represent a single species.

H₂ can be accepted for the navicular and medial cuneiform, but **cannot be accepted** for the talus.

H₃ That *A.afarensis* tarsals are morphologically distinct from either *H.habilis* or *A.africanus* so as to fall outside extant intraspecific ranges of variation.

As a reminder, the hypotheses presented at the beginning of this chapter are presented again.

H₃ can be accepted for the talus. For the navicular it can be accepted for *A.africanus* versus *A.afarensis*, but not for *H.habilis* versus *A.afarensis*.

5.8 Summary

The main finding of this chapter is that there is considerable morphological variation in the fossil record for the tarsals analysed. Table 5.15 (on page 216) shows a summary of the findings (and inferred functional implications) of this study. In some respects this is hardly surprising, because all these specimens are assigned to different taxa, come from different locations often thousands of miles apart, and are (in some cases, like OH 8 and Stw 573) millions of years apart in age. However, what the data do show is that whilst the feet of *A.afarensis*, *A.africanus* and *H.habilis* were all mosaic in their affinities, with a combination of human-like, ape-like and unique features, they were all mosaic in *different* ways to each other.

When considering *A.africanus* and *A.afarensis*, which are roughly contemporaneous taxa, they both show certain adaptations to bipedal locomotion, but, crucially in different parts of the foot. The *A.africanus* foot, as typified by Stw 573, had lost the ability to oppose its hallux, but had retained an ape-like ankle complex, and probably had a moderate degree of arching in the medial longitudinal column. Conversely, the *A.afarensis* remains show that their feet had a human-like ankle joint, which would have resulted in a more efficient transference of weight from the lower leg to the foot throughout the stance phase (Latimer *et al.*, 1986). However, in all likelihood, *A.afarensis* did not probably have a medial longitudinal arch. Furthermore, the partial medial cuneiform from Hadar, Al 333-28, which could not be included in this 3D study since it was missing too many landmarks, has been shown to have retained a degree of hallux abduction on account of its markedly convex hallucial facet (Stern & Susman, 1991; Susman & Stern, 1991; Berillon, 1998, 1999, 2000; Harcourt-Smith, 2002), indicating that *A.afarensis* maintained at least a degree of grasping potential.

The *H.habilis* and *A.africanus* tarsals were, in general, more similar to each other in morphology and inferred function, than either were to those of *A.afarensis*. Both have the derived trait of having lost the ability to oppose the hallux. OH 8, is however, just a little more human-like than Stw 573 in that it is likely to have had a more human-like medial longitudinal arch.

Overall, what these findings highlight is that the data strongly suggest that the feet of different hominin taxa were adapted to the increased requirement for bipedalism in different ways. The implications of this are discussed in the next and final chapter.

	Human-like	Ape-like	Inferred function
<i>A.afarensis</i>			
Talus	Flat trochlea		Human-like movement of leg over foot
Navicular		Highly enlarged tuberosity	Reduced medial longitudinal arch & increased weight bearing on navicular
Medial Cuneiform	Forward facing hallucial facet	Curved hallucial facet	Some degree of hallux opposability (NB. This is a finding of other studies).
<i>A.africanus</i>			
Talus		Sloping trochlea	Ape-like movement of leg over foot
Navicular	Increase in width on lateral side	Slightly enlarged tuberosity	Slightly reduced medial longitudinal arch & increased weight bearing on navicular (less than <i>A.afarensis</i> though)
Medial Cuneiform	Flat, anterior facing hallucial facet		Hallux opposability lost
<i>H.habilis</i>			
Talus		Sloping trochlea	Ape-like movement of leg over foot
Cuboid	Pronounced plantar beak in medial and plantar position		Stable locking mechanism of calcaneocuboid joint during stance phase
Navicular	<ul style="list-style-type: none"> • Wide on lateral side • Reduced tuberosity 		<ul style="list-style-type: none"> • Increased weight transfer through 1st ray • Medial longitudinal arch
Medial Cuneiform	Flat, anterior facing hallucial facet		Hallux opposability lost

Table 5.15 Summary of tarsal affinities and inferred functions as found in this study (except for *A.afarensis* medial cuneiform).

Chapter 6

Summary of Results

The aim of this study has been to investigate tarsal shape variation in extant hominoid taxa, and then to consider fossil hominin tarsals in the context of those findings.

Firstly it is found (Chapter 3) for all extant taxa, that there is no sexual dimorphism in tarsal shape in the forefoot (medial cuneiform, navicular and cuboid). In the hindfoot (talus and calcaneus), there are significant differences between male and female mean shapes for *Pongo* and *Gorilla*, but not for any other taxon (the exception is the *P.paniscus* calcaneus, but the sample is too small to allow error to be discounted). Both these taxa have higher degrees of body-size dimorphism than *Pan* or *Homo* (Smith & Jungers, 1997), and it is concluded that since the great ape hindfoot is generally involved in force transmission rather than grasping, that the sexual dimorphism observed is probably a reflection of this. However, based on Procrustes distances, what shape difference there is between males and females for these taxa is negligible when compared to interspecific differences. Not only that, but the observed differences when warping from the mean male to the mean female shape were, in most cases, hardly visible to the eye. So whilst there is a statistically significant difference between males and female for *Pongo* and *Gorilla* tali and calcanei, it is likely that there is very little difference in functional terms. This is important when considering shape differences between fossils, the implication being that there is no sexual dimorphism in the forefoot (medial cuneiform, navicular and cuboid) whereas, although unlikely, sexual dimorphism cannot be completely ruled out as a source of variation in the fossil hindfoot (talus and calcaneus).

When the extant taxa are compared to each other (Chapter 4), it is found that there is no significant relationship between centroid size and any of the PC axes. For all five tarsals, there is clear separation between three distinct groups on the first two (or sometimes three) PC axes. These groups were: *Pongo*, the African apes, and *Homo sapiens*. These three groups represent, respectively, three distinct locomotor modes: dedicated arborealism, a mosaic of terrestrial quadrupedalism and arboreal climbing, and obligate bipedalism. In the absence of a strong relationship between centroid size

and shape that should reflect allometric size relationships, it is highly likely that the separation between the taxa is mainly due to differences in locomotor mode. Furthermore, the shape differences found in this study strongly support those reported in the literature based on visual appraisal or 2D quantification. The relative phenetic relationships between the taxa (based on distances between Procrustes mean shapes) interestingly differs from bone to bone. With regard to the talus and navicular, the *Homo sapiens* medial cuneiform, cuboid and calcaneus are very distant from the great ape taxa, and separate to the exclusion of them all. This implies that they are relatively more remodelled and specialised, and supports the assertion that the loss of hallux abduction and the increase in mid-tarsal rigidity are two of the most fundamental adaptations of the human foot (Elftman & Manter, 1935b; Morton, 1935; Elftman, 1960; Lewis, 1989; Aiello & Dean, 1990). Whilst the talus and navicular of *Homo sapiens* are distinct in their morphology, they are not as distinct from the African great apes as are those of *Pongo*. These findings are important when considering the taxonomic and functional affinities of isolated fossil pedal specimens, since the variable degree of speciality in the modern human foot indicates that certain bones are more diagnostic of bipedal locomotion than others. Finally it is found that the phenetic relationships (for the calcaneus, talus, cuboid, navicular and medial cuneiform) between the taxa do not match the consensus molecular phylogeny for the extant hominoids, lending further credence to the finding that it is problematic to resolve phylogeny using morphological traits (Collard & Wood, 2000).

When the fossils are included in the analysis (Chapter 5), the results show considerable morphological variation in late Pliocene and early Pleistocene hominin pedal remains. The most human-like and functionally derived foot assemblage is that of *Homo habilis* (OH 8), which, based on the evidence of Chapter 5, had lost the ability to oppose the hallux, had a medial and lateral longitudinal arch and a human-like stable mid-tarsal joint. However, the morphology of the talar trochlea indicates that weight transfer from the leg to the foot was unlikely to have been as efficient as it is in *Homo sapiens*. Based on the previously unmeasured Stw 573 pedal fossils (Littlefoot), *Australopithecus africanus* is found to have also lost the ability to have opposed the hallux, but had a navicular that was not quite as human-like as that of OH 8. This implies that the medial longitudinal arch of Stw 573 was not as pronounced as that of *H. habilis*. The *A. africanus* talar trochlea is similar to that of OH 8 in that its

slanted morphology suggests a more ape-like weight transfer from the leg to the foot during bipedal locomotion (Latimer *et al.*, 1987). The finding for the Stw 573 pedal assemblage challenges its original (and only) description (Clarke & Tobias, 1995), in that the authors suggested that the hallux was opposable to an “intermediate” degree, that the navicular was markedly ape-like, but the talus essentially human-like.

The *Australopithecus afarensis* pedal remains were strikingly different to those of *A.africanus* and *H.habilis*. The *A.afarensis* talar trochlea is flat, indicating that weight transfer from the leg to the foot was very human-like. It has been suggested that this would have allowed for a more efficient transfer of weight from the hindfoot to the forefoot during the stance phase (Latimer *et al.*, 1987). Conversely, the navicular of *A.afarensis* is extremely ape-like with a medial tuberosity that is relatively large even by *Gorilla* standards. This implies a high degree of weight transfer through the navicular into the substrate (Elftman & Manter, 1935a; Sarmiento, 2000), and suggests that *A.afarensis* is unlikely to have had a human-like medial longitudinal arch. The overall conclusion about the fossils analysed is that the medial column of *H.habilis* and *A.africanus* is more human-like distally and more ape-like proximally, whereas that of *A.afarensis* is more human-like proximally and more ape-like distally.

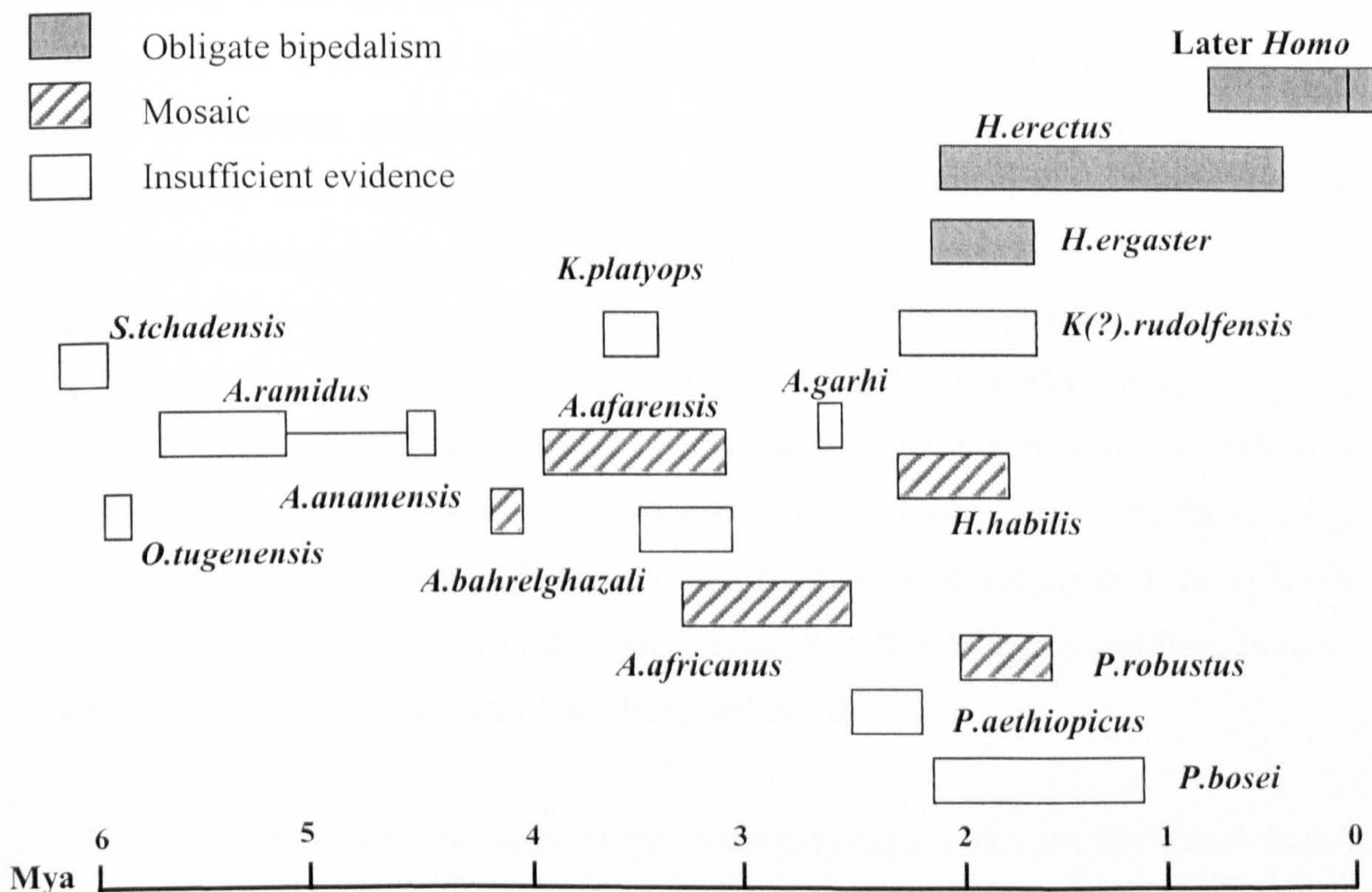


Figure 6.1 Temporal distribution of hominin taxa (adapted from Wood, 2002).

Conclusions

This study is concluded by posing a number of relatively broad questions about hominoid locomotor evolution, and then addressing these questions in light of the findings. For reference, Figure 6.1 displays an up-to-date summary of hominin taxa of the last six million years, and the degrees to which they are considered to have been bipedal.

How do these findings relate to the “problem” taxon, *Homo habilis*?

The taxonomic robusticity of the current *Homo habilis* hypodigm has been questioned a number of times, leading to suggestions that many specimens should be reassigned to a new taxon, *Australopithecus habilis* (Wood, 1974; Wood, 1991; Wood & Collard, 1999; Wood & Richmond, 2000). In a recent review of the criteria needed to assign material to the genus *Homo*, Wood & Collard (1999) suggest that specimens must show “..a postcranial skeleton whose functional morphology is consistent with modern human-like obligate bipedalism and limited facility for climbing” (p.71) and “...reconstructed body proportions that match those of *H.sapiens* more closely than those of the australopiths” (pp.70-71).

This study shows that *Homo habilis* may share a number of synapomorphies with *Homo sapiens* in terms of having a stable locking mechanism in the calcaneocuboid joint, an adducted, unopposable hallux, and medial and lateral longitudinal arches. This implies that, fundamentally, *H.habilis* was a committed biped, with efficient mid-tarsal locking during the stance phase, and a strong toe-off. To quote Latimer & Lovejoy (1990, p.125), “without a grasping hallux, other adaptations to climbing in the hominoid foot would be anatomically superfluous”. Therefore, based on pedal morphology, it is highly unlikely that the taxon OH 8 represents contained a significant arboreal component to its locomotor repertoire. However, the sloping, ape-like talar trochlea of the OH 8 talus, indicating different and perhaps less efficient weight transfer from the leg to the foot, implies that *H.habilis* may not have been an efficient biped in the same way that *Homo sapiens* is.

This finding is at odds with some of the recent suggestions over the taxonomic status of *Homo habilis*. The OH 62 skeleton, currently assigned to *H.habilis* (Johanson *et al.*, 1987), is described as having limb-proportions that are similar to those of

A.africanus, and are more-ape like than human-like, with relatively long upper limbs and short lower limbs (Hartwig-Scherer & Martin, 1991). It has been suggested that this implies a strong, efficient arboreal component to the locomotor repertoires of *H.habilis* (Wood, 1991). As discussed in Chapter 1, there has been much debate over the taxonomic affiliation of OH 8. A number of studies have suggested that there are enough ape-like traits in OH 8 to cast doubt over its designation to the *Homo habilis* hypodigm (e.g. Oxnard, 1972; Lisowski *et al.*, 1974, 1976; Kidd *et al.*, 1996), and it has even been suggested that it is more realistic to assign OH 8 to the genus *Australopithecus* (Wood, 1974b). If this were so, then the logical taxon would be *A.bosei*, which is found at Olduvai Gorge in the same locality and at the same level as OH 8 (Day, 1988). However, this is not compatible with the findings of this study for OH 8, which raises the possibility that the assignation of both OH 62 and OH 8 to the same taxon may be problematic, since OH 8 meets Wood & Collard's (1999) criteria for assignation to the genus *Homo*, but OH 62 does not. It is possible (but needs to be further tested) that OH 62 may represent a different, more arboreal taxon, whereas OH 8 (based on the findings of his study) represents a taxon whose foot was essentially adapted to bipedal locomotion (albeit a different type to that of modern humans), and had lost the crucial mid-tarsal flexibility and hallux opposability that a grasping arboreal foot requires.

However, more recent studies of hominin limb proportions suggests that OH 62 may have had less ape-like limb proportions than have previously been suggested (Hausler, 2001; Richmond *et al.*, 2002). Previous reconstructions of the OH 62 fragmentary femur were based on that of Al 288-1 (Lucy) (Hartwig-Scherer & Martin, 1991; McHenry & Berger, 1998). If the OH 62 femur length is based on that of the OH 34 femur (of a similar age and locality to OH 62), then its body proportions come out as virtually human-like (Hausler, 2001). Even if this is not done, recent research using exact randomisation techniques to assess differences between pairs of fossils shows that OH 62 and Al 288 have limb proportions that are similar enough to fall within extant ranges of variation. The implications of this finding is that OH 62 is still not human-like in its limb proportions, but is less ape-like than *A.africanus* specimens (Richmond *et al.*, 2002). In either case, the problem of assigning OH 8 and OH 62 to the same taxon can possibly be removed in the light of these findings, and the fact that

the morphology of the OH 62 dentition strongly suggests assignment to *H.habilis* (Johanson *et al.*, 1987).

How do these findings relate to various models of hominin foot evolution?

As reviewed in Chapter 1 there are a number of models of foot evolution that have been proposed. All have essentially proposed a process by which a hypothetical ape-like foot of the common ancestor of *Homo* and *Pan*, remodelled to become adapted to full, obligate bipedalism. All models have been relatively “linear” in their approaches, with an ancestral pattern of morphologies, an “intermediate” pattern (often based on available fossil material) and then the modern human pattern. Morton (1936) suggested that the hypothetical “prehuman” foot was not dissimilar to that of *Gorilla*, in having an opposable toe (although not as much as *Pan*), no longitudinal arches, and an enlarged calcaneus. The findings for the *A.affricanus* and *H.habilis* pedal assemblages does not support Morton’s synthesis, in that both taxa had lost the ability to oppose the hallux, and had, to varying degrees, arched longitudinal columns. However, the finding for the *A.afarensis* material is a little more similar to Morton’s model. This study suggests that *A.afarensis* did not have longitudinal arching, and other studies have suggested that *A.afarensis* had a degree of hallux abduction intermediate to *Homo sapiens* and the African great apes (Latimer & Lovejoy, 1982; Stern & Susman, 1983; Deloison, 1991; Stern & Susman, 1991; Susman & Stern, 1991; Berillon, 1998; Berillon, 1999, 2000; Sarmiento, 2000). However, Morton’s (1936) study does not speculate on the morphology of the prehuman foot’s talar trochlea would have been like, which is important when considering the crucial human-like flat trochlea of the *A.afarensis* foot, as shown by this study and others (Latimer *et al.*, 1987).

Lewis’s model (1980a, 1980b, 1989) suggested remodelling of the foot along its subtalar and longitudinal axes. He suggested that the hallux stayed in a “close-packed” abducted position, and that the forefoot realigned towards it until all the metatarsals were in line with each other. However, as discussed in Chapter 1, these axes are difficult to determine and define when using 3D data, and, furthermore, there is a problem of defining the movement of one axis relative to another in terms of which axis is used as the reference axis. There is an assumption that the reference

axis does not move, and this may not be the case. Lewis also postulated in the same work, that ancestral taxa in the Plio-Pleistocene (as represented by OH 8) would have retained some degree of hallux abduction. This is not supported by this study in terms of *H.habilis* and *A.africanus*, which both are shown to have lost the ability to oppose the hallux.

Kidd's (1996, 1999) model states that the lateral side of the hominin foot evolved first, and that this was followed by the medial side. This is based solely on Kidd's interpretation of the OH 8 foot, since Kidd concluded that the OH 8 calcaneocuboid joint (and therefore the lateral longitudinal column) was very human-like, but that the talo-navicular complex (and therefore the medial longitudinal column) was a combination of ape-like and unique in its morphology. This suggestion is not supported by this study, since in the case of OH 8, it is found that there are specialised human-like features on both the lateral (calcaneocuboid joint) and medial (unopposable hallux) sides. Furthermore, the human-like features of the medial columns of *A.africanus* (loss of hallux abduction and wider lateral navicular) and *A.afarensis* (flat, even trochlea) indicate that the criteria for Kidd's model is not displayed in either of those taxa as well.

To summarise, none of the major models of hominin foot evolution proposed can be considered to be wholly correct in the light of the findings of this study. One of the principal differences in this study is that it incorporates the pedal remains of *A.africanus*, *A.afarensis* and *H.habilis*. Morton's (1936) analysis was carried out before the discovery of fossil pedal remains, and he had to base his hypotheses solely on the comparative anatomy of modern extant taxa. More recent studies have concentrated on just the OH 8 foot (Lewis, 1980b, 1989; Kidd, 1996, 1999) or OH 8 and the Hadar remains (Berillon, 1997, 1998, 1999, 2000). There is also a more fundamental problem with these models, and that is the underlying assumption of a single ancestral lineage leading to the modern human form. The findings of this study suggest, from a locomotor point of view, something more complex. This is discussed in the next section.

How do these findings relate to the origins of bipedalism?

As discussed at the start of Chapter 5, there are numerous debates over the origins of bipedalism. This is hardly surprising since it is a unique form of locomotion within all extant primates, and is one of the core functional specialities of modern humans. Much of the discussion has been over the mode of locomotion that preceded bipedalism, or, over how bipedal or not certain taxa were. As with those theories on the evolution of the hominin foot, little attention has been paid to the possibility that different taxa may have developed functionally *different* forms of bipedalism.

This study shows that the feet of *A.afarensis*, *A.africanus* and *H.habilis* all show a mosaic of human-like and ape-like morphologies in the tarsal region. However, the feet of these taxa were mosaic in distinctly different ways, and thus indicate different ways of adapting to bipedalism. The *A.africanus* and *H.habilis* material both share a synapomorphy with *Homo sapiens* in having lost the morphological correlates of hallux opposability. Conversely, they both display a character that is possibly symplesiomorphic with the great apes, in having a sloping trochlea. However, there are distinct differences between these two taxa as well, and, comparatively, *H.habilis* has a more human-like navicular and a very human-like calcaneocuboid joint. Clarke (pers.comm) has suggested that a partial calcaneal fragment belonging to Stw 573 indicates a strongly mobile and ape-like calcaneo-cuboid joint in its owner, but until this analysis is published, this can not be confirmed. As discussed earlier, it is likely that *H.habilis* had more marked longitudinal arching of the foot than did *A.africanus*, but that *A.africanus* had a moderate degree of arching nonetheless. It certainly appears, based on shared characteristics in the talus, medial cuneiforms and naviculars that fall within extant intraspecific ranges of variation, that the *H.habilis* foot is essentially a slightly more human-like “version” of the *A.africanus* foot. This suggests that the two taxa may be closely linked functionally and possibly also phylogenetically.

The *A.afarensis* material shows a markedly different pattern. The talus falls within the modern human range of variation, and has the flat, even trochlea that possibly indicates a more human-like and efficient transmission of force from the leg to the foot (Latimer *et al.*, 1987). However, the *A.afarensis* navicular is a combination of

highly ape-like and unique in its morphology, and strongly suggests the absence of a medial longitudinal arch (Elftman & Manter, 1935a; Sarmiento, 2000) and considerable weight bearing by that bone. Furthermore, as discussed above, the hallux of *A.afarensis* is likely to have retained a degree of opposability, on account of the curved hallucial facet on the medial cuneiform (Berillon, 1998; Berillon, 1999, 2000; Sarmiento, 2000). *A.afarensis*, therefore, possibly shares a synapomorphic feature of the foot with modern humans, but it is different to that shared with humans by *H.habilis* and *A.africanus*. Conversely, *A.afarensis* may share symplesiomorphic features with the great apes that are different to the ones possibly shared with them by *H.habilis* and *A.africanus*.

In summary, based on the morphology and associated function of their foot bones, although *A.afarensis*, *A.africanus* and *H.habilis* all display anatomical adaptations consistent with strong bipedal elements to their locomotor repertoire, none of them were likely to have been bipedal in the way that *Homo sapiens* is, and all of them are likely to have retained an arboreal component to their locomotor repertoire. However, this study also suggests that the feet of these taxa were functionally different to each other, and that two distinct trends may well be evident in the hominin fossil record.

The geological evidence support this assertion. *H.habilis* is geologically much younger (by 1.4 million years) than the *A.afarensis* specimens (Hay, 1971; Walter, 1994), and although having a number of derived human-like features, has a far more primitive and ape-like talus. Whilst not commenting directly on phylogeny, the findings of this study infer that it is unlikely that *H.habilis* is a descendant species of *A.afarensis* based on pedal morphology. The *A.africanus* specimens being considered here (Stw 573) are of a similar age to the *A.afarensis* material (Partridge *et al.*, 1999), and yet, as discussed above, show a different combination of primitive and derived morphologies. This suggests that *A.afarensis* and *A.africanus* were distinct taxa that were adapting to the selection pressure for increased bipedalism in different ways.

The main finding of this thesis is supported by one recent study (Hausler, 2001), which compared limb proportions, and the sacral, pelvic and vertebral morphology of the *A.afarensis* skeleton Al-288, and the undescribed *A.africanus* skeleton Stw 431. Hausler (2001) concluded that the skeletons of both taxa exhibited a mosaic of

adaptations to bipedal locomotion and arboreal climbing, but that the combination of traits was different for each taxa, suggestion at least two distinct adaptations to increased bipedal locomotion in late Pliocene hominins.

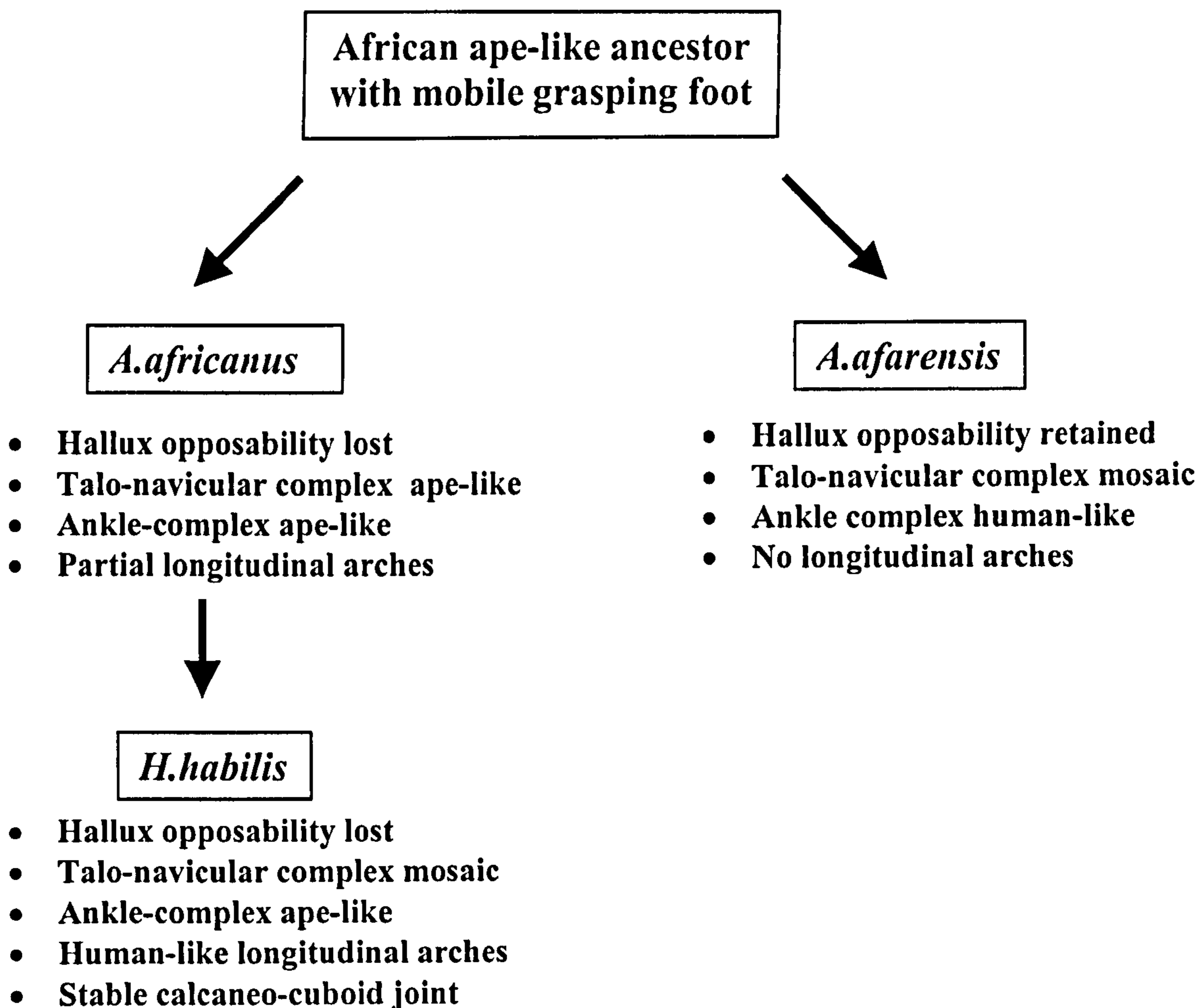


Figure 6.2 Schematic suggesting possible trends in the fossil hominin record based on the findings of this study

Figure 6.2 summarises the findings of this study, and a possible trend in the hominin fossil record that they point to. Based on this, the overall implications for the origins of bipedalism, then, are that it is likely that different hominin taxa existed in the mid to late Pliocene and early Pleistocene with different functional adaptations to the bipedal component of their locomotor repertoire. This strongly correlates with a large number of recent fossil discoveries throughout Africa. Recent discoveries of taxa such as *Kenyanthropus platyops*, *Sahelanthropus tchadensis*, *Orrorin tugenensis* and

Ardipithecus ramidus kadabba, suggest a far wider degree of taxonomic diversity in the African fossil hominin record than had previously been thought (Haile-Selassie, 2001; Leakey *et al.*, 2001; Senut *et al.*, 2001; Brunet *et al.*, 2002; Wood, 2002). At present, the evidence for this diversity is almost exclusively supported by craniodental remains. If such diversity existed, then it is reasonable to assume that there was considerable postcranial diversity as well, and thus at least a degree of diversity in terms of locomotor patterns and repertoire.

This study indicates that in the late Pliocene, there were at least two distinct ways in which the tarsals of different hominin taxa had adapted to bipedal locomotion. This implies that there was more locomotor diversity in the fossil record than has been suggested, and raises questions over whether there was a single origin for bipedalism or not. At the very least, if bipedalism was selected for only once in the hominin radiation, the evidence of this thesis suggests that there were at least two distinct evolutionary pathways responding to that selection pressure.

Appendix

The following graphs are relevant to the results section on centroid size in Chapter 4, Section 4.4.1. They show, for each tarsal in turn, centroid size plotted against those principal component axes that were responsible for separating any or all of the measured taxa.

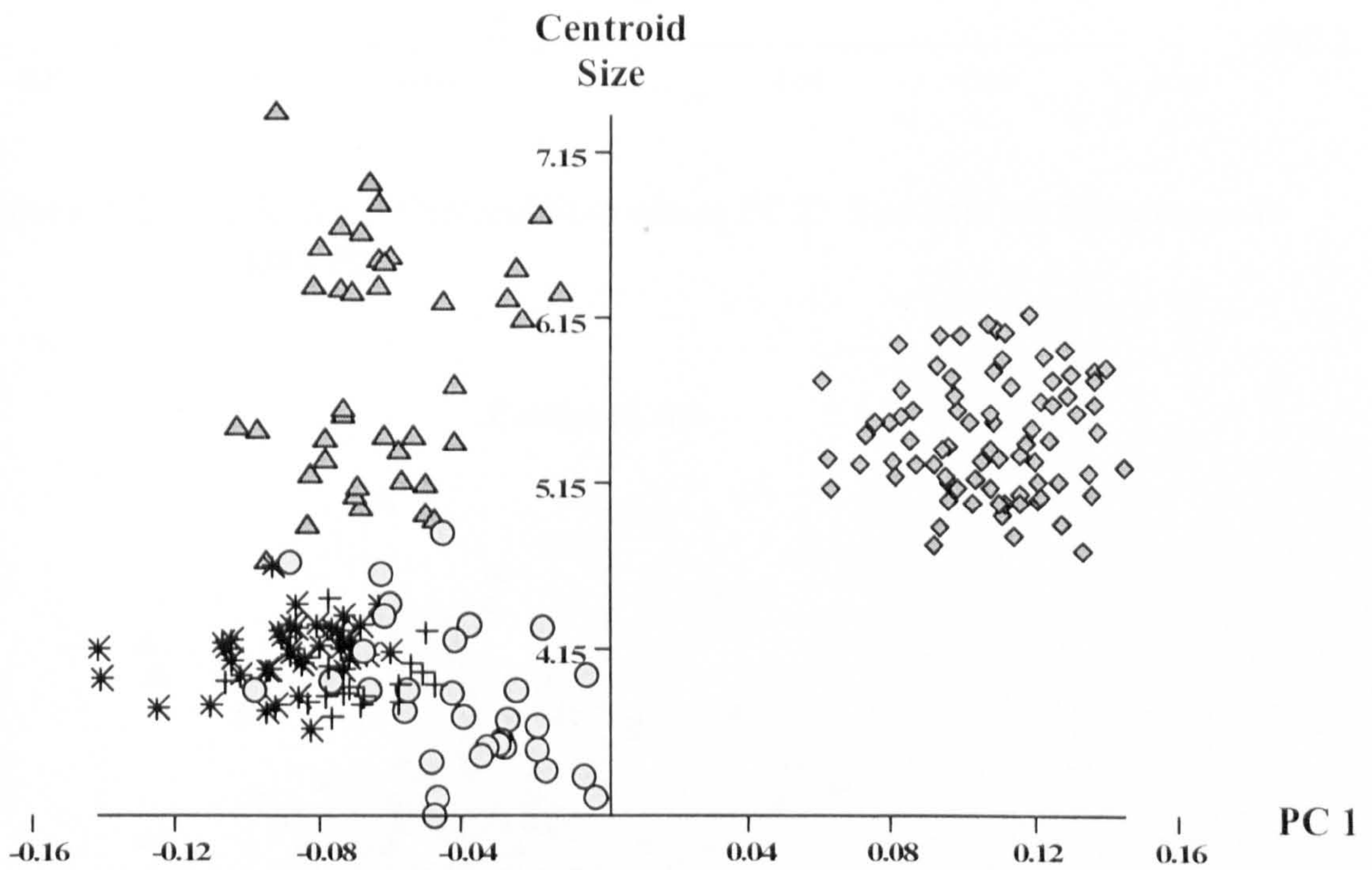


Figure A.1 Calcaneus: Centroid Size versus PC 1. Diamonds: *Homo sapiens*. Stars: *Pan troglodytes*. Crosses: *Pan paniscus*. Triangles: *Gorilla gorilla*. Circles: *Pongo pygmaeus*.

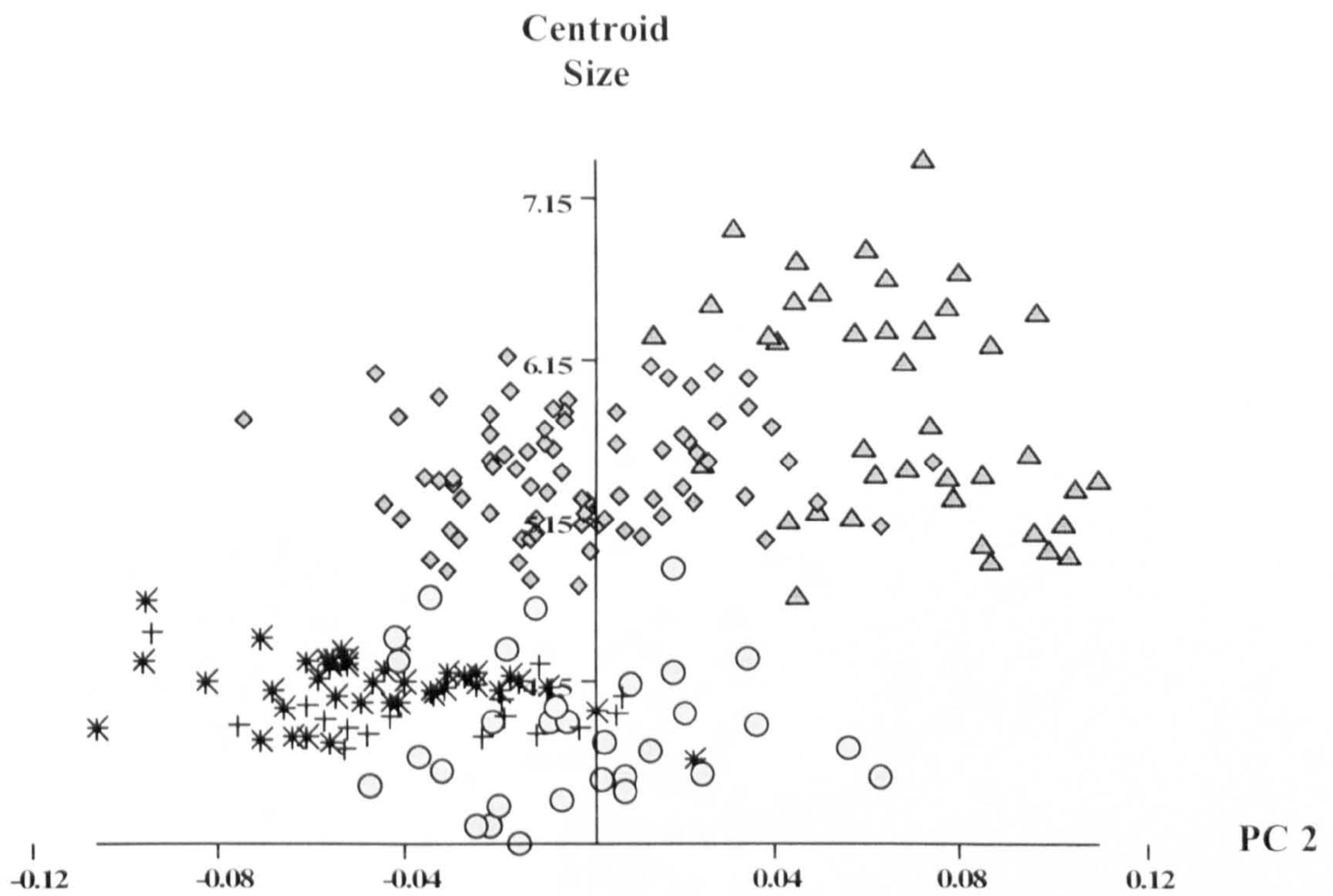


Figure A.2 Calcaneus: Centroid Size versus PC 2. Symbols are the same as in Figure A.1

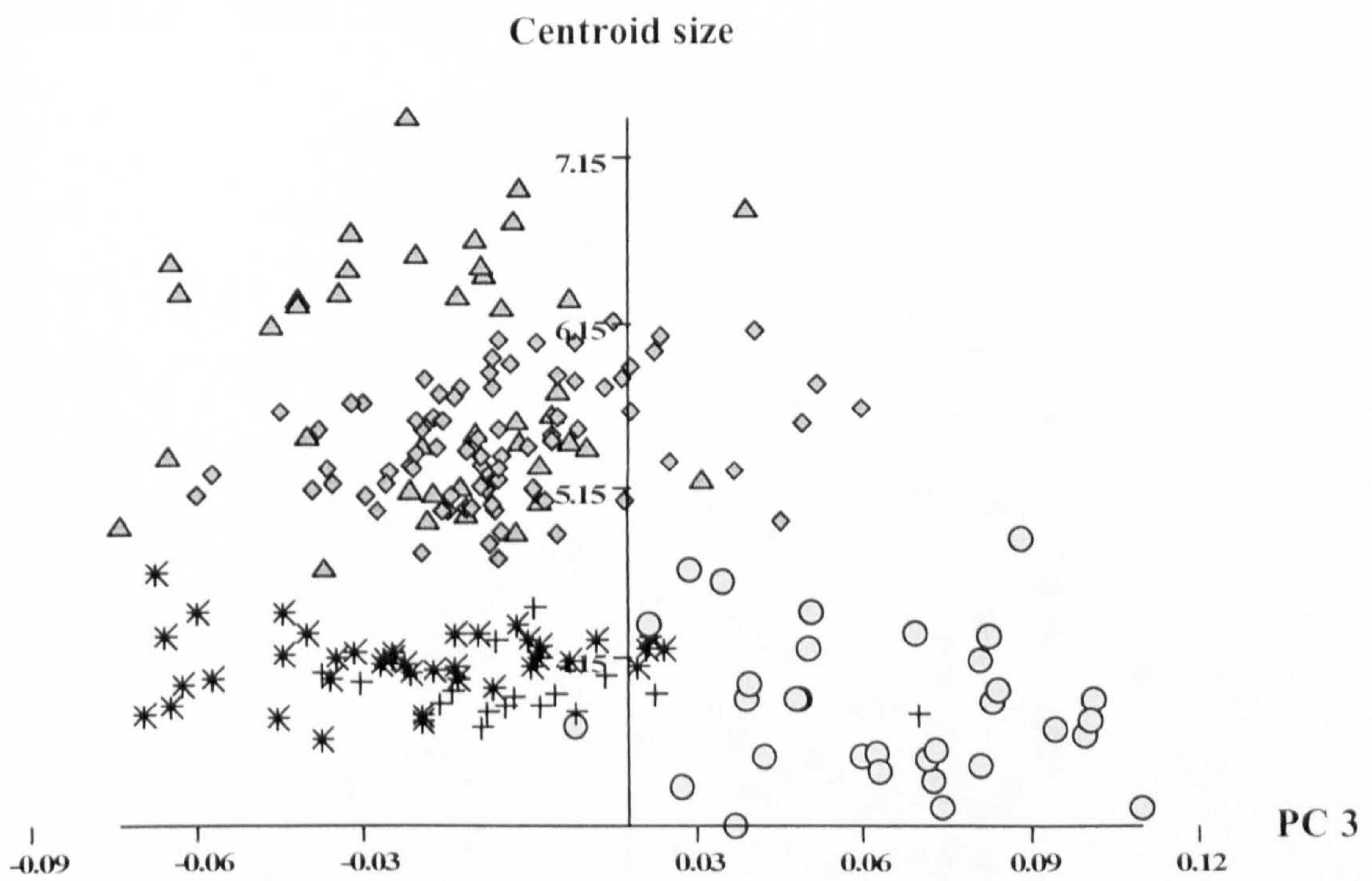


Figure A.3 Calcaneus: Centroid size versus PC 3

Talus

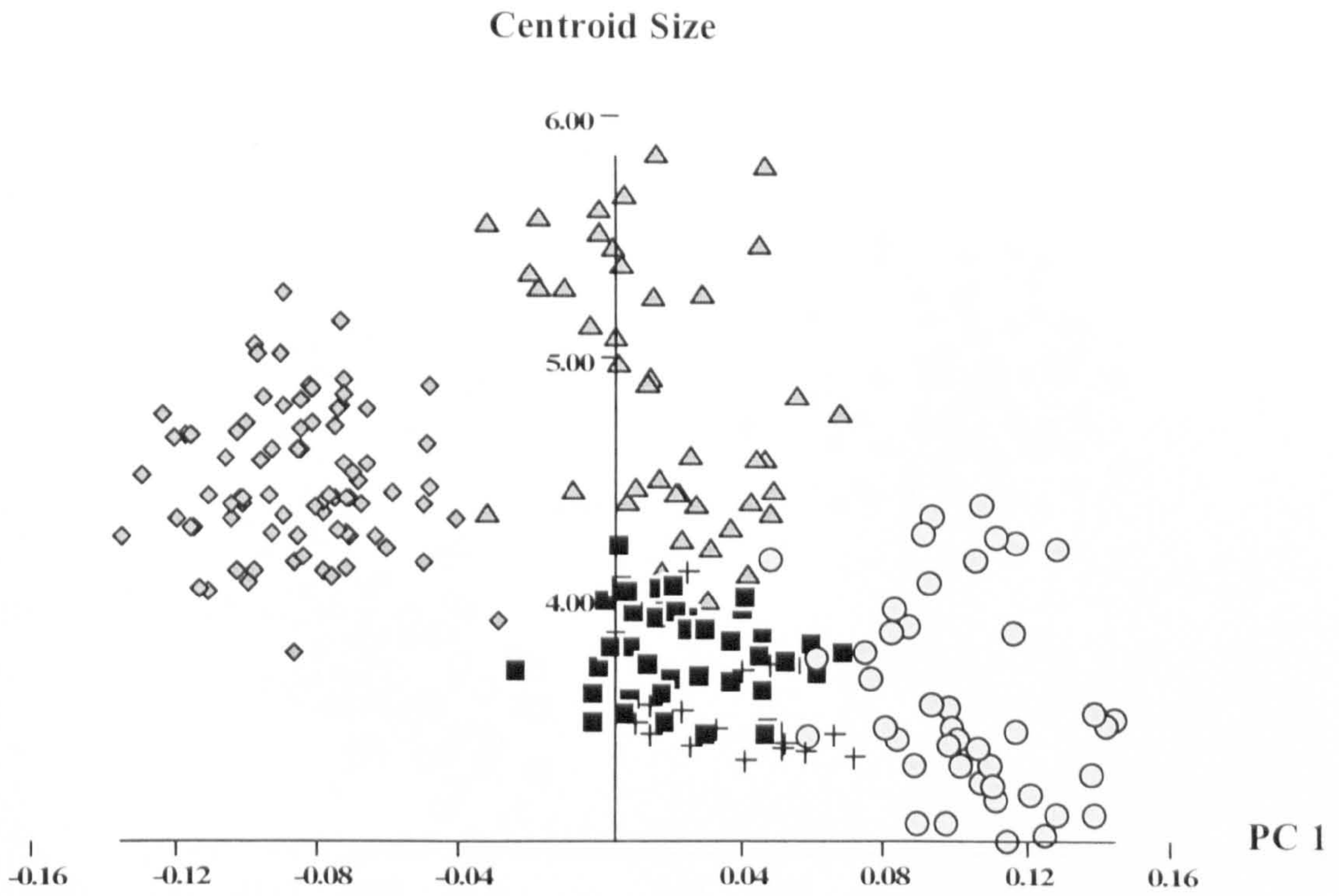


Figure A.4 Talus: Centroid size versus PC 1.

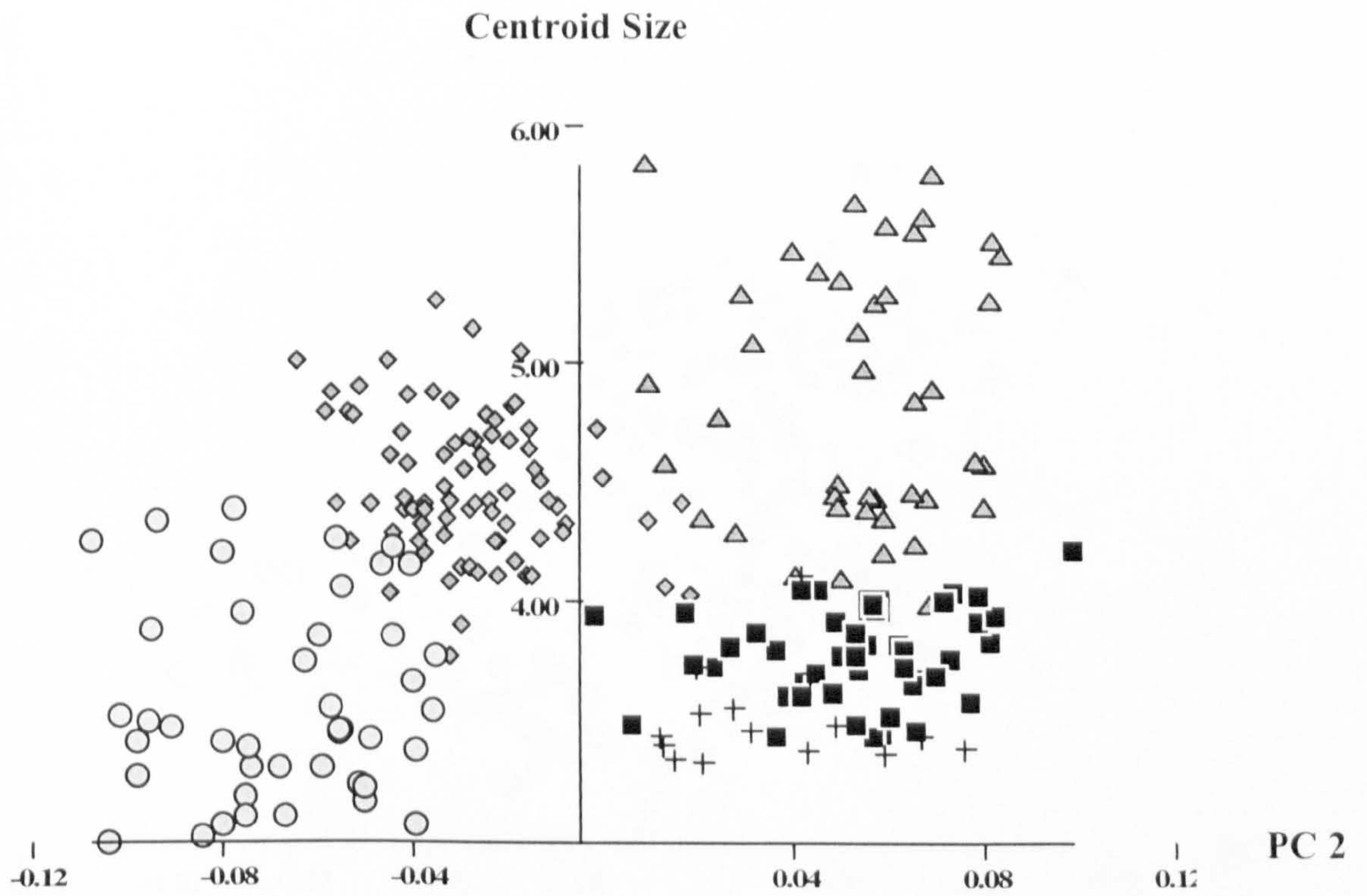


Figure A.5 Talus: Centroid size versus PC 2.

Cuboid

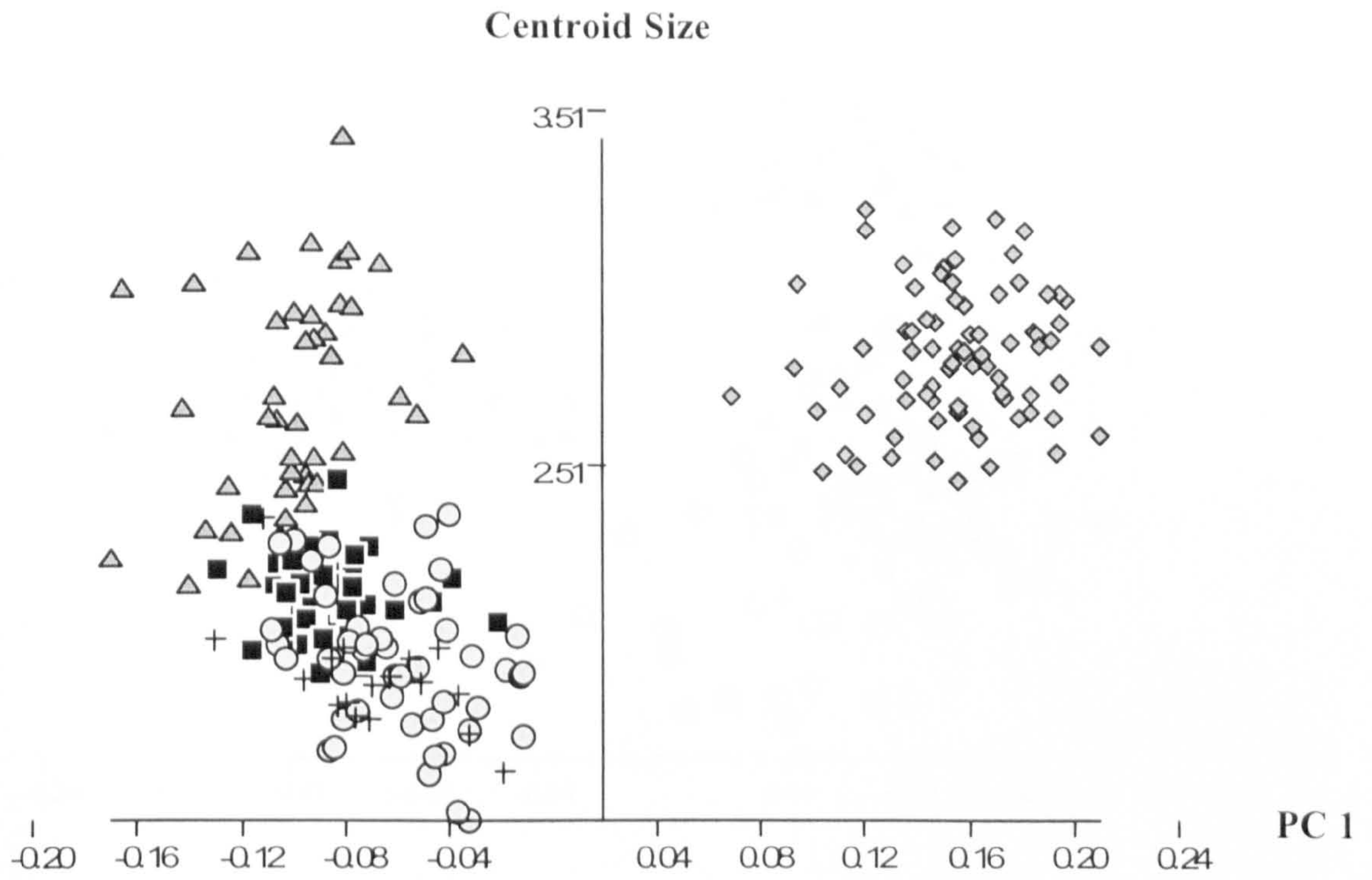


Figure A.6 Cuboid: Centroid Size versus PC 1.

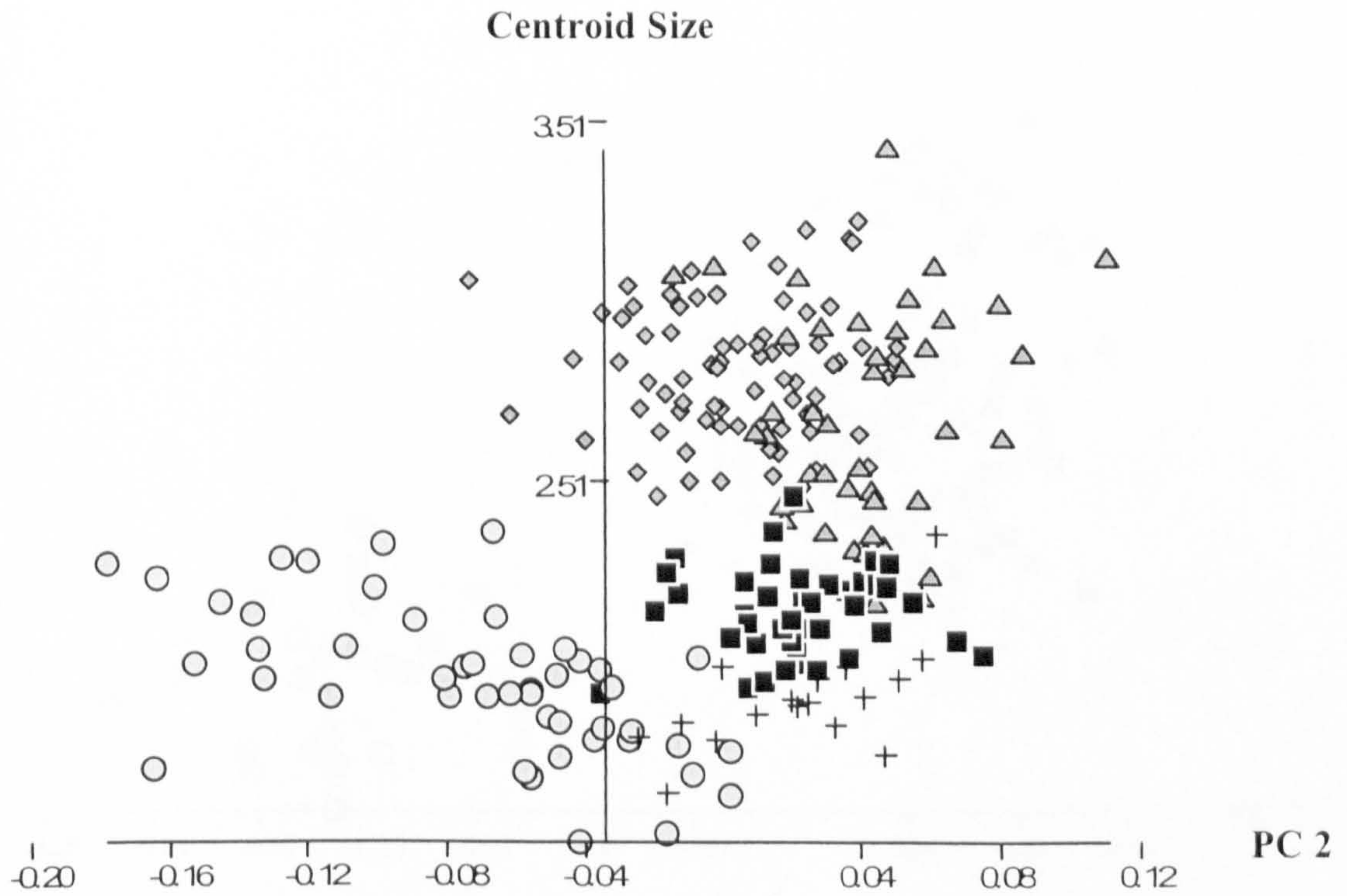


Figure A.7 Cuboid: Centroid Size versus PC 2.

Navicular

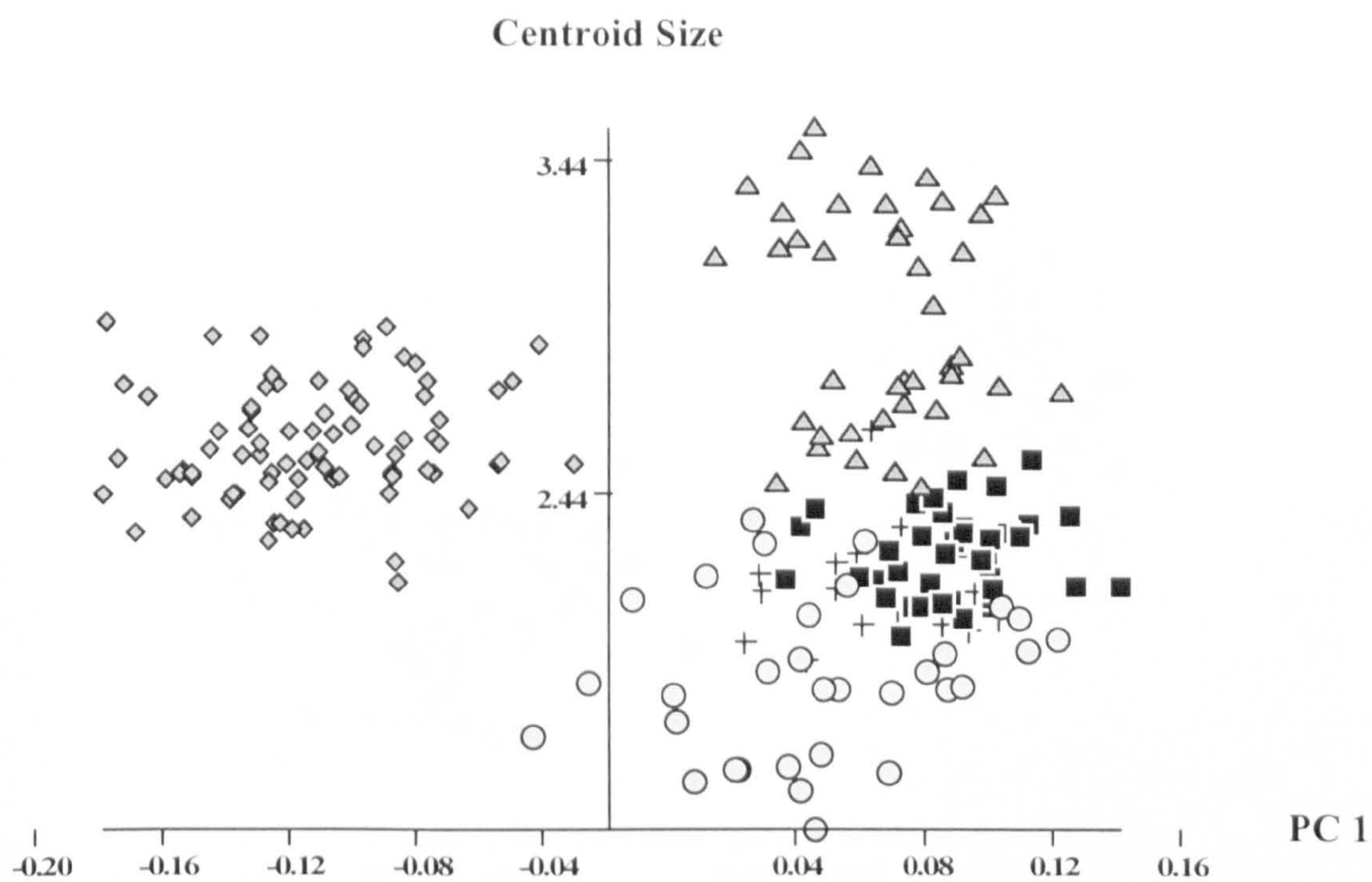


Figure A.8 Navicular: Centroid size versus PC 1.

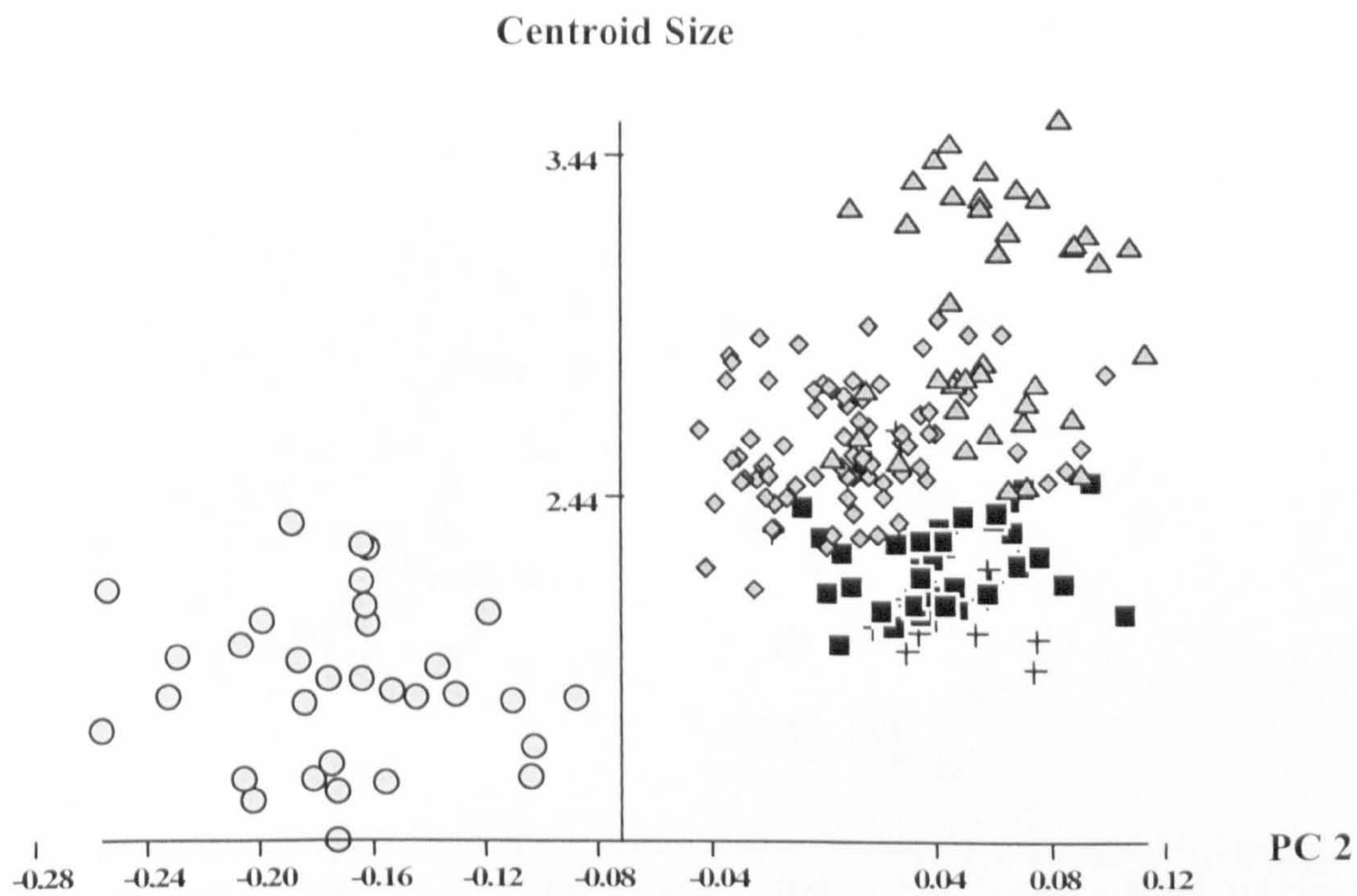


Figure A.9 Navicular: Centroid size versus PC 2.

Medial Cuneiform

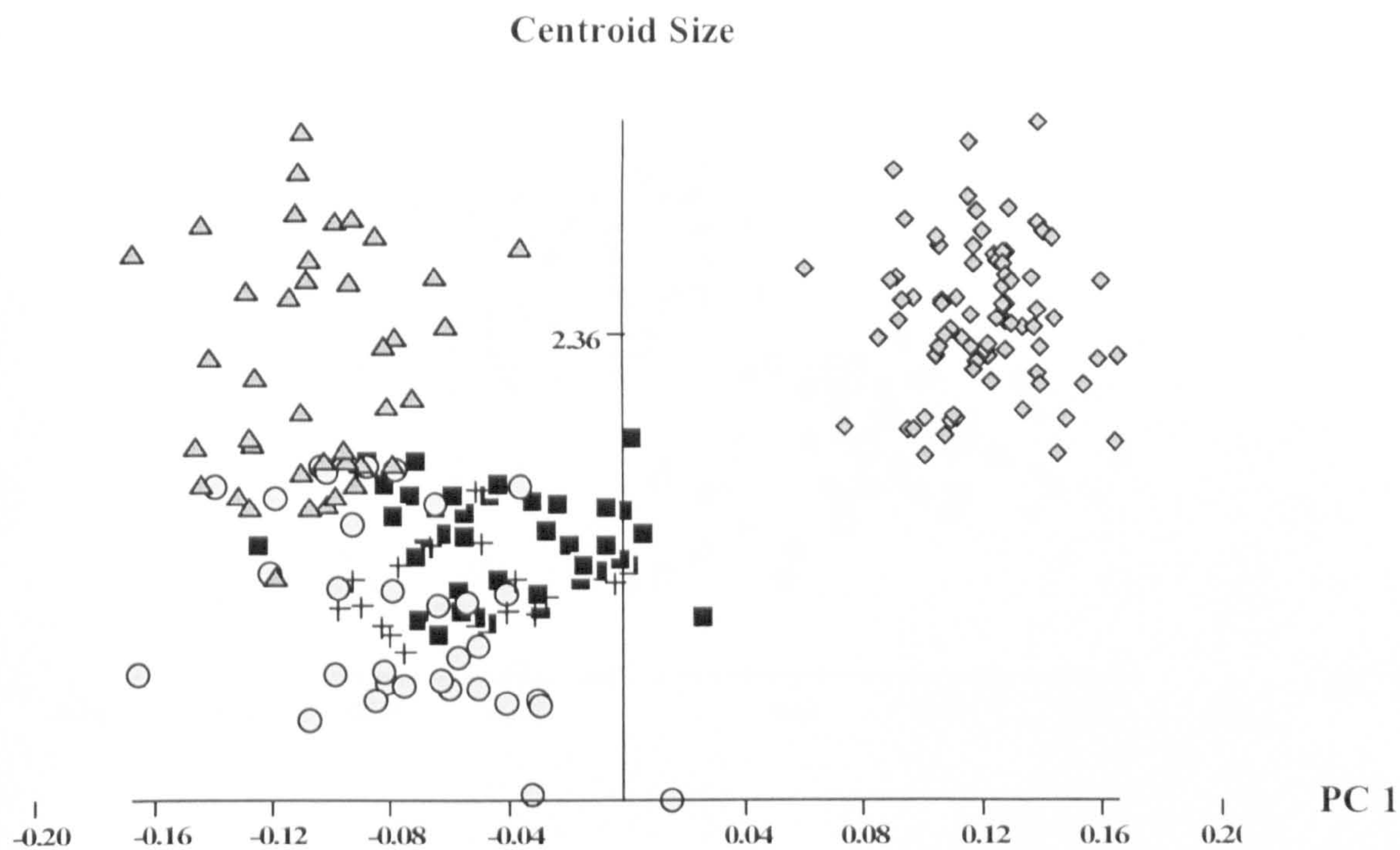


Figure A.10 Medial Cuneiform: Centroid size versus PC 1.

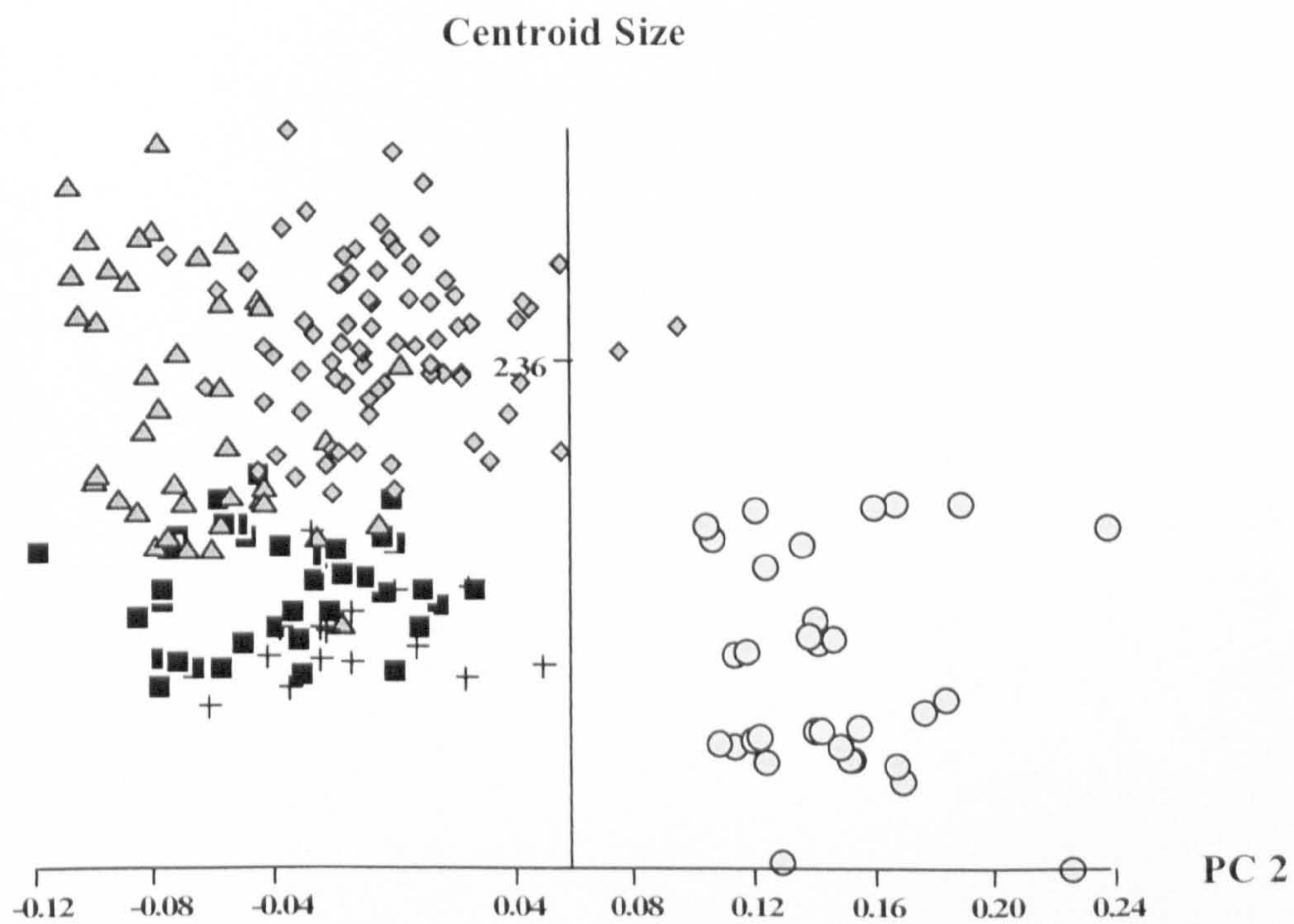


Figure A.11 Medial Cuneiform: Centroid Size versus PC 2

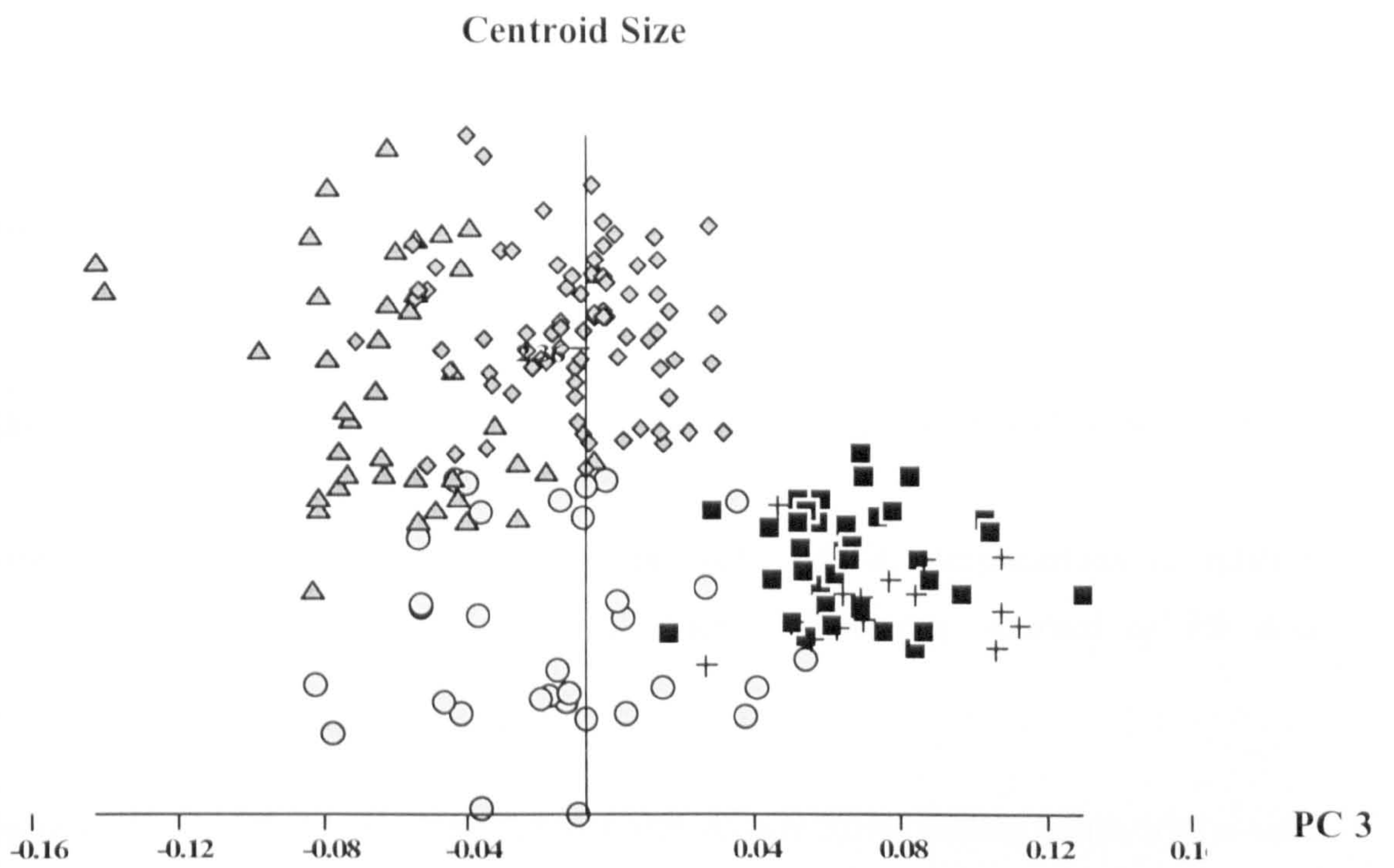


Figure A.12 Medial Cuneiform: Centroid Size versus PC3.

Bibliography

- Aiello, L.C. & Dean, M.C. (1990). *An Introduction to Human Evolutionary Anatomy*. London, Academic Press.
- Aquino, A. & Payne, C. (1999). Function of the plantar fascia. *The Foot*, 9; 73-78.
- Archibald, J.D., Lovejoy, C.O. & Heilpe, K.G. (1972). Implications of relative robusticity in the Olduvai metatarsus. *American Journal of Physical Anthropology*, 37; 93-96.
- Berillon, G. (1997). Quantifying the foot architecture from isolated bones with a view to study fossil hominid foot. Comparative study of the *Homo* and *Pan* calcaneal skeleton. *Biométrie Humaine et Anthropologie*, 15(1-2); 99-106.
- Berillon, G. (1998). Analyse architecturale du pied de Homo, Pan et Gorilla. Application a l'etude des restes isoles d'hominoïdes miocenes et d'hominides fossiles. PhD Thesis, Museum National d'Histoire Naturelle, Paris.
- Berillon, G. (1999). Geometric pattern of the hominoid hallucal tarsometatarsal complex. Quantifying the degree of hallux abduction in early hominids. *Palaeontology*, 328; 627 - 633.
- Berillon, G. (2000). *Le pied des hominoïdes Miocènes et des hominidés fossiles. Architecture, locomotion, évolution*. Paris, CNRS Editions.
- Bojsen-Møller, F. (1979). Calcaneocuboid joint and stability of the longitudinal arch of the foot at high and low gear push off. *Journal of Anatomy London*, 129(1); 165-176.
- Bojsen-Møller, F. & Flagstad, K.E. (1976). Plantar aponeurosis and internal architecture of the ball of the foot. *Journal of Anatomy*, 121(3); 599-611.

- Bookstein, F.L. (1984). A statistical method for biological shape comparisons. *Journal of Theoretical Biology*, 107; 475-520.
- Bookstein, F.L. (1989). Principal warps: thin-plate splines and the decomposition of deformations. *IEEE Transactions in Pattern Analysis and Machine Intelligence*, 11; 567-585.
- Bookstein, F.L. (1991). *Morphometric Tools for Landmark Data: Geometry and Biology* Cambridge, Cambridge University Press.
- Boyer, E.L. (1935). The musculature of the inferior extremity of the orang-utan *Simia satyrus*. *The American Journal of Anatomy*, 56(2); 193-255.
- Broom, R. & Schepers, G.W.H. (1946). *The South African fossil ape-men: the Australopithecinae* Pretoria, Transvaal Museum.
- Brunet, M., Guy, F., Pilbeam, D., Mackaye, H.T., Likius, A., Ahounta, D., Beauvilain, A., Blondel, C., Bocherens, H., Boisserie, J.-R., De Bonis, L., Coppens, Y., Dejax, J., Denys, C., Douring, P., Elsenmann, V., Fanone, G., Fronty, P., Geraads, D., Lehmann, T., Lihoreau, F., Louchart, A., Mahamat, A., Merceron, G., Mochelin, G., Otero, O., Palaez Campomanes, P., Ponce De Leon, M., Rage, J.-C., Sapanet, M., Schuster, M., Sudre, J., Tassy, P., Valentin, X., Vignaud, P., Viriot, L., Zazzo, A. & Zollikofer, C. (2002). A new hominid from Upper Miocene of Chad, Central Africa. *Nature*, 418; 145-151.
- Cant, J.G.H. (1987). Positional behavior of female Bornean orangutans *Pongo pygmaeus*. *American Journal of Primatology*, 12; 71-90.
- Chaplin, G., Jablonski, N.G. & Cable, N.T. (1994). Physiology, thermoregulation and bipedalism. *Journal of Human Evolution*, 27; 497-510.

- Clarke, R.J. (1998). First ever discovery of a well-preserved skull and associated skeleton of *Australopithecus*. *South African Journal of Science*, 94(10); 460-463.
- Clarke, R.J. (1999). Discovery of complete arm and hand of the 3.3 million-year-old *Australopithecus* skeleton from Sterkfontein. *South African Journal of Science*, 95(November/December); 477-480.
- Clarke, R.J. & Tobias, P.V. (1995). Sterkfontein member 2 foot bones of the oldest South African hominid. *Science*, 269; 521-524.
- Cobb, S.N.F. (2001). Form variation in the postnatal facial skeleton of the African apes. PhD Thesis, University College London, London.
- Collard, M. & Wood, B.A. (2000). How reliable are human phylogenetic hypotheses? *Proceedings of the National Academy of Sciences*, 97; 5003-5006.
- Czerniecki, J.M. (1988). Foot and ankle biomechanics in walking and running. *American Journal of Physical Medicine and Rehabilitation*, 67(6); 246-252.
- Dainton, M. (2001). Did our ancestors knuckle-walk? *Nature*, 410; 325-326.
- Day, M.H. (1988). *Guide to fossil man* (4th). Chicago, University of Chicago Press.
- Day, M.H. & Napier, J.R. (1964). Fossil foot bones. *Nature*, 201; 969-970.
- Day, M.H. & Wood, B.A. (1968). Functional affinities of the Olduvai Hominid 8 talus. *Man*, 3; 440-455.
- de Waal, F.B.M. (1997). *Bonobo: The Forgotten Ape* Berkeley, University of California Press.

- Deloison, Y., Ed. (1985). *Comparative study of calcanei of primates on Pan-Australopithecus-Homo relationship*. Hominoid evolution: past, present, future. New York, Alan R. Liss.
- Deloison, Y. (1991). Les australopitheques marchaient - ils comme nous? In: *Origine(s) de la bipédie chez les hominidiés*. Y. Coppens and B. Senut. Paris, Editions du CNRS.
- Doran, D. & Hunt, K.D. (1995). Comparative locomotor behavior of chimpanzees and bonobos: species and habitat differences. In: *Chimpanzee Cultures*. R. W. Wrangham, W. C. McGrew, F. de Waal and P. G. Heltne. Cambridge, MS., Harvard University Press: 93-108.
- Doran, D.M. (1992). The ontogeny of chimpanzee and pygmy chimpanzee locomotor behavior: a case study of pedomorphism and its behavioral correlates. *Journal of Human Evolution*, 23; 139-157.
- Doran, D.M. (1997). Ontogeny of locomotion in mountain gorillas and chimpanzees. *Journal of Human Evolution*, 32; 323-344.
- Dryden, I.L. & Mardia, K.V. (1998). *Statistical Shape Analysis* Chichester, John Wiley & Sons.
- Duncan, A.S., Kappelman, J. & Shapiro, L.J. (1994). Metatarsophalangeal joint function and positional behaviour in *Australopithecus afarensis*. *American Journal of Physical Anthropology*, 93; 67-81.
- Dykyj, D., Ateshian, G.A., Trepal, M.J. & MacDonald, L.R. (2001). Articular geometry of the medial tarsometatarsal joint of the foot: comparison of Metatarsus Primus Adductus and Metatarsus Primus Rectus. *Journal of Foot and Ankle Surgery*, 40(6); 357-365.
- Elftman, H. (1960). The transverse tarsal joint and its control. *Clinical Orthopaedics*, 16; 41-45.

- Elftman, H. & Manter, J. (1935a). Chimpanzee and human feet in bipedal walking. *American Journal of Physical Anthropology*, **20**; 69-79.
- Elftman, H. & Manter, J. (1935b). The evolution of the human foot, with especial reference to the joints. *Journal of Anatomy*, **70**; 56-67.
- Felsenstein, J. (1973). Maximum-Likelihood estimation of evolutionary trees from continuous characters. *American Journal of Human Genetics*, **25**; 471-492.
- Fenart, R. & Deblock, R. (1973). *Pan paniscus* et *Pan troglodytes* Crâniométrie. Etude Comparative et Ontogénique selon les méthodes classiques et vestibulaire. *Annales du Musée Royal de l'Afrique Centrale, Tervuren, Belgique, Serie en 8(Tome 1^o)*; 1-593.
- Gagneux, P. & Varki, A. (2000). Genetic differences between humans and great apes. *Molecular Phylogenetics and Evolution*, **18**(1); 2-13.
- Galdikas, B.M.F. & Teleki, G. (1981). Variations in subsistence activities of female and male pongids: new perspectives on the origins of hominid labor division. *Current Anthropology*, **22**(3); 241-256.
- Gebo, D.L. (1992). Plantigrady and foot adaptation in African apes: implications for hominid origins. *American Journal of Physical Anthropology*, **89**; 29-58.
- Gomberg, D.N. & Latimer, B. (1984). Observations on the transverse tarsal joint of *A. afarensis*, and some comments on the interpretation of behaviour from morphology. *American Journal of Physical Anthropology (Suppl)*, **63**(2); 164.
- Gonder, M.K., Oates, J.F., Disotell, T.R., Forstner, M.R., Morales, J. & Melnick, D.J. (1997). A new west African chimpanzee subspecies? *Nature*, **388**; 337.

- Goodall, C.R. (1991). Procrustes methods and statistical analysis of shape (with discussion). *Journal of the Royal Statistical Society Series B*, **56**; 285-299.
- Gower, J.C. (1975). Generalised Procrustes analysis. *Psychometrika*, **40**; 33-50.
- Groves, C.P. (1970). Population systematics of the gorilla. *Journal of Zoology (Lond.)*, **161**; 287-300.
- Groves, C.P. (1971). Distribution and place of origin of the gorilla. *Man*, **6**; 44-51.
- Haile-Selassie, Y. (2001). Late Miocene hominids from the Middle Awash, Ethiopia. *Nature*, **412**; 178-181.
- Harcourt-Smith, W.E.H. (1997). One Foot in the Past: an Investigation into the degree of hallux abduction of the OH 8 foot. MSc Thesis, University College London, London.
- Harcourt-Smith, W.E.H. & Aiello, L.C. (1999). An investigation into the degree of hallux abduction of the OH 8 foot. *American Journal of Physical Anthropology*, **Supplement 28**; 145.
- Harcourt-Smith, W.E.H., O'Higgins, P. & Aiello, L.C. (2002). 3D morphometrics and the evolution of bipedality. *American Journal of Physical Anthropology*, **Supplement 36**; 109.
- Hartwig-Scherer, S. & Martin, R.D. (1991). Was 'Lucy' more human than the 'child'? Observations on early hominid postcranial skeletons. *Journal of Human Evolution*, **21**; 439-449.
- Hausler, M.F. (2001). Locomotion of *Australopithecus africanus*: implications of the partial skeleton of Stw 431 (Sterkfontein, South Africa). PhD Thesis, University of Zurich, Zurich.

- Hay, R.L. (1971). Geologic Backround of Beds I and II. In: *Olduvai Gorge, Volume 3*. M.D.Leakey. Cambridge, Cambridge University Press.
- Hayafune, N., Hayafune, Y. & Jacob, H.A.C. (1999). Pressure and force distribution characteristics under the normal foot during the push-off phase in gait. *The Foot*, 9; 88-92.
- Helal, B. & Wilson, D. (1988). *The Foot* Edinburgh, Churchill Livingstone.
- Henderson, A. & Wood, B.A. (1977). The functional anatomy of the Olduvai OH 8 foot. *Journal of Anatomy London*, 124; 252.
- Hill, W.C.O. (1969). The nomenclature, taxonomy and distribution of chimpanzees. In: *The Chimpanzee: A Series of Volumes on the Chimpanzee*. G. H. Bourne. Basel, Karger. 1.
- Hunt, K.D. (1993). Sex differences in chimpanzee foraging strategies: implications for the australopithecine toolkit. *American Journal of Physical Anthropology*, Supplement 16; 112.
- Hunt, K.D. (1994). The evolution of human bipedality: ecology and functional morphology. *Journal of Human Evolution*, 26(3); 183-203.
- Hutton, W.C. & Stokes, I.A.F. (1991). The mechanics of the foot. In: *The foot and its disorders*. L. Klenerman. Oxford, Blackwell Scientific Publications: 11-25.
- Huxely, T.H. (1863). *Mans Place in Nature*. London, Macmillan.
- Jenkins, P.D. (1990). *Catalogue of Primates in the British Museum (Natural History) and Elsewhere in the British Isles, Part V: The Apes, Superfamily Hominoidea* London, Natural History Museum Publications.

- Johanson, D.C., Masao, F.T., Eck, G.G., White, T.D., Walter, R.C., Kimbel, W.H., Asfaw, B., Manega, P., Nolessokia, P. & Suwa, G. (1987). New partial skeleton of *Homo habilis* from Olduvai Gorge, Tanzania. *Nature*, **327**; 205-209.
- Keith, A. (1928). The history of the human foot and its bearing on orthopaedic practice. *Journal of Bone and Joint Surgery*, **11**; 10-32.
- Kendall, D.G. (1984). Shape manifolds, Procrustean metrics and complex projective spaces. *Bulletin of the London Mathematical Society*, **16**; 81-121.
- Kidd, R.S. (1995). An investigation into patterns of morphological variation in the proximal tarsus of selected human groups, apes and fossils: a morphometric analysis. PhD Dissertation, The University of Western Australia, Perth.
- Kidd, R.S. (1999). Evolution of the rearfoot. A model of adaptation with evidence from the fossil record. *Journal of the American Podiatric Medical Association*, **89**(1); 2-17.
- Kidd, R.S., O'Higgins, P.O. & Oxnard, C.E. (1996). The OH8 foot: a reappraisal of the hindfoot utilizing a multivariate analysis. *Journal of Human Evolution*, **31**; 269-291.
- Kidd, R.S. & Oxnard, C.E. (2002). Patterns of morphological discrimination in selected human tarsal elements. *American Journal of Physical Anthropology*, **117**(2); 169-182.
- Kinnear, P.R. & Gray, C.D. (1995). *SPSS for Windows made simple* Hove, U.K., Erlbaum UK Taylor & Francis.
- Laitman, J.T. & Jaffe, W.L. (1982). A review of current concepts on the evolution of the human foot. *Foot & Ankle*, **2**(5); 284-290.

- Langdon, J.H., Bruckner, J. & Baker, H.H. (1991). Pedal mechanics and bipedalism in early hominids. In: *Origine(s) de la bipédie chez les hominidés*. Y. Coppens and B. Senut. Paris, Editions du CNRS.
- Latimer, B. & Lovejoy, C.O. (1982). Hominid tarsal, metatarsal, and phalangeal bones recovered from the Hadar formation: 1974-1977 collections. *American Journal of Physical Anthropology*, **57**; 701-719.
- Latimer, B. & Lovejoy, C.O. (1989). The calcaneus of *Australopithecus afarensis* and its implications for the evolution of bipedality. *American Journal of Physical Anthropology*, **78**; 369-386.
- Latimer, B. & Lovejoy, C.O. (1990a). Hallucial tarsometatarsal joint in *Australopithecus afarensis*. *American Journal of Physical Anthropology*, **82**; 125-133.
- Latimer, B. & Lovejoy, C.O. (1990b). Metatarsophalangeal joints of *Australopithecus afarensis*. *American Journal of Physical Anthropology*, **83**; 13-23.
- Latimer, B., Ohman, J.C. & Lovejoy, C.O. (1987). Talocrural joint in African hominoids: implications for *Australopithecus afarensis*. *American Journal of Physical Anthropology*, **74**; 155-175.
- Le Gros Clark, W.E. (1947). Observations on the anatomy of the fossil Australopithecinae. *Journal of Anatomy*, **81**; 300-333.
- Le Gros Clark, W.E. (1967). *Man-apes or ape-men? The story of discoveries in Africa*. (1st). New York, Holt, Rinehart & Winston.
- Leakey, L.S.B. (1960). Recent discoveries at Olduvai Gorge. *Nature*, **188**; 1050-1052.
- Leakey, L.S.B., Evernden, J.F. & Curtis, G.H. (1961). Age of Bed 1, Olduvai Gorge, Tanganyika. *Nature*, **191**; 478-479.

- Leakey, L.S.B., Tobias, P.V. & Napier, J.R. (1964). A new species of the genus *Homo* from Olduvai Gorge. *Nature*, **202**; 7-9.
- Leakey, M.D. & Hay, R.L. (1979). Pliocene footprints in the Laetoli Beds at Laetoli, northern Tanzania. *Nature*, **278**; 317-323.
- Leakey, M.G., Spoor, F., Brown, F.H., Gathogo, P.N., Kiare, C., Leakey, L.N. & McDougall, I. (2001). New hominin genus from Eastern Africa shows diverse middle Pliocene lineages. *Nature*, **410**(433-440).
- Leakey, R.E., Leakey, M.G. & Behrensmeyer, A.K. (1978). The hominid catalogue. In: *Koobi Fora Research Project, Volume 1: The fossil hominids and an introduction to their context, 1968-1974*. M. G. Leakey and R. E. Leakey. Oxford, Clarendon Press.
- Lele, S. (1993). Euclidian distance matrix analysis: estimation of mean form and form difference. *Mathematical Geology*, **25**; 573-602.
- Lele, S. & Richtsmeier, J.T. (1991). Euclidian distance matrix analysis: a coordinate free approach for comparing biological shapes using landmark data. *American Journal of Physical Anthropology*, **86**; 415-427.
- Lewis, O.J. (1972). The evolution of the hallucial tarsometatarsal joint in the Antropoidea. *American Journal of Physical Anthropology*, **37**; 13-34.
- Lewis, O.J. (1980a). The joints of the evolving foot. Part II. The intrinsic joints. *Journal of Anatomy*, **130**(4); 833-857.
- Lewis, O.J. (1980b). The joints of the evolving foot. Part III. The fossil evidence. *Journal of Anatomy London*, **131**(2); 275-298.
- Lewis, O.J. (1981). Functional morphology of the joints of the evolving foot. *Symposia of the Zoological Society of London*, **46**; 169-188.

- Lewis, O.J. (1989). *Functional morphology of the evolving hand and foot* Oxford, Clarendon Press.
- Lewis, P.O. (2001). A likelihood approach to estimating phylogeny from discrete morphological character data. *Systematic Biology*, 50 (6); 913-925.
- Lisowski, F.P. (1967). Angular growth changes and comparisons in the primate talus. *Folia Primatologica*, 7 (2); 81-97.
- Lisowski, F.P., Albrecht, G.H. & Oxnard, C.E. (1974). The form of the talus in some higher primates: a multivariate study. *American Journal of Physical Anthropology*, 41; 191-216.
- Lisowski, F.P., Albrecht, G.H. & Oxnard, C.E. (1976). African fossil tali: further Multivariate studies. *American Journal of Physical Anthropology*, 45; 5-18.
- Lorenzo, C., Arsuaga, J.-L. & Carretero, J.-M. (1999). Hand and foot remains from the Gran Dolina Early Pleistocene site (Sierra de Atapuerca, Spain). *Journal of Human Evolution*, 37; 501-522.
- Mann, R.A. (1988). Gait Analysis. In: *The Foot*. B. Helal and D. Wilson. Edinburgh, Churchill Livingstone. 1: 97-107.
- Mann, R.A. (1991). Overview of foot and ankle biomechanics. In: *Disorders of the foot and ankle*. M. H. Jahss. Philadelphia, W.B.Saunders Company: 385-408.
- Marcus, L.F., Corti, M., Loy, A., Naylor, G.J.P. & Slice, D., Eds. (1996). *Advances in Morphometrics*. New York, Plenum Press.
- Matsusaka, N. (1986). Control of the medial-lateral balance in walking. *Acta Orthopaedica Scandinavica*, 57(6); 555-559.

- McDonald, S.W. & Tavener, G. (1999). Pronation and supination of the foot: confused terminology. *The Foot*, 9; 6-11.
- McHenry, H. & Berger, L.R. (1998). Body proportions of *Australopithecus afarensis* and *A.africanus* and the origin of the genus *Homo*. *Journal of Human Evolution*, 35; 1-22.
- McHenry, H.M. (1992). Body size and proportions in early hominids. *American Journal of Physical Anthropology*, 87; 407-431.
- McKee, J.K. (1996). Faunal evidence and Sterkfontein Member 2 foot bones of early hominid. *Science*, 271; 1301-1302.
- Morton, D.J. (1922). Evolution of the human foot I. *American Journal of Physical Anthropology*, 5; 305-336.
- Morton, D.J. (1924). Evolution of the human foot II. *American Journal of Physical Anthropology*, 7; 1-52.
- Morton, D.J. (1927). Human Origin. Correlation of previous studies of primate feet and posture with other morphologic studies. *American Journal of Physical Anthropology*, 10; 173-203.
- Morton, D.J. (1935). *The human foot. Its evolution, physiology and functional disorders* New York, Columbia University Press.
- Napier, J.R. (1964). The evolution of bipedal walking in the hominids. *Archives de Biologie (Liege)*, 75(Supplement); 673-708.
- Napier, J.R. (1967). The antiquity of human walking. *Scientific American*, 216(4); 56-66.
- Norušis, M.J. (1994). *SPSS professional statistics 6.1*. Chicago, SPSS Inc.

- O'Higgins, P. (2000). The study of morphological variation in the hominid fossil record: biology, landmarks and geometry. *Journal of Anatomy*, **197**; 103-120.
- O'Higgins, P., Chadfield, P. & Jones, N. (2001). Facial growth and the ontogeny of morphological variation within and between the primates *Cebus apella* and *Cercocebus torquatus*. *Journal of Zoology, London*, **254**; 337-357.
- O'Higgins, P. & Jones, N. (1998). Facial growth in *Cercocebus torquatus*: an application of three-dimensional geometric morphometric techniques to the study of morphological variation. *Journal of Anatomy*, **193**; 251-272.
- Olson, T.R. & Seidel, M.R. (1983). The evolutionary basis of some clinical disorders of the human foot: a comparative survey of the living primates. *Foot & Ankle*, **3**(6); 322-341.
- Owen, R. (1866). Contributions to the natural history of the anthropoid apes. On the external characteristics of the gorilla (*Troglodytes gorilla*, Sav.). *Transactions of the Zoological society of London*, **4**; 243-284.
- Oxnard, C.E. (1972). Some African fossil foot bones: a note on the interpolation of fossils into a matrix of extant species. *American Journal of Physical Anthropology*, **37**; 3-12.
- Oxnard, C.E. & Lisowski, F.P. (1980). Functional articulation of some hominid foot bones: implications for the Olduvai Hominid 8 foot. *American Journal of Physical Anthropology*, **52**; 107-117.
- Page, S.L. & Goodman, M. (2001). Catarrhine phylogeny: noncoding DNA evidence for a diphyletic origin of the Mangebys and a for a Human-Chimpanzee clade. *Molecular Phylogenetics and Evolution*, **18**(1); 14-25.
- Partridge, T.C., Shaw, J., Heslop, D. & Clarke, R.J. (1999). The new hominid skeleton from Sterkfontein, South Africa: age and preliminary assessment. *Journal of Quaternary Science*, **14**(4); 293-298.

- Preuschoft, H. (1971). Body posture and mode of locomotion in early Pleistocene Hominids. *Folia Primatologica*, 14; 209-240.
- Reeser, L.A., Susman, R.L. & Stern, J.T. (1983). Electromyographic studies of the human foot: experimental approaches to hominid evolution. *Foot & Ankle*, 3(6); 391-407.
- Remis, M. (1995). Effects of body size and social context on the arboreal activities of lowland gorillas in the Central African Republic. *American Journal of Physical Anthropology*, 97; 413-433.
- Remis, M.J. (1996). Lowland gorillas as seasonal frugivores: use of resources which vary in time and space. *American Journal of Physical Anthropology*, Supplement 22; 196.
- Remis, M.J. (1997a). Tree structure and group composition influence arboreality in lowland gorillas. *American Journal of Physical Anthropology*, Supplement 24; 196.
- Remis, M.J. (1997b). Western lowland gorillas *Gorilla gorilla gorilla* as seasonal frugivores: Use of a variable resource. *American Journal of Primatology*, 43; 87-109.
- Rholf, F.J. (2000). On the use of shape spaces to compare morphometric methods. *Hystrix*, 11(1); 9-25.
- Rholf, F.J. (2002). Bias and error in estimates of mean shape in morphometrics. *In press*.
- Rholf, F.J. & Slice, D. (1990). Extensions of the Procrustes method for the optimal superimposition of landmarks. *Systematic Zoology*, 39; 40-59.
- Richmond, B.G., Aiello, L.C. & Wood, B.A. (2002). Early hominin limb proportions. *Journal of Human Evolution*. *In press*.

- Richmond, B.G., Begun, D.R. & Strait, D.S. (2002). Origin of human bipedalism: the knuckle-walking hypothesis revisited. *Yearbook of Physical Anthropology*, 44(Supplement 33); 71-105.
- Richmond, B.G. & Strait, D.S. (2000). Evidence that humans evolved from a knuckle-walking ancestor. *Nature*, 404; 382-385.
- Robinson, J.T. (1972). *Early hominid posture and locomotion* Chicago, University of Chicago.
- Ruff, C.B., Trinkhaus, E. & Holliday, T.W. (1997). Body mass and encephalisation in Pleistocene *Homo*. *Nature*, 387; 173-176.
- Ruff, C.B. & Walker, A.C. (1993). Body size and body shape. In: *The Nariokotome Homo erectus skeleton*. A. C. Walker and R. E. Leakey. Cambridge, MA, Harvard Press: 234-265.
- Ruvolo, M. (1997). Molecular phylogeny of the hominoids: inferences from multiple independent DNA sequence sets. *Molecular Biology and Evolution*, 14(3); 248-265.
- Sarmiento, E.E. (1994). Terrestrial traits in the hands and feet of gorillas. *American Museum Novitates*(3091); 1-56.
- Sarmiento, E.E. (2000). The Os Navicular of humans, great apes, OH 8, Hadar, and *Oreopithecus*: function, phylogeny, and multivariate analyses. *American Museum Novitates*(3288); 2-38.
- Schultz, A.H. (1930). The skeleton of the trunk and limbs of higher primates. *Human Biology*, 2; 303-438.
- Schultz, A.H. (1963). The relative lengths of the foot skeleton and its main parts in primates. *Symposia of the Zoological Society of London*, 10; 199-206.

- Senut, B., Pickford, M., Gommery, D., Mein, P., Cheboi, K. & Coppens, Y. (2001). First hominid from the Miocene (Lukeino formation, Kenya). *C.R.Acad.Sci.Paris, Earth & Planetary Sciences*, **332**; 137-144.
- Senut, B. & Tardieu, C. (1985). Functional aspects of Plio-Pleistocene hominid limb bones: implications for taxonomy and phylogeny. In: *Ancestors: The Hard Evidence*. E. Delson. New York, Alan R. Liss, Inc.: 193-201.
- Shea, B.T. (1983). Paedomorphosis and neoteny in the pygmy chimpanzee. *Science*, **222**; 521-522.
- Shea, B.T. & Coolidge, H.J. (1988). Craniometric differentiation and systematics in the genus *Pan*. *Journal of Human Evolution*, **17**; 671-685.
- Siegal, A.F. & Benson, R.H. (1982). A robust comparison of biological shapes. *Biometrics*, **38**; 341-350.
- Smith, R.J. (1993). Categories of allometry: body size versus biomechanics. *Journal of Human Evolution*, **24**; 173-182.
- Smith, R.J. & Jungers, W.L. (1997). Body mass in comparative primatology. *Journal of Human Evolution*, **32**; 523-561.
- Spoor, F., Wood, B.A. & Zonneveld, F. (1994). Implications of early hominid labyrinthine morphology for evolution of human bipedal locomotion. *Nature*, **369**; 645-648.
- Stern, J.T. & Susman, R.L. (1983). The locomotor anatomy of *Australopithecus afarensis*. *American Journal of Physical Anthropology*, **60**; 279-317.
- Stern, J.T. & Susman, R.L. (1991). "Total morphological pattern" versus the "magic trait": conflicting approaches to the study of early hominid bipedalism. In: *Origine(s) de la bipédie chez les hominidés*. Y. Coppens and B. Senut. Paris, Editions du CNRS.

- Sugardjito, J. & Cant, J.G.H. (1994). Geographic and sex differences in positional behaviour of orang-utans. *Treubia*, 31(Part 1); 31-41.
- Susman, R.L. (1983). Evolution of the human foot: evidence from Plio-Pleistocene Hominids. *Foot & Ankle*, 3 (6); 365-376.
- Susman, R.L. (1989). New hominid fossils from the Swartkrans formation (1979-1986 Excavations): postcranial specimens. *American Journal of Physical Anthropology*, 79; 451-474.
- Susman, R.L. & Brain, T.M. (1988). New first metatarsal (SKX 5017) from Swartkrans and the gait of *Paranthropus robustus*. *American Journal of Physical Anthropology*, 77; 7-15.
- Susman, R.L. & Stern, J.T. (1982). Functional morphology of *Homo habilis*. *Science*, 217; 931-934.
- Susman, R.L. & Stern, J.T. (1991). Locomotor behavior of early hominids: epistemology and fossil evidence. In: *Origine(s) de la bipédie chez les hominidés*. Y. Coppens and B. Senut. Paris, Editions du CNRS.
- Susman, R.L., Stern, J.T. & Jungers, W.L. (1985). Locomotor adaptations in the Hadar hominids. In: *Ancestors: The Hard Evidence*. E. Delson. New York, Alan R. Liss, Inc.: 184-192.
- Suzuki, R. (1985). Human adult walking. In: *Primate morphophysiology, locomotor analysis and human bipedalism*. S. Kondo. Tokyo, University of Tokyo Press: 3-24.
- Szalay, F.S. & Langdon, J.H. (1986). The foot of *Oreopithecus*: an evolutionary assessment. *Journal of Human Evolution*, 15; 585-621.
- Thompson, D.A.W. (1917). *On Growth and Form* Cambridge, Cambridge University Press.

- Trinkhaus, E. (1983a). Functional aspects of Neanderthal pedal remains. *Foot & Ankle*, 3 (6); 377-390.
- Trinkhaus, E. (1983b). *The Shanidar Neanderthals*. New York, Academic Press.
- Tuttle, R.H. (1968). Propulsive and prehensile capabilities in the hands and feet of the great apes: a preliminary report. VIIIth Congress of Anthropological and Ethnological Sciences, Tokyo.
- Tuttle, R.H. (1970). Postural, propulsive, and prehensile capabilities in the cheiridia of chimpanzees and other great apes. In: *The Chimpanzee*. Bourne. Basel / New York, Karger. 2: 167-253.
- Tuttle, R.H. (1981). Evolution of hominid bipedalism and prehensile capabilities. *Philosophical Transactions of the Royal Society of London Series B*, 292; 89-94.
- Tuttle, R.H. & Rogers, C.M. (1966). Genetic and selective factors in reduction of the hallux in *Pongo pygmaeus*. *American Journal of Physical Anthropology*, 24(2); 191-198.
- Tuttle, R.H., Webb, D.M. & Tuttle, N.I. (1991). Laetoli footprint trails and the evolution of hominid bipedalism. In: *Origine(s) de la bipédie chez les hominidés*. Y. Coppens and B. Senut. Paris, Editions du CNRS.
- Tyson, E. (1699). *Orang-Outang, sive Homo sylvestris: or, the anatomy of a Pygmie compared with that of a monkey, an ape, and a man*. London, John Hoskins, Thomas Bennet & Daniel Brown.
- Volkov, T. (1903). Les variations squelettiques du pied chez les Primates et dans les races humaines. *Bulletin et Mémoires de la Société d'Anthropologie de Paris*, 5(4); 632-708.

- Volkov, T. (1904). Les variations squelettiques du pied chez les Primates et dans les races humaines. *Bulletin et Mémoires de la Société d'Anthropologie de Paris*, 5(5); 1-50, 201-331.
- Vrba, E.S. & Panagos, D.C. (1982). New perspectives on taphonomy, palaeoecology and chronology of the Kromdraai apeman. *Palaeoecology of Africa*, 15; 13-26.
- Walter, R.C. (1994). Age of Lucy and the First Family: single crystal ⁴⁰/₃₉ Ar dating of the Denen Dora and lower Kada Hadar members of the Hadar Formation, Ethiopia. *Geology*, 22; 6-10.
- Wheeler, P. (1988). Stand tall and stay cool. *New Scientist*, 12 May; 62-65.
- Wheeler, P. (1994). The foraging times of bipedal and quadrupedal hominids in open equatorial environments (a reply to Chaplin, Jablonski & Cable, 1994). *Journal of Human Evolution*, 27; 511-517.
- White, T.D. & Suwa, G. (1987). Hominid footprints at Laetoli: facts and interpretations. *American Journal of Physical Anthropology*, 72; 485-514.
- Wood, B.A. (1973). Locomotor affinities of hominoid tali from Kenya. *Nature*, 246; 45-46.
- Wood, B.A. (1974a). A *Homo* talus from East Rudolf, Kenya. *Journal of Anatomy*, 117; 203-204.
- Wood, B.A. (1974b). Olduvai Bed I post-cranial fossils: a reassessment. *Journal of Human Evolution*, 3; 373-378.
- Wood, B.A. (1991). Origin and evolution of the genus *Homo*. *Nature*, 355; 783-790.
- Wood, B.A. (1993). Four legs good, two legs better. *Nature*, 363; 587-588.

Wood, B.A. (2002). Hominid revelations from Chad. *Nature*, 418; 133-135.

Wood, B.A. & Collard, M. (1999). The Human Genus. *Science*, 284; 65-71.

Wood, B.A. & Richmond, B.G. (2000). Human evolution: taxonomy and paleobiology. *Journal of Anatomy*, 106; 19-60.

Wood Jones, F. (1946). *Structure and function as seen in the foot* London, Bailliere, Tindall and Cox.